

Faculty of Engineering

Numerical Modelling on Load Bearing Performance of Combined Stone Column-Piled Raft Foundation in Soft Clay Soil

Danish Ahmed

Doctor of Philosophy
2024

Numerical Modelling on Load Bearing Performance of Combined Stone Column-Piled Raft Foundation in Soft Clay Soil

Danish Ahmed

A thesis submitted

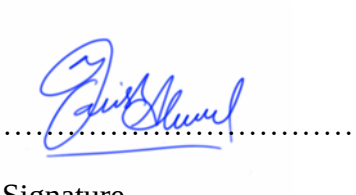
In fulfillment of the requirements for the degree of Doctor of Philosophy

(Civil Engineering)

Faculty of Engineering
UNIVERSITI MALAYSIA SARAWAK
2024

DECLARATION

I declare that the work in this thesis was carried out in accordance with the regulations of Universiti Malaysia Sarawak. Except where due acknowledgements have been made, the work is that of the author alone. The thesis has not been accepted for any degree and is not concurrently submitted in candidature of any other degree.



……

Signature

Name: Danish Ahmed

Matric No.: 17010168

Faculty of Engineering

Universiti Malaysia Sarawak

Date: 03/13/2024

ACKNOWLEDGEMENT

All honour and grandeur go to Allah Almighty who gave me the strength and endurance to carry out this work.

I would like to pay my immense regard and appreciation to my thesis advisor Dr. Siti Noor Linda bt Taib for her consistent guidance, motivation, and feedback during the course of this research work.

I would like to express my appreciation to my co-advisor Dr. Tahar Ayadat for helping me with my research work. I am heartily thankful to the efforts he put in while encouraging and mentoring me. I extend my deepest gratitude to Dr. Alsidqi Hasan who gave astute comments and reviewed my work.

I would also like to thank my friends Ajmal and Saad whose consistent support and encouragement made this journey a lot more pleasant. Thanks guys, you were always there for me.

Last, but most important, I thank my family: My father and my mother for the indescribable support, love, and confidence they provided during course of my studies. My wife for being always there to listen, encourage, motivate me; my brothers for giving me immense support and motivation; and specially my son and daughter for giving me love, comfort, and making my mind relaxed during hard times.

I would like to take this opportunity to acknowledge all the people who contributed directly or indirectly to this thesis.

My sincere gratitude to the Centre for Graduate Studies, for the advice and support given during my period of study in Universiti Malaysia Sarawak.

Finally, I would like to thank the management of the Universiti Malaysia Sarawak for making it possible for me to complete my study here in Sarawak. Thank you all.

ABSTRACT

An important problem encountered by foundation engineers involves soft to very soft (compressible) soils which possess low in-situ undrained shear strength (i.e., cu < 25 kPa). Foundation design in such soils is difficult at best. In many cases, deep foundations may be required to transmit foundation loads to suitable bearing strata below the soft soil deposit. Furthermore, stone columns, which consist of granular material compacted in long cylindrical holes, can be used as a technique for improving the strength and consolidation characteristics of these soils. Their costs are relatively moderate, and their installation requires medium-priced equipment. Stone columns occupy an important place and have a major role in ground treatment methods. Their use for more than 50 years in reinforcing soft soils has demonstrated their usefulness and makes them one of the most attractive methods in improving bearing capacity and reducing settlement. Unlike pile foundations, stone columns make very efficient use of the soil near the surface. These stone columns are ideal for supporting light loads, but less effective when it comes to supporting heavy loads because stone columns cannot transfer the applied stresses to the deeper layers of soil. For heavy constructions, where it is needed to transfer the applied stresses to deeper layers, piles are the most recommended foundation system. However, piles are costly, and their use is expensive. To overcome these technical and economic issues, it might be more appropriate to combine both foundations in one combined foundation system (i.e., stone column and piles used conjugally under raft foundation). In the literature, very limited work has been reported regarding the use of such a system to reinforce soft and compressible soils. Furthermore, no study was carried out to investigate the behaviour of such combined foundation system, to optimize the configuration of stone columns/piles group as combined foundation system, and to develop a theoretical model to predict the carrying capacity of the

combined foundation system in soft soil capped with rigid raft foundation. Therefore, the objectives of this numerical investigation are to study the behaviour (i.e., modes of failure) of this new foundation system in order to optimize the configuration of stone columns/piles to get optimum soil improvement. For this reason, parametric study was conducted to examine the effect of the configuration and arrangement of the combined foundation system on the performance of this type of foundation system on soft soils. Also, an optimization study was conducted aiming to display the geometrical layout of stone columns/pile foundations exhibiting the superlative improvement of the performance of soil foundation. It was observed from the parametric study that combining stone columns and piles in one foundation system, improve the carrying capacity of the system, modify the soil foundation to a new upgraded composite ground, and certainly can reduce the cost of the geotechnical works. Overall, 680 combinations were investigated for this parametric study and based on the optimization study, chief leading sets were selected to get optimum soil improvement. It was noticed that these chief leading sets can increase the bearing capacity of the raft foundation by almost 50% to 90% compared to that of raft foundation resting on stone columns only. Based on the results of the optimization study, the behaviour (i.e., modes of failure) of such combined foundation system under loading was examined and it was observed that the combined foundation system fails by shear in the stone columns and soft soil, and by bearing and shear failure of pile's tip under the rigid raft. The outcome of the observed behaviour (i.e., modes of failure) was used to develop an analytical model for predicting the carrying capacity of the combined system in soft soil.

Keywords: Combined foundation system, Stone columns, Piles, Raft foundation, Performance, Soft soil, Failure Mechanism, Improvement Factor, Parametric study, optimization study, Numerical investigation, Analytical model.

Pemodelan Berangka pada Prestasi Menanggung Beban Asas Rakit Bercorak Tiang Batu Gabungan dalam Tanah Tanah Liat Lembut

ABSTRAK

Masalah penting yang dihadapi oleh jurutera asas melibatkan tanah lembut hingga sangat lembut (boleh mampat) yang mempunyai kekuatan ricih tak bersaliran in-situ yang rendah (iaitu, cu < 25 kPa). Reka bentuk asas dalam tanah sedemikian adalah paling sukar. Dalam kebanyakan kes, asas dalam mungkin diperlukan untuk menghantar beban asas ke strata galas yang sesuai di bawah deposit tanah lembut. Tambahan pula, tiang batu, yang terdiri daripada bahan berbutir yang dipadatkan dalam lubang silinder panjang, boleh digunakan sebagai teknik untuk meningkatkan kekuatan dan ciri penyatuan tanah ini. Kos mereka agak sederhana, dan pemasangannya memerlukan peralatan berharga sederhana. Tiang batu menduduki tempat yang penting dan mempunyai peranan utama dalam kaedah rawatan tanah. Penggunaannya selama lebih daripada 50 tahun dalam mengukuhkan tanah lembut telah menunjukkan kegunaannya dan menjadikannya salah satu kaedah yang paling menarik dalam meningkatkan kapasiti galas dan mengurangkan penyelesaian. Tidak seperti asas cerucuk, tiang batu menggunakan tanah berhampiran permukaan dengan sangat cekap. Tiang batu ini sesuai untuk menyokong beban ringan, tetapi kurang berkesan apabila ia datang untuk menyokong beban berat kerana tiang batu tidak dapat memindahkan tegasan yang dikenakan ke lapisan tanah yang lebih dalam. Untuk pembinaan berat, di mana ia diperlukan untuk memindahkan tegasan yang dikenakan ke lapisan yang lebih dalam, cerucuk adalah sistem asas yang paling disyorkan. Walau bagaimanapun, cerucuk adalah mahal, dan penggunaannya mahal. Untuk mengatasi isu teknikal dan ekonomi ini, mungkin lebih sesuai untuk menggabungkan kedua-dua asas dalam satu sistem asas gabungan (iaitu, tiang batu dan cerucuk yang digunakan secara bersambung di bawah asas

rakit). Dalam literatur, kerja yang sangat terhad telah dilaporkan mengenai penggunaan sistem sedemikian untuk mengukuhkan tanah lembut dan boleh mampat. Tambahan pula, tiada kajian telah dijalankan untuk menyiasat kelakuan sistem asas gabungan tersebut, untuk mengoptimumkan konfigurasi tiang batu/kumpulan cerucuk sebagai sistem asas gabungan, dan untuk membangunkan model teori untuk meramalkan daya tampung sistem asas gabungan dalam bentuk lembut. tanah ditutup dengan asas rakit tegar. Oleh itu, objektif penyiasatan berangka ini adalah untuk mengkaji tingkah laku (iaitu, mod kegagalan) sistem asas baharu ini untuk mengoptimumkan konfigurasi tiang/cerucuk batu untuk mendapatkan pembaikan tanah yang optimum. Atas sebab ini, kajian parametrik telah dijalankan untuk mengkaji kesan konfigurasi dan susunan sistem asas gabungan terhadap prestasi sistem asas jenis ini pada tanah lembut. Juga, kajian pengoptimuman telah dijalankan bertujuan untuk memaparkan susun atur geometri tiang batu/asas cerucuk yang mempamerkan peningkatan superlatif prestasi asas tanah. Ia diperhatikan daripada kajian parametrik bahawa menggabungkan tiang batu dan cerucuk dalam satu sistem asas, meningkatkan daya tampung sistem, mengubah suai asas tanah kepada tanah komposit baru yang dinaik taraf, dan pastinya dapat mengurangkan kos kerja-kerja geoteknik. Secara keseluruhan, 680 kombinasi telah disiasat untuk kajian parametrik ini dan berdasarkan kajian pengoptimuman, set peneraju utama telah dipilih untuk mendapatkan pembaikan tanah yang optimum. Adalah diperhatikan bahawa set peneraju utama ini boleh meningkatkan kapasiti galas asas rakit sebanyak hampir 50% hingga 90% berbanding asas rakit yang terletak pada tiang batu sahaja. Berdasarkan keputusan kajian pengoptimuman, tingkah laku (iaitu, mod kegagalan) sistem asas gabungan tersebut di bawah beban telah diperiksa dan diperhatikan bahawa sistem asas gabungan gagal dengan ricih dalam tiang batu dan tanah lembut, dan dengan galas dan kegagalan ricih hujung cerucuk di bawah

rakit tegar. Hasil daripada tingkah laku yang diperhatikan (iaitu, mod kegagalan) telah digunakan untuk membangunkan model analitikal untuk meramalkan kapasiti tampung sistem gabungan dalam tanah lembut.

Kata kunci: *Sistem asas gabungan, Tiang batu, Cerucuk, Asas rakit, Prestasi, Tanah lembut, Mekanisme Kegagalan, Faktor Penambahbaikan, Kajian parametrik, kajian pengoptimuman, Penyiasatan berangka, Model analisis*

TABLE OF CONTENTS

		Page
DECLARATION		**i**
ACKNOWLEDGEMENT		**ii**
ABSTRACT		**iv**
ABSTRAK		**vi**
TABLE OF CONTENTS		**ix**
LIST OF TABLES		**xiv**
LIST OF FIGURES		**xvi**
LIST OF ABBREVIATIONS AND NOTATIONS		**xxiii**
CHAPTER 1	**INTRODUCTION**	**1**
1.1	Background of the Study	1
1.2	Problem Statement	2
1.3	Hypothesis of Research	3
1.4	Objectives	4
1.5	Motivation of the Research	5
1.6	Scope of Research	6
1.7	Thesis Outline	6
CHAPTER 2	**LITERATURE REVIEW**	**8**

2.1 Introduction 8

2.2 Stone Columns as Ground Improvement 9

2.2.1 Failure Mechanism of Stone Columns 9

2.2.2 Analytical and Numerical Studies of Stone Columns 16

2.3 Piled Raft Foundation 36

2.3.1 Failure Mechanism of Pile Foundation 37

2.3.2 Analytical and Numerical Studies of Pile Foundation 38

2.4 Stone Column and Pile under Raft Foundation 51

2.5 Material Properties and Parameters Available in Literature 58

2.6 Summary 66

CHAPTER 3 METHODOLOGY 72

3.1 Introduction 72

3.2 Numerical Modelling 77

3.2.1 Material Model 77

3.2.1.1 Soil Model 77

3.2.1.2 Stone Columns 80

3.2.1.3 Concrete Raft 80

3.2.1.4 Embedded Pile 80

3.2.2 Geometry and Boundary Conditions 83

3.2.3 Loading Details 84

3.2.4 Meshing 85

3.2.5 3D Models 87

3.2.5.1 3D Model for Stone Columns under Raft Foundation in Soft Soil 89

3.2.5.2 3D Model for Piled Raft Foundation in Soft Soil 91

3.2.5.3 3D Model for Combined Stone Column/Piles Caped with Raft Foundation in Soft Soil 94

3.2.6 Model Validation 100

3.2.6.1 Numerical Validation for Stone Columns under Raft in Soft Soil 101

3.2.6.2 Numerical Validation for Piled Raft Foundation in Soft Soil 103

3.3 Limitation of the Research 106

3.4 Chin's method 107

3.5 Summary 109

CHAPTER 4 RESULTS AND DISCUSSIONS 110

4.1 Overview 110

4.2 Parametric Study of Stone Columns under Raft Foundation in Soft Soil 110

4.2.1 Effect of Stone Columns Spacing 110

4.2.2 Effect of Angle of Friction of Stone Columns 116

4.2.3 Behaviour of Stone Columns Under Raft Foundation in Soft Soil 117

4.3 Parametric Study of Piled Raft Foundation in Soft Soil 121

4.3.1 Effect of Pile Spacing 121

4.3.2 Effect of Pile Diameter 124

4.3.3 Effect of Modulus of Elasticity of Soil 128

4.3.4 Behaviour of Piled Raft Foundation in Soft Soil 130

4.3.5 Improvement Factor (IF_{PR}) for the Piled Raft Foundation System 134

4.4 Parametric Study of Combined Stone Column/Piles Caped with Raft Foundation in Soft Soil 138

4.4.1 Effect of Configuration of Combined Foundation 139

4.4.2 Effect of Diameter of Stone Column and Pile 142

4.4.3 Effect of Length of Stone Column and Pile 145

4.4.4 Effect of Modulus of Elasticity of Soil 148

4.4.5 Effect of Angle of Friction of Stone Column 150

4.4.6 Optimization Study 153

4.4.7 Behaviour of Combined Foundation in Soft Soil 162

4.5 Results Summary 171

CHAPTER 5 THEORETICAL DEVELOPMENT 177

5.1 Overview 177

5.2 Analytical Model for Stone Columns under Raft in Soft Clay Soils 177

5.3 Analytical Model for Piled Raft Foundation in Soft Clayey Soils 180

5.4 Analytical Model for Combined Foundation System in Soft Clayey Soils 190

5.5 Summary 199

CHAPTER 6 CONCLUSION AND RECOMMENDATIONS 200

6.1 Conclusion 200

6.1.1 Stone Columns Under Raft Foundation in Soft Clayey Soils 200

6.1.2 Piled Raft Foundation in Soft Clayey Soils 201

6.1.3 Combined Foundation System Composed of Stone Columns, Piles and Rigid Raft Foundation in Soft Clayey Soils 202

6.2 Recommendations 205

REFERENCES **206**

APPENDICES **222**

LIST OF TABLES

		Page
Table 2.1:	Settlement (mm) for different number of columns. (Castro, 2014)	21
Table 2.2:	Column configurations to investigate influence of other parameters (Micheál & Bryan, 2014)	26
Table 2.3:	Parameters of stone column and piled raft. (Samanta & Bhowmik, 2017)	56
Table 2.4:	Range of parameters available in literature	58
Table 3.1:	Range of parameters used in this numerical investigation	74
Table 3.2:	Range of parameters used for stone columns under raft for present study	91
Table 3.3:	Configuration of stone columns under raft for present study	91
Table 3.4:	Range of parameters of piled raft for present study	93
Table 3.5:	Configuration of piled raft for present study	94
Table 3.6:	Foremost sets in each group	98
Table 3.7:	20 Combinations for parametric study	99
Table 3.8:	Materials properties for combined stone column/piles caped with raft	100
Table 3.9:	Statistical analysis for stone columns model validation	102
Table 3.10:	Material properties (Sinha & Hanna, 2017)	103
Table 3.11:	Statistical analysis for piled raft model validation	105
Table 3.12:	Stress Vs Strain for untreated soil (Raft alone in soft clay)	107
Table 4.1:	Ultimate carrying capacity using Chin's method	115
Table 4.2:	Foremost performed set in each group	161
Table 5.1:	Validation of the present analytical model for stone columns under foundation (Equation 5.1)	180
Table 5.2:	Validation of the present analytical model for piled raft foundation (Equation 5.28)	189

Table 5.3: Calibration of the present analytical model for combined foundation (Equation 5.43) 197

LIST OF FIGURES

Page

Figure 2.1: Stress on the columns (Hughes & Withers, 1974) 10

Figure 2.2: Deformed shape of the model test after applying load (Hu, 1995). 12

Figure 2.3: Deformed shape of single stone column (Hanna et al., 2013) 13

Figure 2.4: Deformed shape of group of stone columns (Hanna et al., 2013) 14

Figure 2.5: Design charts for predicting the mode of failure of soft soils reinforced (Hanna et al., 2013) 16

Figure 2.6: Variation of stone column ultimate load versus stone column spacing for various stone material diameters (Nazari et al., 2014) 18

Figure 2.7: Comparison between bearing capacity values determined (Nazari et al., 2014) 18

Figure 2.8: Critical column length for different area replacement ratios. (Castro, 2014) 20

Figure 2.9: Groups of stone columns for different number of columns. (Castro, 2014) 20

Figure 2.10: Influence of column stiffness upon settlement improvement factors. (Micheál & Bryan, 2014) 23

Figure 2.11: Influence of column strength upon settlement improvement factors. (Micheál & Bryan, 2014) 24

Figure 2.12: Influence of the coefficient of lateral earth pressure upon settlement (Micheál & Bryan, 2014) 24

Figure 2.13: Column configurations to examine the influence of column (Micheál & Bryan, 2014) 25

Figure 2.14: Distribution of total shear strains through a cross-section of a 3x3 group of 8m long columns at A/A_C of (i)3.5, (ii)8.0 and (iii)14.1. (Micheál & Bryan, 2014) 25

Figure 2.15: Load – settlement for the non-reinforced and reinforced soft soil with different spacing ratios (Elsawy & El-Garhy, 2016) 29

Figure 2.16: Bending moment distribution along footing for non-reinforced and reinforced soft soil with different spacing ratios. (Elsawy & El-Garhy, 2016) 29

Figure 2.17: Load – settlement for non-reinforced and reinforced soft soil with different pile lengths (Elsawy & El-Garhy, 2016) 30

Figure 2.18: Deformed mesh for single and group of stone columns under static load (Ziaie & Mohammadi-Haji, 2016) 31

Figure 2.19: Comparison of the load-settlement static curves of unimproved ground and improved ground (Ziaie & Mohammadi-Haji, 2016) 31

Figure 2.20: Variation of lateral displacement of central and periphery stone columns versus normalized depth. (Ziaie & Mohammadi-Haji, 2016) 32

Figure 2.21: Comparison of settlement improvement factors from numerical analysis and analytical methods. (Znamenskii & Syed, 2019) 35

Figure 2.22: Pile skin friction and point bearing. 38

Figure 2.23: Piled raft load displacement relationship. (Elwakil & Azzam, 2016) 39

Figure 2.24: Normalized differential settlements with pile group-raft raft area ratio (stiff clay):(a)3x3 array;(b)4x 4 array. (Cho et al., 2012) 42

Figure 2.25: Piled raft's behaviour comparison between centrifuge test, proposed method analysis and Plaxis 3D foundation analysis. (a) Piled raft with 16 piles (D = 0.6 m; L = 15 m) in dense sand. (b) Piled raft with 16 piles (D = 0.6 m; L = 15m) in loose sand. (c) Piled raft with 9 piles (D = 0.6 m; L = 9 m) in dense sand. (Nguyen et al., 2013) 44

Figure 2.26: Distribution of total bending moment. (a) PLAXIS 3D. (b) SAP 2000. (Nguyen et al., 2013) 45

Figure 2.27: Influence of parameters on the load carrying capacity of piled raft system (Prashant et al., 2013) 46

Figure 2.28: Load-settlement curve (Anhtuan et al., 2014) 47

Figure 2.29: Effect pile spacing on the settlement of the foundation, U_{max}= maximum settlement. (Anhtuan et al., 2014) 47

Figure 2.30: Settlement reduction by increasing number of piles (Paravita & Daniel, 2015) 48

Figure 2.31: Average settlement versus pile length effect with respect to spacing to diameter ratio (*s/d*). (Celik, 2019) 50

Figure 2.32: Schematic diagram of calculating modal to be analyzed. (Liang et al., 2003) 53

Figure 2.33: Effects of cushion elastic modulus on axial stress distribution of piles. (Liang et al., 2003) 53

Figure 2.34: Effects of cushion thickness on axial force of piles to soil. (Liang et al., 2003) 54

Figure 2.35: Effects of cushion thickness on stress ratio of piles to soil. (Liang et al., 2003) 54

Figure 2.36: Schematic diagram of one quarter of the problem modelled in the present study (Samanta & Bhowmik, 2017) 55

Figure 2.37: Pile and stone column within the raft in FEM model. (Samanta & Bhowmik, 2017) 56

Figure 2.38: Settlements (Samanta & Bhowmik, 2017) 57

Figure 3.1: Flow chart of methodology 76

Figure 3.2: Basic concept of elastic perfectly plastic. (Brinkgreve et al., 2013) 80

Figure 3.3: Stiffness at the skin of the pile. (Brinkgreve et al., 2013) 82

Figure 3.4: Stiffness at the foot of the pile. (Brinkgreve et al., 2013) 83

Figure 3.5: 3D model with boundary conditions 84

Figure 3.6: 3D model for Raft 84

Figure 3.7: 3D soil elements (10-node Tetrahedrons) 85

Figure 3.8: Meshing 86

Figure 3.9: Refined meshing for stone columns 86

Figure 3.10: Refined meshing for piled raft 87

Figure 3.11: Refined meshing for combined stone column/piles caped with raft 87

Figure 3.12: 3D model for raft and soil 88

Figure 3.13: Cross-section of raft and soil 89

Figure 3.14: Finite element model for stone columns under raft 90

Figure 3.15: 3D model for stone columns under raft 90

Figure 3.16: Finite element model for piled raft 92

Figure 3.17: 3D model for piled raft 92

Figure 3.18: Finite element model for combined stone column/piles caped with raft 96

Figure 3.19: 3D model for combined stone column/piles caped with raft 96

Figure 3.20: Different configurations (Sets) for combined foundation 97

Figure 3.21: Load vs settlement curves for validation of stone columns under raft 102

Figure 3.22: Stress-Displacement for validation of raft only 104

Figure 3.23: Stress-Displacement for validation of piled raft 104

Figure 3.24: Stress Vs Strain for untreated soil (Raft alone in soft clay) 108

Figure 3.25: Strain/Stress Vs Strain (Chin, 1970) for untreated soil (Raft alone in soft clay) 108

Figure 4.1: Stress Vs Strain for untreated soil and treated soil as a function of *S/D* and $\varphi c = 42^o$ 112

Figure 4.2: Strain/Stress Vs Strain (Chin, 1970) for untreated soil and treated soil as a function of *S/D* and $\varphi c = 42^o$ 112

Figure 4.3: Stress Vs Strain for untreated soil and treated soil as a function of *S/D* and $\varphi c = 45^o$ 113

Figure 4.4: Strain/Stress Vs Strain (Chin, 1970) for untreated soil and treated soil as a function of *S/D* and $\varphi c = 45^o$ 113

Figure 4.5: Stress Vs Strain for untreated soil and treated soil as a function of *S/D* and $\varphi c = 48^o$ 114

Figure 4.6: Strain/Stress Vs Strain (Chin, 1970) for untreated soil and treated soil, as a function of *S/D* and $\varphi c = 48^o$ 114

Figure 4.7: Bearing capacity ratio (*BCR*) as a function of *S/D* and angle of friction 116

Figure 4.8: q_u Vs φc for stone columns under raft 117

Figure 4.9: Behaviour of stone columns under raft for the case *S/D* = 7 119

Figure 4.10: Behaviour of stone columns under raft for the case *S/D* = 6 119

Figure 4.11: Behaviour of stone columns under raft for the case *S/D* = 5 120

Figure 4.12: Behaviour of stone columns under raft for the case *S/D* = 4 120

Figure 4.13: Stress Vs Strain for *L/D* = 50, E_p/E_s =52500 123

Figure 4.14: Strain/Stress Vs Strain (Chin, 1970) for untreated soil and treated soil (*L/D* = 50, E_p/E_s = 52500) 123

Figure 4.15: q_u Vs L/D for untreated soil and treated soil as a function of E_p/E_s and S/D = 7 125

Figure 4.16: qu Vs L/D for untreated soil and treated soil as a function of E_p/E_s and S/D = 6 125

Figure 4.17: q_u Vs L/D for untreated soil and treated soil as a function of E_p/E_s and S/D = 5 126

Figure 4.18: q_u Vs L/D for untreated soil and treated soil as a function of E_p/E_s and S/D = 4 126

Figure 4.19: q_u Vs L/D for untreated soil and treated soil as a function of E_p/E_s and S/D = 3 127

Figure 4.20: q_u Vs E_p/E_s for untreated soil and treated soil as a function of S/D and L/D = 50 129

Figure 4.21: q_u Vs E_p/E_s for untreated soil and treated soil as a function of S/D and L/D = 40 129

Figure 4.22: q_u Vs E_p/E_s for untreated soil and treated soil as a function of S/D and L/D = 33.33 130

Figure 4.23: Behaviour of piled raft for the case (L/D = 40, S/D = 7, E_p/E_s = 52500) 131

Figure 4.24: Behaviour of piled raft for the case (L/D = 40, S/D = 6, E_p/E_s = 52500) 131

Figure 4.25: Behaviour of piled raft for the case (L/D = 40, S/D = 5, E_p/E_s = 52500) 132

Figure 4.26: Behaviour of piled raft for the case (L/D = 40, S/D = 4, E_p/E_s = 52500) 132

Figure 4.27: (a) Behaviour of piled raft for the case (L/D = 40, S/D = 3, E_p/E_s =52500) and (b) Behaviour of stone columns under raft for the case S/D = 4 133

Figure 4.28: Variation of the improvement factor (IF_{PR}) as a function of S/D and L/D = 50 136

Figure 4.29: Variation of the improvement factor (IF_{PR}) as a function of L/D and S/D = 6 137

Figure 4.30: Variation of the improvement factor (IF_{PR}) as a function of E_p/E_s and L/D = 50 137

Figure 4.31: Variation of the improvement factor (IF_{PR}) as a function of E_p/E_s and S/D = 5 138

Figure 4.32: Stress Vs Strain for combined foundation (combination 1) 140

Figure 4.33: Strain/Stress Vs Strain (Chin, 1970) for combined foundation (combination 1) 140

Figure 4.34: Ultimate carrying capacities for combined foundation (combination 1) 142

Figure 4.35: *IF* VS n_A f as a function of L_c/L_p = 1, and D_p/D_c 144

Figure 4.36: *IF* VS n_A as a function of L_c/L_p = 0.9, and D_p/D_c 144

Figure 4.37: *IF* VS n_A as a function of L_c/L_p = 0.8, and D_p/D_c 145

Figure 4.38: *IF* VS n_A as a function of L_c/L_p = 0.6, and D_p/D_c 145

Figure 4.39: *IF* VS n_A as a function of D_p/D_c = 0.6, and L_c/L_p 147

Figure 4.40: *IF* VS n_A as a function of D_p/D_c = 0.5, and L_c/L_p 147

Figure 4.41: *IF* VS n_A as a function of D_p/D_c = 0.4, and L_c/L_p 148

Figure 4.42: *IF* VS n_A as a function of L_c/L_p = 1, and $(E_p + E_c) / E_s$ 149

Figure 4.43: *IF* VS n_A as a function of for L_c/L_p = 0.8, and $(E_p + E_c) / E_s$ 150

Figure 4.44: *IF* VS n_A as a function of L_c/L_p = 1, and φ_c 152

Figure 4.45: *IF* VS n_A as a function of L_c/L_p = 0.8, and φ_c 152

Figure 4.46: Improvement factor (*IF*) for group 1 155

Figure 4.47: Improvement factor (*IF*) for group 2 155

Figure 4.48: Improvement factor (*IF*) for group 3 156

Figure 4.49: Improvement factor (*IF*) for group 4 156

Figure 4.50: Improvement factor (*IF*) for group 5 157

Figure 4.51: Improvement factor (*IF*) for group 6 157

Figure 4.52: Improvement factor (*IF*) for group 7 158

Figure 4.53: Improvement factor (*IF*) for group 8 158

Figure 4.54: Improvement factor (*IF*) for group 9 159

Figure 4.55: Improvement factor (*IF*) for group 10 159

Figure 4.56: Improvement factor (*IF*) for group 11 160

Figure 4.57: Chief leading set no. 28 163

Figure 4.58: Behaviour of chief leading set no. 28, Section A-A 163

Figure 4.59: Behaviour of chief leading set no. 28, Section B-B 164

Figure 4.60: Behaviour of chief leading set no. 28, Section C-C 164

Figure 4.61: Chief leading set no. 33 165

Figure 4.62: Behaviour of chief leading set no. 33, Section A-A 165

Figure 4.63: Behaviourof chief leading set no. 33, Section B-B 166

Figure 4.64: Behaviour of chief leading set no. 33, Section C-C 166

Figure 4.65: Chief leading set no. 4 167

Figure 4.66: Behaviour of chief leading set no. 4, Section A-A 167

Figure 4.67: Behaviour of chief leading set no. 4, Section B-B 168

Figure 4.68: Behaviour of chief leading set no. 4, Section C-C 168

Figure 4.69: Chief leading set no. 12 169

Figure 4.70: Behaviour of chief leading set no. 12, Section A-A 169

Figure 4.71: Behaviour of chief leading set no. 12, Section B-B 170

Figure 4.72: Behaviour of chief leading set no. 12, Section C-C 170

Figure 5.1: Shape of the shear failure at the beginning of the failure mechanism. 182

Figure 5.2: Shape of the shear failure mechanism when the applied load approaches the ultimate load capacity. 182

Figure 5.3: Geometry/configuration of the shear failure mechanism of the piled raft foundation in soft soils 183

Figure 5.4: Observed behaviour (i.e., modes of failure)for the chief leading sets 4 and 28. 191

Figure 5.5: Observed behaviour 195

LIST OF ABBREVIATIONS AND NOTATIONS

A_{col}	Column cross-section
A_g	Actual area of the pile group
A_s	The area replacement ratio
B	Width, width of raft
BCR	Bearing capacity ratio
B_g	Width of pile group
B_r	Width of raft foundation
c	Cohesion, Cohesion of soft soil
c_{comp}	Cohesion of composite (clay+stone column)
c_c	Cohesion of soil (clay)
c_s	Cohesion of stone columns
c_u	Cohesion
C_u	Soil shear strength
c_2	Cohesion of soil supporting the piles
D	Diameter
d	Column diameter
d_c	Diameter of column
D_f	Depth of foundation, Depth of raft
D_p/D_c	Diameter of piles to diameter of stone columns ratio
D_1	Diameter of pile
E	Young's modulus
E_c	Modulus of elasticity of column

E_p	Modulus of elasticity of Pile
E_p/E_s	The modulus of elasticity of pile over soft clay ratio
E_s	Modulus of elasticity of soil
f_{foot}	Base resistance
H	Height or length of pile group
IF	Improvement factor
IF_{PR}	Improvement factor for the piled raft foundation system
K_{foot}	Stiffness at the pile tip
K_n,K_t	Interface stiffness in the normal direction
K_s	Interface stiffness in the axial direction
K_{skin}	Material stiffness matrix of the interface
L	Length, Length of raft
L/D	Length to diameter ratio
L_p/L_c	Length of pile to length to stone column ratio
m, n	Number of piles
n	Stress ratio
n_A	Total area of piles over total area of stone columns under the raft
n_1	Number of piles
p_a	Atmospheric pressure (100 kN/m^2)
Q_p	The bearing at the pile point
Q_s	Skin friction
Q_u	Load transfers from the raft
Q_{u1}	Ultimate composite
Q_{u2}	Ultimate of one pile
q_u	Bearing capacity, Ultimate Carrying Capacity

S	Spacing
SPT	Standard penetration test
S/D	Spacing to diameter ratio
t_n,t_t	Shear stress in the normal direction
t_s	Shear stress in the axial direction
t_{skin}	Traction along the pile
UDL	Uniform distributed load
u_p	Displacement of pile
u_s	Displacement of soil
u^P_{foot}	Displacement of pile at foot
u^S_{foot}	Displacement of soil at foot
v	Poisson's ratio
v_s	Soil Poisson's ratio
α	Configuration factor
γ	Unit weight
γ_c	Unit weight of soft soil (clay)
γ_s	Unit weight of stone columns
γ_{sat}	Unit weight saturated
γ_{unsat}	Unit weight unsaturated
γ_{comp}	Unit weight of the composite
φ_c	Angle of shearing resistance of soft soil, Friction of stone columns
φ_s	Angle of shearing resistance of granular column's material
$\emptyset'$	Angle of friction of stone column
φ_{comp}	Angle of shearing resistance of the composite
φ_2	Angle of shearing resistance of soil supporting the piles

ψ	Dilatancy angle
ε	Strain
σ	Applied Stress

CHAPTER 1

INTRODUCTION

1.1 Background of the Study

In the last few decades, many countries around the world have seen a significant expansion of infrastructure cities outside of their traditional inhibited zones. In these areas and environments, geotechnical engineers have had to deal with totally new types of soil problems, such as collapsible soils, swelling soils, liquefiable soils, soft soils (up to very soft) and peats. The most common type of troublesome soil is soft compressible soil. Usually, these types of soils can be found in lowland areas like floodplains, streams, and lakes. It has been possible nowadays to classify, test, and construct on weakly compressible soft soils.

High compressibility, low undrained shear strength (C_u less than 25 kPa), and low permeability are the main characteristics of these soft soils. For these types of soils, construction problems generally include excessive compression under heavily loaded foundations, insufficient bearing capacity, differential settlement, and instability while excavating and forming embankments. These problems are often overcome by using ground improvement techniques including precompression, sand drains, stone columns, and sand compaction piles, in addition to stabilization through mixtures, soil reinforcement, and pile foundations. As far as weak and soft (compressible) soils are concerned, stone columns and pile foundations are among the common foundation systems (Hughes & Withers, 1974; Michael et al., 2004; Pivarc, 2011; Paravita & Daniel 2015). Piles are employed on soft soils on which foundations have low bearing capacity and high consolidation settlement. They carry load through soft soil to firm stratum through bearing and/or side friction. They are

usually deployed for cases of large loads (such as high-rise building) applied on poorly soils. However, advance planning and heavy equipment are required for driving them. Stone columns consists of crushed coarse aggregates of various size compacted in long cylindrical holes in the ground to ameliorate the performance of soft soils and the rate of consolidation. When installed, stone columns modify the original soil to a composite ground of low compressibility and high shear strength. They are simple and cost saving alternative. They are best suited for small structures (1- 4 stories). Combining stone columns and piles under one foundation as a composite can be a more appropriate foundation for medium rise structures (5 - 9 stories), to the best of authors knowledge, very limited work was reported in literature indicating the use of stone columns and pile foundation together as composite foundation system under raft foundation in soft and compressible soils.

1.2 Problem Statement

Construction on soft and compressible soil is difficult due to soil low shear strength (C_u less than 25 kPa) and high compressibility. In order to overcome this difficulty, stone columns and pile foundations are the most used techniques and very common methods for improving soft soils (Hasan et al., 2009; Michael et al., 2004; Masoumeh & Behzad, 2012). The stone columns or pile group is typically capped by a reinforced concrete block known as the pile cap, which is responsible for making the piles work as a unit.

Stone columns, which consist of granular material compacted in long cylindrical holes, are used as a technique for improving the strength and consolidation characteristics of soft and compressible soil. Unlike pile foundations, stone columns make very efficient use of the soil near the surface and are ideal for light loads; however, foundations with stone columns are less effective at supporting heavy loads because these foundations cannot

transfer the applied stresses to the deeper layers of soil. For heavy structures the strategy of deep foundations (piles) are very effective, because piles penetrate through the weak soil deposits to the stiff soil or bed rock to support the structure's weight.

For the high-rise buildings, the use of piled rafts as a foundation system are very common, piled rafts are defined as a system whose load carrying capacity is determined by the sum of the load carrying capacity of its components (i.e., rafts and piles). The carrying capacity of the raft depends on the type of soil near to the surface or at the shallow level, when the raft is resting on the soft and compressible soil, the raft soil bearing interaction will not be adequate due to the insufficient bearing capacity of soft soil, which minimizes the effect of raft to the whole piled raft load carrying capacity. Therefore, pre-strengthening or improving the soft and compressible soil near to the surface using stone columns before piled raft can improve the overall load carrying capacity of the piled raft.

Combining stone columns and piles in one foundation system, can improve the carrying capacity of the system, modify the soil foundation to a new upgraded composite ground, and reduce the cost of the geotechnical works. Combined foundation system can provide an optimal solution and cost saving alternative to pile, and a more attractive alternative to stone columns in respect to ground improvement and amelioration of the performance of soil foundation. It is believed that the combined foundation is the more suitable foundation for medium rise structures.

1.3 Hypothesis of Research

Problem statement has stated that combining stone columns and piled raft in soft soils can improve the overall performance of foundation system. Improving soft and compressible soils using stone columns before installation of piled raft can improve the load carrying

capacity of piled raft. In the literature, there are no studies reported examining the bearing interaction between a stone column improved soft soil and piled raft foundation. This research requires parametric investigation to optimize the use of stone columns and piles together in one foundation system in soft soil using three-dimensional finite element based analysis. The parameters (for example: diameter of stone columns and piles, length of stone columns and piles, modulus of elasticity of elasticity of soft soils, angle of friction of stone columns and configuration of stone columns and piles together under the raft in soft soils) can influence the carrying capacity of combined foundation system needs further investigation.

1.4 Objectives

The goal of this research is to study the load- bearing performance of a combined foundation system composed of stone columns and piles grouped together under raft foundation, in soft and compressible soil. The research includes a comparative study between this new method (i.e., stone columns and piles combined under raft foundation) and other foundation systems such as a group of stone columns or piled raft foundation.

The main objectives of this research can be summarized as follows:

i. To study the load- bearing performance of

   a. Stone columns under raft foundation in soft and compressible soil via numerical investigation.

   b. Piled raft foundation in soft and compressible soil via numerical investigation.

c. Combined foundation system (i.e., stone columns and piles combined under raft foundation) in soft and compressible soil via numerical investigation.

ii. To optimize the configuration (i.e., number of stone columns and piles and their arrangements under raft) of stone columns/piles group as combined foundation system, and to develop an analytical model to predict the carrying capacity of the combined foundation system, capped with rigid raft foundation, in soft and compressible soil.

Validation of numerical models for stone columns in under raft foundation in soft clay soils and piled raft foundation in soft clayey soils are considered based on the data available in the literature (i.e., Ghazavi & Afshar, 2013; and Sinha & Hanna, 2017).

1.5 Motivation of the Research

Results of this research will provide an understanding of the proposed combined foundation system (stone column – piled raft) in soft and compressible soil. This study will establish the guidelines to comprehend the load-bearing performance for different arrangements of stone columns and piles together under raft in soft and compressible soil. Analytical model for the combined foundation (stone column – piled raft) will be developed based on the performance of these different arrangements of stone columns and piles together under raft which can be used to calculate the bearing capacity.

1.6 Scope of Research

In order to achieve the objectives of this proposed research, a numerical investigation will be carried out using 3D finite element software intended to develop the numerical models for stone columns under raft foundation, piled raft foundation, and the combined foundation system (i.e., stone columns and piles combined together under raft foundation) in soft and compressible soil.

After the development and validation of these numerical models, a parametric study will be carried out (using the three developed numerical models: stone columns under raft foundation, piled raft foundation, and combined foundation system) for the optimization of the configuration of stone columns/piles group as the combined foundation system, and notably to investigate the load-bearing performance of the combined foundation system (stone columns/pile foundation).

Furthermore, analytical models will be developed to predict the load-bearing performance and the carrying capacity of the combined foundation system capped with rigid raft foundation. The theoretical development chapter will present the theoretical framework and concepts to develop these analytical models, and the validation of these analytical models will be conducted using the existing data reported in literature.

1.7 Thesis Outline

This dissertation comprises of 6 chapters, Chapter 1 is an introduction for the proposed research which consists of research background, problem statement, hypothesis, objectives, significance, and scope of research. Chapter 2 is the review of past studies and investigations carried out on the stone columns under the raft in soft soil, piled raft foundation in soft soil and stone columns and piles together under raft as a combined system

in soft soil. Chapter 3 describes the methodology to be used for the proposed research. Chapter 4 presents the results from numerical models for stone columns under the raft in soft soil, piled raft foundation in soft soil and stone columns and piles together under raft as a combined system in soft soil. Chapter 5 presents the analytical models to predict the ultimate carrying capacity for piled raft foundation in soft clayey soils, and combined foundation in soft clayey soils and chapter 6 highlights the conclusions and recommendations from the research.

CHAPTER 2

LITERATURE REVIEW

2.1 Introduction

Numerous studies have been carried out on the foundation improvement techniques such as piling, rafts, raft on piles, preloading compaction, dewatering, soil reinforcing and stone columns to overcome and minimize the adverse effects of soil conditions. In majority cases, it has been observed that stone columns and piled raft foundations are utilized in soft and compressible soils to overcome the low shear strength and compressibility issues.

Stone columns consist of granular materials filled and compacted in long cylindrical holes, this granular material filled in the weak soil at regular intervals to improve the bearing capacity and consolidation characteristics, whereas the piles can be made of timber, reinforced concrete, cast in place concrete and steel which can help to transfer the load to the deeper and stiff soil layers.

There is very limited published work reporting the use of stone columns and pile foundation together under raft foundation to reinforce compressible soils. In these circumstances and according to the objective of this investigation, literature on three main topics are reviewed. Firstly, the performance and behaviour of stone columns under raft foundation in soft soils are outlined. Secondly, the reinforcement of compressible soils by piled raft foundation are described and finally, some limited published works on the combined pile and stone column under raft are discussed.

2.2 Stone Columns as Ground Improvement

Stone columns were originally introduced in 1830 by French military engineers, they constructed columns made of crushed limestones having the diameter of 0.2m and length of 2m in order to support the foundation of iron works artillery arsenal which was situated above soft estuarine in Bayonne (Moreau et al., 1835). Later almost after 100 years use of stone columns appeared in 1930s partially as the result of vibroflotation compaction method for granular material. It was reported by Hughes and Withers (1974), that stone columns having length of 15 m and diameter ranging between 0.5-1.5 m can have the bearing capacity up to 300 kN in soft clayey soils.

2.2.1 Failure Mechanism of Stone Columns

Several researchers have worked on theoretical and experimental study on complex behaviour of stone columns. Hughes and Withers (1974) were among the first one who carried out the laboratory experiments on single granular columns and described that column fails individually by bulging as presented in Figure 2.1. They also have given the concept of unit cell to predict the capacity of these columns, where the sum of capacity of individual columns in a group is the capacity of the group of stone columns.

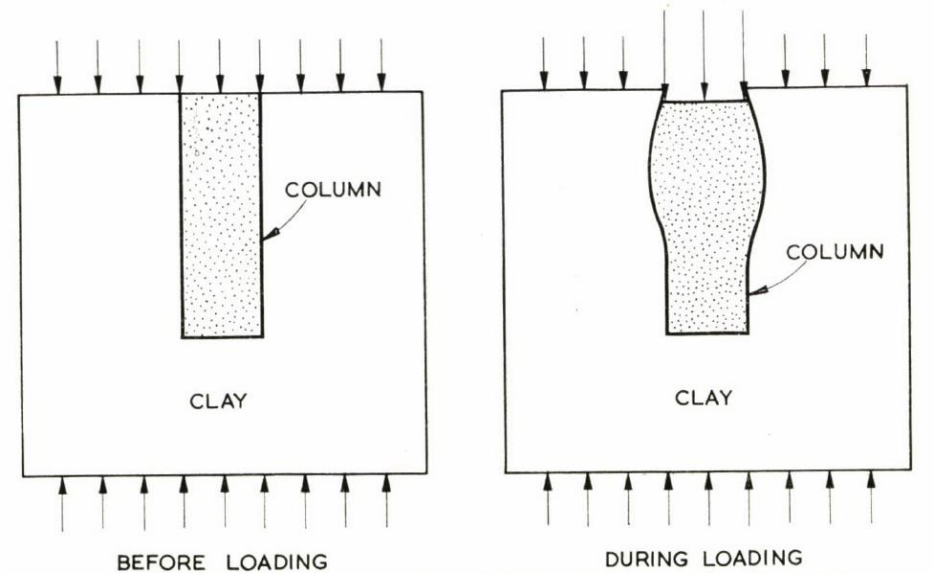


Figure 2.1: Stress on the columns (Hughes & Withers, 1974)

Bachus and Barksdale (1984) performed the experimental investigation on the group of 2×3 columns to understand the effect of adjacent columns. The results obtained from this work shows the difference of failure between outer to inner columns. Inner columns were confined due to adjacent columns that results in preventing the bulging effects. Stone columns in a group may experience different types of failure due to their respective positions and load-bearing performance. Inner stone columns typically carry a greater portion of the load compared to the outer ones. As results, the inner stone columns may experience higher stresses and can fail due to compression or buckling, on the other hand, outer stone columns may fail due to lateral forces or bending. Therefore a detail parametric study is required.

Rao et al. (1997) also have performed experimental study on the group of stone columns, and they have reported that the spacing between the columns equal to three times the diameter of columns ($S = 3D$) have more significance on the group efficiency. They also have reported that smaller spacing between the columns can improve the overall capacity due to confinement as the result of overlapping of bulging zones of adjacent columns. Closely spaced group of stone columns can lead to an increase in the overall bearing capacity

of the foundation due to the load distribution among the stone columns. Load transmitted by the superstructure distributes among the stone columns which can increase the overall capacity of group of stone columns. For this reason a range of spacing and diameter ratio of stone columns should be investigated to study the load bearing performance of group of stone columns under raft in soft soil.

Hu et al. (1997) investigated that the group of stone columns failing in conical shape not bulging because of column interaction as presented in Figure 2.2. Wehr (1999) and Wood et al. (2000) used the finite element analysis to investigate the performance of group of stone columns and reported the conical shape failure because of column interaction, which was also later confirmed by Bae et al. (2002) who conducted a laboratory model test and finite element analysis on a group of stone columns. The conical shape failure pattern in a group of stone columns refers to the failure mode where the soil around the stone columns develops a conical shape due to the load applied on the stone columns, this pattern indicates that the load from the superstructure is effectively transmitted to the surrounding soil. The load distributes radially outwards from each stone column can results in a more uniform stress distribution on the soil mass. The formation of conical shape under the foundation can be considered as a sign of effective engagement of stone columns with large volume of soil which can contribute to the overall bearing capacity. Parameters such as spacing, diameter, and length of stone columns contributes to the load-bearing performance of group of stone columns, these parameters can also have an influence on the conical shape pattern. For example larger stone column diameters and longer lengths can help to distributes the load over a larger area, which can reduce the stress concentrations and may reduce the formation of conical failure zone.

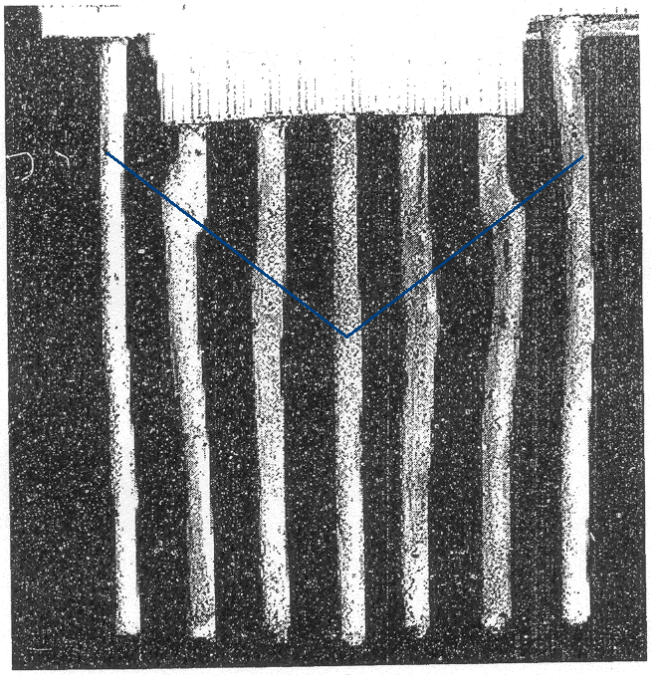


Figure 2.2: Deformed shape of the model test after applying load (Hu, 1995).

Hanna et al. (2013) developed the numerical model to study the performance, behaviour and mode of failure of single stone column and group of stone columns installed in soft clay, based on parametric study (modulus of elasticity, column diameter, spacing, angle of shearing resistance) and they identified bulging mode of failure in individual columns and massive shear failure in group of stone columns (Idrus et al., 2021) as presented in Figure 2.3 and Figure 2.4. It has been observed in their study that the load ratio increases significantly when diameter of stone column to the foundation width ratio is less than 0.6, and the bearing capacity of reinforced foundation improves with the increase in angle of shearing resistance of stone columns. Also, they reported bulging mode failure in the group of stone columns when the area replacement ratio is less than 10%, and the massive shear failure (general, local/punching shear) in between 10% to 35%.

The reason for bulging failure in a group of stone columns versus massive shear failure can be attributed to the different modes of failure and underlying mechanics involved.

Soft clay has low shear strength and can deform easily under lateral loads, when the stone columns subjected to vertical load, the soft clay can exert lateral pressure on the stone columns and may cause them to deform laterally or bulge outwards. This failure mode can be influenced by the factors such as the stiffness, and diameter of the stone columns, spacing between the stone columns, and the properties of the soil (Zukiri et al., 2018). On the other hand, massive shear failure in a group of stone columns in soft clay can occurs when the shear strength of the clay is exceeded. Soft clay has low shear strength and can undergo significant shear deformations when subjected to excessive shear force. In this failure mode the columns can experience sliding or collapse due to the inability of the soft clay to resist the shear force acting on them. The factors that can contribute the massive shear failure include the vertical load on stone columns, the shear strength of the soft clay and the interaction between the stone columns and clay.

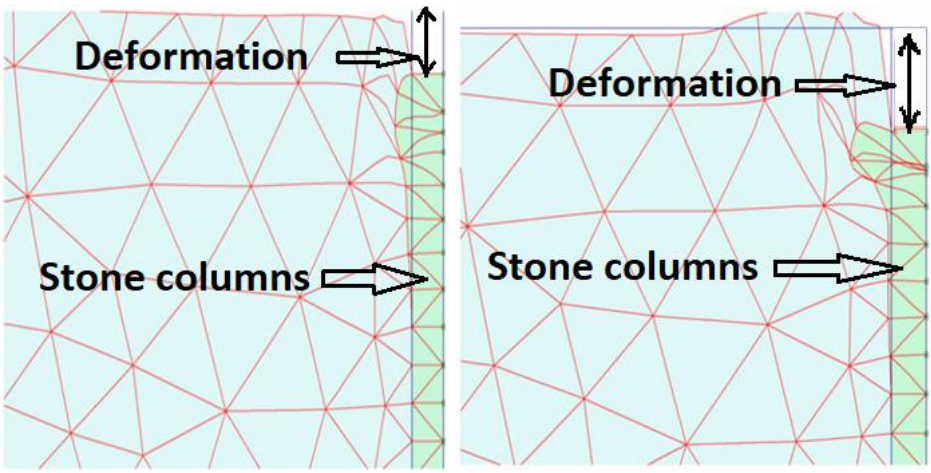


Figure 2.3: Deformed shape of single stone column (Hanna et al., 2013)

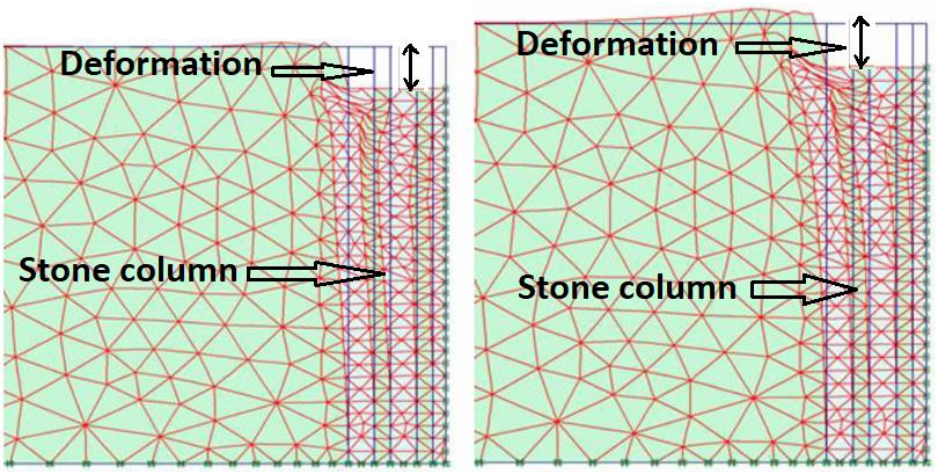
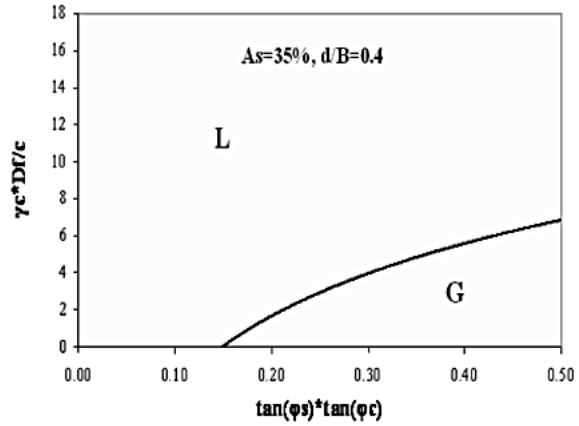
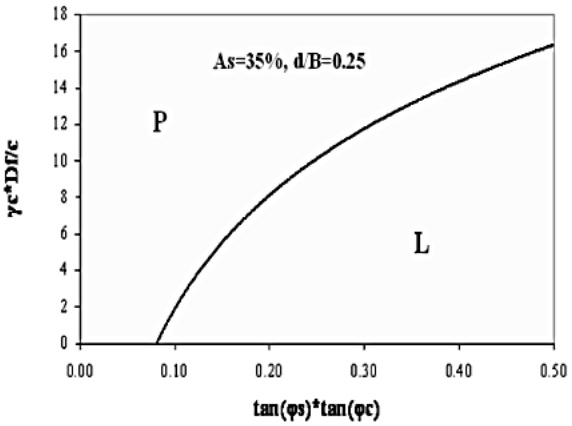


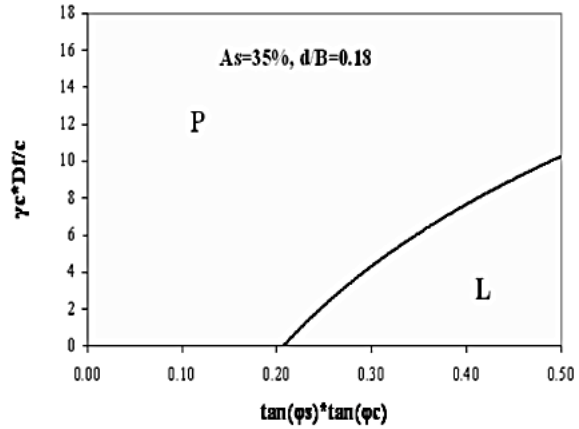
Figure 2.4: Deformed shape of group of stone columns (Hanna et al., 2013)

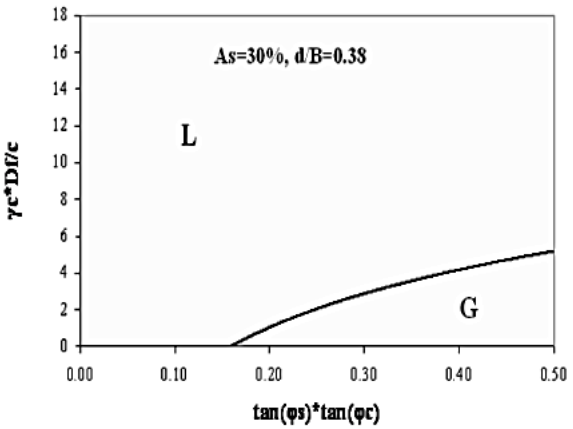
They prepared the design charts to predict the mode of failure (punching, local or general shear failure) of group of stone columns in soft soils presented in Figure 2.5-. The parameters used in developing these charts were: the angle of shearing resistance of soft soil (φ_c), angle of shearing resistance of granular column's material (φ_s), unit weight of soft soil (γ_c), cohesion of soft soil (c), column diameter(d), width (B) and depth (D_f) of the foundation respectively.

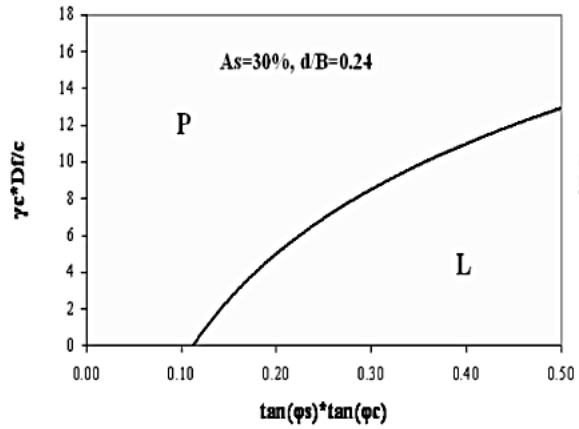
The numerical study performed by Hanna et al. (2013) was limited to the 2D models whereas the 3D models can provide better understanding of load-bearing performance of stone columns under raft in soft soils, Also, the design charts prepared by them can be used to understand and predict the failure modes based on the parameters but not to estimate the bearing capacity.

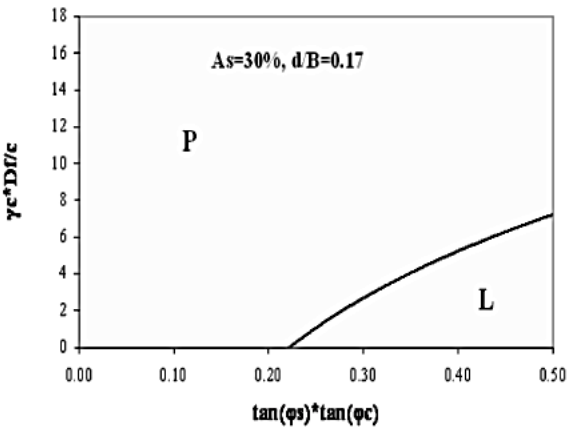

As=35%, d/B=0.4
L
G
γc*Df/c
tan(φs)*tan(φc)


As=35%, d/B=0.25
P
L
γc*Df/c
tan(φs)*tan(φc)


As=35%, d/B=0.18
P
L
γc*Df/c
tan(φs)*tan(φc)


As=30%, d/B=0.38
L
G
γc*Df/c
tan(φs)*tan(φc)


As=30%, d/B=0.24
P
L
γc*Df/c
tan(φs)*tan(φc)


As=30%, d/B=0.17
P
L
γc*Df/c
tan(φs)*tan(φc)

-

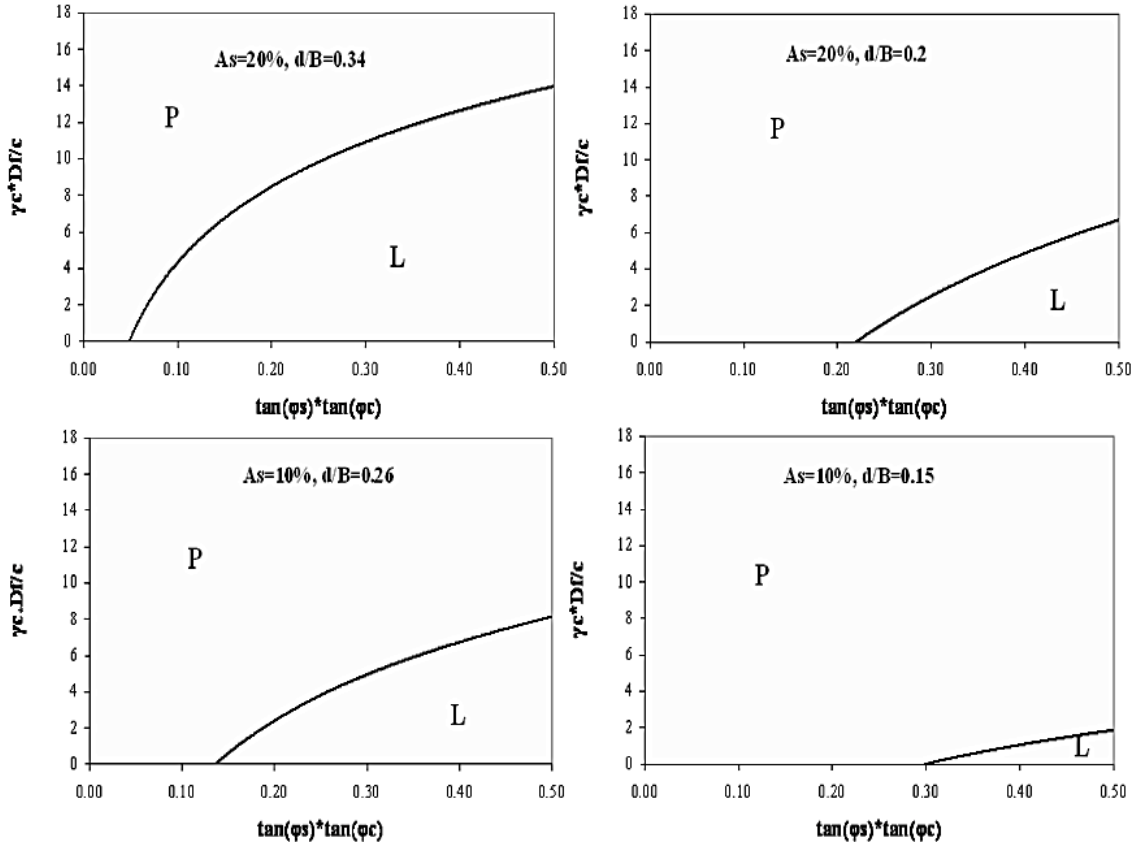


Figure 2.5: Design charts for predicting the mode of failure of soft soils reinforced (Hanna et al., 2013)

2.2.2 Analytical and Numerical Studies of Stone Columns

Many researchers have performed analytical and numerical studies on the performance of stone columns, most of the numerical works are based on the finite element models using computing software that can simulate and solve wide range of problems. Similarly, analytical works have been reported in the literature, most of the analytical models were created and validated based on the parametric study of stone columns that involves the use of experimental and numerical results.

Nazari et al. (2014) introduced a simple analytical method (given in Equation 2.1) for the estimation of ultimate bearing capacity of stone column, the validity of the presented analytical method was verified by using finite element method including the effect of

changes in parameters such as column size, spacing and angle of friction as presented in Figure 2.6 and Figure 2.7. and it was reported that the bearing capacity of stone column increases with the friction angle and diameter of stone columns and bearing capacity decrease with the increase in center-to-center distance between stone columns, similar findings were reported in (Al-Kazzaz & Al-Obaydi, 2021; Naderi et al., 2018; Naseer et al., 2019; Unni et al., 2021).

$$q_{ult} = C_c N_c + \bar{q} N_q + \frac{1}{2} W \gamma_c N_\gamma \qquad \text{Equation 2.1}$$

Where:

$$N_c = 2\frac{cos\frac{\emptyset_c}{2}\sqrt{K_{pc}}}{cos\frac{\emptyset_s}{2}K_{as}}, \qquad N_q = \frac{K_{pc}}{K_{as}}\frac{cos\frac{\emptyset_c}{2}}{cos\frac{\emptyset_s}{2}}, \qquad N_\gamma = tan\eta_a\left[\frac{cos\frac{\emptyset_c}{2}}{cos\frac{\emptyset_s}{2}}\frac{K_{pc}}{K_{as}} - \frac{\gamma_s}{\gamma c}\right]$$

C_c=cohesion for native soil

$\emptyset_c$=internal friction angle of the native soil

$\emptyset_s$=internal friction angle of the stone columns

η_a= the active wedge angle from horizontal direction

K_{as}=lateral active earth pressure coefficient,

K_{pc}=lateral passive earth pressure coefficient,

W=width of continuous strips for each row of stone columns

γ_s=unit weight of stone material,

γ_c=unit weight of soil,

$\bar{q}$ =surcharge pressure on passive region surface.

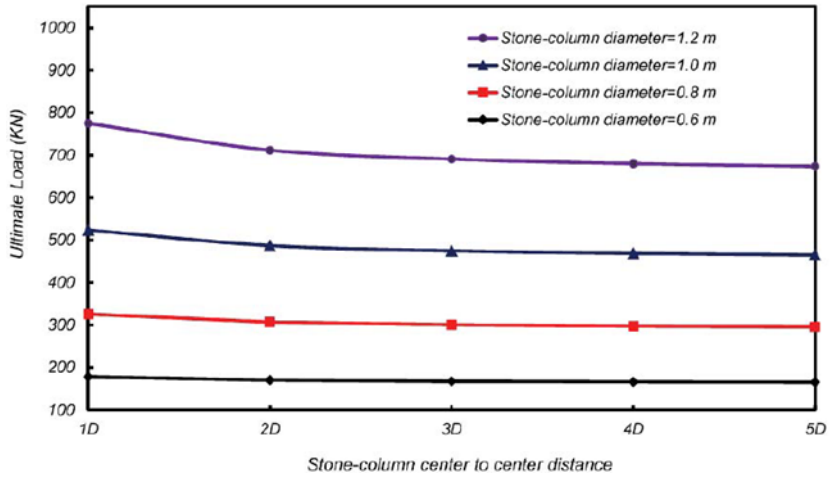


Figure 2.6: Variation of stone column ultimate load versus stone column spacing for various stone material diameters (Nazari et al., 2014)

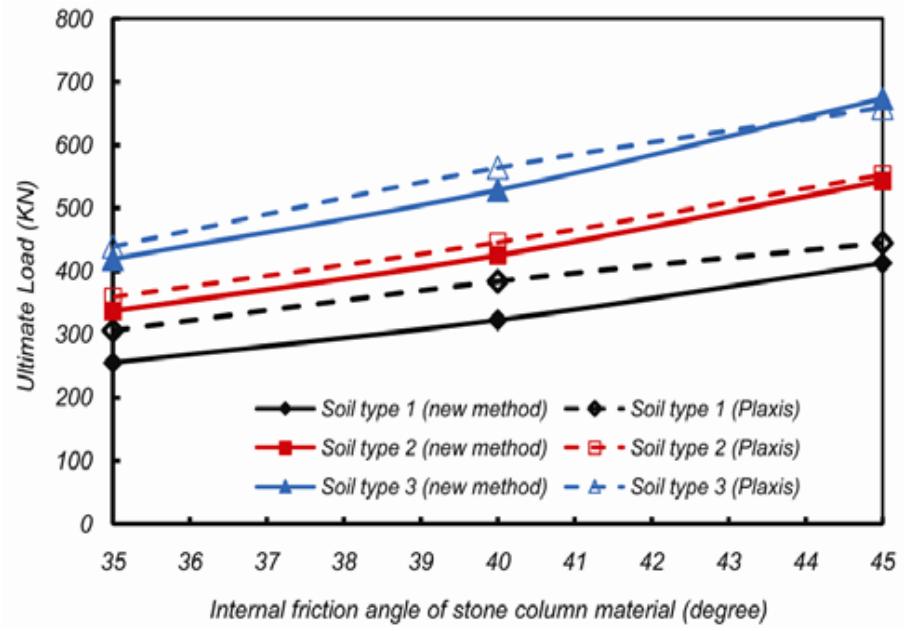


Figure 2.7: Comparison between bearing capacity values determined (Nazari et al., 2014)

It can be observed from Figure 2.6 that with smaller spacing between the stone columns have higher ultimate load carrying capacity and with higher spacing between stone columns the ultimate carrying capacity reduces and become steadier. This shows that there must be an optimal spacing range of stone columns, beyond which the benefit of increased

spacing can diminish. Figure 2.7 shows the effect of internal friction angle of stone columns on the bearing capacity, with the increase in the angle of friction of stone columns the bearing capacity increases, similar conclusions were reported by Khalifa et al. (2018) and Kouklanifar (2023). The angle of friction is a measure of the resistance to sliding between two surfaces in contact. When stone columns are stalled in the ground, they can interact with surrounding soil and can contribute to the overall load-baring capacity.

Castro (2014) studied the performance of groups of stone columns under rigid footing and investigated the effect of column configuration on the load-settlement curves by conducting the 2D and 3D finite element analysis as presented in Figure 2.8 and Figure 2.9 and Table 2.1. It was concluded that uniformly distributed columns are more beneficial, stone column length to diameter ratio has not much effect on settlement, column length more than the width of footing is more efficient, and higher area replacement ratio is less efficient for settlement reduction factor. Later authors Castro et al. (2019) proposed that the critical length of columns can be range between 1.2-2.2D (D = width of footing).

Figure 2.9 shows two sets of arrangement for stone columns under square raft one with stone columns at the corner of square raft and another with stone columns on the sides uniformly. These uniformly distributed stone columns under raft foundation can provide benefits due to the mechanism of load distribution and soil improvement. When stone columns are uniformly placed under a raft foundation, they can share the load from superstructure more evenly. This load sharing mechanism can help to reduce the stress concentration on individual stone columns, which can prevent localized failure. By distributing the load over a large number of stone columns, the overall load-bearing capacity of the foundation system can be increased.

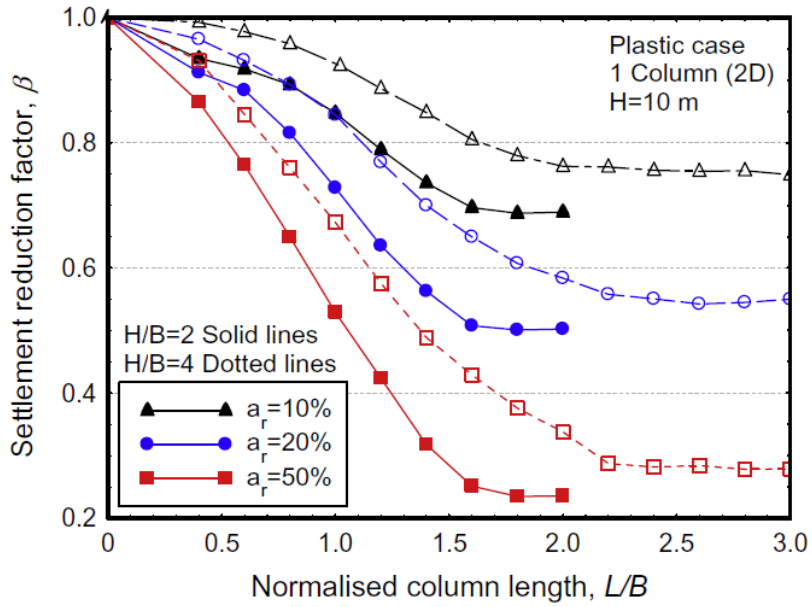


Figure 2.8: Critical column length for different area replacement ratios. (Castro, 2014)

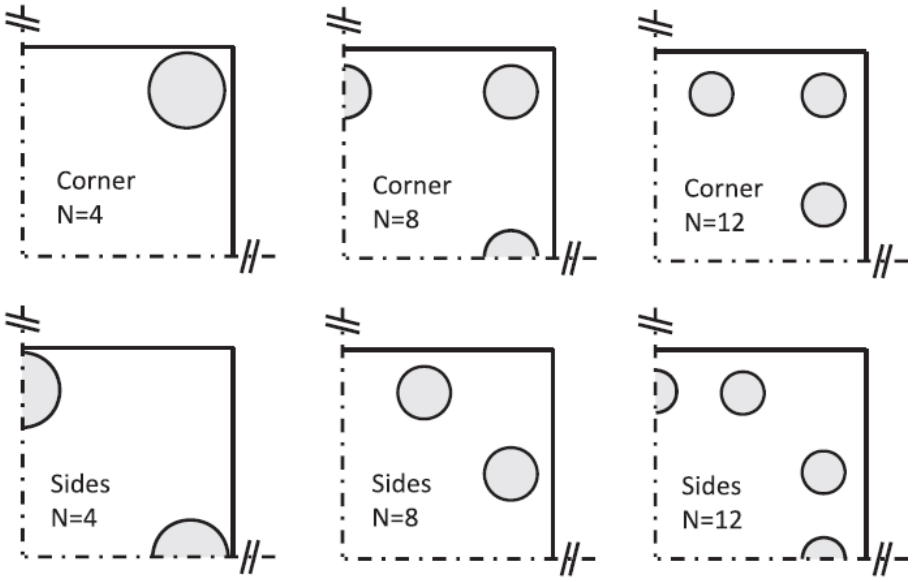


Figure 2.9: Groups of stone columns for different number of columns. (Castro, 2014)

Table 2.1: Settlement (mm) for different number of columns. (Castro, 2014)

	L/D_c	Elastic			Elasto-plastic			Plastic		
		Corner		Sides	Corner		Sides	Corner		Sides
2D	5.6		100.9			123.4			206.6	
Circular	5.6		100.8			123.0			198.5	
N = 1	5.6		99.1			119.8			199.1	
N = 4	11.2	93.4		96.5	118.2		119.1	204.4		198.7
N = 8	15.9	94.7		95.9	118.5		119.0	203.0		198.4
N = 12	19.4	94.8		96.0	118.5		119.1	200.1		198.3
N = 16	22.4	95.2		95.9	118.8		119.1	199.5		198.1
N = 20	25.1	95.4		96.6	118.9		119.3	199.6		197.7
N = 24	27.5	95.3		95.8	118.9		119.4	197.4		194.8

Micheál and Bryan (2014) conducted the 3-D finite element analysis using elastic-plastic soil model to study the influence of variation in the stone column configuration as presented in Figure 2.13 and Figure 2.14 and Table 2.2. Also, they have proposed a simplified method to estimate the settlement. It was reported that the area ratio, column length and number of columns are related to each other. The number of columns near the footing edge has less effect on the settlement. The settlement improvement factor increases with the increase in column stiffness and strength as well as due to the lateral earth confinement *Ko* as shown in Figures 2.10, Figure 2.11, and Figure 2.12, respectively. Similar findings were reported by Hadri et al. (2021). It has also been observed that the columns are more confined in the stiff crust and can bulge in the softer layer of soil.

Stone columns near the edge of a raft foundation can have a reduced effect on the overall performance of the foundation compared to those located closer to the center. This is because the load distribution and settlement behaviour of the foundation can be influenced by the proximity of the stone columns to the load-bearing elements.

When stone columns are placed near the center of a raft foundation, they can effectively distribute the load over a large area and can reduce the stress on the soil and minimize the settlement.

However, when stone columns are located near the edge of raft, their ability to influence the load distribution and settlement patterns can diminished. The load from the superstructure can be directly transmitted to the surrounding soil through the edge of the raft, which can reduce the effectiveness of the stone columns in redistributing the load.

Figure 2.14 shows the deform shapes of the stone columns under raft, a shear zone can be observed in these contour diagrams that when the stone columns are near to the edge of raft, when stone columns are placed near the edge of a raft foundation there is a potential for higher shear zone to develop in the soil adjacent to stone columns. This is due to the interaction between the stone columns and the surrounding soil, which can create a differential shear stress distribution. The magnitude of this shear zone can depend on various factors such as soil properties, stone column configuration and applied loads.

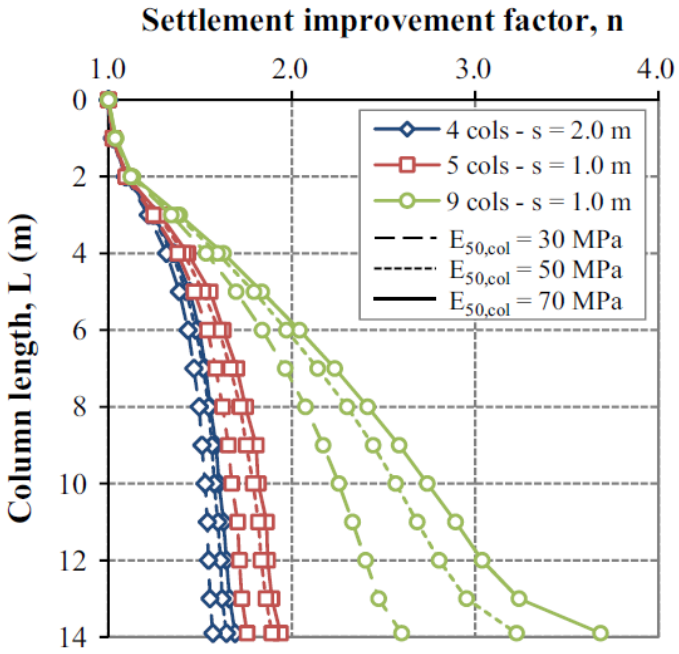


Figure 2.10: Influence of column stiffness upon settlement improvement factors. (Micheál & Bryan, 2014)

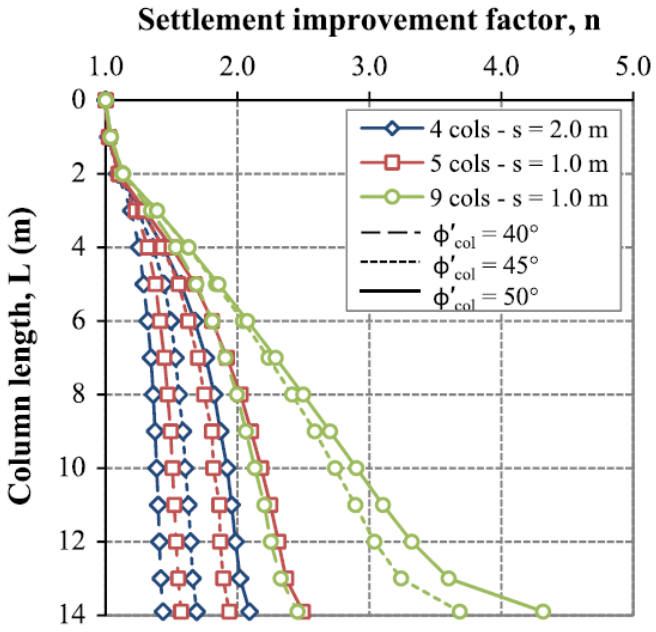


Figure 2.11: Influence of column strength upon settlement improvement factors. (Micheál & Bryan, 2014)

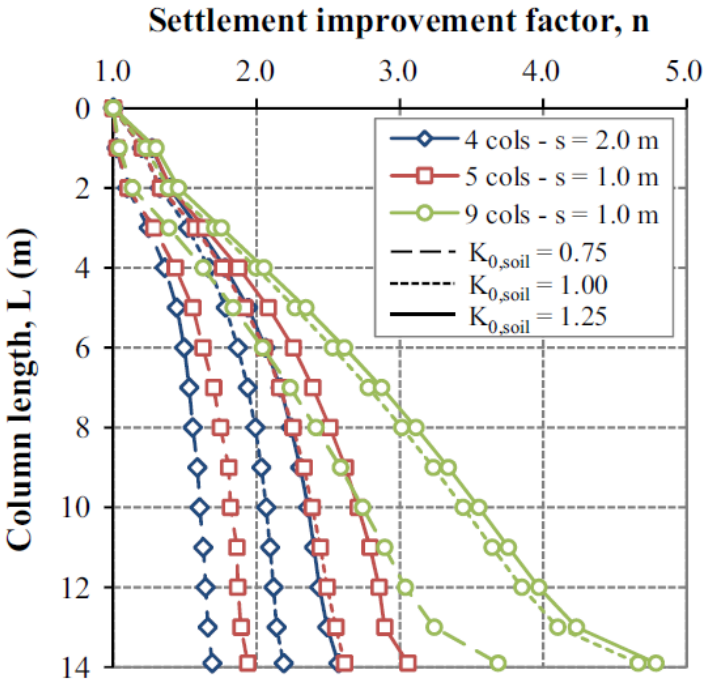


Figure 2.12: Influence of the coefficient of lateral earth pressure upon settlement (Micheál & Bryan, 2014)

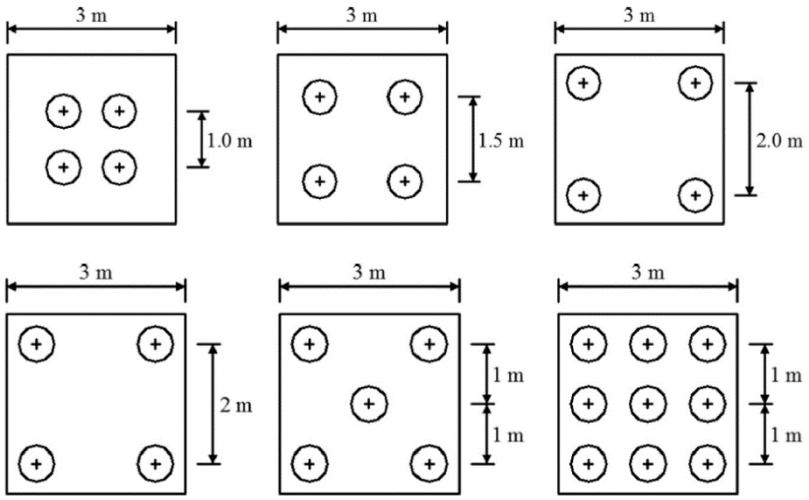


Figure 2.13: Column configurations to examine the influence of column (Micheál & Bryan, 2014)

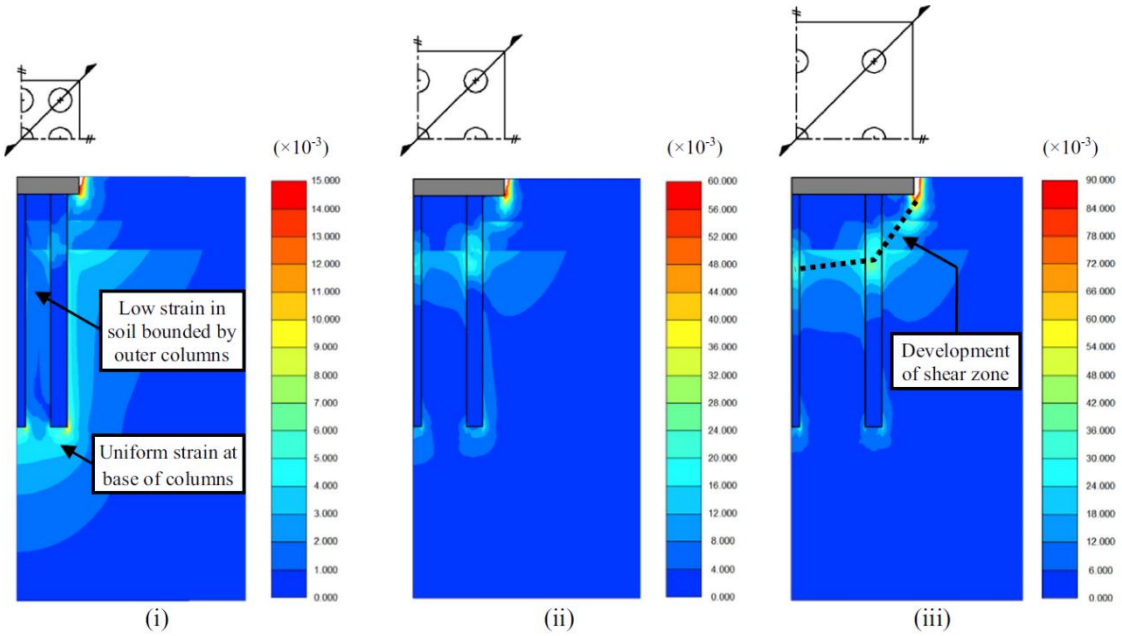


Figure 2.14: Distribution of total shear strains through a cross-section of a 3x3 group of 8m long columns at A/A_C of (i)3.5, (ii)8.0 and (iii)14.1. (Micheál & Bryan, 2014)

Table 2.2: Column configurations to investigate influence of other parameters (Micheál & Bryan, 2014)

No. of columns, *N*	**S (m)**	***B* (m)**	***A/A*$_C$ (-)**	***L* (m)**	***E*$_{50, col}$ (MPa)**	***ϕ*^{0}*col* (º)**
4	1.0	3	8.0	1.0-13.9	70	45
4	1.5	3	8.0	1.0-13.9	70	45
4	2.0	3	8.0	1.0-13.9	70	45
4	2.0	3	8.0	1.0-13.9	30, 50, 70	45
5	1.0	3	6.4	1.0-13.9	30, 50, 70	45
9	1.0	3	3.5	1.0-13.9	30, 50, 70	45
4	2.0	3	8.0	1.0-13.9	70	40, 45, 50
5	1.0	3	6.4	1.0-13.9	70	40, 45, 50
9	1.0	3	3.5	1.0-13.9	70	40, 45, 50

Etezad et al. (2015) proposed an analytical model to estimate the bearing capacity of raft foundation resting on the soft soil reinforced with number of columns. This proposed model can predict the bearing capacity having the concept of composite properties of reinforced soil when subjected to general shear failure. They also have validated their work with available data in the literature and have presented the design procedures and charts for practicing purposes.

Analytical model for estimating the bearing capacity of raft foundation resting on soft soil reinforced with stone columns are given:

$$q_u = \frac{1}{2}\gamma_{comp} B N_\gamma + q N_q + C_{comp} N_c \qquad \text{Equation 2.2}$$

Where:

$C_{comp} =$ Cohesion (soil/columns composite system) $= A_s = C_s + (1 - A_s)C_c$

$\gamma_{comp} =$ Unit Weight (soil/columns composite system) $= A_s\gamma_s + (1 - A_s)\gamma_c$

φ_{comp}=angle of shearing resistance (soil/columns composite system)

$A_s = replacement\ ratio = A_{col}/s^2$

A_{col} = area of column cross-section

s = spacing

C_s = cohesion of stone columns

C_c = cohesion of clay soil

γ_s= unit weight of stone columns

γ_c= unit weight of clay soil

$$\varphi_{comp} = \tan^{-1}[A_s \mu_s \tan \varphi_s + (1 - A_s)\mu_c \tan \varphi_c]$$

$$\mu_s = \frac{n}{1 + (n-1)A_s}$$

$$\mu_c = \frac{1}{1 + (n-1)A_s}$$

φ_s = angle of shearing resistance of stone columns

φ_c = angle of shearing resistance of clay soil

n = stress ratio (between 2 -6) (Mitchell & Katti, 1981)

Elsawy and El-Garhy (2016) have studied the behaviour of reinforcing the soft soil with granular pile (*GP*) under raft foundation using finite element program PLAXIS 3D. A parametric study was performed by changing spacing (*S*), diameter (*d*) and length (*L*) of granular piles (*GP*). In this study, in general they have concluded that the settlement and bending moment reduces with higher value of replacement area ratio and smaller value of spacing ratio, because with the higher replacement ratio the bearing capacity and settlement of the soil under the foundation can be improved (Ahmed & Fattah, 2021; Boumekik et al., 2021; Ng et al., 2021; Znamenskii et al., 2021). They also have concluded that settlement will decrease with the increment in granular pile length as given in Figure 2.15, Figure 2.16, and Figure 2.17.

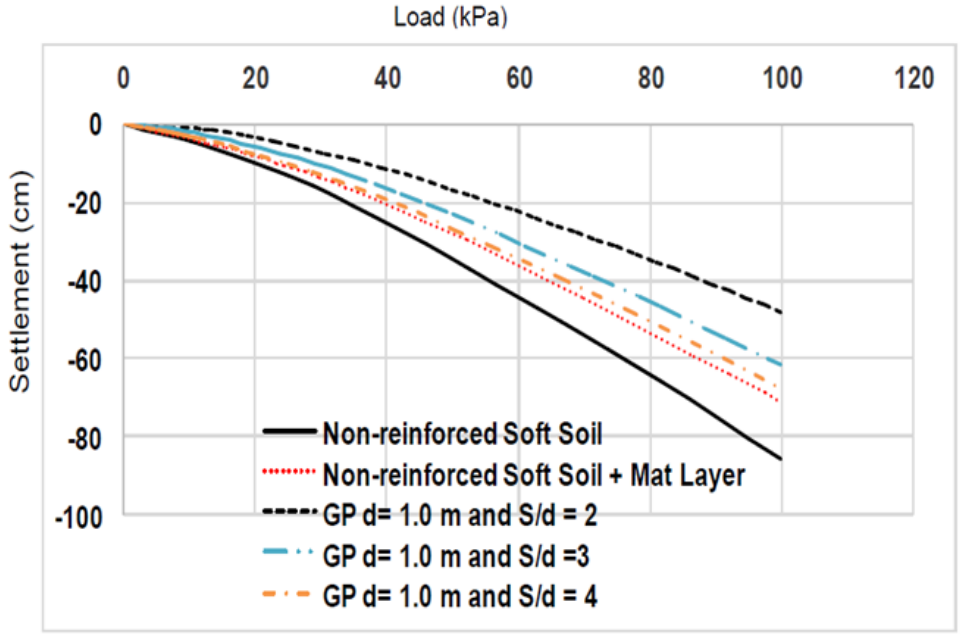


Figure 2.15: Load – settlement for the non-reinforced and reinforced soft soil with different spacing ratios (Elsawy & El-Garhy, 2016)

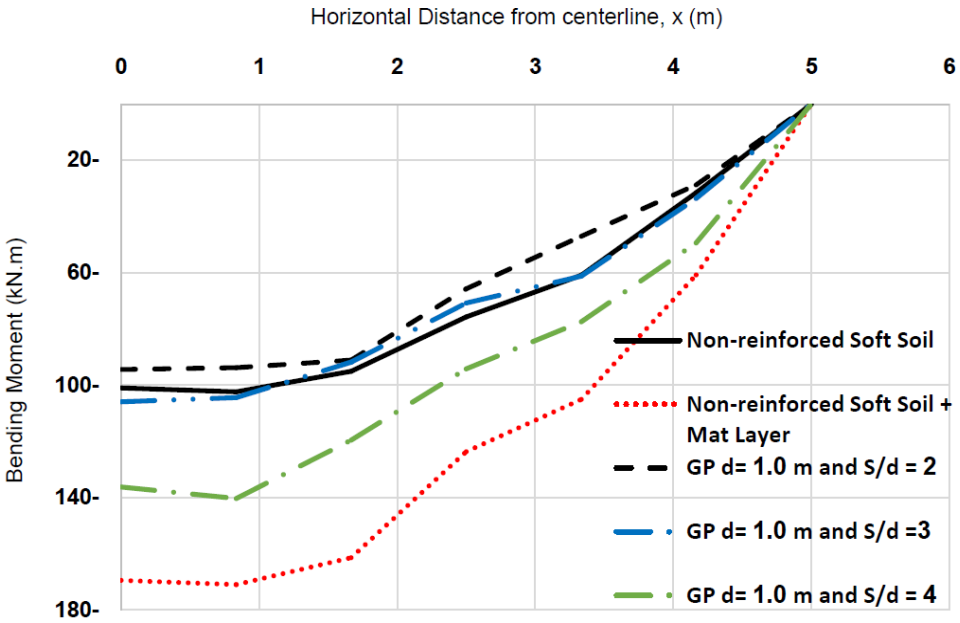


Figure 2.16: Bending moment distribution along footing for non-reinforced and reinforced soft soil with different spacing ratios. (Elsawy & El-Garhy, 2016)

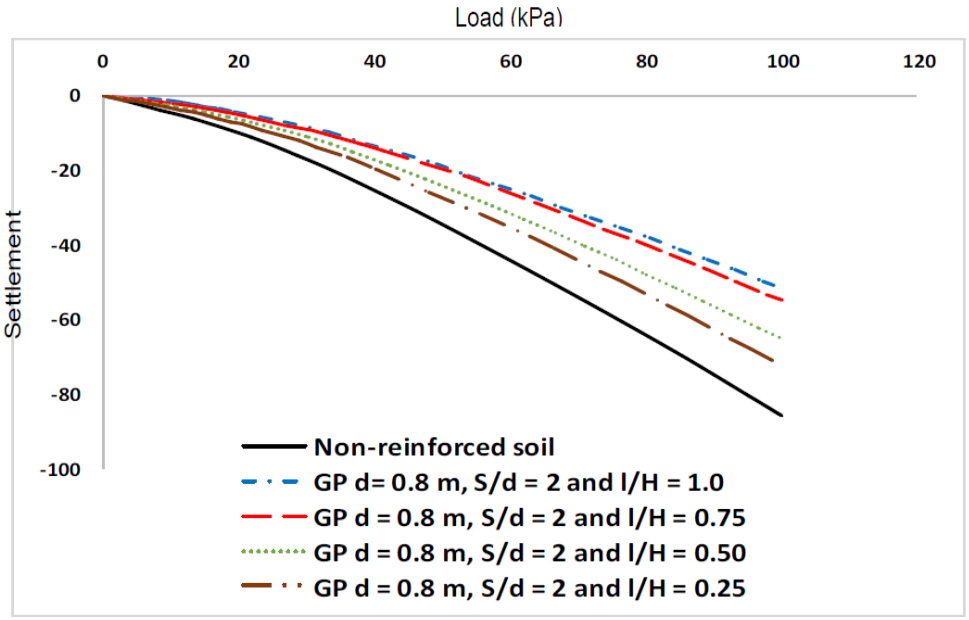


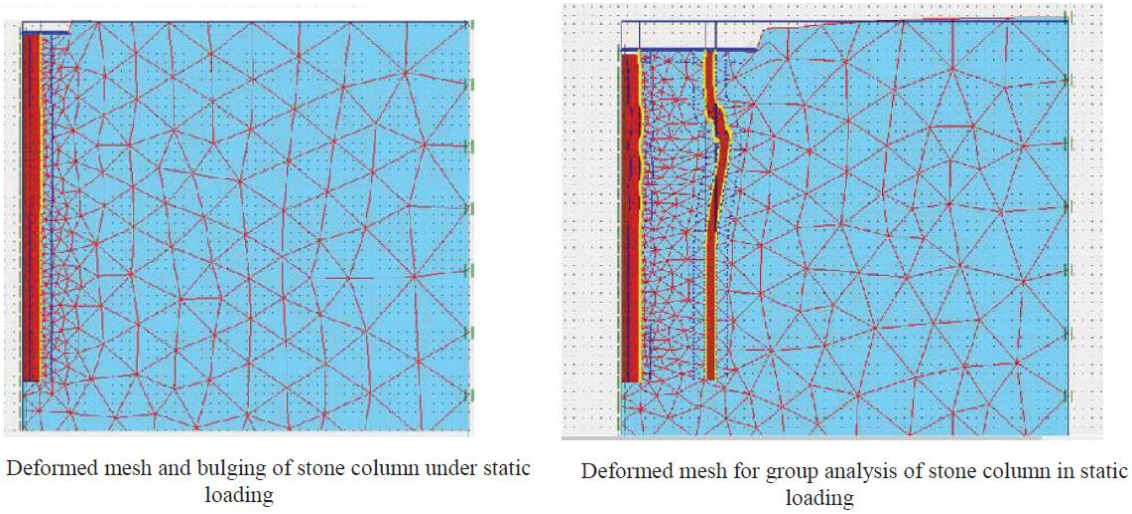
Figure 2.17: Load – settlement for non-reinforced and reinforced soft soil with different pile lengths (Elsawy & El-Garhy, 2016)

Ziaie and Mohammadi-Haji (2016) have conducted the numerical finite element simulations for the validation of test results obtained from the displacement control loading test on stone columns. They investigated the use of stone columns under raft foundation as presented in Figure 2.18 and Figure 2.19.

They have reported that the use of single and group of stone columns under footing can increase the bearing capacity by 60% to 100% under static loads, similar outcomes were stated by Karkush and Jabbar (2019), and it was also concluded that in group of stone columns fails due to bulging near the centre and columns fails due to lateral deformation near the edge as shown in Figure 2.20. Similar findings were reported by Bachus and Barksdale (1984).

Figure 2.19 shows the bearing capacity of improved ground and unimproved ground. The curves show the bearing capacity of ground improved by 100% by using group of stone columns under footing. Figure 2.20 shows the variation of lateral displacement in columns

when placed at the center and near the edge of footing, it can be observed from the curves that the bulging failure occurred with the center column and lateral displacement occurred at the column near the edge of the footing. (Where: Y = distance of point on column from the top of column and L = column total length)



Deformed mesh and bulging of stone column under static loading

Deformed mesh for group analysis of stone column in static loading

Figure 2.18: Deformed mesh for single and group of stone columns under static load (Ziaie & Mohammadi-Haji, 2016)

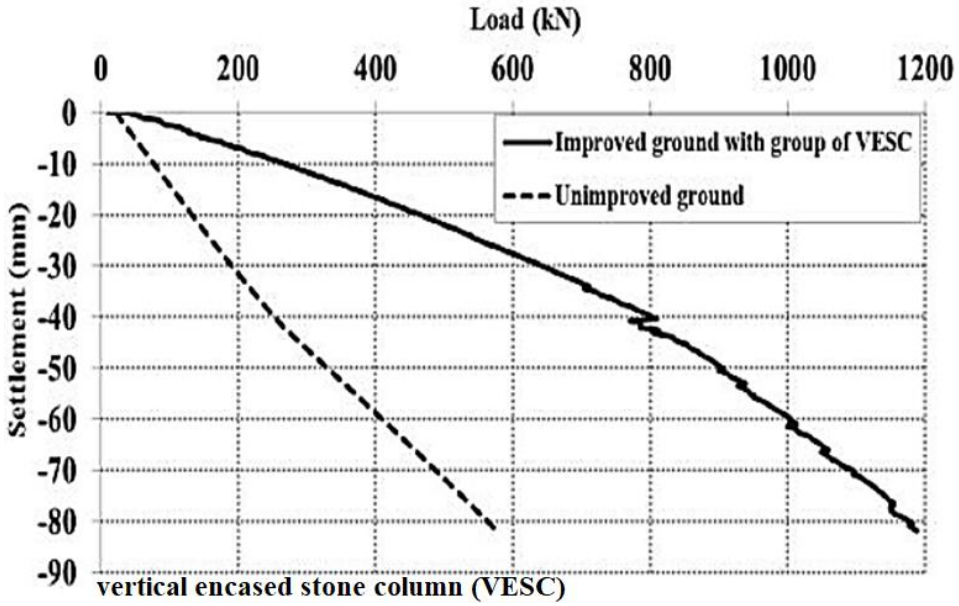


Figure 2.19: Comparison of the load-settlement static curves of unimproved ground and improved ground (Ziaie & Mohammadi-Haji, 2016)

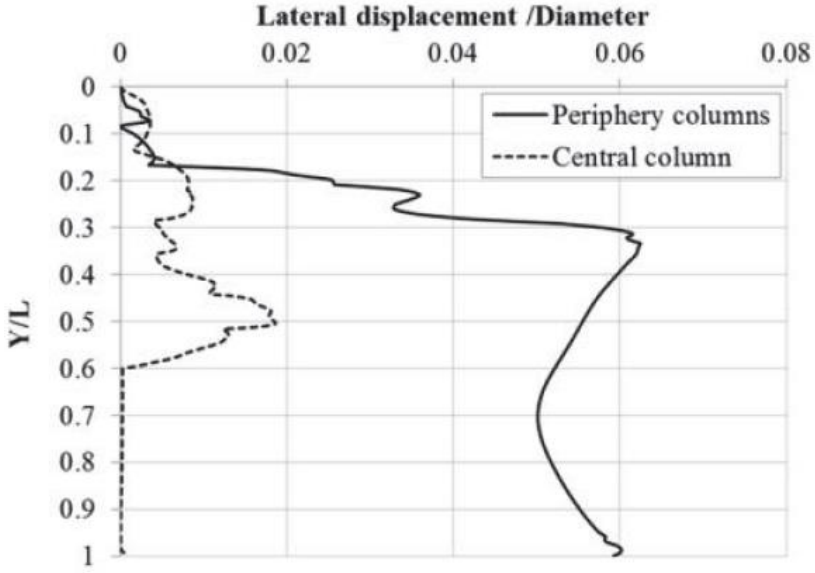


Figure 2.20: Variation of lateral displacement of central and periphery stone columns versus normalized depth. (Ziaie & Mohammadi-Haji, 2016)

Fattah et al. (2017) have developed the generalized equation to estimate the carrying capacity of floating group of stone columns installed in clay with different diameters and *L/D* ratios. They have used SPSS (Statical Package for the Social Sciences) program to perform statical analysis on experimental work and previous studies and develop new carrying capacity equation (Equation 2.3)

$$q_u = 15.34 C_u^{0.401} A_s^{0.266} N_s^{0.084} \left(L/D\right)^{0.526} \quad \text{Equation 2.3}$$

Where:

C_u *= the undrained shear strength kPa*

A_s *= the area replacement ratio*

L/D *= length to diameter ratio*

Etezad et al. (2018) presented an analytical model that can estimate the bearing capacity of raft foundation on soft clay when reinforced with stone columns. Mostly stone

columns fail in bulging and in general shear, but their proposed model can estimate the bearing capacity of raft foundation on stone columns when subjected to local or punching shear failure mechanisms. The proposed analytical models were also validated with the experimental and numerical data from literature.

Analytical model for local shear failure is developed by Etezad et al. (2018) is given below:

$$q_u = \frac{1}{2} B \left(\gamma_c N_{\gamma_c} - \gamma_{comp} N_{\gamma_{comp}} \right) + q N_q + C_{comp} N_{comp} + C_c N_{C_c} \quad \text{Equation 2.4}$$

Where:

B = width of raft

γ_c *= unit weight of clay soil*

γ_{comp} *= unit weight (soil/columns composite system)*

C_{comp} *= Cohesion (soil/columns composite system)*

C_c *= Cohesion of clay soil*

$N_{\gamma_c}, N_{\gamma_{comp}}, N_q, N_{comp}, N_{C_c}$ *= bearing capacity factors in form of design charts*

Analytical model for the punching shear failure is given below:

$$q_u = \frac{1}{2} B \left(\gamma_s N_{\gamma_s} - \gamma_c N_{\gamma_c} \right) + q \left(N_{q_s} - N_{q_c} \right) + C_s N_{C_s} - C_c N_{C_c} \quad \text{Equation 2.5}$$

Where:

$N_{\gamma_s} = \left[K_{p_s} A_s^2 \cos(\psi - \varphi_s) \right] / 2 \cos^2 \psi - (A_s \tan \psi)/2$

$N_{q_s} = \left[K_{q_s} A_s \cos(\psi - \varphi_s) \right] / \cos \psi$

$$N_{c_s} = A_s \tan\psi - K_{c_s} A_s \cos(\psi - \varphi_s) / \cos\psi$$

$$N_{\gamma_c} = \left[K_{p_c}(1 - A_s)^2 \cos(\psi - \varphi_c)/2\cos^2\psi\right] - [(1 - A_s)\tan\psi/2]$$

$$N_{q_c} = K_{q_c}(1 - A_s)\cos(\psi - \varphi_c)/\cos\psi$$

$$N_{c_c} = (1 - A_s)\tan\psi - \left[K_{c_c}(1 - A_s)\cos(\psi - \varphi_c)/\cos\psi\right]$$

$$\psi = A_s \frac{(\varphi_s - \varphi_c)}{2} + \frac{\pi}{4} + \frac{\varphi_c}{2}$$

K_γ taken from section 11 of Caquot and Kerisel (1948).

$$K_q = \frac{K_\gamma}{\cos(\beta - \lambda)}$$

$$K_c = \frac{\frac{1}{\cos\varphi} - K_q}{\tan\varphi}$$

β = *slope of ground surface*

$\lambda = 90^o - \psi$

Ng (2018) performed a 3D numerical analysis of single stone column to observe the effect of angle of friction of stone column, the shear strength of surrounding soil and modular ratio. He proposed and validated a new method to predict the ultimate bearing capacity of single stone column when fails under bulging and punching.

$$q_{ult} = (\emptyset' - 15)C_u + 50 \qquad \text{Equation 2.6}$$

Where:

$\emptyset'$ = *angle of friction of stone column*

C_u = shear strength of surrounding soil

Madun et al. (2018) performed a finite element analysis on stone columns using PLAXIS 2D to investigate the effects of stone columns diameter and length on loading capacity and settlement. The results showed longer columns lengths resulted in a lower settlement of soil (Nazariafshar et al., 2019), while larger column diameters resulted in a higher load bearing capacity of soil. Moreover, it was also concluded that for better design of stone columns each factor diameter and length should be optimized independently.

Znamenskii and Syed (2019) have performed a 3D numerical analysis on a footing resting on soft clay reinforced with stone columns and compared the numerical results with the existing four different analytical methods, (a) Priee's (1995) method, (b) Castro and Sagaseta (2009) method, (c) Ballam and Booker (1981) method and (d) Castro (2014) method. The results obtained from their numerical study and analytical method shows the similar trends (Figure 2.21).

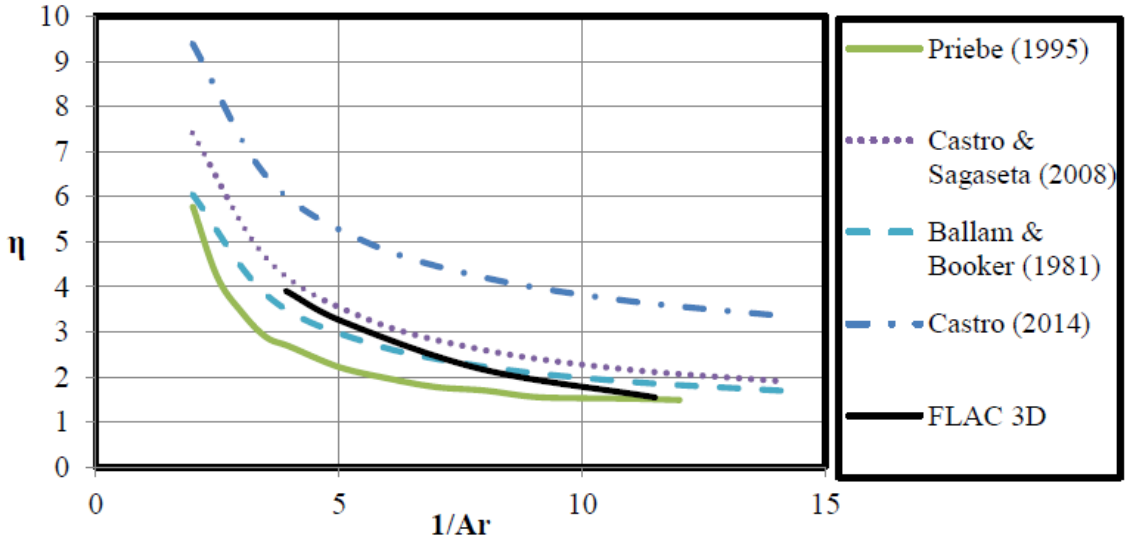


Figure 2.21: Comparison of settlement improvement factors from numerical analysis and analytical methods. (Znamenskii & Syed, 2019)

Grizi et al. (2022) carried out an 3D finite element parametric investigation using PLAXIS 3D in order to examine the influence of these parameters on the settlement of stone

columns to support the shallow foundations. From this study it was concluded that using both drained and undrained analysis, the modelling of well-characterized soft soil profile can be used to predict the long-term settlements. It was also concluded that the presence of a stiff crust layer affect stone columns deformation in a significant way which is not captured by laboratory.

A stiff layer can help to distribute the applied load more evenly, it can reduce the stress concentration at the column-soil interface by preventing excessive settlement and by improving load bearing capacity of the stone columns. Also stiff crust layer can resist the downward movement of the stone columns which can minimize the settlement.

Sakr et al. (2022) performed a numerical study on ordinary stone columns and encased stone columns in soft clay using PLAXIS 3D. Different set of parameters were selected to study the behaviour of stone columns. It was concluded that as the angle of internal friction for ordinary stone columns increased, the ultimate bearing capacity increased and settlement decreased (Saxena & Roy, 2022). Furthermore, it was found that the increase in *BCR* (Bearing capacity ratio) of the encased stone column over untreated soil for two diameters of columns (D = 0.4 m and 0.6 m) was 227% and 200%, respectively at 45° internal friction.

2.3 Piled Raft Foundation

Piles are generally made of steel, concrete, or timber. Pile foundations are the long slender which are used to support the structure and heavy loads. In the piled raft foundation system, piles penetrate through the weak soil deposits to the stiff soil or bed rock to support the raft foundation.

The concept of pile foundation was started in 50's (Zeevaert, 1957) when the friction piles were used to reduce the settlement of building on the highly compressible volcanic clay of Mexico City and the first time it was recommended to use the combination of shallow and deep foundations. Later in 70s and onwards many researchers have proposed the idea of combined piled raft foundation system (Burland et al., 1977; Davis & Poulos, 1972; Hooper, 1973)

2.3.1 Failure Mechanism of Pile Foundation

The main purpose of using pile foundations is to reduce the settlements and to increase the bearing capacity of raft foundation. Also, for designing the raft foundation on the soft clay soil two aspects are mainly considered as the limiting factor the bearing capacity and the excessive settlements of raft foundation. If the piled raft foundations are placed on clay soil, then excessive settlements can be an issue (Jendeby, 1986). The failure of pile foundation also depends on the properties of soil surrounding the pile shaft as well as soils around the toe of the piles because when the load transfers from the raft (Q_u) to the piles, are resisted by the skin friction (Q_s) developed at the shaft of the pile and the bearing (Q_p) at the pile point (pile toe) as in Figure 2.22. The ground failure can occur if the stresses in the soil near the shaft and toe exceeds the strength of the soil. (Bergfelt, 1957; Brandtzaeg & Elvegaten, 1957; Charles et al., 2001; Fan et al., 2014; Golder & Skipp, 1957; Gonzalez-Nicieza et al., 2007; Gayarre et al., 2009; Hussein et al., 2012; Kozubal et al., 2014; Lopez Opeyemi, 2009; Zhang & Dasaka, 2010).

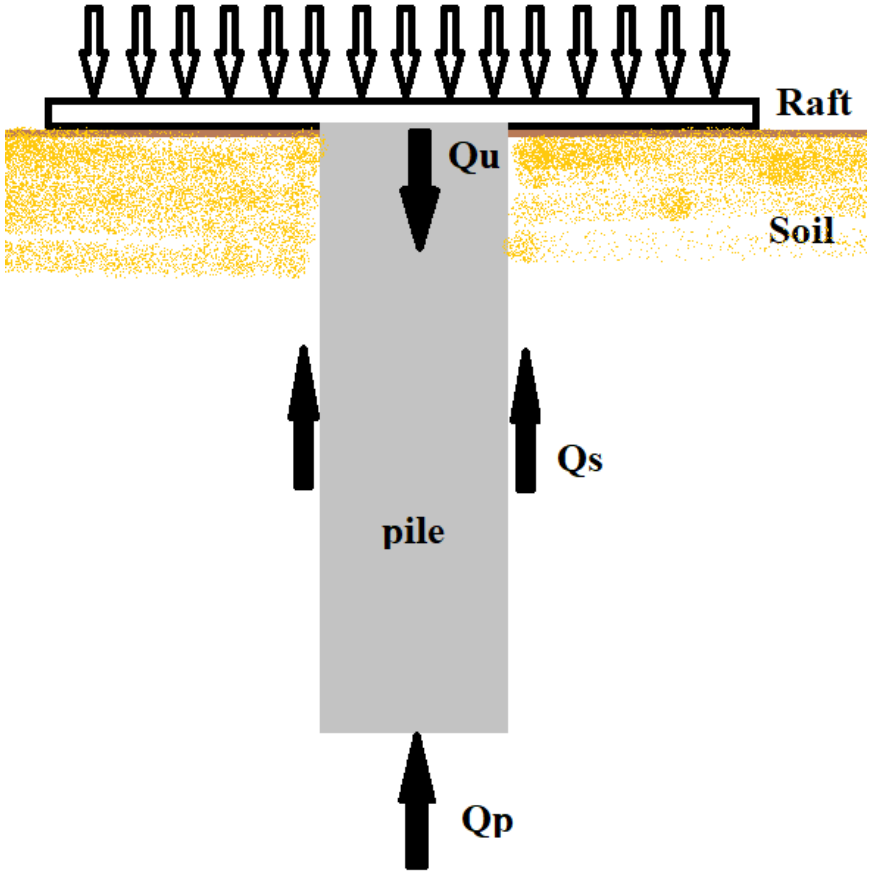


Figure 2.22: Pile skin friction and point bearing.

2.3.2 Analytical and Numerical Studies of Pile Foundation

Likewise, many researchers have contributed either experimentally, theoretically, or numerically on the behaviour of piled raft foundation to study the different aspects of piled raft foundation. Most of the research and investigations are focused on the settlement characteristics of combined piled raft foundation with various arrangements of pile groups using experimental and numerical models as given in Figure 2.23.

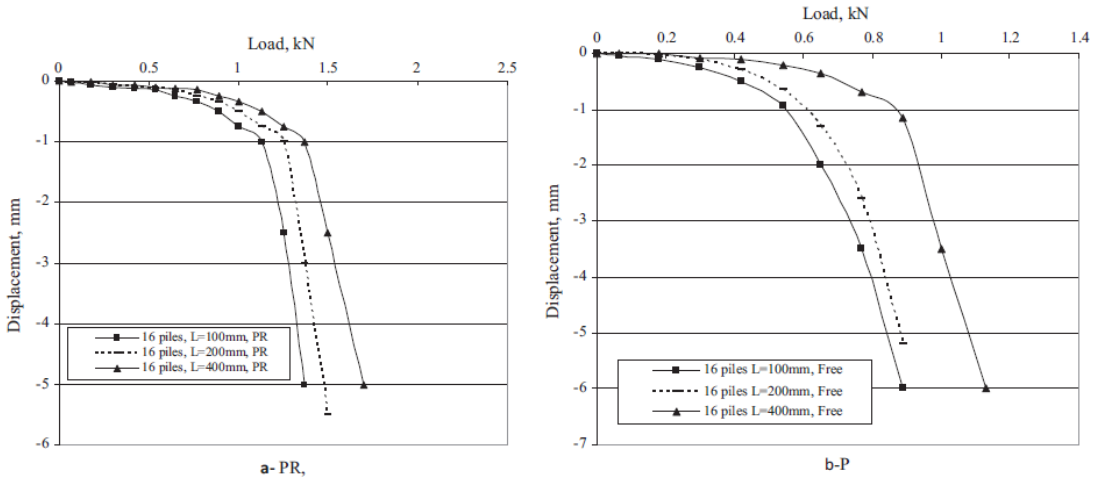


Figure 2.23: Piled raft load displacement relationship. (Elwakil & Azzam, 2016)

Elwakil and Azzam (2016) presented the load displacement relation of piled raft. Figure 2.23 shows the effect of varying length of piles on the ultimate load capacity of the foundation. It can be observed from these curves as the length of pile increases the ultimate load capacity is increasing. This is because longer piles generally increases the bearing capacity of the foundation. The longer the pile the deeper they penetrate into the stronger soil layers, which can allow the piles to transfer the load to more stable soil layers that can increase the overall bearing capacity of foundation.

Tan and Chow (2004) have discussed two categories for the design of piled raft foundations on soft soil, first for low-rise buildings (less than 3-storeys) and second medium rise buildings (2 to 5-storeys). Short length piles were used for the low-rise buildings directly under the concentrated loads to control local deformations whereas for medium rise buildings piles with varying length were used, longest piles in the middle and shorter piles at the edge of foundation were provided to control the differential settlement. They also have discussed many designed case histories to validate their proposed design approach.

For low rise buildings, shorter piles are generally sufficient to support the relatively lighter load. They can be designed to penetrate the upper layers of the soft soil and transfer

the load to more competent soil layers below. The length of the short pile can depend on the specific soil condition and the load applied. For medium-rise buildings, a combination longer piles in the middle and shorter piles on the edges can be an effective solution. This approach can take into account the variation in load across the building's footprint.

Placing longer piles in the middle of the building helps to distribute the heavier loads from the central area to the deeper soil layers. Longer piles can provide better bearing capacity and improved settlement control, shorter piles on the edges of the building can penetrate to the upper layers of the soft soils to support the lighter loads. They can help to provide a transition between the stiffer central portion of foundation and the outer edges where the load ae lower. The specific lengths and arrangements of the piles can depends on the various factors such as soil properties, building loads and site conditions.

Sanctis and Mandolini (2006) have proposed a criterion to evaluate the ultimate vertical load of piled raft using bearing capacity theories. The proposed criterion is a guide to measure the safety factor of vertically loaded piled raft. A comprehensive parametric study was also performed using 3D finite element program ABAQUS to a capped pile, unpiled rafts, pile groups and piled raft resting on clay, to define the failure load coefficients for the interaction between the raft and pile group at failure. The relation for coefficient is given below.

$$\xi_{PR} = \frac{Q_{PR,ult}}{Q_{UR,ult} + Q_{G,ult}} = \frac{FS_{PR}}{FS_{UR} + FS_G} \qquad \text{Equation 2.7}$$

Where:

$Q_{PR,ult}$ *= the bearing capacity of piled raft*

$Q_{UR,ult}$ = *the bearing capacity of unpiled raft*

$Q_{G,ult}$ = *the bearing capacity of pile groups*

$FS_{PR} = Q_{PR,ult}/Q$

$FS_{UR} = Q_{UR,ult}/Q$

$FS_G = Q_{G,ult}/Q$

Q = the load that should be applied to the unpiled raft.

Poulos et al. (2011) have used the principles of limit state design approach for the piled raft foundation design under tall buildings. The finite element analysis of a full-scale building using PLAXIS 3D were also used which showed smaller lateral deflections because of the larger lateral stiffness of piles than the raft foundations.

Cho et al. (2012) have investigated the behaviour of a square raft foundation using 3D finite element analysis (ABAQUS, 2010) under vertical loading. In this study different pile arrangements and loading on the raft were examined. Also, finite element model 3D elasto-plastic FE analysis with slip interface between soil and pile contact were used to evaluate the results. They have concluded that the length of piles has less effect than the number of piles for controlling the settlement, it was also observed that the higher area replacement ratio is required in soft clay than the stiff clay for minimizing differential settlement as presented in Figure 2.24.

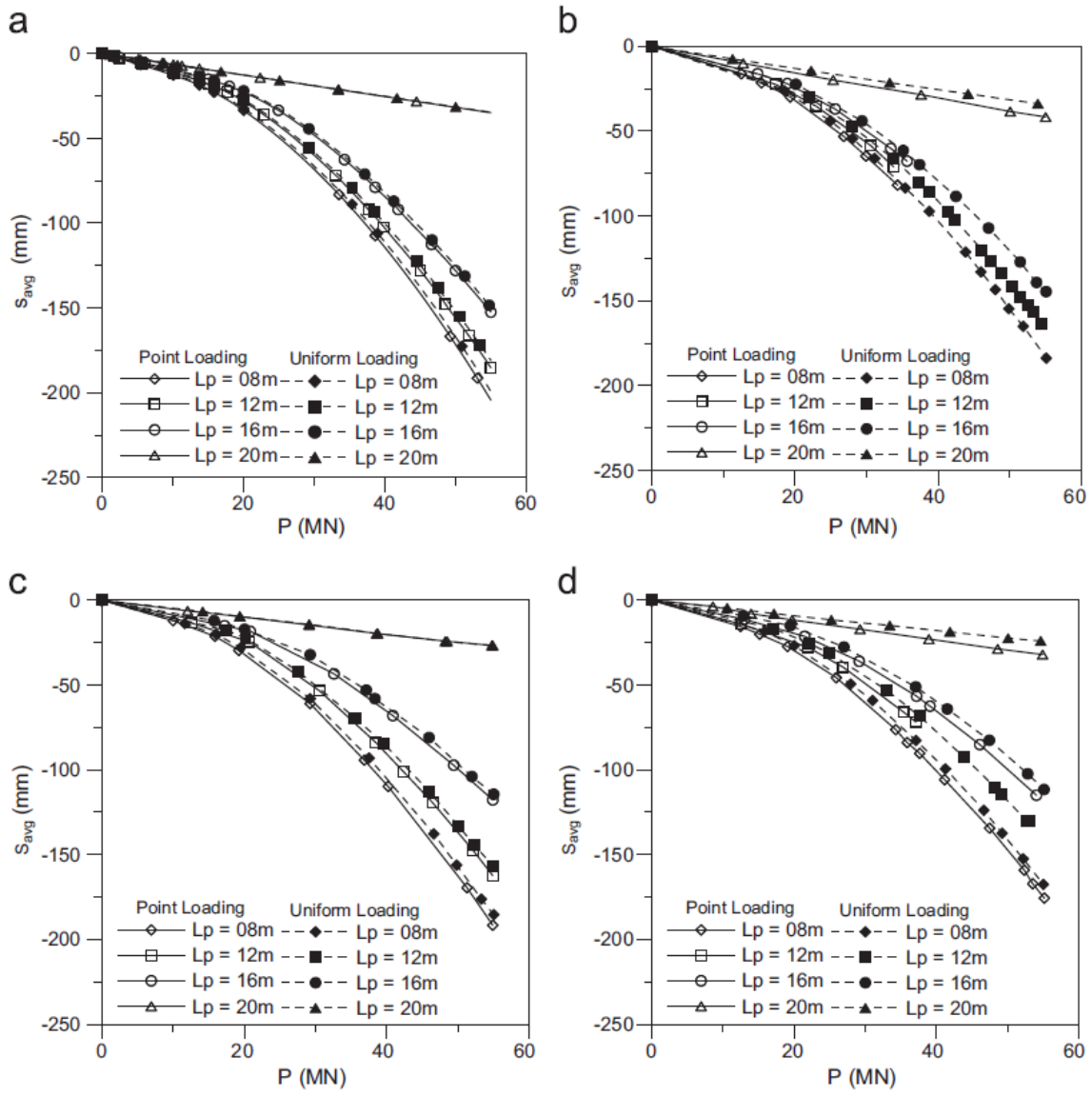


Figure 2.24: Normalized differential settlements with pile group-raft raft area ratio (stiff clay):(a)3x3 array;(b)4x 4 array. (Cho et al., 2012)

Figure 2.24 shows load-settlement curves of piled raft with various configurations, and varying number of piles with point load and uniform load on raft. It can be seen from these curves that with increasing pile length, the settlement of the raft is reducing, the type of loading (point load or uniform load) has no significance on the raft settlement. It can also be observed that with smaller spacing between the piles, settlement can decrease.

Watcharasawe et al. (2017) performed the consolidation analysis on the piled raft foundation of 8 story and 25 story buildings when placed in clayey soil in Bangkok using 3D numerical modelling. Parametric study was conducted to study the effect on raft depth and load carried by piles, and it was concluded that the consolidation has strong impact on the load carried by piles, the percentage of load shared by the piles can increase up to 12 percent for low rise and 6 percent for high rise buildings. The load sharing behaviour of piles in piled raft foundation may undergo changes after consolidation of underlying soil. Consolidation settlement occurs when excess pore water pressure is dissipated over time. The influence of the consolidation on load sharing can vary depending on several factors, including soil properties, piles characteristics, and nature of the consolidation process.

Consolidation settlement can lead to increased load sharing among the piles. This happens because the increased soil stiffness allows for better load transfer from the raft to the piles for this reason the piles that initially carried smaller portion of the loads may experience an increase in their load share after consolidation.

Nguyen et al. (2013) investigated the use of piles under raft foundation using Plaxis 3D. The behaviour and performance of pile under raft was investigated using different parameters like pile length, pile arrangement, raft thickness and it was concluded in general that the increase in raft thickness, pile length, number of piles can reduce the total and differential settlement. These are presented in Figure 2.25 and Figure 2.26.

Increasing the raft thickness can distribute the load over a larger area which can reduce the stress transferred to the underlying soil, longer piles can penetrate deeper into more competent soil layer which can provide enhanced load bearing capacity and reduced settlement, and increasing number of piles under the raft foundation can enhance the load

distribution, more piles can help to evenly distribute the applied load which can help to reduce the load intensity on each individual pile and controls the settlement of the whole foundation (Deb & Pal, 2022; Elsawwaf et al., 2022; Ghalesari & Choobbasti, 2018; Mali & Singh, 2020;). In Figure 2.25, It can be observed from the graph (a) that the settlement in the raft is less due to the dense soil, and from graph (b) higher settlements can be observed when the soil is loose. Also, graph (a) and (b) shows having more number of piles under the raft can increase the load carrying capacity of the foundation system.

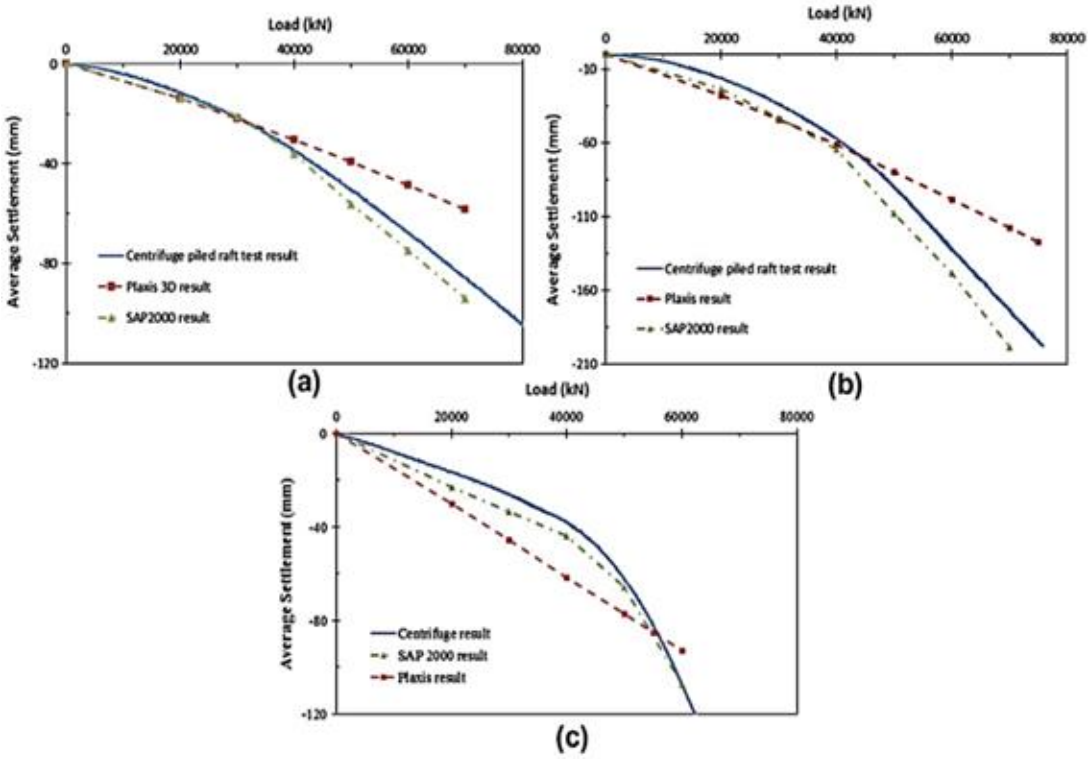


Figure 2.25: Piled raft's behaviour comparison between centrifuge test, proposed method analysis and Plaxis 3D foundation analysis. (a) Piled raft with 16 piles (D = 0.6 m; L = 15 m) in dense sand. (b) Piled raft with 16 piles (D = 0.6 m; L = 15m) in loose sand. (c) Piled raft with 9 piles (D = 0.6 m; L = 9 m) in dense sand. (Nguyen et al., 2013)

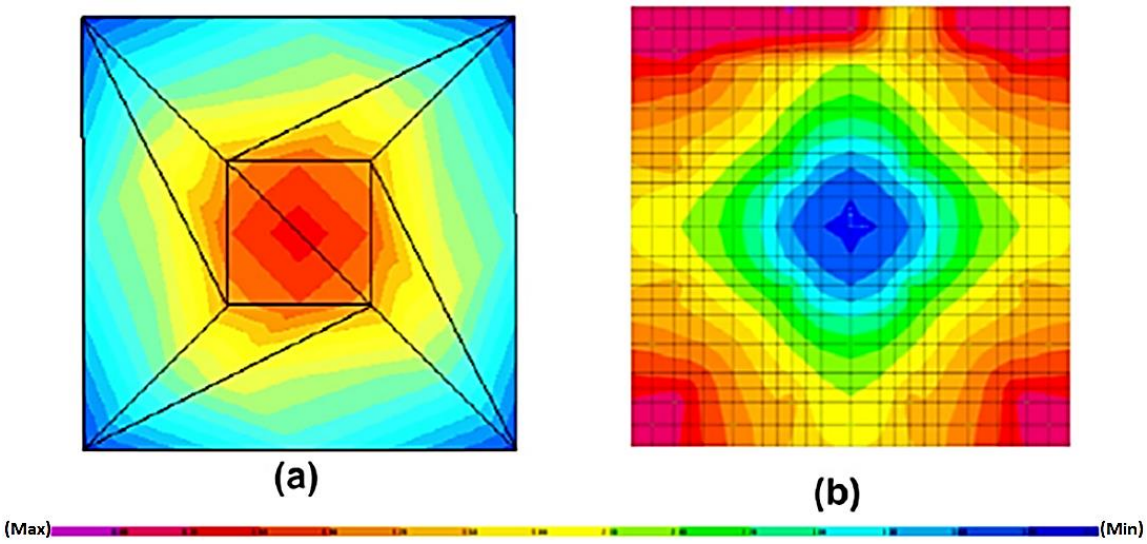


Figure 2.26: Distribution of total bending moment. (a) PLAXIS 3D. (b) SAP 2000. (Nguyen et al., 2013)

Prashant et al. (2013) have presented the study for the optimization of piled raft foundation based on the variation of parameters such as pile raft aspect ratio, pile spacing to diameter ratio, thickness of raft, and pile to raft area ratio using PLAXIS 3D as presented in Figure 2.27. They also have suggested some guidelines based on the parametric study for the optimization of piles under raft as a combined system. It was concluded that the increase in pile diameter, pile aspect ratio, raft thickness (2.3 to 2.5 times the thickness required for punching shear), pile to raft ratio can help to reduce the differential settlements and increase the load carrying capacity.

It can be observed from the Figure 2.27(a) that with the decrease in the diameter of piles the spacing over diameter ratio increase which improves the load carrying capacity of piled raft, Figure 2.27(b) shows the influence of aspect ratio (length/ diameter of pile), the increase in the carrying capacity can be seen with higher aspect ratio. By comparing Figure 2.27(b, c, and d) it can be noticed that with increasing number of piles under raft the carrying capacity of piled raft can be improved.

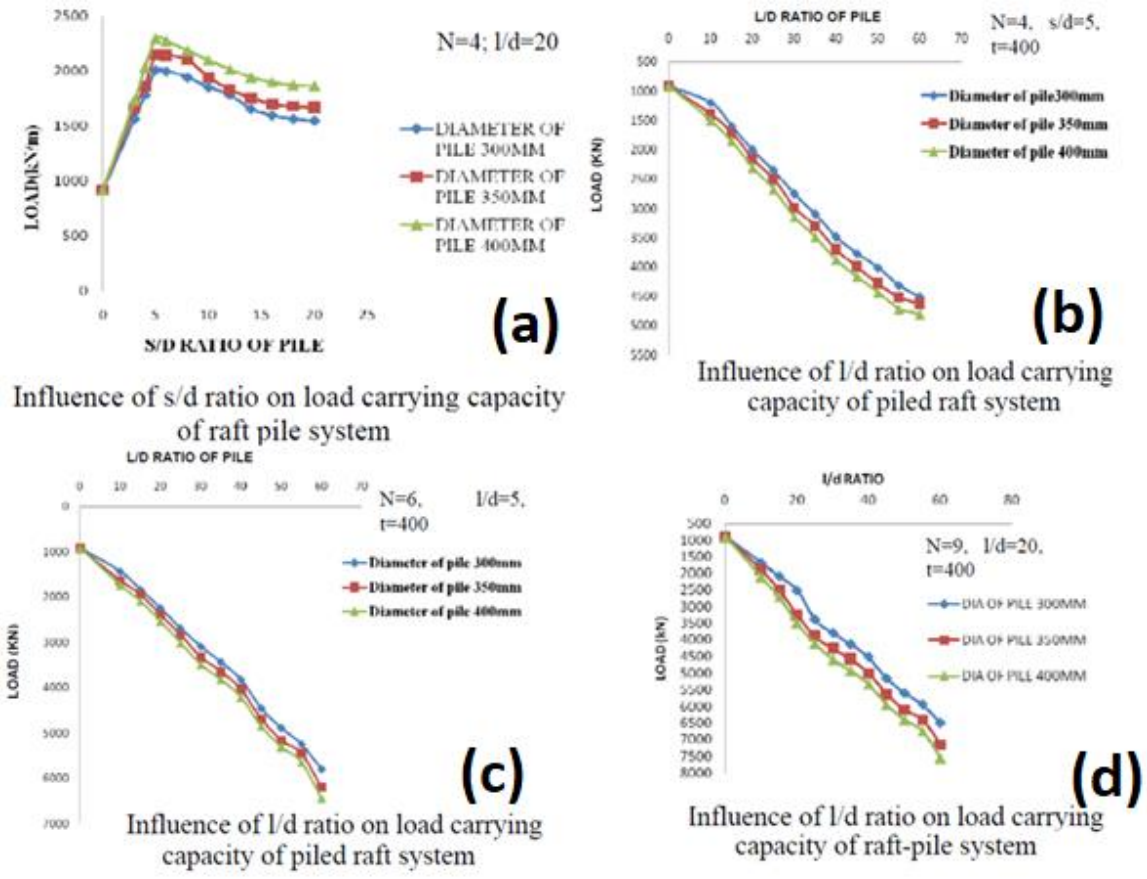
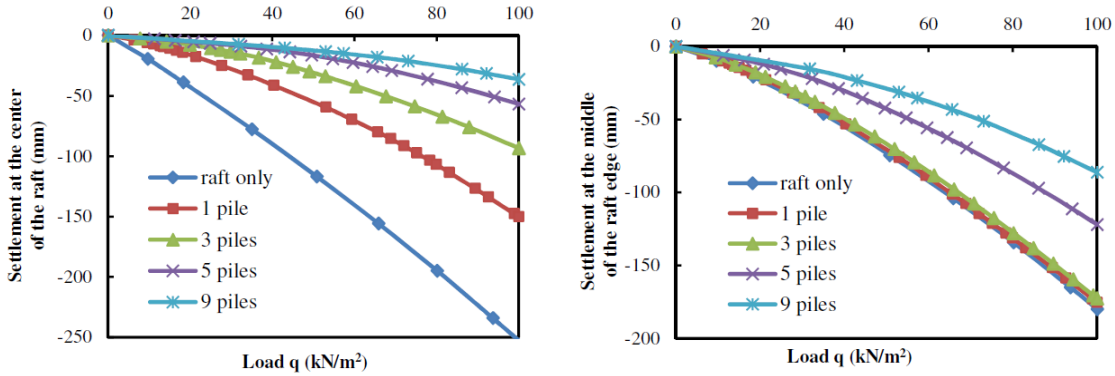


Figure 2.27: Influence of parameters on the load carrying capacity of piled raft system (Prashant et al., 2013)

A parametric study has been carried out by Anhtuan et al. (2014) to study the behaviour of piled raft foundation using PLAXIS 3D and they have reported the decrease in the settlement when the number of pile and length is increased and increase in the settlement when the spacing of piles increase (Al-Jubair & Abbas, 2014; Khanmohammadi & Fakharian, 2018; Mali & Singh, 2019) as given in Figure 2.28 and Figure 2.29. These figures show the effect of number of piles on the settlement, it can be seen from the curves that the settlement of the foundation is decreasing with the increasing number of piles. This can be understood by the fact that when multiple piles are installed within a foundation system, they interact with each other which helps for load sharing. This load sharing mechanism helps to

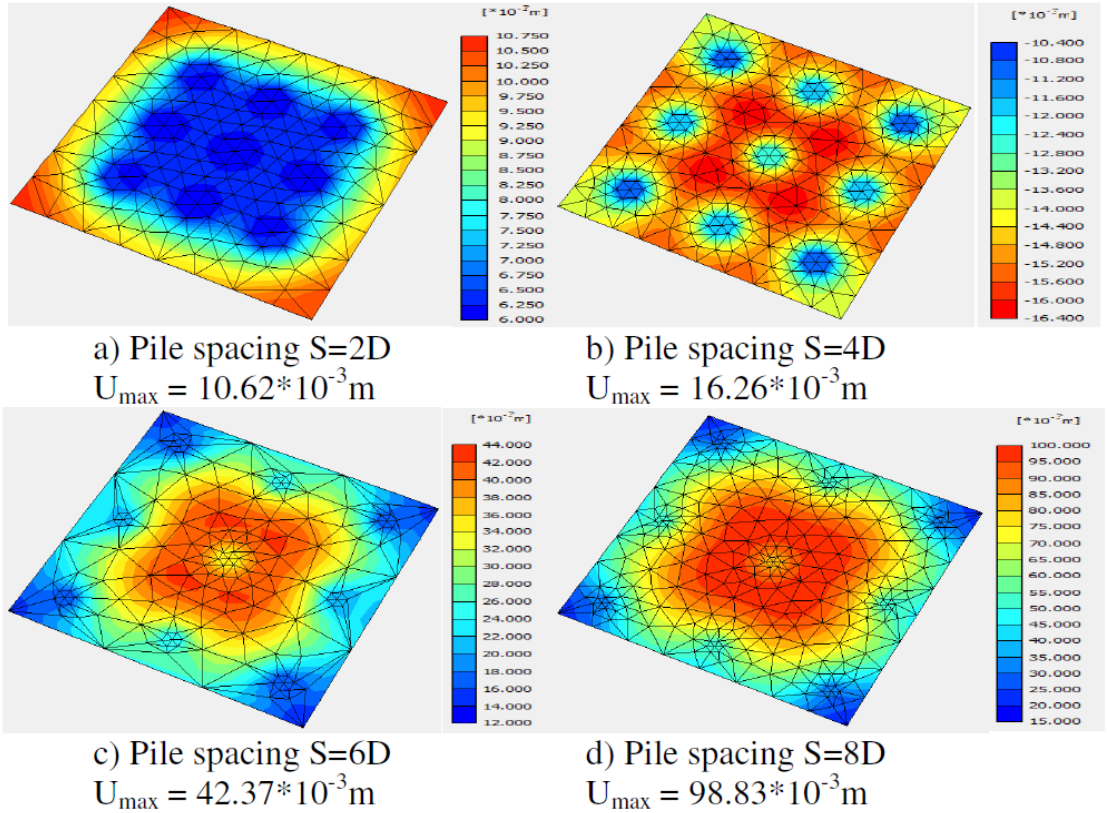
redistribute the applied load among the piles and reduces the stress and settlement on each pile (Deb et al., 2022).



Load-settlement curve at the centre of the raft

Load-settlement curve at the middle of the raft edge

Figure 2.28: Load-settlement curve (Anhtuan et al., 2014)



a) Pile spacing S=2D
U_{max} = 10.62*10^{-3}m

b) Pile spacing S=4D
U_{max} = 16.26*10^{-3}m

c) Pile spacing S=6D
U_{max} = 42.37*10^{-3}m

d) Pile spacing S=8D
U_{max} = 98.83*10^{-3}m

Figure 2.29: Effect pile spacing on the settlement of the foundation, U_{max}= maximum settlement. (Anhtuan et al., 2014)

Paravita and Daniel (2015) have conducted the finite element analysis on raft foundation with and without piles using PLAXIS 2D to study the effect of the number of piles on the settlement as presented in Figure 2.30. They have concluded that by increasing the number of piles the settlement of piled raft foundation can reduce, and the optimum number of piles should be calculated in pile raft foundation system to control the foundation settlement effectively and economically. In Figure 2.30 the relation between number of piles and settlement is presented, it can be noticed from the curve that settlement reduces with the increasing number of piles (Ferchat et al., 2021; Kumar & Kumar, 2018; Mali & Singh, 2021; Patil et al., 2016). Also, it can be observed that having number of piles more than 8, settlement in the foundation reduces with slow rate.

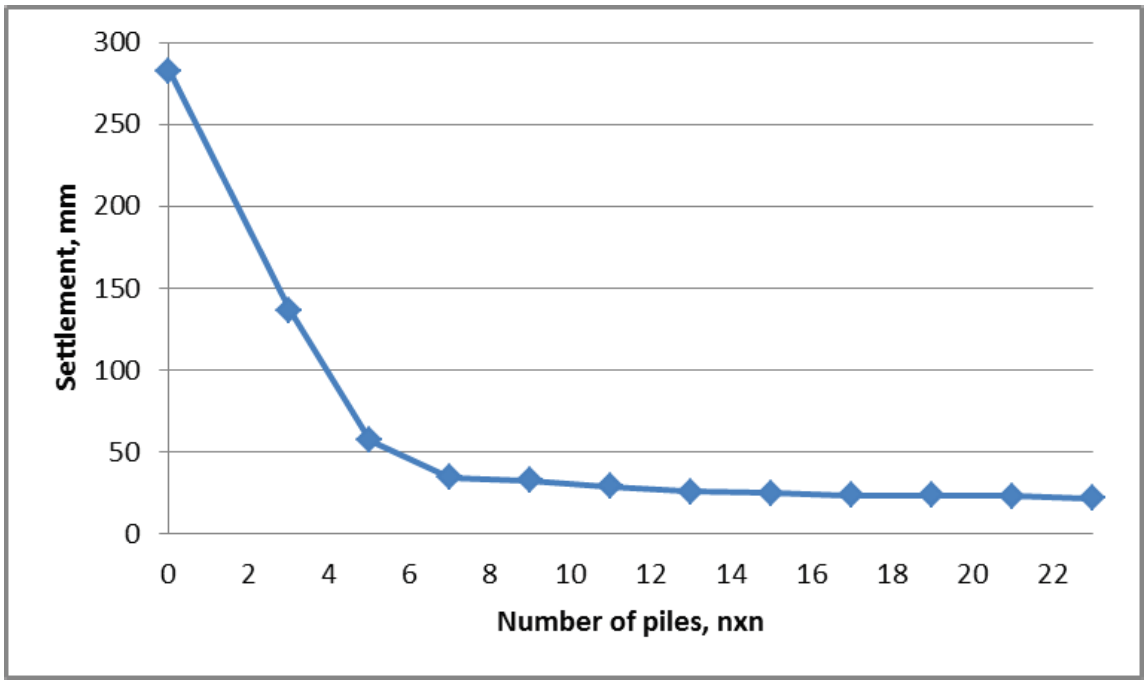


Figure 2.30: Settlement reduction by increasing number of piles (Paravita & Daniel, 2015)

Celik (2019) presented a design concept of piled raft foundation system that was prepared by combining 2D finite element method with equivalent pier. The results obtained from the proposed design concept were compared with equivalent raft and equivalent pier

method in sandy soil. It was concluded that the proposed analysis can make similar settlement predictions as it can be seen in Figure 2.31.

Following are the equations used for new design concept:

$$\textit{Pile group stiffness} = K_p = n^{1-e}K_1 \qquad \text{Equation 2.8}$$

Where:

K_1 *= pile head stiffness*

n = number of piles

$$\textit{Piled raft stiffness} = K_{pr} = \frac{1-0.6\left(K_r/K_p\right)}{1-0.64\left(K_r/K_p\right)}K_p$$

$$\textit{Ratio of load carried by raft and group piles} = \frac{P_r}{P_p} = \frac{0.2K_r}{1-0.8\left(K_r/K_p\right)K_p}$$

$$\textit{Stiffness of raft} = K_r = \frac{2.25GB}{1-\upsilon}$$

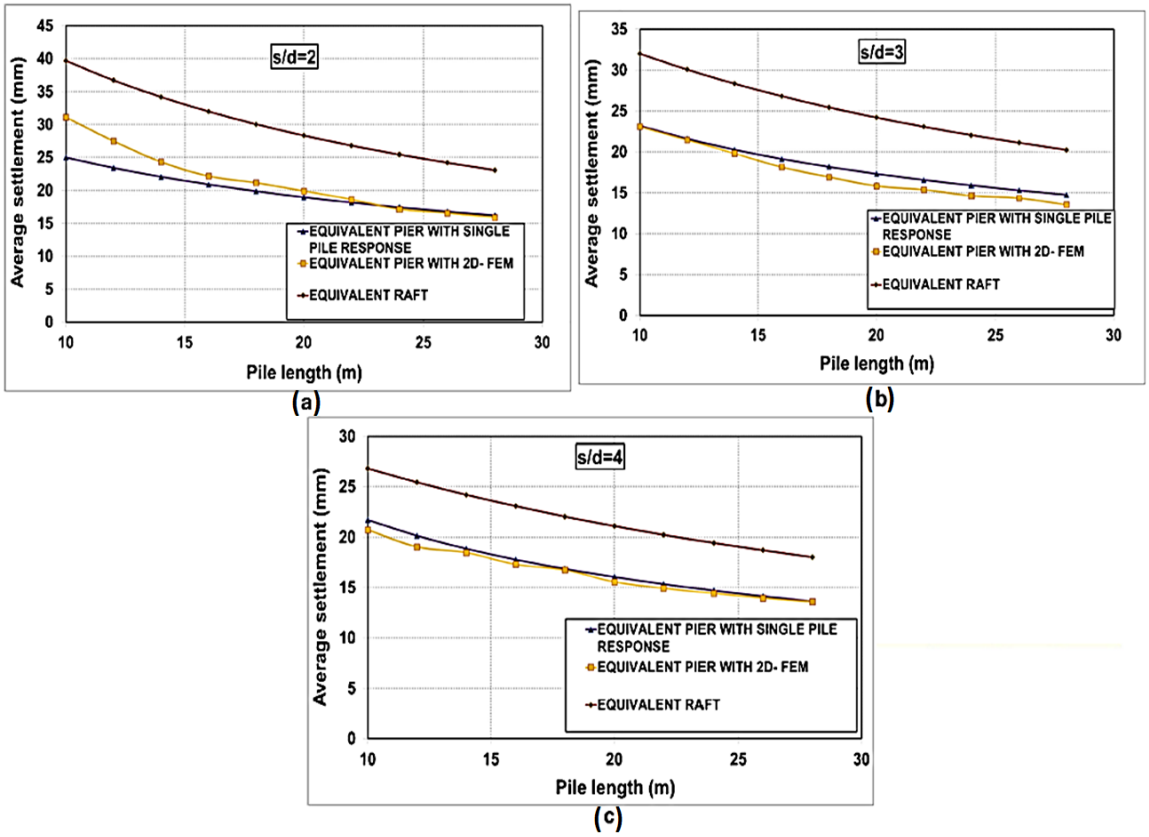


Figure 2.31: Average settlement versus pile length effect with respect to spacing to diameter ratio (*s/d*). (Celik, 2019)

Figure 2.31 presents the influence of pile length on the average settlement. It can be noticed that with the increase in pile length the average settlement reduces. The reduction in settlement can be attributed by the fact that, longer piles penetrate deeper into the soil, allowing then to reach stronger soil layers, which can reduce the stress and settlement on the foundation (Lodha et al., 2019).

Abdel-Azim et al. (2020) performed a 3D finite element analysis on a piled raft foundation of Messeturm building in Germany using Plaxis 3D to investigate the performance of foundation in Frankfurt over-consolidated clay. Piled raft foundation was evaluated based on total settlement, differential settlement and pile skin friction and it was concluded that the piled raft foundation is the optimized foundation solution for high rise buildings.

Elsawwaf et al. (2022) conducted a numerical investigation to study the effect of length of pile, diameter of pile, and number of piles in soft clay using PLAXIS 3D. It was reported that settlement and differential settlement of foundation decreased with the increase in pile length and number. It was also reported that the load sharing ratio of piles increases by 13.7, 36, and 58% with the range of pile length to diameter ratio from 10 to 30 and number of piles 4, 9, and 16 respectively.

Amornfa et al. (2022) compares monitoring data from real world with 3D numerical simulations using PLAXIS 3D, a parametric study of piled raft was conducted on the Ho Chi Minh sub soil. According to the results, total and differential settlement decreased with increased pile length, pile number and embedding raft depth. Moreover, it as also reported that the raft could share 66% of building's load by being located in the second layer of stiff clay.

2.4 Stone Column and Pile under Raft Foundation

So far very few works have been reported in the literature on the use of combined stone column and pile under the raft.

Liang et al. (2003) proposed the concept of combining two types of pile system under raft such as short pile made of flexible materials and long piles made of rigid material. ANSYS program was used for finite element analysis to study the behaviour of seven-story building foundation with different parameter including ratio of length to diameter, elastic moduli of piles, thickness and elastic modulus of cushion as presented in Figure 2.32. It was reported that the elastic modulus of piles are more effective in long piles to control the settlement than the short piles, thickness of cushion has significant effect on the load sharing

ratio of piles to subsoils and decrease in modulus of elasticity of cushion can decrease the stress concentration of long piles as given in Figure 2.33, Figure 2.34 and Figure 2.35.

It can be observed from Figure 2.33 that when the stiffness of cushion increases the load on the pile is increasing, this can be understand by the fact that when the elastic modulus of the cushion layer in increased, it becomes stiffer and less flexible. This increased stiffness can affect the load distribution within foundation system, as a result, the stiffer cushion layer transmits a larger portion of load directly to the center long pile, increasing its load compared to the surrounding piles.

Figure 2.34 and Figure 2.35 shows the effect of cushion thickness on axil force of piles. It can be noticed from the curves that with the increase in the thickness of cushion the axil stress on the long center pile decreases, increasing the thickness of cushion layer can provides a greater area load distribution. As a result, the load can spread more evenly across the foundation system, reducing the load concentration on the center long pile.

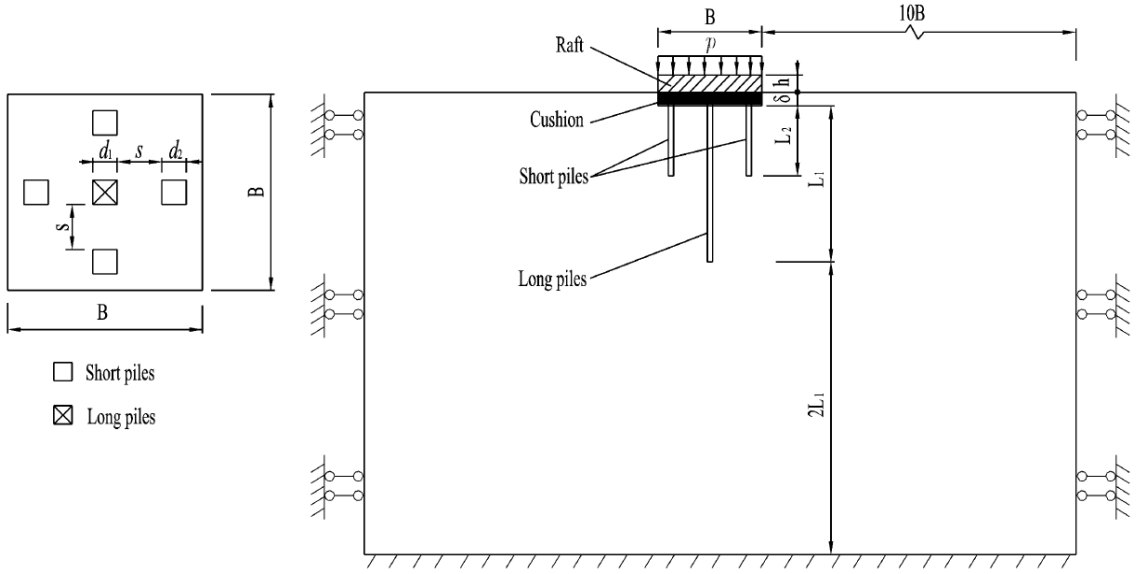


Figure 2.32: Schematic diagram of calculating modal to be analyzed. (Liang et al., 2003)

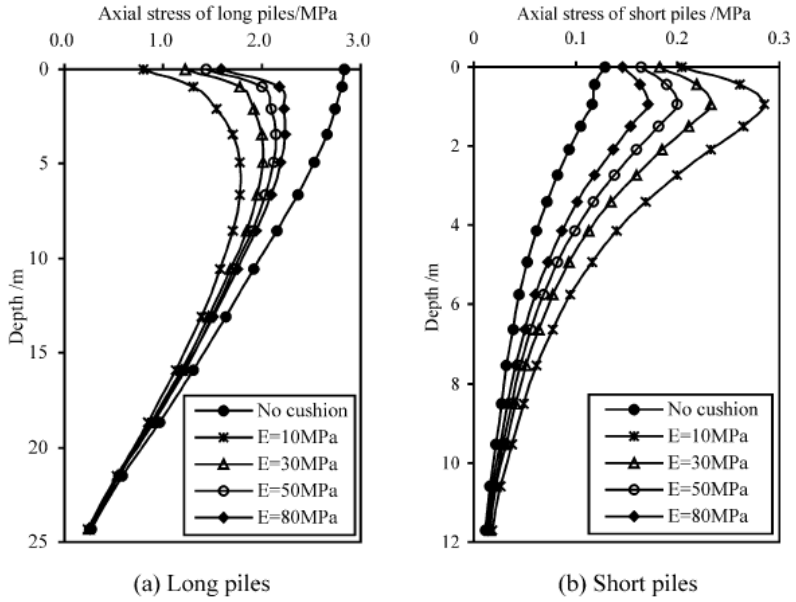


Figure 2.33: Effects of cushion elastic modulus on axial stress distribution of piles. (Liang et al., 2003)

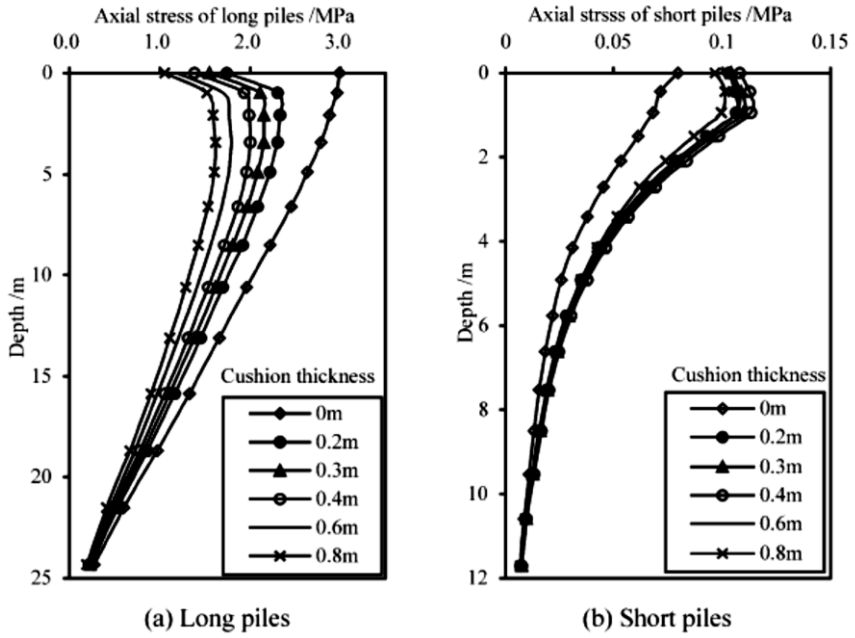


Figure 2.34: Effects of cushion thickness on axial force of piles to soil. (Liang et al., 2003)

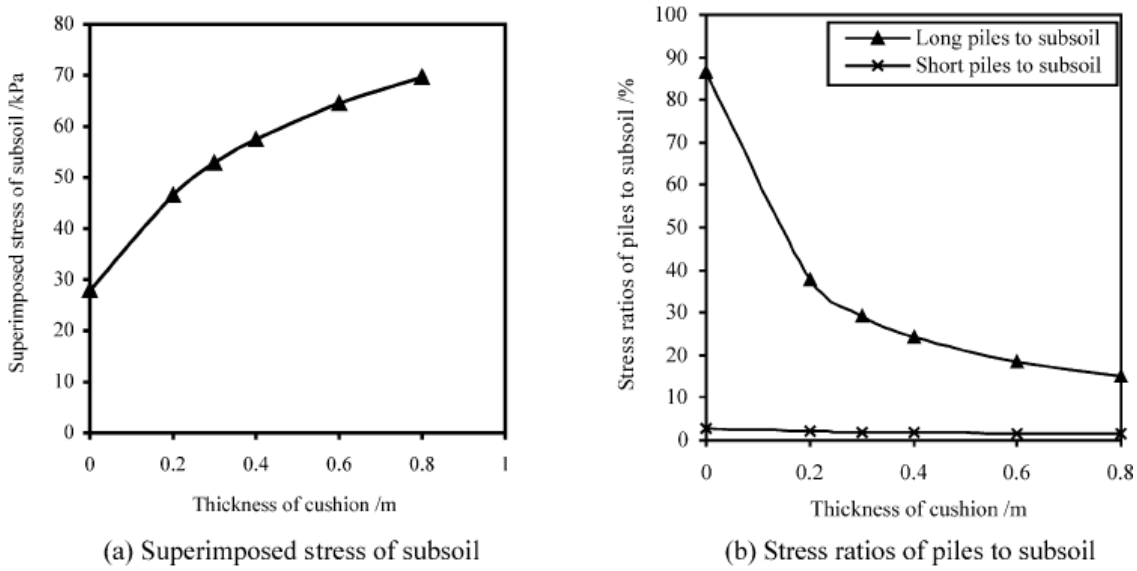


Figure 2.35: Effects of cushion thickness on stress ratio of piles to soil. (Liang et al., 2003)

Samanta and Bhowmik (2017) have conducted the numerical analysis of the piled raft foundation in soft soil improved with stone columns see Figure 2.36 and Figure 2.37. PLAXIS 3D was used to study the influence of parameters (Table 2.3) on the total and differential settlements of the foundation as presented in Figure 2.38. They have concluded

that the increase in the length of the pile increases the percentage of load shared by piles whereas by increasing the diameter of stone columns results in higher portion of load shared by stone columns which played a significant role in reducing the settlement of foundation. The length of stone columns helps to control the settlement, but it has no effect in sharing the load percentage. Increase in angle of friction of stone columns and thickness of raft foundation increases the percentage of load shared by stone columns and help to reduce the foundation settlement. It was also reported that using pile slenderness equal to 40 and area replacement ratio equal to 25% results in balanced share of loads between stone columns and piles.

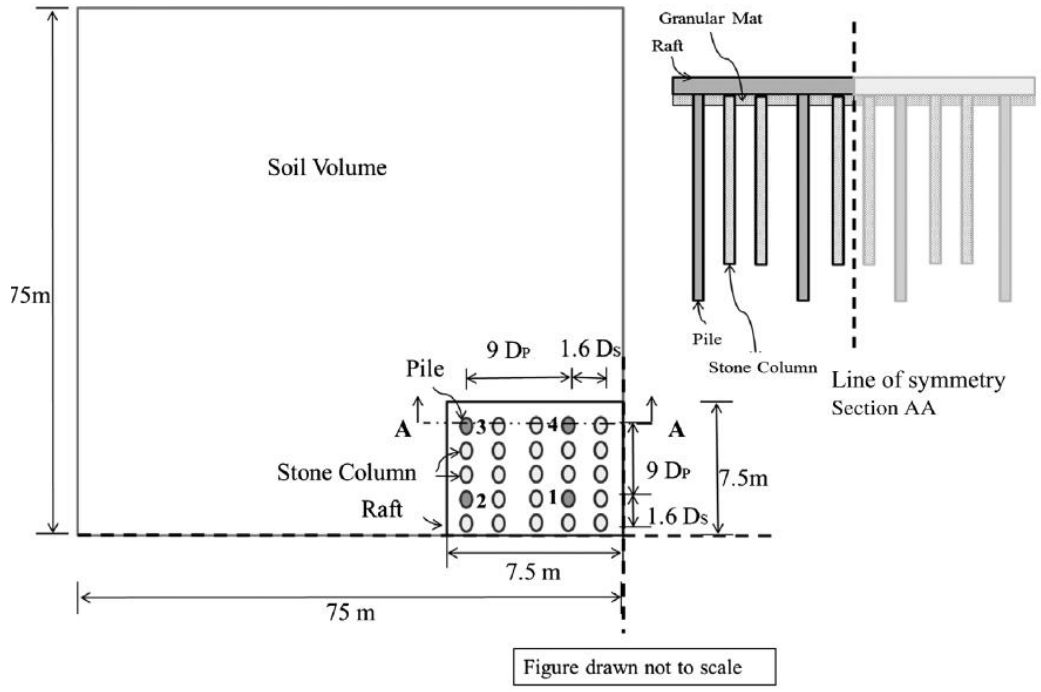


Figure 2.36: Schematic diagram of one quarter of the problem modelled in the present study (Samanta & Bhowmik, 2017)

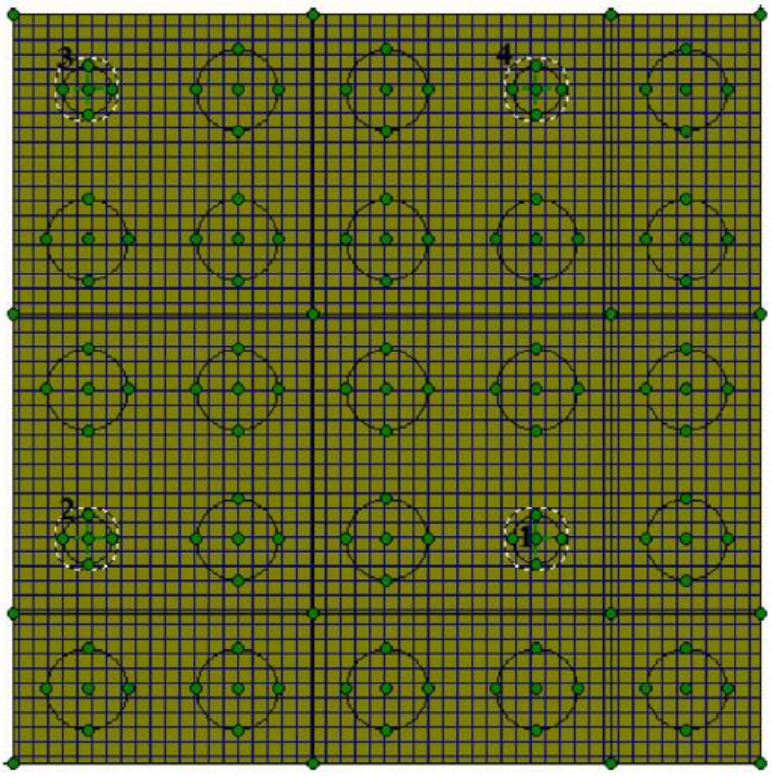


Figure 2.37: Pile and stone column within the raft in FEM model. (Samanta & Bhowmik, 2017)

Table 2.3: Parameters of stone column and piled raft. (Samanta & Bhowmik, 2017)

Parameters				
	Slenderness ratio, *L/D*	**Area replacement ratio (%)**	**Angle of internal friction, *φ* (º)**	**Thickness of raft (m)**
Stone column	5, 10, 15,20, 25	10, 15, 20, 25	36, 40, 43, 45	-
Pile	40, 50, 60	-	-	-
Raft	-	-	-	1, 1.5, 2, 2.5

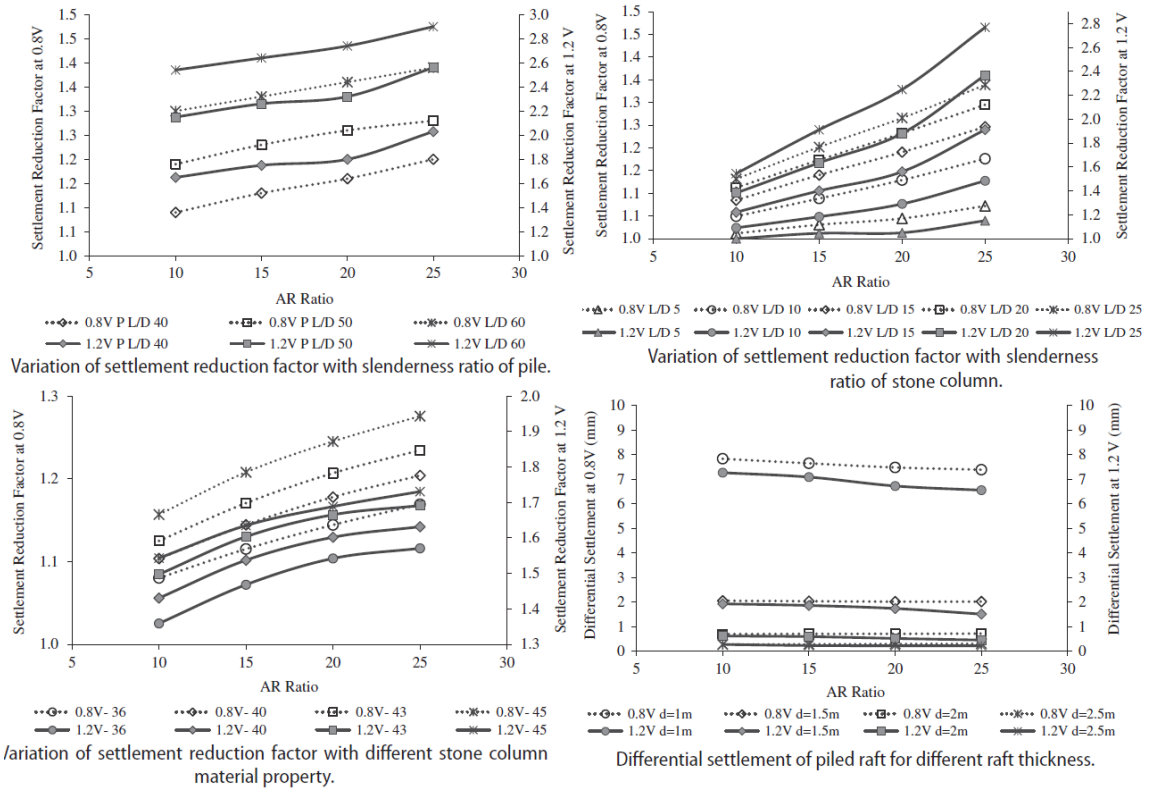


Figure 2.38: Settlements (Samanta & Bhowmik, 2017)

2.5 Material Properties and Parameters Available in Literature

Table 2.4 shows the material properties and parameters available in literature used for experimental and numerical works for foundations with stone columns, pile foundations and combined foundation systems.

Table 2.4: Range of parameters available in literature

Material	Properties		Source
Soft Clay	Unit weight, γ_{unsat}, γ_{sat}	14 – 21, 16 – 22 kN/m^3	Budhu (2000)
		19, 20 kN/m^3	Sinha (2013)
		17.5, 18.5 kN/m^3	Lee et al. (2010)
		17, 18 kN/m^3	Tran et al. (2012)
		16, 17 kN/m^3	Kardgar (2018)
		16, 17 kN/m^3	Samanta & Bhowmik (2017)
		18 kN/m^3	Sharma & Kumar (2021)
		16, 17 kN/m^3	Mali & Singh (2018)
		16 kN/m^3	Ng et al. (2021)
		17 kN/m^3	Al-Kazzaz & Al-Obaydi (2021)
		13.6, 18.3 kN/m^3	Bhaumik et al. (2021)
	Young's modulus, E_s	2 - 15 MPa	Bowles (1982)
		1.5 – 3 MPa	Kolar & Nemec (1989)
		1 – 15 MPa	Budhu (2000)
		15 – 30 MPa	Budhu (2000)
		54 MPa	Sinha (2013)
		16.8 MPa	Lee et al. (2010)
		0.3 – 6.3 MPa	Tran et al. (2012)
		5 MPa	Kardgar (2018)
		5 MPa	Samanta & Bhowmik (2017)
		1.5 – 14 MPa	Hanna et al. (2013)

		4 MPa	Sharma & Kumar (2021)
		25 MPa	Mali & Singh (2018)
		3 MPa	Ng et al. (2021)
		10 MPa	Al-Kazzaz & Al-Obaydi (2021)
		2.15 MPa	Bhaumik et al. (2021)
	Poisson's ratio, v_s	0.1 – 0.3	Bowles (1982)
		0.35 – 0.45	Barksdale & Bachus (1983)
		0.3, 0.4	Balaam (1985)
		0.3	Lee & Pande (1998)
		0.35 – 0.4	Budhu (2000)
		0.3 – 0.35	Budhu (2000)
		0.15 – 0.25	Das (2000)
		0.2 – 0.5	Das (2000)
		0.15	Sinha (2013)
		0.4	Lee et al. (2010)
		0.33	Tran et al. (2012)
		0.25	Kardgar (2018)
		0.35	Samanta & Bhowmik (2017)
		0.15 – 0.45	Hanna et al. (2013)
		0.35	Sharma & Kumar (2021)
		0.495	Mali & Singh (2018)
		0.3	Ng et al. (2021)
		0.35	Al-Kazzaz & Al-Obaydi (2021)
		0.47	Bhaumik et al. (2021)
	Angle of friction, φ	15 – 30°	Budhu (2000)
		20°	Sinha (2013)
		20°	Tran et al. (2012)
		25°	Kardgar (2018)

		0°	Samanta & Bhowmik (2017)
		30°	Sharma & Kumar (2021)
		0°	Mali & Singh (2018)
		0°	Ng et al. (2021)
		20°	Al-Kazzaz & Al-Obaydi (2021)
		0°	Bhaumik et al. (2021)
	Cohesion, c	20 kPa	Sinha (2013)
		41.4 kPa	Lee et al. (2010)
		5 kPa	Tran et al. (2012)
		3 kPa	Kardgar (2018)
		20 kPa	Samanta & Bhowmik (2017)
		15 kPa	Sharma & Kumar (2021)
		25 kPa	Ng et al. (2021)
		10 kPa	Al-Kazzaz & Al-Obaydi. (2021)
		7 kPa	Bhaumik et al. (2021)
Sand	Unit weight, γ_{unsat}, γ_{sat}	16, 20 kN/m^3	Alkhorshid (2012)
		20 kN/m^3	Samanta & Bhowmik (2017)
		15.5 kN/m^3	Naseer et al. (2019)
		18-21.5 kN/m^3	Hataf et al. (2020)
		17 kN/m^3	Hadri et al. (2021)
		15.5, 18.5 kN/m^3	Bhaumik et al. (2021)
	Young's modulus, E_s	20 MPa	Alkhorshid (2012)
		45 MPa	Samanta & Bhowmik (2017)
		25 MPa	Naseer et al. (2019)
		70, 90, and 120 Mpa	Hataf et al. (2020)
		45 MPa	Hadri et al. (2021)

		20 MPa	Bhaumik et al. (2021)
	Poisson's ratio, v_s	0.3	Alkhorshid (2012)
		0.3	Samanta & Bhowmik (2017)
		0.2 – 0.45	Hanna et al. (2013)
		0.3	Naseer et al. (2019)
		0.15-0.25	Hataf et al. (2020)
		0.3	Bhaumik et al. (2021)
	Angle of friction, φ	30°	Alkhorshid (2012)
		40°	Samanta & Bhowmik (2017)
		38° – 45°	Hanna et al. (2013)
		30°	Naseer et al. (2019)
		38° – 44°	Hataf et al. (2020
		30°	Hadri et al. (2021)
		30°	Bhaumik et al. (2021)
	Cohesion, c	0	Samanta & Bhowmik (2017)
		1 kPa	Hadri et al. (2021)
		1 kPa	Hataf et al. (2020)
		0.3 kPa	Bhaumik et al. (2021)
Stone Column	Unit weight, γ_{unsat}, γ_{sat}	16.5, 20.2 kN/m^3	Barksdale & Bachus (1983)
		15 - 17, 20 – 22 kN/m^3	Budhu (2000)
		13 – 16, 18 – 20 kN/m^3	Budhu (2000)
		19.5, 20.5 kN/m^3	Kardgar (2018)
		17, 18 kN/m^3	Fattah & Majeed (2012)
		20 kN/m^3	Sharma & Kumar (2021)
		18 kN/m^3	Ng et al. (2021)
		20 kN/m^3	Al-Kazzaz & Al-Obaydi (2021)
		16.62, 20.1 kN/m^3	Bhaumik et al. (2021)

	Young's modulus, E_s	48 MPa	Datye et al. (1982)
		96 - 192 MPa	Bowles (1982)
		48 - 81 MPa	Bowles (1982)
		80 – 500 MPa	Kolar & Nemec (1989)
		40 – 80 MPa	Budhu (2000)
		52 MPa	Kardgar (2018)
		100 MPa	Fattah & Majeed (2012)
		35 MPa	Samanta & Bhowmik (2017)
		35 – 175 MPa	Hanna et al. (2013)
		40 MPa	Sharma & Kumar (2021)
		30 MPa	Ng et al. (2021)
		50 MPa	Al-Kazzaz & Al-Obaydi (2021)
		55 Mpa	Bhaumik et al. (2021)
	Poisson's ratio, v_s	0.2 - 0.4	Bowles (1982)
		0.3	Balaam (1985)
		0.2 - 0.25	Kolar & Nemec (1989)
		0.3	Lee & Pande (1998)
		0.25 – 0.35	Budhu (2000)
		0.3 – 0.45	Das (2000)
		0.35	Wright & Touquet (2004)
		0.3	Kardgar (2018)
		0.3	Fattah & Majeed (2012)
		0.3	Samanta & Bhowmik (2017)
		0.3	Hanna et al. (2013)
		0.3	Sharma & Kumar (2021)
		0.3	Ng et al. (2021)
		0.3	Al-Kazzaz and Al-Obaydi (2021)

		0.3	Bhaumik et al. (2021)
	Angle of friction, φ	38° - 42°	Barksdale & Bachus (1983)
		44°	Kardgar (2018)
		40°	Fattah & Majeed (2012)
		36°, 40°, 43°, 45°	Samanta & Bhowmik (2017)
		40°	Hanna et al. (2013)
		44°	Sharma & Kumar (2021)
		40°	Ng et al. (2021)
		40°	Al-Kazzaz & Al-Obaydi (2021)
		43°	Bhaumik et al. (2021)
	Cohesion, c	44 kPa	Kardgar (2018)
		0	Fattah & Majeed (2012)
		0	Samanta & Bhowmik (2017)
		0	Hanna et al. (2013)
		0.1 kPa	Ng et al. (2021)
		0.2 kPa	Al-Kazzaz & Al-Obaydi (2021)
		0.3 kPa	Bhaumik et al. (2021)
	Stone columns diameter	1 m	Hanna et al. (2013)
		0.7, 0.8, 0.9, 1, 1.2 m	Sharma & Kumar (2021)
		1 m	Ng et al. (2021)
		0.75 m	Al-Kazzaz & Al-Obaydi (2021)
		1 m	Bhaumik et al. (2021)
	Stone column length	5D, 10D, 15D	Samanta & Bhowmik (2017)
		14 m, 20 m	Hanna et al. (2013)
		6 m	Sharma & Kumar (2021)

		10 m 2D, 4D, 6D and 8D 20 m	Ng et al. (2021) Al-Kazzaz & Al-Obaydi (2021) Bhaumik et al. (2021)
	Stone column Spacing	1.6D 1 m 3D, 4D, and 5D 1.4m 9 m, 4 m, and 1.5m	Samanta & Bhowmik (2017) Sharma & Kumar (2021) Al-Kazzaz & Al-Obaydi (2021) Boumekik et al. (2021) Bhaumik et al. (2021)
Raft	Young's modulus, E_r	34000 MPa 40000 MPa 68000 MPa 25000 MPa 25000 MPa 30000 MPa 25000 MPa 30000 MPa	Sinha (2013) Lee et al. (2010) Tran et al. (2012) Kardgar (2018) Samanta & Bhowmik (2017) Sharma & Kumar (2021) Mali & Singh (2018) Al-Kazzaz & Al-Obaydi (2021)
	Poisson's ratio, v_r	0.2 0.16 0.15 0.2 0.2 0.2	Sinha (2013) Lee et al. (2010) Tran et al. (2012) Kardgar (2018) Samanta & Bhowmik (2017) Al-Kazzaz & Al-Obaydi (2021)
	Raft Size	24 x 24 x 2 m 10 x 10 x 1 m 1.4 x 1.4 x 0.75 m	Sinha (2013) Lee et al. (2010) Tran et al. (2012)

		7.5 x7.5 x 1, 1.5, 2, 2.5 m 4.8 x 4.8 x 1m 45 x 45 x 1, 2, 3 m 23 x 23 x 0.8 m 15 x 15 x 1.5 m	Samanta & Bhowmik (2017) Sharma & Kumar (2021) Mali & Singh (2018) Al-Kazzaz & Al-Obaydi (2021) Mali & Singh (2021)
Pile	Young's modulus, E_p **(Concrete)**	25000 MPa 40000 MPa 68000 MPa 25000 MPa 30000 MPa 25000 MPa	Sinha (2013) Lee et al. (2010) Tran et al. (2012) Samanta & Bhowmik (2017) Sharma &U Kumar (2021) Mali & Singh (2018)
	Young's modulus, E_p **(Steel)**	210000 MPa 210000 MPa 210000 MPa	Yao et al. (2016) Baca et al. (2021) Kim et al. (2021)
	Pile diameter	1 m 0.5 m 0.4 m 0.5 m 0.5, 1, 1.5, 2 m 0.4 m 0.5, 1, 1.5m 0.3 m	Sinha (2013) Lee et al. (2010) Tran et al. (2012) Sharma & Kumar (2021) Mali & Singh (2018) Baca et al. (2021) Mali & Singh (2021) Kim et al. (2021)
	Pile length	15 m 8, 12 ,16, 20 m 10 m 6m 10, 20, 30 m 15, 20, 30, 40, 50 m	Sinha (2013) Lee et al. (2010) Tran et al. (2012) Sharma & Kumar (2021) Mali & Singh (2018) Mali & Singh (2021)

		5 m	Kim et al. (2021)
	Pile Spacing	2D, 3D, 4D, 6D, 7D, 8D, 10D	Sinha (2013)
		3D, 4D, 6D, 9 D	Lee et al. (2010)
		2D, 4D	Tran et al. (2012)
		9D	Samanta & Bhowmik (2017)
		2D	Sharma & Kumar (2021)
		4.5D, 9D, 18D, 36D	Mali & Singh (2018)
		3, 4, 5 m	Mali &Singh (2021)

2.6 Summary

This chapter reviewed the reported works from the literature regarding (a) stone columns, (b) piled raft foundation and (c) stone columns and piles together under raft foundation in soft and compressible soil.

Most of the research work has been carried out to investigate the effect of parameters on the load-bearing performance and settlement of foundations. So far what has been discussed, it can be concluded that the change in parameters for any type of foundation system (stone under raft, pile under raft, stone, and pile under raft in soft soil) can make the notable effect on the load-bearing performance and settlement of foundations.

Many researchers have investigated the performance of stone columns under raft, using parametric study, the key parameters that can affect the performance of the foundation reported in literature mostly include, Stone columns spacing, diameter, angle of friction of stone columns and length of stone columns (Ahmed & Fattah, 2021; Al-Kazzaz & Al-Obaydi, 2021; Bachus & Barksdale, 1984; Boumekik et al., 2021; Castro et al., 2019; Elsawy & El-Garhy, 2016; Grizi et al., 2022; Hanna et al., 2013; Haji, 2016; Hadri et al., 2021; Idrus

et al., 2021; Karkush & Jabbar, 2019; Kouklanifar, 2023; Khalifa et al., 2018; Micheál & Bryan, 2014; Madun et al., 2018; Naderi et al., 2018; Naseer et al., 2019; Ng et al., 2021; Rao et al., 1997; Sakr et al., 2022; Saxena & Roy, 2022; Unni et al., 2021; Ziaie & Mohammadi-Haji, 2016; Nazariafshar et al., 2019; Zukiri et al., 2018; Znamenskii & Syed, 2019; Znamenskii et al., 2021).

The spacing, diameter, angle of friction, and length of stone columns all play important roles in the load-bearing performance of a foundation. Each parameter influences the load distribution, bearing capacity improvement, settlement control, and overall stability of the foundation system.

The spacing between stone columns determines the size of the loaded area between columns and affects load distribution. Closer spacing results in smaller loaded areas and more evenly distributed loads, reducing stresses on individual columns. It improves load transfer and helps control settlement.

The diameter of stone columns influences their load-bearing capacity. Larger diameter columns can support higher loads due to their increased contact area with the surrounding soil. They also provide more stiffness and improve settlement control.

The angle of friction between the stone columns and the surrounding soil is a crucial parameter affecting load transfer and bearing capacity. It represents the resistance to shear between the columns and the soil. A higher angle of friction increases the load-bearing capacity and improves stability.

The length of stone columns impacts their load-bearing capacity and settlement control. Longer columns provide a greater depth of improvement, allowing for greater load

transfer to deeper, more competent soil layers. Longer columns can also enhance settlement control by improving the stiffness and drainage characteristics of the soil over a greater depth. The stone columns typically extend from the foundation level to a specified depth within the soft clay soil. Beyond this depth, the load transfer mechanism relies on the surrounding soil. Once the stone columns have reached the specified depth, their length does not directly impact the load-bearing performance of the foundation.

Similarly, piled raft foundation system is also studied by many researchers and it is reported in the literature that the performance of a piled raft can be influenced by several factors, including pile length, pile diameter, aspect ratio, number of piles, pile spacing and raft foundation thickness (Al-Jubair & Abbas, 2014; Anhtuan et al., 2014; Abdel-Azim et al., 2020; Amornfa et al., 2022; Cho et al., 2012; Celik, 2019; Deb & Pal, 2022; Deb et al., 2022; Elsawwaf et al., 2022; Elwakil & Azzam, 2016; Ferchat et al., 2021; Ghalesari & Choobbasti, 2018; Kumar & Kumar, 2018; Khanmohammadi & Fakharian, 2018; Lodha et al., 2019; Mali & Singh, 2019; Mali & Singh, 2020; Mali & Singh, 2021; Nguyen et al., 2013; Poulos et al., 2011; Prashant et al., 2013; Paravita & Daniel., 2015; Patil et al., 2016; Tan & Chow, 2004; Watcharasawe et al., 2017). These factors play important roles in distributing loads, improving bearing capacity, controlling settlement, and ensuring overall stability.

The length of piles in soft clay affects the depth of load transfer and the zone of influence. Longer piles can reach stronger and more competent soil layers, enhancing load-bearing capacity and stability. They provide a greater depth of improvement and can control settlement more effectively.

The diameter of piles influences their load-bearing capacity and the area of contact with the surrounding soil. Larger diameter piles generally have higher load-bearing capacities due to increased contact area and skin friction. They can distribute loads more efficiently and reduce stresses on individual piles.

The aspect ratio is the ratio of the pile length to its diameter. It affects the load transfer mechanism and the performance of piles in soft soil. A higher aspect ratio can increase the load-carrying capacity of the pile, as it allows for more interaction with the soil. However, excessively high aspect ratios may lead to issues such as pile buckling or reduced lateral stability.

The number of piles in a raft foundation affects load distribution and overall bearing capacity. Increasing the number of piles spreads the load over a larger area, reducing the individual pile stresses and promoting more uniform settlement.

The spacing between piles can influence the load distribution, settlement control, and overall stability. Closer pile spacing can leads to more evenly distributed loads and reduced stresses on individual piles. It can help control differential settlement and improve overall stability. Wider pile spacing concentrates loads on individual piles, potentially leading to higher stresses and differential settlement.

The thickness of the raft foundation has an impact on load distribution and settlement control. A thicker raft can distribute loads over a larger area, reducing stresses and promoting more uniform settlement. It can also provide additional stiffness and stability to the foundation system.

In general, the notable effect of stone columns can only be seen in shallow foundations whereas the pile foundation can be used to support the excessive load by resting on the stiff and hard soil layers, and the use of pile foundations are not economical.

As far as for combined foundation system (i.e. Stone column and pile under raft foundation) very few studies have been reported in the literature. Liang et al. (2003) used ANSYS program to study the behaviour of seven-story building foundation with different parameter including ratio of length to diameter, elastic moduli of piles, thickness, and elastic modulus of cushion. In this study new concept of combining two types of pile system under raft was proposed, such as short pile made of flexible materials and long piles made of rigid material. This study mainly investigated the effect of cushion on the performance of short and long piles.

Samanta and Bhowmik (2017) have investigated the combined foundation system (stone columns and piles combined under raft in soft soil) with the variation in parameters and they have concluded that the change in length, spacing, friction angles, area replacement ratio, diameter of stone columns/piles and the thickness of raft can change the percentage of shared load on the stone columns and piles. This study was performed based on only one type of configuration of combining stone columns and piles under raft in soft clay.

Combined stone column and pile system can be more complex compared to using either technique individually. It requires careful consideration of various factors, including the interaction between the stone columns and piles, load-bearing performance, and the behaviour of the soft soil.

There is no data available in the literature related to the configuration of combined system or optimization of the number of stone columns with number of piles under raft foundation as a combined system to improve the performance of raft foundation in soft soils. For this reason, a detail parametric study is required to study the load-bearing performance of combined stone columns and piles under raft in soft soils. The key parameters reported in literature that effects the performance of either ground improvement technique stone columns or piles, needs to be used to investigate the performance of combined system.

CHAPTER 3

METHODOLOGY

3.1 Introduction

Combined foundations (i.e., stone columns combined with piles under raft) are the most attractive solution for optimizing the cost and performance of foundations in soft soils. There are two types of weak soils commonly available in different regions of the world that are soft (compressible) clay and peat. In this present study soft (compressible) clay soil is used and considered for the combine foundation system. Peat does not provide sufficient lateral confinement to the stone columns, and when the lateral support is significantly low, column can fail by bulging (Prasad et al., 2012).

The methodology used to treat this subject is based on numerical investigation and analysis using 3D finite element modelling. Similar methodologies can be found in the literature (Abas, 2015; Etezad, 2007; Omeman, 2012; Sinha, 2013; Sheil, 2014; Tschuchnigg, 2012) and all these investigations were performed based on the numerical approaches, either for stone columns under raft or for the piled raft foundations. Generally, a numerical model consists of a complex system of equations with boundary conditions, which can be validated with real test data or with accepted numerical data.

The parameters used in the numerical study are given in Table 3.1. The different parameters listed in this table were deduced from field data (i.e., taken from the range of data used in practice and reported in the literature for soft soils and stone columns, etc.). This research is carried out in different steps as shown Figure 3.1 and summarized as follows:

1. Development and validation (Chapter 3: Ghazavi & Afshar, 2013; Sinha & Hanna, 2017) of numerical models for stone columns under raft foundation and piled raft foundation in a soft soil.

2. Development and validation of numerical model concerning combined foundation system (i.e., stone columns/piles capped with rigid raft foundation) in soft soil.

3. Parametric study performed using the three developed numerical models (stone columns under raft foundation, piled raft foundation, and combined foundation system). Different configurations were investigated (i.e., different diameters, spacing and number, ratio of piles to stone columns area, etc.), as shown in Table 3.1.

4. Behaviour (i.e., modes of failure) under loading for the combined foundation system investigated and compared to the existing behaviour of other foundation systems, such as piled raft foundation and stone columns under raft foundation.

5. Optimization of the configuration stone columns/piles in the combined foundation system and development of an analytical model to predict the carrying capacity of the combined foundation system capped with rigid raft foundation in compressible soil.

Combining stone columns and piles under a raft foundation in soft soil create a new type of foundation system that can provide an enhanced load-bearing capacity and improved stability. There is no data available in the literature regarding the specific combination of

stone columns and piles under a raft foundation in soft soil that can be used for numerical modelling. But the there are many existing data available in the literature for modelling stone columns, piles, and raft foundations in soft soil individually. For this reason present study rely on existing literature and data as a starting point for modelling and analysis. To understand the influence of different parameters on the behaviour of combined foundation system, a wide range of numerical input parameters are collected from the literature.

For the present numerical study, the details of parameters selected for the raft, stone columns and piles are given in Table 3.1, these range of parameters are associated with the types of cases encountered in real life. Furthermore, each parameter was individually examined to determine the ultimate carrying capacity of the foundation systems (i.e., stone columns under raft foundation in soft clay, piled raft foundation in soft clay, and combined stone columns/piles under raft foundation in soft clay).

Table 3.1: Range of parameters used in this numerical investigation

Material	**Properties**	
Soft Clay	Unit weight, γ_{unsat}, γ_{sat}	17, 18 kN/m^3
	Young's modulus, E_s	4, 6 and 8 MPa
	Poisson's ratio, v_s	0.5
	Angle of friction, φ	0°
	Cohesion, c	25 kPa
Sand	Unit weight, γ_{unsat}, γ_{sat}	17.5, 19.5 kN/m^3
	Young's modulus, E_s	28 MPa
	Poisson's ratio, v_s	0.3
	Angle of friction, φ	42°

	Cohesion, c	0
Stone Column	Unit weight, γ_{unsat}, γ_{sat}	19, 20 kN/m^3
	Young's modulus, E_s	80 MPa
	Poisson's ratio, v_s	0.3
	Angle of friction, φ	42°, 45°, 48°
	Cohesion, c	0
	Stone columns diameter	1 m
	Stone column length	20, 18, 16, 12 m
	S/D (spacing / diameter of stone column)	7, 6, 5, 4 m/m
Raft	Young's modulus, E_r	27.8 GPa
	Poisson's ratio, v_r	0.15
	Raft Size	20 m x 20 m
	Raft Thickness	2 m
Pile (steel tube pile)	Young's modulus, E_p	210 GPa
	Pile diameter	0.4, 0.5, 0.6 m
	Pile length	20 m
	S/D (spacing / diameter of pile)	7, 6, 5, 4, 3 m/m

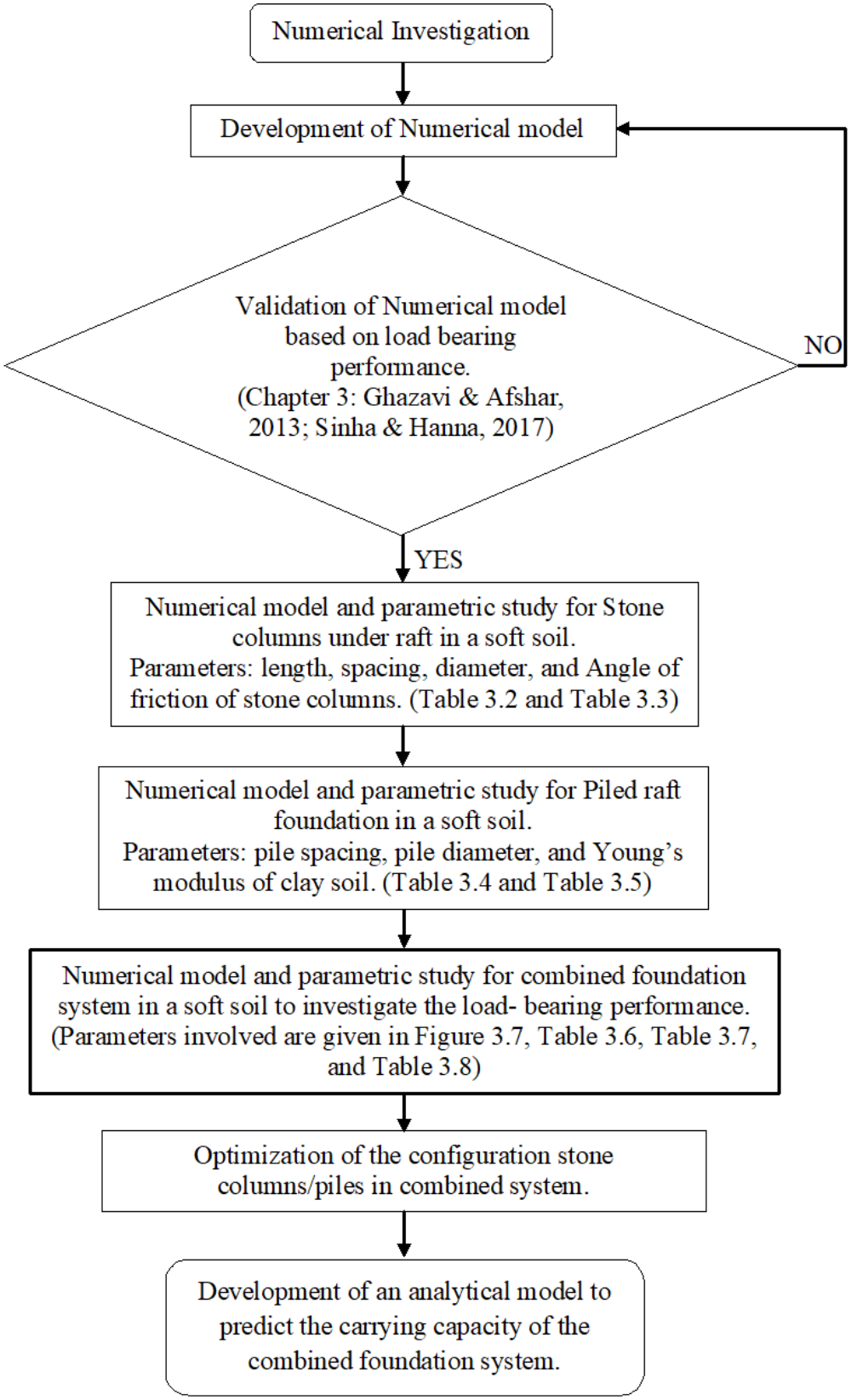


Figure 3.1: Flow chart of methodology

3.2 Numerical Modelling

In the past few decades many advancements have been made in the numerical modelling software (for example Plaxis 3D, ANSYS, ABAQUS etc.), numerical modelling is widely used in the previous geotechnical studies for the validation and research work, these software packages are designed to predict the carrying capacity and settlements, as well as they idealize the real behaviour and performance of actual foundations and soils.

In the present study numerical analysis and modelling are performed using the geotechnical finite element program Plaxis 3D. Plaxis was developed first in 1987 at Delft University of Technology for the Dutch ministry of public works. Its 3D version was released in 2010, it is a three-dimensional finite element program, which is mainly used for nonlinear analysis in geotechnical studies. This program provides a user-friendly interface that helps to create all kind of configuration for foundations and soils, it also provides auto meshing option which reduces the overall time for generating the model mesh and analysis.

3.2.1 Material Model

Selecting the material properties and material model in any type of numerical modelling is very important to have an accurate simulation. Plaxis 3D provides material model for all kind of elements involved in geotechnical studies for example (raft, pile, column, soil etc.).

3.2.1.1 Soil Model

In the present study and investigation, Mohr-Coulomb model was considered for modelling all the soil elements and a drained behaviour is assumed for all the soil materials (present research is focused on long-term settlement). When considering the drained condition for soft clay under a raft foundation using Mohr-Coulomb model, the model

assumes that excess pore water pressures have dissipated, and the soil is fully consolidated. But the water table in the model can still have several effects on the behaviour of the soil. The water table can exert the hydrostatic pressure, which can reduce the effective stress and can decrease the shear strength parameters of the soil. Different layers of soil were modelled using elastic perfectly plastic. The basic concept of elastic perfectly plastic condition is given in Figure 3.2.

Mohr-Coulomb model works with five very common parameters Young's modulus E, Poisson's ratio v, Cohesion c, Friction angle φ, and Dilatancy angle ψ. Worthwhile to note that, the Mohr-Coulomb elastic-perfectly plastic model was adopted in the present study because it is convenient to limit equilibrium state, which is adopted when developing the analytical model. Furthermore, several numerical analyses, reported in literature, which employed the Mohr-Coulomb model, were in good agreement with physical modelling or experimental data (Etezad et al., 2015; Samangani & Naderi, 2022).

The Mohr-Coulomb model is commonly used for studying the bearing capacity of foundations in soft soil. The model provides a simplified representation of the shear strength and stress-strain performance of soils, including soft clay. Normally Mohr-Coulomb model considers two main parameters which include cohesion and angle of internal friction. These parameters represent the shear strength properties of the soil. The cohesion accounts for the soil's inherent strength, while the angle of internal friction represents the soil's resistance to shear deformation.

When studying the bearing capacity of a foundation in soft clay using the Mohr-Coulomb model, the model can be used to analyse the shear strength of the soil and determine the maximum load that the foundation can safely support without failure. It is

important to note that Mohr-Coulomb model simplifies the representation of soft clay's complex behaviour. Where soft clay can exhibit significant time-dependent and consolidation-related behaviours, which may require more advanced soil models for accurate predictions.

Compared to these advanced soil models that account for complex behaviours, the Mohr-Coulomb model is simpler and computationally faster. This can make it more convenient for initial or preliminary analyses of foundation bearing capacity and settlement in soft clay. The Mohr-Coulomb model requires fewer input parameters (cohesion and angle of internal friction) compared to advanced models that consider additional parameters related to time-dependent behaviour, strain-hardening, or strain-softening. This simplicity reduces the data requirements and computational effort needed for analysis, making it a faster option for quick assessments or conceptual designs.

For the present study coefficient of earth pressure at rest (*Ko*) is calculated separately for each soil model using simple equation.

$$K_o = 1 - \sin\varphi \qquad \text{Equation 3.1}$$

Where φ is the angle of friction of soil.

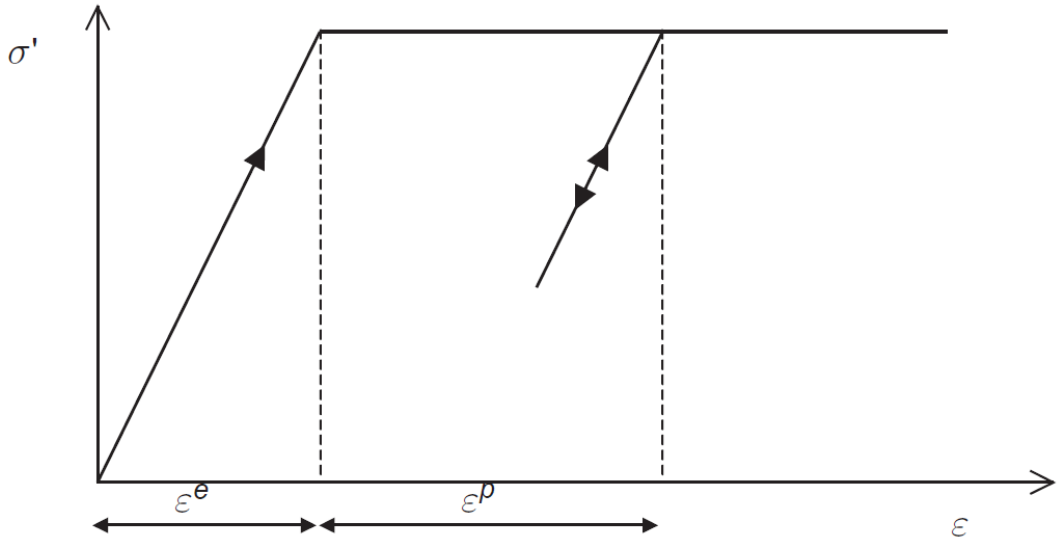


Figure 3.2: Basic concept of elastic perfectly plastic. (Brinkgreve et al., 2013)

3.2.1.2 Stone Columns

Stone columns were also modelled using elastic-perfectly-plastic Mohr-Coulomb failure criteria. Granular stone columns material properties were selected from the data available in literature as given in Table 3.1 and drained condition was considered for cohesionless materials.

3.2.1.3 Concrete Raft

Concrete raft was modelled using linear elastic model, which works as an isotropic elasticity relation between stress and strain which is based on the Hooke's law. Linear elastic model mainly requires two parameters Young's modulus *E* and Poisson's ratio *v*. This model is suitable for modelling stiff structural elements.

3.2.1.4 Embedded Pile

The skin resistance and foot resistance of the pile are defined in Equation 3.2 until Equation 3.4, respectively.

$$t_{skin} = K_{skin} u_{rel} \qquad \text{Equation 3.2}$$

Where:

$t_{skin} = \ traction\ along\ the\ pile$

$K_{skin} = material\ stiffness\ matrix\ of\ the\ interface$

$u_{rel} = u_p - u_s$

The constitutive equation to define the skin resistance can be interpreted from Figure 3.3.

$$\begin{bmatrix} t_s \\ t_n \\ t_t \end{bmatrix} = \begin{bmatrix} K_s & 0 & 0 \\ 0 & K_n & 0 \\ 0 & 0 & K_t \end{bmatrix} \begin{bmatrix} u_s^p - u_s^s \\ u_n^p - u_n^s \\ u_t^p - u_t^s \end{bmatrix}$$ Equation 3.3

Where:

$t_s = shear\ stress\ in\ the\ axial\ direction$

$t_n, t_t = shear\ stress\ in\ the\ normal\ direction$

$K_s = interface\ stiffness\ in\ the\ axial\ direction$

$K_n, K_t = interface\ stiffness\ in\ the\ normal\ direction$

$u_p = displacement\ of\ pile$

$u_s = displacement\ of\ soil$

$u_s^p = displacement\ of\ pile\ in\ the\ axial\ direction$

$u_s^s = displacement\ of\ soil\ in\ the\ axial\ direction$

$u_n^p, u_t^p = \ displacement\ of\ pile\ in\ the\ normal\ direction$

$u_n^s, u_t^s = \ displacement\ of\ soil\ in\ the\ normal\ direction$

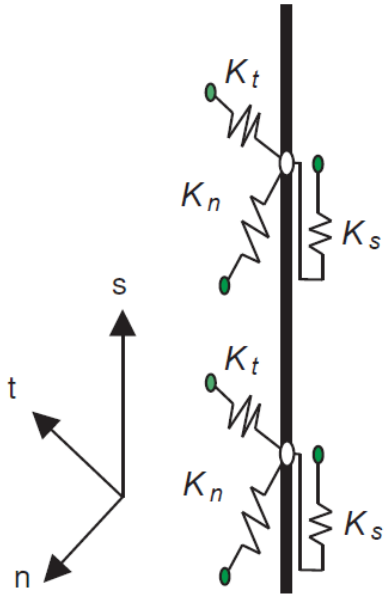


Figure 3.3: Stiffness at the skin of the pile. (Brinkgreve et al., 2013)

The constitutive equation to define the foot resistance of the pile can be interpret from Figure 3.4

$$f_{foot} = K_{foot}\left(u^{p}_{foot} - u^{s}_{foot}\right) \qquad \text{Equation 3.4}$$

Where:

$f_{foot} = base\ resistance$

$K_{foot} = stiffness\ at\ the\ pile\ tip$

$u^{p}_{foot} = displacement\ of\ pile\ at\ foot$

$u^{s}_{foot} = displacement\ of\ soil\ at\ foot$

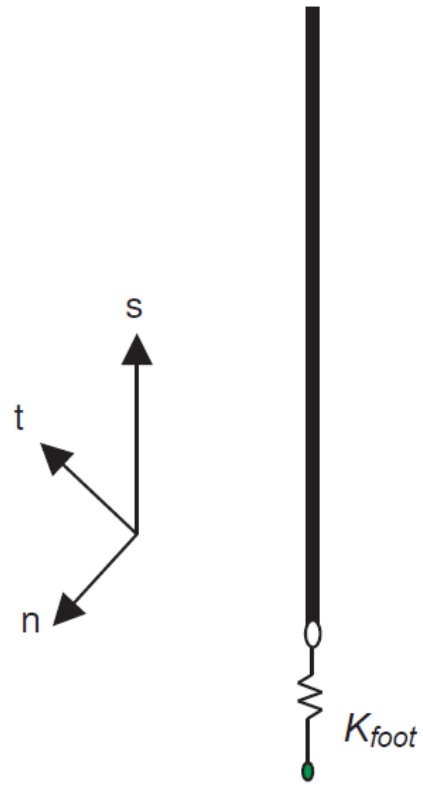


Figure 3.4: Stiffness at the foot of the pile. (Brinkgreve et al., 2013)

3.2.2 Geometry and Boundary Conditions

The geometry of the three-dimensional model was selected based on trial to avoid the horizontal and vertical stress confinements. A study was carried out on the boundary extent and after several trials the overall size of complete 3D model was selected as 100m x 100m x 40m. Where the 3D model consists of square 20 m x 20 m x 2 m rigid raft resting on 20 m of soft clay and below the soft clay a 20 m thick layer of sand is situated. For the boundary condition of the 3D model, fixed support was considered at the bottom and the roller supports were assumed on the vertical boundaries as shown in Figure 3.5.

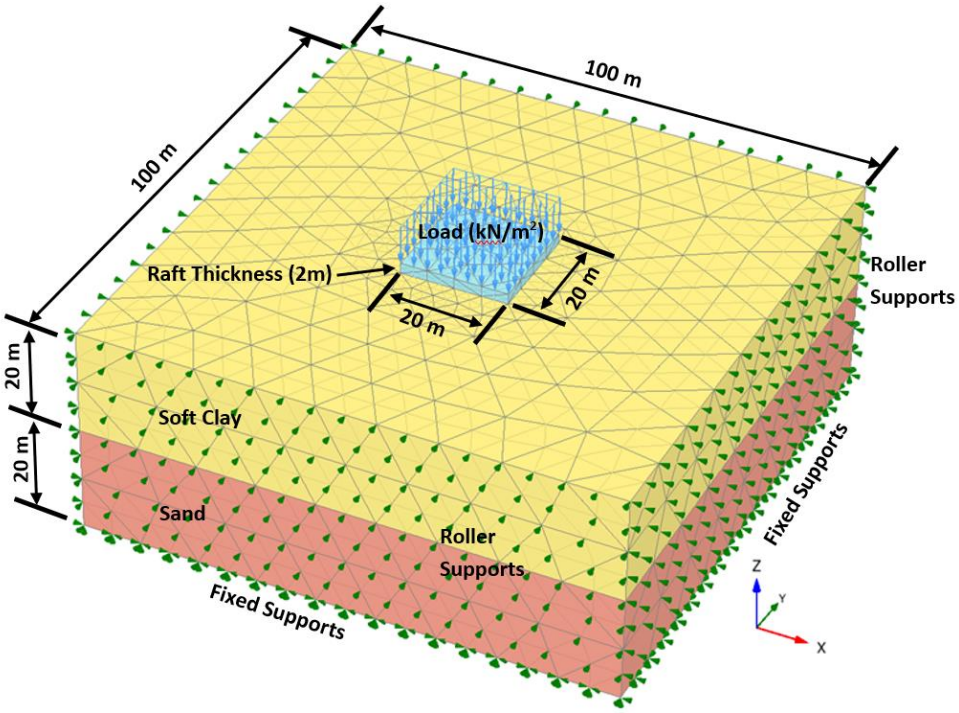


Figure 3.5: 3D model with boundary conditions

3.2.3 Loading Details

A uniform distributed load was applied on the surface of 20 m x 20 m rigid raft as shown in Figure 3.6.

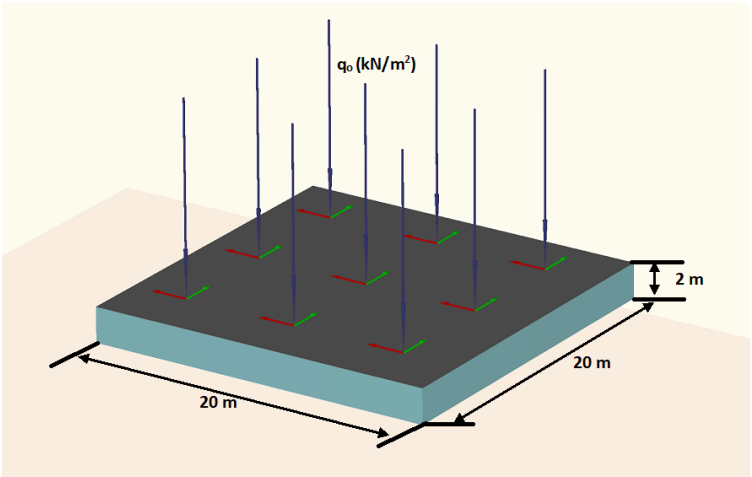


Figure 3.6: 3D model for Raft

3.2.4 Meshing

The mesh size plays an important role in any finite element modelling, using fine mesh one can capture results very close to real behaviour of the model and consume more time for analysis and vice versa.

In the present study 10-noded tetrahedral elements were used to create 3D model for all the soil elements which also includes stone columns as given in Figure 3.7, medium mesh size was used globally for all the model and it was refined to fine to very fine near the region where critical stresses and displacements were expected to capture the real behaviour of the model and to reduce the overall time for the analysis as shown in Figure 3.8, Figure 3.9, Figure 3.10 and Figure 3.11.

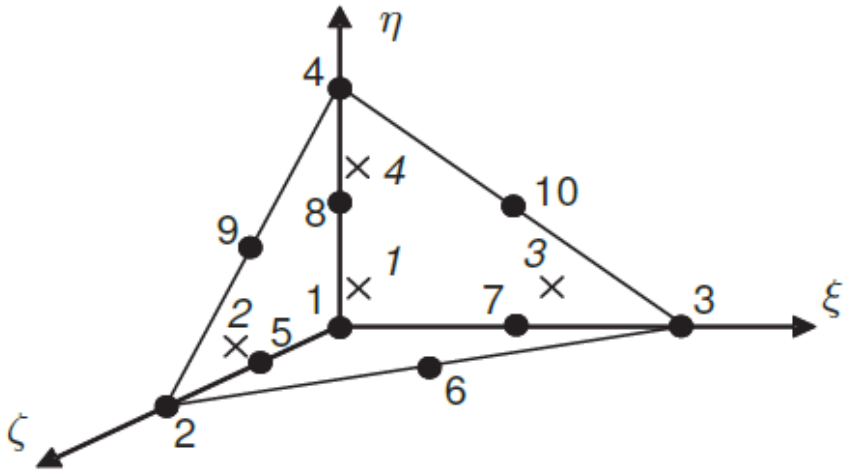


Figure 3.7: 3D soil elements (10-node Tetrahedrons)

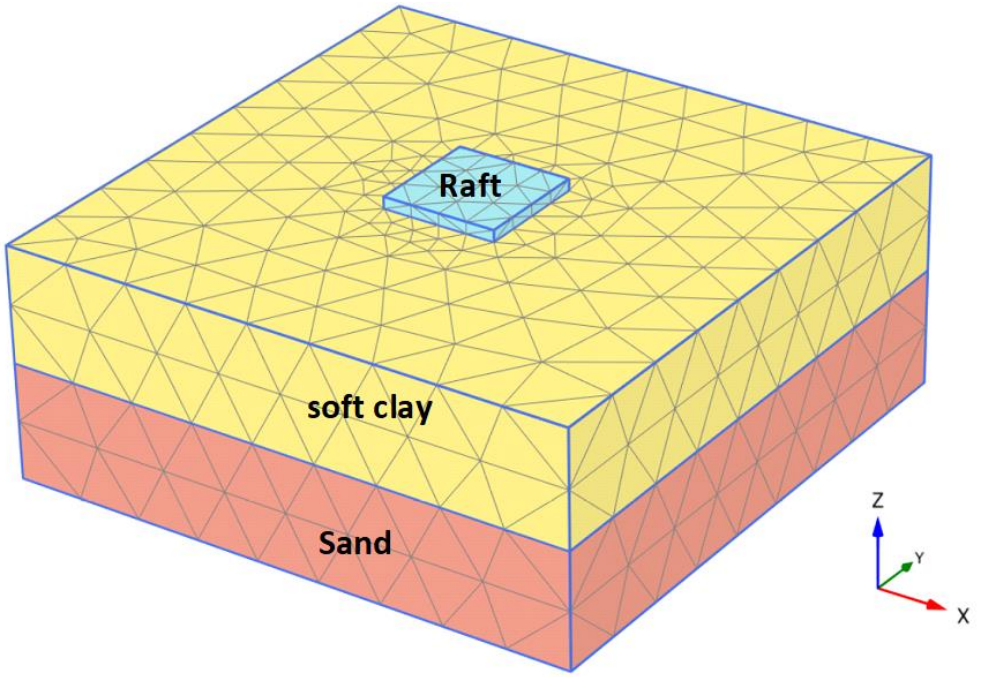


Figure 3.8: Meshing

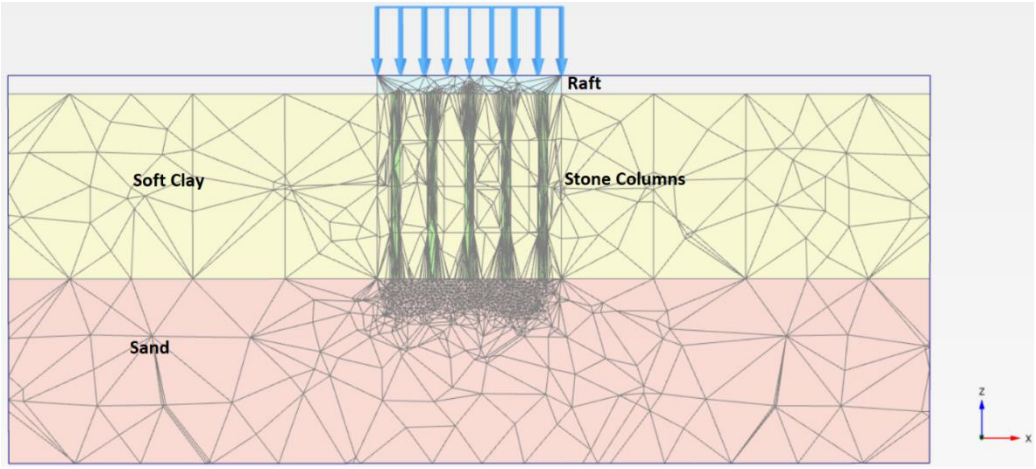


Figure 3.9: Refined meshing for stone columns

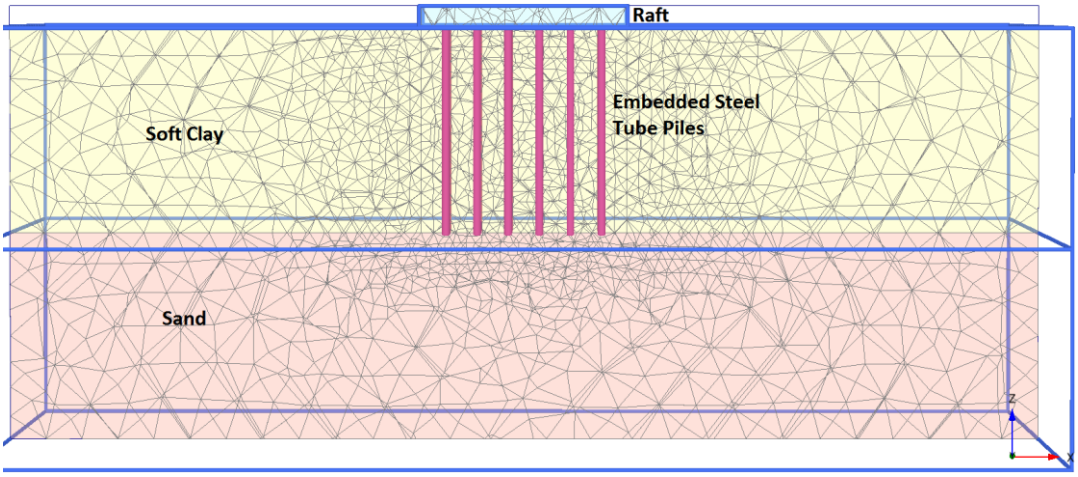


Figure 3.10: Refined meshing for piled raft

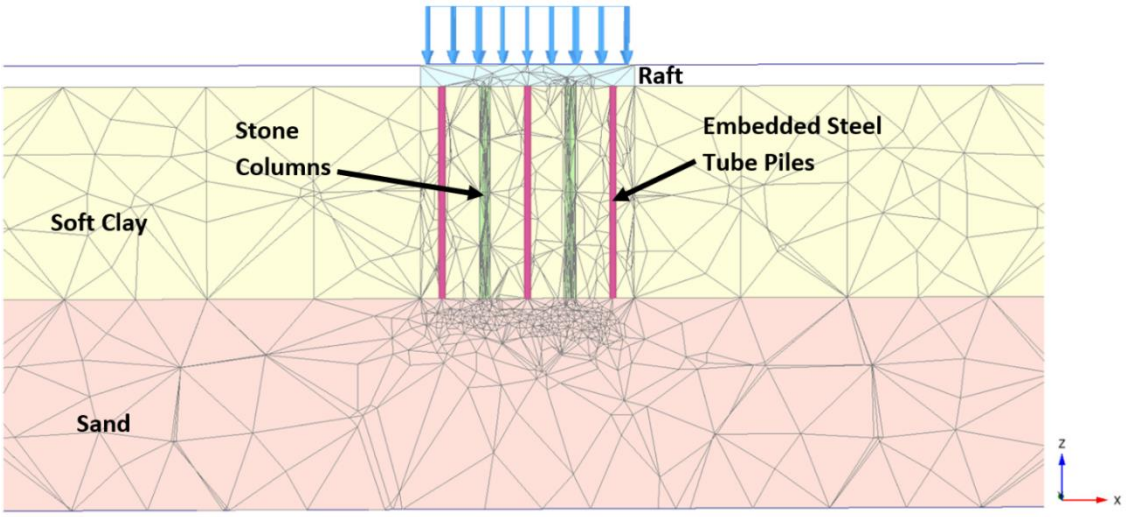


Figure 3.11: Refined meshing for combined stone column/piles caped with raft

3.2.5 3D Models

As explained in section 3.1 three major finite element models were considered to perform the parametric study, as well as to investigate the behaviour of (a) stone columns under raft in soft soil (treated soil with stone columns), (b) piled raft in soft soil (treated soil with piles), and (c) stone columns/piles capped with rigid raft in soft soil. Figure 3.12 and Figure 3.13 show the 3D model of soil layers and raft foundation alone without stone columns or piles (untreated soil). For all the models the water table is considered fixed at the

ground level. The presence of a fixed water table at the ground level can influence the shear strength of the soft clay. The water table exerts hydrostatic pressure, which can reduce the effective stresses. This reduction in effective stresses can lead to a decrease in the shear strength parameters, such as cohesion and friction angle, which can affect the overall stability and bearing capacity of the raft foundation.

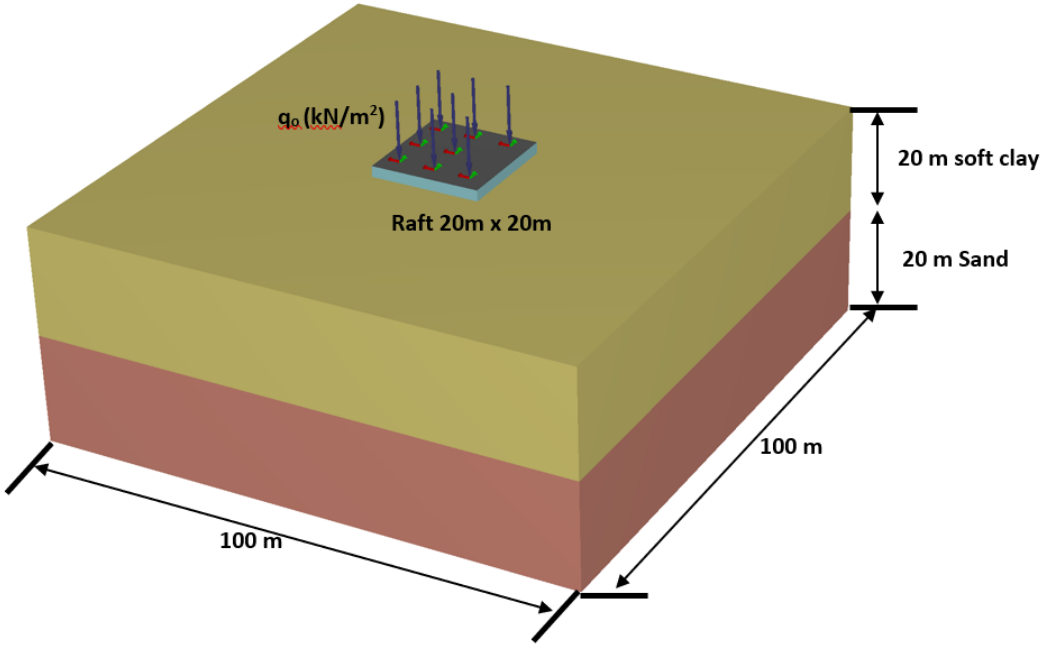


Figure 3.12: 3D model for raft and soil

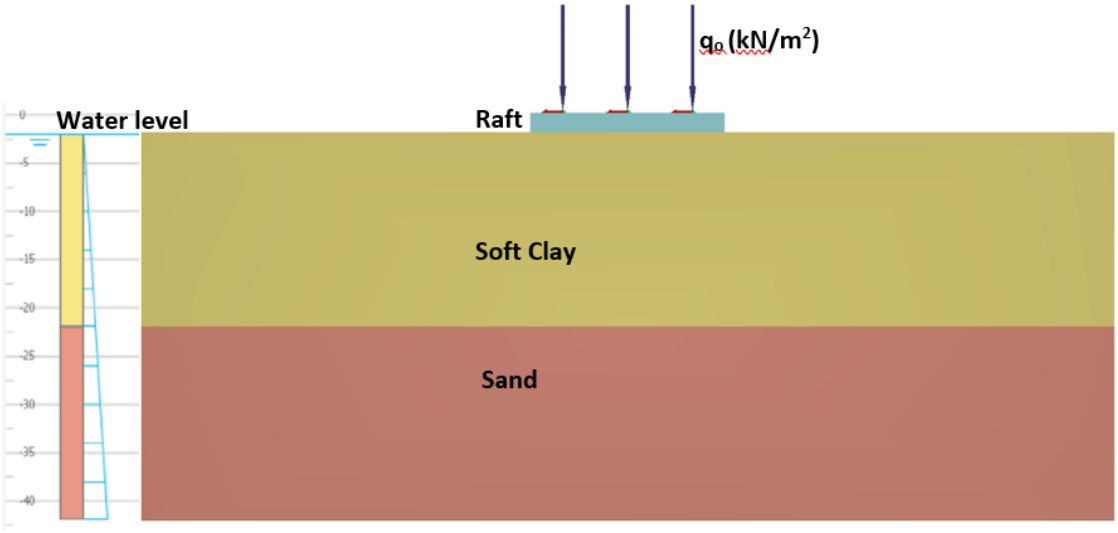


Figure 3.13: Cross-section of raft and soil

3.2.5.1 3D Model for Stone Columns under Raft Foundation in Soft Soil

In this configuration, 3D model consists of square 20 m x 20 m rigid raft resting on the treated soft clay and below the soft clay a thick layer of sand is situated. The soil was treated using the stone columns as shown in Figure 3.14 and Figure 3.15.

Table 3.2 and Table 3.3 show the parameters used for geometric configuration and material properties for stone columns under raft foundation in soft soil, in this study four different spacing to diameter ratio (*S/D*) were used and for each different (*S/D*) ratio three different angle of frictions of stone columns (φ_c) were examined.

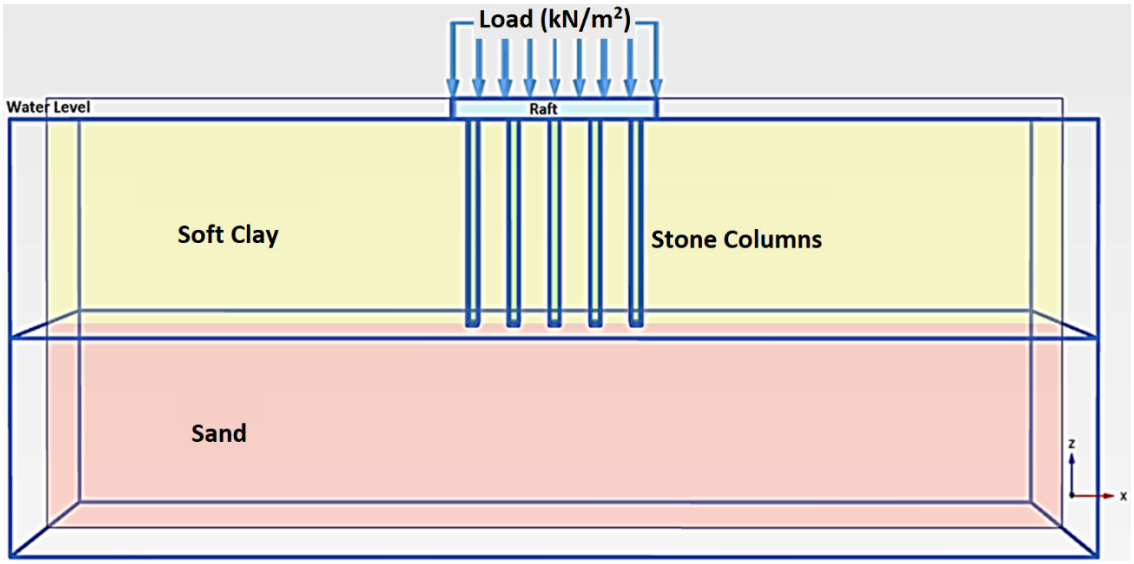


Figure 3.14: Finite element model for stone columns under raft

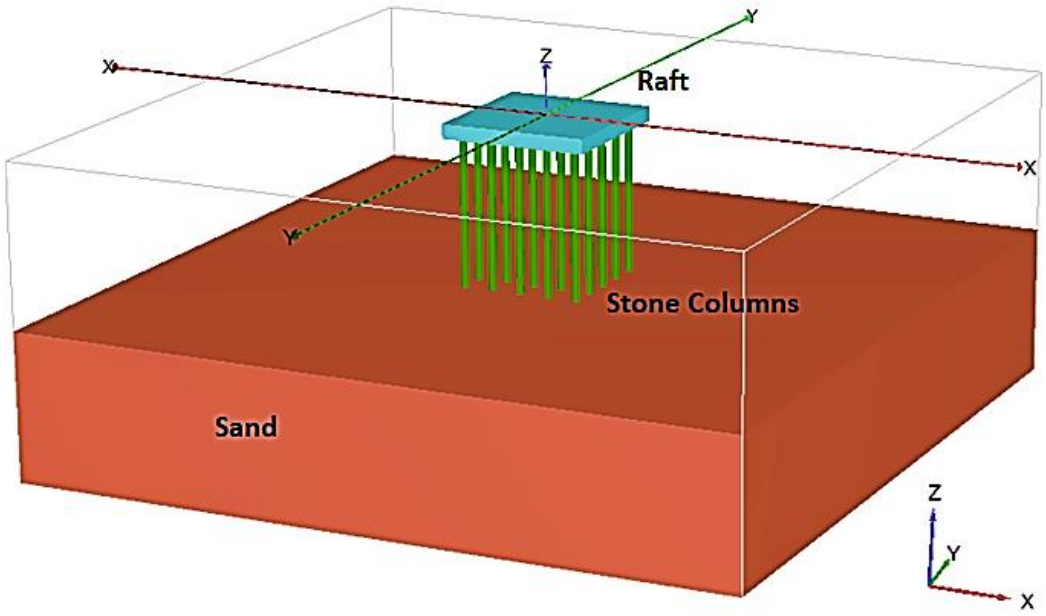


Figure 3.15: 3D model for stone columns under raft

Table 3.2: Range of parameters used for stone columns under raft for present study

Properties	Soft Clay	Sand	Stone Column	Raft
Unit weight, γ_{unsat}, γ_{sat}	17, 18 kN/m^3	17.5, 19.5 kN/m^3	19, 20 kN/m^3	-
Young's modulus, E	4 MPa	28 MPa	80 MPa	27.8 GPa
Poisson's ratio, v	0.5	0.3	0.3	0.15
Angle of friction, φ	0°	42°	42°, 45°, 48°	-
Cohesion, c	25 kPa	0	0	-

Table 3.3: Configuration of stone columns under raft for present study

Parameters	Unit	Value
Raft Size	m x m	20 x 20
Raft Thickness	m	2
Stone Column Length	m	20
Stone Column Diameter	m	1
S/D (spacing / diameter of stone column)	m/m	7, 6, 5, 4
Number of Columns (for each spacing)	-	4, 9, 16, 25

3.2.5.2 3D Model for Piled Raft Foundation in Soft Soil

In this configuration, 3D model consist of square 20 m x 20 m rigid raft resting on the group of piles in soft clay soil and below the soft clay a thick layer of sand is situated as shown in Figure 3.16 and Figure 3.17.

Table 3.4 and Table 3.5 show the parameters used for geometric configuration and material properties for piled raft foundation in soft soil. In this study three different diameters were used and for each diameter five different spacings and three different modulus of elasticities were examined.

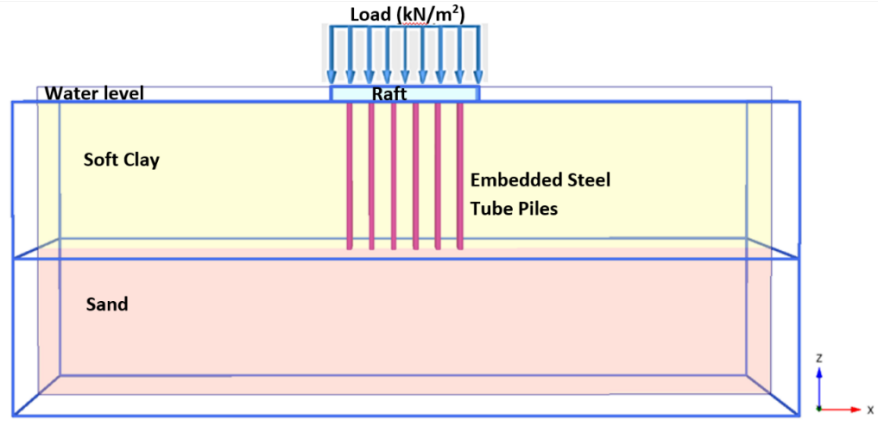


Figure 3.16: Finite element model for piled raft

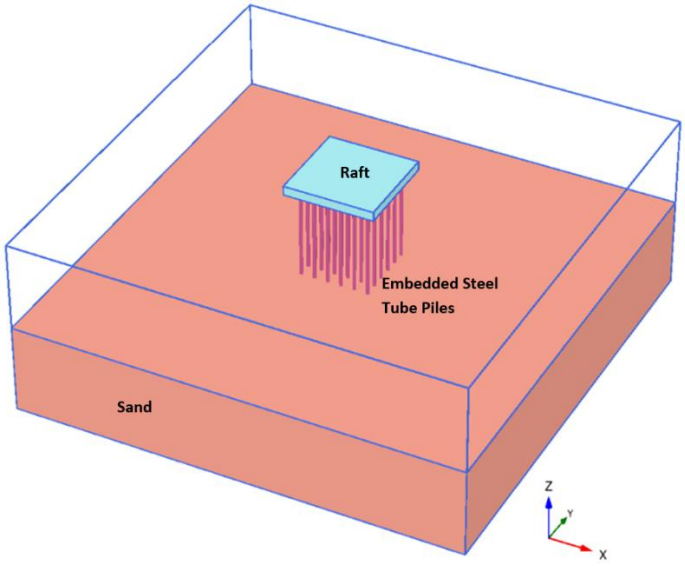


Figure 3.17: 3D model for piled raft

Table 3.4: Range of parameters of piled raft for present study

Material	Properties	
Soft Clay	Unit weight, γ_{unsat}, γ_{sat}	17, 18 kN/m^3
	Young's modulus, E_s	4, 6 and 8 MPa
	Poisson's ratio, v_s	0.5
	Angle of friction, φ	0°
	Cohesion, c	25 kPa
Sand	Unit weight, γ_{unsat}, γ_{sat}	17.5, 19.5 kN/m^3
	Young's modulus, E_s	28 MPa
	Poisson's ratio, v_s	0.3
	Angle of friction, φ	42°
	Cohesion, c	0
Raft	Young's modulus, E_r	27.8 GPa
	Poisson's ratio, v_r	0.15
Pile	Young's modulus, E_p	210 GPa

Table 3.5: Configuration of piled raft for present study

Parameters	Unit	Value
Raft Size	m x m	20 x 20
Raft Thickness	m	2
Pile Length	m	20
Pile Diameter	m	0.4, 0.5, 0.6
S/D (spacing / diameter of pile)	m/m	7, 6, 5, 4, 3
Number of Piles (for each spacing)	-	25, 36, 49, 81 and 121

3.2.5.3 3D Model for Combined Stone Column/Piles Caped with Raft Foundation in Soft Soil

For the combined foundation system, the three-dimensional model consists of 20 m x 20 m rigid raft resting on soft clay treated with group of stone columns and piles together and below the soft clay a thick layer of sand is situated as shown in Figure 3.18 and Figure 3.19.

The square raft was considered for stone columns and piles to be arranged in symmetry for combined foundation system. To achieve this symmetry in the arrangement of stone columns and piles, it was considered to divide the 20 m x 20 m raft in to 5 x 5 grid sections. So that the stone columns and piles can be arranged in a symmetrical pattern within each grid section which can help to ensure the uniformity of load distribution and to avoid any eccentric load from the foundation.

In this investigation group of 25 stone columns and piles are arranged in 34 different configurations (sets) as in Figure 3.20. Each of the configuration (set) is categorized into 11 groups based on number of piles in each group, for example in group no. 1 all the sets having

four piles are grouped together (set # 2, 8, 24, 25) as it can be seen in Table 3.6. The configurations of column-piles arrangement were adopted in respect to the piles number and their emplacement in each configuration. The number and positioning of the piles were varied to cover a wide range of conceivable combinations.

Furthermore, every set was considered in 20 combinations for parametric study, depending on the size of stone columns/piles and material properties for stone columns and soft soils as given in Table 3.7 and Table 3.8. It can also be observed from these tables that the stone columns diameter is kept constant where the diameter of the piles are varying because of two reasons, first the purpose of stone columns in combined system is to pre-strengthened the soft clay, so to get the maximum influence on the improvement of the foundation one diameter of stone columns is selected in the higher range, secondly it is selected to maintain the clear spacing between the stone columns, because very close spacing can results in uneven load distribution in the ground. Also, the length of the pile is kept constant because the piles are considered to be resting on the thick layer of sand (Figure 3.19), on the other hand varied length of stone columns is used to study the influence of stone columns length on the load-bearing performance of combined foundation system.

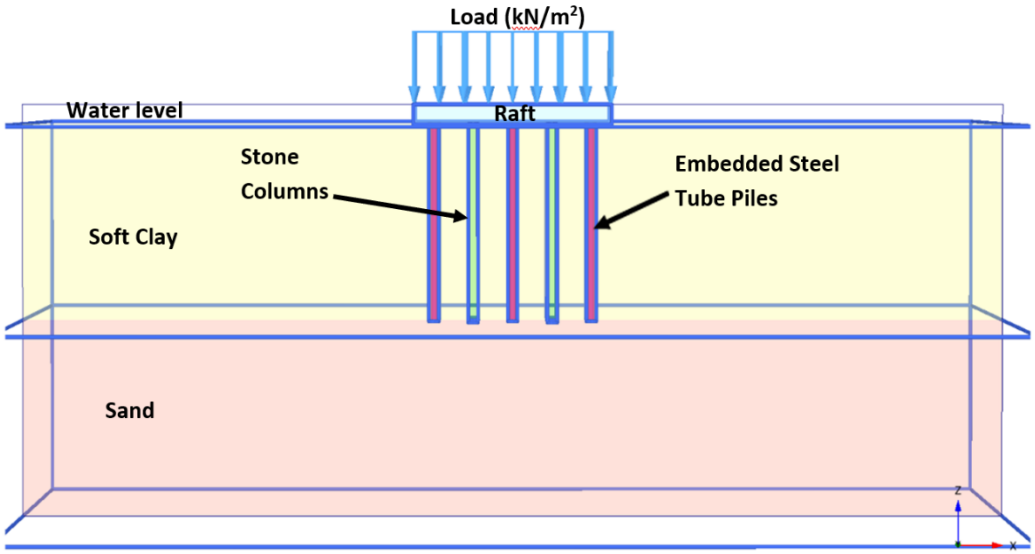


Figure 3.18: Finite element model for combined stone column/piles caped with raft

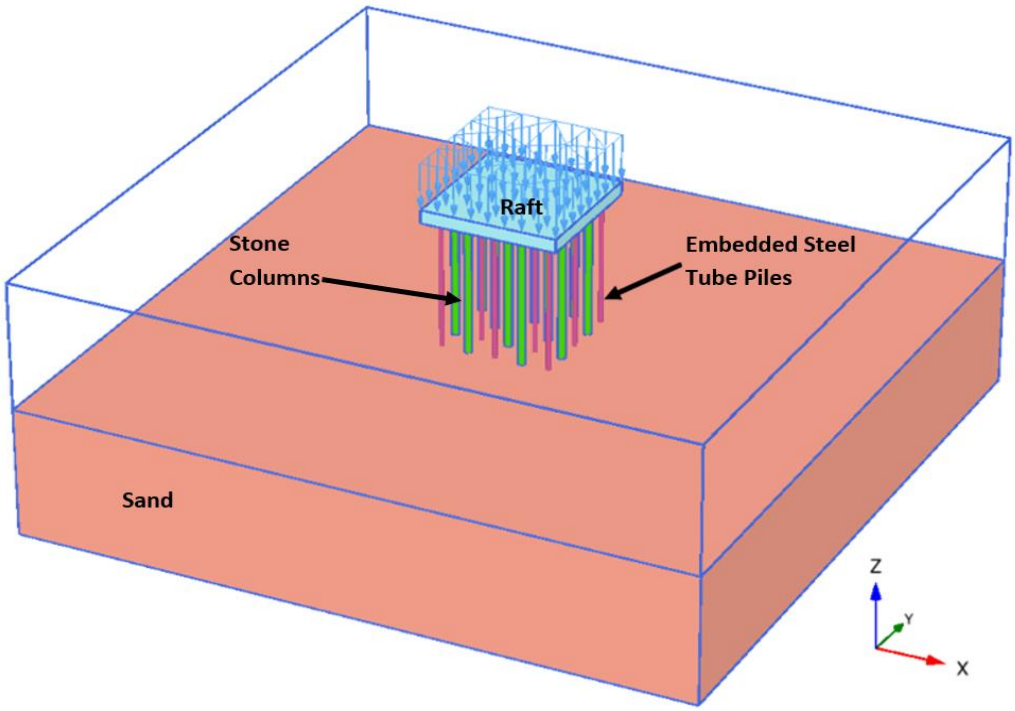


Figure 3.19: 3D model for combined stone column/piles caped with raft

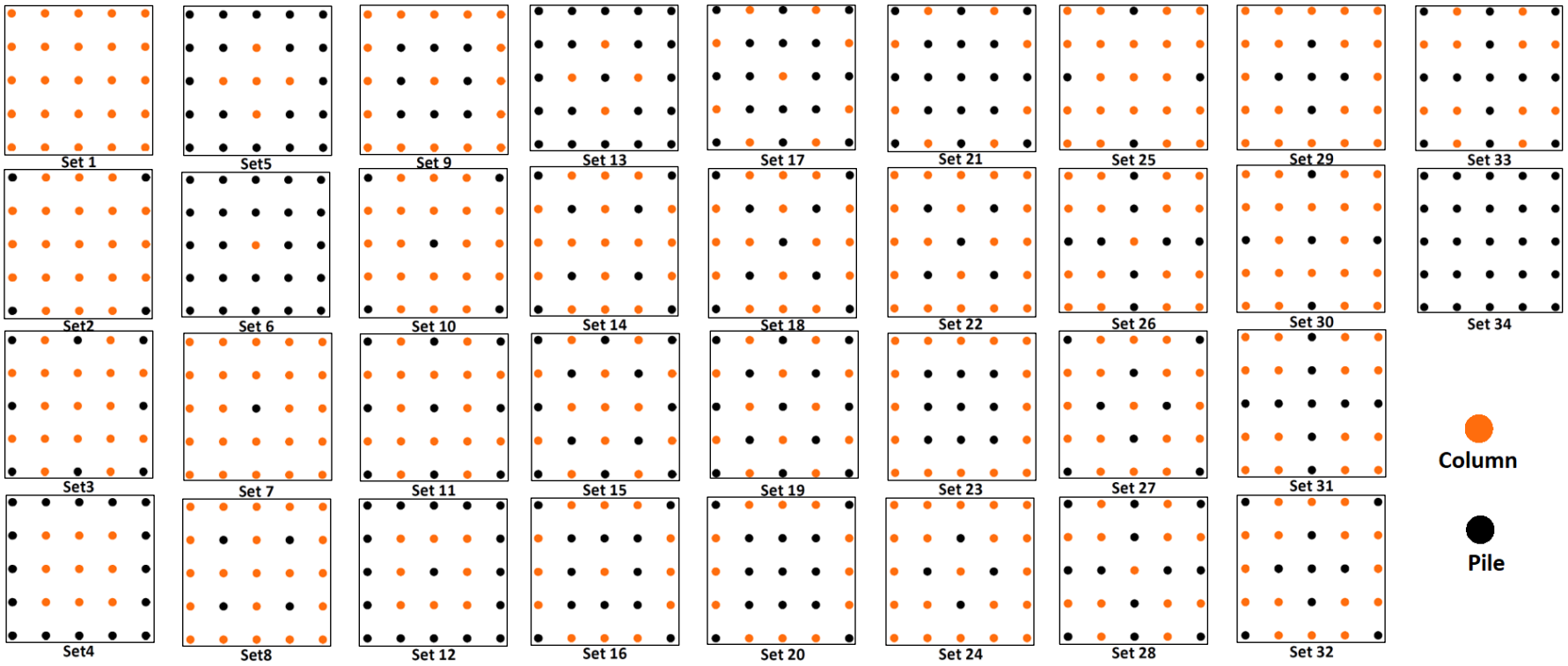


Figure 3.20: Different configurations (Sets) for combined foundation

Table 3.6: Foremost sets in each group

Group No.	No. of piles	Distribution of sets in each group (Figure 3.20)
1	4	2, 8, 24, 25
2	5	10, 22, 29, 30
3	8	3, 9, 14, 26, 27
4	9	11, 18, 23, 31, 32
5	12	15, 16, 28
6	13	19, 20, 33
7	16	4, 17
8	17	12, 21
9	20	5
10	21	13
11	24	6

Table 3.7: 20 Combinations for parametric study

Combination No.	Stone Column Length (m)	Stone Column Diameter (m)	Pile Length (m)	Pile Diameter (m)	Young's Modulus for Soft Clay (MPa)	Angle of friction for Stone Columns (degree)
1	20	1	20	0.6	4	45
2	20	1	20	0.5	4	45
3	20	1	20	0.4	4	45
4	18	1	20	0.6	4	45
5	18	1	20	0.5	4	45
6	18	1	20	0.4	4	45
7	16	1	20	0.6	4	45
8	16	1	20	0.5	4	45
9	16	1	20	0.4	4	45
10	12	1	20	0.6	4	45
11	12	1	20	0.5	4	45
12	12	1	20	0.4	4	45
13	20	1	20	0.5	8	45
14	20	1	20	0.5	6	45
15	16	1	20	0.5	8	45
16	16	1	20	0.5	6	45
17	20	1	20	0.5	4	48
18	20	1	20	0.5	4	42
19	16	1	20	0.5	4	48
20	16	1	20	0.5	4	42

Table 3.8: Materials properties for combined stone column/piles caped with raft

Properties	Soft Clay	Sand	Stone Column	Pile	Raft
Unit weight, γ (kN/m^3)	17, 18	17.5, 19.5	19, 20	-	-
Young's modulus, E_s (MPa)	4, 6, 8	28	80	210×103	27.8×103
Poisson's ratio, v_s	0.5	0.3	0.3	-	0.15
Angle of friction, φ (^{o})	0	42	42, 45, 48	-	-
Cohesion, c (kPa)	25	0	0	-	-
Diameter (m)	-	-	1	0.4, 0.5, 0.6	-
Length (m)	-	-	20, 18, 16, 12	20	-

3.2.6 Model Validation

As discussed in the literature review chapter, very limited studies are reported in the literature about the performance of combined foundation system and its behaviour under loading. Therefore, only two types of numerical models are considered for validation.

1. Stone columns under raft in soft soils

2. Piled raft in soft soils

Validation of Plaxis 3D model was conducted to assess the accuracy of the soil model in predicting the load-bearing performance of raft with stone columns in clay soil and piled raft foundation in clay soil. The accuracy of the model depends on the soil parameters and the sensitivity of mesh. For both cases (Stone columns under raft in soft soils and piled raft in soft soils) soil parameters were checked for soil model and mesh sensitivity were checked to finalize the size of mesh that can also be applied for the present study.

The numerical model developed in this investigation was validated for two cases separately, in this instance soft soil reinforced with stone columns alone (case #1), and soft soil strengthened with piles (case #2). For case #1, the numerical results obtained in this study for stone columns alone were validated against the experimental results reported in literature by Ghazavi and Afshar (2013). However, for case #2, the results of the present numerical analysis for piled raft foundation were endorsed against the numerical results proclaimed in literature by Sinha and Hanna (2017).

3.2.6.1 Numerical Validation for Stone Columns under Raft in Soft Soil

Experimental test results were used from the literature (Ghazavi & Afshar, 2013) to validate the numerical model for stone columns under raft in soft soils, the experimental test setup consists of large test box of 120 cm x 120 cm x 90 cm, carrying the bed of clay in it with maximum depth of 500 mm and reinforced with a single stone column 100 mm in diameter, also a stiff steel plate with 200 mm in diameter and 30 mm in thickness were used for loading on the stone column. Figure 3.21 shows promising match between the results obtained from numerical model and the experimental data. The comparisons of the results are shown in Table 3.9, where acceptable agreement is apparent. Furthermore, the coefficient of variation, defined as the ratio of the standard deviation to the mean (which is a measure of the dispersion of a data set), was less than 1 for all the results, indicating a relatively low variation in the results.

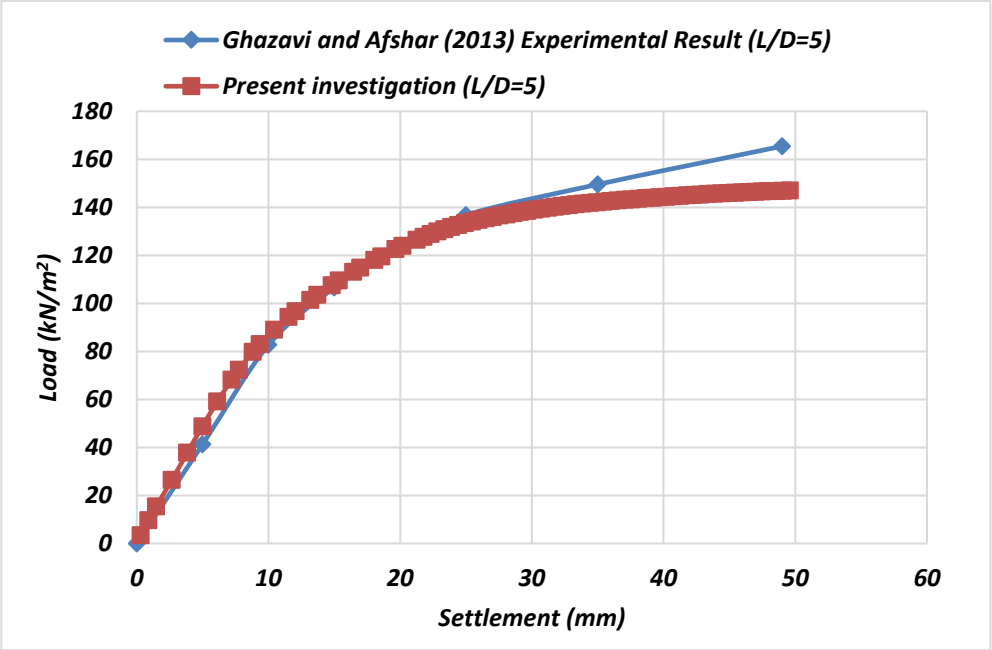


Figure 3.21: Load vs settlement curves for validation of stone columns under raft

Table 3.9: Statistical analysis for stone columns model validation

Settlement (m)	Ghazavi and Afshar (2013)	PLAXIS 3D	Difference (%)	mean	Standard deviation	Coefficient of variation
	Load (kN/m^2) from literature	Load (kN/m^2) from present work				
0.005	41.36	49.00	18.46	45.18	5.40	0.1195
0.010	82.73	86.50	4.56	84.61	2.67	0.0315
0.015	106.59	108.00	1.32	107.30	1.00	0.0093
0.020	124.09	123.50	0.48	123.80	0.42	0.0034
0.025	136.82	133.50	2.43	135.16	2.35	0.0174
0.035	149.55	143.00	4.38	146.27	4.63	0.0316
0.049	165.45	146.50	11.45	155.98	13.40	0.0859

3.2.6.2 Numerical Validation for Piled Raft Foundation in Soft Soil

The numerical study for piled raft foundation in soft soil is validated by modelling the results reported in literature (Sinha & Hanna, 2017). A 24 m square raft foundation of 2 m thickness in untreated and treated soil (16 piles, $S = 6D$ of 1.0 m diameter) were used and 0.5 MPa UDL was applied on the raft in their study. Table 3.10 shows the material properties used for their soil, pile, and raft. However, Figure 3.22 and Figure 3.23 show good agreement between present work and reported results. The comparisons of the results are shown in Table 3.11, where acceptable agreement is apparent. Furthermore, the coefficient of variation, defined as the ratio of the standard deviation to the mean (which is a measure of the dispersion of a data set), was less than 1 for all the results, indicating a relatively low variation in the results.

Table 3.10: Material properties (Sinha & Hanna, 2017)

Parameter	Unit	Clay	Limestone	Pile	Raft
Young's modulus, E_s	MPa	54	2000	25000	34000
Poisson's ratio, v_s	-	0.15	0.25	0.2	0.2
unit weight, γ	kN/m^3	19	22	25	25
Angle of internal friction, Φ	°	20	15		
Cohesion, c	kPa	20	1000		

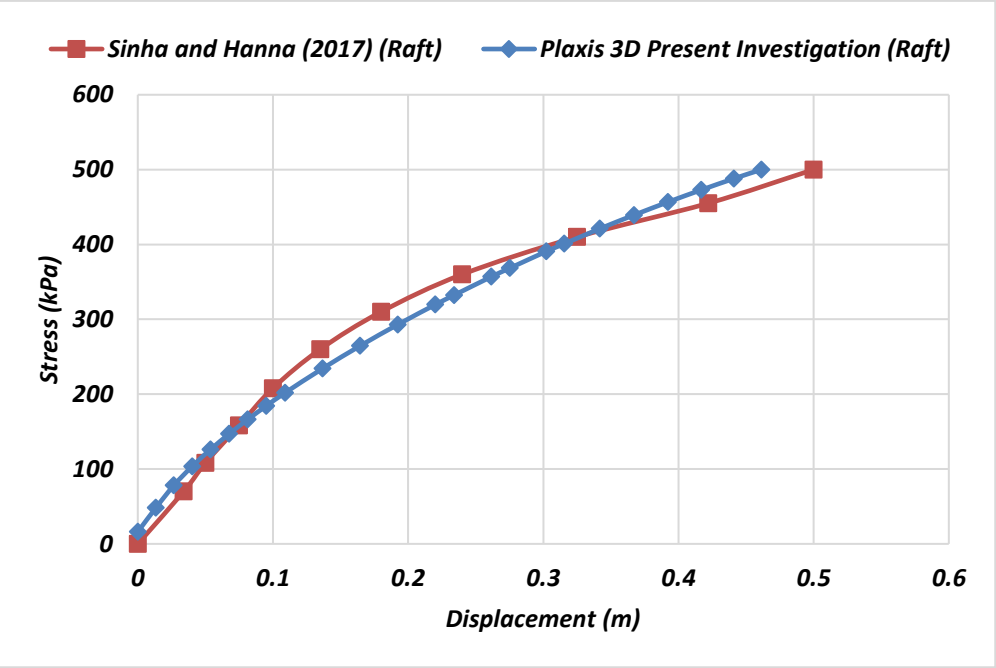


Figure 3.22: Stress-Displacement for validation of raft only

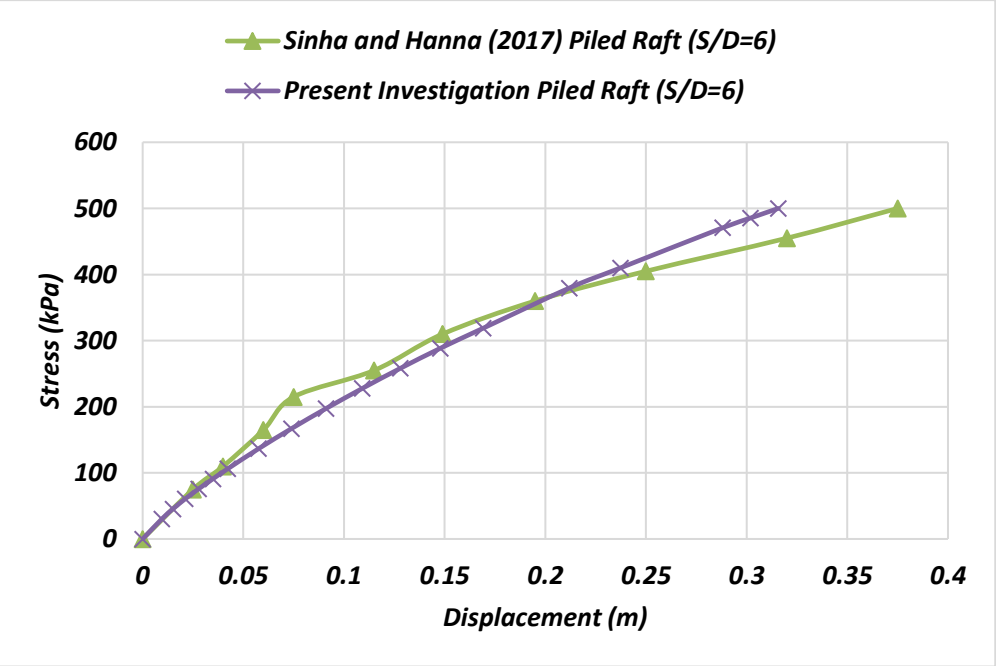


Figure 3.23: Stress-Displacement for validation of piled raft

Table 3.11: Statistical analysis for piled raft model validation

Displacement (m)	Sinha and Hanna (2017) (RAFT ONLY)	PLAXIS 3D (RAFT ONLY)	Difference (%)	mean	Standard deviation	Coefficient of variation
	Stress (kPa) from literature	Stress (kPa) from present work				
0.05	108.00	120.00	11.11	114.00	8.49	0.0744
0.10	208.00	190.00	8.65	199.00	12.73	0.0640
0.15	276.00	250.00	9.42	263.00	18.38	0.0699
0.20	327.00	300.00	8.26	313.50	19.09	0.0609
0.25	365.00	345.00	5.48	355.00	14.14	0.0398
0.30	396.00	387.00	2.27	391.50	6.36	0.0163
0.35	422.00	427.00	1.18	424.50	3.54	0.0083
0.40	444.00	460.00	3.60	452.00	11.31	0.0250
0.46	477.00	497.00	4.19	487.00	14.14	0.0290
Displacement (m)	**Sinha and Hanna (2017) (PILED RAFT)**	**PLAXIS 3D (PILED RAFT)**	**Difference (%)**	**mean**	**Standard deviation**	**Coefficient of variation**
	Stress (kPa) from literature	**Stress (kPa) from present work**				
0.05	135.00	120.00	11.11	127.50	10.61	0.0832
0.10	240.00	213.00	11.25	226.50	19.09	0.0843
0.15	311.00	293.00	5.79	302.00	12.73	0.0421
0.20	365.00	363.00	0.55	364.00	1.41	0.0039
0.25	405.00	423.00	4.44	414.00	12.73	0.0307
0.30	440.00	482.00	9.55	461.00	29.70	0.0644

3.3 Limitation of the Research

1. Present numerical work is limited to one layer of soft clay underlined by dense sand. Studying the use of stone columns and piles in soft clay soil is not limited to this type of soil alone. These ground improvement techniques can also be applied to other types of soil, depending on their characteristics and engineering requirements. However, soft clay soil is often a challenging soil type that requires particular attention due to its low strength, high compressibility, and potential for excessive settlement.
2. Arrangement of piles and columns are square shaped. The square shape provides symmetry and uniform load distribution.
3. Steel tube piles are investigated in present study. For steel tube piles PLAXIS 3D provides a built-in material models and properties for steel, which makes it very simple to correctly represent the behaviour of steel tube piles.
4. Only one type of geometry and model size is considered in the present study. The chosen geometry and the model size is aligned with the type of soil and foundation selected for the present investigation, geometry and model size can vary based on different type of foundations and soil conditions.

3.4 Chin's method

For the present work the stress-strain curves could not show any sign of failure (drop in stress accompanied by an increase in strain), Chin's method (Chin, 1970) was applied to estimate the ultimate load bearing capacity of the raft foundation under different conditions. In this method each strain value first must be divided by its corresponding stress as shown in Table 3.12 and the resulting values must be plotted against the strains as shown in Figure 3.24 and Figure 3.25. When the plotted values fall in straight lines it indicates the load approach's fault tension and the ultimate load efficiency (q_u) can be determined by measuring the reverse slope (m) of this straight line.

$$q_u = \frac{1}{m} \qquad \text{Equation 3.5}$$

Table 3.12: Stress Vs Strain for untreated soil (Raft alone in soft clay)

Applied Stress, σ (kN/m^2)	**Strain, ε (%)**	**Strain/Stress, ε/σ (% / kN/m^2)**
46.43468	0.59656	0.01285
59.14962	0.89250	0.01509
77.40340	1.49971	0.01938
91.00316	2.11585	0.02325
101.06875	2.73584	0.02707
108.36567	3.35397	0.03095
113.95533	3.96595	0.03480
117.91402	4.56892	0.03875

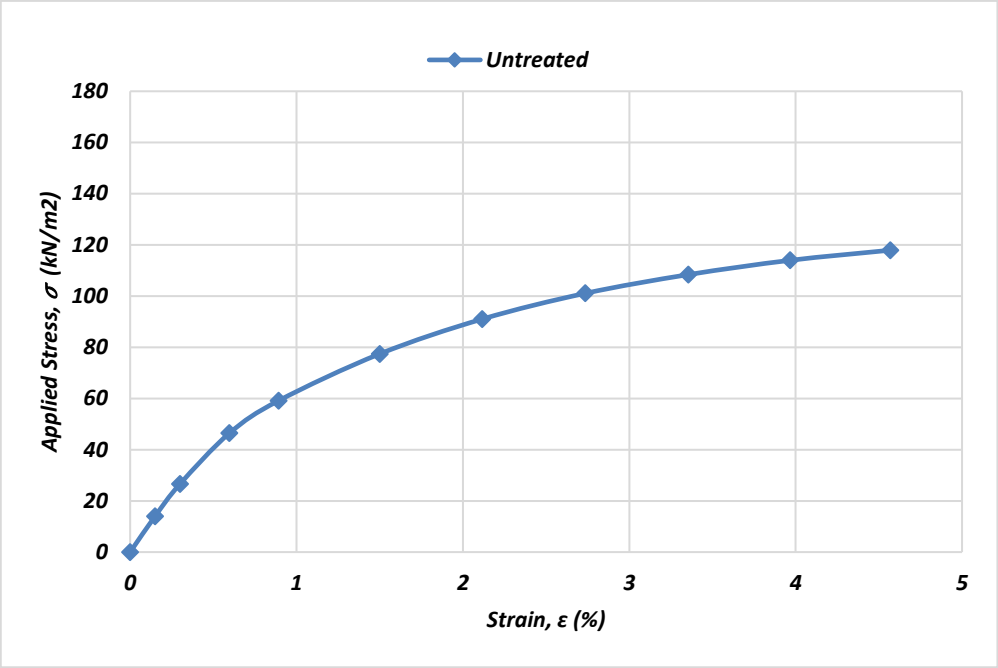


Figure 3.24: Stress Vs Strain for untreated soil (Raft alone in soft clay)

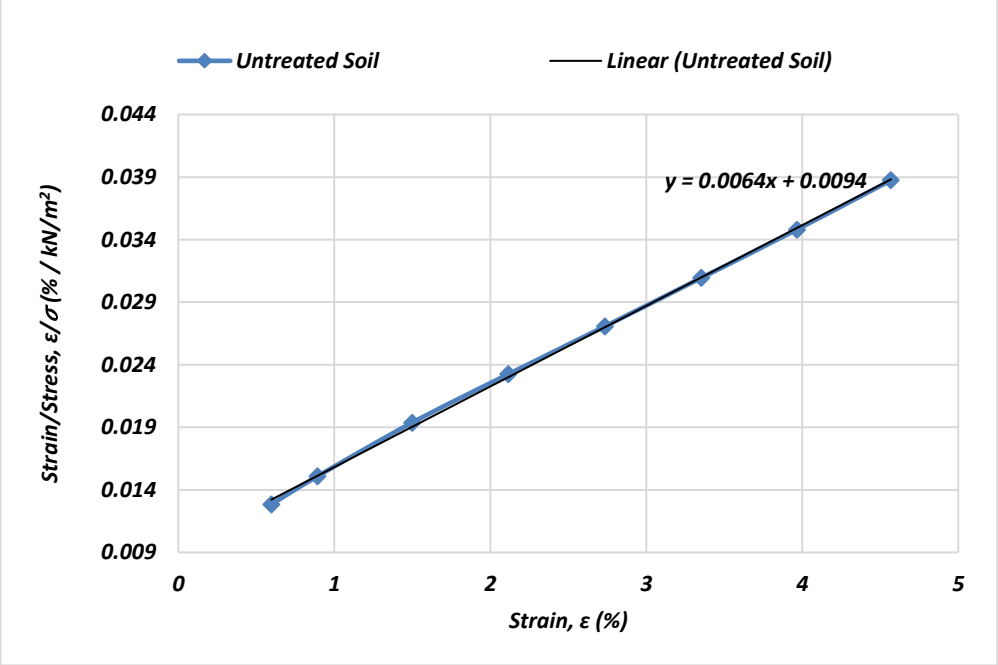


Figure 3.25: Strain/Stress Vs Strain (Chin, 1970) for untreated soil (Raft alone in soft clay)

3.5 Summary

This chapter provides all the steps considered to carry out this present research. The methodology used in this study is based on numerical investigation using PLAXIS 3D. The detailed process of developing three-dimensional finite element model and the descriptions of all the elements and components used in these models are discussed in this chapter. A total of three numerical models were considered (a) stone columns under raft, (b) piled raft foundations and (c) combined foundation (i.e., stone columns/piles capped with rigid raft foundation).

Also, parameters are selected very carefully from the range of data used in practice and reported in literature for parametric study of all three developed numerical models.

Finally, the model validation for stone columns under raft in soft soils and piled raft in soft soils are presented which shows the great agreement between the present work and reported results from the literature.

CHAPTER 4

RESULTS AND DISCUSSIONS

4.1 Overview

A detail parametric study is required for three developed models to investigate the different configurations (i.e., different diameters, spacing and number, ratio of piles to stone columns area, etc.).

The effect of parameters on the performance of the three types of foundation system (i.e., stone columns under raft foundation in soft soil, piled raft foundation in a soft soil and stone columns/piles capped with rigid raft foundation in soft soil) is studied. Moreover, the behaviour of these foundation system under loading is examined and the results obtained from these parametric studies are discussed in the following subsections.

4.2 Parametric Study of Stone Columns under Raft Foundation in Soft Soil

Table 3.2 and Table 3.3 show the range of parameters and material properties used to perform the parametric study for stone columns under raft foundation in soft soils. A certain range of parameters (i.e. spacing, diameter and angle of friction of stone columns) is considered. The load-bearing performance of this foundation system is analyzed, as well as the results of the parametric study is utilized to understand the bearing capacity ratio (*BCR*) of stone columns under raft foundation in soft soil.

4.2.1 Effect of Stone Columns Spacing

A range of spacing over diameter ratios of stone columns were selected (*S/D* = 7, 6, 5, 4) to study the influence of spacing of stone columns on the ultimate capacity of stone

columns under raft foundation in soft soils, the stress strain relations were established for the raft foundations on both untreated soil (raft resting on soft clay alone) and treated soil (stone columns with raft in soft clay soil) , for each spacing over diameter ratios (*S/D*), and angle of friction of stone columns as shown in Figure 4.1, Figure 4.3, and Figure 4.5. A significant difference in carrying capacity can be noted between the raft foundation on the untreated soil and treated soil with stone columns.

Also, the results show that the carrying capacity of raft on untreated soft soil has lowest load bearing capacity, whereas the carrying capacity of raft on treated soft soil is increasing with decrease in (*S/D*) of the stone columns (Table 4.1) similar findings were reported in (Al-Kazzaz & Al-Obaydi, 2021; Nazari et al., 2014; Naderi et al., 2018; Naseer et al., 2019; Unni et al., 2021)., whereas on the other hand stress-strain diagram shows strain rate increases with an increase in the spacing to diameter ratio (*S/D*) of stone columns for a given stress this can be understand by the fact that larger spacing to diameter ratio (*S/D)* means wider spacing between the stone columns which can results in more flexible system with higher strains under the applied stress. Meanwhile there is no clear sign of failure can be observed in the stress-strain curves. Therefore, Chins Stability Method (Chin, 1970) was used to predict the ultimate carrying capacity of the foundation system. Table 4.1 shows that the load bearing capacity of the foundation system is increasing with the decrease in the (*S/D*) of the stone columns this can be understand by the fact that the decrease in spacing between the stone columns can have a greater number of stone columns which can be distribute uniformly under the raft foundation, due to this uniformly distribution of stone columns the load can be shared more evenly, which can improve the overall performance of the foundation system (Castro, 2014).

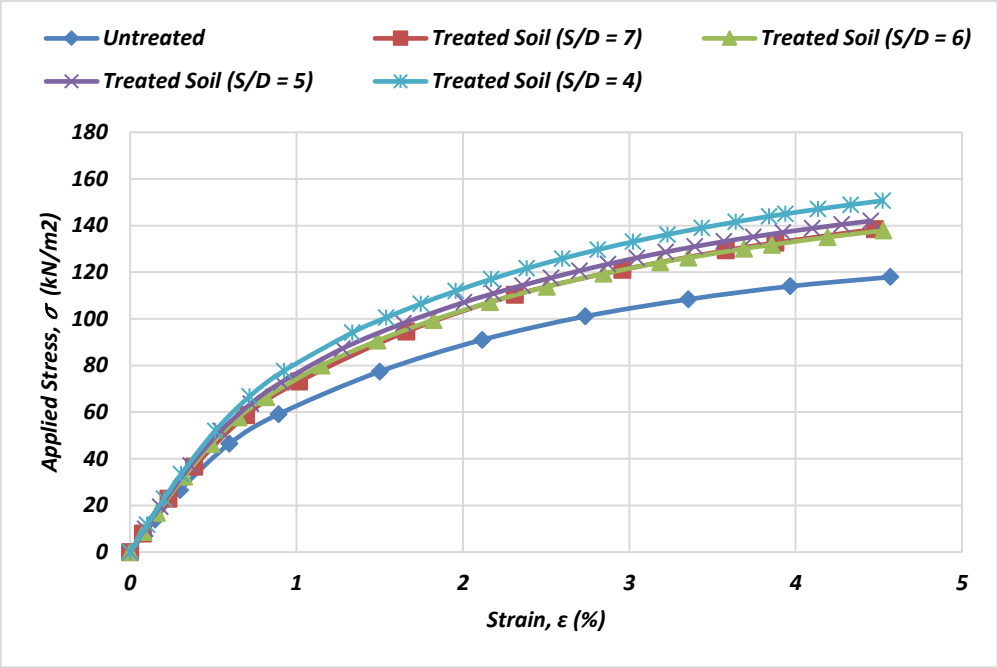


Figure 4.1: Stress Vs Strain for untreated soil and treated soil as a function of *S/D* and φ_c = 42°

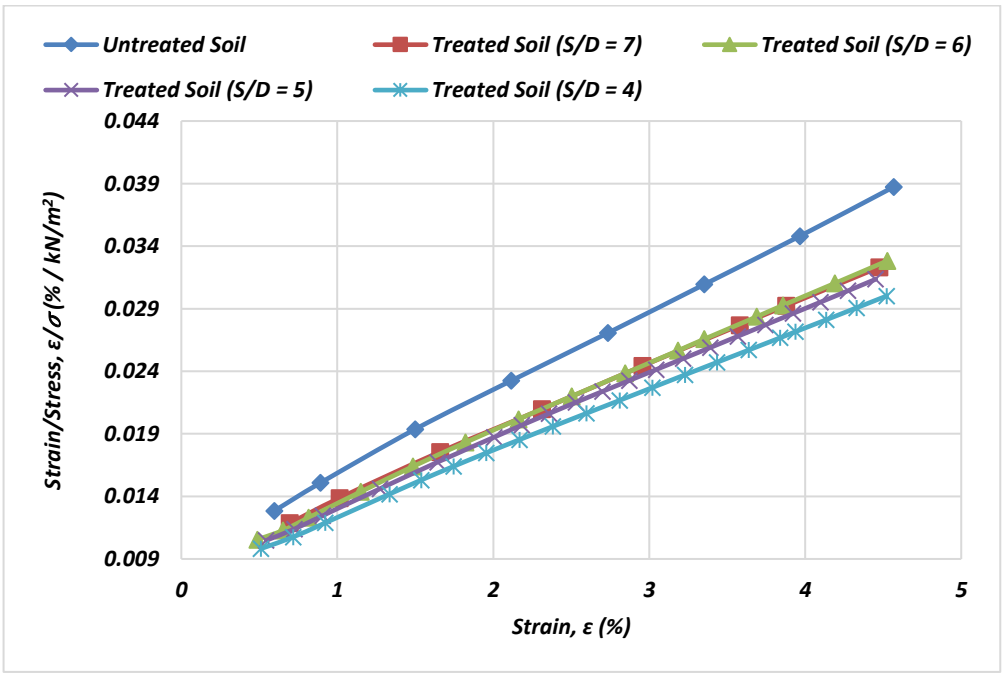


Figure 4.2: Strain/Stress Vs Strain (Chin, 1970) for untreated soil and treated soil as a function of *S/D* and φ_c = 42°

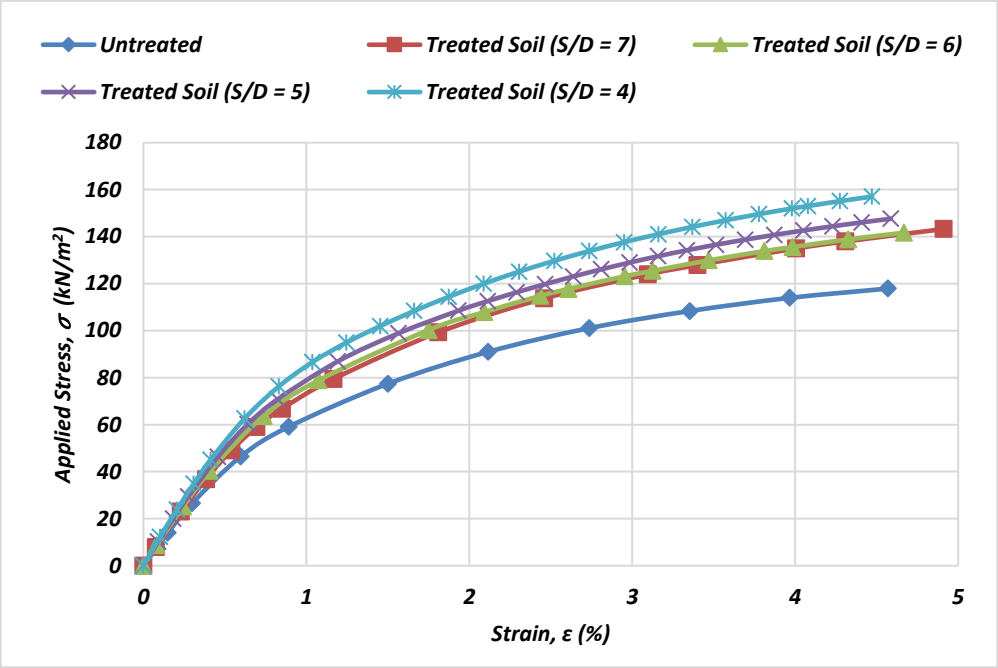


Figure 4.3: Stress Vs Strain for untreated soil and treated soil as a function of *S/D* and $\varphi_c = 45^o$

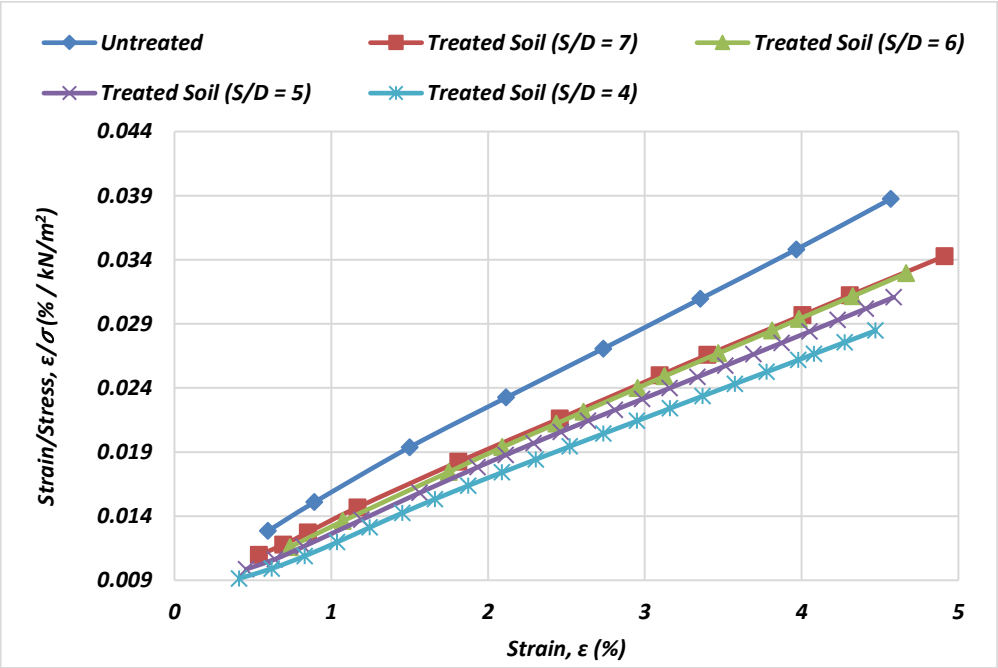


Figure 4.4: Strain/Stress Vs Strain (Chin, 1970) for untreated soil and treated soil as a function of *S/D* and $\varphi_c = 45^o$

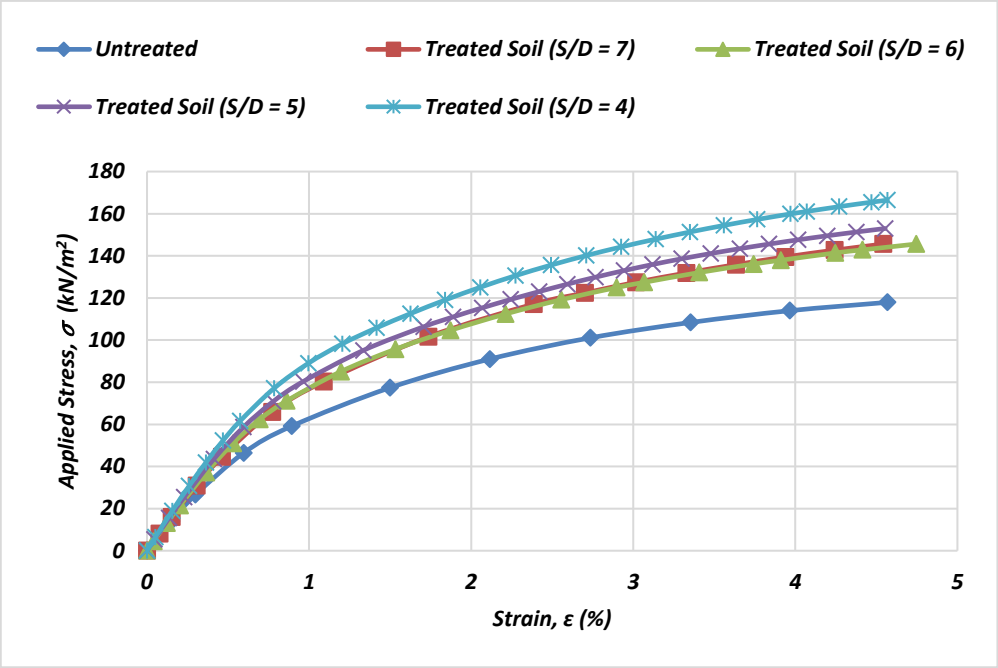


Figure 4.5: Stress Vs Strain for untreated soil and treated soil as a function of *S/D* and φ_c = 48°

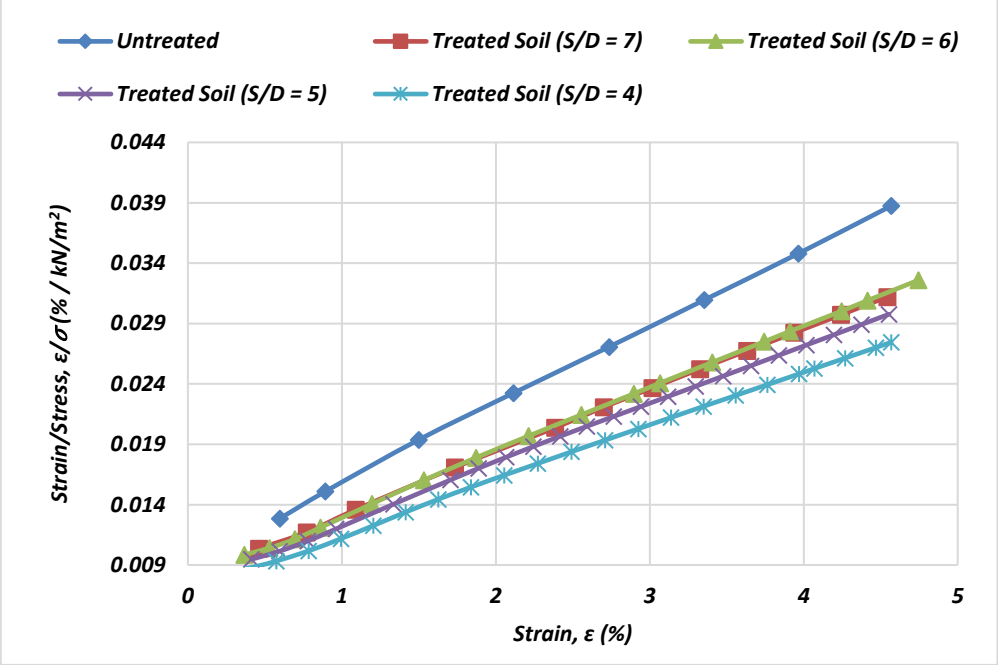


Figure 4.6: Strain/Stress Vs Strain (Chin, 1970) for untreated soil and treated soil, as a function of *S/D* and φ_c = 48°

Table 4.1: Ultimate carrying capacity using Chin's method

	q_u (kN/m^2)		
S/D	$\varphi_c = 42^o$	$\varphi_c = 45^o$	$\varphi_c = 48^o$
7	185.85	189.75	198.91
6	184.16	186.61	196.47
5	188.29	198.37	208.37
4	201.34	212.16	226.77
Untreated	153.36	153.36	153.36

The term bearing capacity ratio (*BCR*) was introduced to understand the effect of spacing-diameter ratio (*S/D*) and angle of friction of stone columns (φ_c). Bearing capacity ratio is described as the ratio between the ultimate load bearing capacity of raft foundation on treated soft soil to that of raft foundation on untreated soft soil. For this purpose, a graph was established for the relation of bearing capacity ratio (*BCR*) verses the spacing-diameter ratio (*S/D*) for each angle of friction of stone columns (φ_c). It can be observed from Figure 4.7 that the ratio (*S/D*) of stone columns have no influence on the bearing capacity when (*S/D*) is greater than 7, whereas the bearing capacity ratio (*BCR*) can be improved when the ratio (*S/D*) is 4 or less. Al-Kazzaz and Al-Obaydi (2021) reported that there is a 10.2, 8.7, and 4.0% improvement in soil bearing for spacings (3, 4 and 5), respectively. Figure 4.7 also shows the positive influence of angle of friction (φ_c) on the bearing capacity ratio (*BCR*). It is observed that the increase in the angle of friction of stone columns (φ_c) can increase the ultimate load bearing capacity of the foundation system on treated soft clayey soil. This can

be described by the fact that the stone columns with higher angle of friction have good interlocking between their granular particles and have good shear strength.

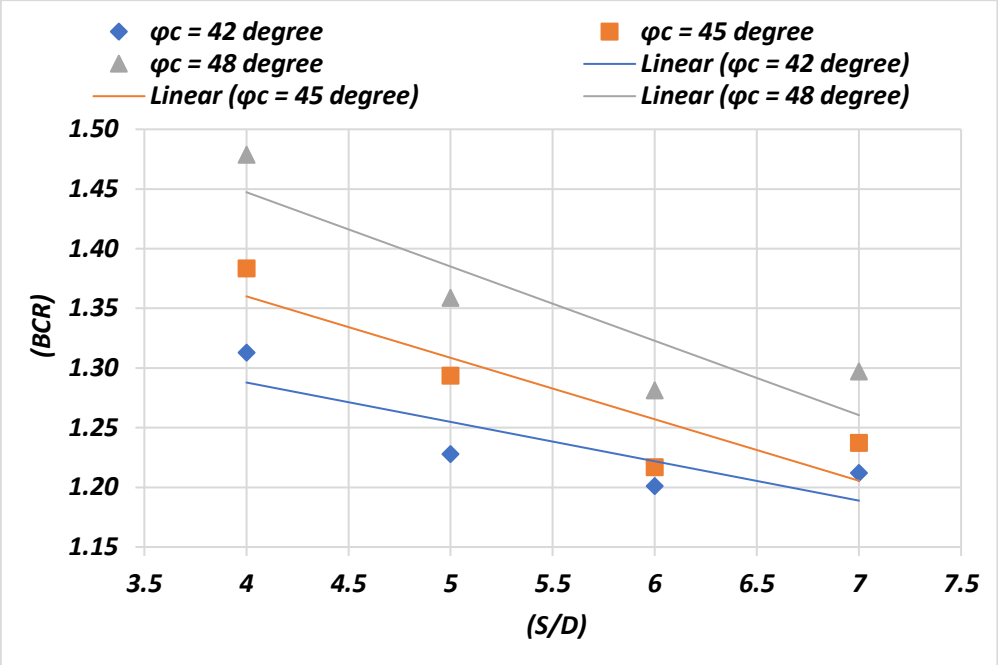


Figure 4.7: Bearing capacity ratio (*BCR*) as a function of *S/D* and angle of friction

4.2.2 Effect of Angle of Friction of Stone Columns

Apart from the effect of geometric properties of the foundation system, properties of the foundation materials can also have considerable effect on the performance of foundation system. Therefore, certain range of angle of friction of stone columns are considered to examine the performance of raft foundation on treated soil with stone columns. To study the influence of angle of friction of stone columns three values were selected φ_c = 42°, 45°, and 48°. Ultimate carrying capacity verses angle of friction of stone columns (*qu* Vs φ_c) were plotted for various spacing over diameter ratio (*S/D*) of stone columns as shown in Figure 4.8. In general, it can be observed from this graph that the ultimate capacity of foundation system increases with increase in angle of friction of stone columns (Table 4.1). Ng and Ann

(2014) reported the similar findings that the performance of footing resting on the stone columns increases with the increase in angle of friction of stone columns.

Angle of friction of stone columns represents the internal friction between the individual particles of stone columns, increasing the angle of friction of stone columns can affect and improve the load-bearing performance of the foundation, with bigger values of angle of friction, the stone columns can better resist the shear force which can enhance the overall performance of the foundation system.

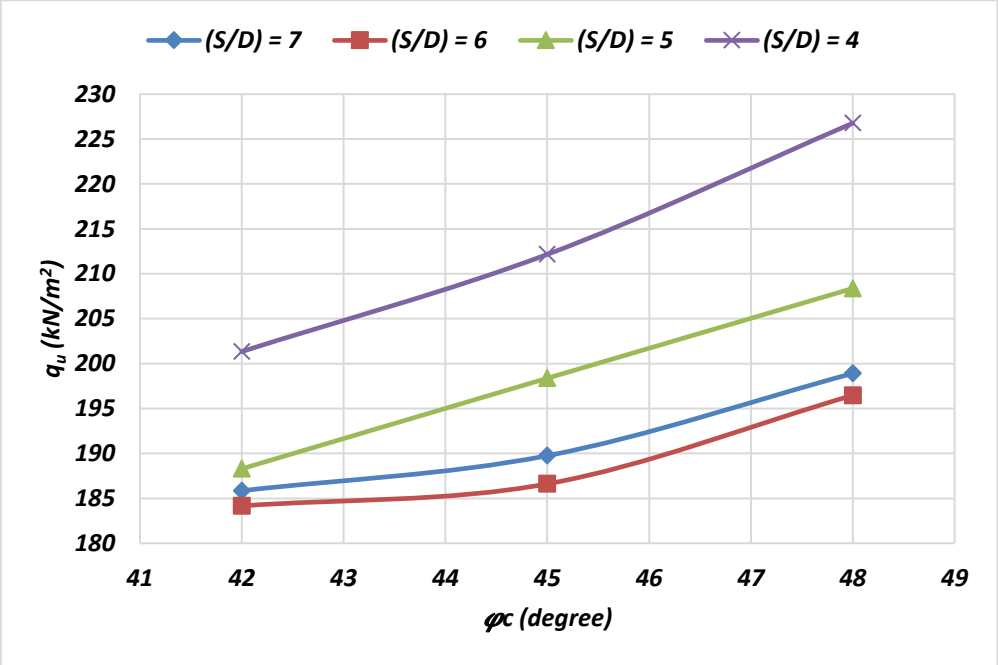


Figure 4.8: q_u Vs φ_c for stone columns under raft

4.2.3 Behaviour of Stone Columns Under Raft Foundation in Soft Soil

Failure of group of stone columns under the raft is either by bulging or massive shear failure (Hanna et al., 2013). Failure mode observed in the present study for the group of stone columns under raft foundation in soft clay shows that most of the failure occurs due to the shear in columns and soils in the surrounding regions. The contour diagrams in Figure 4.9 displays that the larger shear failure occurs in this foundation system when the spacing

over diameter ratio (*S/D*) of stone columns are bigger, it can be observed from Figure 4.9, Figure 4.10, Figure 4.11, and Figure 4.12 that the intensity of shear failure reduces with the smaller spacing over diameter ratio (*S/D*) of stone columns, the contour diagrams shows the higher strain values in the soil under the raft with bigger spacing over diameter ratio (*S/D*) of stone columns, similar findings were described in the contour diagram reported by (Micheál & Bryan, 2014).

The balance between the spacing and diameter of stone columns in a raft foundation system can play a critical role in determining the failure mechanism of the raft foundation in soft clay. The relationship between these two factors can affect the load distribution, consolidation behaviour, and overall stability. The balance between spacing and diameter of stone columns depends on several factors which includes soil properties, applied loads, and design objectives.

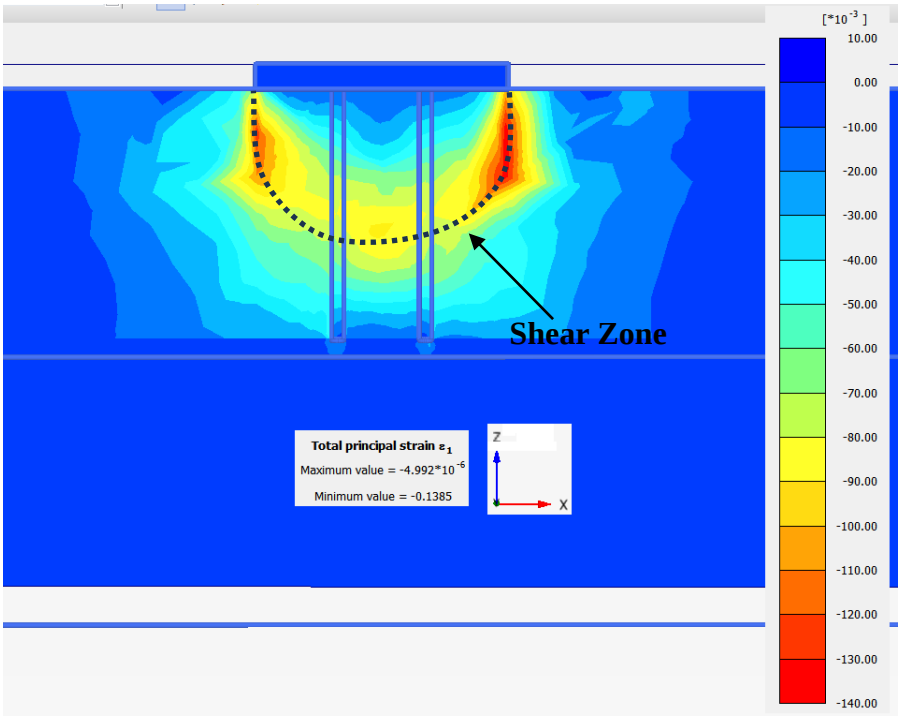


Figure 4.9: Behaviour of stone columns under raft for the case *S/D* = 7

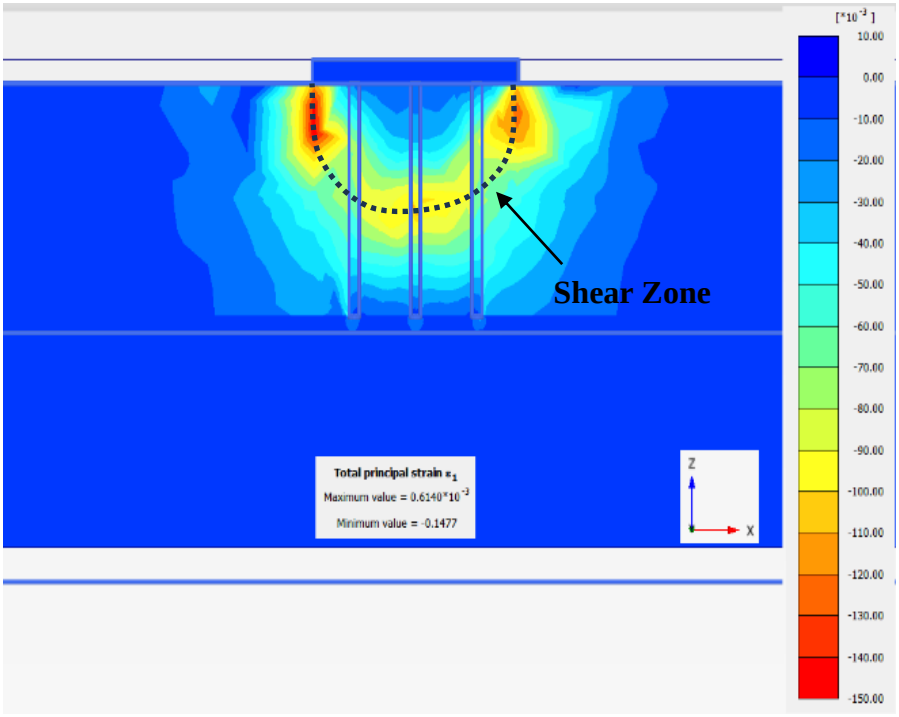


Figure 4.10: Behaviour of stone columns under raft for the case *S/D* = 6

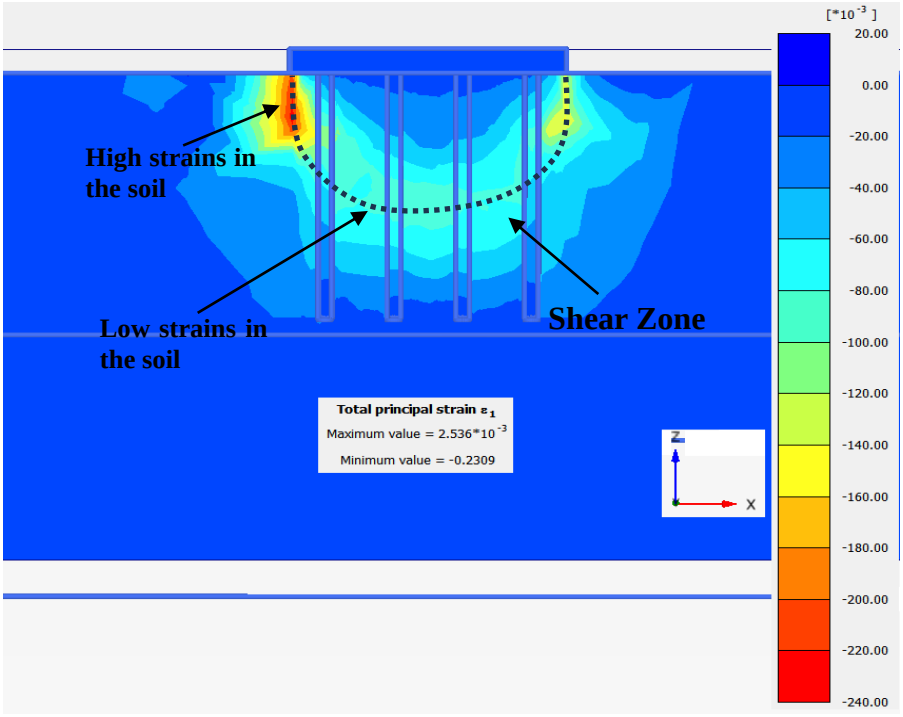


Figure 4.11: Behaviour of stone columns under raft for the case *S/D* = 5

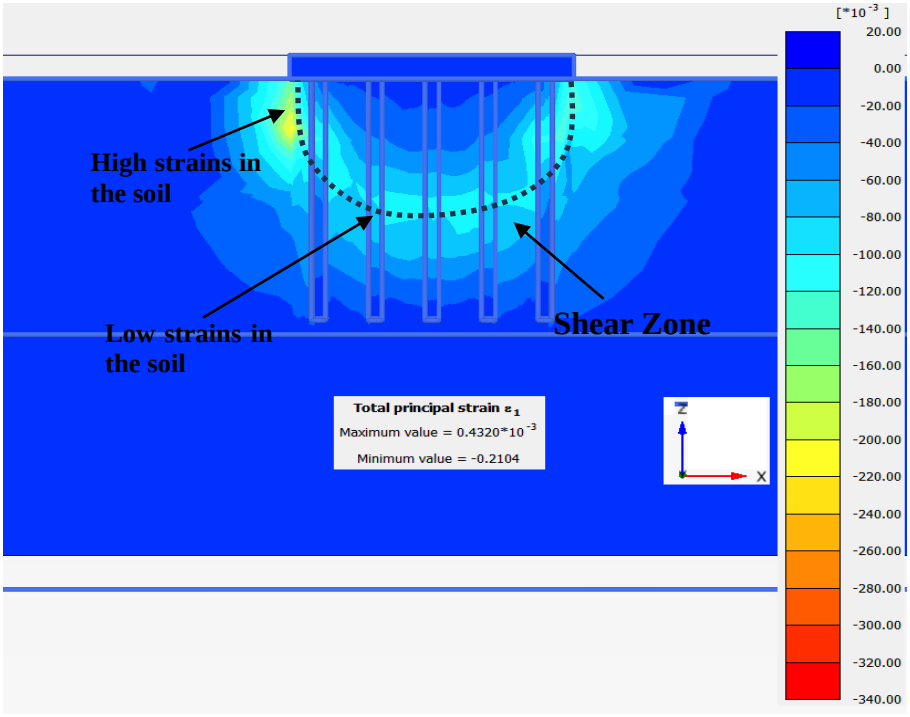


Figure 4.12: Behaviour of stone columns under raft for the case *S/D* = 4

The spacing, diameter, and angle of friction of stone columns are interconnected and their combined effects determine the overall performance of the raft foundation in soft clay.

Closer spacing between the stone columns can provide more points of load transfer which can result in better load distribution and reduced settlement, larger diameter stone columns generally have higher load-bearing capacity and can better distribute loads to the surrounding soil and a higher angle of friction of stone columns can provide better shear strength. Optimizing the spacing, diameter, and angle of friction of the stone columns can help in achieving improved load-bearing performance of the foundation.

4.3 Parametric Study of Piled Raft Foundation in Soft Soil

Table 3.4 and Table 3.5 show the range of parameters and material properties used to perform the parametric study for piled raft foundation in soft soils. A certain range of parameters is considered to investigate the effect of geometry (i.e. piles length, diameter, and spacing) of the foundation system, as well as the effect of rigidity ratio between piles materials and clay (E_p/E_s) are used to examine the performance of piled raft foundation system in soft clayey soils. The behaviour of this foundation system is also examined under the loading as well as the results of the parametric study is utilized to develop a semi-empirical model for the determination of the improvement factor (IF_{PR}) for the piled raft foundation system.

4.3.1 Effect of Pile Spacing

To study the effect of spacing on the ultimate capacity of piled raft foundation in soft soil, five different spacings were used as shown in Table 3.5. The stress strain relations (Stress Vs Strain) for the raft foundation on untreated soil (raft resting on soft clay alone) and treated soil (Piled raft in soft clay) were established for each different set of spacing over diameter ratio of piles (S/D) and the rigidity ratio between piles materials and clay (i.e., the modulus of elasticity of pile over the modulus of elasticity of soft clay ratio = E_p/E_s) as

shown in Figure 4.13, and the remaining stress strain relations are given in Appendix A. A significant difference of carrying capacity can be noted between the raft foundation and piled raft foundation. Also, the results show that the carrying capacity of piled raft foundation system increases with the decrease in pile spacing and the strain increases with the increase in pile spacing for the given stress. Meanwhile there is no clear sign of failure can be observed in the stress-strain curves therefore Chins Stability Method (Chin, 1970) is used to predict the ultimate carrying capacity of the foundation system as given in Figure 4.14, and the remaining figures are given in Appendix B.

The spacing to diameter ratio of piles in a raft foundation system can influence the overall performance of the foundation in soft clay. Pile group with an appropriate spacing-to-diameter ratio can enhance the load-bearing capacity of the foundation by effectively distributing the applied loads to the surrounding soil. The configuration of group of piles can influence the strains and stresses within the piles and the surrounding soil. A well-balanced spacing to diameter ratio of the pile can help to distribute the loads uniformly among the piles, which can result in lower stresses and strains within each pile and vice versa.

Stone columns in combination with a piled raft foundation in soft clay can potentially complement the spacing to diameter ratio of the piles and can improve the overall performance of the foundation system. Stone columns can help to distribute the load from the raft to a wider area of the soil. The use of stone columns can increase the load-bearing capacity of the soil, which can reduce the load sharing to the individual piles in the piled raft foundation. As a result, the spacing between the piles may be increased while still achieving the desired carrying capacity of the foundation system, this allows for a higher spacing to diameter ratio of piles.

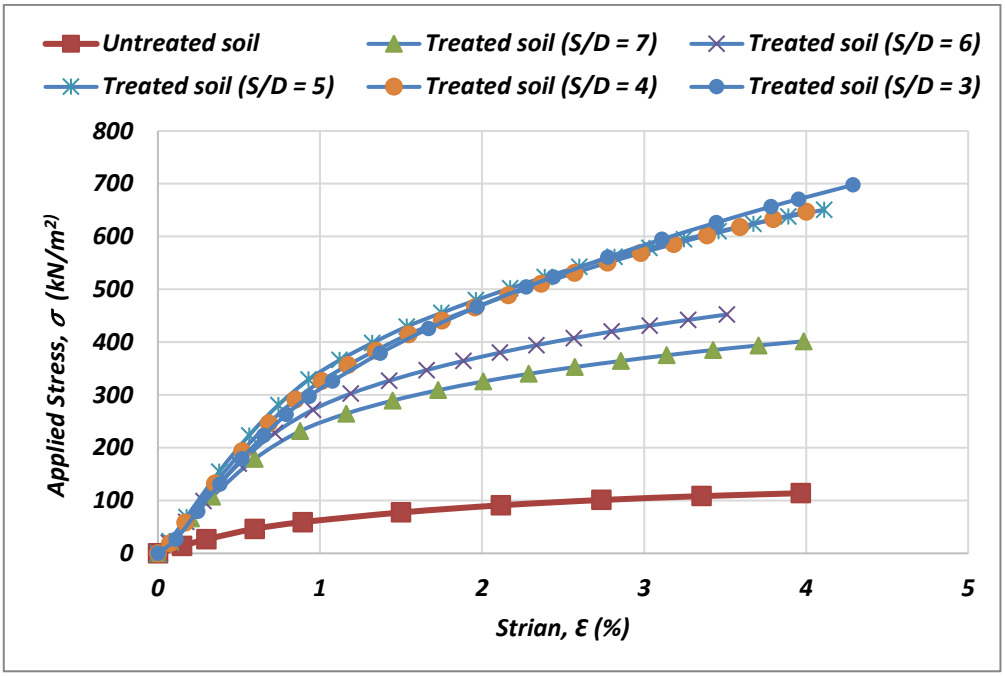


Figure 4.13: Stress Vs Strain for L/D = 50, E_p/E_s =52500

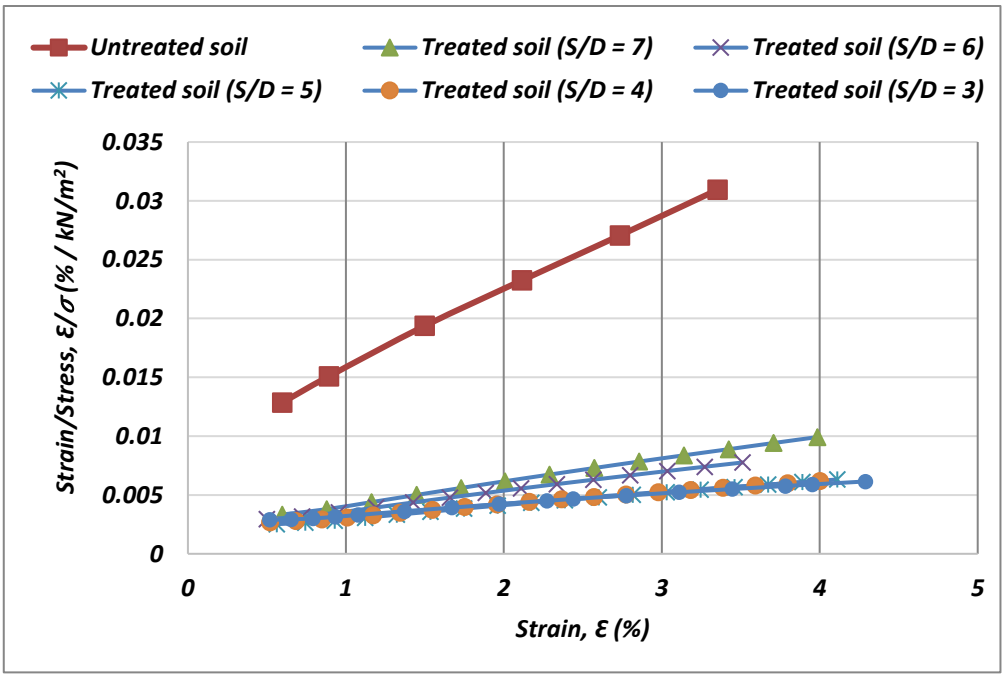


Figure 4.14: Strain/Stress Vs Strain (Chin, 1970) for untreated soil and treated soil (L/D = 50, E_p/E_s = 52500)

4.3.2 Effect of Pile Diameter

The diameter of pile is another important geometric parameter that can affect the performance of the piled raft foundation system. To study the effect of pile diameter on the ultimate capacity of piled raft foundation in soft soil three different diameters were considered as shown in Table 3.5, for this purpose five graphs were established for the relation of ultimate carrying capacity verses the length to diameter ratio of pile (*L/D*) for each different set of spacing over diameter ratio of piles (*S/D*) and the rigidity ratio between piles materials and clay (E_p/E_s) as shown in Figure 4.15, Figure 4.16, Figure 4.17, Figure 4.18, and Figure 4.19. A similar trend can be observed in these graphs which illustrate that the ultimate carrying capacity of the foundation system increases with the decrease in length to diameter ratio of pile (*L/D*), which shows that the increase in diameter of piles can increase the ultimate carrying capacity of the piled foundation in soft clay. Prashant et al. (2013) concluded that the increase in pile diameter reduces the differential settlement and increases the load carrying capacity of foundation.

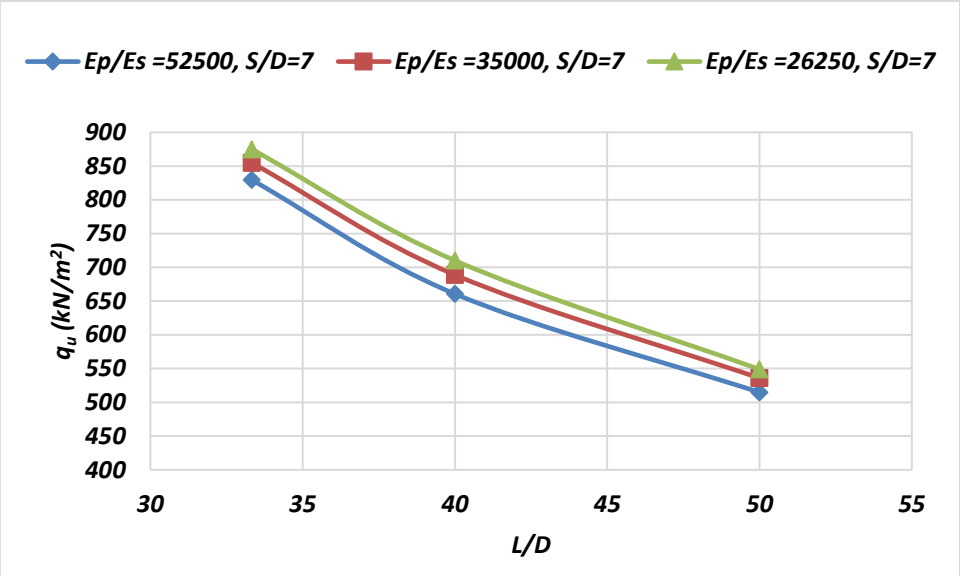


Figure 4.15: q_u Vs *L/D* for untreated soil and treated soil as a function of E_p/E_s and *S/D* = 7

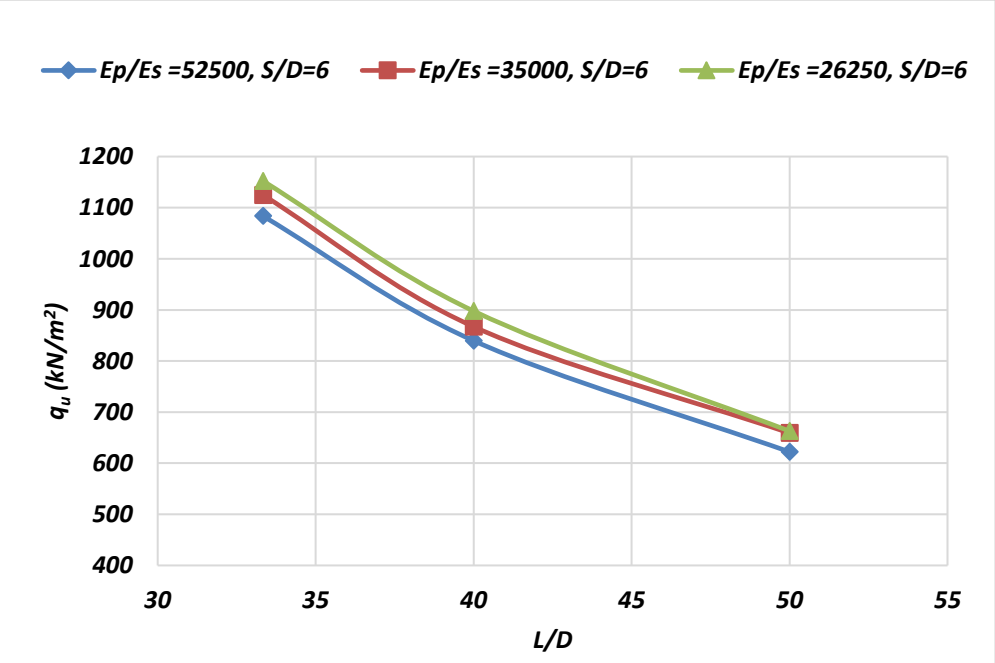


Figure 4.16: *qu* Vs *L/D* for untreated soil and treated soil as a function of E_p/E_s and *S/D* = 6

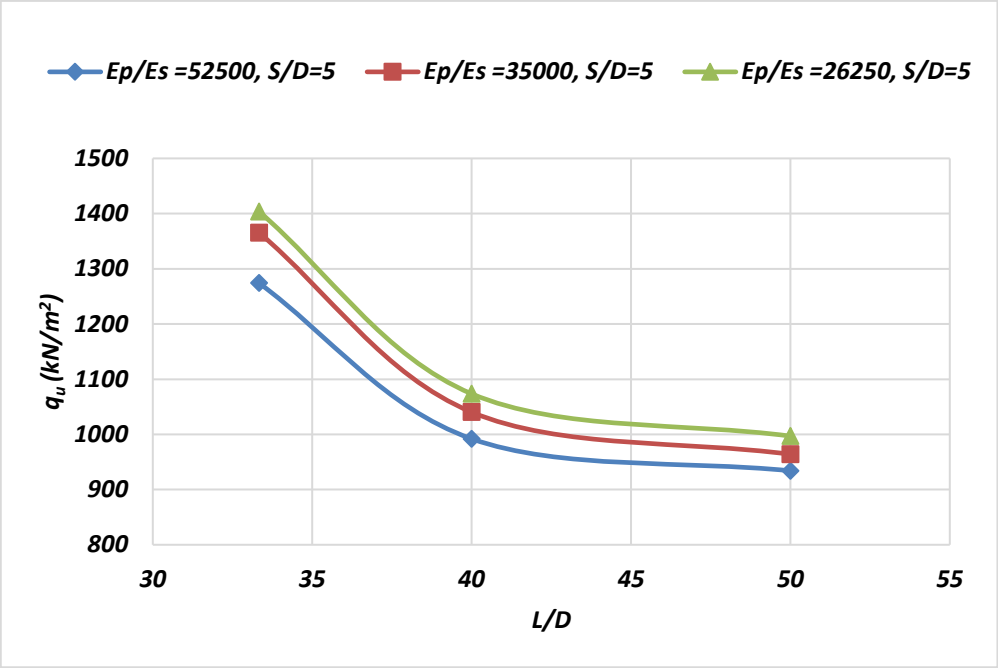


Figure 4.17: q_u Vs L/D for untreated soil and treated soil as a function of E_p/E_s and S/D = 5

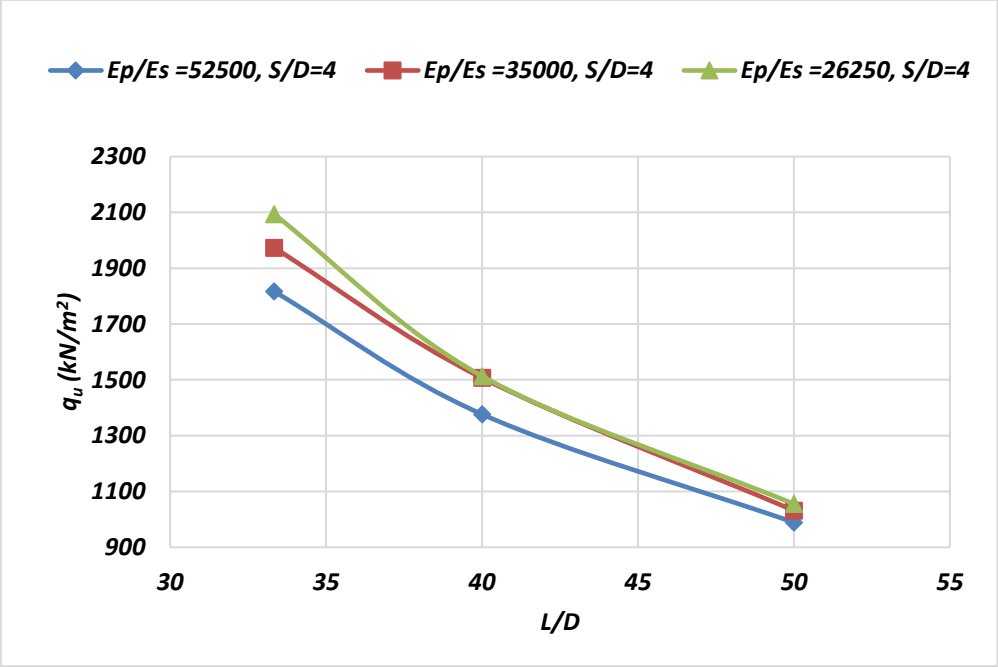


Figure 4.18: q_u Vs L/D for untreated soil and treated soil as a function of E_p/E_s and S/D = 4

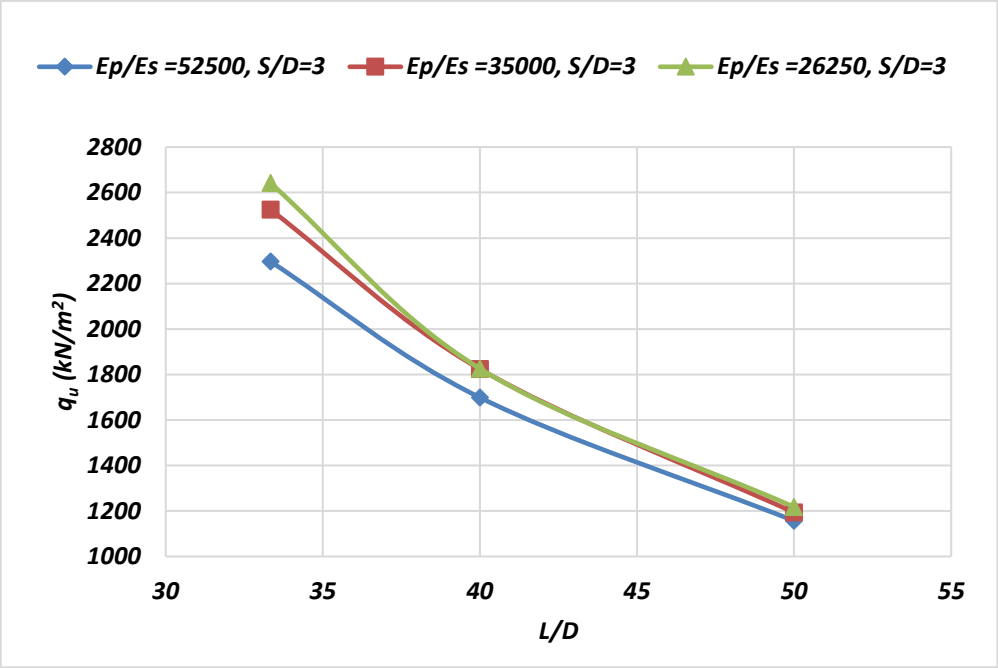


Figure 4.19: q_u Vs L/D for untreated soil and treated soil as a function of E_p/E_s and S/D = 3

The length and diameter of piles in a piled raft foundation system are the critical parameters in determining the load-bearing performance of the foundation. Longer piles can penetrate deeper into the soil, allowing for greater load transfer to deeper soil layers. Larger diameter piles can provide bigger cross-sectional area of piles, which can improve the load-bearing capacity by providing more skin friction and end-bearing resistance. Achieving a balance between length and diameter is important to optimize the load-bearing capacity of the piled raft system. (Cho et al., 2012; Deb & Pal, 2022; Elwakil & Azzam, 2016; Elsawwaf et al., 2022; Ghalesari & Choobbasti, 2018; Mali & Singh, 2020; Nguyen et al., 2013).

To determine the balance between length and diameter for the piles in a piled raft foundation in soft clay, factors (i.e. soil properties, required carrying capacity, and settlements) should be considered for appropriate design calculations.

4.3.3 Effect of Modulus of Elasticity of Soil

Modulus of elasticity is one of the mechanical properties of the foundation materials that can have influence on the performance of piled raft foundation system. Modulus of elasticity of raft and piles are not considered because they are rigid component of the foundation, and their modulus of elasticity is way higher than the soils. Therefore, only modulus of elasticity of clay soil is considered to examine the performance of piled raft foundation under the load. To study the influence of modulus of elasticity of soft clay three values were selected E_s = 4, 6 and 8 MPa (Table 3.4). Ultimate carrying capacity verses the rigidity ratio between piles materials and clay (E_p/E_s) were plotted for various spacing over diameter ratio of piles (S/D = 7, 6, 5, 4, 3) as shown in Figure 4.20, Figure 4.21, and Figure 4.22. In general, it can be noticed from these graphs that the ultimate capacity of foundation system gradually increasing with decrease in the modulus of elasticity of pile over modulus of elasticity of soft clay ratio (E_p/E_s).

The modulus of elasticity is a measure of the stiffness of the soil, and it reflects the soil's ability to resist deformation under applied loads. The modulus of elasticity can influence the load distribution within the soil under the piled raft foundation. A higher modulus of elasticity indicates a stiffer soil, which can result in a more uniform distribution of applied loads among the piles. As a result, a higher modulus of elasticity enhance the bearing capacity of the piled raft foundation system.

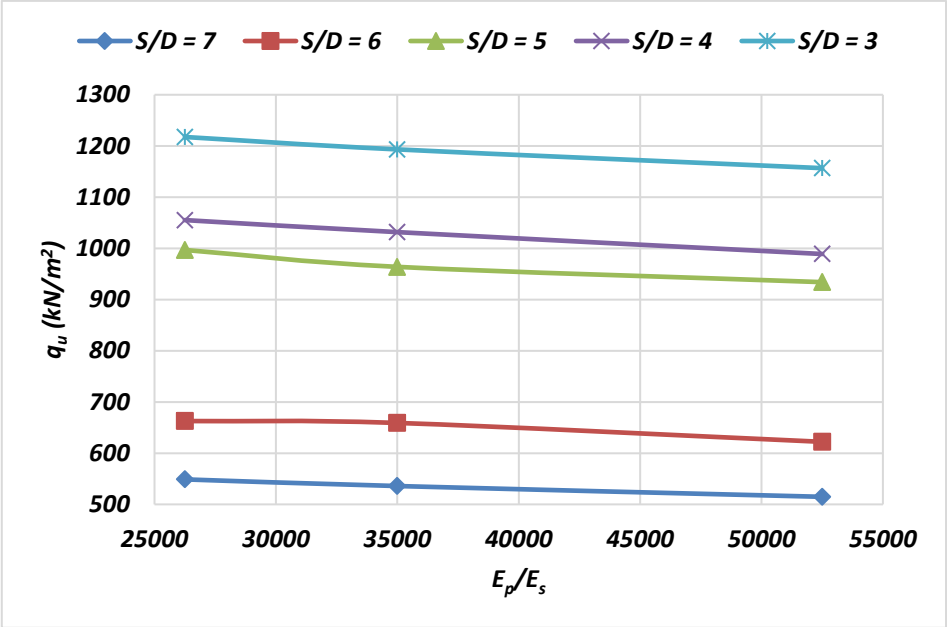


Figure 4.20: q_u Vs E_p/E_s for untreated soil and treated soil as a function of *S/D* and *L/D* = 50

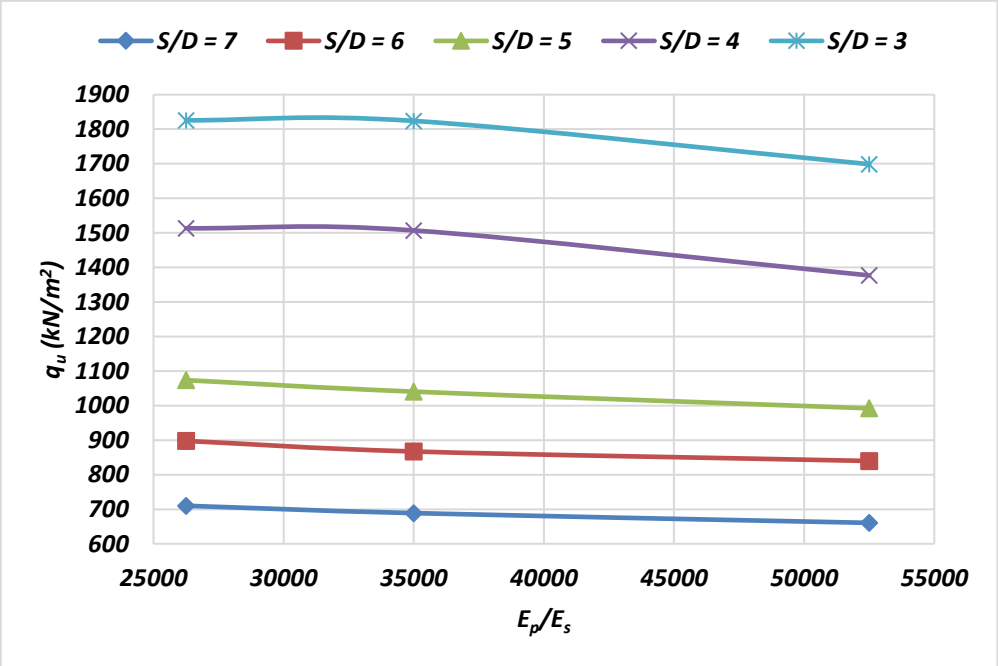


Figure 4.21: q_u Vs E_p/E_s for untreated soil and treated soil as a function of *S/D* and *L/D* = 40

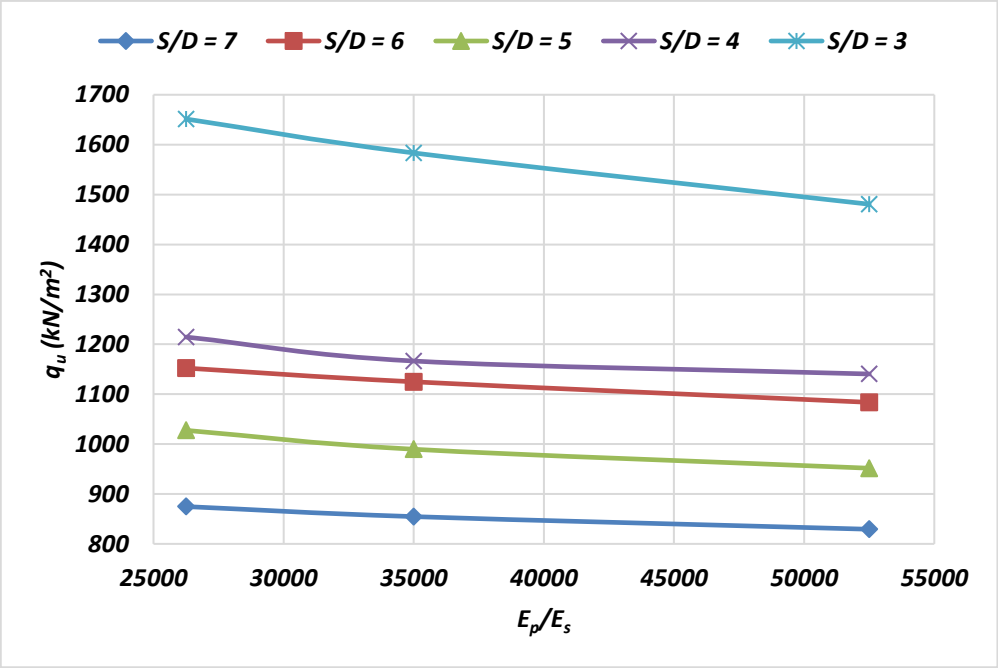


Figure 4.22: q_u Vs E_p/E_s for untreated soil and treated soil as a function of *S/D* and *L/D* = 33.33

4.3.4 Behaviour of Piled Raft Foundation in Soft Soil

The ground failure can occur in the piled raft foundation system if the stresses in the soil near the shaft and toe exceeds the strength of the soil. Behaviour observed in the present study for the piled raft foundation under loading shows that the foundation system fails by bearing at the tip of the piles and by shear along the side of the piles group as shown in Figure 4.23, Figure 4.24, Figure 4.25, Figure 4.26, and Figure 4.27.

Soft clay soils have low shear strength and can undergo shear failure when subjected to excessive loading, the soil adjacent to the sides of the pile group can experience lateral shearing forces which can be the cause of shear failure. The bearing capacity failure can occur at the tip of the pile when the applied load exceeds the bearing capacity of the soil in that region. It can be clearly seen from the figures that the shear failure contours along the side of the piles forms a straight line from the edge of the raft to the edge of the base of the piles group which overall creates a trapezoidal shape.

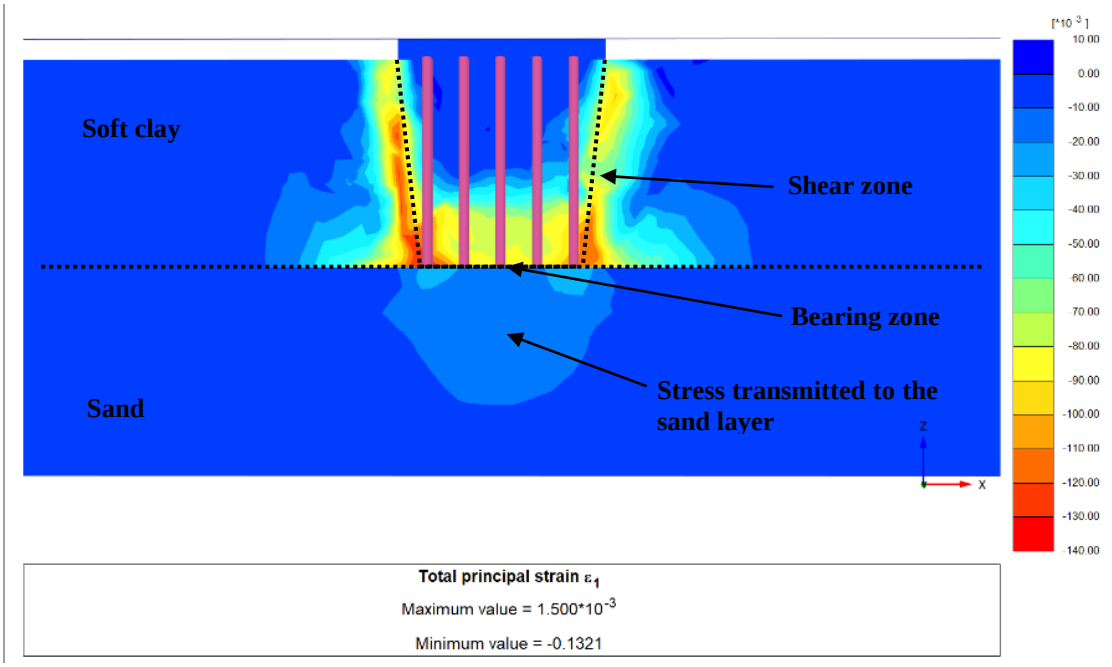


Figure 4.23: Behaviour of piled raft for the case (L/D = 40, S/D = 7, E_p/E_s =52500)

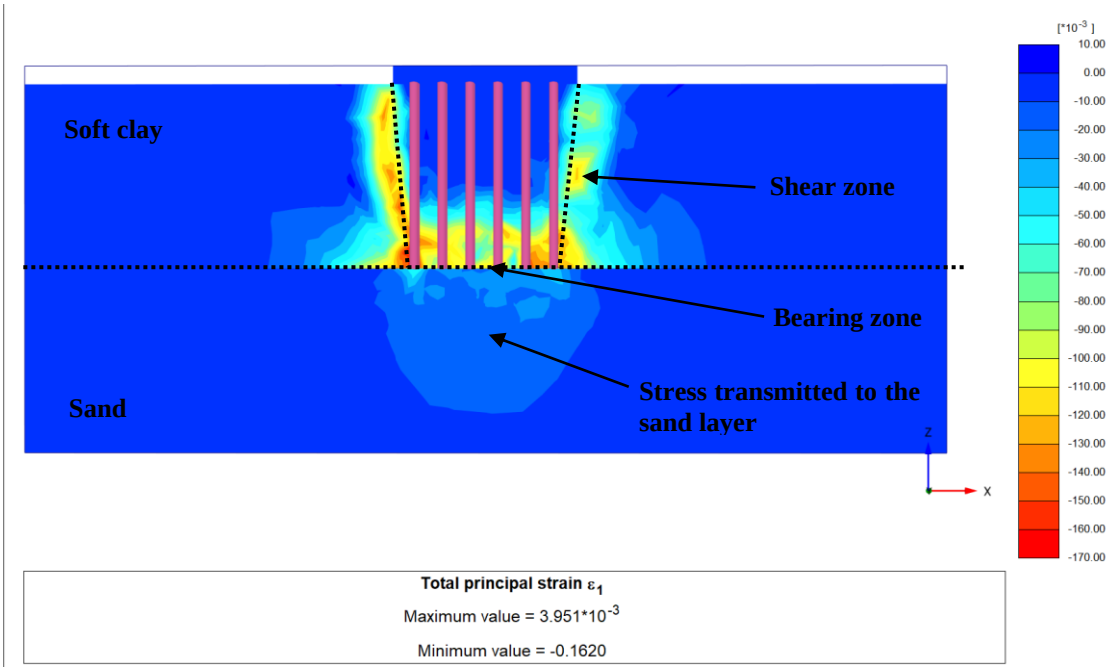


Figure 4.24: Behaviour of piled raft for the case (L/D = 40, S/D = 6, E_p/E_s =52500)

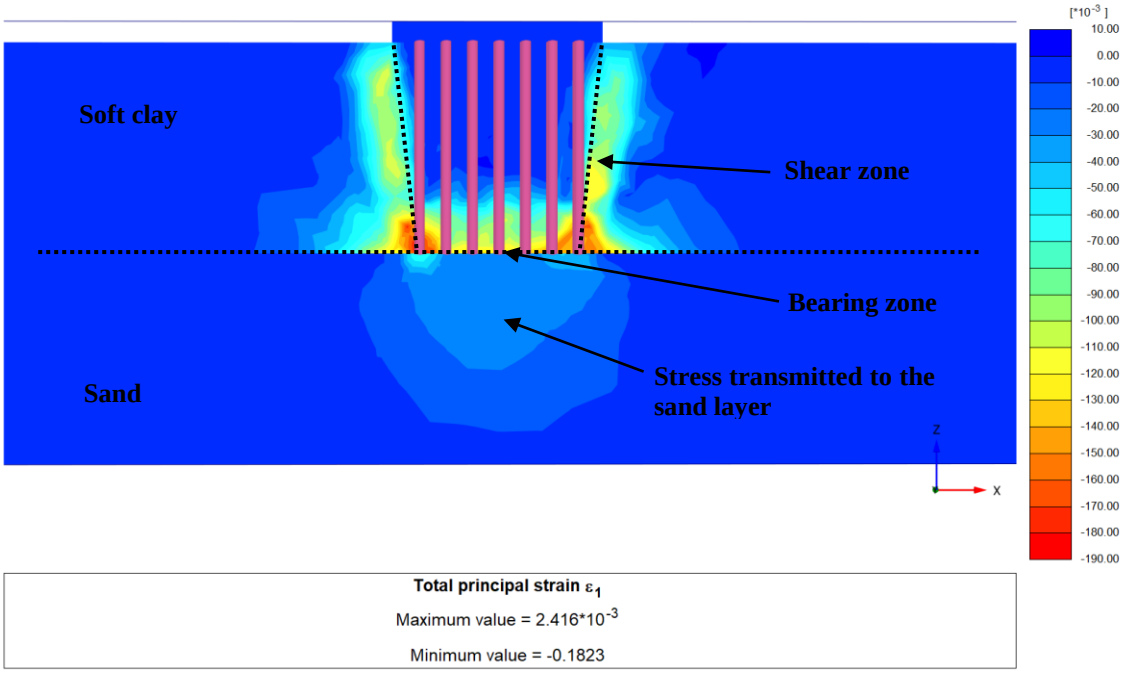


Figure 4.25: Behaviour of piled raft for the case (L/D = 40, S/D = 5, E_p/E_s =52500)

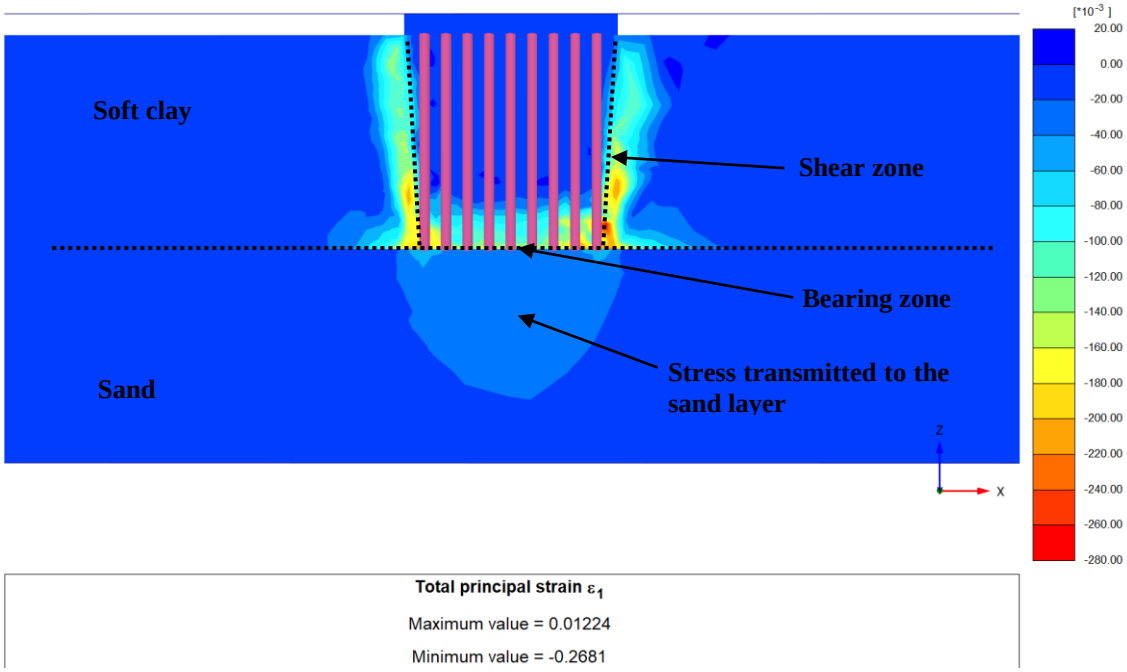


Figure 4.26: Behaviour of piled raft for the case (L/D = 40, S/D = 4, E_p/E_s =52500)

Figure 4.27 shows the comparison of (a) behaviour of piled raft in soft clay under loading and (b) behaviour of stone columns under raft in soft clay under loading. It can be observed from these contour diagrams that the stone columns mostly failed due to shear in

the soil and stone columns under the raft, and the stress do not transmit to the sand layer. Whereas, for piled raft fails with the combination of shear on the side of group of piles and bearing failure at the tip of the pile group and the stresses transmitted to the sand layer beneath the tip of the piles.

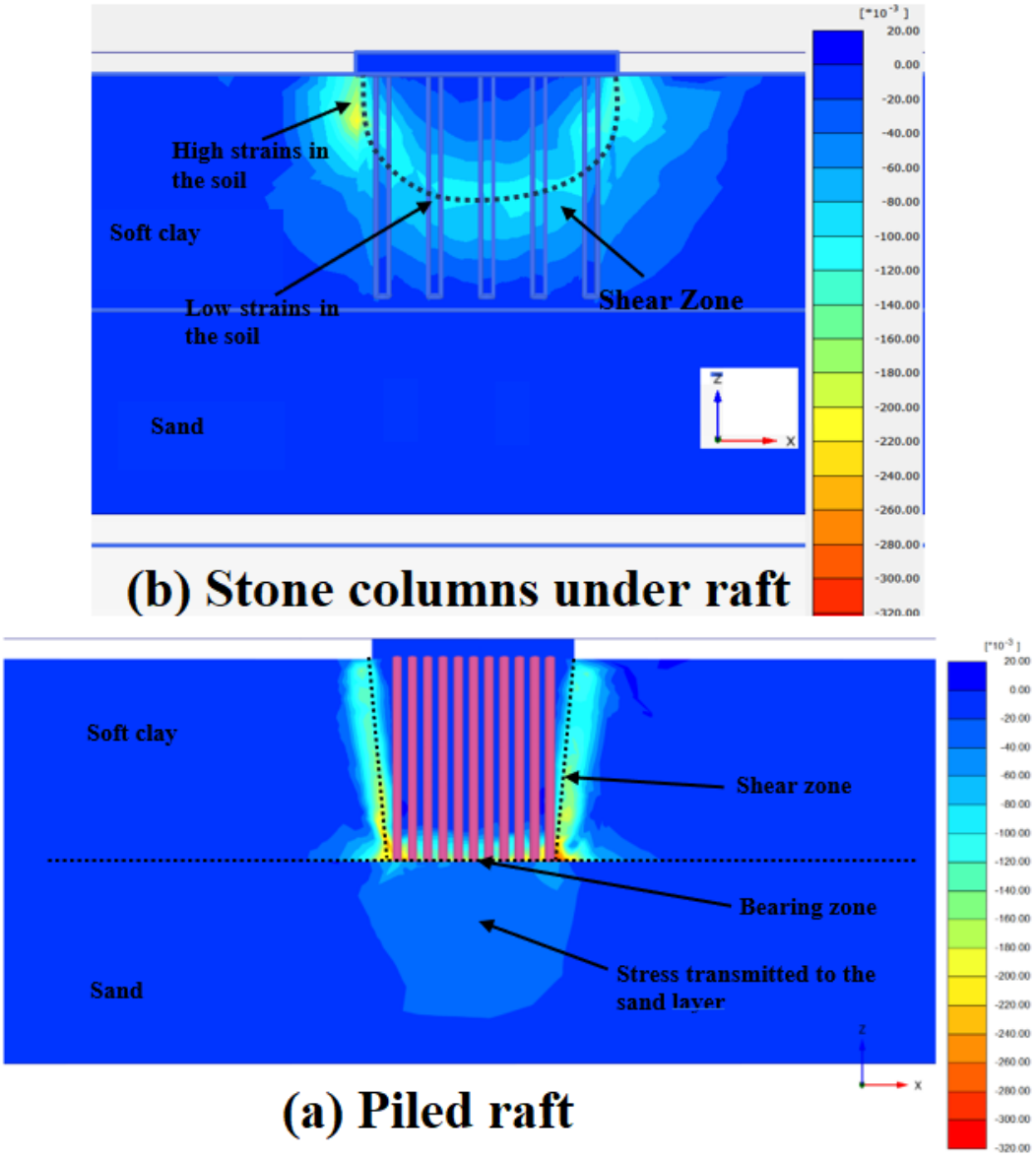


Figure 4.27: (a) Behaviour of piled raft for the case (L/D = 40, S/D = 3, E_p/E_s =52500) and (b) Behaviour of stone columns under raft for the case S/D = 4

4.3.5 Improvement Factor (IF_{PR}) for the Piled Raft Foundation System

To show the effect of pile spacing and its rigidity on the carrying capacity of the piled raft foundation system, the term improvement factor (IF_{PR}) was introduced. It is defined as the ratio between the ultimate carrying capacity of piled raft foundation to that of raft foundation alone. The variation of this improvement factor (IF_{PR}) with the ratios (S/D = 7, 6, 5, 4, 3) and (L/D = 50, 40, 33.33) are presented in Figure 4.28 and Figure 4.29, respectively. It is clearly indicated that the performance of piled raft foundation on soft soil is significantly impacted by the pile spacing. The relationship between (IF_{PR}) and (S/D) can be considered linear (Figure 4.28 and Figure 4.29).

Furthermore, it can be deduced from these figures that, when the spacing to diameter ratio exceeds 10 (S/D> 10), piles have little or no effect on the ultimate carrying capacity of this foundation system. In this case, the raft can be considered as acting alone on the soft soil. Accordingly:

When S/D>10: Raft foundation can be considered as acting alone.

When S/D<10: Carrying capacity of piled raft = Capacity of raft foundation × IF_{PR}

This finding indicates that when the ratio S/D is less than 10, the piled raft foundation concept is a better alternative than the raft foundation alone. Banerjee (1970) concluded that piles interact even beyond distances of 8 diameters. Moreover, the results obtained illustrate that the load carried by a raft increases with a reduction in the pile length and the number of piles, which is in accordance with Elwakil and Azzam (2016). The improvement factor is reduced from 5.25 for S/D = 3 to 2.25 for S/D = 7, which corresponds to a reduction of about 60%.

In the piled raft foundation system, typically the load coming from the superstructure is shared between the raft and piles. When the spacing to diameter ratio exceeds 10, the piles contribute less to load bearing capacity, and a bigger proportion of the load is transferred to the soil (soft clay) through the raft, which makes the raft contributing more or alone in the soft clay. Stone columns in combination with a piled raft foundation in soft clay can potentially complement the spacing to diameter ratio of the piles and can improve the overall performance of the foundation system.

According to the results presented in Figure 4.28 and Figure 4.29, and using a least square regression, the following expression was established for the estimation of the improvement factor of such a foundation system:

$$IF = -a \times \frac{S}{D} - b \times \frac{L}{D} + c \qquad \text{Equation 4.1}$$

$a, b, = \text{Coefficient}$

$c = f\left(\frac{E_p}{E_s}\right)$

$S = Spacing\ of\ piles$

$D = Diameter\ of\ piles$

$L = Length\ of\ piles$

Figure 4.30 and Figure 4.31 show the effect of the ratio between the modulus of elasticity of piles and soft soil (E_p/E_s) on the improvement factor (IF_{PR}). It can be noted from these figures that the improvement factor is lower for piles with higher modulus of elasticity (higher rigidity). This can be explained by the fact that rigid piles penetrate more easily in

the layer of sand situated beneath the layer of soft soil. However, it is worth noting that this ratio is commonly applied as a governing parameter for pile settlement analysis rather than for carrying capacity. For the range of parameters considered in this investigation, the improvement factor (IF_{PR}) can be expressed by:

$$IF_{PR} = \left(4.3 \times 10^{-6} \frac{E_p}{E_s} - 1.1\right)\frac{S}{D} - \left(4 \times 10^{-5} \frac{E_p}{E_s} - 8.2\right) \qquad \text{Equation 4.2}$$

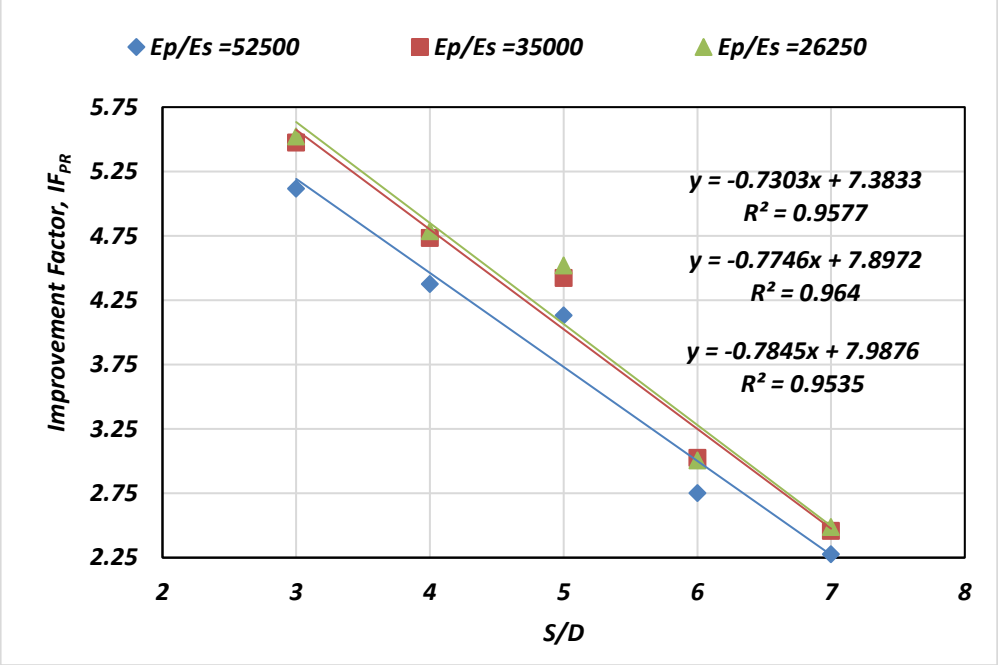


Figure 4.28: Variation of the improvement factor (IF_{PR}) as a function of *S/D* and *L/D* = 50

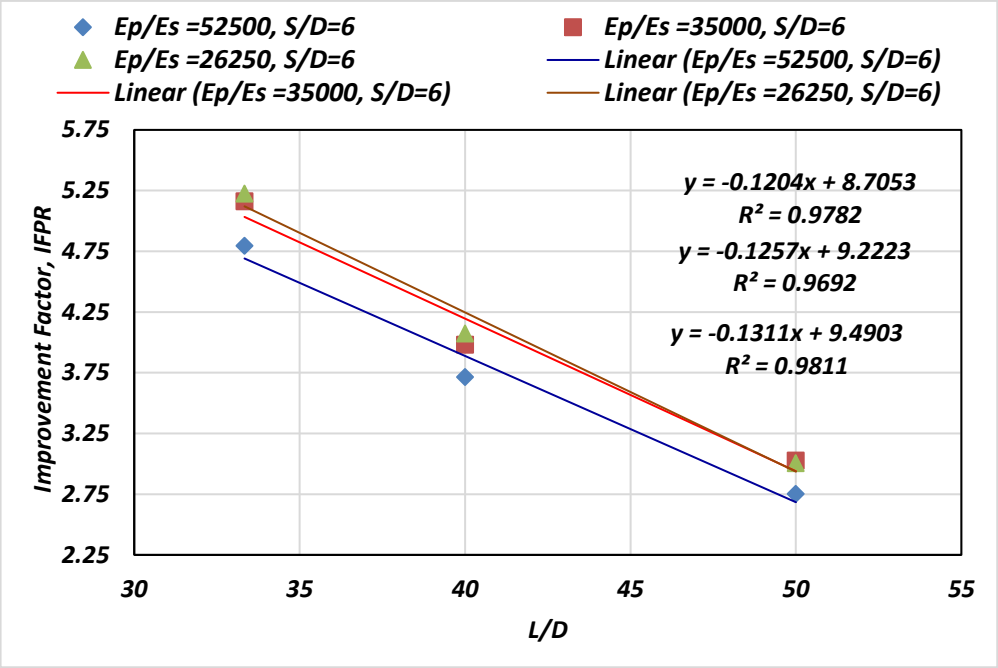


Figure 4.29: Variation of the improvement factor (IF_{PR}) as a function of L/D and S/D = 6

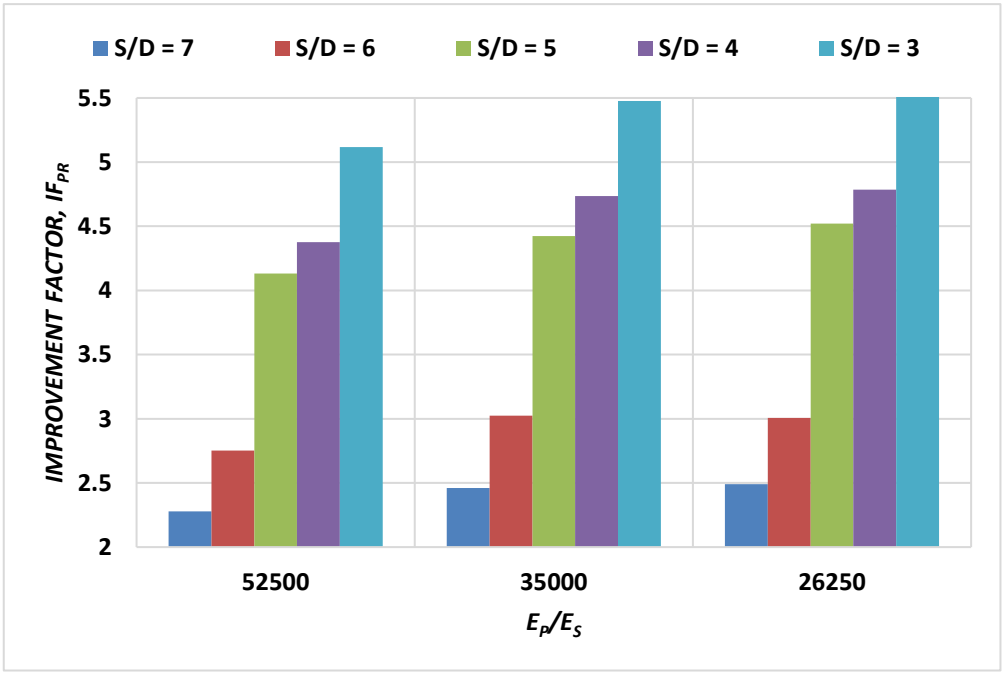


Figure 4.30: Variation of the improvement factor (IF_{PR}) as a function of E_p/E_s and L/D = 50

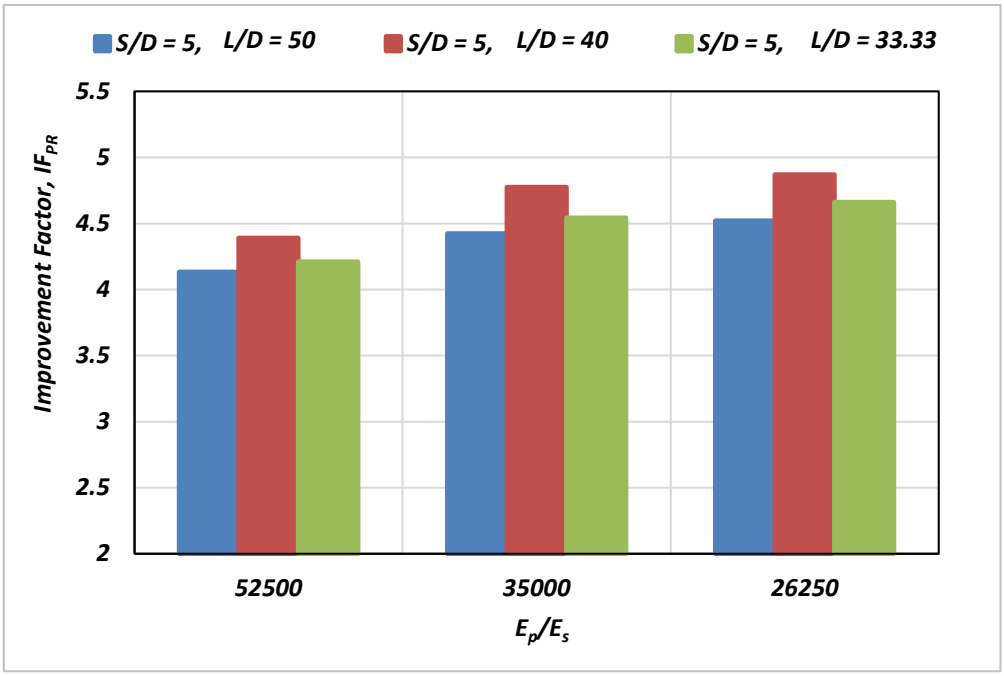


Figure 4.31: Variation of the improvement factor (IF_{PR}) as a function of E_p/E_s and S/D = 5

4.4 Parametric Study of Combined Stone Column/Piles Caped with Raft Foundation in Soft Soil

For the parametric study of combined stone columns/piles caped with raft foundation in soft clay, 34 different configurations (sets) were used as shown in Figure 3.20. The basic model consists of 20m x 20m square raft foundation resting on the soft clay treated with group of 25 stone columns and piles combined in a square form and over all underlined by the thick layer of sand as given in Figure 3.18 and Figure 3.19. Out of 34 configurations (sets), different sets were grouped and total 11 groups were created based on the number of piles in each group as shown in Table 3.6. Furthermore, every set was considered for 20 combinations depending on the parameters (i.e., stone columns/pile length, diameter, materials properties of soils and columns) as given in Table 3.7.

Overall, 680 combinations were investigated for this parametric study, the parameters and the material properties used in this investigation are given in Table no. 3.8 and Table 3.8.

4.4.1 Effect of Configuration of Combined Foundation

To study the effect of configuration on the performance of combined foundation system 34 sets with different configuration were selected. Each configuration has 25 pile/columns combined under raft except the set 1 and set 34 which have only stone columns and piles under raft, respectively. Each one of the sets has a unique arrangement of stone column and piles combined under raft from one another as shown in Figure 3.20.

The stress strain relation (Stress Vs Strain) for the combined foundation system were established for 34 different sets for each combination. The stress strain relation for combination 1 is presented in Figure 4.32 and the stress strain relations for the remaining combinations are shown in Appendix C. Significant difference of carrying capacity can be noted between stone columns with raft foundation (set 1) and piled raft foundation (set 34). Also, the results show that with the increase in number of piles in configurations (sets) increases the overall capacity of combined foundation system in clayey soil. The stress-strain curves of the combined foundation does not show any clear sign of failure; therefore, Chin's stability method (Chin, 1970) is used to predict the ultimate carrying capacity of the foundation system as shown in Figure 4.33 (the remaining plots for all other combinations are presented in Appendix D).

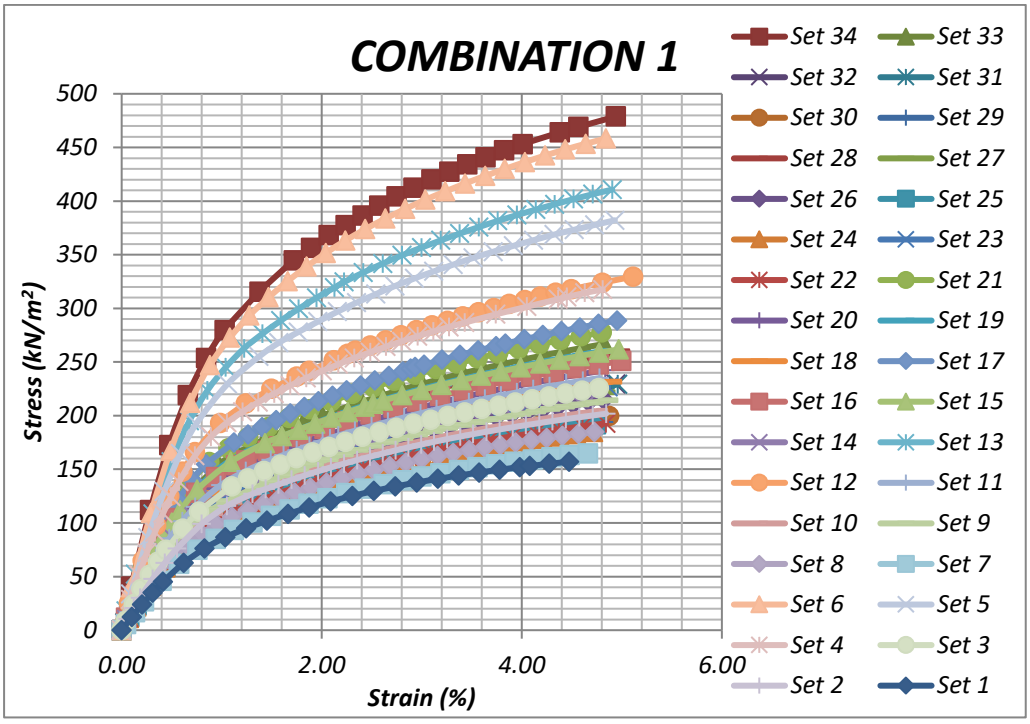


Figure 4.32: Stress Vs Strain for combined foundation (combination 1)

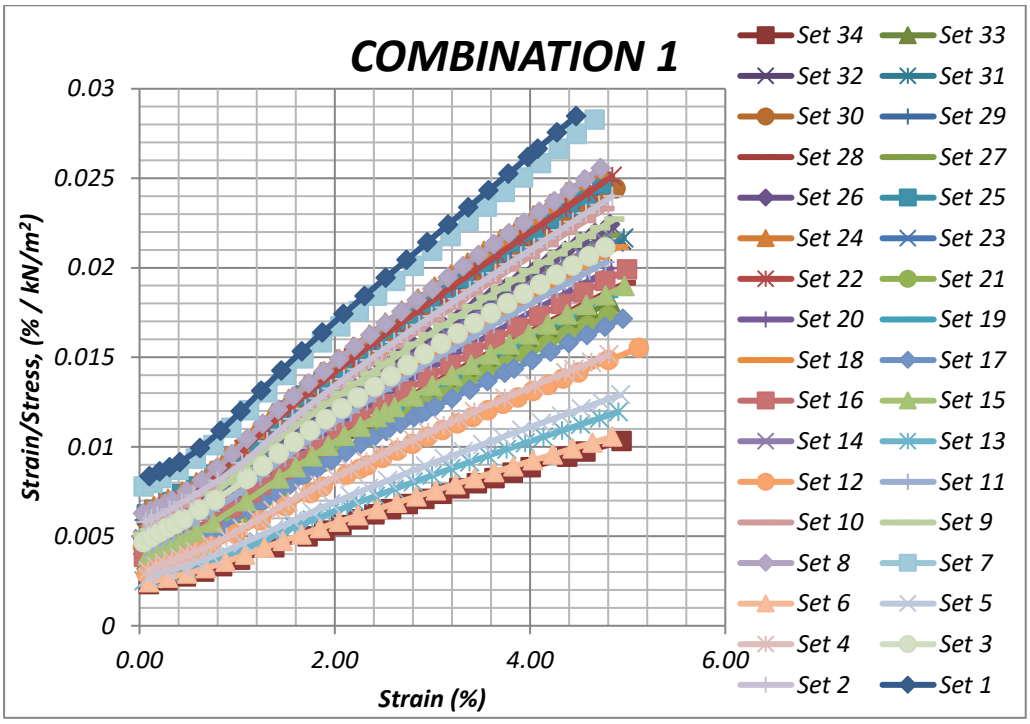


Figure 4.33: Strain/Stress Vs Strain (Chin, 1970) for combined foundation (combination 1)

Furthermore, after finding the ultimate carrying capacity using Chin's method, all 34 configurations (sets) of the combined foundation were presented in column charts to observe the comparison of their ultimate carrying capacity for all 20 combinations as given in Figure 4.34 for the first combination and the comparisons for the remaining combinations are presented in Appendix E. As mentioned before, these charts present the same observations that is configurations (sets) with increasing number of piles increases the carrying capacity of the combined foundation systems (increases the capacity of raft foundation with stone columns ranging between 3.5% to 180%). Set number 6, 13 and 34 have the highest possible number of piles and they show the major differences in their capacities with other configurations (sets).

Sets can be categorised based on their carrying capacity, it can be observed from the chart that sets can be divided into to three categories high (q_u between 500-700 kN/m^2), moderate (q_u between 300-500 kN/m^2), and low (q_u between 200-300 kN/m^2). It can be noticed from these categories that there are different range of number piles used in each category. In the high category the number of piles used are ranging between 21-20 piles, for moderate category the number of piles used are ranging between 12-20 piles, and for low category the number of piles used ranging between 0-9 piles, this indicates that the carrying capacity of the combined foundation system is increasing with the increasing number of piles.

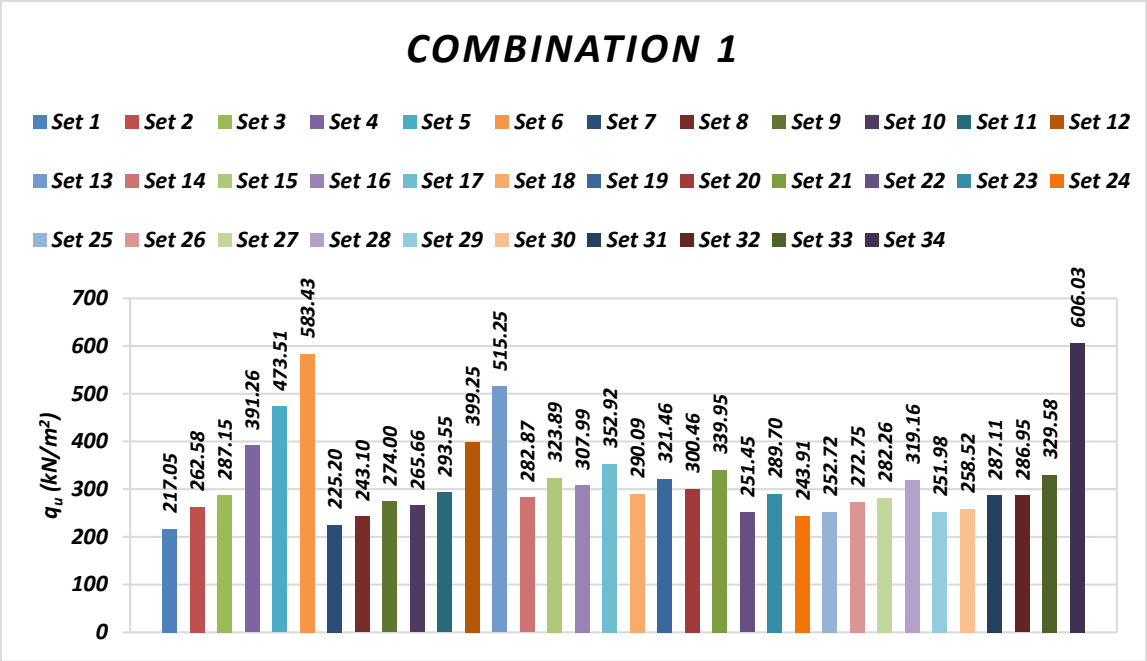


Figure 4.34: Ultimate carrying capacities for combined foundation (combination 1)

4.4.2 Effect of Diameter of Stone Column and Pile

The diameter of stone columns and piles is one of the dominating variables in this parametric study of combined foundation systems, which can influence the performance of this foundation system. To study the effect of stone columns and piles diameters three diameter of piles to diameter of stone columns ratio (D_p/D_c) were selected (D_p/D_c = 0.6, 0.5, 0.4). To clearly show the effect of diameter ratio of piles and stone columns (D_p/D_c) on the ultimate carrying capacity of the combined foundation system, the term improvement factor (*IF*) was introduced, it is defined as the ratio between the ultimate carrying capacity of combined foundation to that of raft foundation with stone columns only. For this purpose, four graphs with different L_p/L_c (i.e., length of pile to length to stone column) were established for the relation of improvement factor (*IF*) versus the area ratio of piles and stone columns ($n_A = \sum Ap/\sum Ac$ = total area of piles over total area of stone columns under the raft) with varying set of diameter ratio (D_p/D_c). Each point of the different curves shown in these

figures was identified by its corresponding group number. Only chief sets were considered in the construction of these individual curves.

It can be observed from Figure 4.35, Figure 4.36, Figure 4.37, and Figure 4.38 that with increasing the diameter ratio (D_p/D_c, with increasing D_p) the area ratio ($n_A = \sum A_p/\sum A_c$) increases which improves the overall performance of combined foundation system as well as improvement factor (*IF*). Samanta and Bhowmik (2017) reported that the performance of the whole combined foundation system improved when the area replacement ratio increased. The diameter of the stone columns and piles can affect the overall bearing capacity of the foundation system. Larger diameter elements generally provide higher bearing capacity, allowing for increased structural loads to be safely supported.

A general divergence can be seen in the curves from *IF* = 1.4, means the curves are very close to each other in the first few groups (group 1 to 5) and after *IF* = 1.4 the difference between groups increases, this is because in the first few groups the number of piles are less and the difference between area ratio ($n_A = \sum A_p/\sum A_c$) is small, but after group 5 the difference between area ratio ($n_A = \sum A_p/\sum A_c$) increases due to more number of piles in each group increases, which shows the divergence in the curves from *IF* = 1.4. Also a curving of plots towards the plateau can be observed in these curves when L_c/L_p = 0.9, 0.8, 0.6. and on the other hand the curves continued to rise when L_c/L_p = 1, which shows that the length of stone column is dominating in the performance of combined system and can contribute until the critical length L_c/L_p = 0.6.

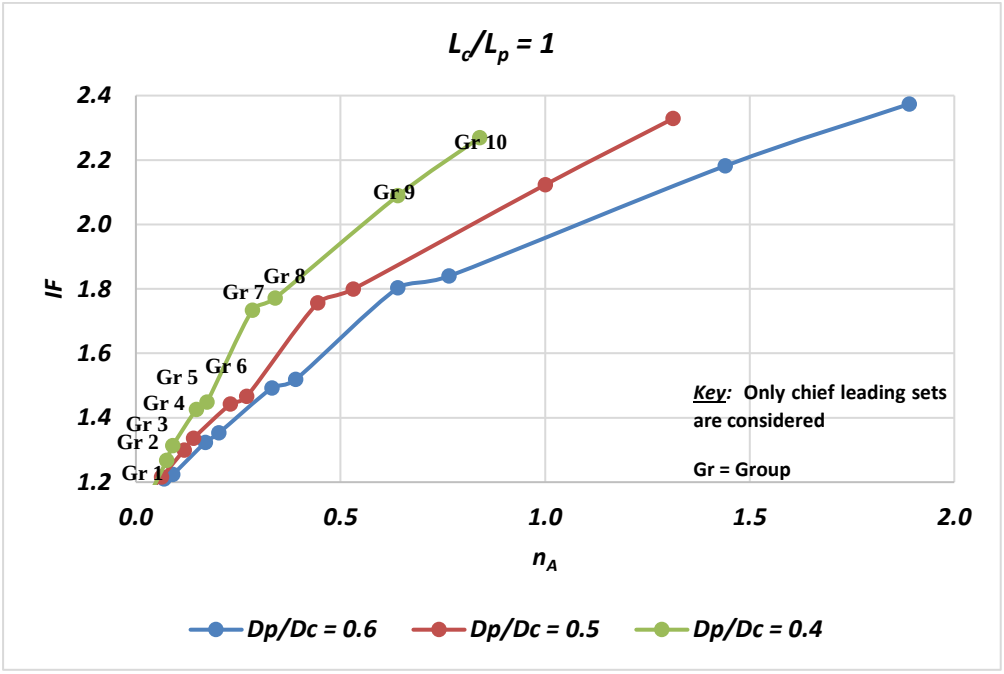


Figure 4.35: *IF* VS n_A f as a function of L_c/L_p = 1, and D_p/D_c

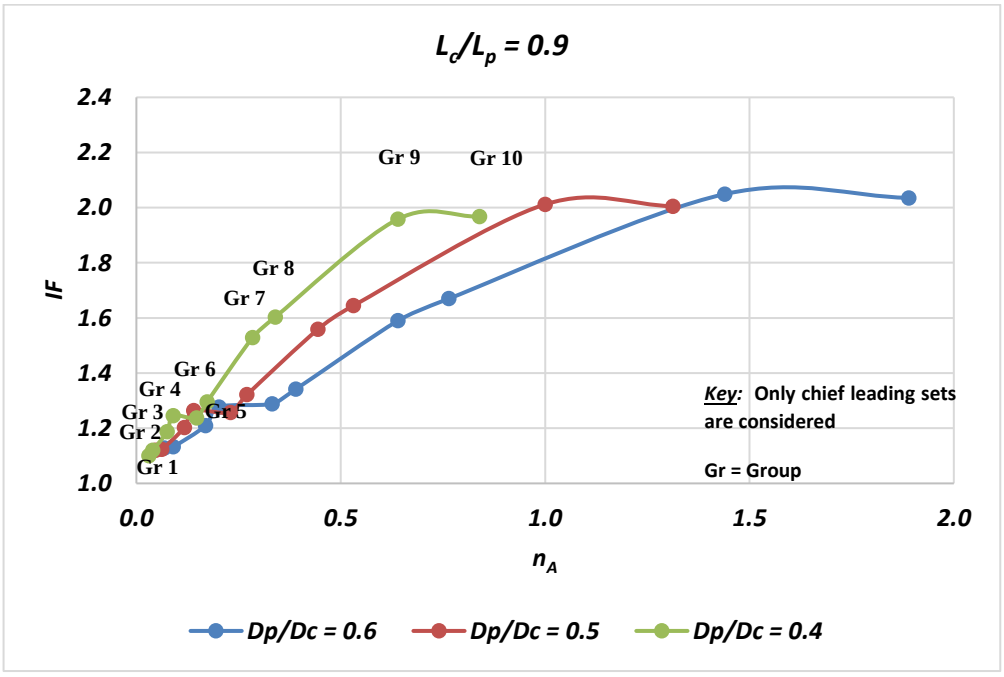


Figure 4.36: *IF* VS n_A as a function of L_c/L_p = 0.9, and D_p/D_c

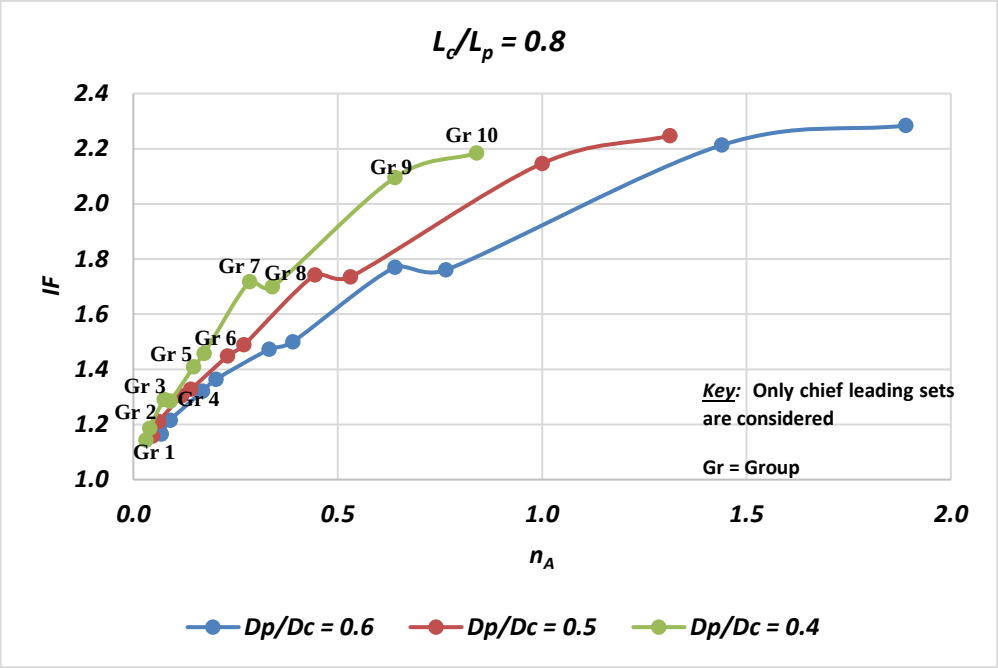


Figure 4.37: *IF* VS n_A as a function of L_c/L_p = 0.8, and D_p/D_c

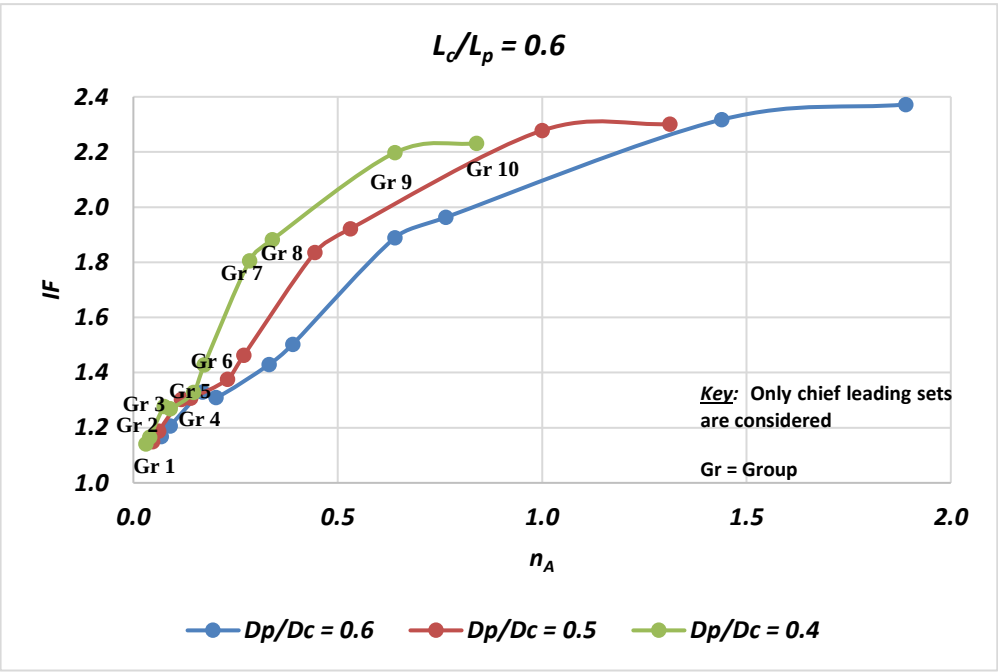


Figure 4.38: *IF* VS n_A as a function of L_c/L_p = 0.6, and D_p/D_c

4.4.3 Effect of Length of Stone Column and Pile

To study the effect of length of stone columns and piles on the performance of combined foundation system, four different length ratios of stone columns and piles (L_c/L_p)

were selected (i.e., L_c/L_p = 1, 0.9, 0.8, 0.6). Therefore, three graphs with varying D_p/D_c (i.e., diameter of pile to diameter of stone column ratio) were established for the relation of improvement factor (*IF*) and area ratio of piles and stone columns ($n_A = \sum Ap/\sum Ac$ = total area of piles to total area of stone columns under raft) for each set of length ratios of stone columns and piles (L_c/L_p) as shown in Figure 4.39, Figure 4.40, and Figure 4.41. Each point of the different curves shown in these figures was identified by its corresponding group number. Only chief sets were considered in the construction of these individual curves. It can be observed from each graph, that with the decrease in length ratios of stone columns and piles (L_c/L_p) the improvement factor (*IF*) increases. This can be attributed to the fact that, beyond the critical length (L_c equal to six times D_c) stone columns do not contribute extra benefit improvement factor (*IF*) but they help to reduce settlement by penetrating the firm layer of soil, reported by (Ayadat, 2022), Furthermore, a similar trend can also be observed in these graphs which illustrate that the improvement factor (*IF*) increases with the increase in the area ratio ($n_A = \sum Ap/\sum Ac$).

A general decline of the improvement factor (*IF*) can be noticed from these curves with the decrease in the diameter ratio (D_p/D_c), this is because as the pile diameter decreases, the available surface area for skin friction decreases which can leads to a decrease in the skin friction resistance and it can also results in reducing the piles ability to resist axial and lateral loads, which can reduce its contribution to the overall load-bearing capacity of the foundation. These curves also show that there is a sharp rise in improvement factor (*IF*) from group 5-7 this is because the number of piles in these groups increases from 12 to 16 which shows big change in improvement factor (*IF*). Also the curve stabilizes from group 9 to group 10 this is because the difference in the number of piles in these group is 1 pile (group 9 has 20 piles and group 10 has 21 piles respectively).

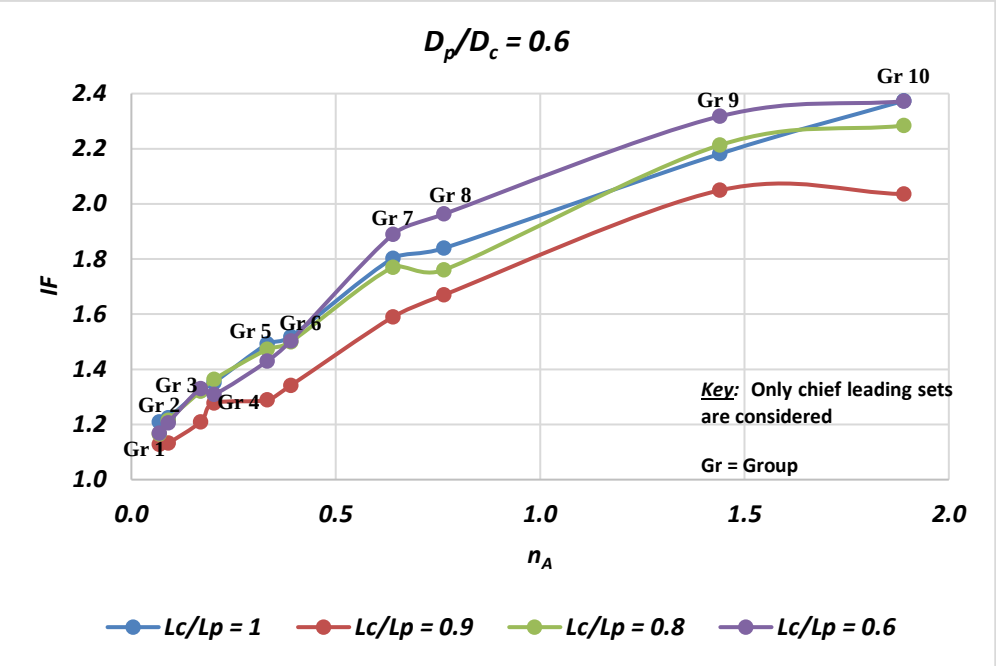


Figure 4.39: *IF* VS n_A as a function of D_p/D_c = 0.6, and L_c/L_p

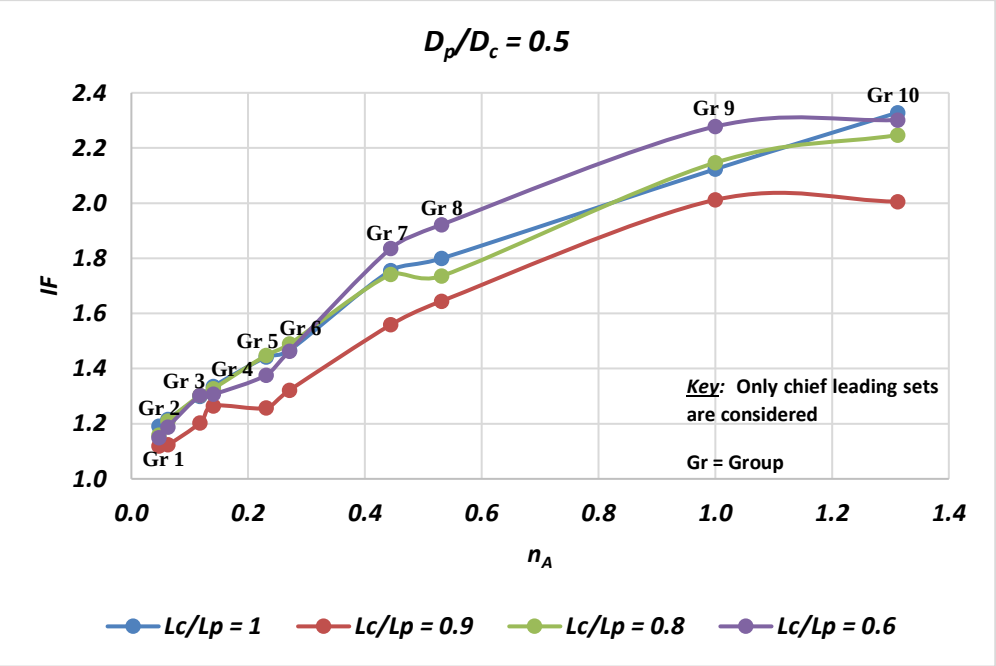


Figure 4.40: *IF* VS n_A as a function of D_p/D_c = 0.5, and L_c/L_p

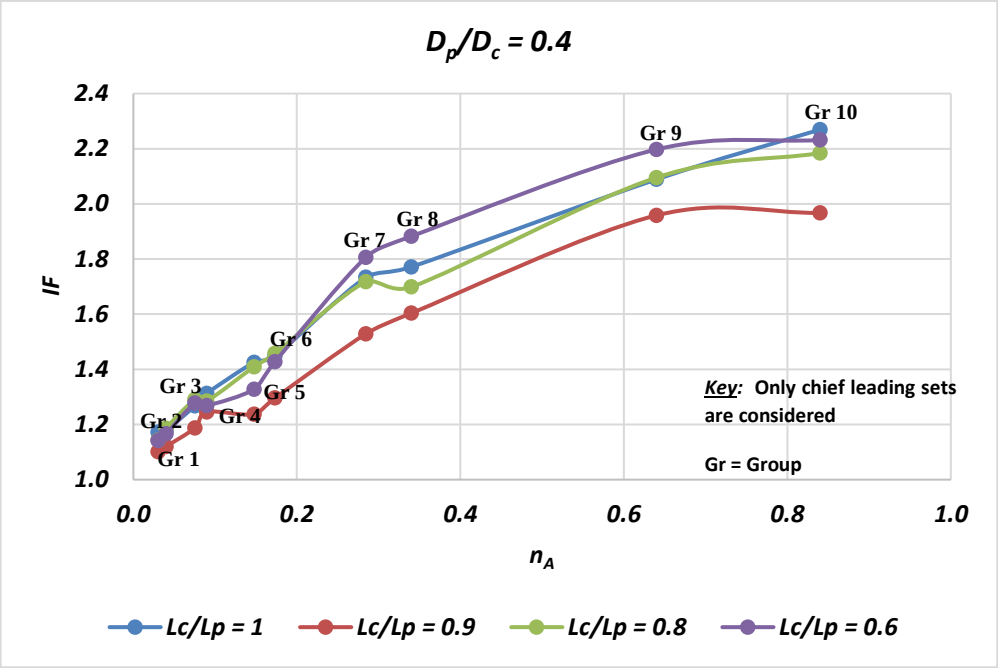


Figure 4.41: *IF* VS n_A as a function of D_p/D_c = 0.4, and L_c/L_p

4.4.4 Effect of Modulus of Elasticity of Soil

Modulus of elasticity of soil in combined foundation system is one of the influencing mechanical properties that can affect the performance of this foundation system. For this study only modulus of clay soil is considered to examine the performance of combined foundation system under the load. To study the influence of modulus of elasticity of soft clay soil three values were selected (E_s = 4, 6, and 8 MPa). Therefore, two graphs with different length ratios of stone columns and piles (L_c/L_p) were established for the relation of improvement factor (*IF*) versus the area ratio of piles and stone columns ($n_A = \sum Ap/\sum Ac$ = total area of piles to total area of stone columns under raft) with varying sets of rigidity ratio (i.e., sum of modulus of elasticity of piles and columns to modulus of elasticity of soil ratio = $((E_p + E_c)/E_s)$ as shown in Figure 4.42, and Figure 4.43. Each point of the different curves shown in these figures was identified by its corresponding group number. Only chief sets were considered in the construction of these individual curves. It can be illustrated from both

graphs that the improvement factor (*IF*) slightly increases with decrease in the rigidity ratio ($(E_p + E_c)/ E_s$).

This shows that with the increase in the modulus of elasticity of the soft clay soil the distribution of the load among the piles and the stone columns can be uniform which can enhance the performance of the foundation system, similar findings are presented in the parametric study of piled raft foundation in the present research. These curves show a sharp rise in improvement factor (*IF*) from group 5-7 because the number of piles in these groups increases from 12 to 16. It also shows that the curve stabilizes from group 9 to group 10 this is because the difference in the number of piles in these group is 1 pile (group 9 has 20 piles and group 10 has 21 piles respectively).

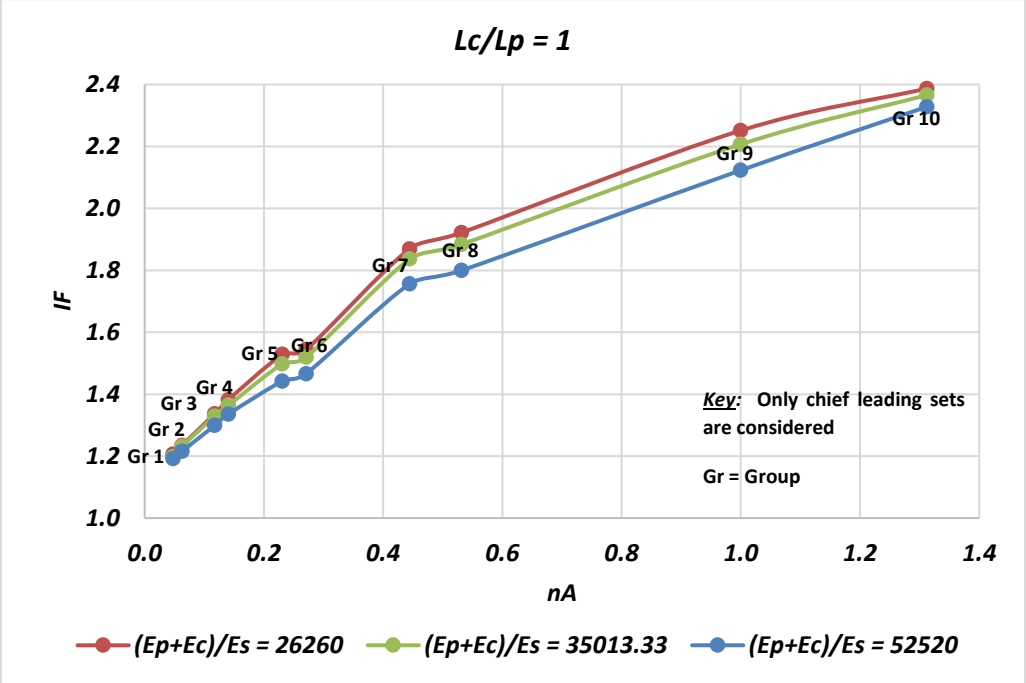


Figure 4.42: *IF* VS n_A as a function of L_c/L_p = 1, and $(E_p + E_c) / E_s$

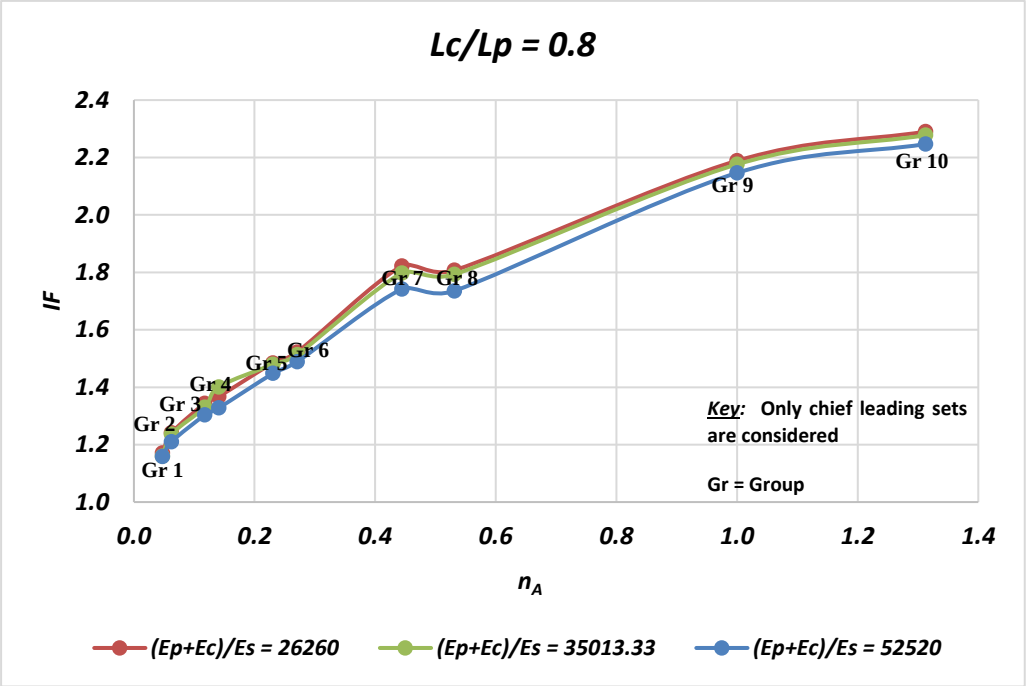


Figure 4.43: *IF* VS n_A as a function of for L_c/L_p = 0.8, and $(E_p + E_c) / E_s$

4.4.5 Effect of Angle of Friction of Stone Column

Angle of friction can also have a considerable effect on the performance of the foundation system. Therefore, certain range angle of friction of stone columns are considered to examine the performance of this combined foundation system. To study the influence of angle of friction of stone columns three values were selected (φ_c = 42°, 45°, and 48°). To do so, two graphs with different length ratios of stone columns and piles (L_c/L_p) were established for the relation of improvement factor (*IF*) versus the area ratio of piles and stone columns ($n_A = \sum Ap/\sum Ac$) for each set of angles of friction of stone column (φ_c) as shown in Figure 4.44, and Figure 4.45. Each point of the different curves shown in these figures was identified by its corresponding group number. Only chief sets were considered in the construction of these individual curves.

A similar trend can be observed in these graphs which illustrate that the improvement factor (*IF*) increases with the decrease in the angle of friction of stone columns. This is

because improvement factor (*IF*) is the ratio of carrying capacity of stone column/pile combined under raft to the carrying capacity of raft on stone columns, so when the angle of friction of stone columns increases it increases the carrying capacity of raft on the stone columns alone which reduces the overall the improvement factor (*IF*) with respective area ratios of piles and columns ($n_A = \sum Ap/\sum Ac$).

Angle of friction of stone columns represents the internal friction between the individual particles of stone columns, increasing the angle of friction of stone columns can affect and improve the load-bearing performance of the foundation, with bigger values of angle of friction, the stone columns can better resist the shear force which can enhance the overall performance of the foundation system. Similar findings are presented in the parametric study of stone columns under raft foundation in the present research.

These curves also show different stages in improvement factor (*IF*), there is a general rise observed in the improvement factor (*IF*) between the groups, but the most notable stages are in between group 5 to 6, group 7 to 8, and group 9 to 10. For group 5 to 6 and group 7 to 8 difference between the number of piles in each group is one, for this case the dominating factor to influence the improvement factor (*IF*) can the length of stone columns, soil properties, and configuration of the piled raft system. For group 9 to 10 the curve stabilizes this can be due to the difference in the number of piles in these group is 1 pile (group 9 has 20 piles and group 10 has 21 piles respectively) and critical length of the stone columns.

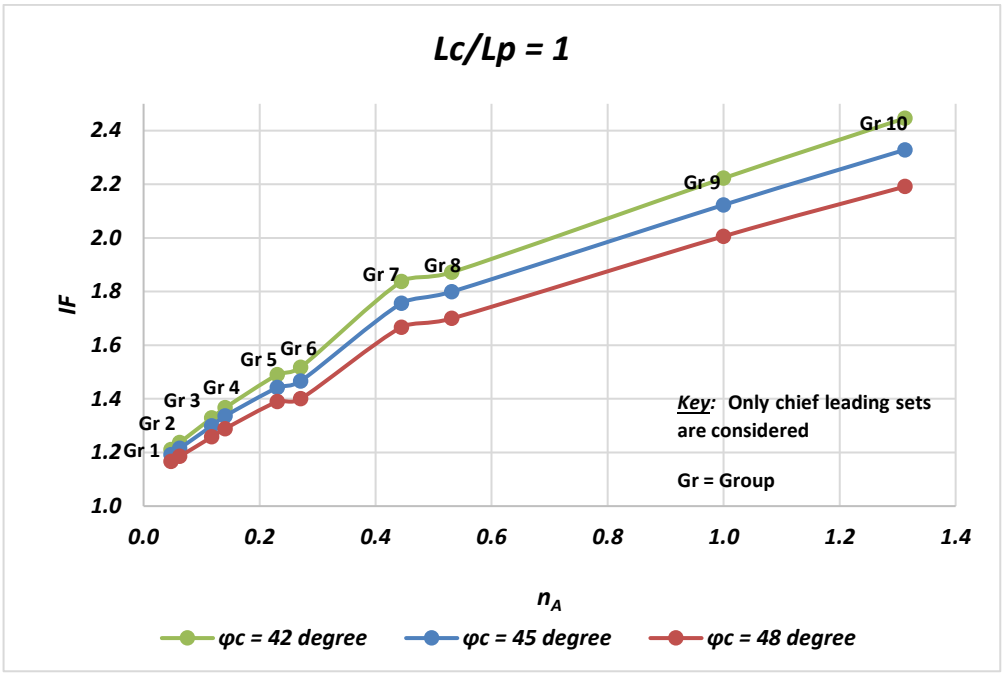


Figure 4.44: *IF* VS n_A as a function of L_c/L_p = 1, and φ_c

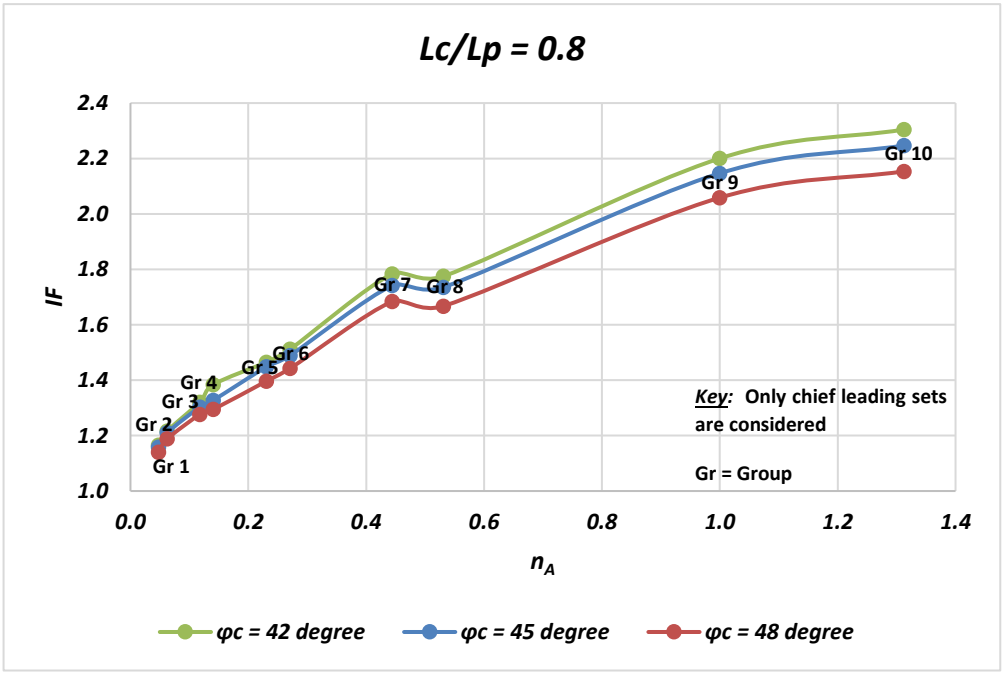


Figure 4.45: *IF* VS n_A as a function of L_c/L_p = 0.8, and φ_c

4.4.6 Optimization Study

As discussed earlier 34 configuration or sets of stone columns/piles combined under the raft were considered for all 20 combinations depending on the dimensions of stone columns/piles and properties of stone columns material and soft soils.

All 34 configurations or sets were grouped into 11 groups based on the number of piles present in each configuration as shown in Figure 3.20, a detail optimization study was conducted on these 11 groups through 34 sets for each combination. A total of 680 finite element model simulations were tested and studied for the combined foundation system in soft soils and ultimate carrying capacities of these different models were determined using Chin's method (Chin, 1970).

Furthermore, improvement factor (*IF*) was introduced and calculated for all 680 models which is defined as the ratio between the ultimate carrying capacity of combined foundation to that of raft foundation with stone columns only, after calculating the improvement factor (*IF*) for all 680 sets, leading sets with highest improvement factor (*IF*) in each group for all 20 combinations were selected as shown in Appendix F. The optimization study to find the chief leading set is conducted based on the highest improvement factor (*IF*).

Typical results for the leading 20 combinations of all 11 groups are shown in Figure 4.46, Figure 4.47, Figure 4.48, Figure 4.49, Figure 4.50, Figure 4.51, Figure 4.52, Figure 4.53, Figure 4.54, Figure 4.55, and 4.56, each chart shows the leading chief set of their group having the highest improvement factor (*IF*) and foremost profound set in each group are presented in Table 4.2. In this table 11 leading sets were compared based on their improvement factor (*IF*) and sets 28, 33, 4, and 12 were selected as the chief leading sets.

Sets 28 and 33 have the similar layout because the piles in these sets were positioned in the center of the raft in the form of a plus sign (+). While, in layout of sets 4 and 12, the piles are positioned on the edges of raft as given in Figure 3.20. The configuration of these chief leading sets show that the stone columns and piles are arranged in a way that somehow the stone columns are confined between the piles and piles are placed on the edge of the raft. Placing stone columns between the piles can improve the load distribution. By confining the stone columns between the piles, the load from the raft can be distributed more evenly and can reduce the stress concentration on individual piles and the raft itself. Micheál and Bryan (2014) reported that when stone columns placed near the edge of raft, their ability to influence the load distribution and settlement patterns can diminished.

Placing piles on the edge of the raft can helps to distribute the applied loads more evenly across the raft. By providing additional load-bearing elements at the perimeter of the raft, the piles can help in reducing stress concentrations and improve load distribution which can result in improving overall load-carrying capacity of combined foundation.

It is important to note that although sets 5, 13 and 16 have the highest improvement factor, but they were not selected because in this case stone columns are almost 100% replaced with piles, which is not the purpose of the present investigation. On the other hand, sets 2, 10, 3, and 11 were discarded because they have lower improvement factor. It is imperative to note that the chief leading sets (i.e., sets 28, 33, 4, and 12) have better performance than the raft foundation resting on stone columns only. It was deduced that according to the obtained values of the improvement factor, the chief leading sets can increase the bearing capacity of the raft foundation by almost 50% to 90% (Table 4.2) compared to that of raft foundation resting on stone columns only.

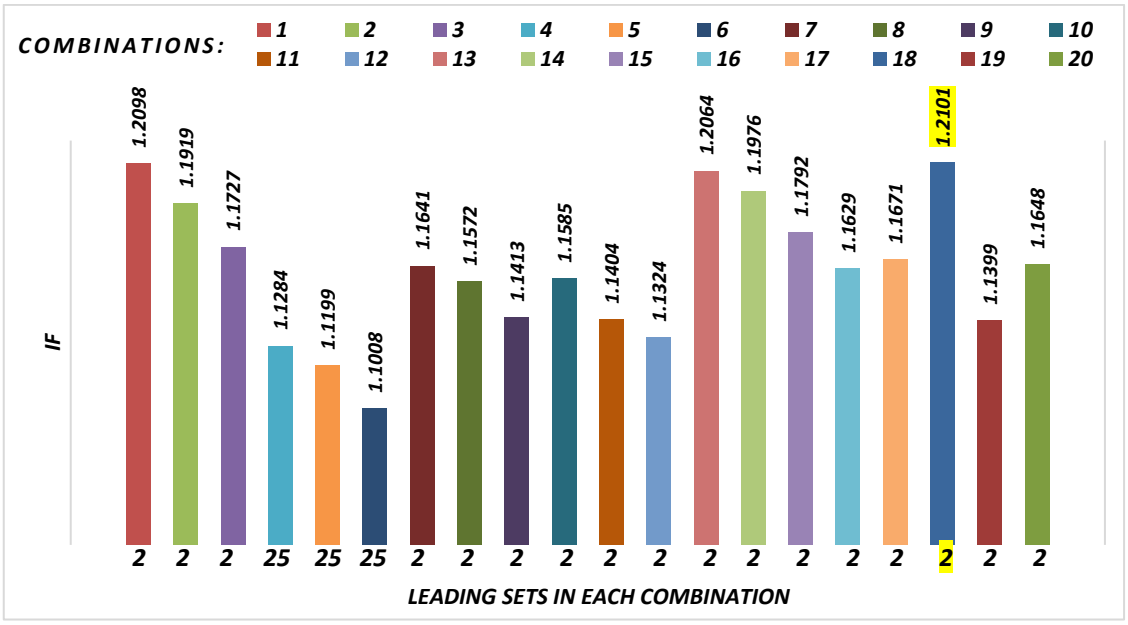


Figure 4.46: Improvement factor (*IF*) for group 1

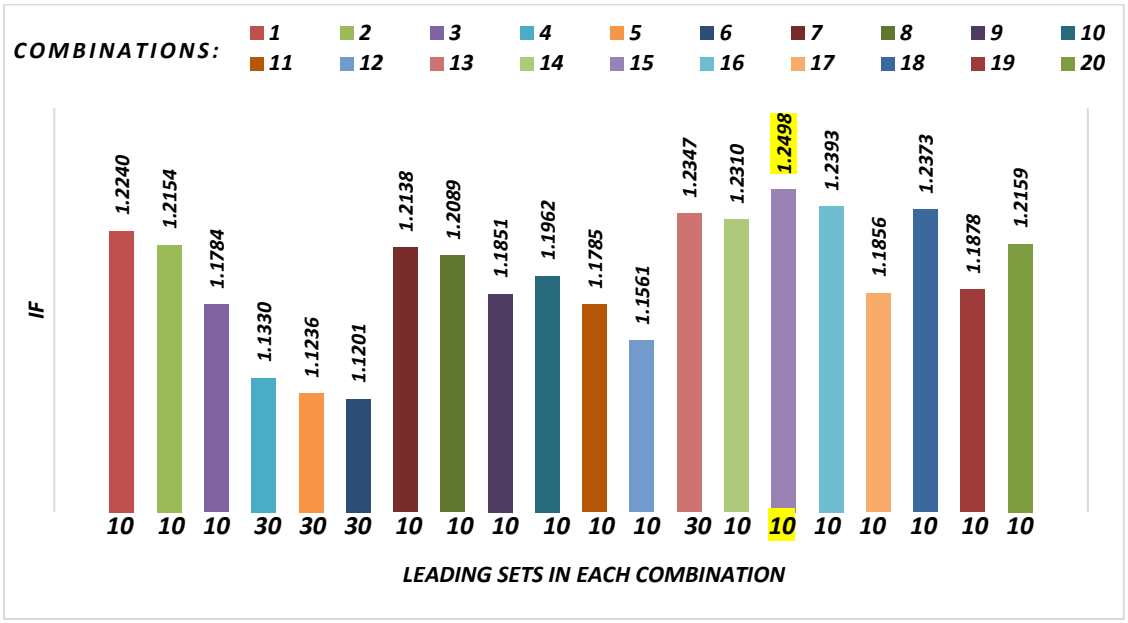


Figure 4.47: Improvement factor (*IF*) for group 2

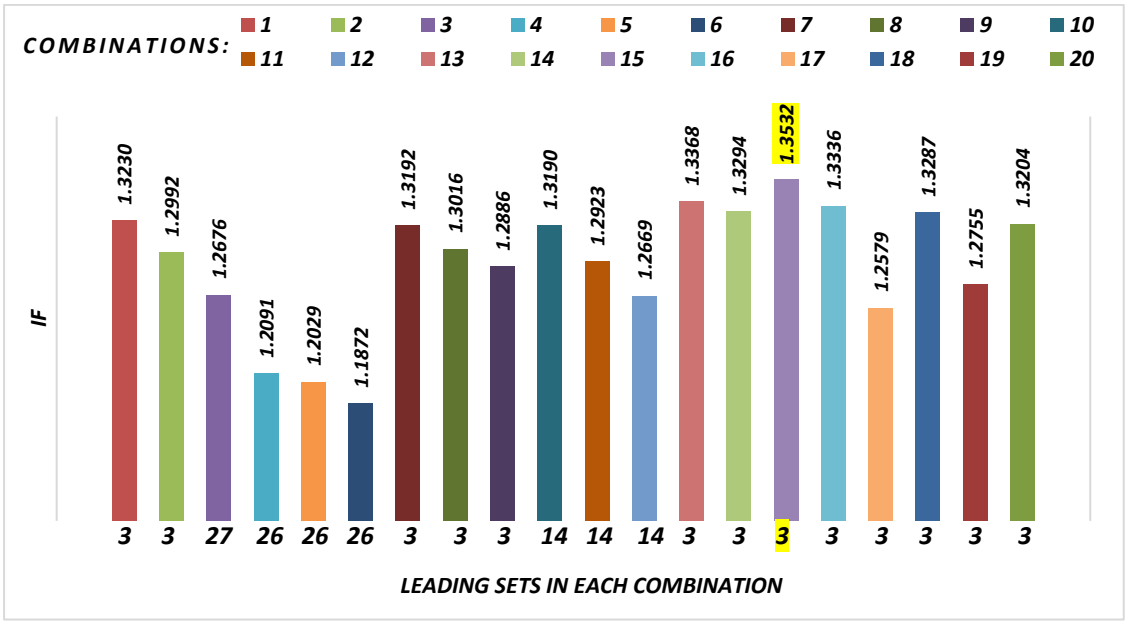


Figure 4.48: Improvement factor (*IF*) for group 3

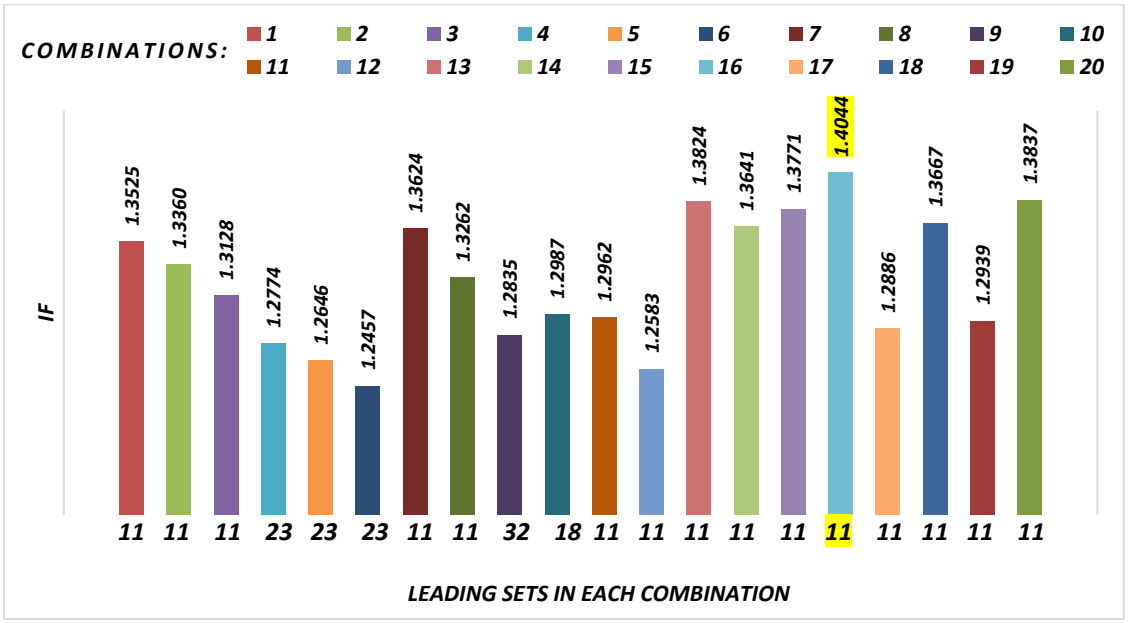


Figure 4.49: Improvement factor (*IF*) for group 4

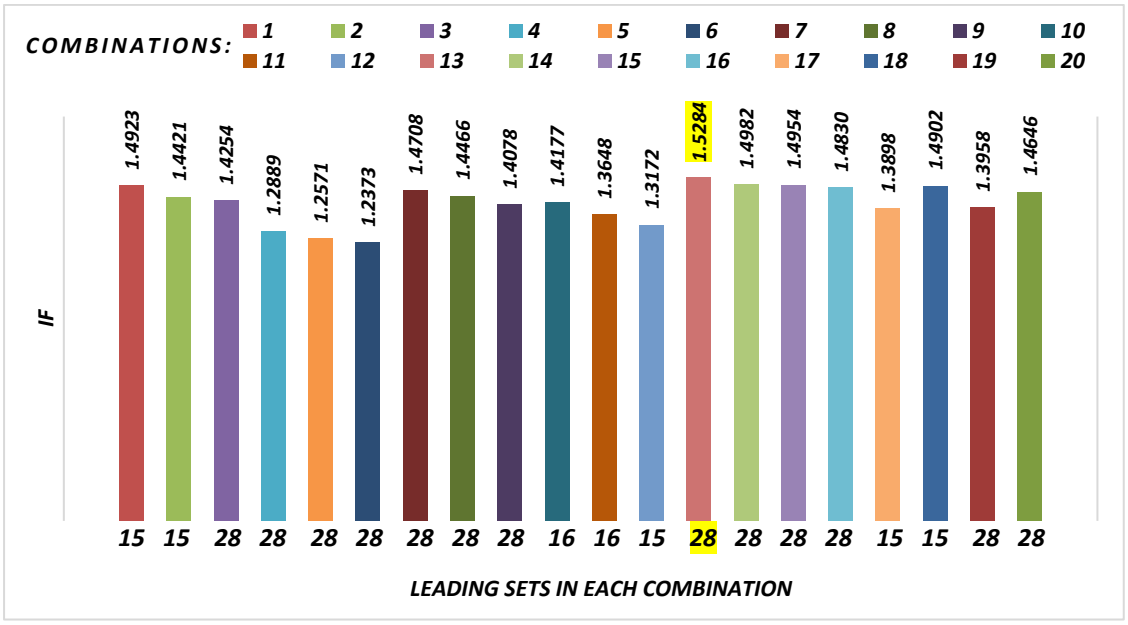


Figure 4.50: Improvement factor (*IF*) for group 5

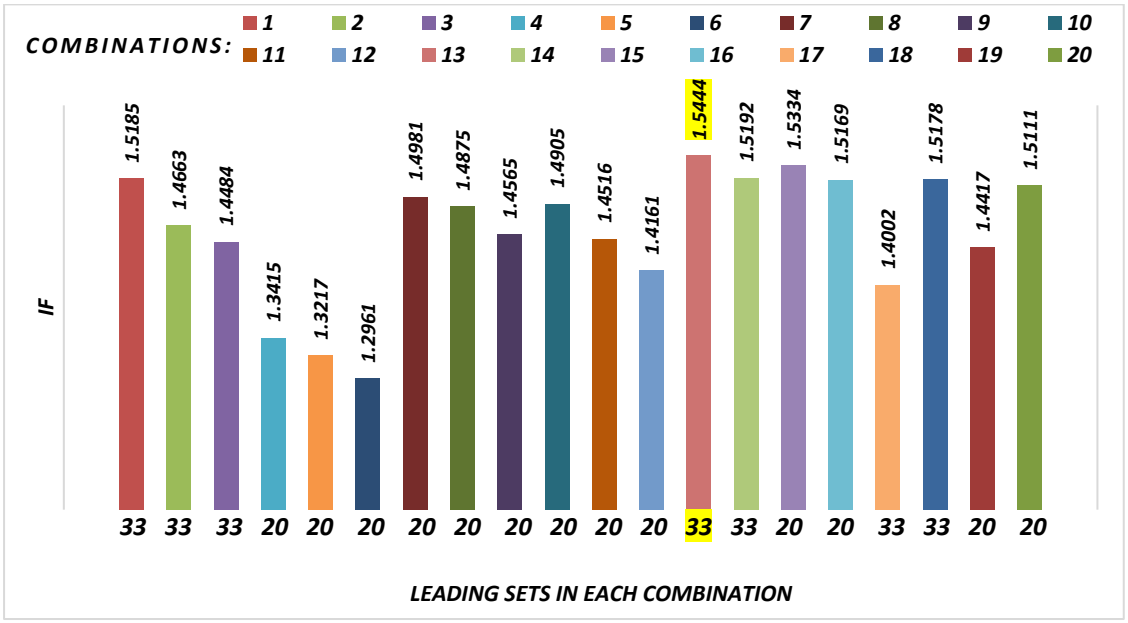


Figure 4.51: Improvement factor (*IF*) for group 6

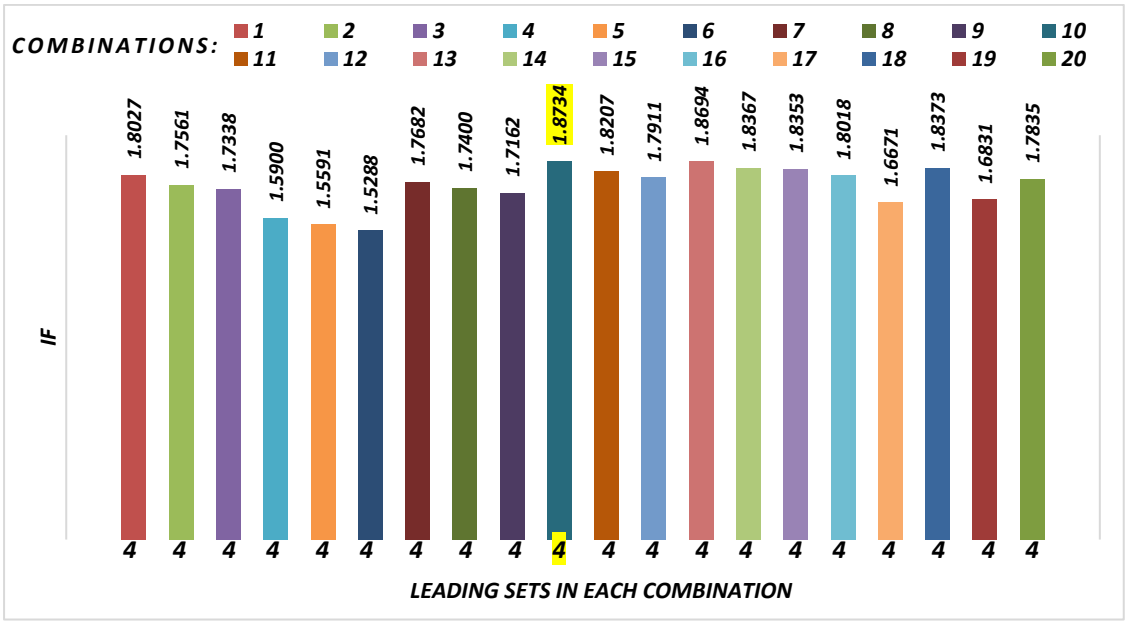


Figure 4.52: Improvement factor (*IF*) for group 7

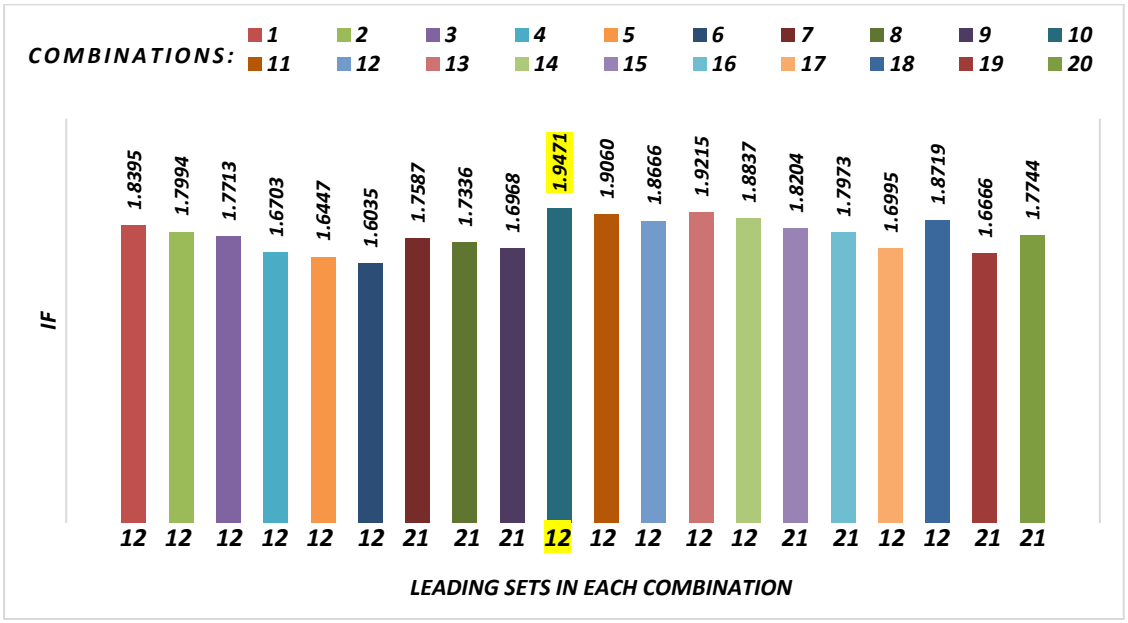


Figure 4.53: Improvement factor (*IF*) for group 8

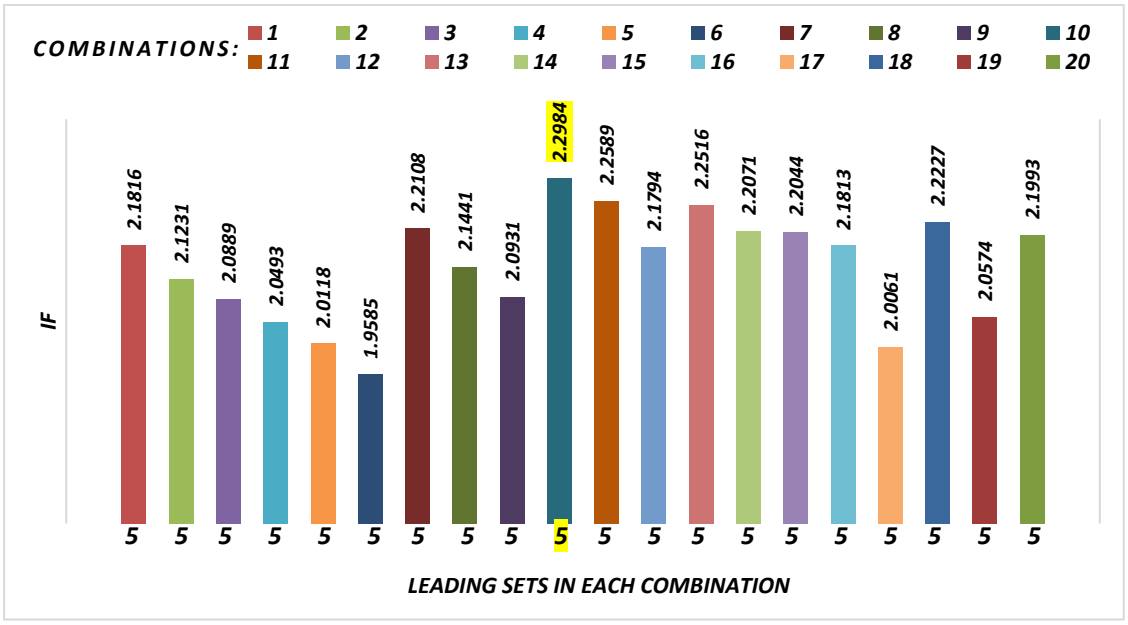


Figure 4.54: Improvement factor (*IF*) for group 9

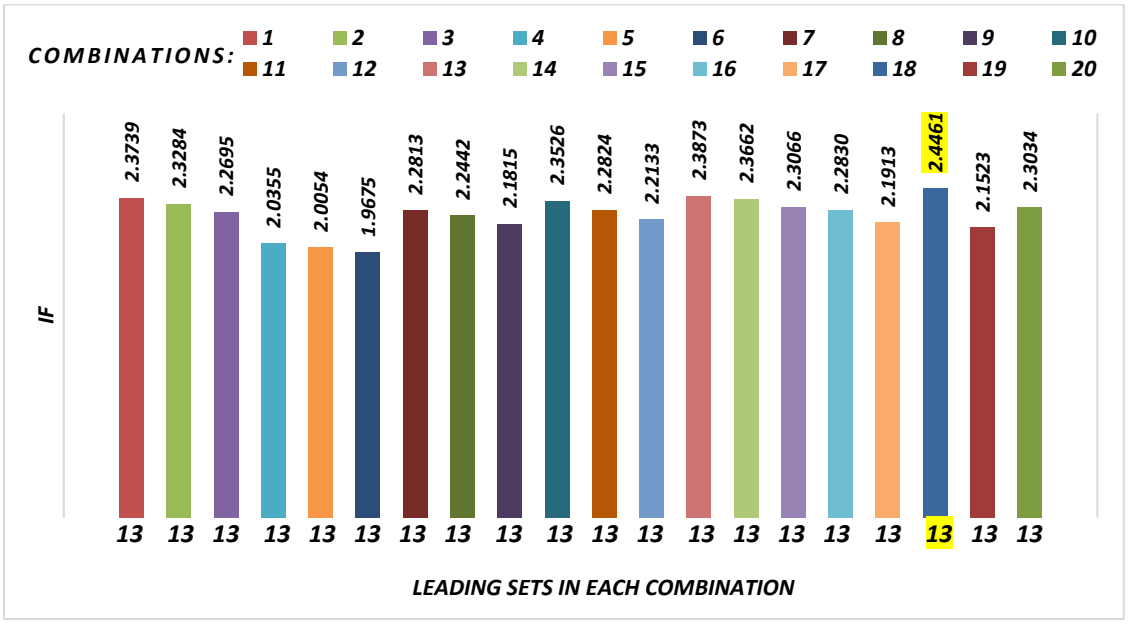


Figure 4.55: Improvement factor (*IF*) for group 10

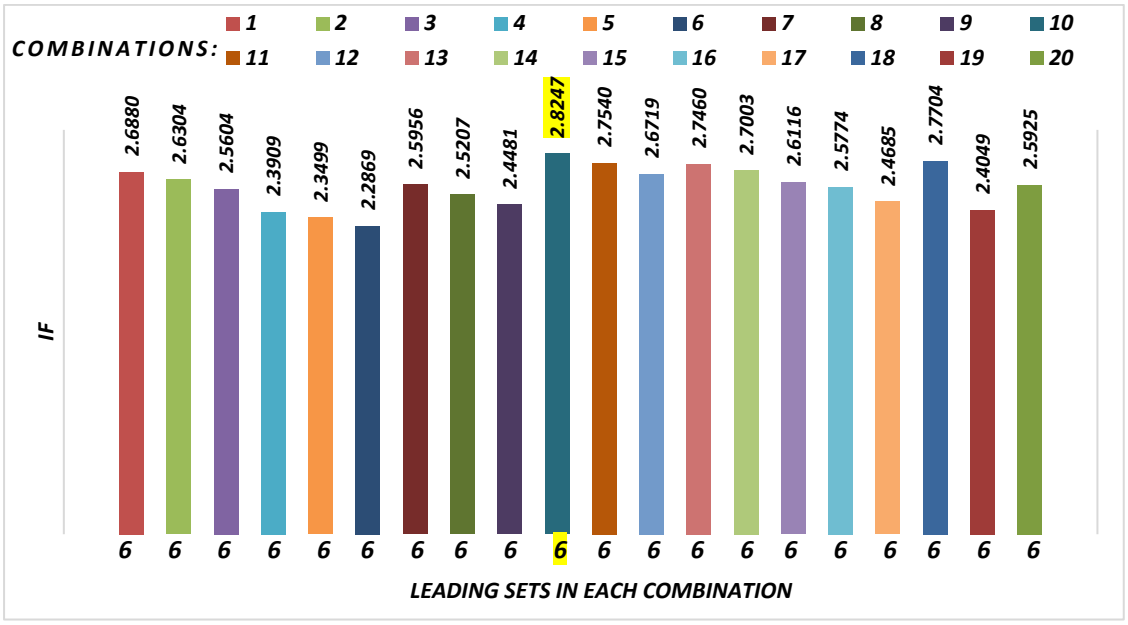


Figure 4.56: Improvement factor (*IF*) for group 11

Table 4.2: Foremost performed set in each group

Group No.	No. of piles in each group	Distribution of sets in each group	Leading set in each group	
			Set	***IF***
1	4	2, 8, 24, 25	2	1.2101
2	5	10, 22, 29, 30	10	1.2498
3	8	3, 9, 14, 26, 27	3	1.3532
4	9	11, 18, 23, 31, 32	11	1.4044
5	12	15, 16, 28	**28***	**1.5284**
6	13	19, 20, 33	**33***	**1.5444**
7	16	4, 17	**4***	**1.8734**
8	17	12, 21	**12***	**1.9471**
9	20	5	5	2.2984
10	21	13	13	2.4461
11	24	6	6	2.8247

(*, chief leading sets based on highest improvement factor)

4.4.7 Behaviour of Combined Foundation in Soft Soil

Behaviour observed in this present study for the stone columns/ piles combined under raft foundation in soft soils are presented in Appendix G. The couture diagrams for all 34 configurations for one of the combinations are presented in these figures, because the similar trends of failure were noticed for all 20 combinations. The general trend of failure for combined foundation system shows that the foundation fails due to shear failure in columns and bearing failure of piles under the raft. Except raft foundation resting on stone columns alone (Set 1) which fails by shear (Hanna et al., 2013) and raft foundation on group of piles (Set 34) which fails by bearing at the base of group piles and by shear near the side of the piles group as shown in appendix B. Similar findings are presented in the parametric study of stone columns under raft foundation and piled raft foundation in the present research.

Furthermore, based on the results from the optimization study the behaviour (i.e., modes of failure) of the chief leading sets (i.e., sets 28, 33, 4, and 12) under loading was examined and presented in Figure 4.57 to Figure 4.72. It is clear from these figures that the failure of the combined foundation system starts slightly from the center of the raft and noticeably extends to its edges. Moreover, due to the presence of the stone columns in the foundation system, the piles do not interact, and the stress transmitted by the piles to the soil does not overlap. Therefore, the load-carrying capacity of the piles is not reduced which contribute to the improvement of the geotechnical performance of the combined foundation system.

This can be attributed by the fact that the presence of stone columns between the piles can modify these pile group effects (pile interaction). The stone columns can influence the soil response and stress distribution around the piles, potentially altering the overall

behaviour of the combined system. This interaction between the stone columns and the piles needs to be considered in the design to ensure an accurate assessment of the foundation's performance.

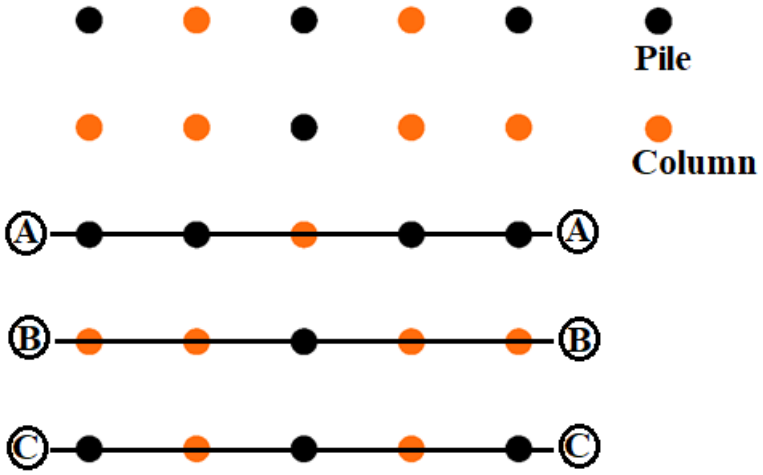


Figure 4.57: Chief leading set no. 28

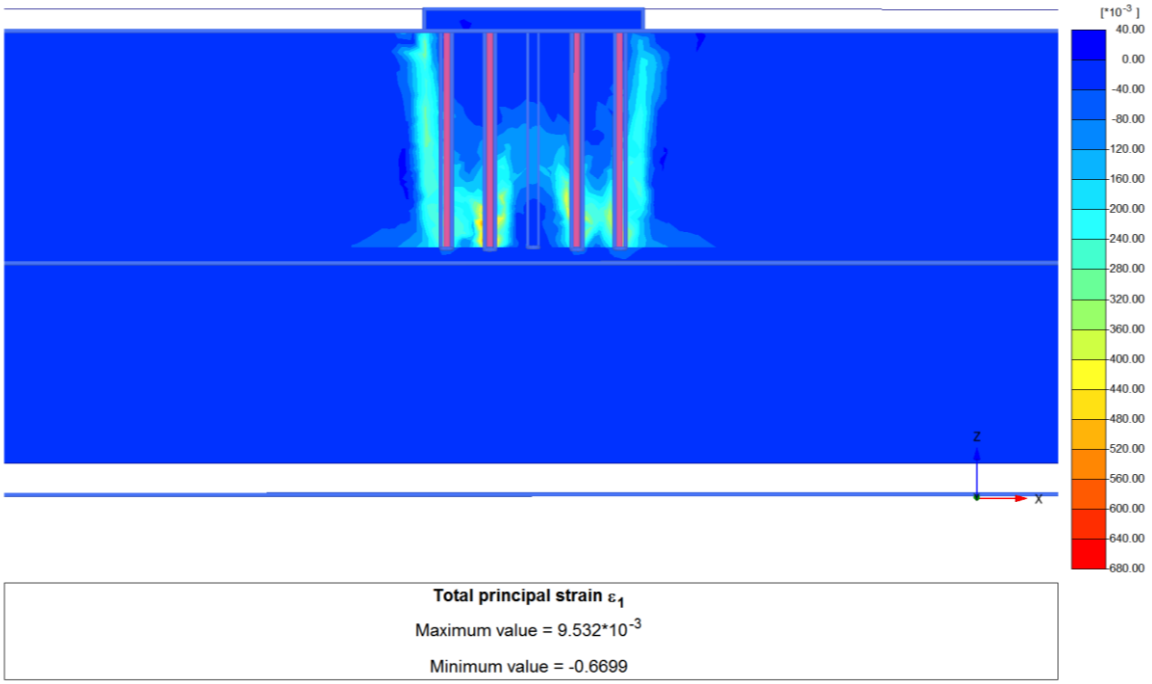


Figure 4.58: Behaviour of chief leading set no. 28, Section A-A

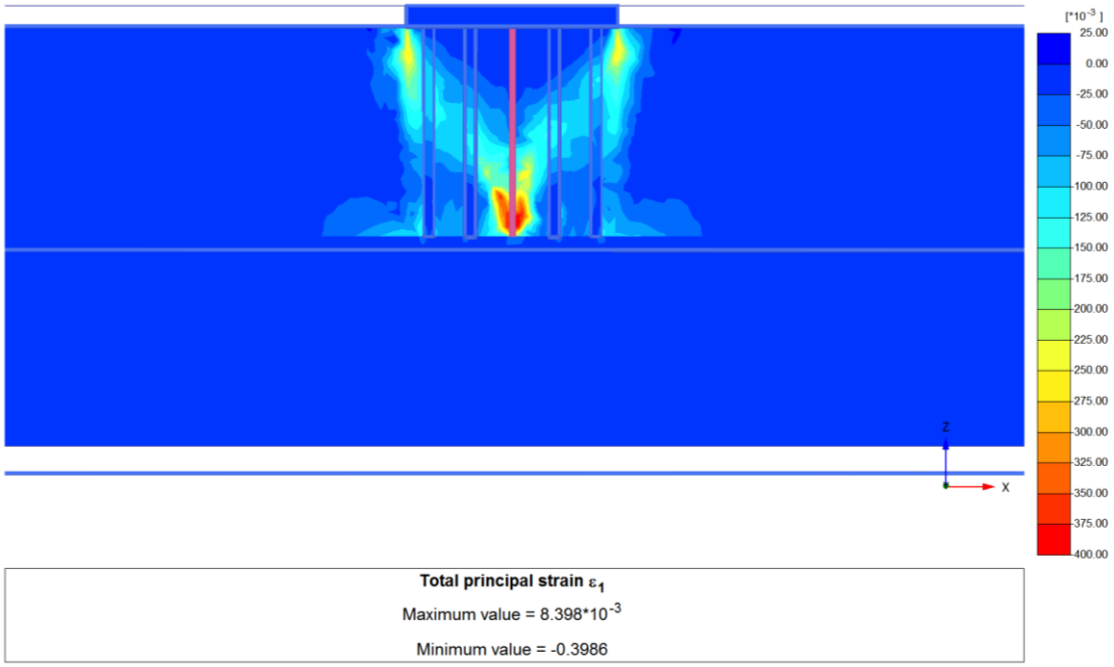


Figure 4.59: Behaviour of chief leading set no. 28, Section B-B

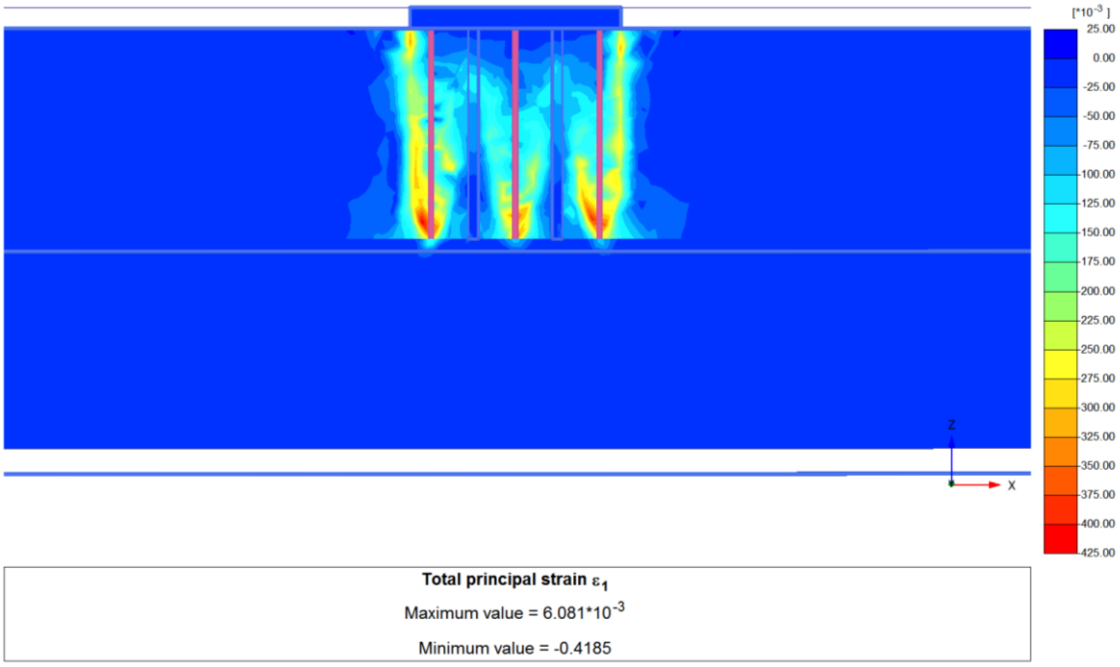


Figure 4.60: Behaviour of chief leading set no. 28, Section C-C

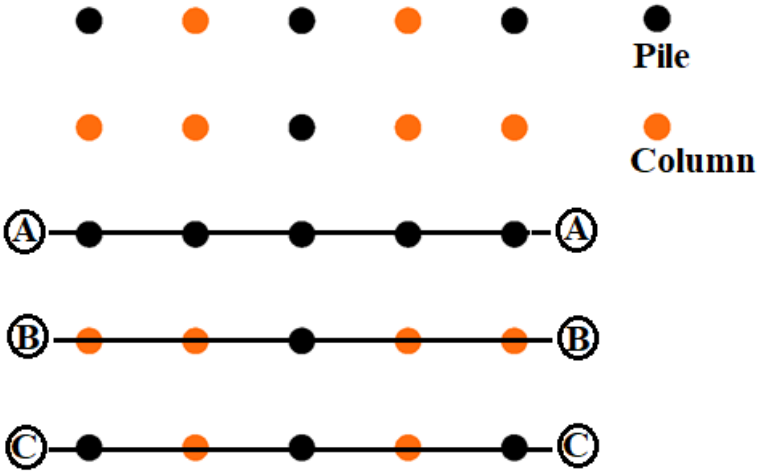


Figure 4.61: Chief leading set no. 33

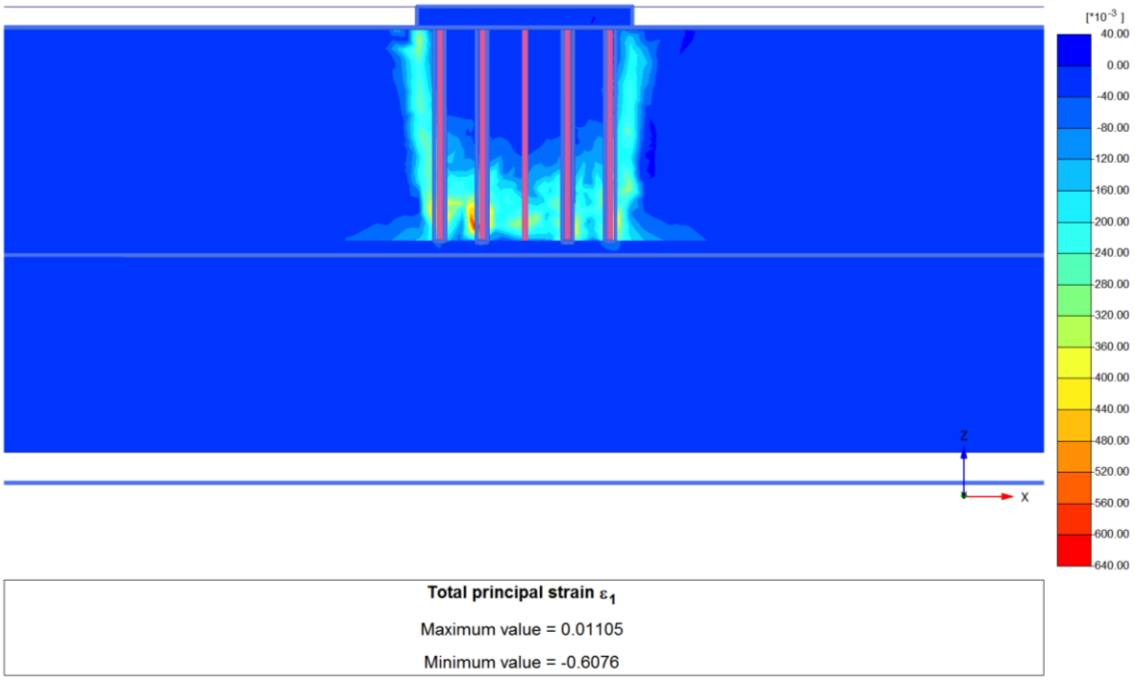


Figure 4.62: Behaviour of chief leading set no. 33, Section A-A

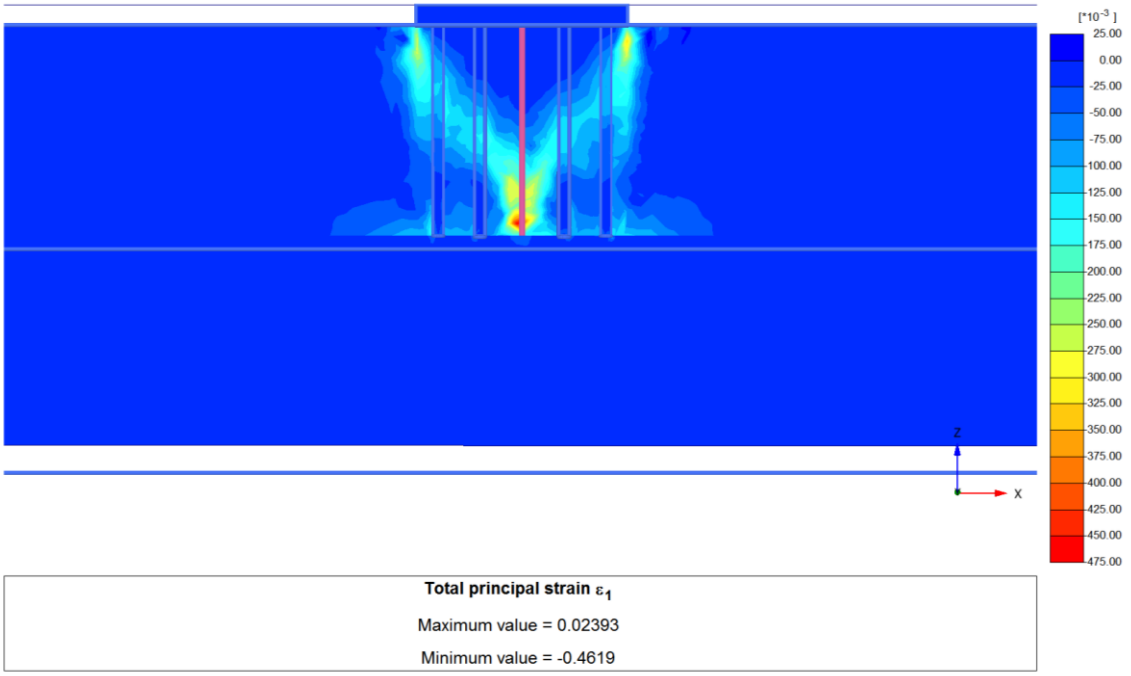


Figure 4.63: Behaviourof chief leading set no. 33, Section B-B

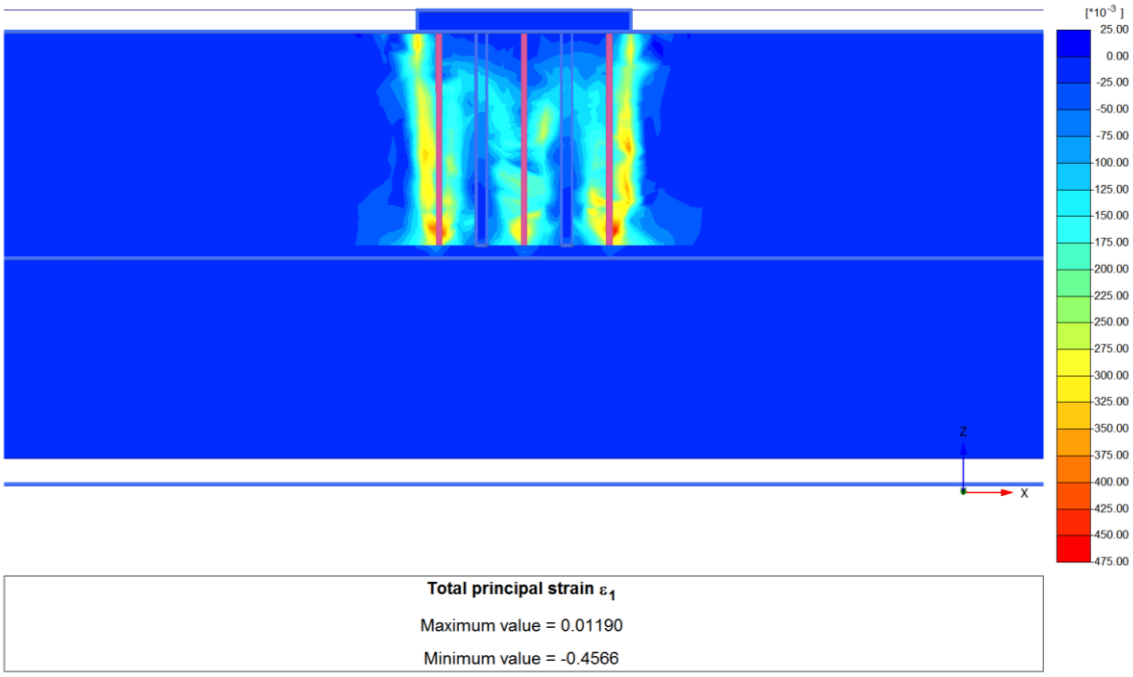


Figure 4.64: Behaviour of chief leading set no. 33, Section C-C

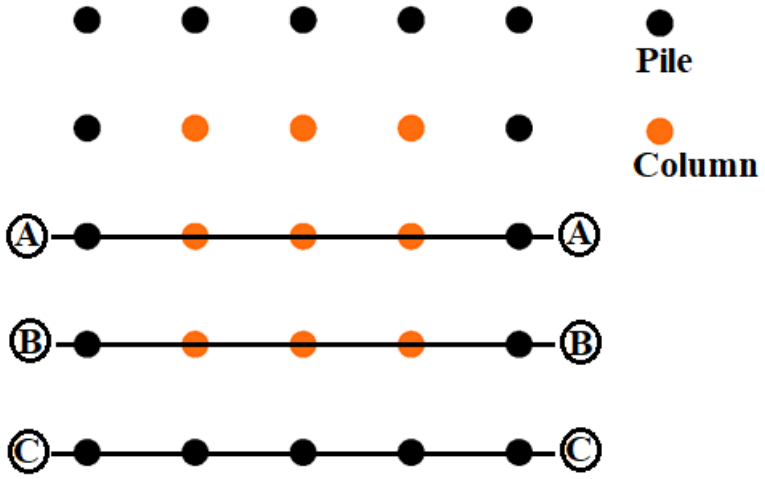


Figure 4.65: Chief leading set no. 4

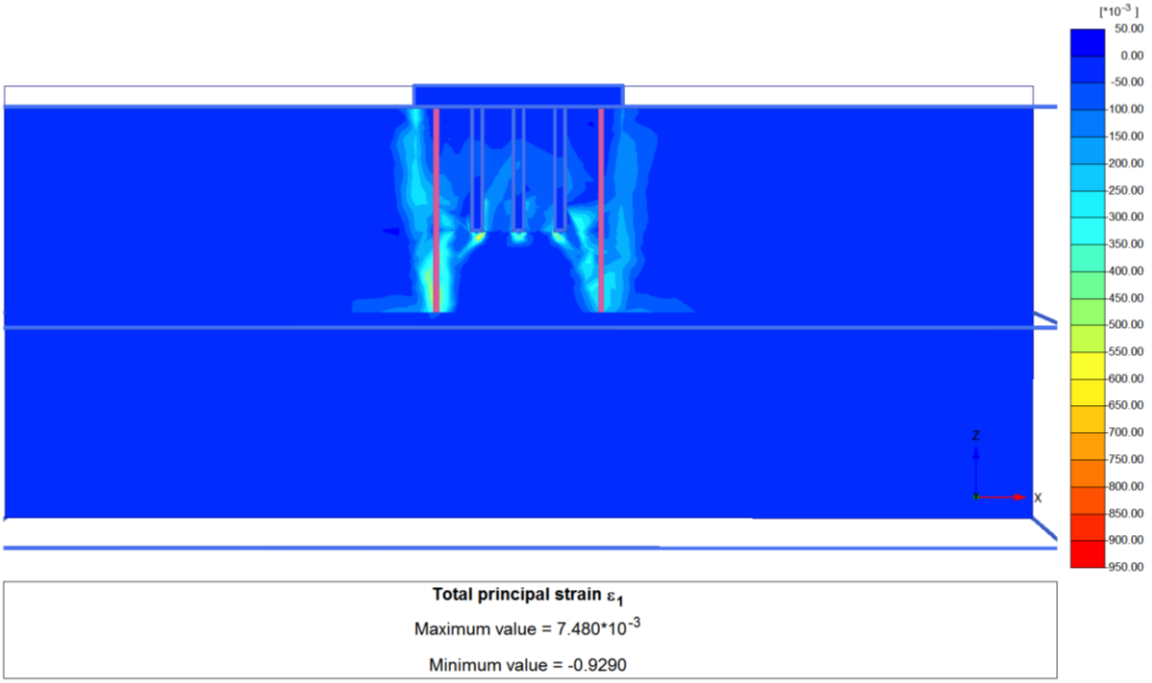


Figure 4.66: Behaviour of chief leading set no. 4, Section A-A

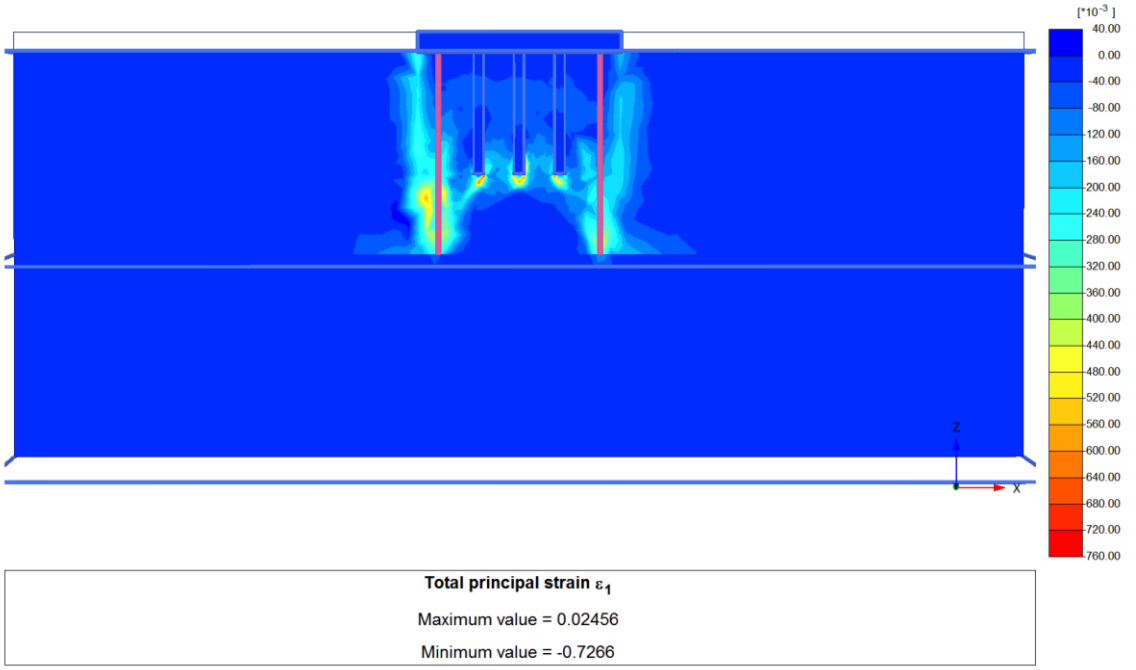


Figure 4.67: Behaviour of chief leading set no. 4, Section B-B

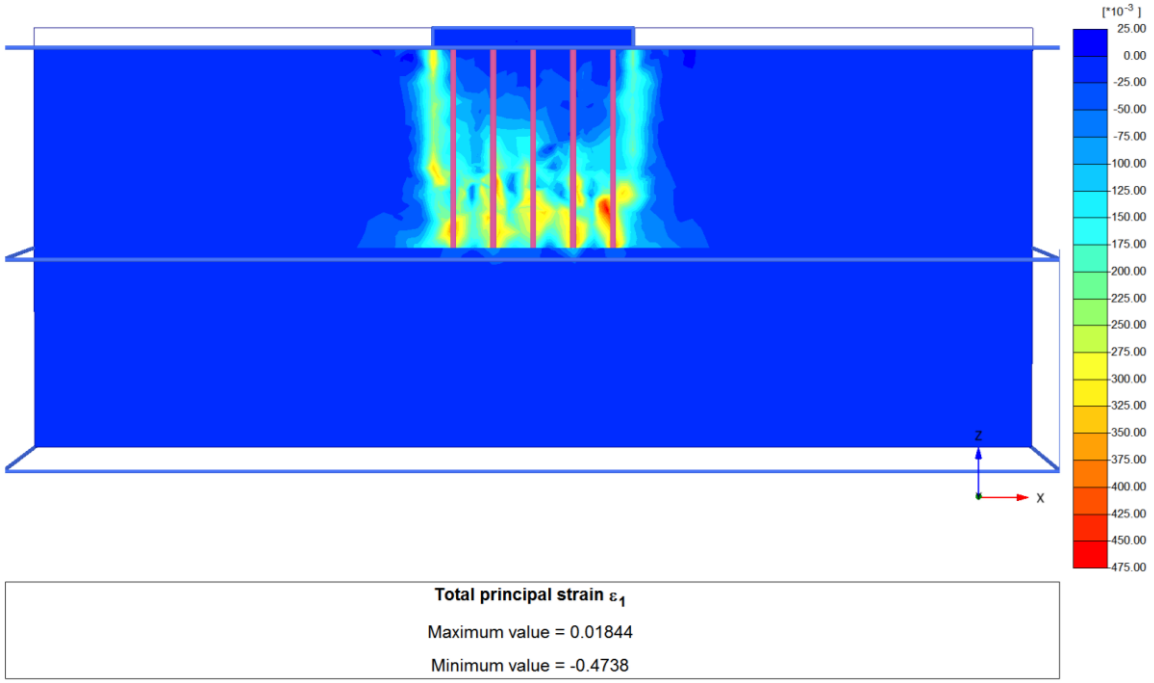


Figure 4.68: Behaviour of chief leading set no. 4, Section C-C

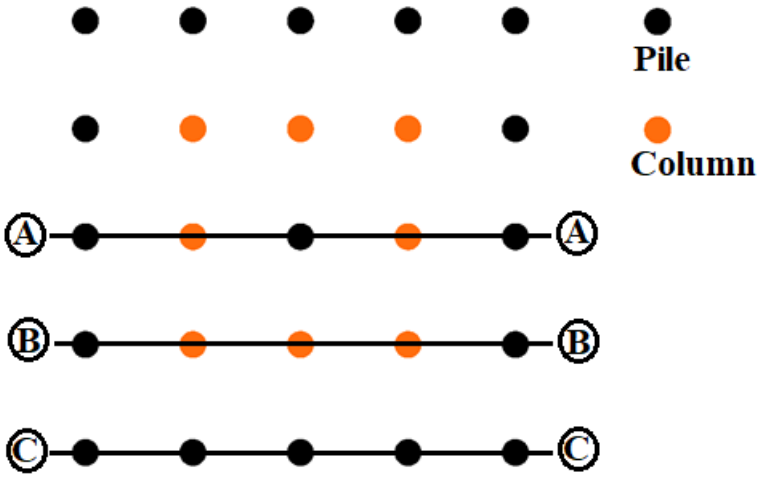


Figure 4.69: Chief leading set no. 12

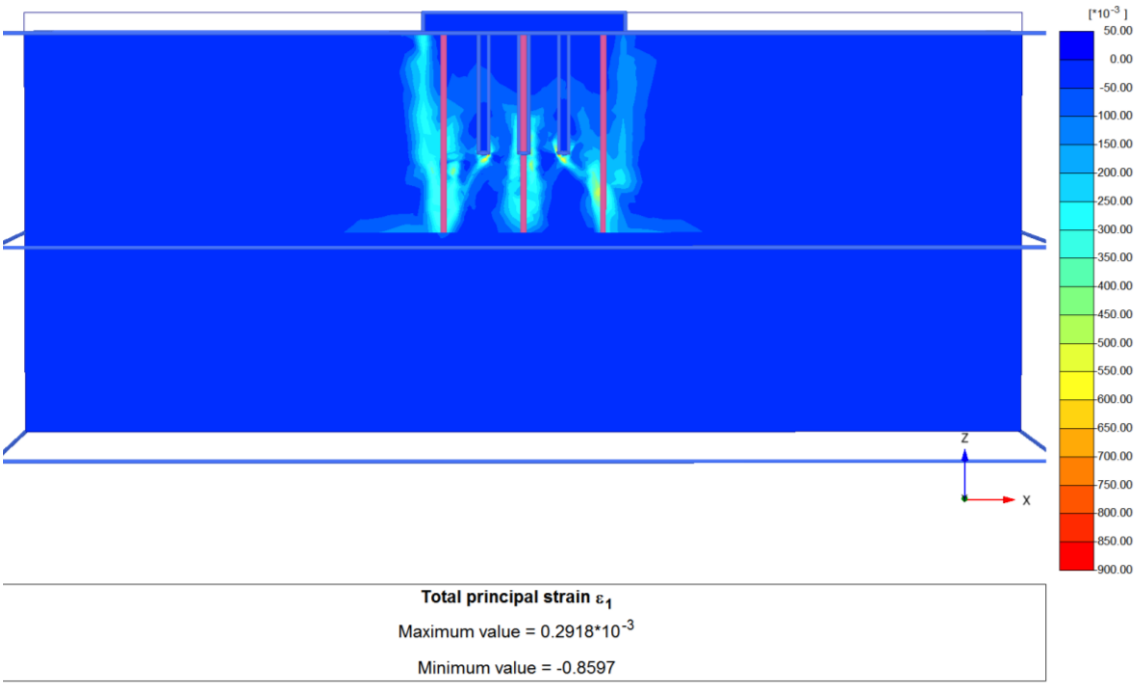


Figure 4.70: Behaviour of chief leading set no. 12, Section A-A

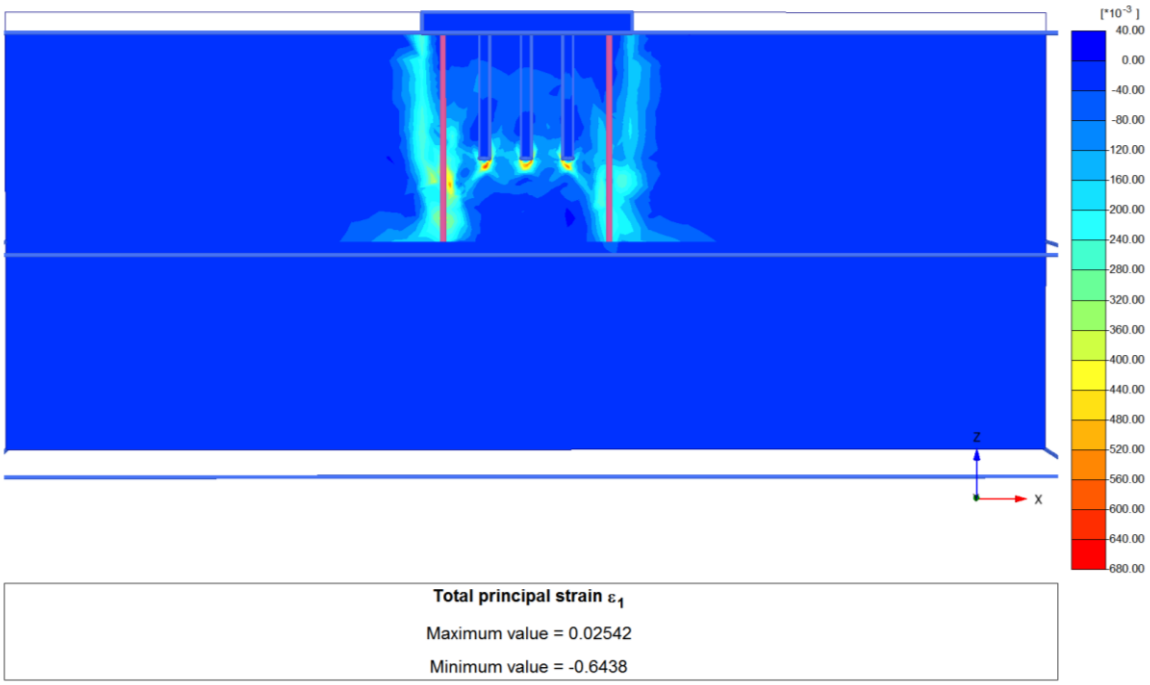


Figure 4.71: Behaviour of chief leading set no. 12, Section B-B

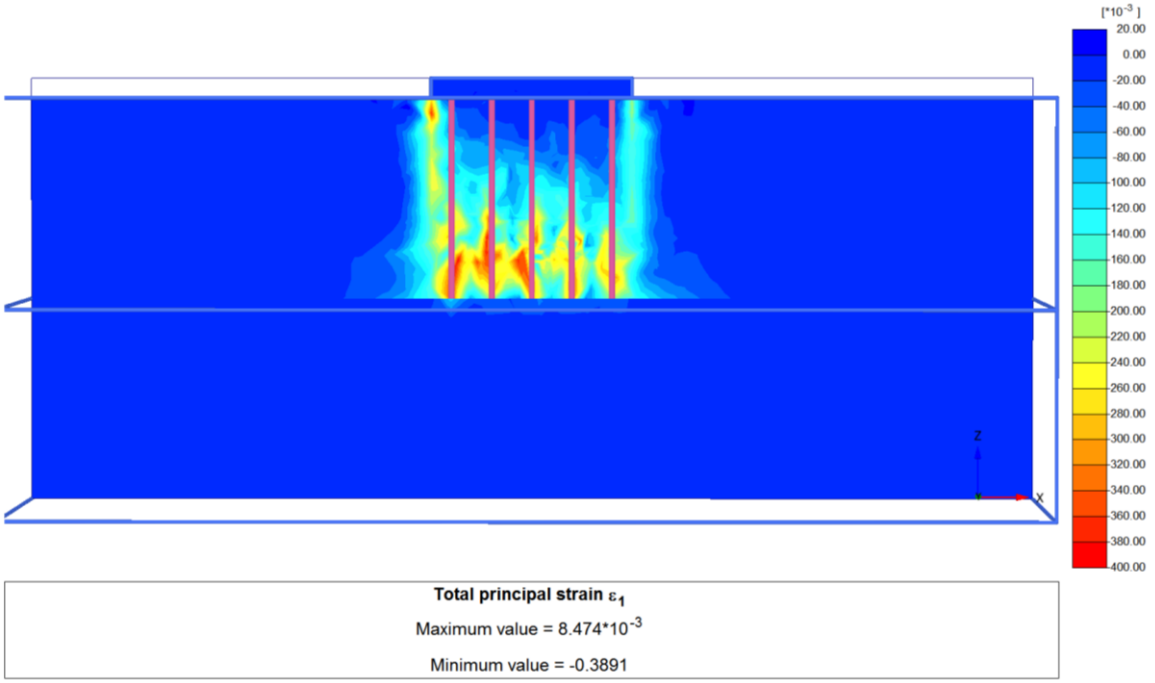


Figure 4.72: Behaviour of chief leading set no. 12, Section C-C

4.5 Results Summary

Numerical modeling was performed for (a) stone columns under raft in soft clay, (b) piled raft in soft clay and (c) stone columns/piles capped with rigid raft in soft clay, to conduct the parametric study as well as to investigate the behaviour (i.e., modes of failure). The results obtained from these numerical and parametric investigations are summarized in this section.

The parametric study for stone columns under raft foundation in soft clay presents the influence of spacing and angle of friction of stone columns on the ultimate carrying capacity of the foundation system. It was observed from this investigation that the raft foundation alone on the soft clay has the lowest carrying capacity whereas the carrying capacity of raft on the treated clay with stone columns increases with the decrease in the spacing to diameter ratio of stone columns (*S/D*), similar findings were reported in (Al-Kazzaz & Al-Obaydi, 2021; Elsawy & El-Garhy, 2016; Nazari et al., 2014; Naderi et al., 2018; Naseer et al., 2019; Rao et al., 1997; Unni et al., 2021). It also shows that with the decrease in spacing between the stone columns can have a greater number of stone columns which can be distributed uniformly under the raft foundation and can result in more even load distribution, which can improve the overall performance of the foundation system (Castro, 2014).

Also, the effect of angle of friction of stone columns shows that the ultimate carrying capacity of stone columns under raft foundation increases with an increase in the angle of friction of stone columns as it was reported by Ng and Ann (2014), Hanna et al. (2013), and Nazari et al. (2014). The behaviour of stone columns with raft foundation under load shows that the foundation systems were mostly failed because of shear both in columns and the

soils in the surrounding regions, larger shear failure was observed with the increasing spacing to diameter ratio of stone columns (*S/D*), the intensity of shear failure reduces with the smaller spacing over diameter ratio (*S/D*) of stone columns, the contour diagrams shows the higher strain values in the soil under the raft with bigger spacing over diameter ratio (*S/D*) of stone columns, similar findings were described in the contour diagram reported by Micheál and Bryan (2014), also reported by Hanna et al. (2013). Furthermore, the effect of spacing -diameter ratio (*S/D*) and the angle of friction of stone columns on bearing capacity ratio (*BCR*) were studied and it was deduced from this study that the ratio (*S/D*) of stone columns have no influence on the bearing capacity when (*S/D*) is greater than 7, whereas the bearing capacity ratio (*BCR*) can be improved when the ratio (*S/D*) is 4 or less. Similar findings were reported by Fattah et al. (2017), it was reported that the bearing improvement ratio (bearing capacity of treated-to-untreated soil) increased with decreasing spacing of stone columns. It was also reported that a higher improvement ratio can be achieved when the spacing -diameter ratio (*S/D*) of stone columns is 2.5. In addition to that Al-Kazzaz and Al-Obaydi (2021) reported that there is a 10.2, 8.7, and 4.0% improvement in soil bearing for spacings (3, 4 and 5), respectively. Also, present study for stone columns under raft foundation shows the positive influence of angle of friction (φ_c) on the bearing capacity ratio (*BCR*), increase in the angle of friction of stone columns (φ_c) can increase the ultimate load bearing capacity of the foundation system on treated soft clayey soil, similar results were reported by Ng and Ann (2014). This can be described by the fact that the stone columns with higher angle of friction have good interlocking between their granular particles and have good shear strength.

The parametric study of piled raft foundation in soft clay presents the influence of pile spacing, diameter and modulus of elasticity of clay soil on the carrying capacity of piled

raft foundation system. In this study each parameter was isolated and individually examined to determine its impact on the ultimate carrying capacity of piled raft foundation system. The results obtained from this investigation shows that the ultimate carrying capacity of piled raft foundation increases when piles spacing decreases and diameter of piles and modulus of elasticity of clay soil increases as it was also reported by Prashant et al. (2013) and Anhtuan et al. (2014). It was deduced from the failure mechanism investigation of piled raft foundation on soft clay that the foundation system fails by bearing at the tip of the piles and by shear along the side of the piles group which form it to a trapezoidal shape. Additionally, the improvement factor (IF_{PR}) for the raft foundation was introduced to show the effect of pile spacing and rigidity on the carrying capacity ratio of piled raft foundation system. It was concluded from this study that when the spacing to diameter ratio exceeds 10 (S/D> 10), piles have little or no effect on the ultimate carrying capacity of this foundation system. In this case, the raft can be considered as acting alone on the soft soil. Accordingly:

When S/D>10: Raft foundation can be considered as acting alone.

When S/D<10: Carrying capacity of piled raft = Capacity of raft foundation × IF_{PR}

This finding indicates that when the ratio S/D is less than 10, the piled raft foundation concept is a better alternative than the raft foundation alone. Banerjee (1970) concluded that piles interact even beyond distances of 8 diameters. Moreover, the results obtained illustrate that the load carried by a raft increases with a reduction in the pile length and the number of piles, which is in accordance with Elwakil and Azzam (2016). The improvement factor is reduced from 5.25 for S/D = 3 to 2.25 for S/D = 7, which corresponds to a reduction of about 60%. A well-balanced spacing to diameter ratio of the pile can help to distribute the loads

uniformly among the piles, which can result in lower stresses and strains within each pile and vice versa.

Also, the present study for piled raft foundation shows the effect of the ratio between the modulus of elasticity of piles and soft soil (E_p/E_s) on the improvement factor (IF_{PR}). It was observed from the study that the improvement factor is lower for piles with higher modulus of elasticity (higher rigidity). This can be explained by the fact that rigid piles penetrate more easily in the layer of sand situated beneath the layer of soft soil. However, it is worth noting that this ratio is commonly applied as a governing parameter for pile settlement analysis rather than for carrying capacity. Also higher modulus of elasticity indicates a stiffer soil, which can result in a more uniform distribution of applied loads among the piles and as a result, a higher modulus of elasticity can enhance the bearing capacity of the piled raft foundation system.

Finally, for the parametric study of combined stone columns/piles /raft foundation installed soft clay was conducted to examine the effect of configuration, diameter ratio for stone columns and piles, length ratio of stone columns and piles, modulus of elasticity of clay soil, and angle of friction of stone columns on the ultimate carrying capacity of combined foundation system. The results obtained from this parametric study presents that the ultimate carrying capacity of the combined foundation system increases with the increasing number of piles in each configuration (Sets). It was also observed from this study that the carrying capacity of this foundation system improves with the increase in diameter ratio of piles and columns (D_p/D_c), angle of friction of stone columns (φ_c), modulus of elasticity of clay soil, and with the decrease in the length ration of stone columns and piles (Lc/Lp). Similar behaviour of combined foundation system was reported by Samanta and

Bhowmik (2017), and Sharma and Kumar (2021). It was also noticed that beyond the critical length (L_c equal to six times D_c) stone columns do not contribute extra benefit improvement factor (*IF*) but they help to reduce settlement by penetrating the firm layer of soil, reported by (Ayadat, 2022).

Moreover, improvement factor (*IF*) for the combined foundation system was introduced to perform the optimization study. Improvement factor (*IF*) is defined as the ratio between the ultimate carrying of combined foundation to that of raft foundation with stone columns only. From this optimization study four chief leading sets were selected based on their optimum improvement factor (*IF*), in which first two sets the piles were positioned in the center of the raft in the form of plus (+). While in the other two sets the piles were positioned on the edges of the raft. According to this study the chief leading sets can increase the bearing capacity of the raft foundation by almost 50% to 90% (Table 4.2). The configuration of these chief leading sets show that the stone columns and piles are arranged in a way that stone columns are confined between the piles and piles are placed on the edge of the raft. Micheál and Bryan (2014) reported that when stone columns placed near the edge of raft, their ability to influence the load distribution and settlement patterns can diminished. Placing piles on the edge of the raft can helps to distribute the applied loads more evenly across the raft which can result in improving overall load-carrying capacity of combined foundation.

The behaviour (i.e., modes of failure) observed for the combined foundation system shows that the foundation fails due to shear in columns and by bearing failure at the base of piles under the raft, and notably the failure modes of chief leading sets show that the failure of the combined foundation system starts slightly from the center of the raft and noticeably

extends to its edges. Similar findings are presented in the parametric study of stone columns under raft foundation and piled raft foundation in the present research. Furthermore, due to the presence of the stone columns in the foundation system, the piles do not interact, and the stress transmitted by the piles to the soil doesn't overlap. Therefore, the load-carrying capacity of the piles is not reduced which contribute to the improvement of the geotechnical performance of the combined foundation system, the presence of stone columns between the piles can influence the soil response and stress distribution around the piles, which can affect the overall behaviour of the combined system.

CHAPTER 5

THEORETICAL DEVELOPMENT

5.1 Overview

The results from the numerical models presented in Chapter 4 are used to develop the theoretical and analytical models for (1) Stone columns under raft in soft clay soil (2) Piled raft foundation in soft clay and mainly for (3) Combined foundation (i.e., stone columns/piles caped with raft foundation in soft clay). The analytical models presented in this chapter are developed based on the behaviour (i.e., modes of failure) of the foundation systems obtained from the numerical models to predict their carrying capacities.

5.2 Analytical Model for Stone Columns under Raft in Soft Clay Soils

The ultimate carrying capacity of stone columns under raft in soft clay soil can be defined as the carrying capacity of raft on the composite soil (columns material/soft clay), which can be represented as.

$$Q_{u1} = \left(BL - n_1 \frac{\pi D_1^2}{4}\right) q_{u1} \qquad \text{Equation 5.1}$$

q_{u1} can be determined by the general equation of Meyerhof as follows (Das & Sivakugan, 2019):

Where:

$$q_{u1} = c_{comp}\bar{N}_c + q_1\bar{N}_q + \frac{1}{2}B\gamma_{comp}\bar{N}_\gamma \qquad \text{Equation 5.2}$$

$$\bar{N}_c = N_c\left(1 + \frac{B}{L}\frac{N_q}{N_c}\right)\left(1 + 0.4\frac{D_f}{B}\right)$$

$$\bar{N}_q = N_q\left(1 + \frac{B}{L}\tan\varphi_{comp}\right)\left[1 + 2\tan\varphi_{comp}\left(1 - \sin\varphi_{comp}\right)^2\frac{D_f}{B}\right]$$

$$\bar{N}_\gamma = N_\gamma\left(1 - 0.4\frac{B}{L}\right)$$

$$N_c = \left(N_q - 1\right)\cot\varphi_{comp}$$

$$N_q = \tan^2\left(\frac{\pi}{4} + \frac{\varphi_{comp}}{2}\right)\left(e^{\pi\tan\varphi_{comp}}\right)$$

$$N_\gamma = 2\left(N_q + 1\right)\tan\varphi_{comp}$$

$B = width\ of\ raft$

$L = Length\ of\ raft$

$c_{comp} = Cohesion\ of\ composite\ (clay + stone\ column)$

$\gamma_{comp} = Unit\ weight\ of\ the\ composite$

$\varphi_{comp} = Angle\ of\ shearing\ resistance\ of\ the\ composite$

$n_1 = Number\ of\ piles$

$D_1 = Diameter\ of\ pile$

According to Etezad et al. (2015), the different soil parameters of the composite can be determined using Equations 5.3 to 5.7:

$$q_1 = \gamma_{comp}D_f$$

$D_f = Depth\ of\ raft$

$$c_{comp} = A_s c_s + (1 - A_s)c_c \qquad \text{Equation 5.3}$$

$$\gamma_{comp} = A_s\gamma_s + (1 - A_s)\gamma_c \qquad \text{Equation 5.4}$$

$and\ A_s = Replacement\ ratio\ (Area\ of\ stone\ columns\ over\ the\ area\ of\ the\ raft\ )$

$A_{col} = Column\ cross-section$

$c_s = Cohesion\ of\ stone\ columns$

$c_c = Cohesion\ of\ soil\ (clay)$

$\gamma_s = Unit\ weight\ of\ stone\ columns$

$\gamma_c = Unit\ weight\ of\ soil\ (clay)$

$$\varphi_{comp} = \tan^{-1}[A_s\mu_s \tan\varphi_s + (1 - A_s)\mu_c \tan\varphi_c] \quad \text{Equation 5.5}$$

$$\mu_s = \frac{n}{1 + (n-1)A_s} \quad \text{Equation 5.6}$$

$$\mu_c = \frac{1}{1 + (n-1)A_s} \quad \text{Equation 5.7}$$

$\varphi_s =\ angle\ of\ shearing\ resistance\ of\ stone\ columns$

$\varphi_c =\ angle\ of\ shearing\ resistance\ of\ clay\ soil$

n = stress ratio = 2 - 6 (Mitchell & Katti, 1981), and 1.5 - 2.0 (Lawton et al., 1991)

A comparison between the measured and calculated values of the ultimate carrying capacity (Equation 5.1) of stone columns under raft foundation in soft soils was undertaken. The results of this comparison are shown in Table 5.1, where acceptable agreement is apparent.

Table 5.1: Validation of the present analytical model for stone columns under foundation (Equation 5.1)

	D (m)	L (m)	S/D	Q_u (kN/m^2) Plaxis 3D	Q_u (kN/m^2) Analytical Model (Equation 5.1)	Difference (%)
Current study	1	20.00	4.00	212.16	268.44	(26.53)
	1	20.00	5.00	198.37	245.48	(23.75)
	1	20.00	6.00	186.61	221.61	(18.75)
	1	20.00	7.00	189.75	205.74	(8.43)

5.3 Analytical Model for Piled Raft Foundation in Soft Clayey Soils

Numerical models were used to study the behaviour of raft with piles in soft clayey soil under loading. It was deduced that foundation failure occurs at the base of piles by bearing as well as by shear on inclined/curved plans near the side of the pile group (Figures 5.1 and Figure 5.2). In the 2-D plan, the failure by shear of the foundation system was observed at the beginning of the failure to have a trapezoidal form (i.e., linear, or straight line from the edge of the raft to the edge of the base of the pile group). However, when the applied load approached the ultimate load capacity of this foundation system, the shape of the failure mode was observed to take the form of a hyperbolic curve, which can be expressed by the following equation (Figure 5.3):

$$Z = -aX^2 + b \qquad \text{Equation 5.8}$$

The proposed Equation 5.1 represents the function of the failure contour caused by shear around the piled raft foundation. It represents the function of the delineations or delimits caused by the shaft only. Concerning the beginning of the behaviour of the

foundation system, it is worth noting that when the width of the raft foundation is larger than the width of the pile group, the shear failure along the side of the observed trapezoid can be presented by a straight line. This line passes from the corner edge of the raft to the base corner of the pile group with an angle to the vertical (θ):

$$tan(\theta) = \frac{B_r - B_g}{2H} \qquad \text{Equation 5.9}$$

Where:

B_r= Width of raft foundation

B_g = Width of pile group

H = Height or length of pile group

Recent studies have shown that there is a major concentration of stress shading at the bottom of piles, which indicates a significant amount of stress (El-Mossallamy et al., 2009; Horikoshi & Randolph, 1999). According to their failure diagram, the load transfer mechanism begins at the lower third of the pile length. The system behaves as if embedded blocks are equivalent to pier-one units. The present numerical analysis provided a better understanding of the failure patterns of the piled raft soil system. This confirmed that the transmitted stresses concentrated at the bottom of piles lead to failure by bearing. However, the failure extends by a shearing process at the side of the pile group, from the bottom edge of the pile group to the edge of the raft, on hyperbolic plans.

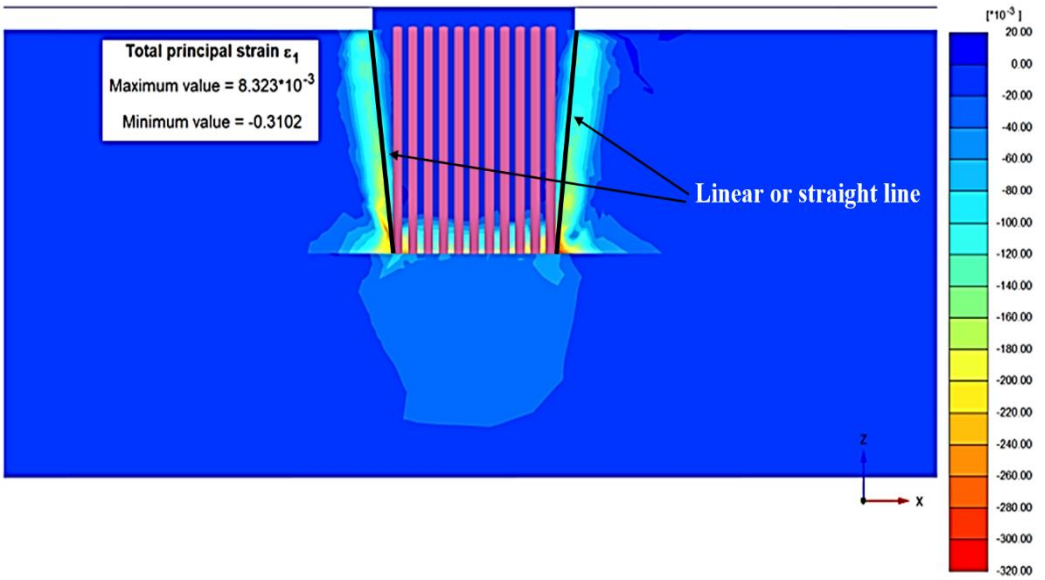


Figure 5.1: Shape of the shear failure at the beginning of the failure mechanism.

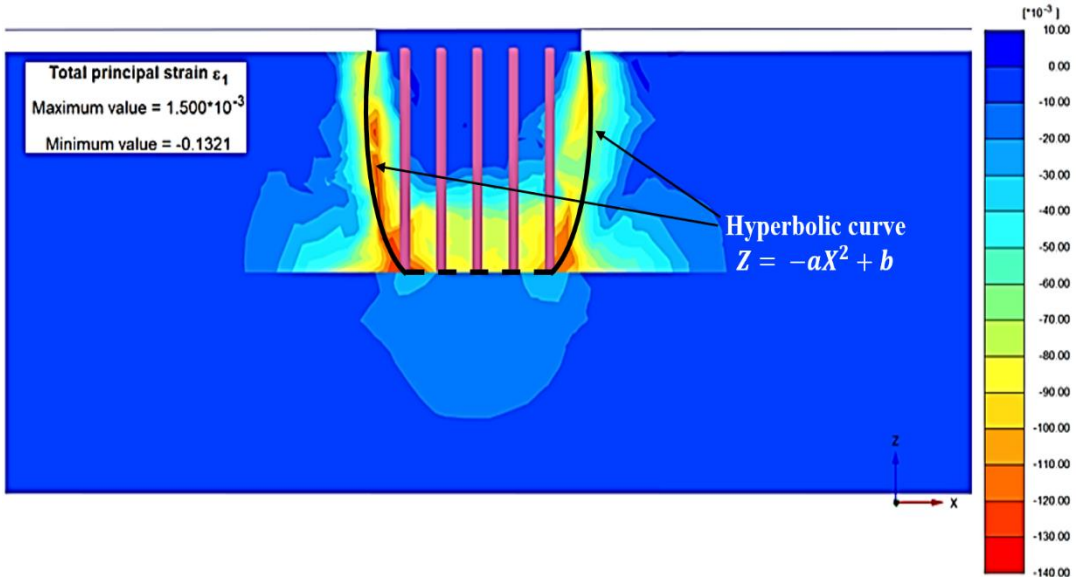


Figure 5.2: Shape of the shear failure mechanism when the applied load approaches the ultimate load capacity.

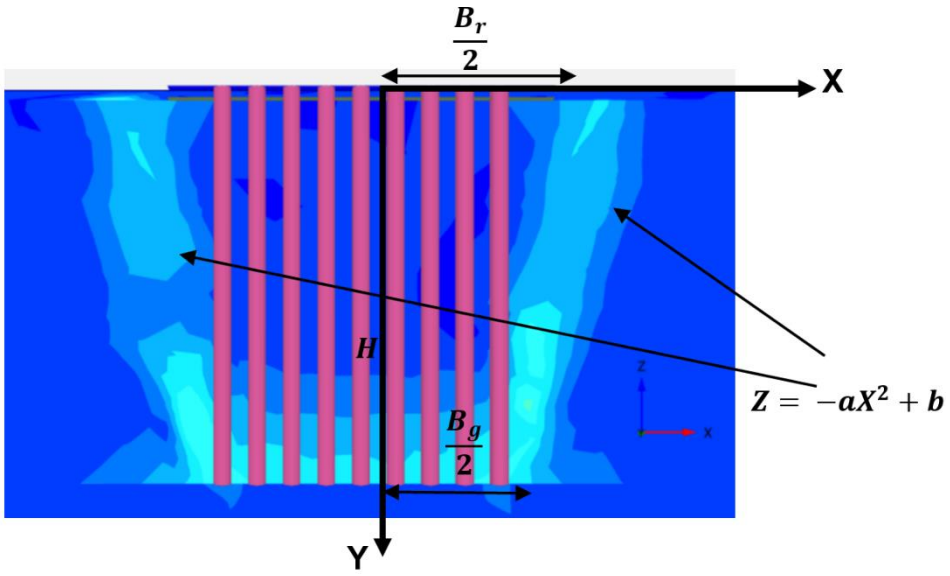


Figure 5.3: Geometry/configuration of the shear failure mechanism of the piled raft foundation in soft soils

An analytical model was developed to predict the ultimate carrying capacity of this foundation system based on the observed behaviour. As mentioned previously, the final shape of the failure mode can be expressed by Equation 5.8) (Figure 5.3):

$$Z = -aX^2 + b$$

By considering the boundary conditions:

$$Z = 0 \qquad X = \frac{B_r}{2}$$ Equation 5.10

$$Z = H \qquad X = \frac{B_g}{2}$$ Equation 5.11

We obtain:

$$a = \frac{H}{\left(\frac{B_r}{2}\right)^2 - \left(\frac{B_g}{2}\right)^2}$$ Equation 5.12

$$b = \left(\frac{B_r}{2}\right)^2 \left[\frac{H}{\left(\frac{B_r}{2}\right)^2 - \left(\frac{B_g}{2}\right)^2}\right]$$ Equation 5.13

From Equation 5.8:

$$X = \left(\frac{b - Z}{a}\right)^{1/2} = f(Z)$$ Equation 5.14

The side area of the curved shear failure plane can be computed by:

$$A_1 = \int_0^H f(Z)\, dZ = \int_0^H \left(\frac{b - Z}{a}\right)^{1/n} dZ$$ Equation 5.15

Let's consider:

$$m = \frac{1}{2}$$

$$\frac{Z}{a} = Y$$

$$\frac{b}{a} = C$$

$$Therefore\ when\ \ Z = 0 \Rightarrow\ Y = 0, \qquad and\ when\ Z = H \Rightarrow\ \ Y = \frac{H}{a}$$

$$Also \quad dZ = a\, dY$$

By replacing in Equation 5.15, we get:

$$A_1 = \int_0^{\frac{H}{a}} (C - Y)^m\, a\, dY = a \int_0^{\frac{H}{a}} (C - Y)^m\ dY$$ Equation 5.16

$$\Rightarrow A_1 = -\left[a\frac{(C-Y)^{m+1}}{m+1}\right]_0^{\frac{H}{a}} = -a\frac{\left(c-\frac{H}{a}\right)^{m+1}}{m+1} + \frac{aC^{m+1}}{m+1}$$ Equation 5.17

Therefore:

$$\overline{A_1} = \frac{A_1}{cos\theta}$$

$$Where\ cos\theta = \frac{H}{\sqrt{\left(\frac{B_r}{2}-\frac{B_g}{2}\right)^2 + H^2}}$$

$$\overline{A_1} = \frac{-a}{(m+1)H}\left(C-\frac{H}{a}\right)^{m+1}\left[\sqrt{\left(\frac{B_r}{2}-\frac{B_g}{2}\right)^2 + H^2}\right] +$$ Equation 5.18

$$\frac{a}{(m+1)H}C^{m+1}\left[\sqrt{\left(\frac{B_r}{2}-\frac{B_g}{2}\right)^2 + H^2}\right]$$

From Equation 5.12 and Equation 5.13:

$$C = \frac{b}{a} = \left(\frac{B_r}{2}\right)^2$$

Therefore:

$$\overline{A_1}$$ Equation 5.19

$$= -\frac{\frac{H}{\sqrt{\left(\frac{B_r}{2}\right)^2 - \left(\frac{B_g}{2}\right)^2}}}{\left(\frac{1}{2}+1\right)H}\left[\left(\frac{B_r}{2}\right)^2\right.$$

$$\left. - \frac{H}{\frac{H}{\sqrt{\left(\frac{B_r}{2}\right)^2 - \left(\frac{B_g}{2}\right)^2}}}\right]^{\frac{1}{2}+1} \left[\sqrt{\left(\frac{B_r}{2} - \frac{B_g}{2}\right)^2 + H^2}\right]$$

$$+ \frac{\frac{H}{\sqrt{\left(\frac{B_r}{2}\right)^2 - \left(\frac{B_g}{2}\right)^2}}}{\left(\frac{1}{2}+1\right)H}\left(\frac{B_r}{2}\right)^{2\left(\frac{1}{2}+1\right)}\left[\sqrt{\left(\frac{B_r}{2} - \frac{B_g}{2}\right)^2 + H^2}\right]$$

So:

$$\overline{A_1} = \frac{1}{\left[\left(\frac{B_r}{2}\right)^2 - \left(\frac{B_g}{2}\right)^2\right]\left(\frac{1}{2}+1\right)}$$ Equation 5.20

$$\sqrt{\left(\frac{B_r}{2} - \frac{B_g}{2}\right)^2 + H^2}\left[-\left(\frac{B_g}{2}\right)^{2\left(\frac{1}{2}+1\right)} + \left(\frac{B_r}{2}\right)^{2\left(\frac{1}{2}+1\right)}\right]$$

i.e.

$$\overline{A_1} = \frac{\sqrt{\left(\frac{B_r}{2} - \frac{B_g}{2}\right)^2 + H^2}}{\left(\frac{3}{2}\right)\left[\left(\frac{B_r}{2}\right)^2 - \left(\frac{B_g}{2}\right)^2\right]}\left[\left(\frac{B_r}{2}\right)^3 - \left(\frac{B_g}{2}\right)^3\right]$$ Equation 5.21

Similarly, for the other side of the curved shear failure plan:

$$\overline{A_2} = \frac{\sqrt{\left(\frac{L_r}{2} - \frac{L_g}{2}\right)^2 + H^2}}{\left(\frac{3}{2}\right)\left[\left(\frac{L_r}{2}\right)^2 - \left(\frac{L_g}{2}\right)^2\right]}\left[\left(\frac{L_r}{2}\right)^3 - \left(\frac{L_g}{2}\right)^3\right] \quad \text{Equation 5.22}$$

Therefore:

$$A_{Total} = 2(\overline{A_1} + \overline{A_2}) \quad \text{Equation 5.23}$$

So:

$$A_{Total} = 2\frac{\sqrt{\left(\frac{B_r}{2} - \frac{B_g}{2}\right)^2 + H^2}}{\left(\frac{3}{2}\right)\left[\left(\frac{B_r}{2}\right)^2 - \left(\frac{B_g}{2}\right)^2\right]}\left[\left(\frac{B_r}{2}\right)^3 - \left(\frac{B_g}{2}\right)^3\right] + \quad \text{Equation 5.24}$$

$$2\frac{\sqrt{\left(\frac{L_r}{2} - \frac{L_g}{2}\right)^2 + H^2}}{\left(\frac{3}{2}\right)\left[\left(\frac{L_r}{2}\right)^2 - \left(\frac{L_g}{2}\right)^2\right]}\left[\left(\frac{L_r}{2}\right)^3 - \left(\frac{L_g}{2}\right)^3\right]$$

As observed from the piled raft foundation failure mode, the ultimate carrying capacity (Q_u) can be computed as:

$$Q_u = Q_p + Q_s \quad \text{Equation 5.25}$$

Based on the formula of Meyerhof for foundation on sand:

$$Q_p = 0.5\gamma B_r \overline{N_\gamma} A_g \quad \text{Equation 5.26}$$

And by taking (Q_s) as:

$$Q_s = \sum_{i=0}^{n} A_i f_i = A_{total} \times C_u$$ Equation 5.27

Finally:

$$Q_u = 0.5\gamma B_r \overline{N_\gamma} A_g + A_{total} \times C_u$$ Equation 5.28

Where:

A_g = Actual area of the pile group ($A_g = (m \times n) \times \left(\frac{\pi}{4} \times D^2\right)$)

$m \times n$ = Number of piles

$\overline{N_\gamma} = N_\gamma F_{\gamma s} F_{\gamma d} F_{\gamma i}$

$F_{\gamma s} = 1 - 0.4\left(\frac{B_g}{L_g}\right)$

$F_{\gamma d} = 1$

$F_{\gamma i} = 1$

So:

$$\overline{N_\gamma} = N_\gamma \left[1 - 0.4\left(\frac{B_g}{L_g}\right)\right]$$ Equation 5.29

The results of this numerical investigation for piled raft in soft clay and data previously reported in the literature were used to validate the proposed analytical model (Equation 5.28). A comparison between the measured and calculated values of the ultimate carrying capacity (Equation 5.28) of raft foundation with piles in soft soils was undertaken. The results of this comparison are shown in Table 5.2, where acceptable agreement is apparent. The calculated values for the mean and the standard deviation of the results grouped in Table 5.2 are 10.45 and 7.52, respectively. Furthermore, the coefficient of

variation, defined as the ratio of the standard deviation to the mean (which is a measure of the dispersion of a dataset), was less than 1, indicating a relatively low variation in the results.

Table 5.2: Validation of the present analytical model for piled raft foundation (Equation 5.28)

Current study	***D* (m)**	***L* (m)**	***S/D***	**Q_u (kN/m^2) Plaxis 3D**	**Q_u (kN/m^2) Analytical Model (Equation 5.28)**	**Difference (%)**
	0.40	20.00	3.00	1156.65	1450.47	(25.40)
	0.40	20.00	4.00	988.99	1074.85	(8.68)
	0.40	20.00	5.00	934.04	916.85	1.84
	0.40	20.00	6.00	622.20	649.29	(4.35)
	0.40	20.00	7.00	514.79	544.27	(5.73)
Elwakil, and Azzam (2016)	***D* (m)**	***L* (m)**	***S/D***	**Q_u (kN) Experimental Work**	**Q_u (kN) Analytical Model (Equation 5.21)**	**Difference (%)**
	0.01	0.40	3.13	1.70	1.37	19.45
	0.01	0.20	3.13	1.50	1.26	16.04
	0.01	0.10	3.13	1.30	1.20	7.35
El-Garhy et al. (2013)	***D* (m)**	***L* (m)**	***S/D***	**Q_u (kN) Experimental Work**	**Q_u (kN) Analytical Model (Equation 5.21)**	**Difference (%)**
	0.01	0.50	3.00	15.50	14.69	5.26

5.4 Analytical Model for Combined Foundation System in Soft Clayey Soils

Behaviour (i.e., modes of failure) of the combined foundation system (i.e., stone columns/piles caped with raft) in soft soil under loading were obtained from the numerical models. These failure modes show that the foundation system fails due to shear in columns and by bearing at the base of piles as shown in Figure 5.4. It is clear from this figure that the failure of combined foundation system starts slightly from the center of the raft and extends noticeably to its edges and due to the presence of the stone columns in the foundation system the stresses transmitted by piles to the soil does not overlap. The outcome of the observed behaviour (i.e., modes of failure) was used to develop an analytical model for the prediction of the ultimate carrying capacity of the combined foundation system, using the limit equilibrium method of analysis and the principal of homogeneous composite material (i.e., homogeneous columns material/soft clay).

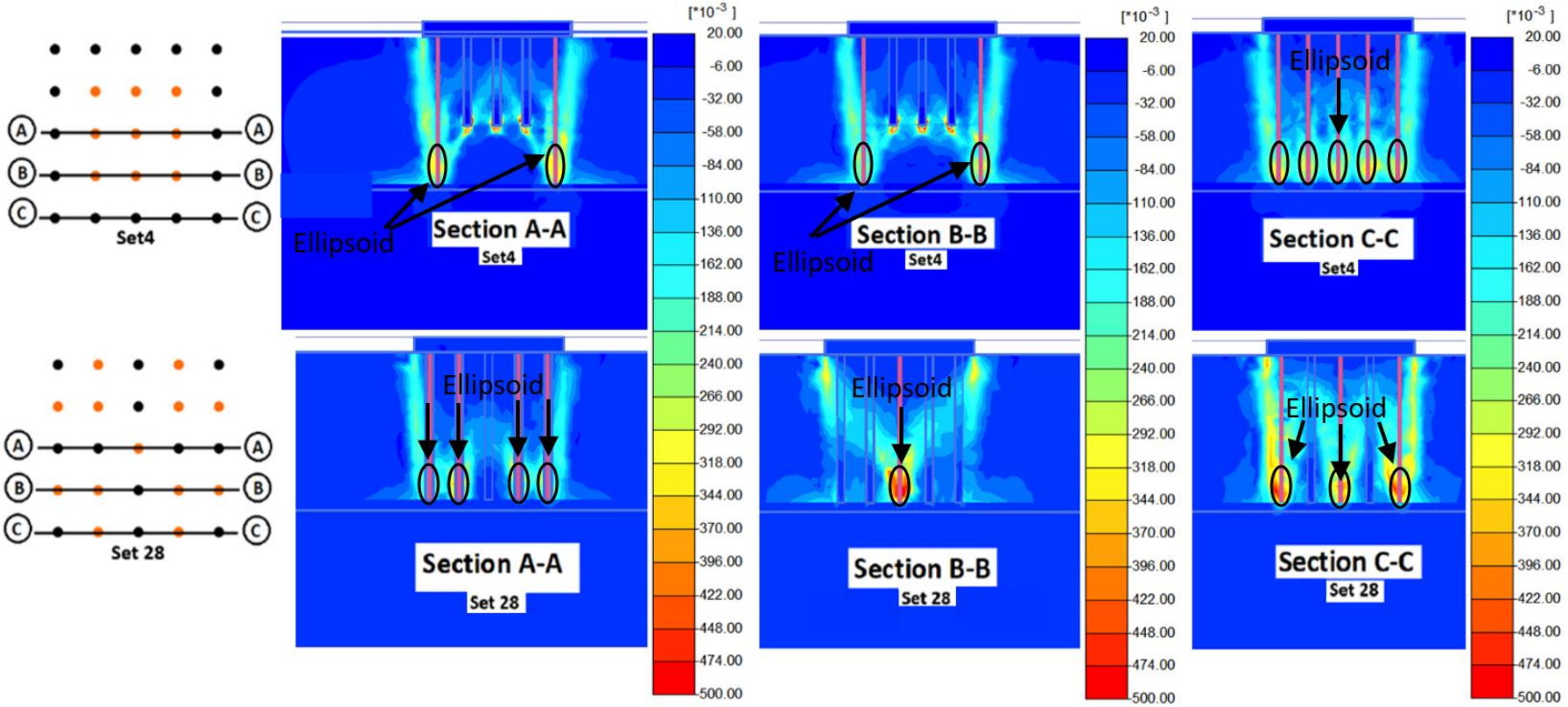


Figure 5.4: Observed behaviour (i.e., modes of failure)for the chief leading sets 4 and 28.

The ultimate carrying capacity of combined foundation can be defined as the sum of carrying capacity of raft on the composite soil (columns material/soft clay) and the carrying capacity of piles, which can be represented as.

$$Q_u = \alpha(Q_{u1} + n_1 Q_{u2}) \qquad \text{Equation 5.30}$$

Where:

$Q_{u1} = Ultimate\ composite$

$Q_{u2} = Ultimate\ of\ one\ pile$

$\alpha = configuration\ factor$ (Appendix H)

$n_1 = Number\ of\ piles$

The ultimate carrying capacity of raft on the composite soil can be estimated as

$$Q_{u1} = \left(BL - n_1 \frac{\pi D_1^2}{4}\right) q_{u1} \qquad \text{Equation 5.31}$$

q_{u1} can be determined by the general equation of Meyerhof as follows (Das & Sivakugan, 2019):

Where:

$$q_{u1} = c_{comp}\bar{N}_c + q_1\bar{N}_q + \frac{1}{2}B\gamma_{comp}\bar{N}_\gamma \qquad \text{Equation 5.32}$$

$$\bar{N}_c = N_c\left(1 + \frac{B}{L}\frac{N_q}{N_c}\right)\left(1 + 0.4\frac{D_f}{B}\right)$$

$$\bar{N}_q = N_q\left(1 + \frac{B}{L}\tan\varphi_{comp}\right)\left[1 + 2\tan\varphi_{comp}\left(1 - \sin\varphi_{comp}\right)^2\frac{D_f}{B}\right]$$

$$\bar{N}_\gamma = N_\gamma\left(1 - 0.4\frac{B}{L}\right)$$

$$N_c = \left(N_q - 1\right) \cot \varphi_{comp}$$

$$N_q = \tan^2 \left(\frac{\pi}{4} + \frac{\varphi_{comp}}{2}\right) \left(e^{\pi \tan \varphi_{comp}}\right)$$

$$N_\gamma = 2\left(N_q + 1\right) \tan \varphi_{comp}$$

$B = width\ of\ raft$

$L = Length\ of\ raft$

$c_{comp} = Cohesion\ of\ composite\ (clay + stone\ column)$

$\gamma_{comp} = Unit\ weight\ of\ the\ composite$

$\varphi_{comp} = Angle\ of\ shearing\ resistance\ of\ the\ composite$

$n_1 = Number\ of\ piles$

$D_1 = Diameter\ of\ pile$

According to Etezad et al. (2015), the different soil parameters of the composite can be determined using Equations 5.33 to 5.37:

$$q_1 = \gamma_{comp} D_f$$

$D_f = Depth\ of\ raft$

$$c_{comp} = A_s c_s + (1 - A_s) c_c \qquad \text{Equation 5.33}$$

$$\gamma_{comp} = A_s \gamma_s + (1 - A_s) \gamma_c \qquad \text{Equation 5.34}$$

$and\ A_s = Replacement\ ratio\ (Area\ of\ stone\ columns\ over\ the\ area\ of\ the\ raft\ )$

$A_{col} = Column\ cross - section$

$c_s = Cohesion\ of\ stone\ columns$

$c_c = Cohesion\ of\ soil\ (clay)$

$\gamma_s = Unit\ weight\ of\ stone\ columns$

$\gamma_c = Unit\ weight\ of\ soil\ (clay)$

$$\varphi_{comp} = \tan^{-1}[A_s \mu_s \tan \varphi_s + (1 - A_s)\mu_c \tan \varphi_c] \quad \text{Equation 5.35}$$

$$\mu_s = \frac{n}{1 + (n-1)A_s} \quad \text{Equation 5.36}$$

$$\mu_c = \frac{1}{1 + (n-1)A_s} \quad \text{Equation 5.37}$$

$\varphi_s = \ angle\ of\ shearing\ resistance\ of\ stone\ columns$

$\varphi_c = \ angle\ of\ shearing\ resistance\ of\ clay\ soil$

n = stress ratio (between 2 -6) (Mitchell & Katti, 1981)

The ultimate carrying capacity of a pile can be estimated by calculating the point bearing of pile at the pile tip and by skin or frictional resistance of pile. According to the behaviour observed from the numerical models of the combined foundation system, the shear failure occurred in the soil near the piles tips which take the shape of ellipsoid as given in Figure 4.5 and Figure 5.5. The surface area of this shear failure plane was used to estimate the skin or frictional resistance of the pile.

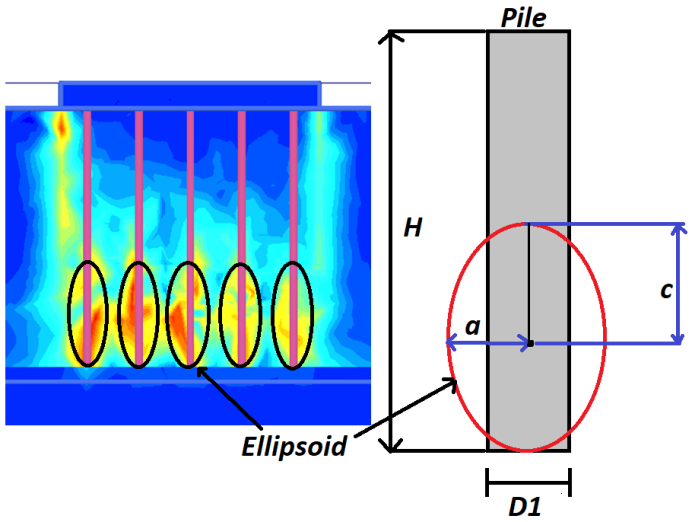


Figure 5.5: Observed behaviour

Therefore, the ultimate carrying capacity of pile (Q_{u2}) can be computed as:

$$Q_{u2} = \left[\frac{\pi D_1^2}{4}\left(q_2 N_q^* + c_2 N_c^*\right)\right] + c_u\left[2\pi a^2\left(1 + \frac{c}{ae} arc\sin e\right)\right] \quad \text{Equation 5.38}$$

$$q_2 = \left(\gamma_{comp} \times H\right) or \left(0.5 p_a \tan \varphi_2\right) \quad \text{Equation 5.39}$$

$p_a = Atmospheric\ pressure\ (100\ kN/m^2)$

$c_u = c_c = Cohesion\ of\ clay$

$c_2 = 0, c_2 = Cohesion\ of\ soil\ supporting\ the\ piles$

$\varphi_2 = Angle\ of\ shearing\ resistance\ of\ soil\ supporting\ the\ piles$

$N_q^*\ and\ N_c^* = f(\varphi_2)$

$a\ and\ C = f(D_1)$

$$e^2 = 1 - \frac{a^2}{c^2}$$

$$a = 3D_1$$

$$c = 7D_1$$

$$Q_{u2} = \left[\frac{\pi D_1^2}{4}\left(q_2 N_q^*\right)\right] + c_u\left[2\pi a^2\left(1 + \frac{c}{ae} arc\sin e\right)\right] \quad \text{Equation 5.40}$$

$$Q_{u2} = q_2\left[\frac{\pi D_1^2}{4} N_q^*\right] + c_u\left[2\pi a^2\left(1 + \frac{c}{ae} arc\sin e\right)\right] \quad \text{Equation 5.41}$$

$$Q_{u2} = q_2\bar{\bar{N}}_q + c_u\bar{\bar{N}}_c \quad \text{Equation 5.42}$$

Where:

$$\bar{\bar{N}}_q = \frac{\pi D_1^2}{4} N_q^*$$

$$\bar{\bar{N}}_c = \left[2\pi a^2\left(1 + \frac{c}{ae} arc\sin e\right)\right]$$

By substituting the carrying capacity of raft on composite soil (Q_{u1})and carrying capacity of pile (Q_{u2}) in Equation 5.30, the ultimate carrying capacity of combined foundation system can be expressed as.

$$\boldsymbol{Q_u} = \quad \text{Equation 5.43}$$

$$\boldsymbol{\alpha}\left[\begin{array}{c}\left(\boldsymbol{BL} - \boldsymbol{n_1}\dfrac{\boldsymbol{\pi D_1^2}}{\boldsymbol{4}}\right)\left(\boldsymbol{c_{comp}}\bar{\boldsymbol{N}}_{\boldsymbol{c}} + \boldsymbol{q_1}\bar{\boldsymbol{N}}_{\boldsymbol{q}} + \dfrac{\boldsymbol{1}}{\boldsymbol{2}}\boldsymbol{B\gamma_{comp}}\bar{\boldsymbol{N}}_{\boldsymbol{\gamma}}\right) + \\ \boldsymbol{n_1}\left(\boldsymbol{q_2}\bar{\bar{\boldsymbol{N}}}_{\boldsymbol{q}} + \boldsymbol{c_u}\bar{\bar{\boldsymbol{N}}}_{\boldsymbol{c}}\right)\end{array}\right]$$

In order to calibrate the analytical model, the results obtained by Equation 5.43 were compared to the results of the present numerical analysis. An admissible discrepancy was noted between the different evaluated results. This divergence can be attributed to the assumptions considered in the derivation process of the analytical model. As a means of confining or narrowing the divergence between the different results, the parameter α was introduced in Equation 5.43. It is defined as the ratio between the results obtained by the numerical model and those computed from Equation 5.43. The different values of this

parameter are summarized in Table 5.3. By excluding the last three values of this parameter, an average value of α = 0.71 was adopted for the present investigation with a standard derivation of 0.03. Subsequently, the analytical model was validated against the results of the work reported by Sharma and Kumar (2021). As mentioned previously very few works were reported in literature concerning the use of combined stone columns and pile under raft foundation. The comparison reveals that the analytical model slightly overestimates the carrying capacity of the combined foundation system (10.5 to 13.7%).

Table 5.3: Calibration of the present analytical model for combined foundation (Equation 5.43)

	Set No.	n_1	n_c	D_1 (m)	D_2 (m)	H (m)	S (m)	D_f (m)	L, B (m)	Q_u (kN/m^2) Plaxis 3D	Q_u (kN/m^2) Analytical Model (Eq. 5.43)	α
Current study	2	4	21	0.6	1	20	4	2	20	262.58	356.03	0.74
	8	4	21	0.6	1	20	4	2	20	243.1	356.03	0.68
	24	4	21	0.6	1	20	4	2	20	243.91	356.03	0.69
	25	4	21	0.6	1	20	4	2	20	252.72	356.03	0.71
	10	5	20	0.6	1	20	4	2	20	265.66	366.54	0.72
	22	5	20	0.6	1	20	4	2	20	251.45	366.54	0.69
	29	5	20	0.6	1	20	4	2	20	251.98	366.54	0.69
	30	5	20	0.6	1	20	4	2	20	258.52	366.54	0.71
	3	8	17	0.6	1	20	4	2	20	287.15	398.59	0.72
	9	8	17	0.6	1	20	4	2	20	274	398.59	0.69
	14	8	17	0.6	1	20	4	2	20	282.87	398.59	0.71
	26	8	17	0.6	1	20	4	2	20	272.75	398.59	0.68
	27	8	17	0.6	1	20	4	2	20	282.26	398.59	0.71

	11	9	16	0.6	1	20	4	2	20	293.55	409.44	0.72
	18	9	16	0.6	1	20	4	2	20	290.09	409.44	0.71
	23	9	16	0.6	1	20	4	2	20	289.7	409.44	0.71
	31	9	16	0.6	1	20	4	2	20	287.11	409.44	0.70
	32	9	16	0.6	1	20	4	2	20	286.95	409.44	0.70
	15	12	13	0.6	1	20	4	2	20	323.89	442.46	0.73
	16	12	13	0.6	1	20	4	2	20	307.99	442.46	0.70
	28	12	13	0.6	1	20	4	2	20	319.16	442.46	0.72
	19	13	12	0.6	1	20	4	2	20	321.46	453.63	0.71
	20	13	12	0.6	1	20	4	2	20	300.46	453.63	0.66
	33	13	12	0.6	1	20	4	2	20	329.58	453.63	0.73
	4	16	9	0.6	1	20	4	2	20	391.26	487.57	0.80
	17	16	9	0.6	1	20	4	2	20	352.92	487.57	0.72
	12	17	8	0.6	1	20	4	2	20	399.25	499.03	0.80
	21	17	8	0.6	1	20	4	2	20	339.95	499.03	0.68
	5	20	5	0.6	1	20	4	2	20	473.51	533.84	0.89
	13	21	4	0.6	1	20	4	2	20	515.25	545.58	0.94
	6	24	1	0.6	1	20	4	2	20	583.43	581.20	1.00
Sharma and Kumar (2021)	Piles with CSC 0.7m ø	4	5	0.5	0.7	6	1	1	4.8	284.29	317.71	-
	Piles with CSC 0.8m ø	4	5	0.5	0.8	6	1	1	4.8	299.48	347.05	-

5.5 Summary

This chapter presents the analytical models for (i) stone columns under foundation in soft clay soils (ii) piled raft foundation in soft clayey soils, and (iii) combined foundation in soft clayey soils. The behaviour (i.e., modes of failure) of the foundation systems obtained from numerical models were used to develop these analytical models for predicting the carrying capacity of foundation systems.

The ultimate carrying capacity of stone columns under raft in soft clay soil was formulated as the carrying capacity of raft on the composite soil (columns material/soft clay), the analytical model to predict the ultimate carrying capacity for the piled raft was established based on the final shape of failure mode of the foundation (hyperbolic curve) as given in Figure 5.3, and for the combined foundation system an analytical model for the prediction of the ultimate carrying capacity was developed based on the outcome of the observed behaviour (i.e., modes of failure) of the combined foundation system, using the limit equilibrium method of analysis and the principal of homogeneous composite material (i.e., homogeneous columns material/soft clay).

Additionally, the results from numerical investigations for stone columns under foundation in soft clay soils, piled raft foundation in soft clayey soils, and combined foundation in soft clayey soils and the data reported in the literature were used to validate the proposed analytical models. A comparison between the measured and calculated values of the ultimate carrying capacity of the foundations was performed and a promising agreement in the results were observed.

CHAPTER 6

CONCLUSION AND RECOMMENDATIONS

6.1 Conclusion

The main goal of this research is to study the geotechnical performance of a combined foundation system composed of stone columns and piles grouped together under a raft foundation in soft clay soil and to compare its performance with other foundation systems, such as piled raft foundation and stone columns under raft foundation. For this reason, detailed numerical investigations were performed for three types of foundation systems (a) stone columns under raft in soft clay, (b) piled raft in soft clay, and (c) stone columns/piles capped with rigid raft in soft clay using PLAXIS 3D, and the following conclusions are drawn from their parametric studies.

6.1.1 Stone Columns Under Raft Foundation in Soft Clayey Soils

1. The ultimate load carrying capacity (q_u) of the foundation system increases with the decrease in ratio (*S/D*) spacing over diameter of stone columns.
2. The ratio (*S/D*) of stone columns have no influence on the bearing capacity when (*S/D*) is greater than 7. On the other hand the bearing capacity ratio (*BCR*) improves when the ratio (*S/D*) is 4 or less.
3. The increase in the angle of friction of stone columns (φ_c) increases the ultimate load carrying capacity (q_u) of the foundation system on treated soft soil which also indicates that (*BCR*) is higher for the higher angle of friction of stone columns.
4. The assembly of stone columns installed under a rigid raft foundation in soft clayey soil were failed mostly because of shear both in columns and the soil in the surrounding regions.

5. An analytical model to predict the ultimate carrying capacity of stone columns installed under a rigid raft foundation in soft clayey soil was developed (Equation 5.1) and a comparison between the measured and calculated values of the ultimate carrying capacity (Equation 5.1) of stone columns under raft foundation in soft soils was undertaken. The results of this comparison are shown in Table 5.1, where acceptable agreement is apparent.

6.1.2 Piled Raft Foundation in Soft Clayey Soils

1. There is no significant difference in the general trend of the stress-strain curves of the piled raft foundation on soft soils apart from the decreasing rate of strain for a given stress with the increase of the ratio of spacing to pile diameter (*S/D*), as the foundation system approaches its ultimate stress.
2. The ultimate carrying capacities of the piled raft foundation decreased with increase in the ratio (*S/D*).
3. The piles spacing significantly affect the performance of the piled raft foundation on soft soil. The relationship between the improvement factor (I_{FPR}) and (*S/D*) can be considered as linear. Moreover, when the ratio *S/D* is greater than 10 (*S/D* > 10), the influence of piles on the ultimate carrying capacity of piled raft foundation is not significant.
4. The improvement factor (I_{FPR}) is lower for the more rigid piles. This can be explained by the fact that the rigid piles penetrate more easily in the layer of sand situated beneath the layer of the soft soil.
5. Based on the parametric study, a semi-empirical model to predict the ultimate carrying capacity of the piled raft foundation was developed.

6. According to the observed behaviour (i.e., modes of failure), the foundation system fails through bearing at the base of the pile group and also through shearing on inclined/curved plans near the sides of the pile group. It was observed in two-dimensional planes that failure of the foundation system by shear began to have a trapezoidal form (that is, a linear or straight line from the edge of the raft to the bottom edge of the pile group). The failure mode, however, takes the form of a hyperbolic curve when the applied load approaches the ultimate capacity of the foundation system.
7. Based on the observed behaviour (i.e., modes of failure), an analytical model to predict the ultimate carrying capacity of the piled raft foundation was developed (Equation 5.28). A more reliable and trustworthy prediction method should be based on the actual or observed behaviour. Safe and cost-effective geotechnical design of piled raft foundation is critically dependent on the representativeness of the failure modes. A comparison between the measured and calculated values of the ultimate carrying capacity (Equation 5.28) of raft foundation with piles in soft soils was undertaken. The results of this comparison are shown in Table 5.2, where acceptable agreement is apparent.

6.1.3 Combined Foundation System Composed of Stone Columns, Piles and Rigid Raft Foundation in Soft Clayey Soils

1. It was concluded from the parametric study, conducted on 680 combinations, that combining stone columns and piles in one foundation system, improve the carrying capacity of the system, modify the soil foundation to a new upgraded composite ground, and certainly reduce the cost of the geotechnical works.

2. The ultimate carrying capacity of the combined foundation system increases with the increasing number of piles in each configuration (Sets).
3. It was also observed from this study that the carrying capacity of this foundation system improves with the increase in diameter ratio of piles and columns (D_p/D_c), angle of friction of stone columns (φ_c), modulus of elasticity of clay soil, and with the decrease in the length ration of stone columns and piles (L_c/L_p).

   The diameter of the stone columns and piles can affect the overall bearing capacity of the foundation system. Larger diameter elements generally provide higher bearing capacity, allowing for increased structural loads to be safely supported. The Angle of friction of stone columns represents the internal friction between the individual particles of stone columns, increasing the angle of friction of stone columns can affect and improve the load-bearing performance of the foundation, with bigger values of angle of friction, the stone columns can better resist the shear force which can enhance the overall performance of the foundation system. For the higher values modulus of elasticity of the soft clay soil the distribution of the load among the piles and the stone columns can be uniform which can improve the performance of the foundation system. Where the length of the stone columns and piles affects the overall bearing capacity of the foundation system. Longer elements can penetrate deeper into competent soil layers, increasing the effective bearing area and providing greater load-carrying capacity.

   Load transfer mechanisms and bearing capacities can be affected by the diameter and length of the stone columns and piles, as well as their angle of friction. Foundation systems with larger diameter and longer elements can carry more load due to their increased contact area and improved shear resistance.

4. Based on the optimization study the sets 28, 33, 4, and 12 are considered the chief leading sets (i.e., the sets having the highest improvement factor). The configuration of these chief leading sets show that the stone columns and piles are arranged in a way that stone columns are confined between the piles and piles are placed on the edge of the raft. These chief leading sets can increase the bearing capacity of the raft foundation by almost 50% to 90% compared to that of raft foundation resting on stone columns only.
5. It was observed that the failure of the combined foundation system starts from the center of the raft and extend to its edges.
6. Due to the presence of the stone columns in the foundation system, the piles do not interact, and the stress transmitted by the piles to the soil does not overlap.
7. An analytical model for the prediction of the ultimate carrying capacity of the combined foundation system, using the limit equilibrium method of analysis and the principal of the homogeneous composite (columns' material/soft clay) material, was developed. To validate the proposed analytical model (Equation 5.43) data for the combined foundation systems reported in the literature were used. A comparison between the measured and calculated values of the ultimate carrying capacity (Equation 5.43) of combined foundation system (i.e., stone column/ piles caped with raft in soft soil) was undertaken. The results of this comparison are given in Table 5.3, where a promising agreement in the results can be observed between the measured and calculated ultimate carrying capacities of combined foundation system.

6.2 Recommendations

- Full scale laboratory test for combined foundation system is required to support the theories presented in this present study.
- The numerical investigation for combined foundation system should be extended for multilayer soils.
- Extend the present study for combined foundation system with encapsulated and stabilized stone columns.
- Extend the numerical study for combined foundation system under dynamic loadings.
- Extend the numerical investigation to study the performance of combined foundation system in sandy soil.

REFERENCES

Alkhorshid, N. R. (2012). *Numerical Analysis of Soft Clay Reinforced with Stone Columns*. Master Thesis, Eastern Mediterranean University, North Cyprus.

Al-Jubair, H. S., & Abbas, S. A. (2014). Finite Element Analyses of Laterally Loaded Pile Groups in Um Qaser Port. *International Journal of Scientific & Engineering Research*, 5(11), ISSN 2229-5518.

Anhtuan, V., Ducphong, P., Tuonglai, N., & Yu, H. (2014). 3D Finite Element Analysis on Behaviour of Piled Raft Foundations. *Applied Mechanics and Materials*, 580–583, 3–8. https://doi.org/10.4028/www.scientific.net/AMM.580-583.3

Abas, H. A. M. (2015). *Performance and Design Optimization of Stone Column in Sabkha Soils*. Doctoral dissertation, King Fahd university of petroleum and minerals, Saudi Arabia.

Abdel-Azim, O. A., Abdel-Rahman, K., & El-Mossallamy, Y. M. (2020). Numerical Investigation of Optimized Piled Raft Foundation for High-Rise Building in Germany. *Innovative Infrastructure Solutions*, 5(11), https://doi.org/10.1007/s41062-019-0258-4.

Al-Kazzaz, Z. A., & Al-Obaydi, M. A. (2021). Effect of Spacing between Stone Columns on the Behavior of Soft Soil. *E3S Web Conferences*, 318 01006, https://doi.org/10.1051/e3sconf/202131801006

Ahmed, A. A., & Fattah, M. Y. (2021). Distribution of Stresses Below Footings Supported by Stone Columns. *Journal of Engineering Science and Technology*, 16(2), 1719–1732.

Amornfa, K., Quang, H. T., & Tuan, T. V. (2022). 3D numerical analysis of piled raft

foundation for Ho Chi Minh City subsoil conditions. *Geomechanics and Engineering*, 29(2), 183–192. https://doi.org/10.12989/GAE.2022.29.2.183

Ayadat, T. (2022). Geotechnical Performance of Encapsulated and Stabilized Stone Columns in a Collapsible Soil. *International Journal of Geomechanics*, 22(6), 04022057. https://doi.org/10.1061/(ASCE)GM.1943-5622.0002368

Bergfelt, A. (1957). The Axial and Lateral Load Bearing Capacity and Failure By Buckling of Piles in Soft Clay.

Brandtzaeg, A., & Elvegaten, E. H. (1957). Buckling Tests of Slender Steel Piles in Soft Quick Clay. *Proceedings 4th International Conference on Soil Mechanics and Foundation Engineering*, London 2, 19–23.

Banerjee, P. K. (1970). Discussion on "Settlement and Construction Aspects", Behaviour of Piles. *Proceedings of Conference Organized by the Institution of Civil Engineering in London*, September, 207.

Burland, J. B., Broms, B. B., & de Mello, V. F. B. (1977). Behavior of Foundations and Structures. *Proceedings of 9th International Conference on Soil Mechanics and Foundation Engineering*, Tokyo, Session 2, 495–546.

Bowles, J. E. (1982). *Foundation Analysis and Design*. McGraw Hill, 3rd ed., USA.

Barksdale, R. D., & Bachus, R. C. (1983). *Design and Construction of Stone Columns*. Report No. FHWA/RD-83/026, Federal Highway Administration, U.S.A, 1.

Bachus, R. C., & Barksdale, R. D. (1984). Vertical and Lateral Behaviour of Model Stone Columns. *In Proceedings of the International Conference on In-situ Soil and Rock Reinforcement*, Paris, 99–104.

Balaam, N. P., & Booker, J. R. (1985). Effect of Stone Column Yield on Settlement of Rigid Foundations in Stabilized Clay. *Internation Journal for Numerical and Analytical*

Methods in Geomechanics, 9(4), 331-351.

Budhu, M. (2000). *Soil Mechanics and Foundations*. John Wiley & Sons, INC., 1st ed., New York.

Bae, W. S., Bang, W. S., & Byung, C. A. (2002). Behavior of Foundation System Improved with Stone Columns. *The Proceedings of the 12th International Offshore and Polar Engineering Conference*, Japan, 675–678.

Brinkgreve, R., Swolfs, W., & Engin, E. (2013). *PLAXIS User's Manual*. Balkema, Rotterdam, The Netherlands.

Balakumar, V., Oh, E., Bolton, M., & Balasubramaniam, A. S. (2013). A Design Method for Piled Raft Foundations. *Proceedings of the 18th International Conference on Soil Mechanics and Geotechnical Engineering*, Paris.

Baca, M., Ivannikov, A. L., & Rybak, J. (2021). Numerical Modelling of Various Aspects of Pipe Pile Static Load Test. *Energies*, 14(24), 8598. https://doi.org/10.3390/en14248598

Bhaumik, M., Singh, S. P., & Biswas, M. (2021). Behavior of Rigid Footing Rested on a Group of Stone Column, In: Patel, S., Solanki, C.H., Reddy, K.R., & Shukla, S.K. (eds) *Proceedings of the Indian Geotechnical Conference* 2019, *Lecture Notes in Civil Engineering*, 133. Springer, Singapore. https://doi.org/10.1007/978-981-33-6346-5_37.

Boumekik, N. E. I., Labed, M., Mellas, M., & Mabrouki, A. (2021). Optimization of the Ultimate Bearing Capacity of Reinforced Soft Soils through the Concept of the Critical Length of Stone Columns. *Civil Engineering Journal*, 7(9).

Caquot, A., & Kerisel. J. (1948). Tables for the Calculation of Passive Pressure, Active Pressure and Bearing Capacity of Foundations. *Gautier-Villars*, Paris.

Chin, F. K. (1972). The Inverse Slope as a Prediction of Ultimate Bearing Capacity of Piles. *In Proceedings of the Second Southeast Asian Conference on Soil Engineerin*, 83–91.

Charles, W. W. N., Yau, T. L. Y., Jonathan H. M. L., & Tang, W. H. (2001). New Failure Load Criterion for Large Diameter Bored Piles in Weathered Geomaterials. *Journal of Geotechnical and Geoenviromental Engineering*, 127(6), 488–498.

Castro, J., & Sagaseta, C. (2009). Consolidation Around Stone Columns. Influence of Column Deformation. *The International Journal for Numerical and Analytical Methods in Geomechanics*, 33(7), 851–877.

Cho, J., Lee, J.-H., Jeong, S., & Lee, J. (2012). The Settlement Behavior of Piled Raft in Clay Soils. *Ocean Engineering*, Volume 53,153–163.

Castro, J. (2014). Numerical Modelling of Stone Columns Beneath a Rigid Footing. *Computers and Geotechnics*, Volume 60, 77–87.

Celik, F. (2019). An Analytical Approach for Piled-Raft Foundation Design Based on Equivalent Pier and Raft Analyses by Using 2D Finite Element Method. *Arabian Journal of Geosciences*, 12(14), 429. https://doi.org/10.1007/s12517-019-4579-6

Castro, J., Miranda, M., Costa, A. D., Cañizal, J., & Sagaseta, C. (2019). Critical length of stone columns. *Proceedings of the XVII European Conference on Soil Mechanics and Geotechnical Engineering, Geotechnical Engineering, foundation of the future*, 1182–1189. https://doi.org/10.32075/17ECSMGE-2019-0220

Davis, E. H., & Poulos, H. G. (1972). The Analysis of Piled Raft Systems. *Australian Geomechanics Journal*, G2: 21–27.

Datye, K. R. (1982). Settlement and Bearing Capacity of Foundation System with Stone Columns. *Proceeding Symposium on Soil & Rock Improvement Techniques*

Including Geotextiles, Reinforced Earth and Modern Piling Methods, AIT, Bangkok, Thailand.

Das, B. M. (2000). *Fundamentals of Geotechnical Engineering*. Brooks/Cole, 1st ed., USA.

De Sanctis, L., & Mandolini, A. (2006). Bearing Capacity of Piled Rafts on Soft Clay Soils. *Journal of Geotechnical and Geo-environmental Engineering*, 132(12), 1600–1610. https://doi.org/10.1061/(ASCE)1090-0241(2006)132:12(1600)

Das, B. M. & Sivakugan, N. (2019). *Principles of Foundation Engineering*. 9th Edition, Cengage Learning, ISBN-13: 978-1-337-70503-5.

Deb, P., & Pal, S. K. (2022). Structural and Geotechnical Aspects of Piled Raft Foundation Through Numerical Analysis. *Marine Georesources & Geotechnology*, 40(7), 823–846. https://doi.org/10.1080/1064119X.2021.1943083

Etezad. B. M. (2007). *Geotechnical Performance of Group of Stone Columns*. Doctoral dissertation, Concordia University, Montreal, Quebec, Canada.

El-Garhy, B., Galil, A. A., Youssef, A.-F., & Raia, M. A. (2013). Behavior of Raft on Settlement Reducing Piles: Experimental Model Study. *Journal of Rock Mechanics and Geotechnical Engineering*, 5(5), 389–399. https://doi.org/10.1016/j.jrmge.2013.07.005

Etezad, M., Hanna, A. M., & Ayadat. T. (2015). Bearing Capacity of a Group of Stone Columns in Soft Soil. *International Journal of Geomechanics*, 15(2), 04014043. https://doi.org/10.1061/(ASCE)GM.1943-5622.0000393.

Elsawy, M., & El-Garhy, B. (2016). Behavior of Raft Foundation Resting on Improved Soft Soil with Conventional Granular Piles. *Journal of Scientific and Engineering Research*, 3(4), 428-434.

Elwakil, A. Z., & Azzam, W. R. (2016). Experimental and Numerical Study of Piled Raft

System. *Alexandria Engineering Journal*, 55(1), 547–560.

Etezad, M., Hanna, A. M., & Khalifa, M. (2018). Bearing Capacity of a Group of Stone Columns in Soft Soil Subjected to Local or Punching Shear Failures. *International Journal of Geomechanics*, 18(12), 04018169. https://doi.org/10.1061/(ASCE)GM.1943-5622.0001300

Elsawwaf, M., Shahien, M., Nasr, A. & Magdy, A. (2022). The Behavior of Piled Rafts in Soft Clay: Numerical Investigation. *Journal of the Mechanical Behavior of Materials*, 31(1), 426–434. https://doi.org/10.1515/jmbm-2022-0050.

Fattah, M. Y., & Majeed, Q. G. (2012). Finite Element Analysis of Geogrid Encased Stone Columns. *Geotechnical and Geological Engineering*, 30(4), 713–726. https://doi.org/10.1007/s10706-011-9488-8

Fan, H., Huang, Q., & Liang, R. (2014). Reliability Analysis of Piles in Spatially Varying Soils Considering Multiple Failure Modes. *Journal of Computers and Geotechnics*, 57, 97–104. https://doi.org/10.1016/j.compgeo.2014.01.009

Fattah, M. Y., Al-Neami, M. A., & Al-Suhaily, A. S. (2017). Estimation of Bearing Capacity of Floating Group Of Stone Columns. *Engineering Science and Technology, An International Journal*, 20(3), 1166–1172.

Ferchat, A., Benmebarek, S., & Houhou, M. N. (2021). 3D numerical analysis of piled raft interaction in drained soft clay conditions. *Arabian Journal of Geosciences*, 14(5), 394. https://doi.org/10.1007/s12517-021-06783-3

Golder, H. Q., & Skipp, B. O. (1957). The Buckling of Piles in Soft Clay. *Proceedings of the 4th International Conference on Soil Mechanics and Foundation Engineering*, London, 35–39.

Gonzalez-Nicieza, C., Alvarez-Fernandez, M. I., Alvarez-Vigil, A. E., & Menendez-Dıaz,

A. (2007). Forensic Analysis of Foundation Failure in Gypsiferous Ground. *Journal of Engineering Failure Analysis*, 15(6).

Ghazavi, M., & Afshar, J. N. (2013). Bearing Capacity of Geosynthetic Encased Stone Columns. *Geotextiles and Geomembranes*, 10(2), 47–53.

Ghalesari, A. T., & Choobbasti., A. J. (2018). Numerical Analysis of Settlement and Bearing Behaviour of Piled Raft in Babol Clay. *European Journal of Environmental and Civil Engineering*, 22(8), 978-1003. DOI: 10.1080/19648189.2016.1229230

Grizi, A., Al-Ani, W., & Wanatowski, D. (2022). Numerical Analysis of the Settlement Behavior of Soft Soil Improved with Stone Columns. *Applied Sciences*, 12(11), 5293. https://doi.org/10.3390/app12115293

Hooper, J. A. (1973). Observations on The Behavior of A Piled-Raft Systems. *Geotechnique*, 28(1), 65–83.

Hughes, J. M., & Withers, N. J. (1974). Reinforcing of Soft Cohesive Soils with Stone Columns. *Ground Engineering*, 7(3), 42–49.

Hu, W., Wood, D. M., & Stewart, W. (1997). Ground Improvement Using Stone Column Foundations: Result of Model Tests. *International Conference on Ground Improvement Techniques*, 247–256.

Horikoshi, K., & Randolph, M. F. (1999). Estimation of Overall Settlement of Piled Rafts. Soils and Foundations, 39(2), 59–68. https://doi.org/10.3208/sandf.39.2_59

Hasan, A., Seyhan, F., Isa, V., & Zeki, G. (2009). Soil and Foundation Stability Improvement by Stone Column: A Case Study in Adapazari City, Turkey. *Scientific Research and Essay*, 4(10), 972-983.

Hussein, M. H., McGillivray, R. T., & Brown, D. A. (2012). Knowledge Is Bliss-A Case for Supplemental Pile Testing to Ascertain Fidelity. *Full-Scale Testing and Foundation*

Design, 322–332. https://doi.org/10.1061/9780784412084.0024

Hanna, A. M., Etezad, M., & Ayadat, T. (2013). Mode of Failure of a Group of Stone Columns in Soft Soil. *International Journal of Geomechanics*, 13(1), 87–96. https://doi.org/10.1061/(ASCE)GM.1943-5622.0000175

Hataf, N., Nabipour, N., & Sadr, A. (2020). Experimental and numerical study on the bearing capacity of encased stone columns. *International Journal of Geo-Engineering*, 11(1), 4. https://doi.org/10.1186/s40703-020-00111-6

Hadri, S., Messast, S., & Bekkouche, S. R. (2021). Numerical Analysis of the Performance of Stone Columns Used for Ground Improvement. *Jordan Journal of Civil Engineering*, 15(2).

Idrus, J., Shien, N. K., Nujid, M. M., & Abdullah, N. H. H. (2023). *A review of stone columns performance in soft soils*. 040003. https://doi.org/10.1063/5.0111958

Jendeby, L. (1986). Friction Piled Foundations in Soft Clay - A Study of Load Transfer and Settlements. Chalmers University of Technology, Gothenburg.

Kolar, V., & Nemec, I. (1989). Modeling of Soil-Structure Interaction. *Elsevier*, New York.

Kozubal, J., Puła, W., & Stach, M. (2014). Reliability Assessment of a Single Pile in Unsaturated Substrate under Climate Factors Influence. *Procedia Engineering*, Volume 91, 310–316. https://doi.org/10.1016/j.proeng.2014.12.066

Kardgar, H. (2018). Investigation of The Bearing Capacity of Foundations on Encased Stone Columns Using Finite Element Method. *International Journal of Integrated Engineering*, 10(1), 103–108.

Khalifa, M., Etezad, M., Hanna, A., & Sabry, M. (2018). Bearing Capacity of Strip Foundation on Soft Soil Reinforced with Stone Columns Using Method of Slices. In W. Frikha, S. Varaksin, & A. Viana Da Fonseca (Eds.), *Soil Testing, Soil Stability*

and Ground Improvement (pp. 79–91). Springer International Publishing. https://doi.org/10.1007/978-3-319-61902-6_8

Khanmohammadi, M., & Fakharian, K. (2018). Evaluation of performance of piled-raft foundations on soft clay: A case study. *Geomechanics and Engineering*, 14(1), 43–50. https://doi.org/10.12989/GAE.2018.14.1.043

Kumar, V., & Kumar, A. (2018). An experimental study to analyse the behaviour of piled-raft foundation model under the application of vertical load. *Innovative Infrastructure Solutions*, 3(1), 35. https://doi.org/10.1007/s41062-018-0141-8

Karkush, M. O., & Jabbar, A. (2019). Improvement of Soft Soil Using Linear Distributed Floating Stone Columns under Foundation Subjected to Static and Cyclic Loading. *Civil Engineering Journal*, 5(3), 702. https://doi.org/10.28991/cej-2019-03091280

Kim, U., Kim, J., Kim, J., Min, B., & Choi, H. (2021). Development of Expandable Steel Pipe Piles to Improve Bearing Capacity. *Journal of the Korean GEO-Environmental Society*, 22(12), 5–13. https://doi.org/10.14481/JKGES.2021.22.12.5

Kouklanifar, M. (2023). A New Analytical Approach for Determination of the Bearing Capacity of a Strip Foundation on a Granular Trench. *International Journal of Geomechanics*, 23(7), 04023107. https://doi.org/10.1061/(ASCE)GM.1943-5622.0002568

Lawton, E. C., Fragaszy, R. J., & Hardcastle, J. H. (1991). Stress Ratio Effects on Collapse of Compacted Clayey Sand. *Journal of Geotechnical Engineering*, 117(5), 714–730. https://doi.org/10.1061/(ASCE)0733-9410(1991)117:5(714)

Lee, J. S. & Pande, G. N. (1998). Analysis of stone-column reinforced foundations. *International Journal for Numerical and Analytical Methods in Geomechanics*, 22(12), 1001–1020.

Liang, F.-Y., Chen, L.-Z., & Shi, X.-G. (2003). Numerical analysis of composite piled raft with cushion subjected to vertical load. *Computers and Geotechnics*, 30(6), 443–453. https://doi.org/10.1016/S0266-352X(03)00057-0

López Gayarre, F., González-Nicieza, C., Alvarez-Fernández, M. I., & Álvarez-Vigil, A. E. (2010). Forensic analysis of a pile foundation failure. *Engineering Failure Analysis*, 17(2), 486–497. https://doi.org/10.1016/j.engfailanal.2009.09.008

Lee, J., Kim, Y., & Jeong, S. (2010). Three-dimensional analysis of bearing behavior of piled raft on soft clay. *Computers and Geotechnics*, 37(1–2), 103–114. https://doi.org/10.1016/j.compgeo.2009.07.009

Lodha, M., Arora, R. P., & Solanki, A. (2021). Finite Element Analysis of Piled Raft Foundation in Clay and Sand. In S. Patel, C. H. Solanki, K. R. Reddy, & S. K. Shukla (Eds.), *Proceedings of the Indian Geotechnical Conference 2019* (Vol. 137, pp. 525–535). Springer Singapore. https://doi.org/10.1007/978-981-33-6466-0_48

Moreau, Neil., & Mary. (1835). Foundations-emploi du Sable. *Annales des Ponts et Chaussees, Memoires*, No. 224, 171-214.

Mitchell, J. K., & Katti, R. K. (1981). Soil Improvement State-of-The-Art Report. *Proceedings of 10th International Conference on Soil Mechanics and Foundation Engineering*, Balkema, Rotterdam, Netherlands, 509–565.

Michael, M. B., Roberto, C., & Gerd, G. (2004). Experimental and Numerical Investigation of The Behaviour of Piles in Soft Soils Under Monotonic And Alternating Loading. *13th World Conference on Earthquake Engineering Vancouver*, B.C., Canada Paper No. 2964.

Mossallamy, Y. M., Lutz, B., & Duerrwang, R. (2009). Special Aspects Related To The Behavior of Piled Raft Foundation. *In Proceedings of the 17th International*

Conference on Soil Mechanics and Geotechnical Engineering, 1, 2, 3 and 4, 1366-1369. IOS Press.

Masoumeh, M., & Behzad, K. (2012). Soft Soil Stabilization Using Stone Columns—A Review. *Electronic Journal of Geotechnical Engineering*, Volume 17.

Micheál, M. K., & Bryan, A. McCabe. (2014). Settlement Performance of Pad Footings on Soft Clay Supported By Stone Columns: A Numerical Study. *Soils and Foundations*, 54(4), 760–776. https://doi.org/10.1016/j.sandf.2014.06.011

Mali, S., & Singh, B. (2018). Behavior of large piled-raft foundation on clay soil. *Ocean Engineering*, Volume 149, 205–216. https://doi.org/10.1016/j.oceaneng.2017.12.029

Madun, A., Meghzili, S. A., Tajudin, S., Yusof, M. F., Zainalabidin, M. H., Al-Gheethi, A. A., Dan, M. F. M., & Ismail, M. A. M. (2018). Mathematical solution of the stone column effect on the load bearing capacity and settlement using numerical analysis. *Journal of Physics: Conference Series*, 995, 012036. https://doi.org/10.1088/1742-6596/995/1/012036

Mali, S., & Singh, B. (2019). Behavior of large piled raft foundation on different soil profiles for different loadings and different pile raft configurations. *Innovative Infrastructure Solutions*, 4(1), 8. https://doi.org/10.1007/s41062-018-0193-9

Mali, S., & Singh, B. (2020). 3D Numerical Modeling of Large Piled-Raft Foundation on Clayey Soils for Different Loadings and Pile-Raft Configurations. *Studia Geotechnica et Mechanica*, 42(1), 1–17.

Mali, S., & Singh, B. (2021). Assessing the effect of governing parameters of bearing capacity determination of small piled rafts on clay soil. *Arabian Journal of Geosciences*, 14(22), 2261. https://doi.org/10.1007/s12517-021-08609-8

Mugahed, S. M., Azzam, W. R, Mohamed, M. K. (2022). Behaviour of Encased Stone Columns in Soft Clay. *Journal of Engineering Research*, 6(3), 71-75. https://doi.org/10.21608/erjeng.2022.151915.1084

Nguyen, D. D. C., Kim, D.-S., & Jo, S.-B. (2014). Parametric study for optimal design of large piled raft foundations on sand. *Computers and Geotechnics*, 55, 14–26. https://doi.org/10.1016/j.compgeo.2013.07.014

Ng, K. S., & Ann, T. S. (2014). Parametric study on the settlement improvement factor of stone column groups. https://doi.org/10.13140/2.1.5092.8328

Nazari, A. J., & Ghazavi, M. (2014). A Simple Analytical Method For Calculation Of Bearing Capacity Of Stone-Column. *International Journal of Civil Engineering*, 12(1), 15–25.

Ng, K. S. (2018). Numerical study on bearing capacity of single stone column. *International Journal of Geo-Engineering*, 9(1), 9. https://doi.org/10.1186/s40703-018-0077-z.

Naderi, E., Asakereh, A., & Dehghani, M. (2018). Bearing Capacity of Strip Footing on Clay Slope Reinforced with Stone Columns. *Arabian Journal for Science and Engineering*, 43(10), 5559–5572. https://doi.org/10.1007/s13369-018-3231-1

Nazariafshar, J., Mehrannia, N., Kalantary, F., & Ganjian, N. (2019). Bearing Capacity of Group of Stone Columns with Granular Blankets. *International Journal of Civil Engineering*, 17(2), 253–263. https://doi.org/10.1007/s40999-017-0271-y

Naseer, S., Sarfraz Faiz, M., Iqbal, S., & Jamil, S. M. (2019). Laboratory and numerical based analysis of floating sand columns in clayey soil. *International Journal of Geo-Engineering*, 10(1), 10. https://doi.org/10.1186/s40703-019-0106-6

Ng, K. S., Idrus, J., & Chew, Y. M. (2021). Bearing Capacity of Stone Column Reinforced Foundation Subjected to Inclined Loadings. *International Journal of Geosynthetics*

and Ground Engineering, 7(3), 62. https://doi.org/10.1007/s40891-021-00307-5

Opeyemi, D. A. (2009). Probabilistic Failure Analysis of Static Pile Capacity for Steel in Cohesive and Cohesionless Soils. *The Electronic Journal of Geotechnical Engineering*, Volume 14.

Omemean. Z. M., (2012). *Load Sharing of Piled-Raft Foundations in Sand Subjected to Vertical Loads*. Doctoral dissertation, Concordia University, Montreal, Quebec, Canada.

Priebe, H. J. (1995). The Design Of Vibro Replacement. *Ground Engineering*, 31–37.

Poulos, H. G., Small, J. C., & Chow, H. (2011). Piled Raft Foundations for Tall Buildings. *Geotechnical Engineering Journal of the SEAGS & AGSSEA*, 42(2), ISSN 0046-5828.

Pivarč, J. (2011). Stone Columns—Determination of the soil improvement factor. *Slovak Journal of Civil Engineering*, 19(3), 17–21. https://doi.org/10.2478/v10189-011-0014-z

Prasad, A., Kazemian, S., Kalantari, B., & Bujang B. K. H. (2012). A Behavior of Reinforced Vibrocompacted Stone Column in Peat. *Pertanika Journal of Science and Technology*, 20(2), 221–241.

Prashant, G., Harvinder, S., & Jagadanand, J. (2013). Optimisation of Piled-Raft Foundation. *UKIERI Concrete Congress - Innovations in Concrete Construction*.

Paravita, S. W., & Daniel, T. 2015. Analysis of Piled Raft Foundation on Soft Soil Using PLAXIS 2D. *Procedia Engineering*, Volume 125, 363–367. https://doi.org/10.1016/j.proeng.2015.11.083

Patil, J. D., Vasanvala, S. A., & Solanki, C. H. (2016). An Experimental Study on Behaviour of Piled Raft Foundation. *Indian Geotechnical Journal*, 46(1), 16–24.

https://doi.org/10.1007/s40098-015-0145-7

Plaban D, P., Debnath, B., Reang, R. B., & Pal, S. K. (2022). Structural Analysis of Piled Raft Foundation in Soft Soil: An Experimental Simulation and Parametric Study with Numerical Method. *Ocean Engineering*, Volume 261, 112139. https://doi.org/10.1016/j.oceaneng.2022.112139

Rao, N. S., Reddy, K. M., & Rumar, P. H. (1997). Studies on Groups of Stone Columns in Soft Clays. *Geotechnical Engineering-Bangkok*, 28(2), 165–182.

Sinha, A. (2013). *3-D Modeling of Piled Raft Foundation.* Doctoral dissertation. Concordia University, Montreal, Quebec, Canada.

Sheil. B. B. (2014). *Numerical and Analytical Modelling of Friction Pile Group Settlement Performance in Clay*. Doctoral dissertation, National University of Ireland.

Samanta, M., & Bhowmik, R. (2019). 3D numerical analysis of piled raft foundation in stone column improved soft soil. *International Journal of Geotechnical Engineering*, 13(5), 474–483. https://doi.org/10.1080/19386362.2017.1368139

Sinha, A., & Hanna, A. M. (2017). 3D Numerical Model for Piled Raft Foundation. *International Journal of Geomechanics*, 17(2), 04016055. https://doi.org/10.1061/(ASCE)GM.1943-5622.0000674

Sharma, S., & Kumar, S. J. (2021). Behaviour of Raft Foundation Supported by Stone Columns and Combination with Rigid Piles in Soft Clay Soils: 3D Numerical Study. *International Research Journal of Engineering and Technology*, 8(9).

Samangani, A. Y. & Naderi, R. (2022). Numerical and Large-Scale Laboratory Study of Rock Column Groups in Sandy Soil Behavior Improvement. *Advances in Civil Engineering*, 1–11. https://doi.org/10.1155/2022/9259093

Saxena, S., & Roy, L. B. (2022). Suitability Analysis of Stone Column Materials with

PLAXIS. *Engineering, Technology & Applied Science Research*, 12(2), 8421–8425. https://doi.org/10.48084/etasr.4761

Tan, Y. C., & Chow, C. M. (2004). Design of Piled Raft Foundation on Soft Ground. *GSM-IEM Forum: The roles of engineering geology and geotechnical engineering in construction works*, Kuala Lumpur.

Tran, T. V., Kimura, M., & Boonyatee, T. (2012). 3D FE Analysis of Effect of Ground Subsidence and Piled Spacing on Ultimate Bearing Capacity of Piled Raft and Axial Force of Piles in Piled Raft. *Open Journal of Civil Engineering*, 02(04), 206–213. https://doi.org/10.4236/ojce.2012.24027

Tschuchnigg. F. (2012). *3D Finite Element Modelling of Deep Foundations Employing an Embedded Pile Formulation*. Doctoral dissertation, Graz University of Technology.

Unni, S., Jerom, A., Prakash, J., Jessian, S. C., & R, S. (2021). Parametric Study on Bearing Capacity of Geosynthetic Encased Stone Column Installed in Soft Clay. *SSRN Electronic Journal*. https://doi.org/10.2139/ssrn.3988280

Wehr, W. (1999). Schottersäulen – Das Verhalten Von Einzelnen Säulen Und Säulengruppen. *Geotechnik,* 22(1), 40–47. (In German).

Wood, D. M., Hu, W., & Nash, D. F. T. (2000). Group Effects In Stone Column Foundations: Model Tests. *Geotechnique*, 50(6), 689–698.

Wright, H., & Touquet J.-L. (2004). Calcul Des Colonnes Ballastées Sous Un Dallage – Comparaison Des Résultats De Différentes Méthodes. *Proceedings International Symposium on Gorund Improvement*, Paris, 333-346. (In French).

Watcharasawe, K., Kitiyodom, P., & Jongpradist, P. (2017). 3-D Numerical Analysis of Consolidation Effect on Piled Raft Foundation in Bangkok Subsoil Condition. *International Journal of GEOMATE*, 12(31).

https://doi.org/10.21660/2017.31.6529

Yao, A., Jiantao, Z., & Yijun, Z. (2016). Study on the Dynamic Response of the Steel Pipe Pile Foundation During Construction of Neighborhood Deep Excavation. *Procedia Engineering*, Volume 165, 58–68. https://doi.org/10.1016/j.proeng.2016.11.735

Zeevaert, L. (1957). Compensated Friction-Pile Foundation to Reduce The Settlement of Buildings on The Highly Compressible Volcanic Clay of Mexico City. *In Proceedings of the 4th International Conference on Soil Mechanics and Foundation Engineering*, 81-86.

Zhang, L. M., & Dasaka, S. M. (2010). Uncertainties in Geologic Profiles Versus Variability in Pile Founding Depth. *Journal of Geotechnical and Geoenvironmental Engineering*, 136(11), 1475–1488.

Ziaie, M. R., & Mohammadi-Haji, B. (2016). Circular Raft Footings Strengthened by Stone Columns under Static Loads. *International Journal of Civil, Environmental, Structural, Construction and Architectural Engineering*, 10(9).

Znamenskii, V. V., & Sayed, D. A. (2019). Comparison between Analytical Method and Numerical Model for Footings on Soft Clay Supported by Stone Columns. *Journal of Physics: Conference Series*, 1425(1), 012075. https://doi.org/10.1088/1742-6596/1425/1/012075

Znamenskii, V. V., Hegazy, O. M., & Sayed, D. A. (2021). The 3D numerical model of the stone column in soft clay soils. *Journal of Physics: Conference Series*, 1928(1), 012011. https://doi.org/10.1088/1742-6596/1928/1/012011

APPENDICES

Appendix A: (STRESS VS STRAIN FOR PILED RAFT FOUNDATION)

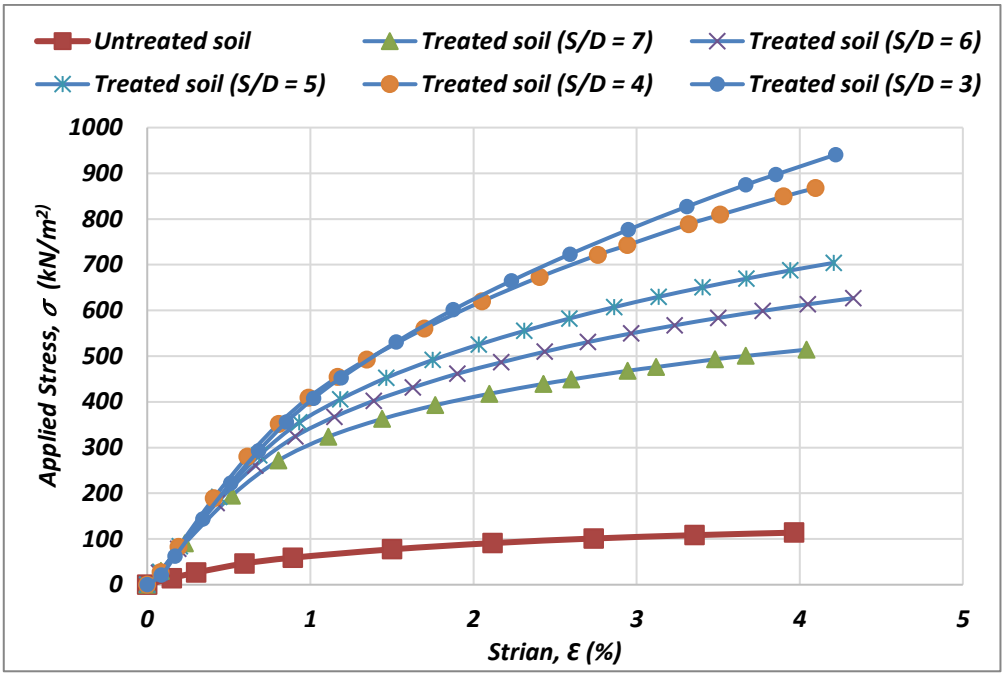


Figure A.1: Stress Vs Strain for *L/D* = 40, Ep/Es = 52500

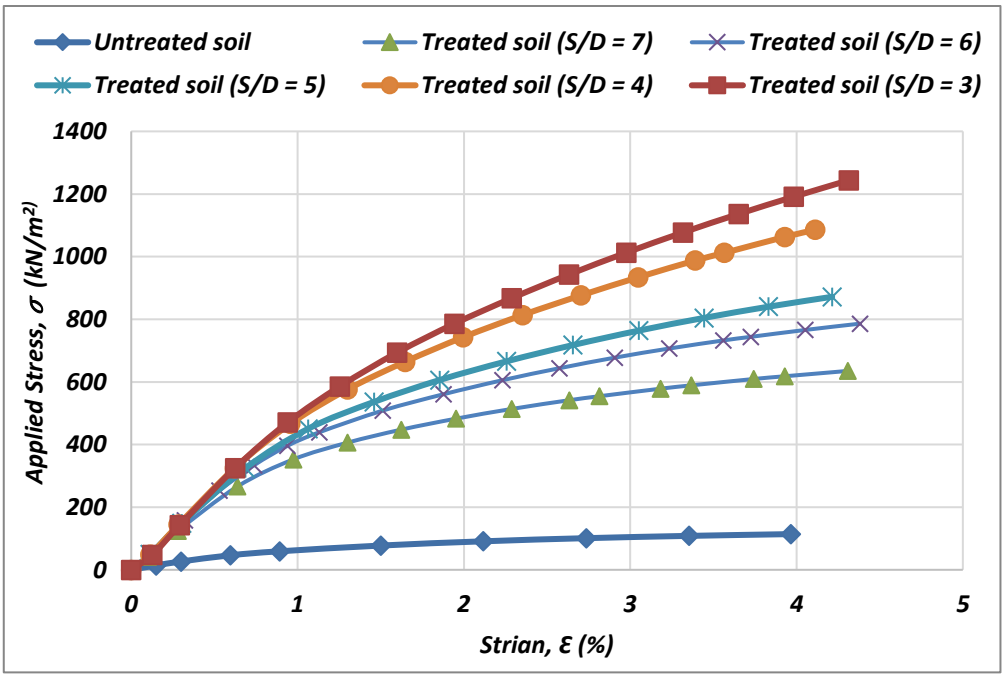


Figure A.2: Stress Vs Strain for *L/D* = 33.33, Ep/Es = 52500

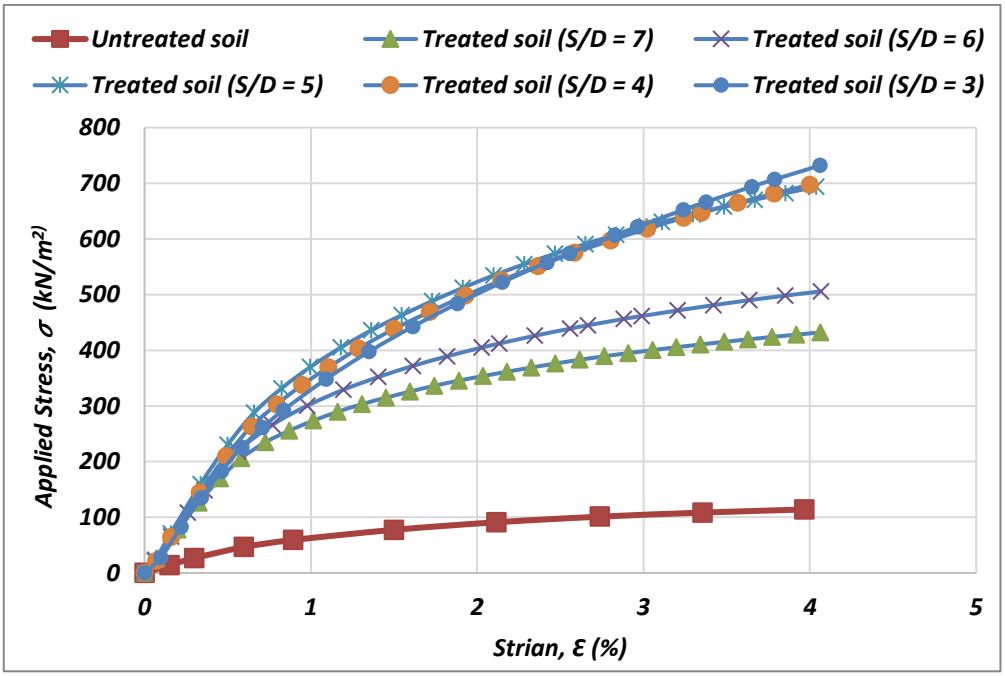


Figure A.3: Stress Vs Strain for *L/D* = 50, Ep/Es = 35000

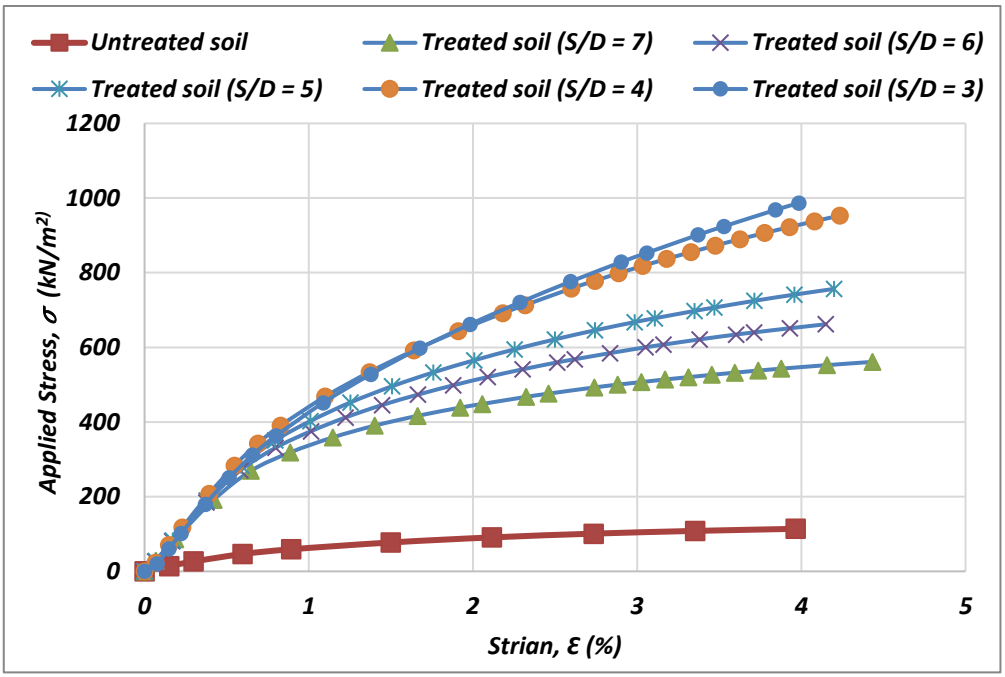


Figure A.4: Stress Vs Strain for *L/D* = 40, Ep/Es = 35000

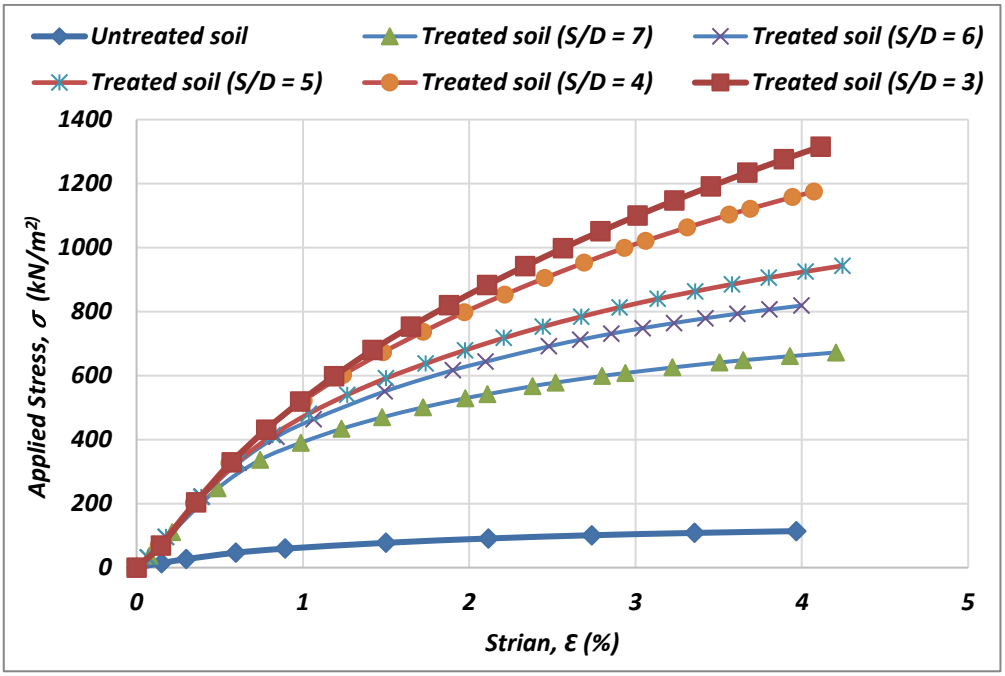


Figure A.5: Stress Vs Strain for *L/D* = 33.33, Ep/Es = 35000

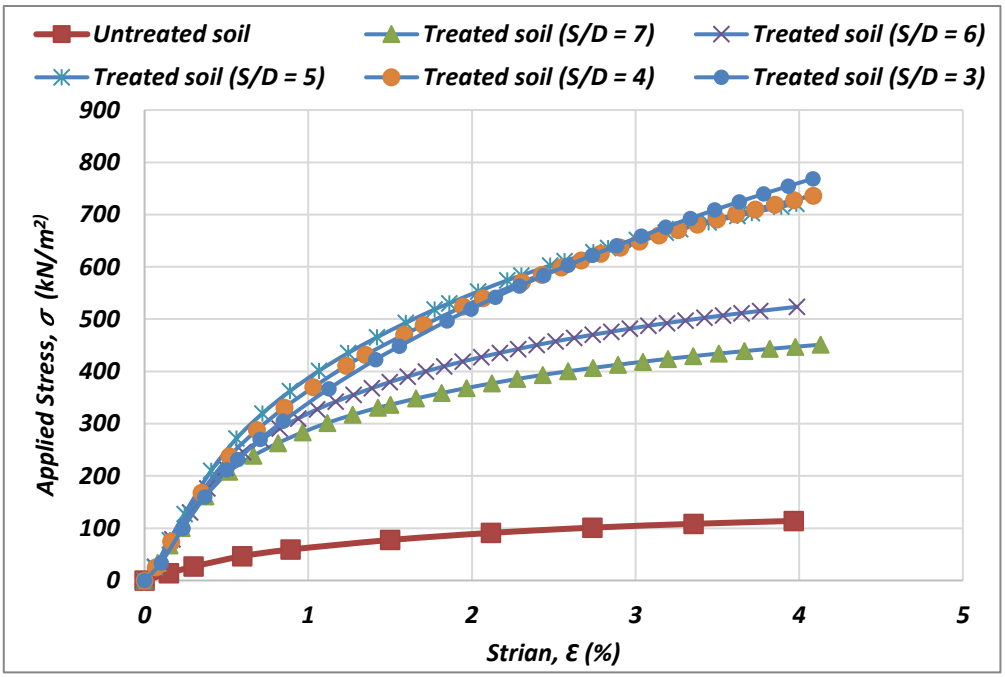


Figure A.6: Stress Vs Strain for *L/D* = 50, Ep/Es = 26250

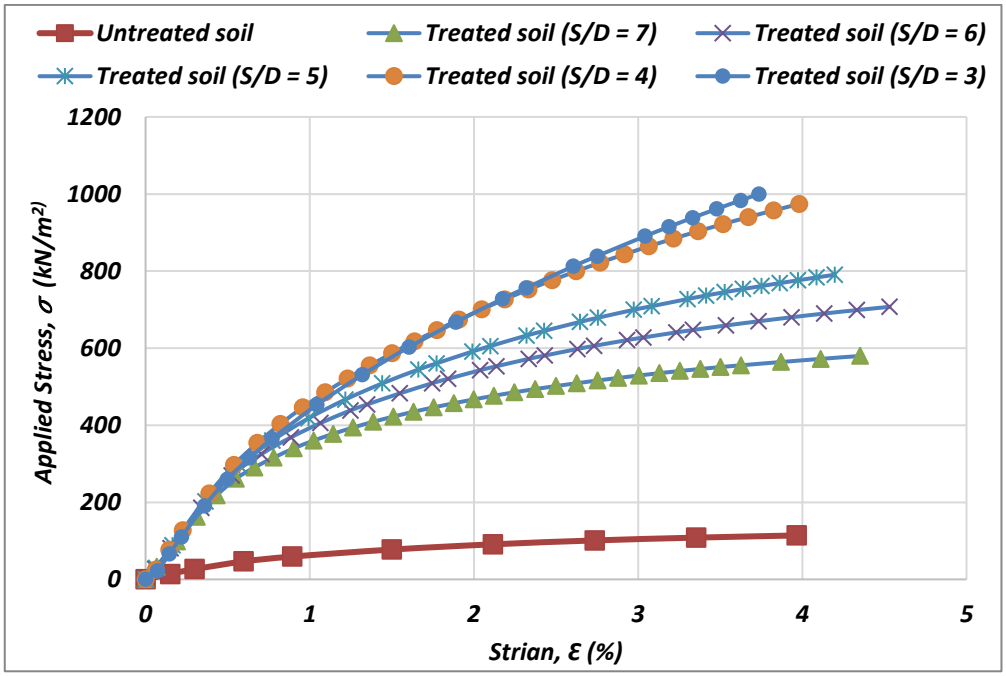


Figure A.7: Stress Vs Strain for *L/D* = 40, Ep/Es = 26250

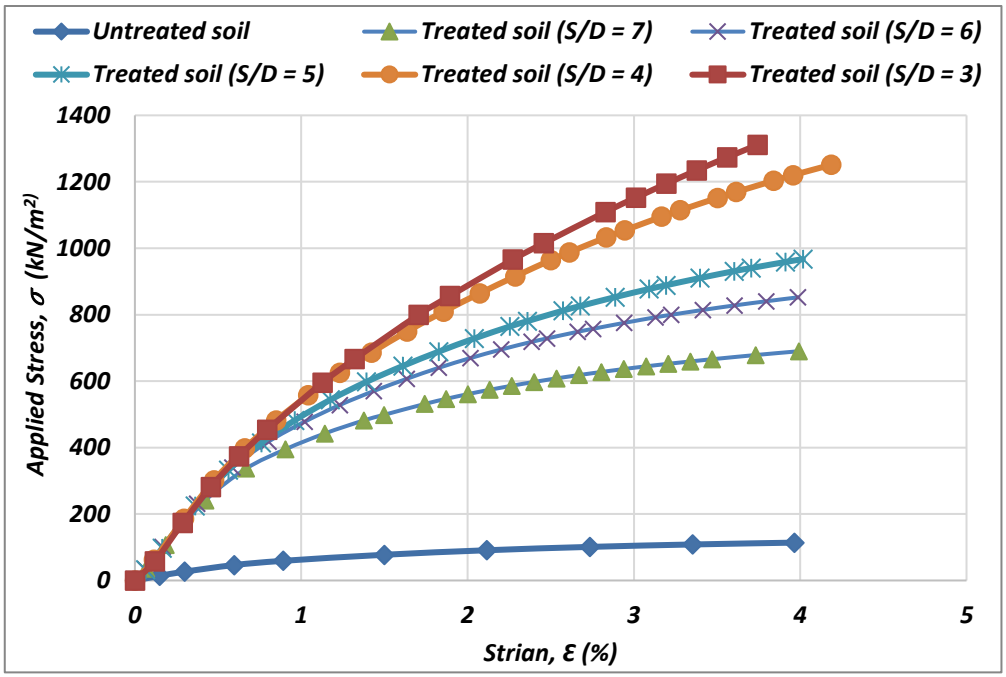


Figure A.8: Stress Vs Strain for *L/D* = 33.33, Ep/Es = 26250

Appendix B: (STRAIN/STRESS VS STRAIN (CHIN 1970) FOR PILED RAFT FOUNDATION)

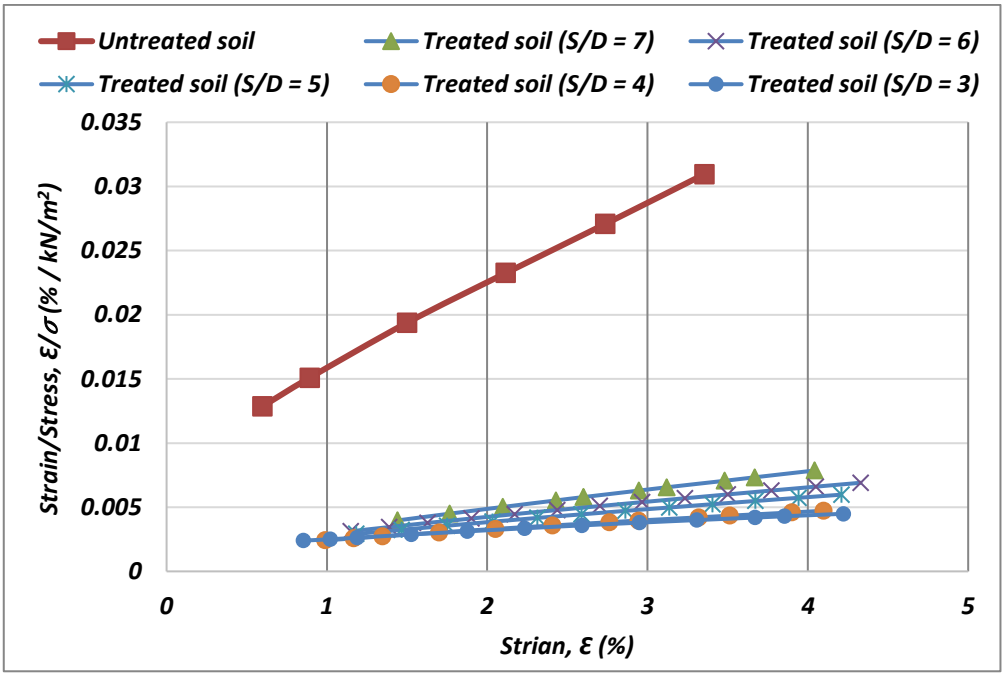


Figure B.1: Strain/Stress Vs Strain (Chin 1970) for untreated soil and treated soil (*L/D* = 40, Ep/Es = 52500)

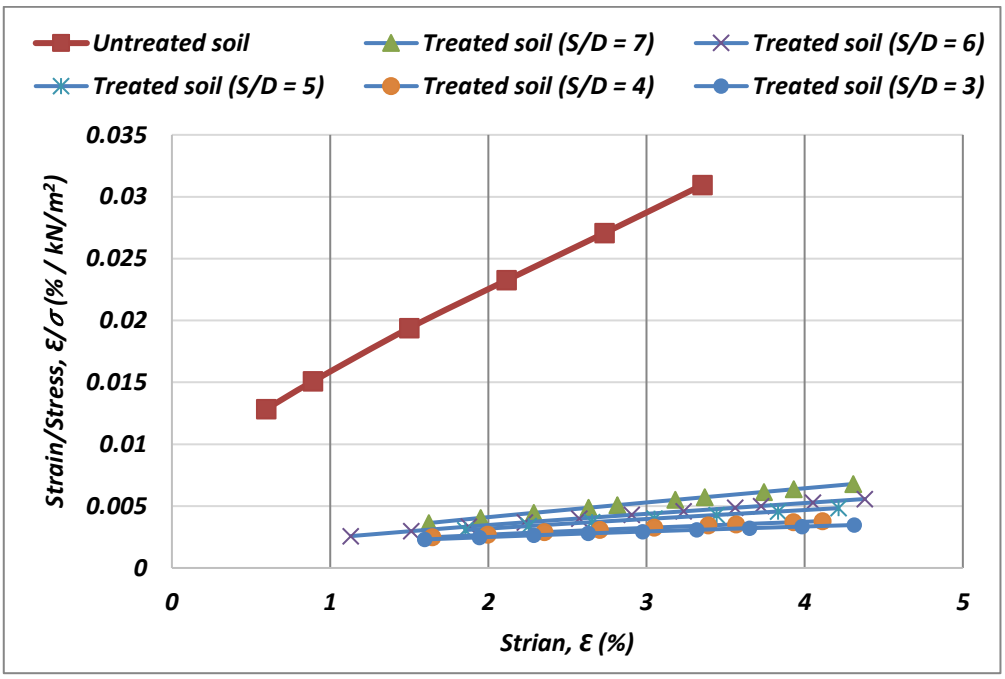


Figure B.2: Strain/Stress Vs Strain (Chin 1970) for untreated soil and treated soil (*L/D* = 33.33, Ep/Es = 52500)

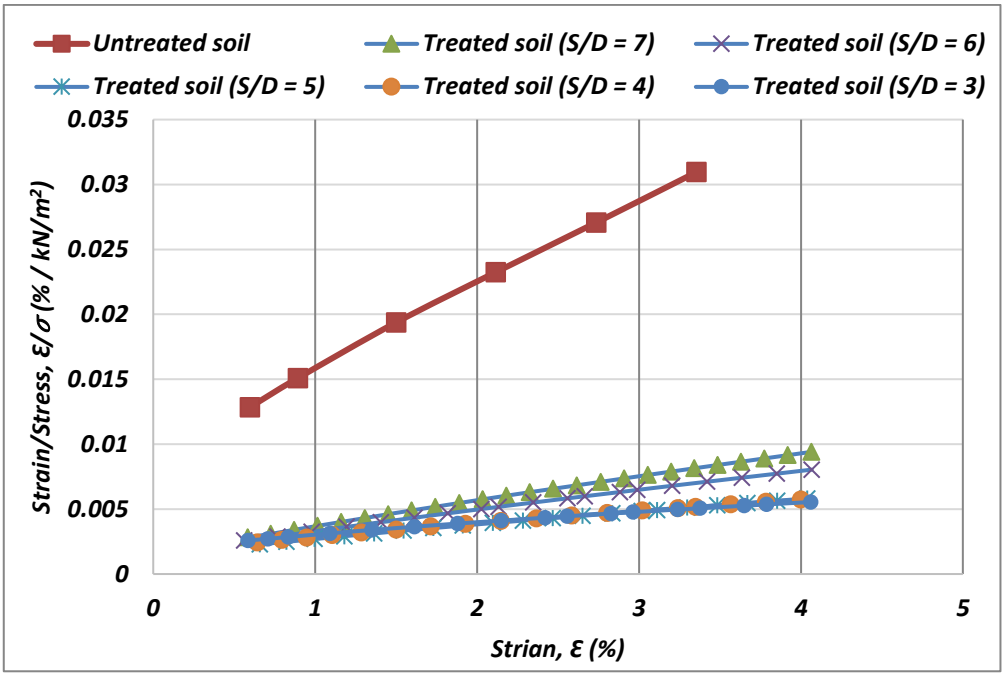


Figure B.3: Strain/Stress Vs Strain (Chin 1970) for untreated soil and treated soil (*L/D* = 50, Ep/Es = 35000)

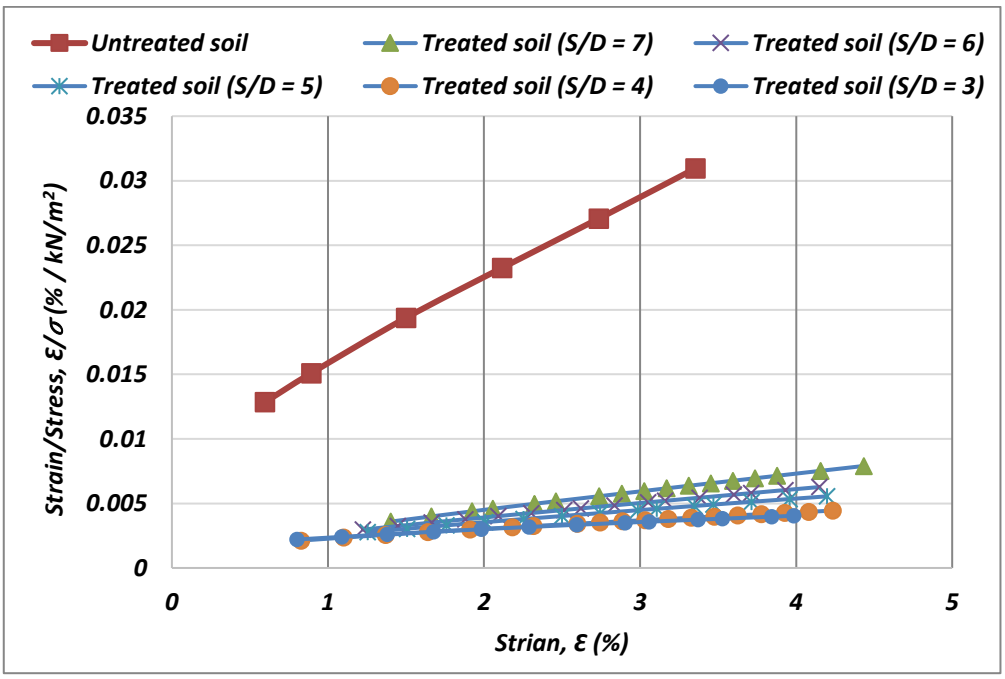


Figure B.4: Strain/Stress Vs Strain (Chin 1970) for untreated soil and treated soil (*L/D* = 40, Ep/Es = 35000)

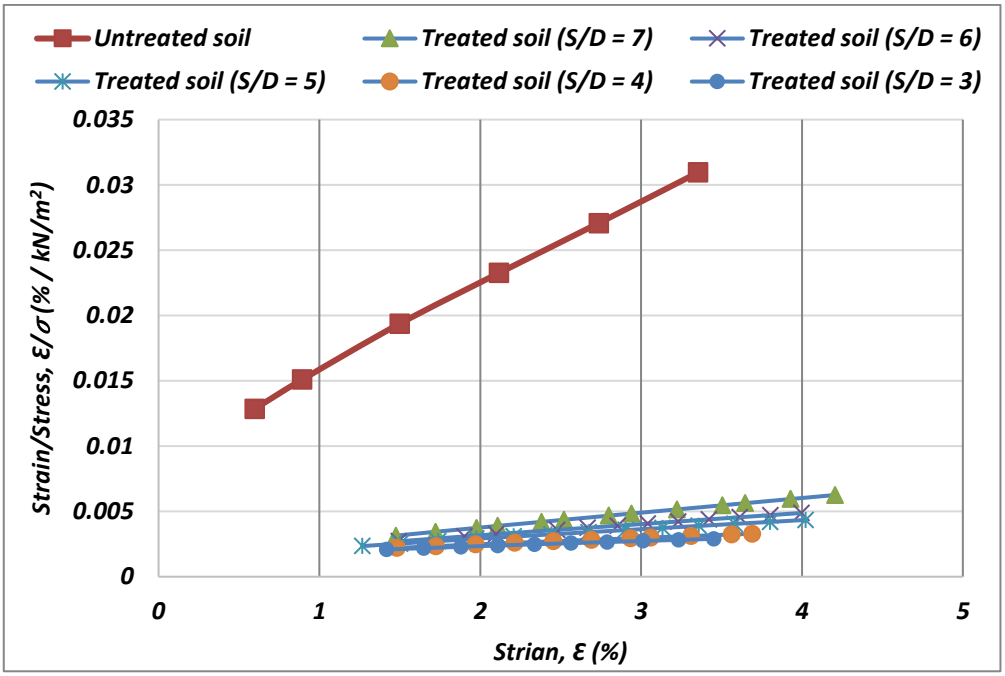


Figure B.5: Strain/Stress Vs Strain (Chin 1970) for untreated soil and treated soil (*L/D* = 33.33, Ep/Es = 35000)

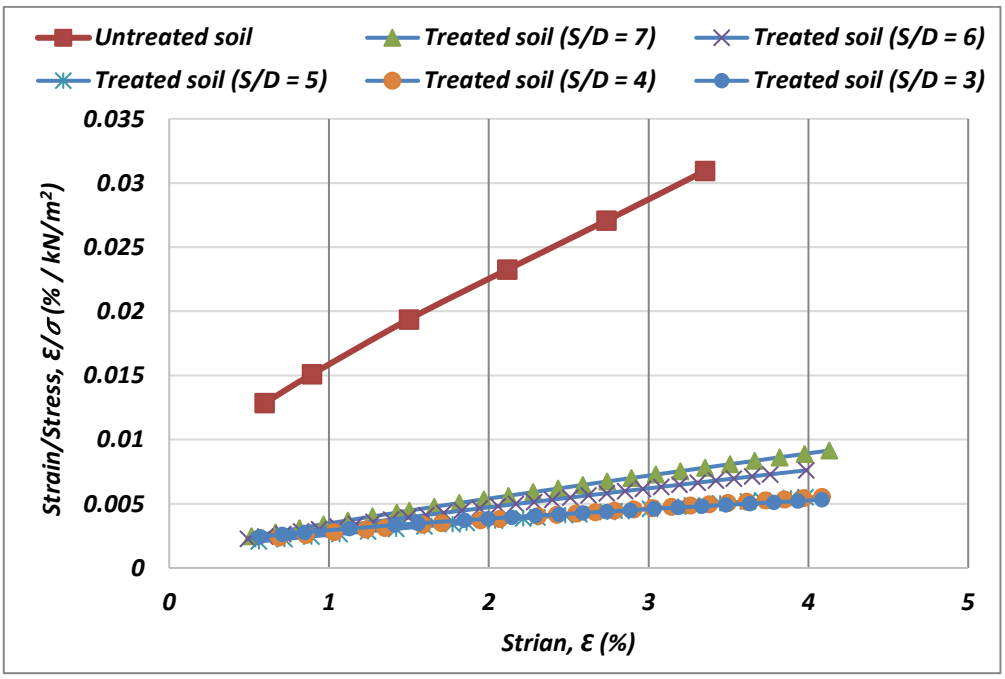


Figure B.6: Strain/Stress Vs Strain (Chin 1970) for untreated soil and treated soil (*L/D* = 50, Ep/Es = 26250)

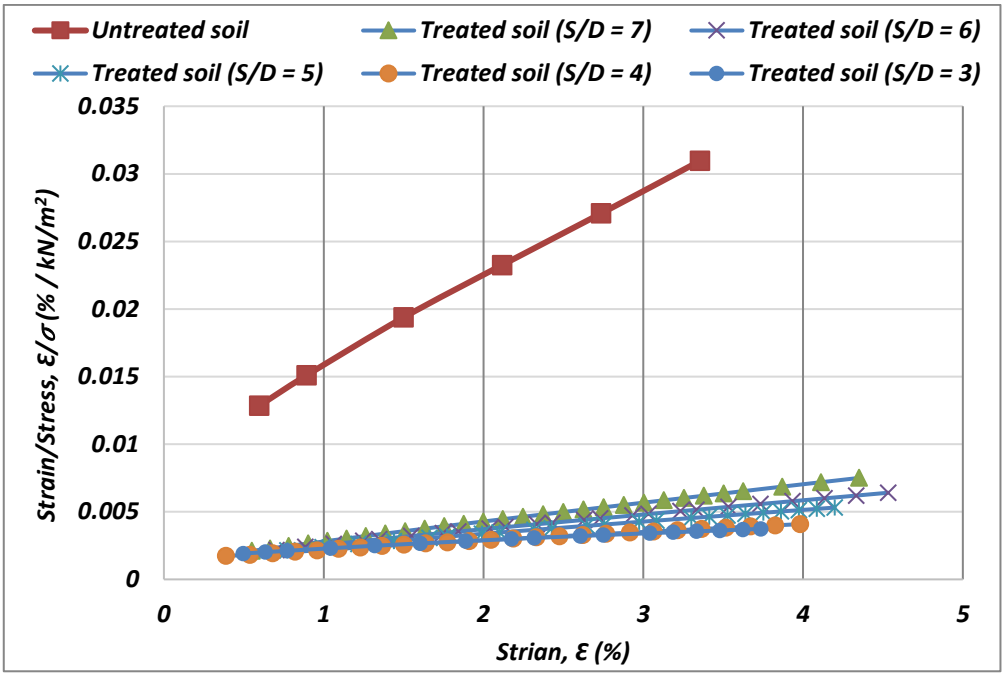


Figure B.7: Strain/Stress Vs Strain (Chin 1970) for untreated soil and treated soil (*L/D* = 40, Ep/Es = 26250)

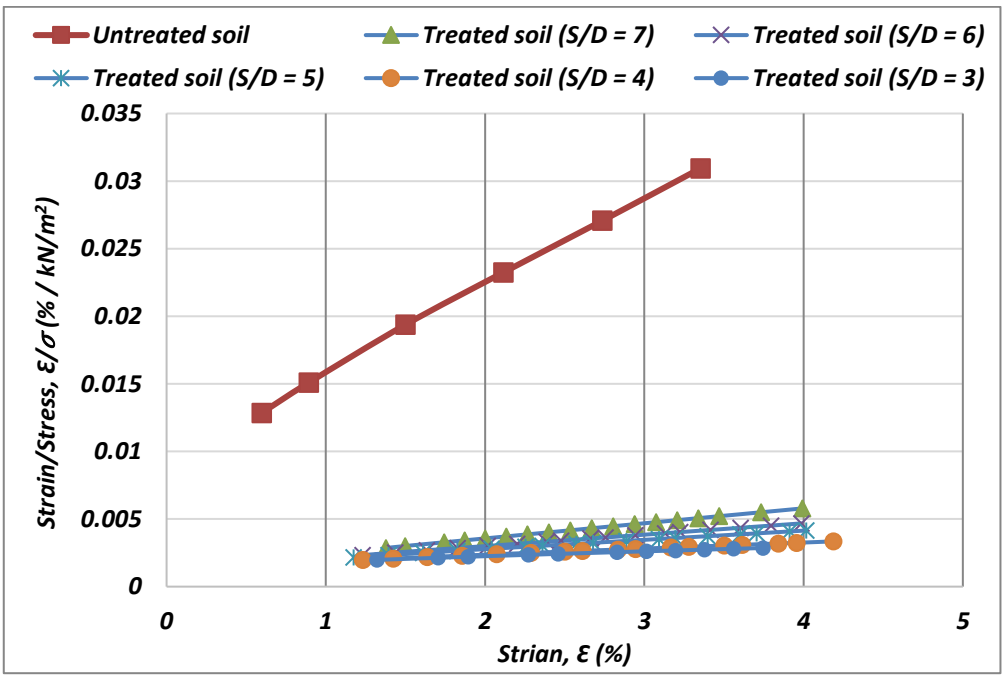


Figure B.8: Strain/Stress Vs Strain (Chin 1970) for untreated soil and treated soil (*L/D* = 33.33, Ep/Es = 26250)

Appendix C: (STRESS VS STRAIN FOR COMBINED FOUNDATION)

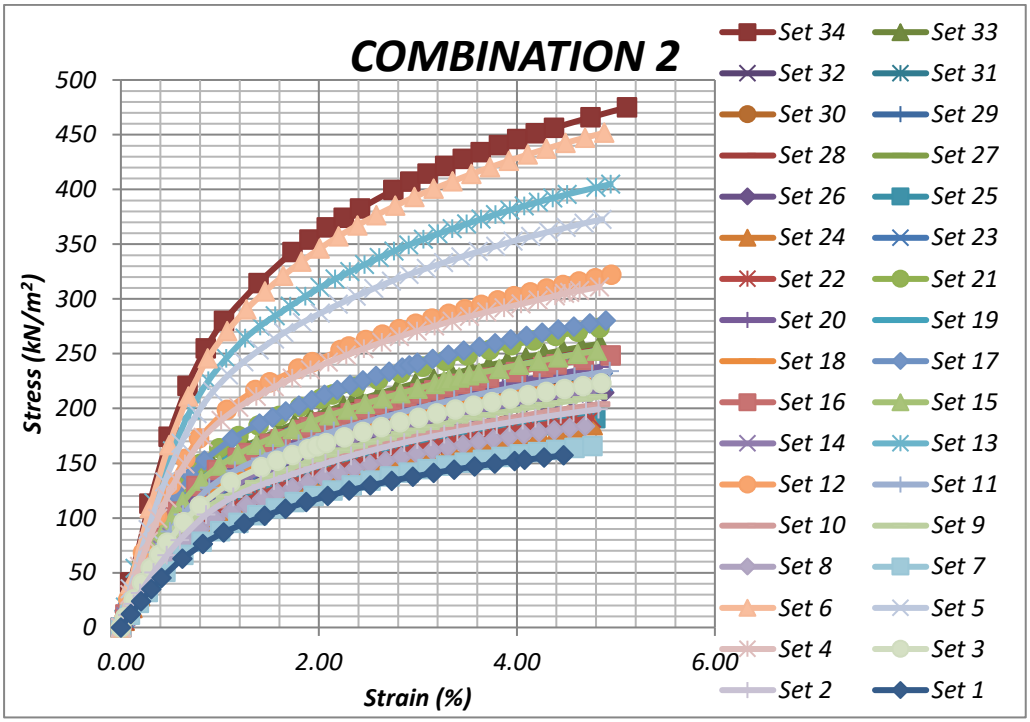


Figure C.1: Stress Vs Strain for combined foundation (combination 2)

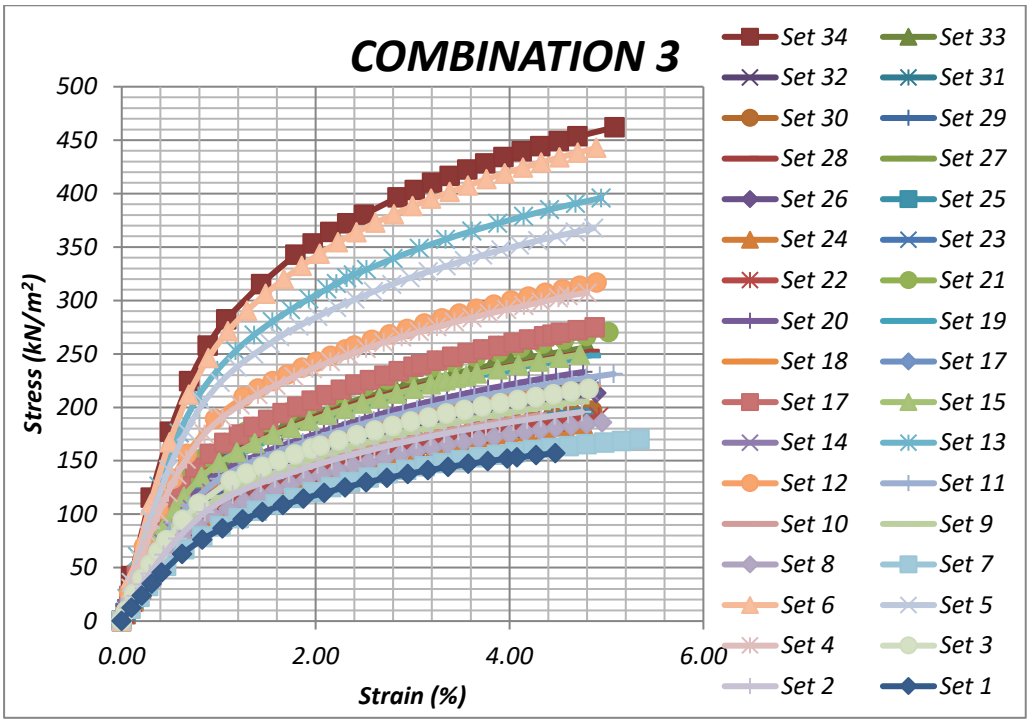


Figure C.2: Stress Vs Strain for combined foundation (combination 3)

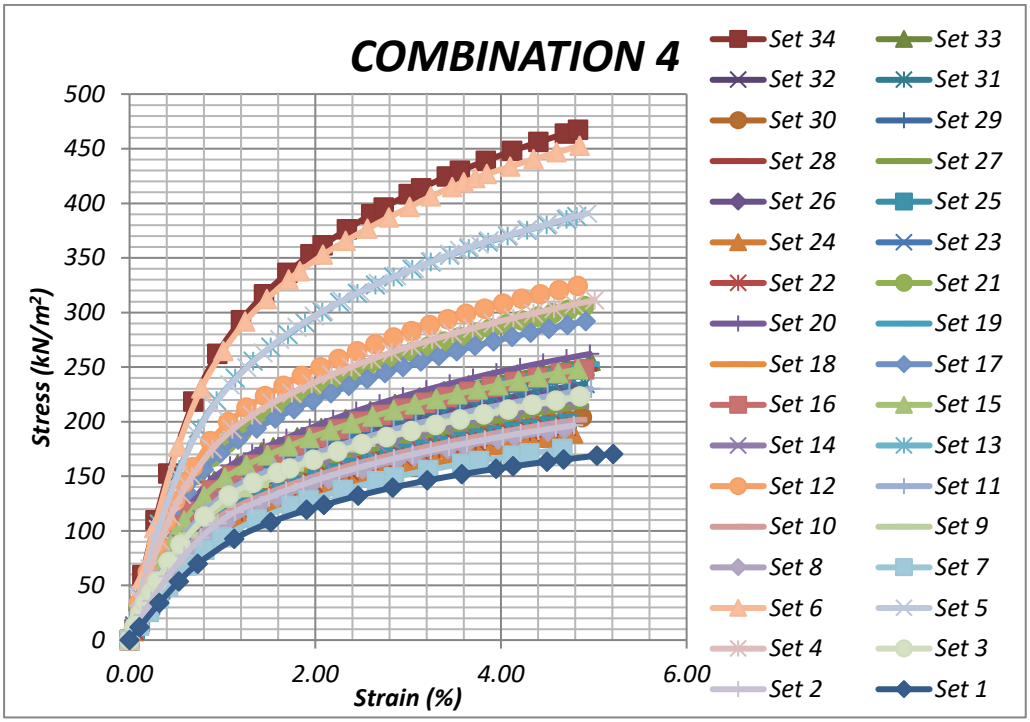


Figure C.3: Stress Vs Strain for combined foundation (combination 4)

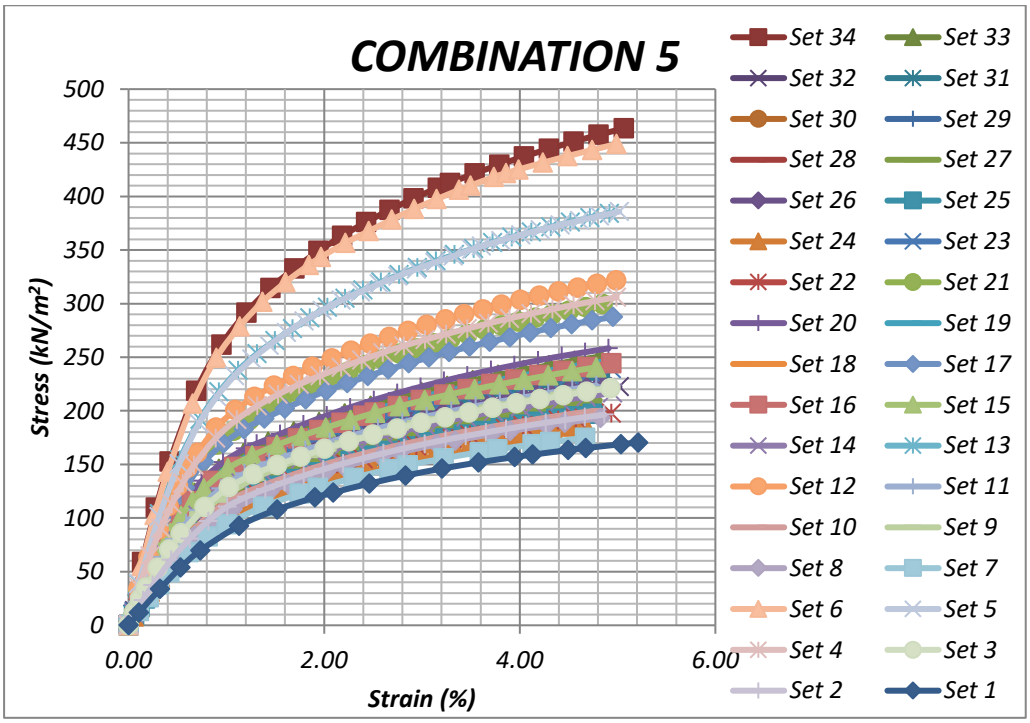


Figure C.4: Stress Vs Strain for combined foundation (combination 5)

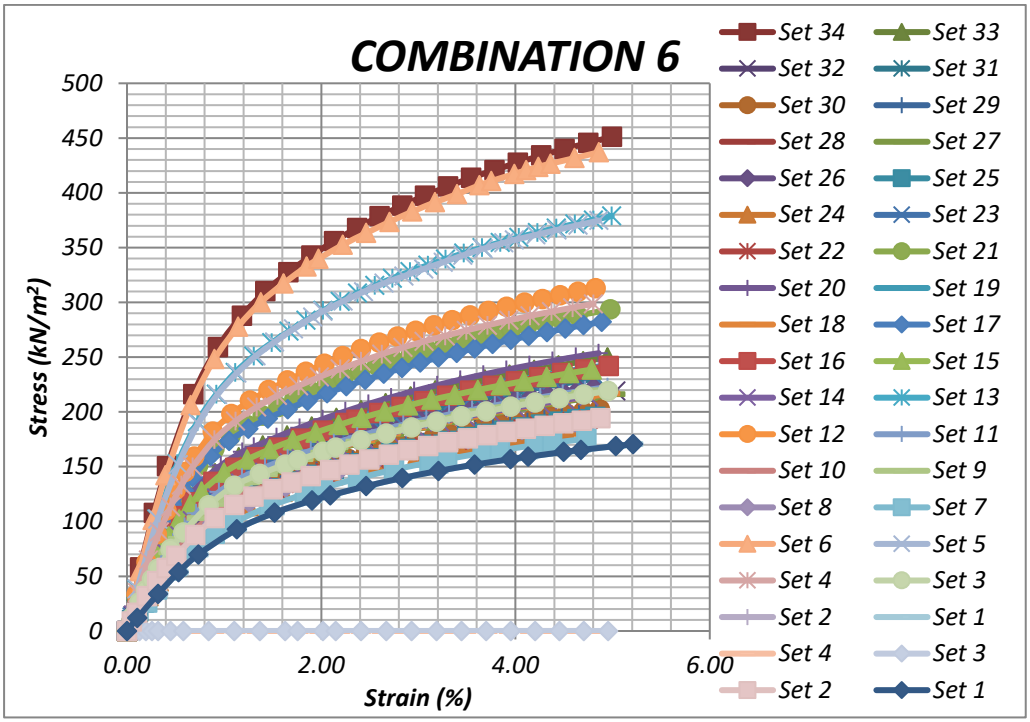


Figure C.5: Stress Vs Strain for combined foundation (combination 6)

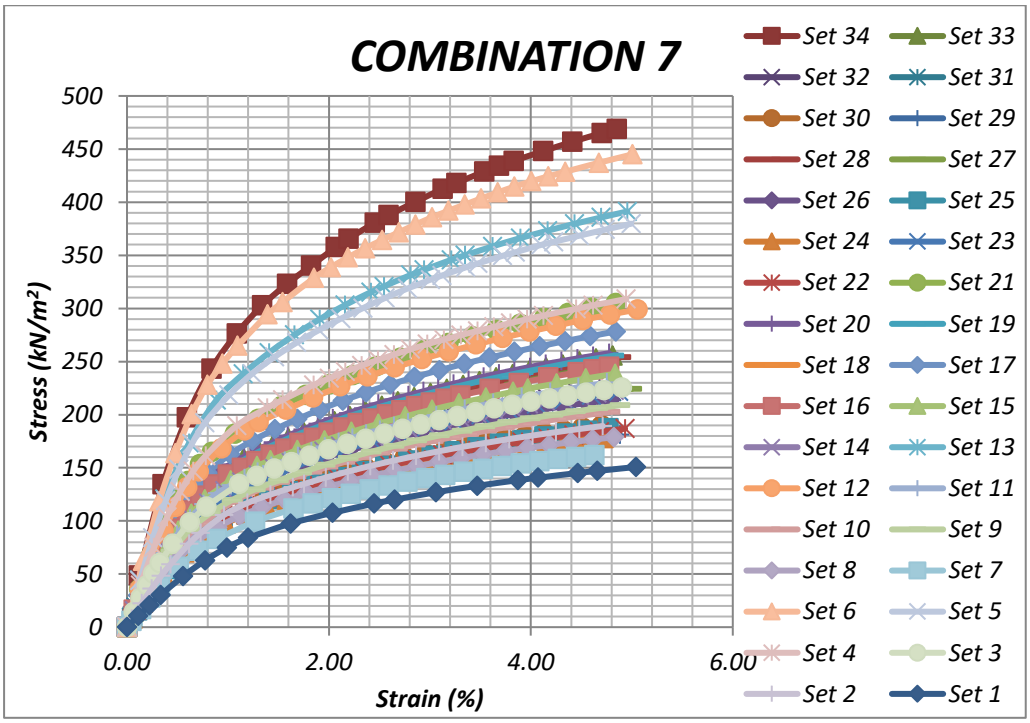


Figure C.6: Stress Vs Strain for combined foundation (combination 7)

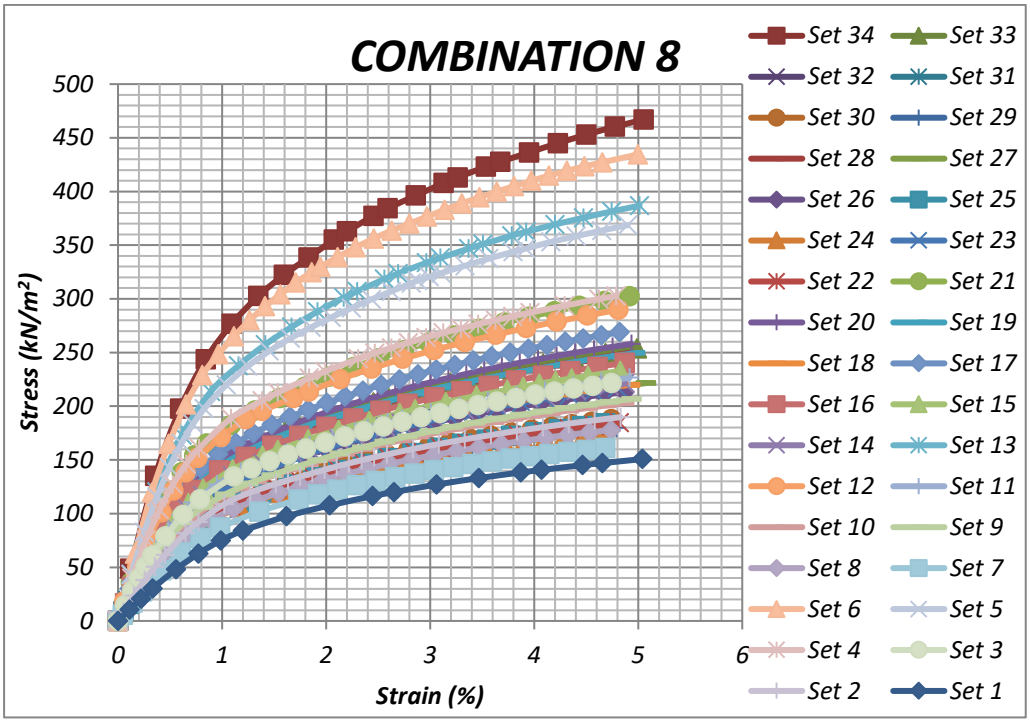


Figure C.7: Stress Vs Strain for combined foundation (combination 8)

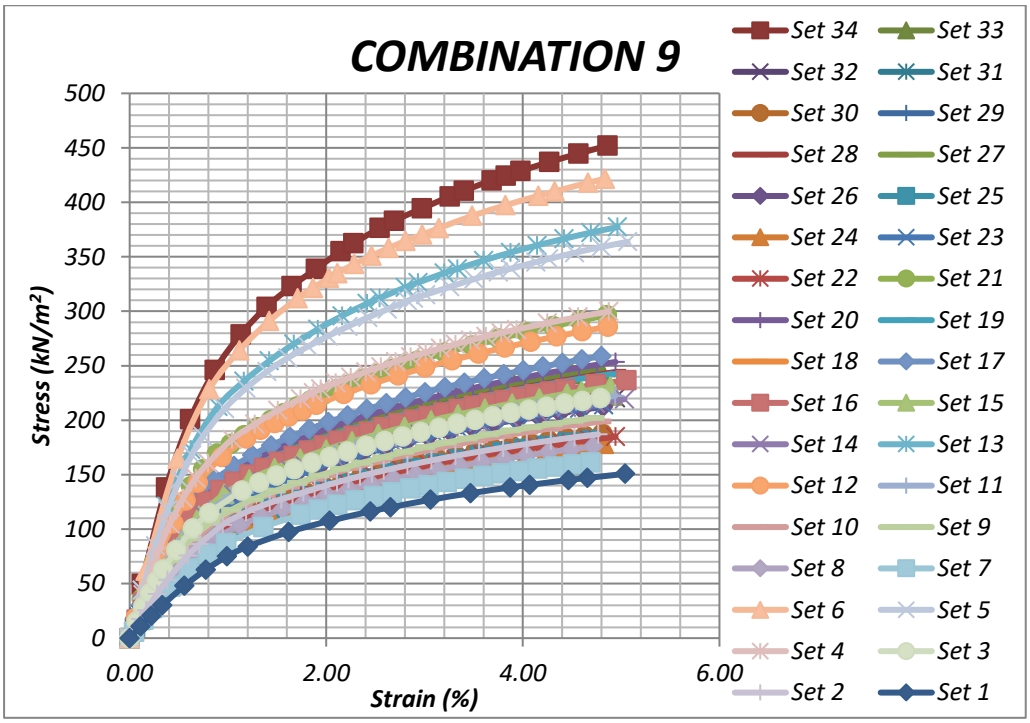


Figure C.8: Stress Vs Strain for combined foundation (combination 9)

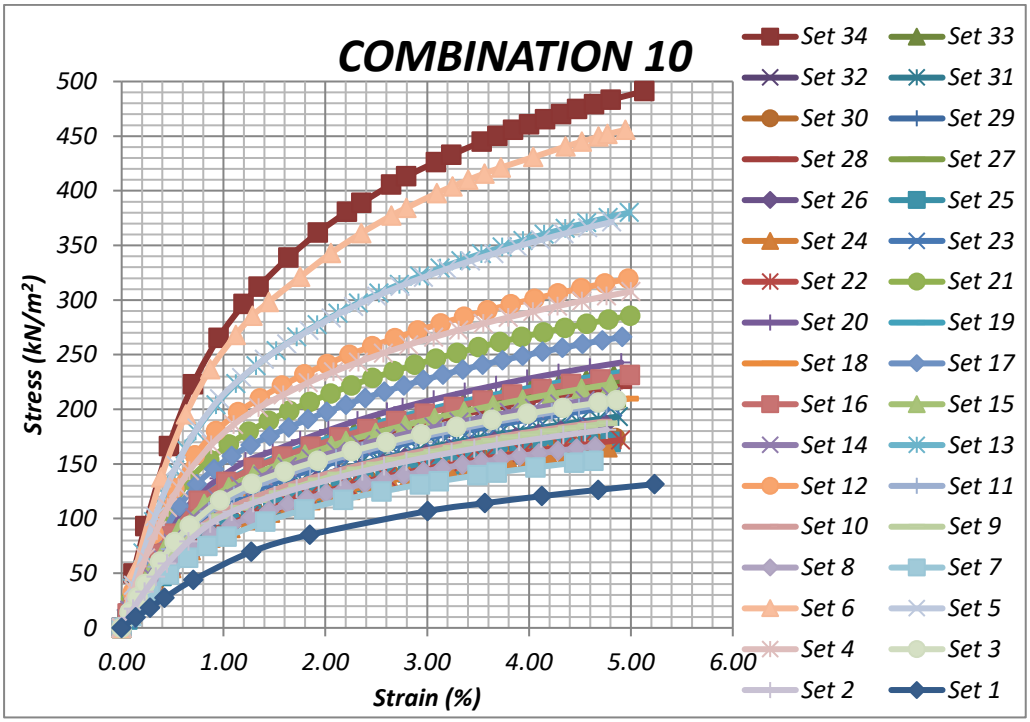


Figure C.9: Stress Vs Strain for combined foundation (combination 10)

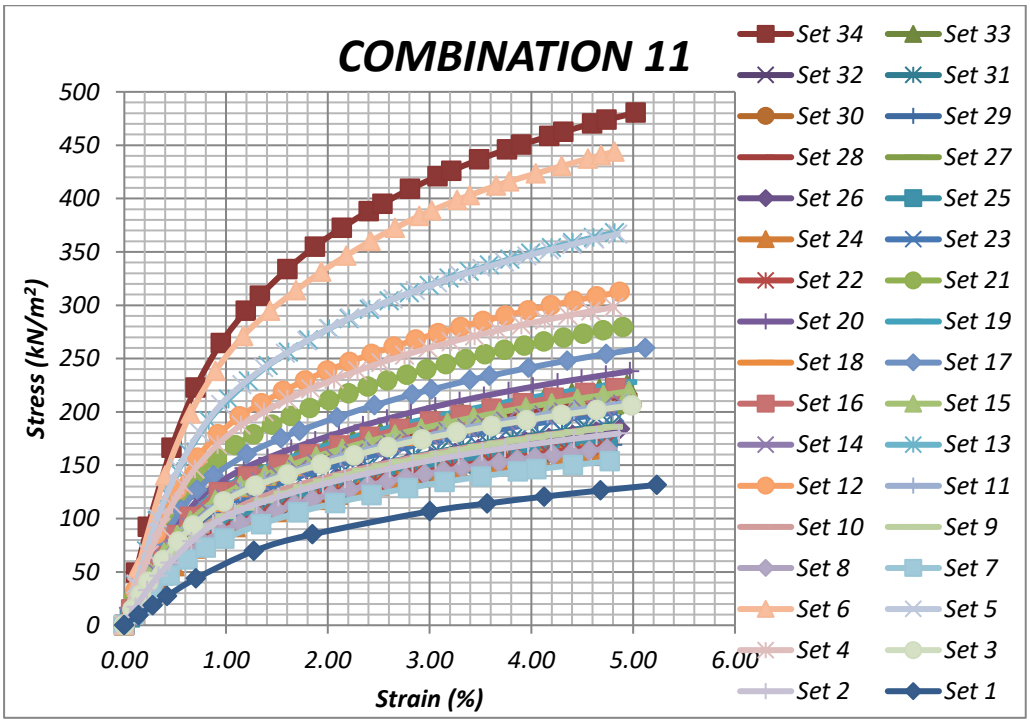


Figure C.10: Stress Vs Strain for combined foundation (combination 11)

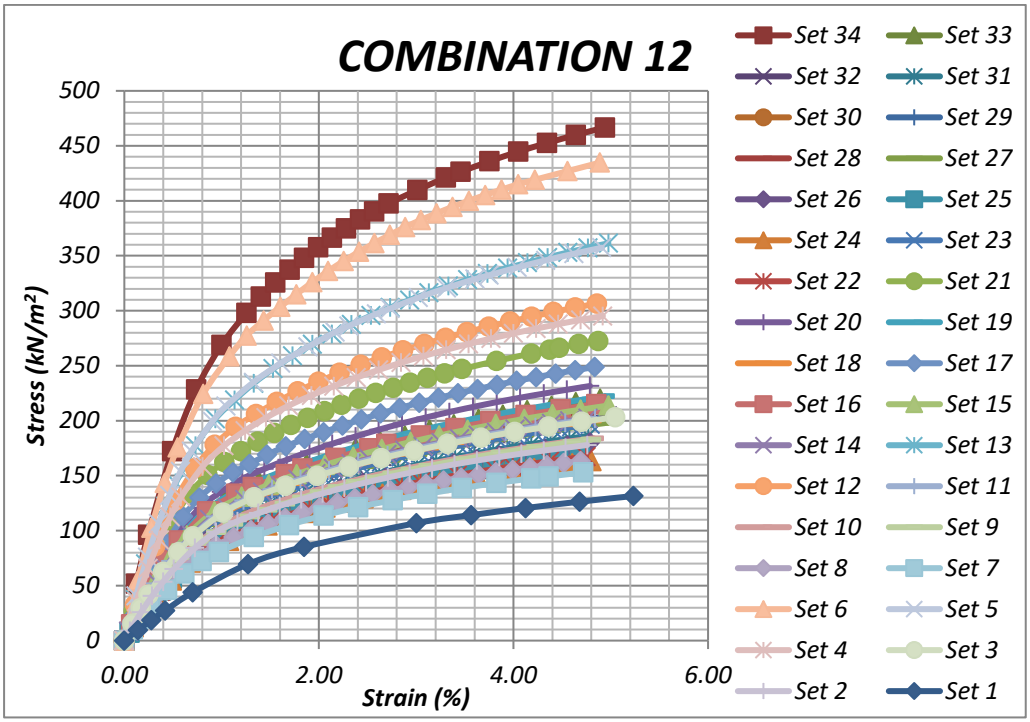


Figure C.11: Stress Vs Strain for combined foundation (combination 12)

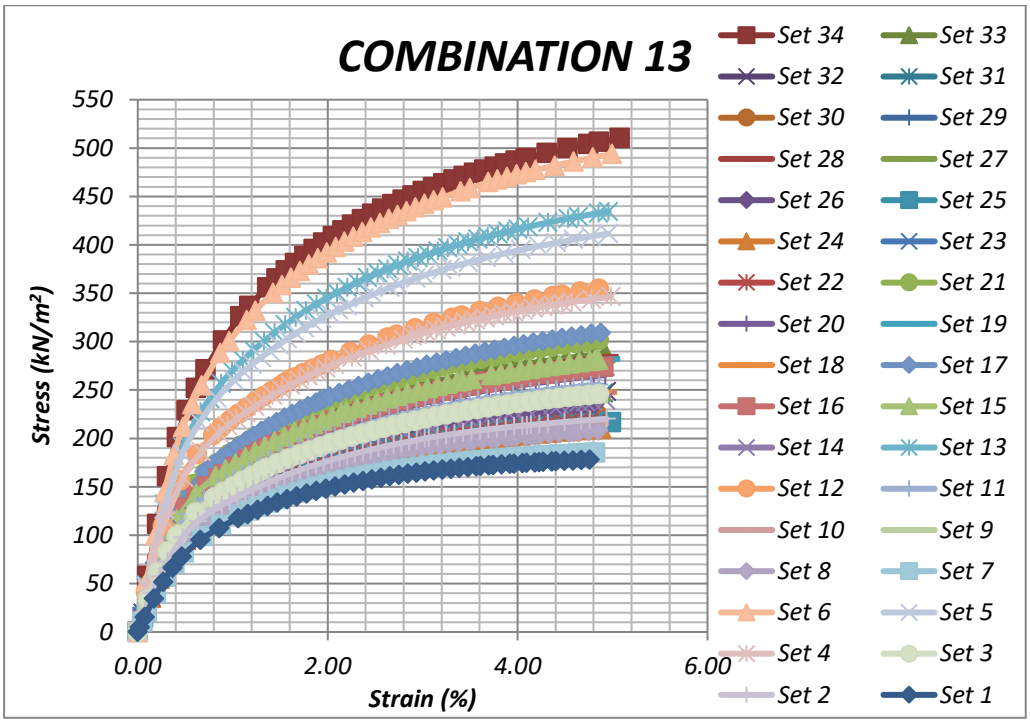


Figure C.12: Stress Vs Strain for combined foundation (combination 13)

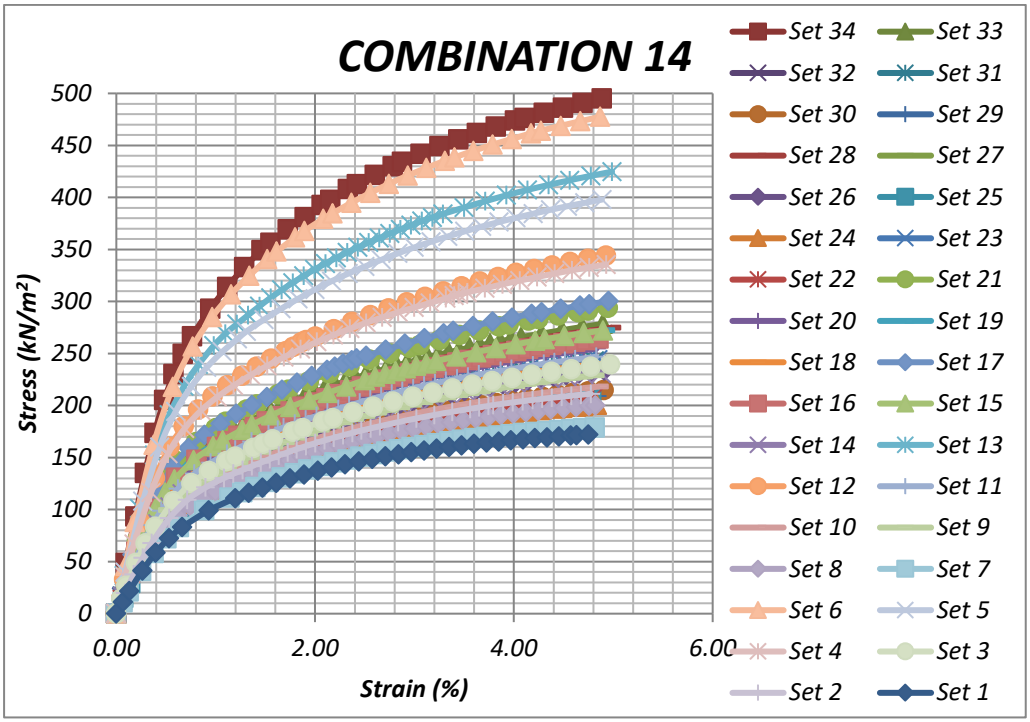


Figure C.13: Stress Vs Strain for combined foundation (combination 14)

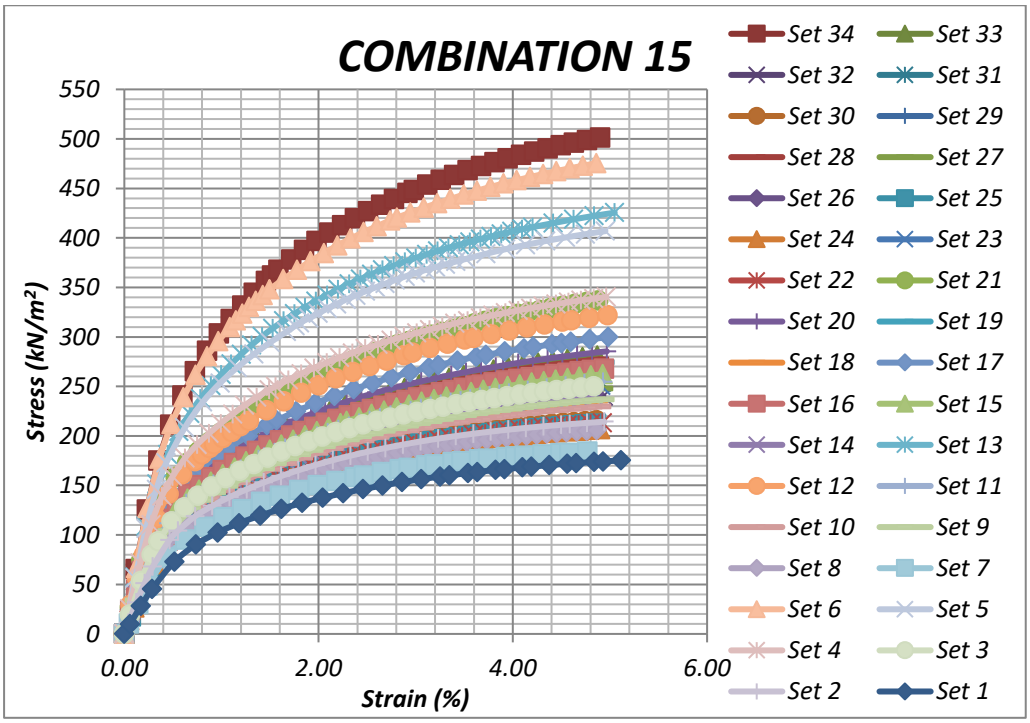


Figure C.14: Stress Vs Strain for combined foundation (combination 15)

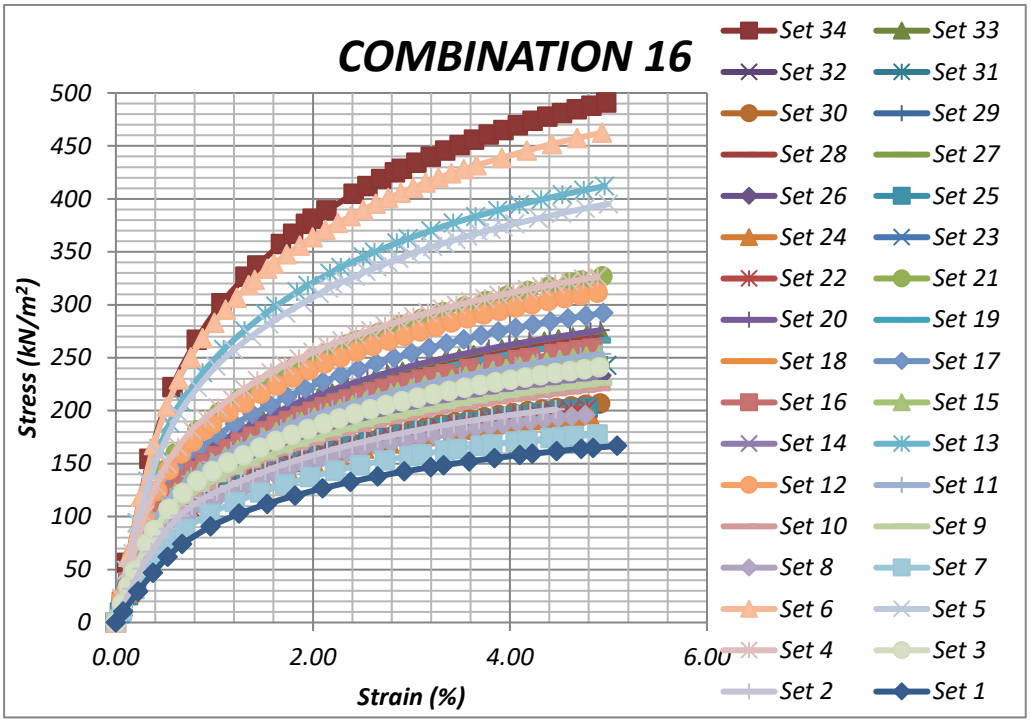


Figure C.15: Stress Vs Strain for combined foundation (combination 16)

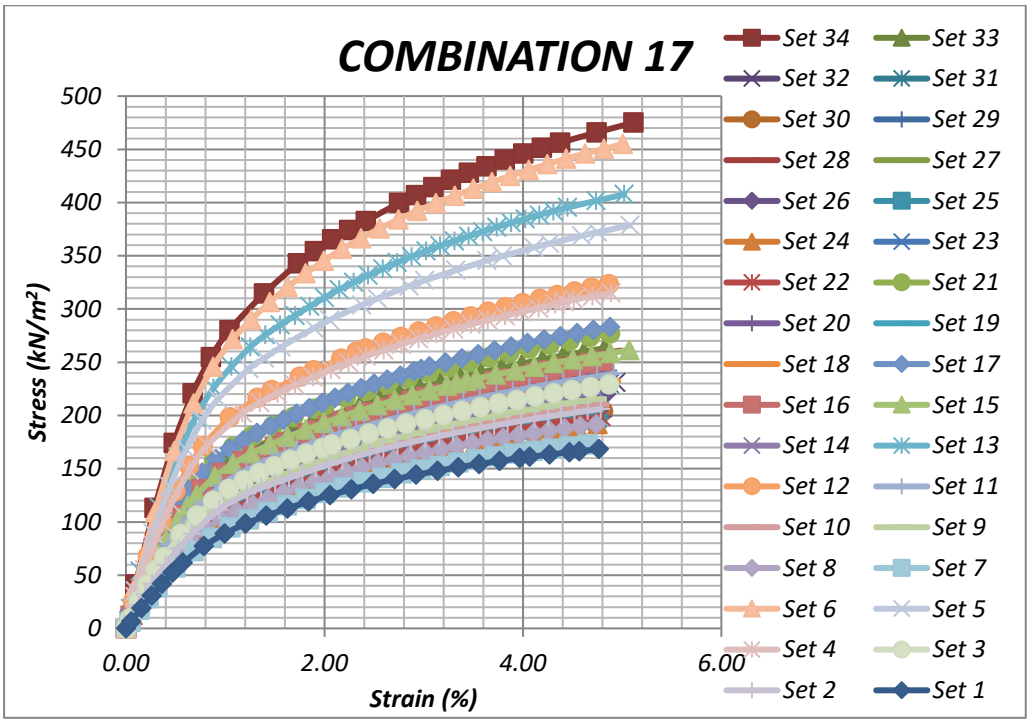


Figure C.16: Stress Vs Strain for combined foundation (combination 17)

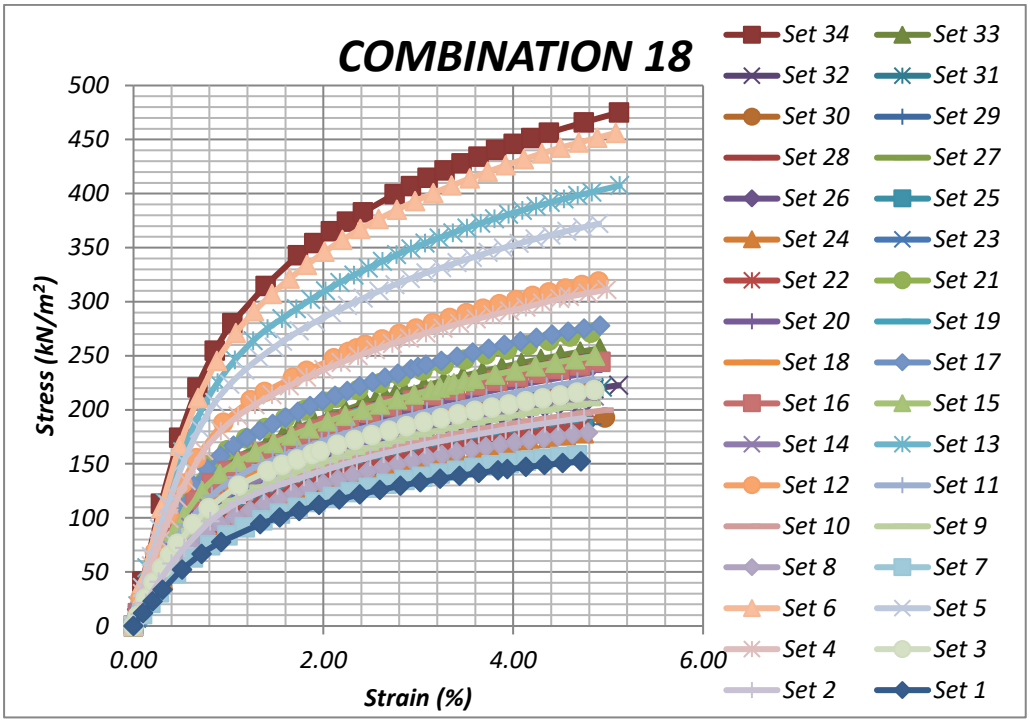


Figure C.17: Stress Vs Strain for combined foundation (combination 18)

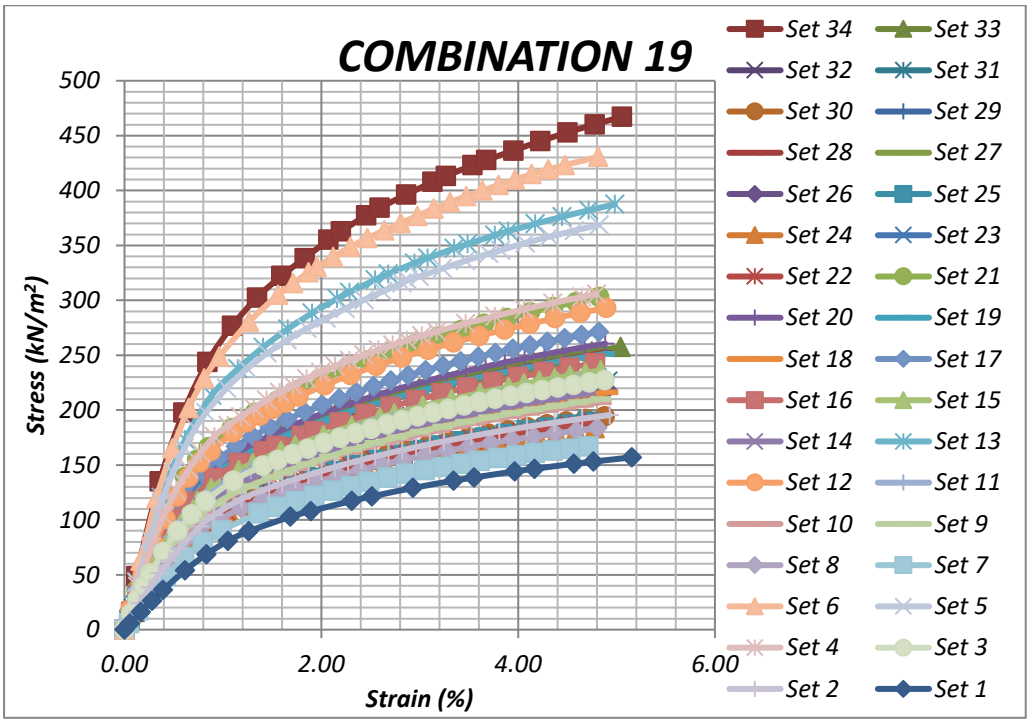


Figure C.18: Stress Vs Strain for combined foundation (combination 19)

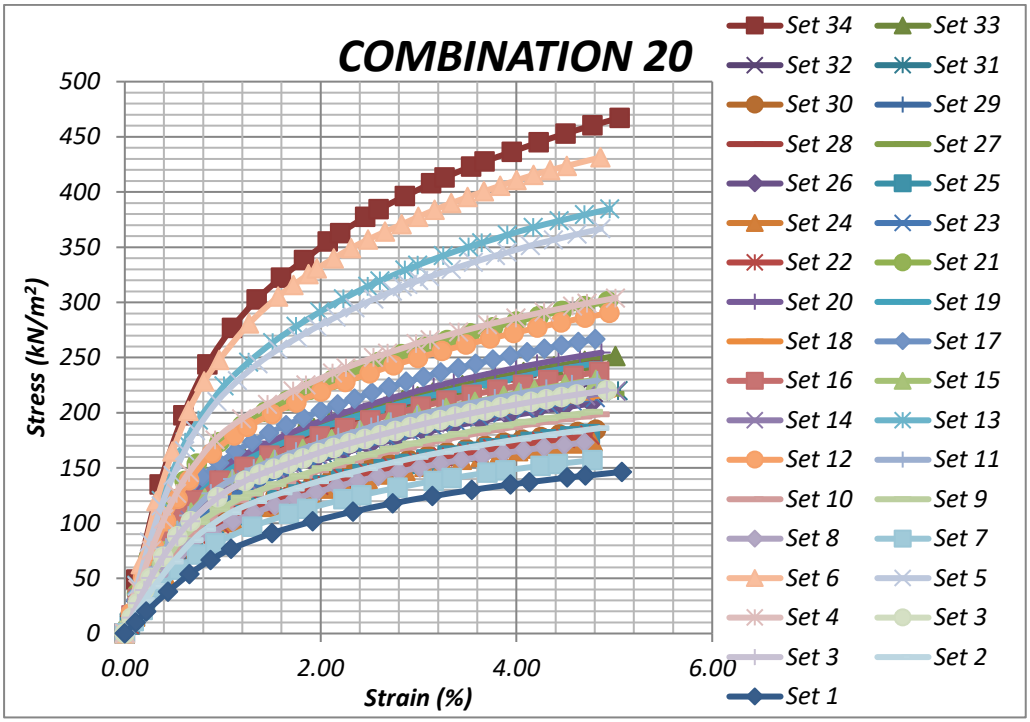


Figure C.19: Stress Vs Strain for combined foundation (combination 20)

Appendix D (STRAIN/STRESS VS STRAIN (CHIN 1970) FOR COMBINED FOUNDATION)

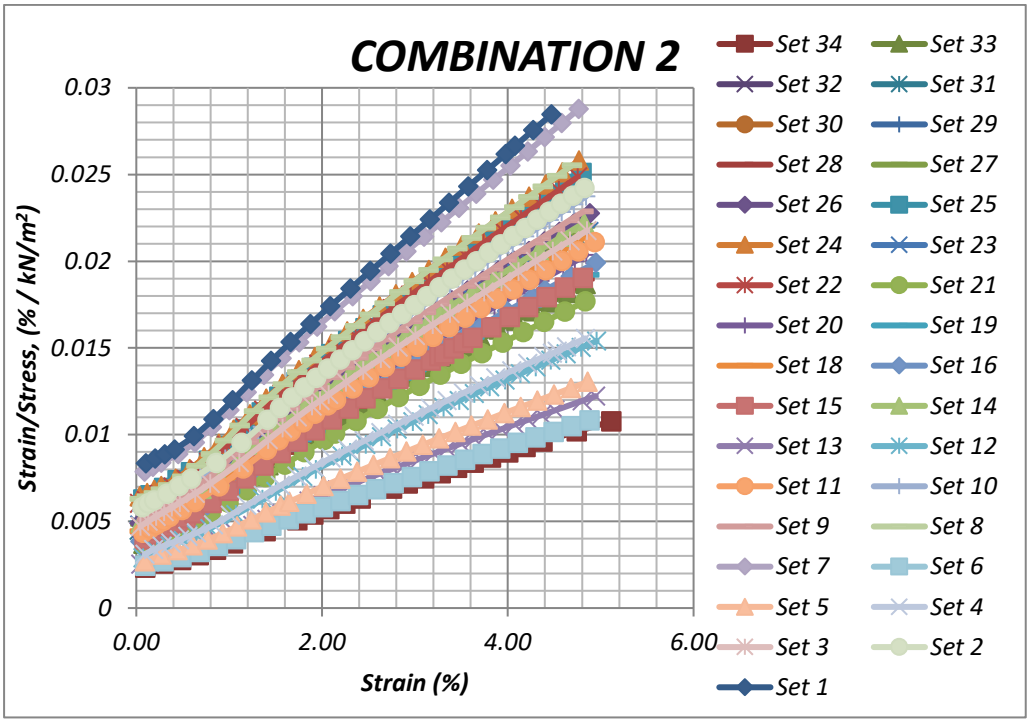


Figure D.1: Strain/Stress Vs Strain (Chin, 1970) for combined foundation (combination 2)

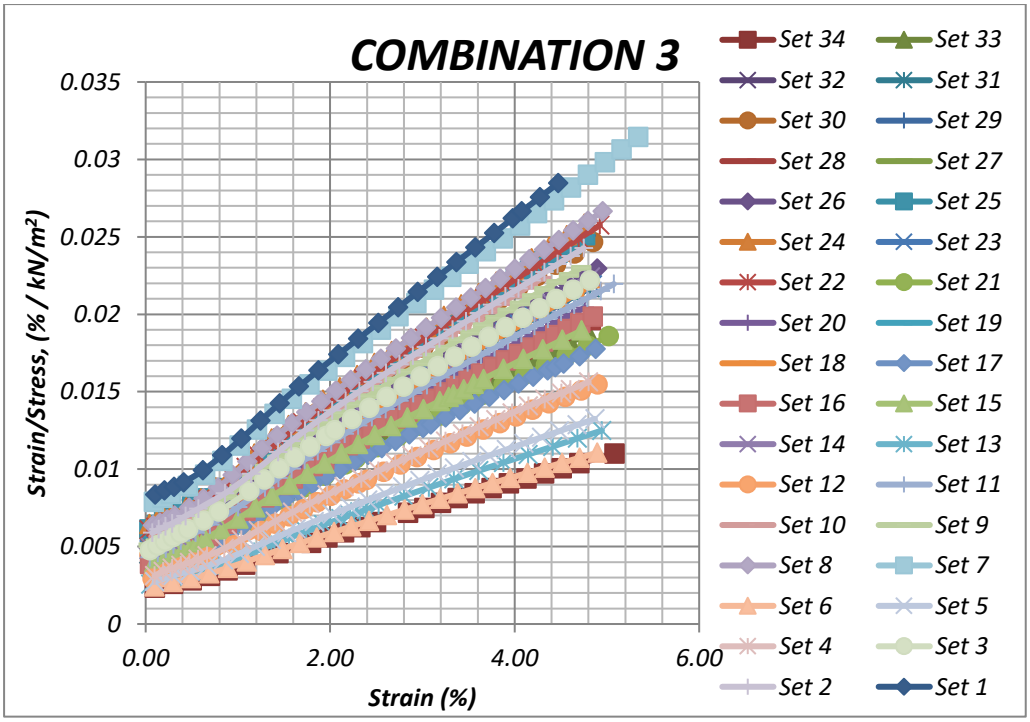


Figure D.2: Strain/Stress Vs Strain (Chin, 1970) for combined foundation (combination 3)

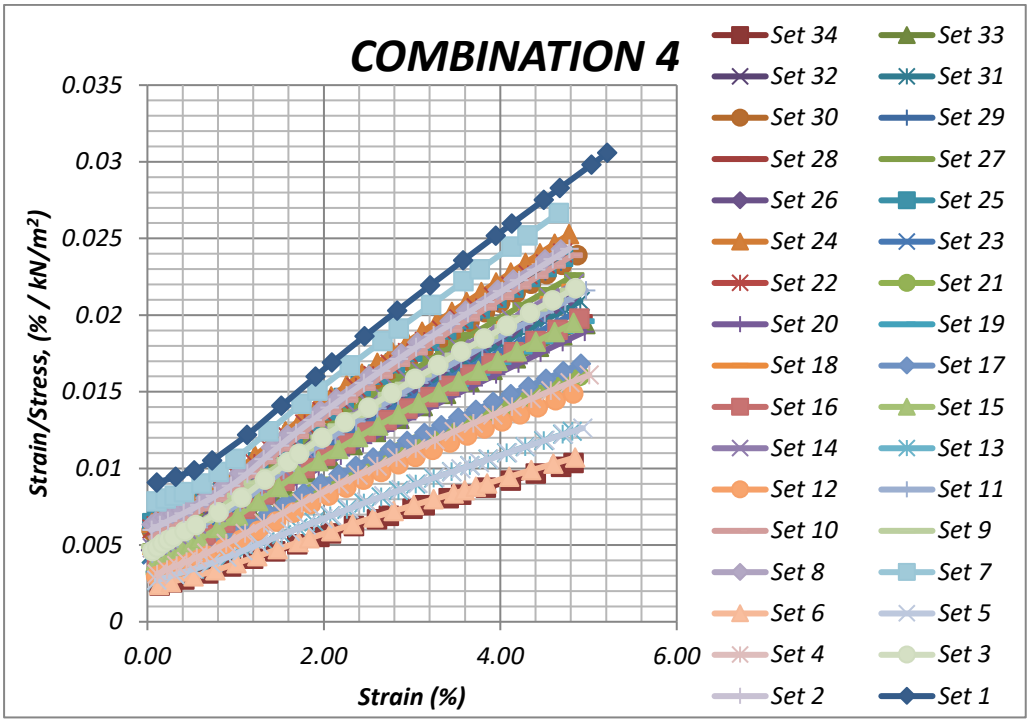


Figure D.3: Strain/Stress Vs Strain (Chin, 1970) for combined foundation (combination 4)

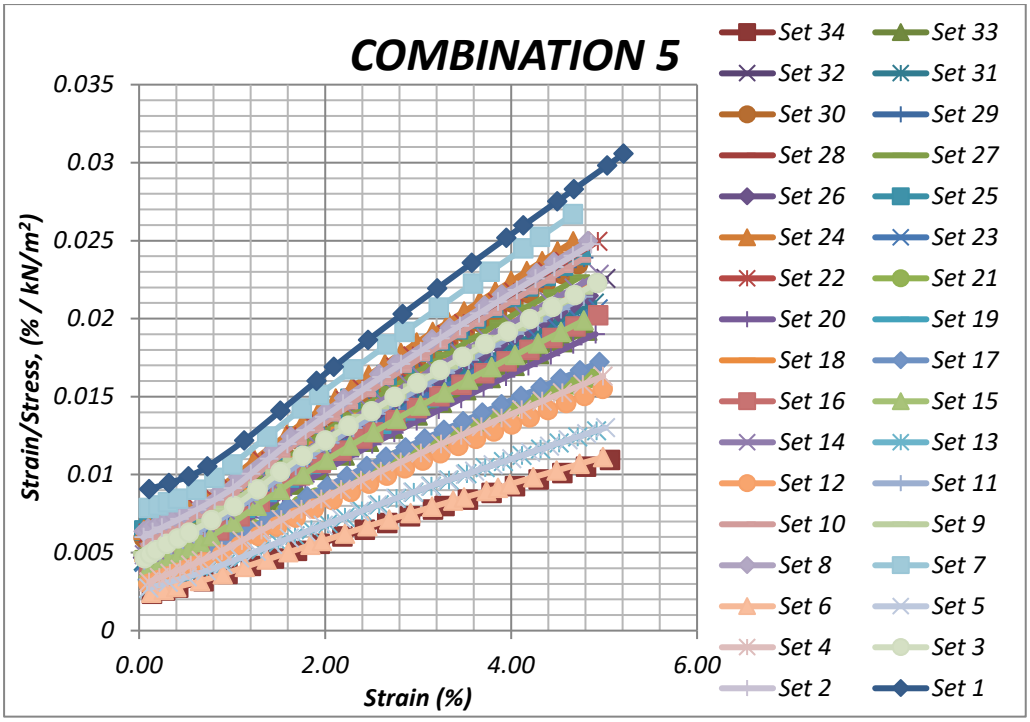


Figure D.4: Strain/Stress Vs Strain (Chin, 1970) for combined foundation (combination 5)

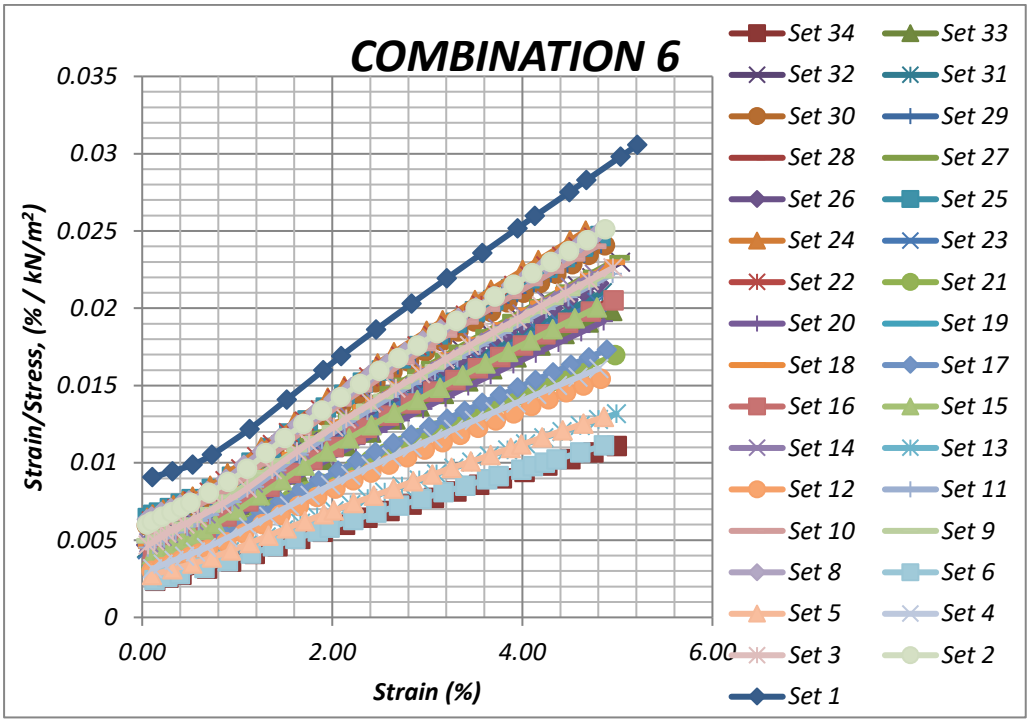


Figure D.5: Strain/Stress Vs Strain (Chin, 1970) for combined foundation (combination 6)

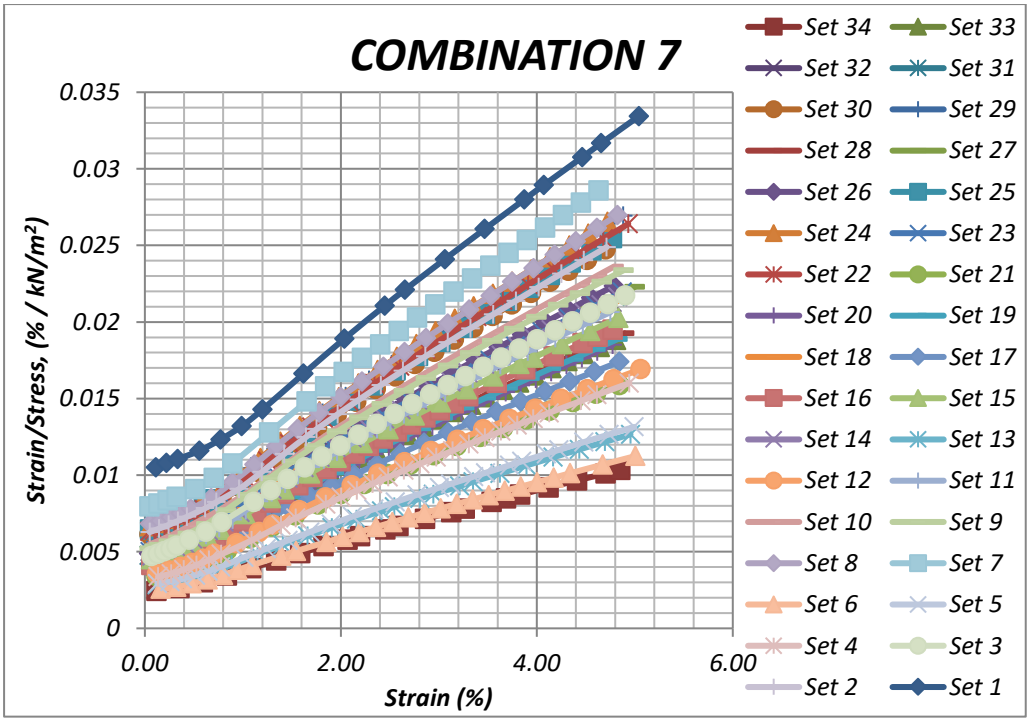


Figure D.6: Strain/Stress Vs Strain (Chin, 1970) for combined foundation (combination 7)

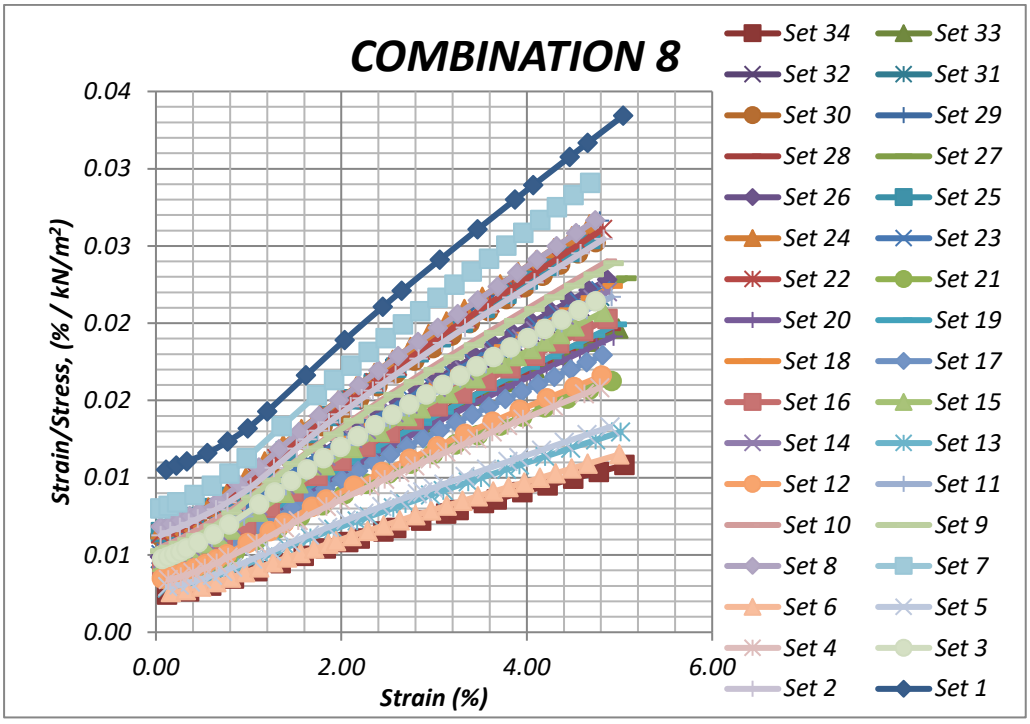


Figure D.7: Strain/Stress Vs Strain (Chin, 1970) for combined foundation (combination 8)

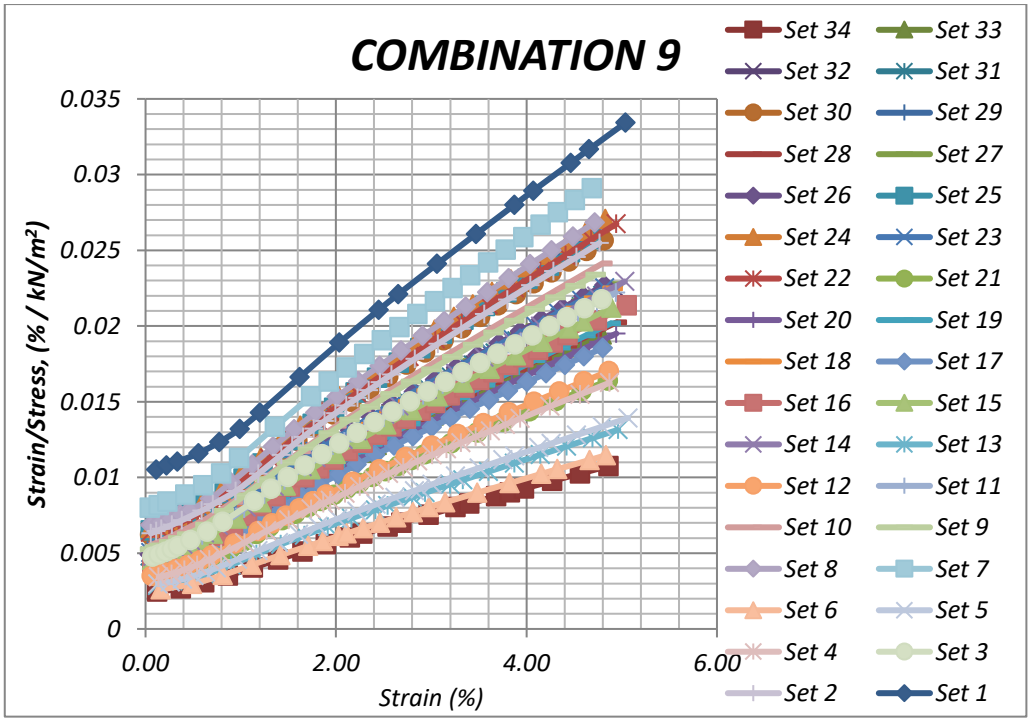


Figure D.8: Strain/Stress Vs Strain (Chin, 1970) for combined foundation (combination 9)

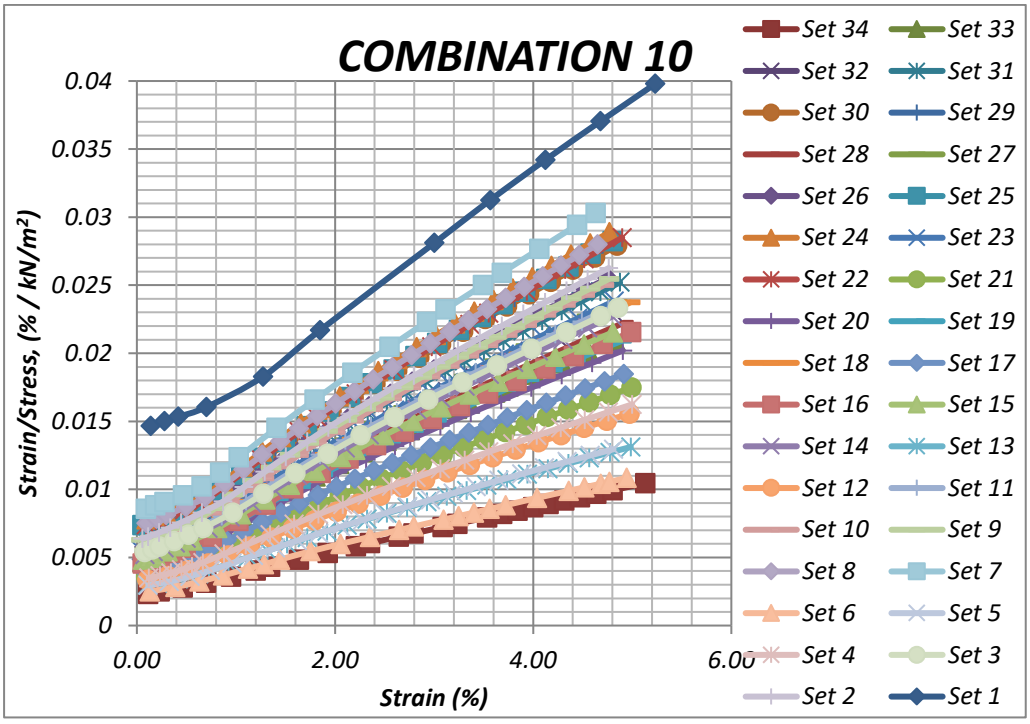


Figure D.9: Strain/Stress Vs Strain (Chin, 1970) for combined foundation (combination 10)

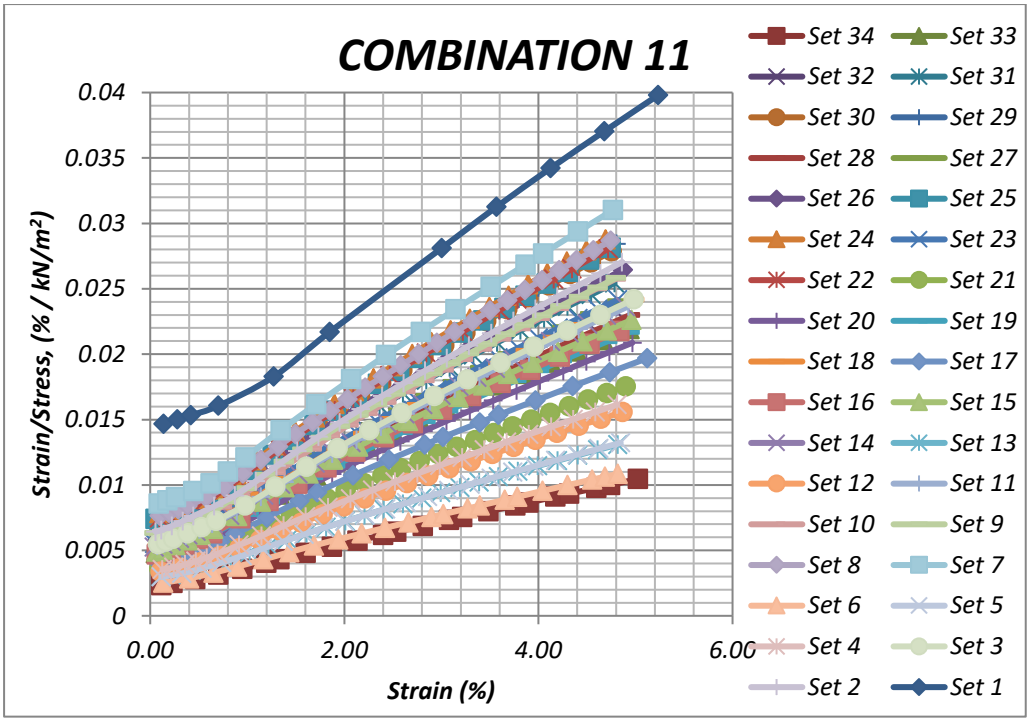


Figure D.10: Strain/Stress Vs Strain (Chin, 1970) for combined foundation (combination 11)

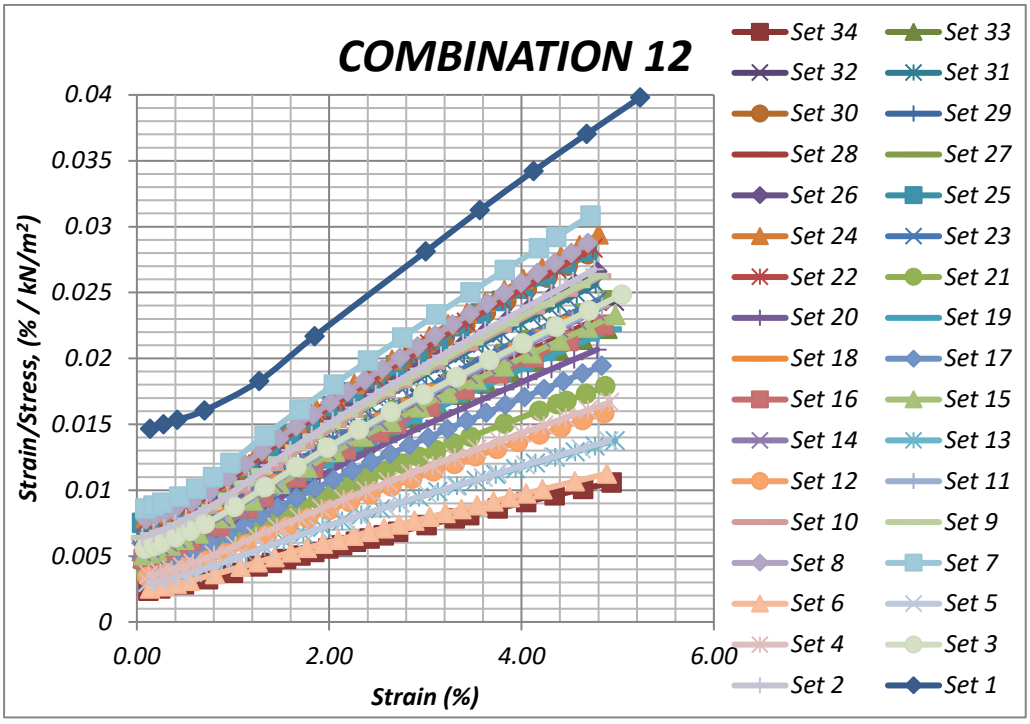


Figure D.11: Strain/Stress Vs Strain (Chin, 1970) for combined foundation (combination 12)

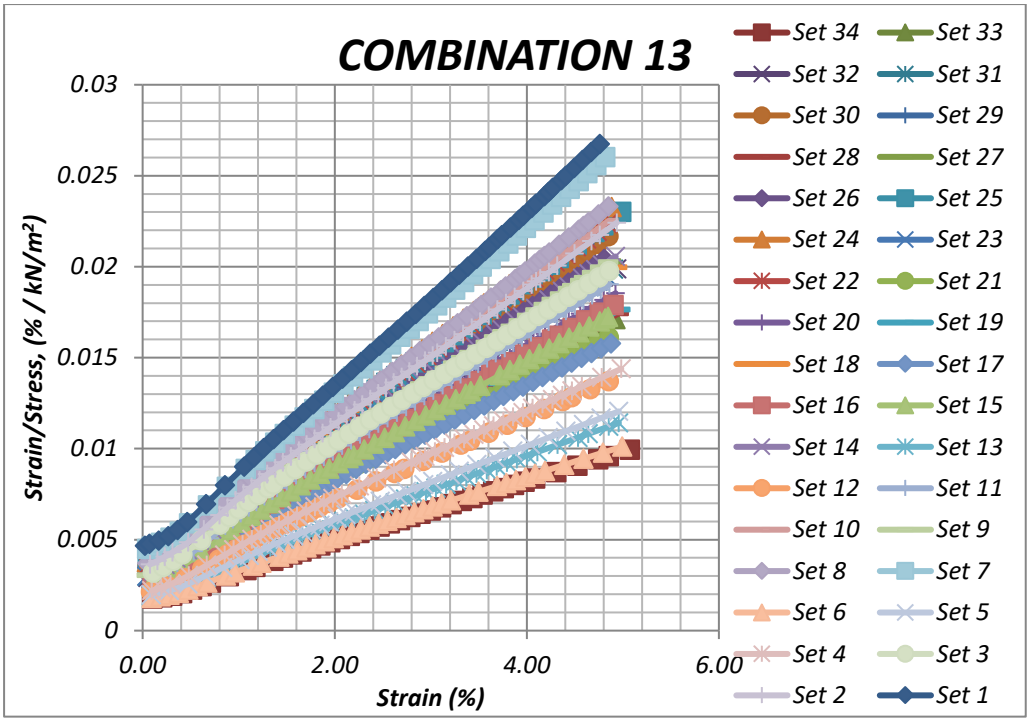


Figure D.12: Strain/Stress Vs Strain (Chin, 1970) for combined foundation (combination 13)

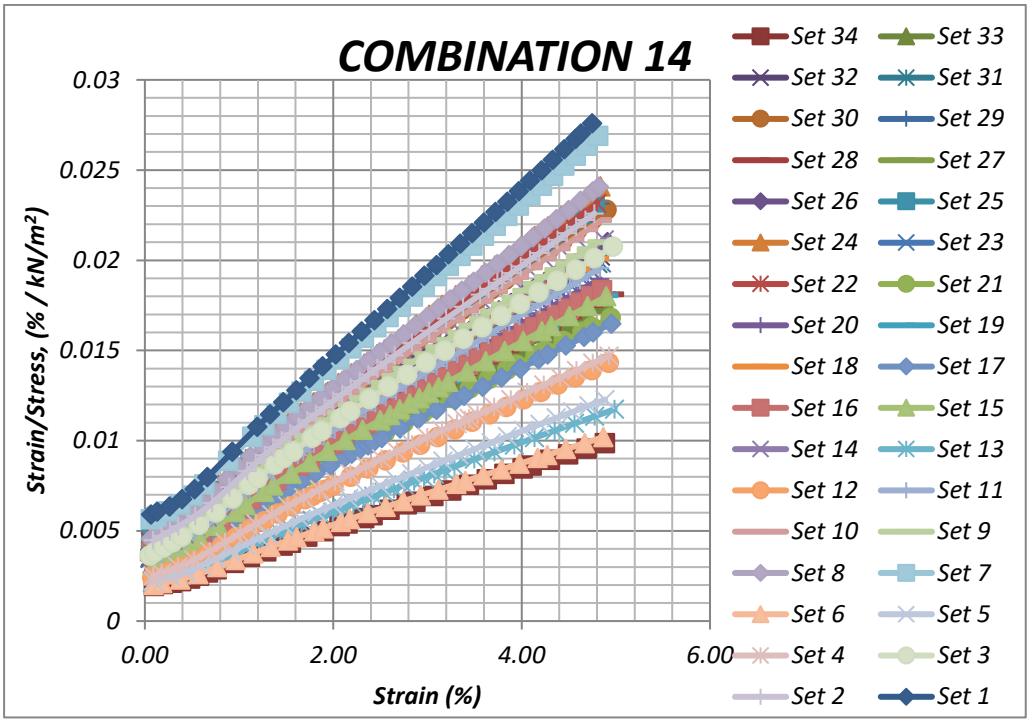


Figure D.13: Strain/Stress Vs Strain (Chin, 1970) for combined foundation (combination 14)

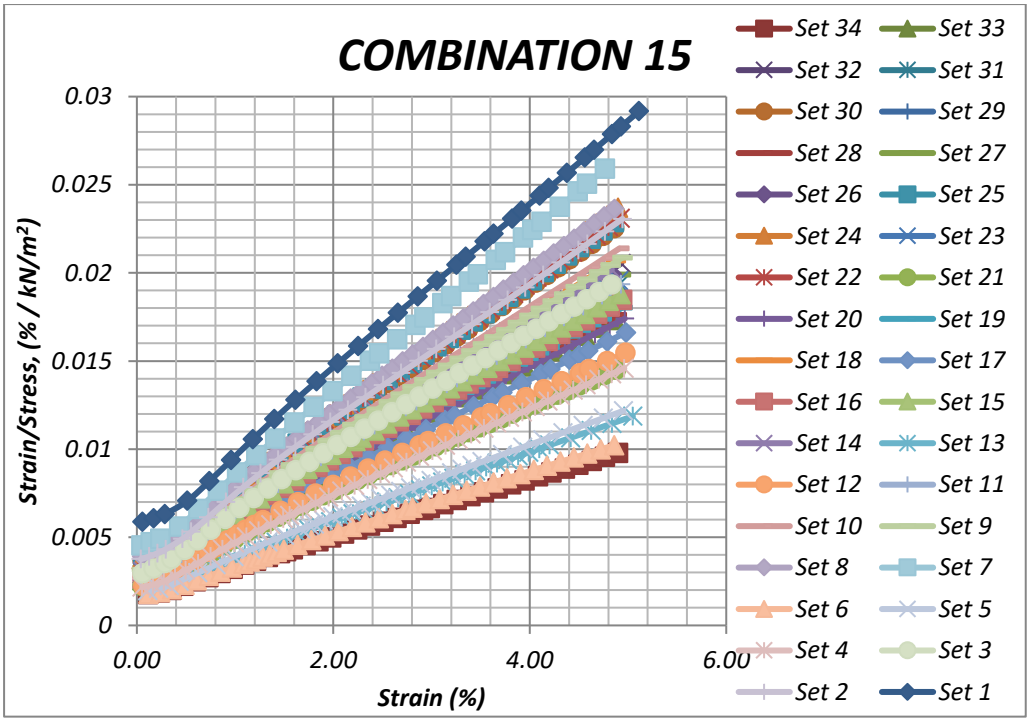


Figure D.14: Strain/Stress Vs Strain (Chin, 1970) for combined foundation (combination 15)

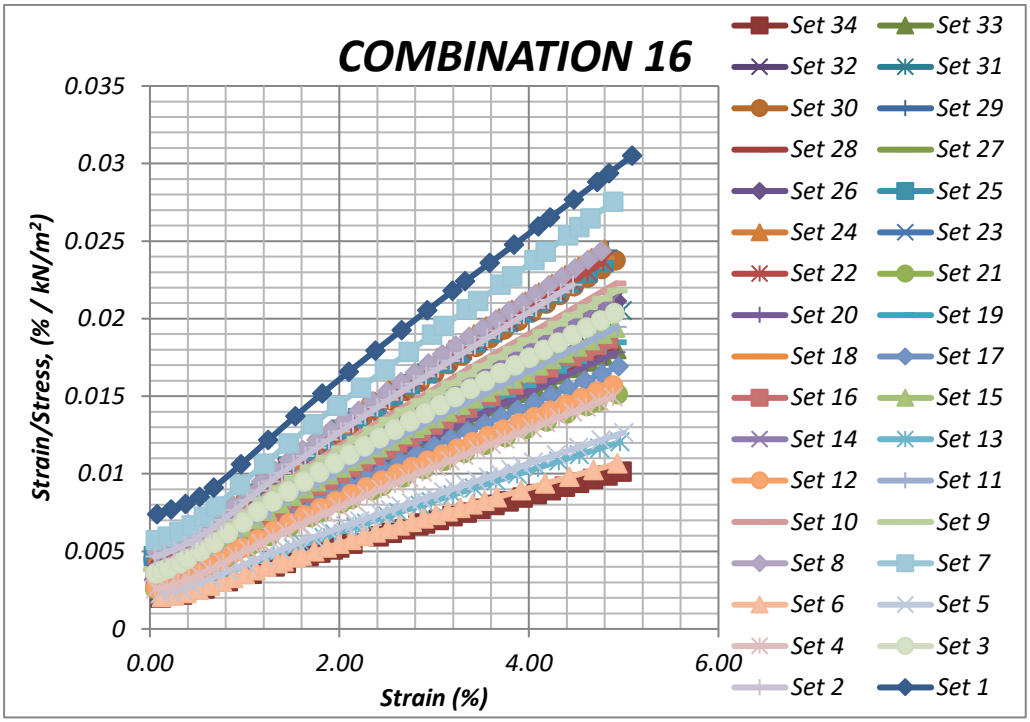


Figure D.15: Strain/Stress Vs Strain (Chin, 1970) for combined foundation (combination 16)

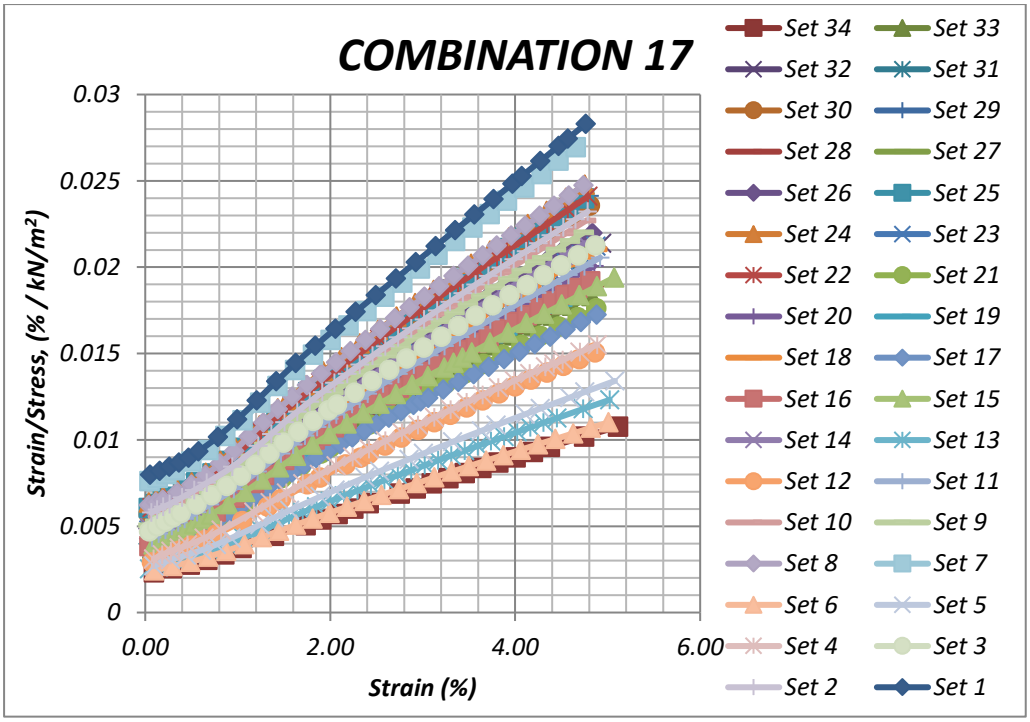


Figure D.16: Strain/Stress Vs Strain (Chin, 1970) for combined foundation (combination 17)

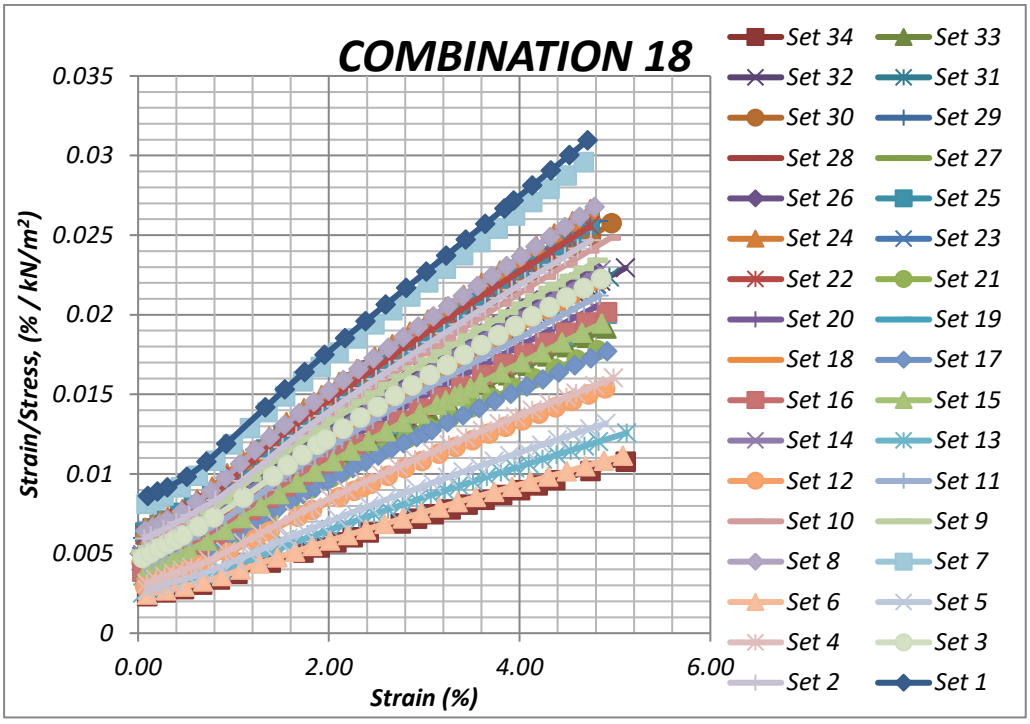


Figure D.17: Strain/Stress Vs Strain (Chin, 1970) for combined foundation (combination 18)

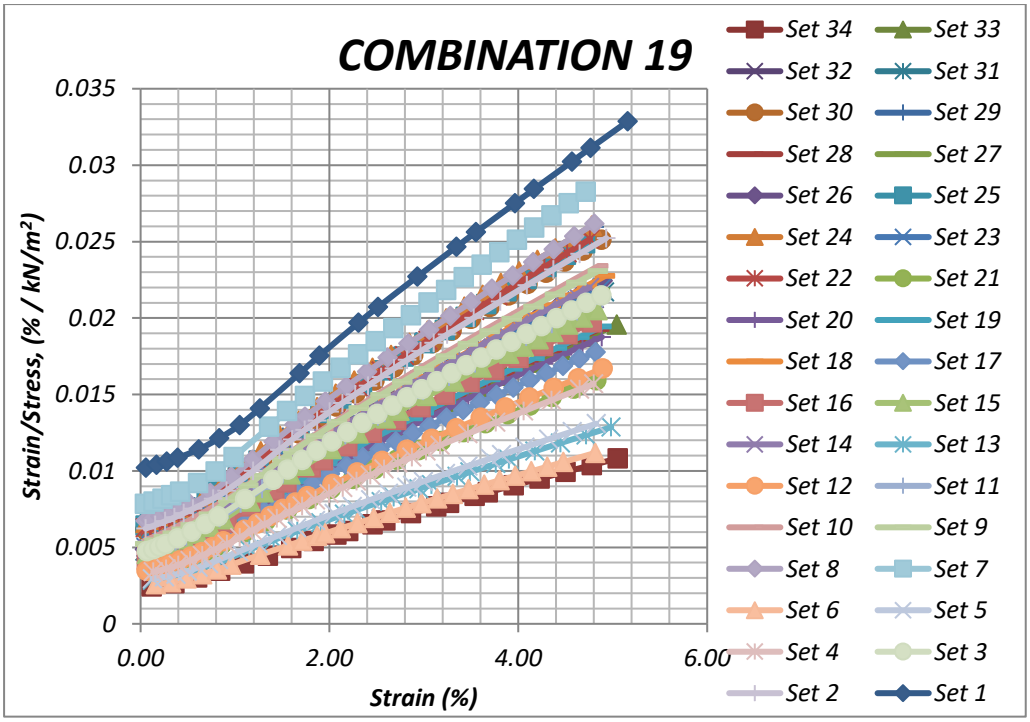


Figure D.18: Strain/Stress Vs Strain (Chin, 1970) for combined foundation (combination 19)

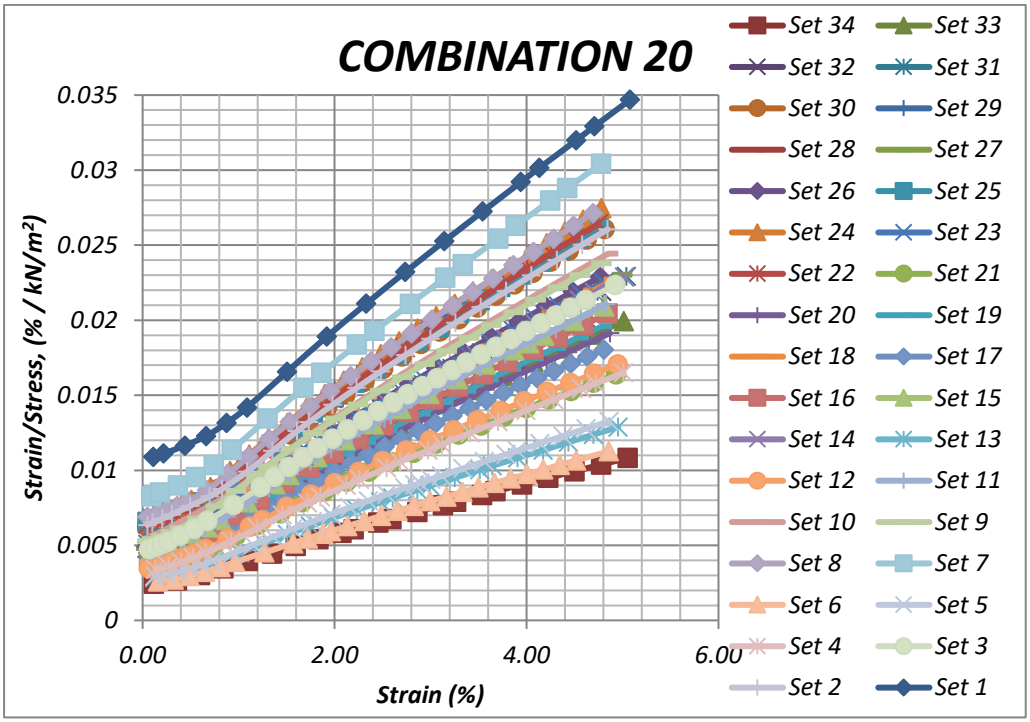


Figure D.19: Strain/Stress Vs Strain (Chin, 1970) for combined foundation (combination 20)

Appendix E (ULTIMATE CARRYING CAPACITIES FOR COMBINED FOUNDATION)

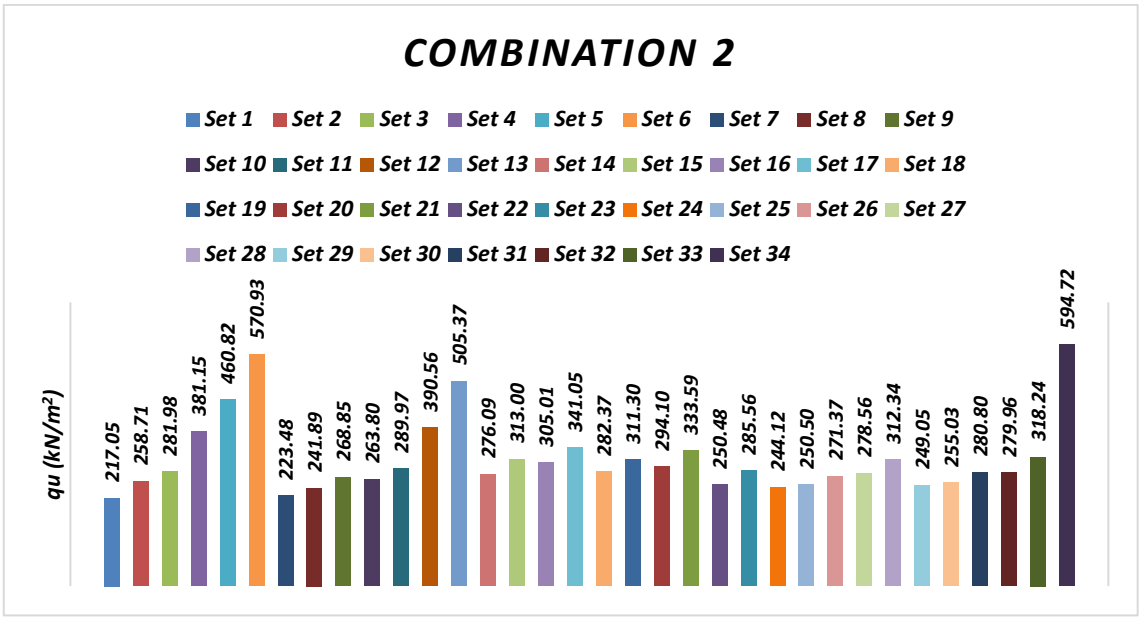


Figure E.1: Ultimate carrying capacities for combined foundation (combination 2)

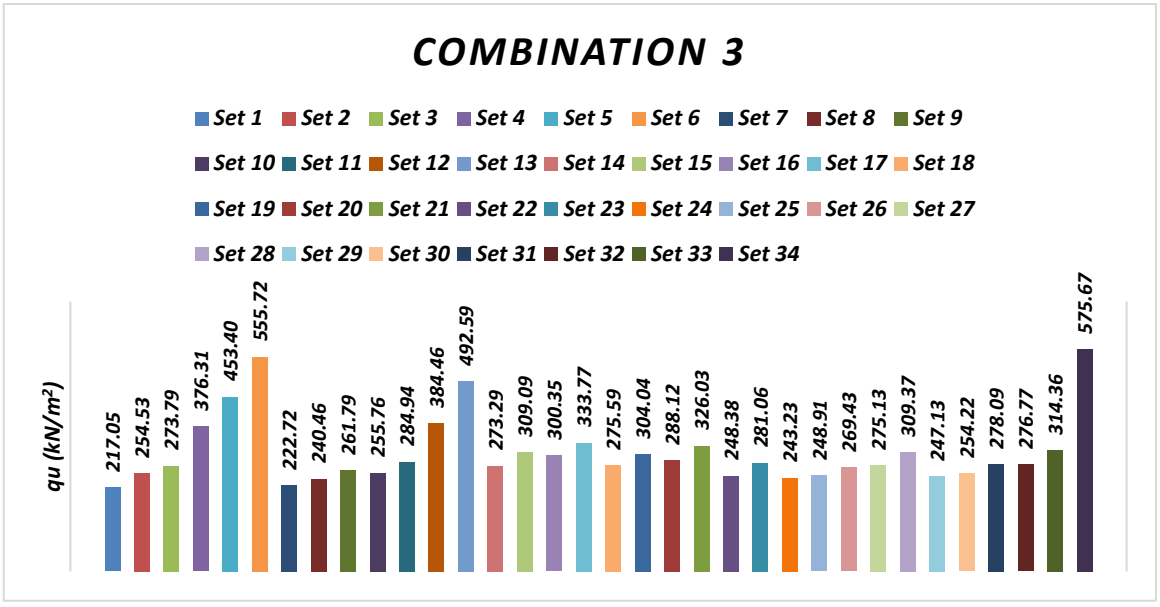


Figure E.2: Ultimate carrying capacities for combined foundation (combination 3)

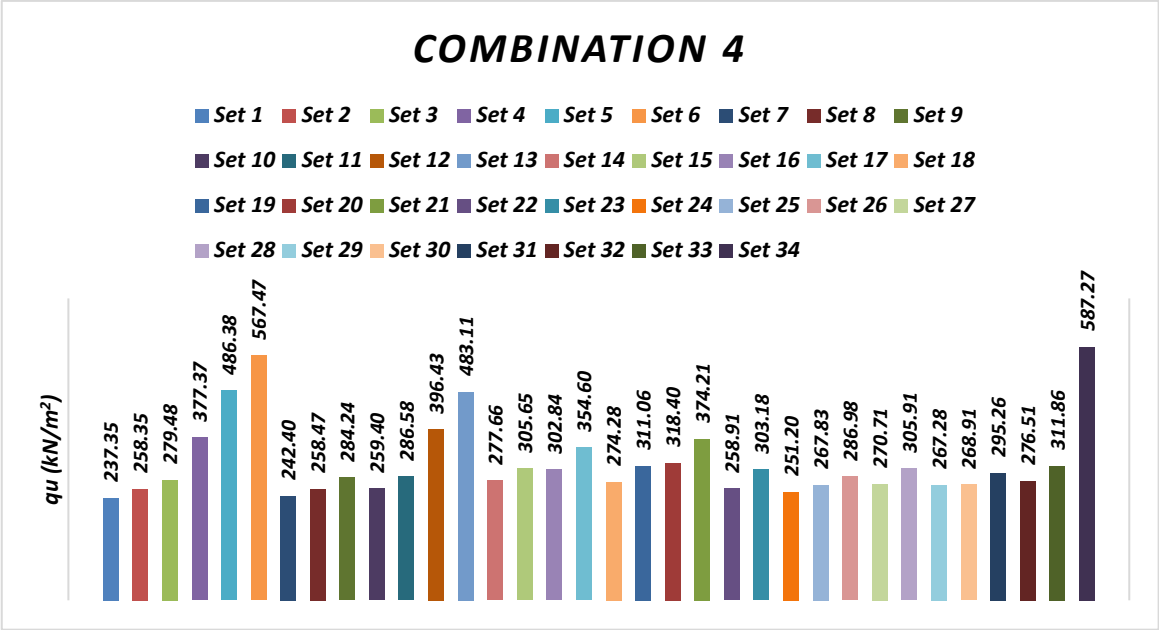


Figure E.3: Ultimate carrying capacities for combined foundation (combination 4)

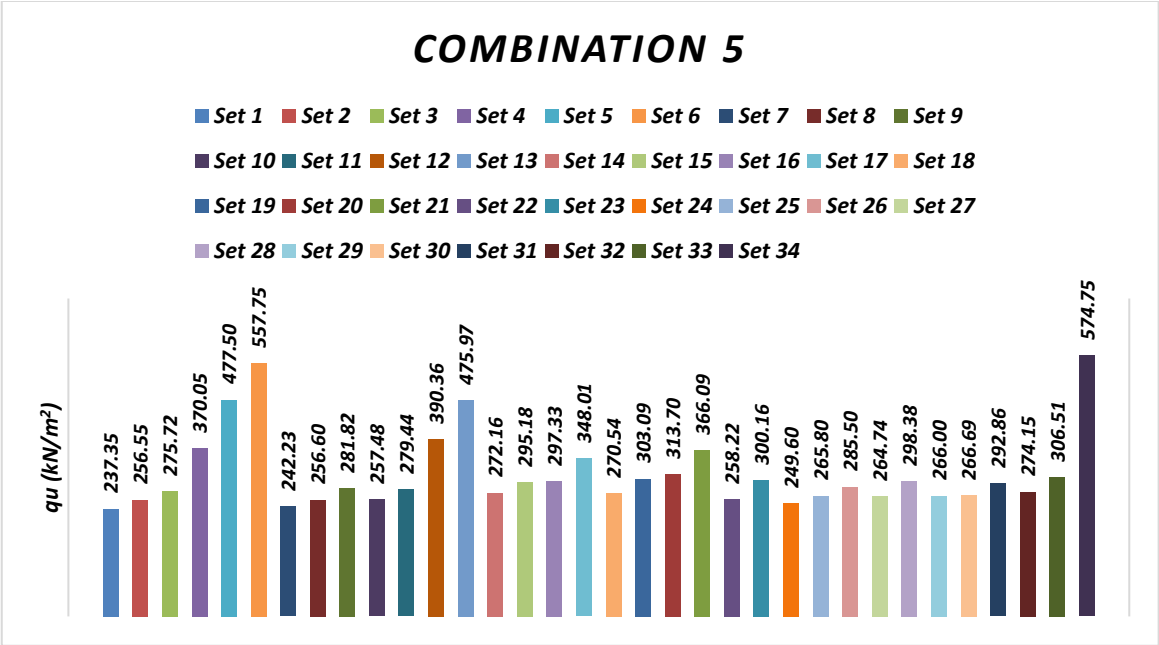


Figure E.4: Ultimate carrying capacities for combined foundation (combination 5)

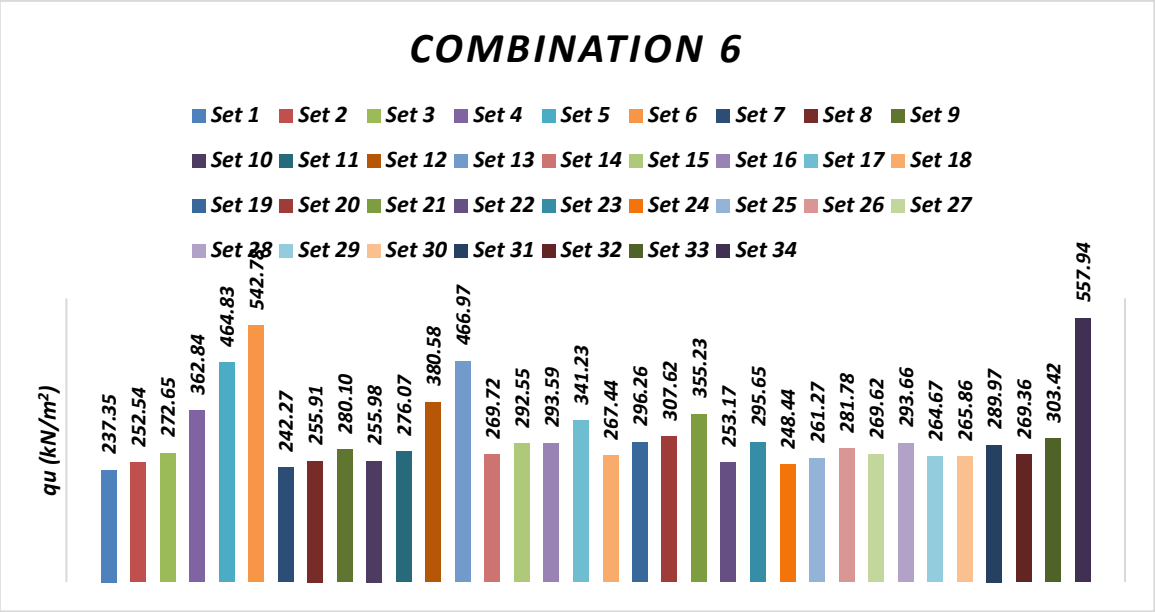


Figure E.5: Ultimate carrying capacities for combined foundation (combination 6)

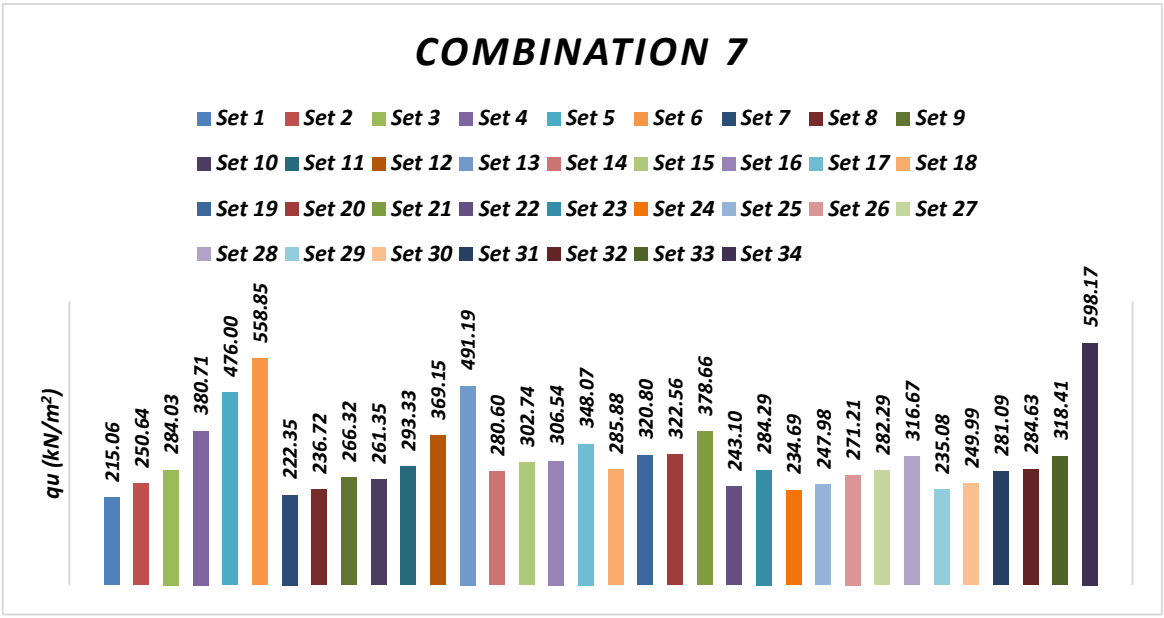


Figure E.6: Ultimate carrying capacities for combined foundation (combination 7)

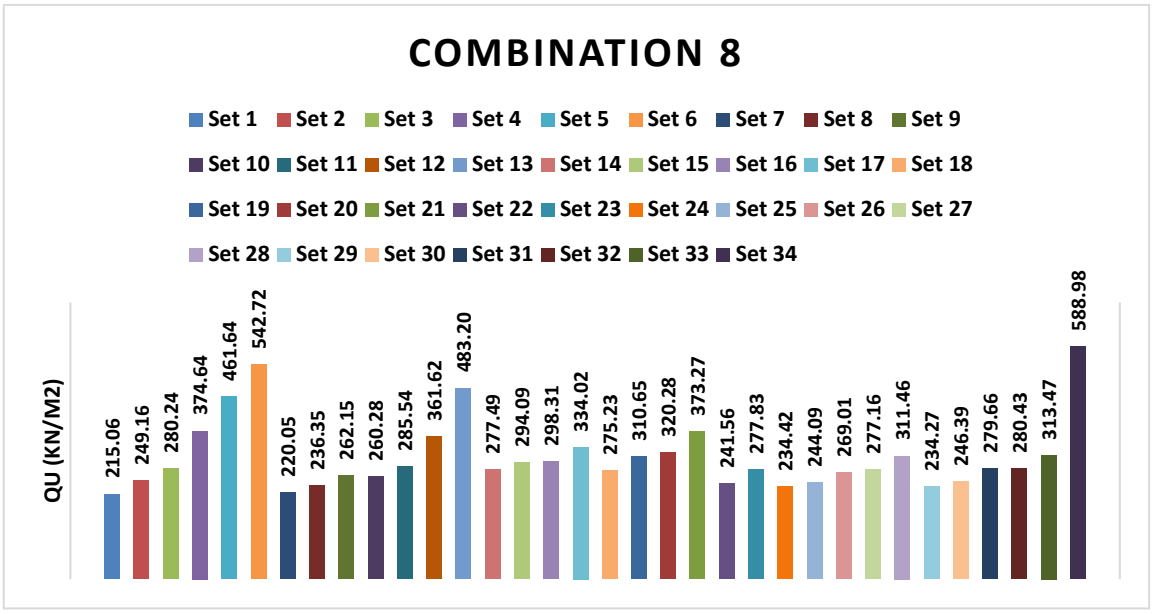


Figure E.7: Ultimate carrying capacities for combined foundation (combination 8)

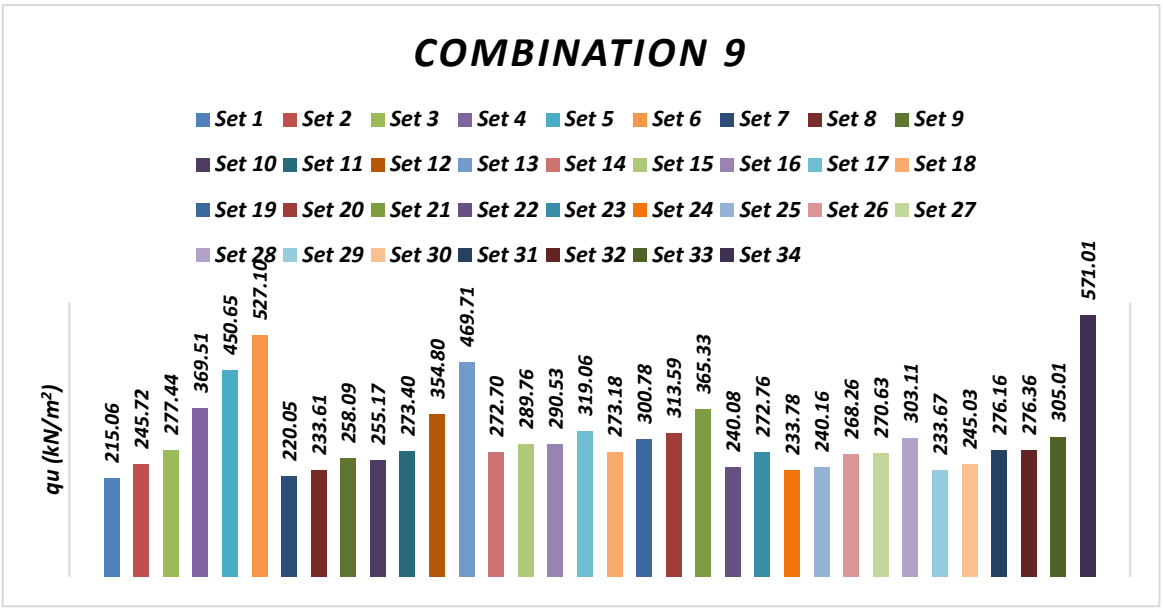


Figure E.8: Ultimate carrying capacities for combined foundation (combination 9)

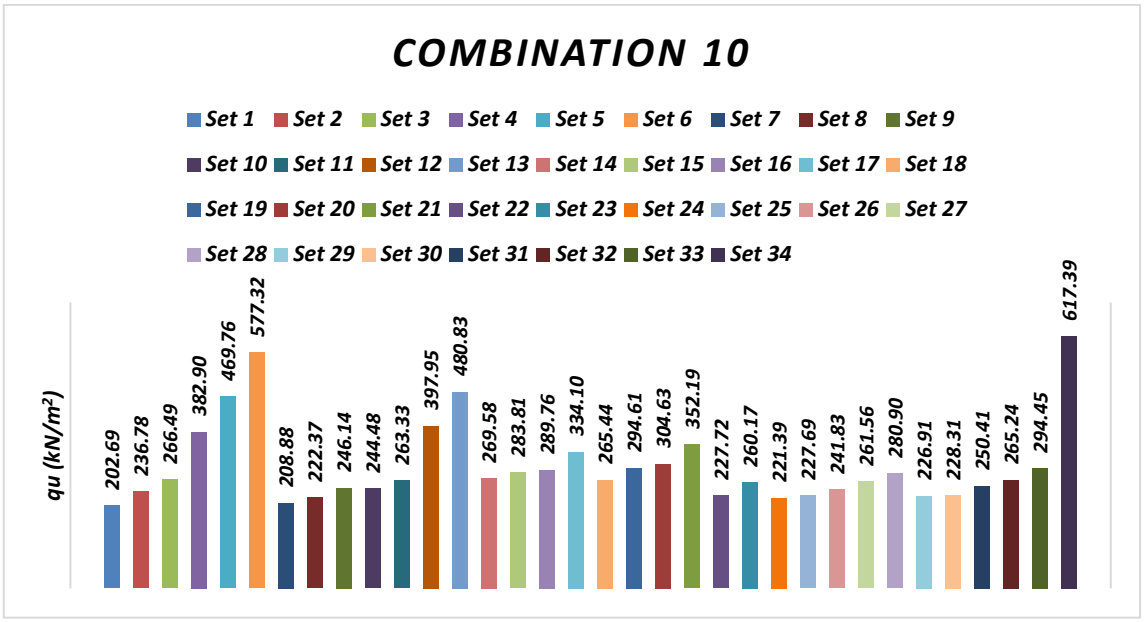


Figure E.9: Ultimate carrying capacities for combined foundation (combination 10)

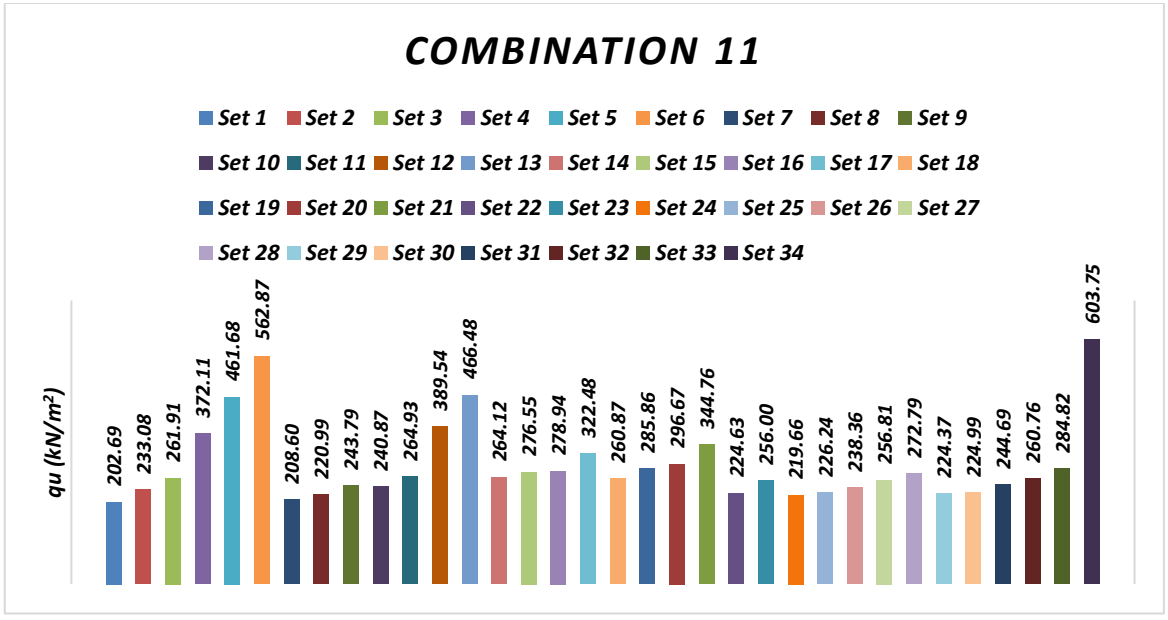


Figure E.10: Ultimate carrying capacities for combined foundation (combination 11)

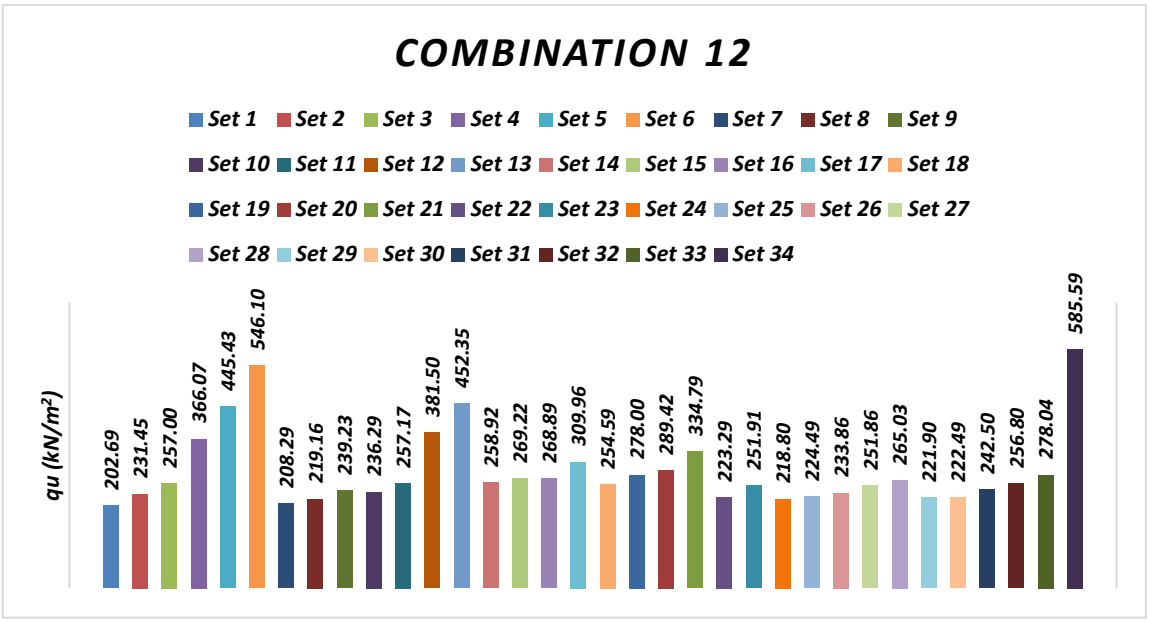


Figure E.11: Ultimate carrying capacities for combined foundation (combination 12)

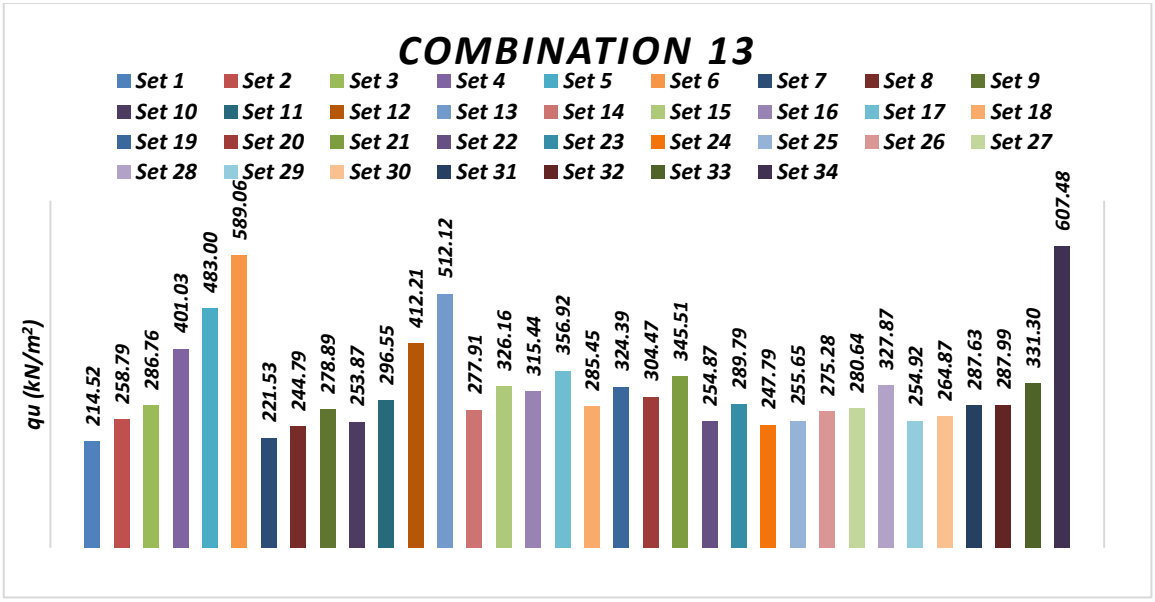


Figure E.12: Ultimate carrying capacities for combined foundation (combination 13)

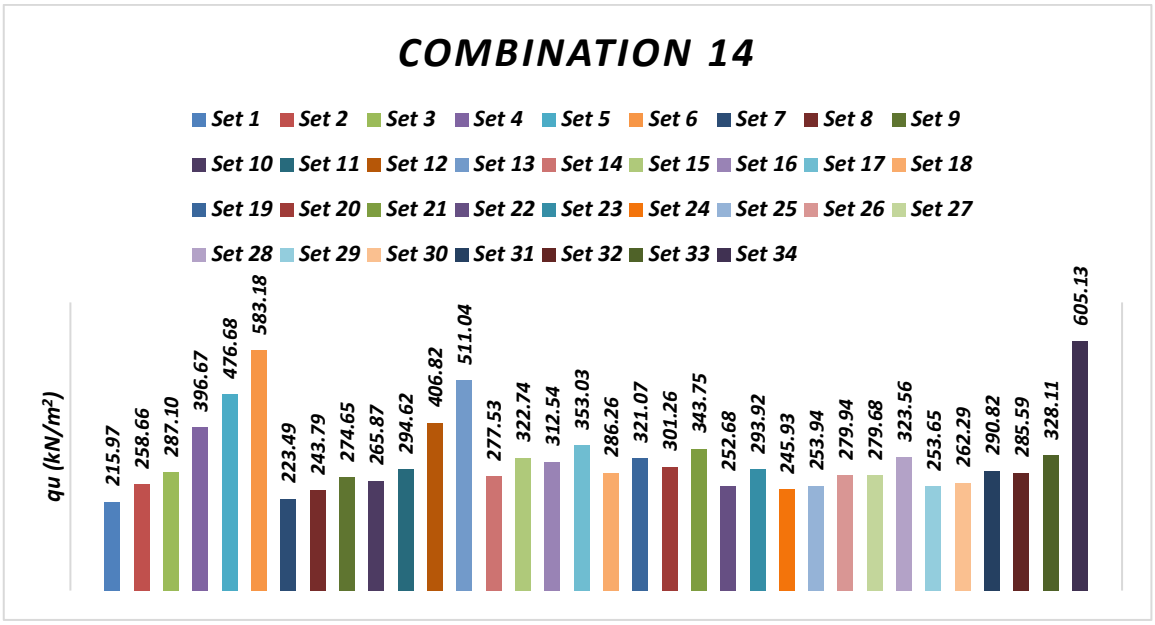


Figure E.13: Ultimate carrying capacities for combined foundation (combination 14)

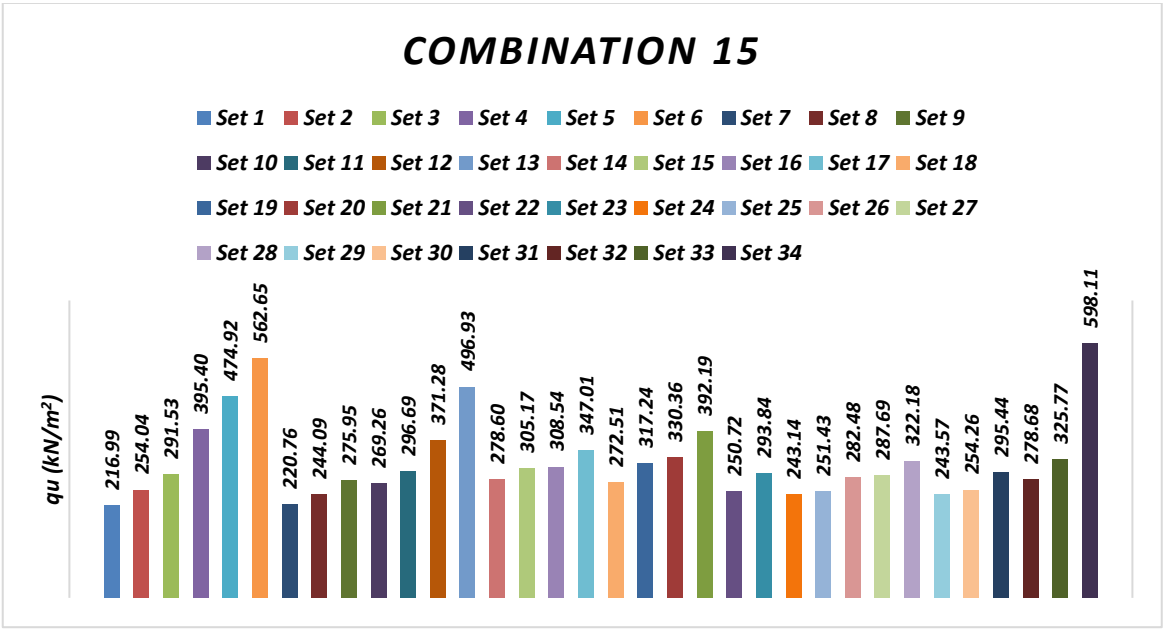


Figure E.14: Ultimate carrying capacities for combined foundation (combination 15)

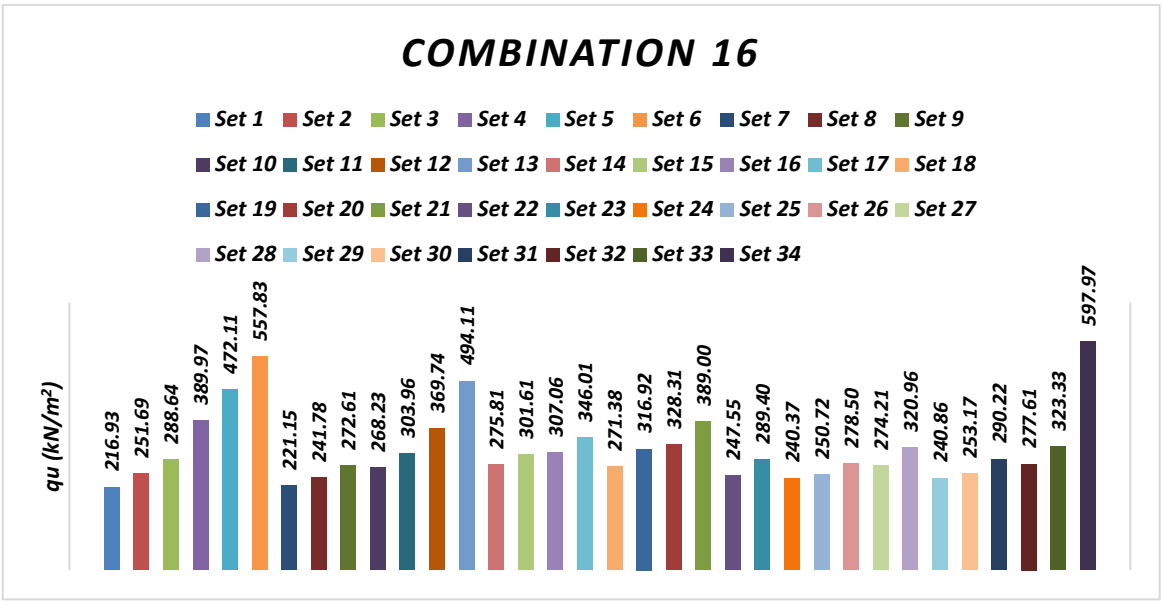


Figure E.15: Ultimate carrying capacities for combined foundation (combination 16)

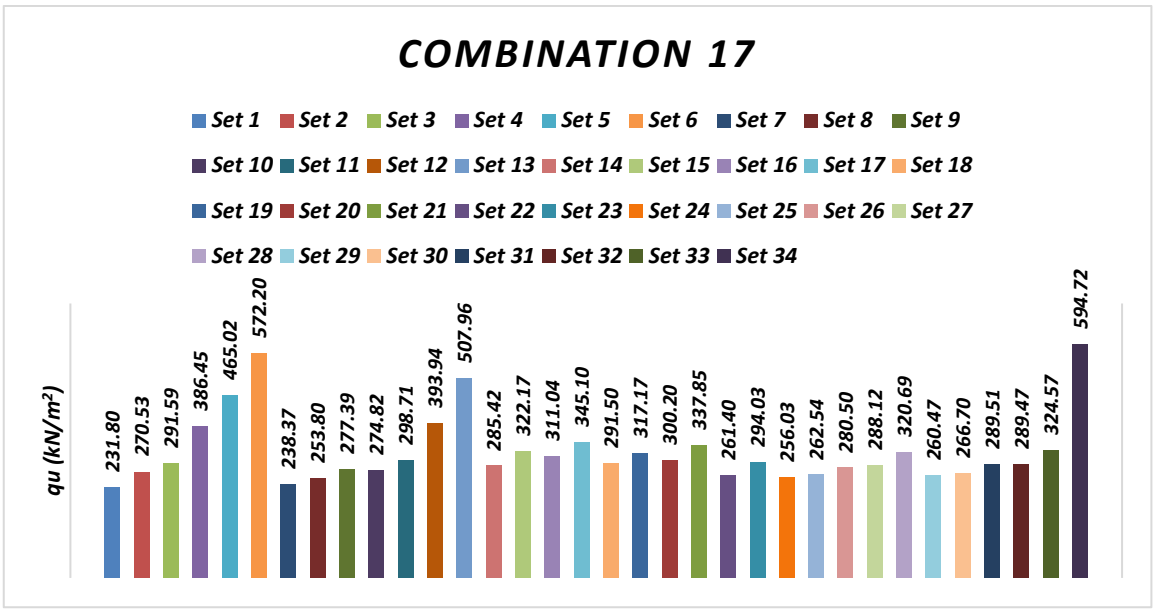


Figure E.16: Ultimate carrying capacities for combined foundation (combination 17)

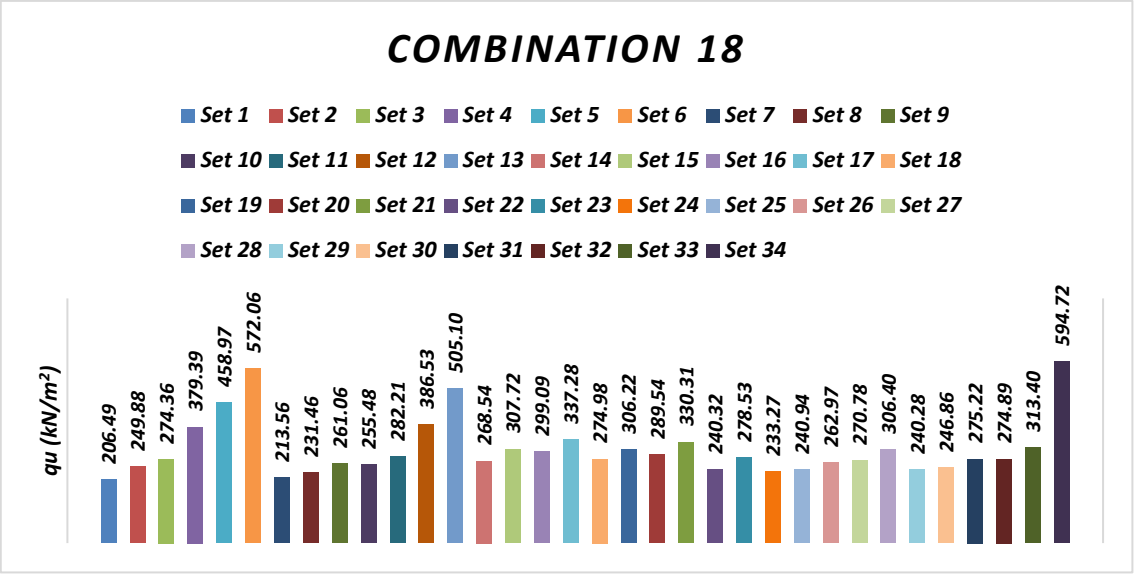


Figure E.17: Ultimate carrying capacities for combined foundation (combination 18)

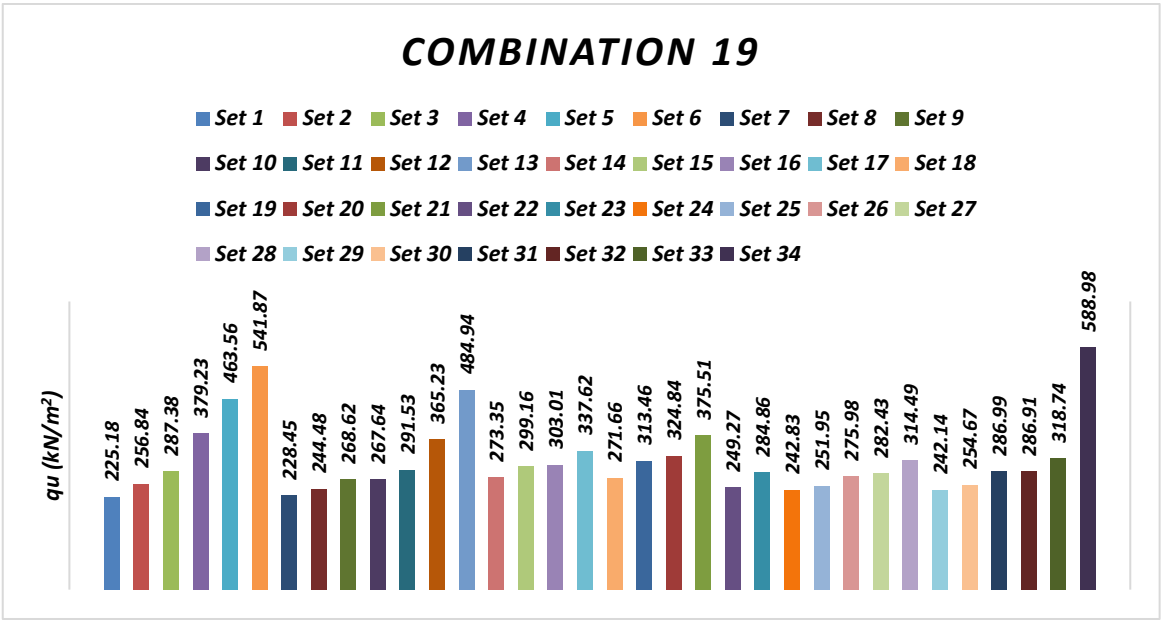


Figure E.18: Ultimate carrying capacities for combined foundation (combination 19)

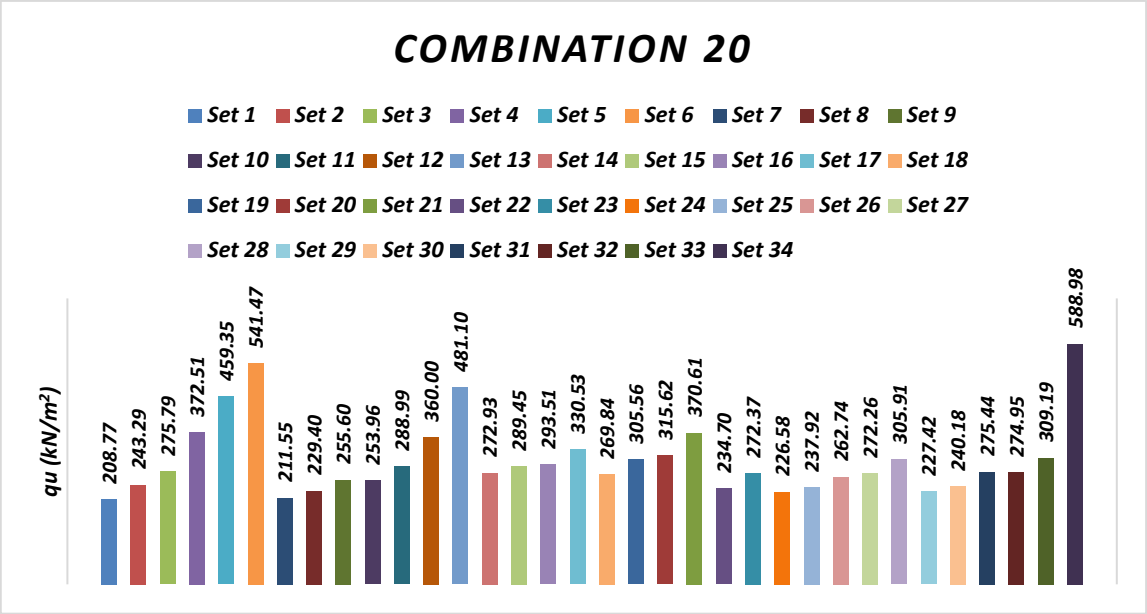


Figure E.19: Ultimate carrying capacities for combined foundation (combination 20)

Appendix F (OPTIMIZATION STUDY)

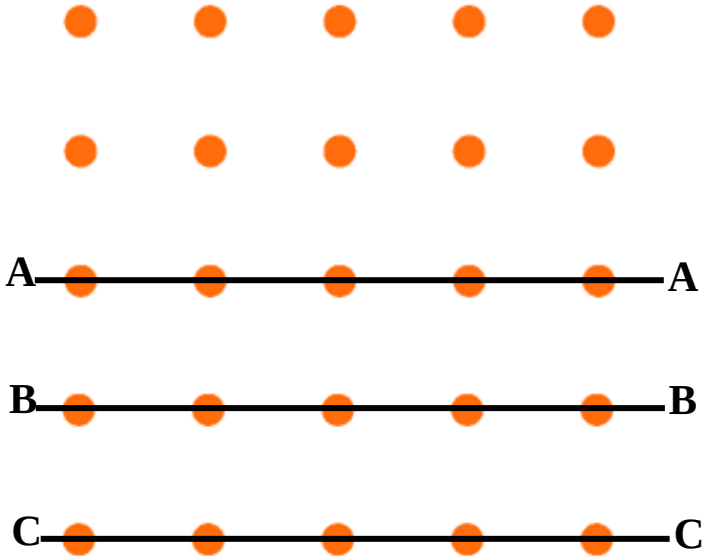
Combination No.	Group 1		Group 2		Group 3		Group 4		Group 5		Group 6		Group 7		Group 8		Group 9		Group 10		Group 11	
	Set No.	IF	Set No.	IF	Set No.	IF	Set No.	IF	Set No.	IF	Set No.	IF	Set No.	IF	Set No.	IF	Set No.	IF	Set No.	IF	Set No.	IF
1	**2**	1.2098	**10**	1.2240	**3**	1.3230	**11**	1.3525	**15**	1.4923	19	1.4811	**4**	1.8027	**12**	1.8395	**5**	2.1816	**13**	2.3739	**6**	2.6880
	8	1.1200	22	1.1585	9	1.2624	18	1.3366	16	1.4190	20	1.3843	17	1.6260	21	1.5662						
	24	1.1238	29	1.1610	14	1.3033	23	1.3347	28	1.4705	**33**	1.5185										
	25	1.1643	30	1.1911	26	1.2567	31	1.3228														
					27	1.3005	32	1.3221														
2	**2**	1.1919	**10**	1.2154	**3**	1.2992	**11**	1.3360	**15**	1.4421	19	1.4343	**4**	1.7561	**12**	1.7994	**5**	2.1231	**13**	2.3284	**6**	2.6304
	8	1.1145	22	1.1541	9	1.2387	18	1.3010	16	1.4053	20	1.3550	17	1.5713	21	1.5370						
	24	1.1247	29	1.1474	14	1.2720	23	1.3157	28	1.4391	**33**	1.4663										
	25	1.1541	30	1.1750	26	1.2503	31	1.2937														
					27	1.2834	32	1.2899														
3	**2**	1.1727	**10**	1.1784	3	1.2614	**11**	1.3128	15	1.4241	19	1.4008	**4**	1.7338	**12**	1.7713	**5**	2.0889	**13**	2.2695	**6**	2.5604
	8	1.1079	22	1.1444	9	1.2061	18	1.2697	16	1.3838	20	1.3274	17	1.5378	21	1.5021						
	24	1.1206	29	1.1386	14	1.2591	23	1.2949	**28**	1.4254	**33**	1.4484										
	25	1.1468	30	1.1713	26	1.2413	31	1.2813														
					27	1.2676	32	1.2752														
4	2	1.0885	10	1.0929	3	1.1775	11	1.2074	15	1.2878	19	1.3106	**4**	1.5900	**12**	1.6703	**5**	2.0493	**13**	2.0355	**6**	2.3909
	8	1.0890	22	1.0909	9	1.1976	18	1.1556	16	1.2759	**20**	1.3415	17	1.4940	21	1.5767						
	24	1.0584	29	1.1261	14	1.1699	**23**	1.2774	**28**	1.2889	33	1.3140										
	25	1.1284	**30**	1.1330	**26**	1.2091	31	1.2440														
					27	1.1406	32	1.1650														
5	2	1.0809	10	1.0848	3	1.1617	11	1.1774	15	1.2437	19	1.2770	**4**	1.5591	**12**	1.6447	**5**	2.0118	**13**	2.0054	**6**	2.3499
	8	1.0811	22	1.0879	9	1.1874	18	1.1399	16	1.2527	**20**	1.3217	17	1.4663	21	1.5424						
	24	1.0516	29	1.1207	14	1.1467	**23**	1.2646	**28**	1.2571	33	1.2914										
	25	1.1199	**30**	1.1236	**26**	1.2029	31	1.2339														
					27	1.1154	32	1.1551														

Combination No.	Group 1		Group 2		Group 3		Group 4		Group 5		Group 6		Group 7		Group 8		Group 9		Group 10		Group 11	
	Set No.	IF	Set No.	IF	Set No.	IF	Set No.	IF	Set No.	IF	Set No.	IF	Set No.	IF	Set No.	IF	Set No.	IF	Set No.	IF	Set No.	IF
6	2	1.0640	10	1.0785	3	1.1487	11	1.1632	15	1.2326	19	1.2482	**4**	1.5288	**12**	1.6035	**5**	1.9585	**13**	1.9675	**6**	2.2869
	8	1.0782	22	1.0667	9	1.1801	18	1.1268	16	1.2370	**20**	1.2961	17	1.4377	21	1.4967						
	24	1.0468	29	1.1151	14	1.1364	**23**	1.2457	**28**	1.2373	33	1.2784										
	25	1.1008	**30**	1.1201	**26**	1.1872	31	1.2217														
					27	1.1360	32	1.1349														
7	**Set No.**	**IF**	**Set No.**	**IF**	**Set No.**	**IF**	**Set No.**	**IF**	**Set No.**	**IF**	**Set No.**	**IF**	**Set No.**	**IF**	**Set No.**	**IF**	**Set No.**	**IF**	**Set No.**	**IF**	**Set No.**	**IF**
	2	1.1641	**10**	1.2138	**3**	1.3192	**11**	1.3624	15	1.4061	19	1.4900	**4**	1.7682	12	1.7145	**5**	2.2108	**13**	2.2813	**6**	2.5956
	8	1.0994	22	1.1291	9	1.2369	18	1.3278	16	1.4237	**20**	1.4981	17	1.6166	**21**	1.7587						
	24	1.0900	29	1.0918	14	1.3033	23	1.3204	**28**	1.4708	33	1.4789										
	25	1.1517	30	1.1611	26	1.2596	31	1.3055														
					27	1.3111	32	1.3220														
8	**Set No.**	**IF**	**Set No.**	**IF**	**Set No.**	**IF**	**Set No.**	**IF**	**Set No.**	**IF**	**Set No.**	**IF**	**Set No.**	**IF**	**Set No.**	**IF**	**Set No.**	**IF**	**Set No.**	**IF**	**Set No.**	**IF**
	2	1.1572	**10**	1.2089	**3**	1.3016	**11**	1.3262	15	1.3659	19	1.4428	**4**	1.7400	12	1.6795	**5**	2.1441	**13**	2.2442	**6**	2.5207
	8	1.0977	22	1.1219	9	1.2176	18	1.2783	16	1.3855	**20**	1.4875	17	1.5513	**21**	1.7336						
	24	1.0888	29	1.0881	14	1.2888	23	1.2904	**28**	1.4466	33	1.4559										
	25	1.1337	30	1.1444	26	1.2494	31	1.2989														
					27	1.2873	32	1.3024														
9	**Set No.**	**IF**	**Set No.**	**IF**	**Set No.**	**IF**	**Set No.**	**IF**	**Set No.**	**IF**	**Set No.**	**IF**	**Set No.**	**IF**	**Set No.**	**IF**	**Set No.**	**IF**	**Set No.**	**IF**	**Set No.**	**IF**
	2	1.1413	**10**	1.1851	**3**	1.2886	11	1.2698	15	1.3458	19	1.3970	**4**	1.7162	12	1.6479	**5**	2.0931	**13**	2.1815	**6**	2.4481
	8	1.0850	22	1.1150	9	1.1987	18	1.2688	16	1.3494	**20**	1.4565	17	1.4819	**21**	1.6968						
	24	1.0858	29	1.0853	14	1.2666	23	1.2668	**28**	1.4078	33	1.4166										
	25	1.1154	30	1.1381	26	1.2459	31	1.2826														
					27	1.2569	**32**	1.2835														
10	**Set No.**	**IF**	**Set No.**	**IF**	**Set No.**	**IF**	**Set No.**	**IF**	**Set No.**	**IF**	**Set No.**	**IF**	**Set No.**	**IF**	**Set No.**	**IF**	**Set No.**	**IF**	**Set No.**	**IF**	**Set No.**	**IF**
	2	1.1585	**10**	1.1962	3	1.3039	11	1.2884	15	1.3886	19	1.4414	**4**	1.8734	**12**	1.9471	**5**	2.2984	**13**	2.3526	**6**	2.8247
	8	1.0880	22	1.1142	9	1.2043	**18**	1.2987	**16**	1.4177	**20**	1.4905	17	1.6347	21	1.7232						
	24	1.0832	29	1.1102	**14**	1.3190	23	1.2729	28	1.3744	33	1.4407										
	25	1.1141	30	1.1171	26	1.1832	31	1.2252														
					27	1.2798	32	1.2978														

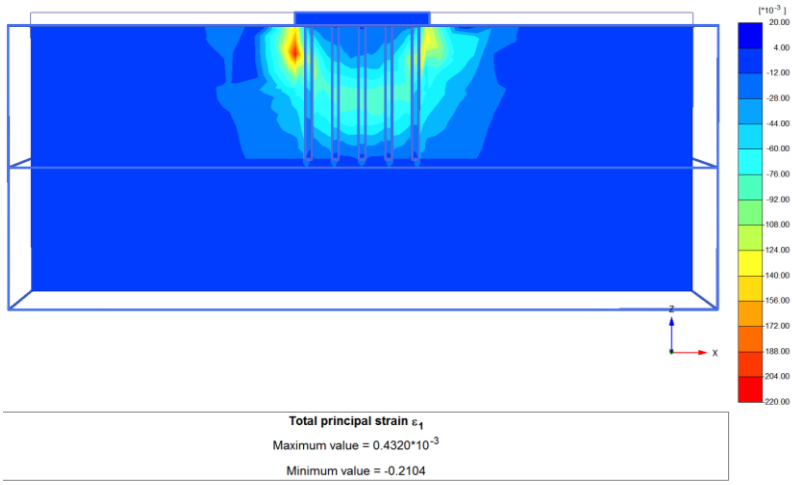
Combination No.	Group 1		Group 2		Group 3		Group 4		Group 5		Group 6		Group 7		Group 8		Group 9		Group 10		Group 11	
	Set No.	IF	Set No.	IF	Set No.	IF	Set No.	IF	Set No.	IF	Set No.	IF	Set No.	IF	Set No.	IF	Set No.	IF	Set No.	IF	Set No.	IF
11	**2**	1.1404	**10**	1.1785	3	1.2815	**11**	1.2962	15	1.3531	19	1.3986	**4**	1.8207	**12**	1.9060	**5**	2.2589	**13**	2.2824	**6**	2.7540
	8	1.0812	22	1.0991	9	1.1928	18	1.2764	**16**	1.3648	**20**	1.4516	17	1.5778	21	1.6868						
	24	1.0748	29	1.0978	**14**	1.2923	23	1.2526	28	1.3347	33	1.3936										
	25	1.1069	30	1.1008	26	1.1662	31	1.1972														
					27	1.2565	32	1.2759														
12	**2**	1.1324	**10**	1.1561	3	1.2574	**11**	1.2583	15	1.3172	19	1.3602	**4**	1.7911	**12**	1.8666	**5**	2.1794	**13**	2.2133	**6**	2.6719
	8	1.0723	22	1.0925	9	1.1705	18	1.2456	16	1.3156	**20**	1.4161	17	1.5166	21	1.6381						
	24	1.0706	29	1.0857	**14**	1.2669	23	1.2325	28	1.2968	33	1.3604										
	25	1.0984	30	1.0886	26	1.1442	31	1.1865														
					27	1.2323	32	1.2565														
13	**2**	1.2064	10	1.1834	**3**	1.3368	**11**	1.3824	15	1.5204	19	1.5122	**4**	1.8694	**12**	1.9215	**5**	2.2516	**13**	2.3873	**6**	2.7460
	8	1.1411	22	1.1881	9	1.3001	18	1.3306	16	1.4705	20	1.4193	17	1.6638	21	1.6106						
	24	1.1551	29	1.1883	14	1.2955	23	1.3509	**28**	1.5284	**33**	1.5444										
	25	1.1917	**30**	1.2347	26	1.2832	31	1.3408														
					27	1.3082	32	1.3425														
14	**2**	1.1976	**10**	1.2310	**3**	1.3294	**11**	1.3641	15	1.4944	19	1.4866	**4**	1.8367	**12**	1.8837	**5**	2.2071	**13**	2.3662	**6**	2.7003
	8	1.1288	22	1.1700	9	1.2717	18	1.3255	16	1.4471	20	1.3949	17	1.6346	21	1.5917						
	24	1.1387	29	1.1745	14	1.2850	23	1.3609	**28**	1.4982	**33**	1.5192										
	25	1.1758	30	1.2145	26	1.2962	31	1.3466														
					27	1.2950	32	1.3224														
15	**2**	1.1792	**10**	1.2498	**3**	1.3532	**11**	1.3771	15	1.4165	19	1.4725	**4**	1.8353	12	1.7234	**5**	2.2044	**13**	2.3066	**6**	2.6116
	8	1.1330	22	1.1638	9	1.2809	18	1.2649	16	1.4322	**20**	1.5334	17	1.6107	**21**	1.8204						
	24	1.1286	29	1.1306	14	1.2932	23	1.3639	**28**	1.4954	33	1.5121										
	25	1.1670	30	1.1802	26	1.3112	31	1.3713														
					27	1.3354	32	1.2935														

Combination No.	Group 1		Group 2		Group 3		Group 4		Group 5		Group 6		Group 7		Group 8		Group 9		Group 10		Group 11	
	Set No.	IF	Set No.	IF	Set No.	IF	Set No.	IF	Set No.	IF	Set No.	IF	Set No.	IF	Set No.	IF	Set No.	IF	Set No.	IF	Set No.	IF
16	**2**	1.1629	**10**	1.2393	**3**	1.3336	**11**	1.4044	15	1.3935	19	1.4643	**4**	1.8018	12	1.7083	**5**	2.1813	**13**	2.2830	**6**	2.5774
	8	1.1171	22	1.1438	9	1.2596	18	1.2539	16	1.4188	**20**	1.5169	17	1.5987	**21**	1.7973						
	24	1.1106	29	1.1129	14	1.2744	23	1.3372	**28**	1.4830	33	1.4939										
	25	1.1584	30	1.1698	26	1.2868	31	1.3410														
					27	1.2669	32	1.2827														
17	**2**	1.1671	**10**	1.1856	**3**	1.2579	**11**	1.2886	**15**	1.3898	19	1.3683	**4**	1.6671	**12**	1.6995	**5**	2.0061	**13**	2.1913	**6**	2.4685
	8	1.0949	22	1.1277	9	1.1967	18	1.2575	16	1.3418	20	1.2951	17	1.4888	21	1.4575						
	24	1.1045	29	1.1237	14	1.2313	23	1.2684	28	1.3834	**33**	1.4002										
	25	1.1326	30	1.1506	26	1.2101	31	1.2489														
					27	1.2429	32	1.2488														
18	**2**	1.2101	**10**	1.2373	**3**	1.3287	**11**	1.3667	**15**	1.4902	19	1.4830	**4**	1.8373	**12**	1.8719	**5**	2.2227	**13**	2.4461	**6**	2.7704
	8	1.1209	22	1.1639	9	1.2643	18	1.3317	16	1.4485	20	1.4022	17	1.6334	21	1.5996						
	24	1.1297	29	1.1636	14	1.3005	23	1.3489	28	1.4838	**33**	1.5178										
	25	1.1669	30	1.1955	26	1.2735	31	1.3329														
					27	1.3114	32	1.3312														
19	**2**	1.1399	**10**	1.1878	**3**	1.2755	**11**	1.2939	15	1.3278	19	1.3912	**4**	1.6831	12	1.6210	**5**	2.0574	**13**	2.1523	**6**	2.4049
	8	1.0851	22	1.1063	9	1.1922	18	1.2057	16	1.3449	**20**	1.4417	17	1.4984	**21**	1.6666						
	24	1.0778	29	1.0747	14	1.2132	23	1.2643	**28**	1.3958	33	1.4147										
	25	1.1182	30	1.1303	26	1.2249	31	1.2737														
					27	1.2535	32	1.2734														
20	**2**	1.1648	**10**	1.2159	**3**	1.3204	**11**	1.3837	15	1.3858	19	1.4630	**4**	1.7835	12	1.7236	**5**	2.1993	**13**	2.3034	**6**	2.5925
	8	1.0983	22	1.1237	9	1.2238	18	1.2920	16	1.4053	**20**	1.5111	17	1.5825	**21**	1.7744						
	24	1.0849	29	1.0888	14	1.3068	23	1.3041	**28**	1.4646	33	1.4804										
	25	1.1391	30	1.1499	26	1.2580	31	1.3188														
					27	1.3035	32	1.3164														

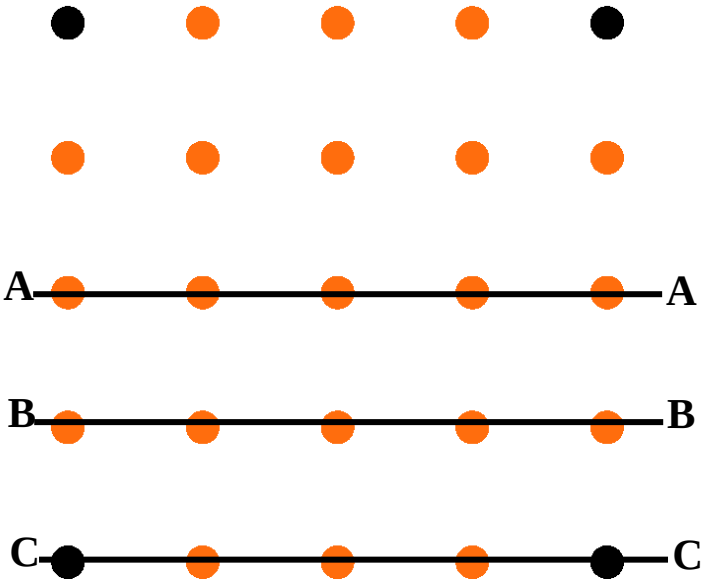
Appendix G (BEHAVIOUR OF COMBINED FOUNDATION)



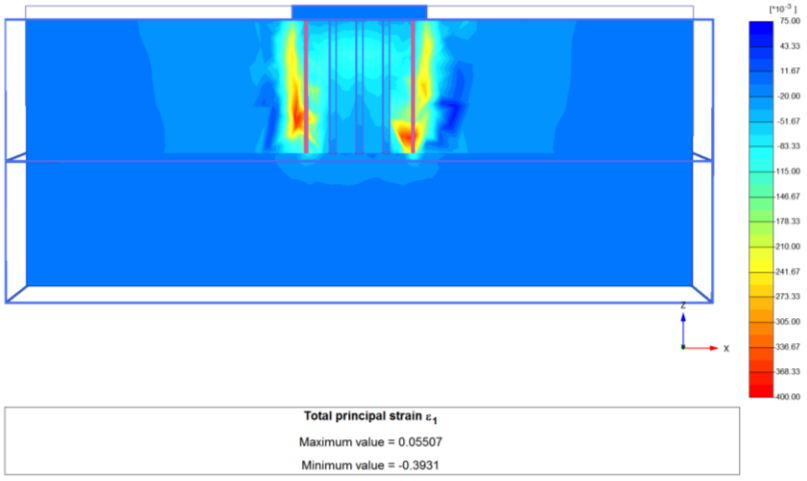
Set 1



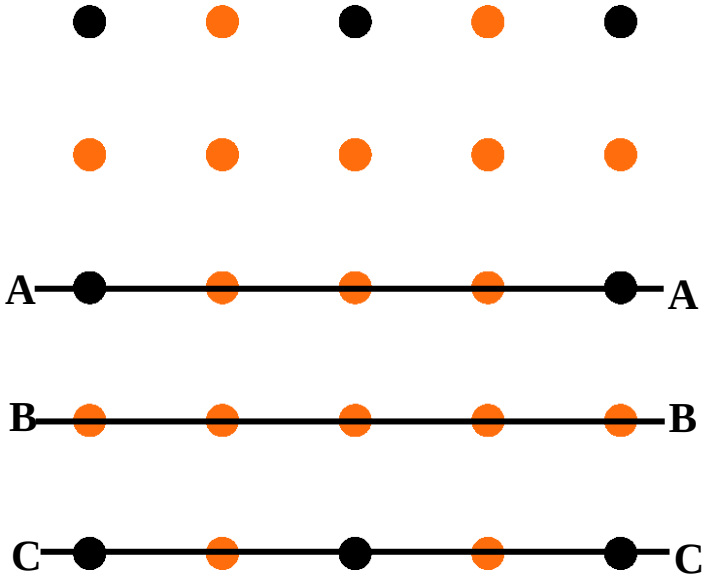
Set 1 Section A-A



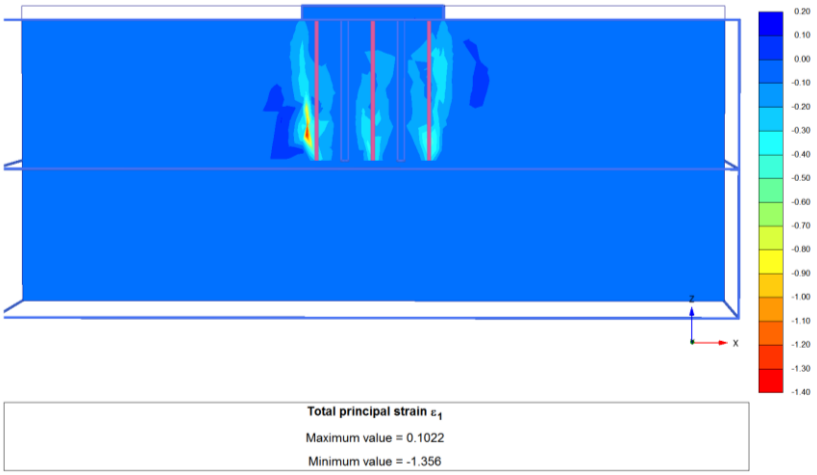
Set2



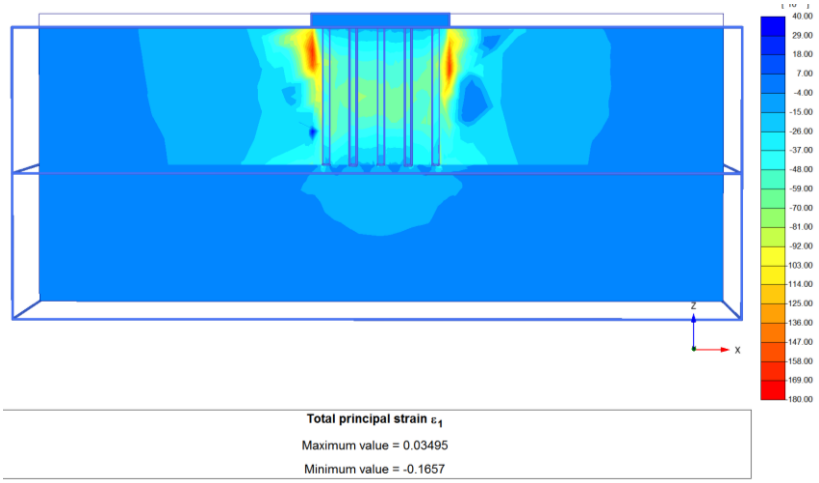
Set2 Section C-C



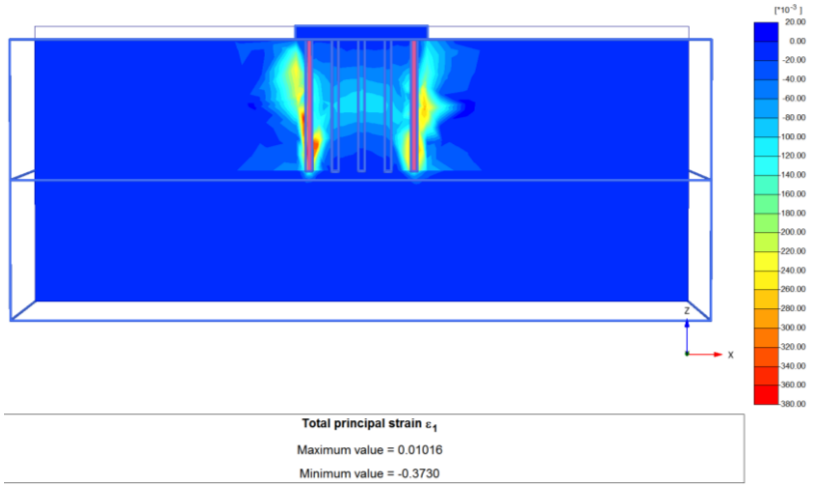
Set3



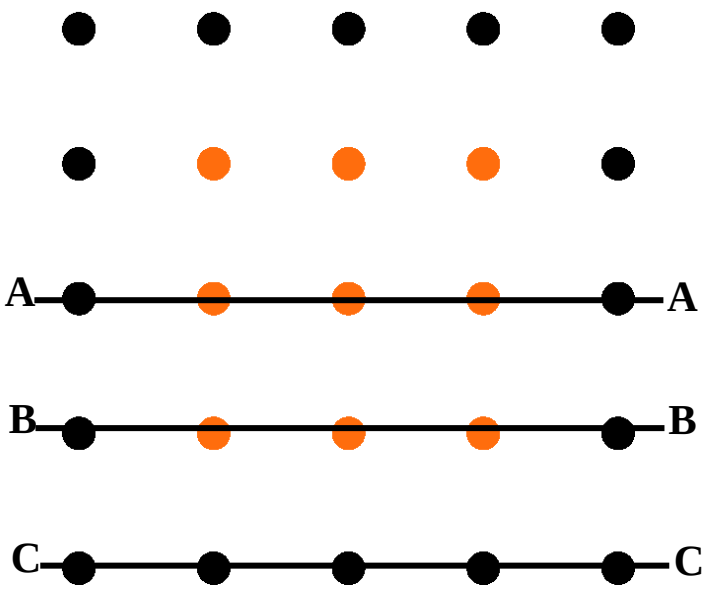
Set3 Section-C-C



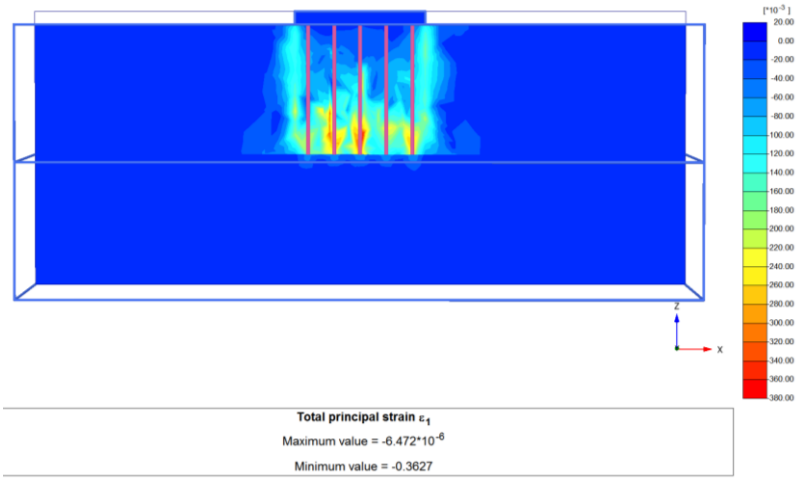
Set3 Section B-B



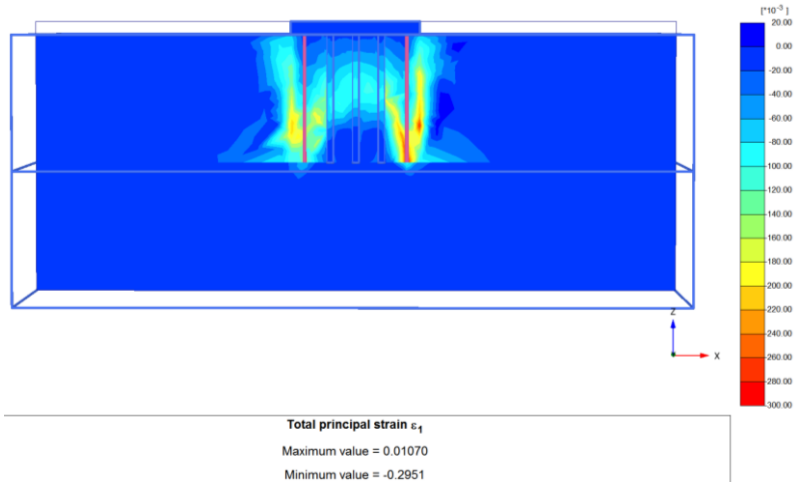
Set3 Section A-A



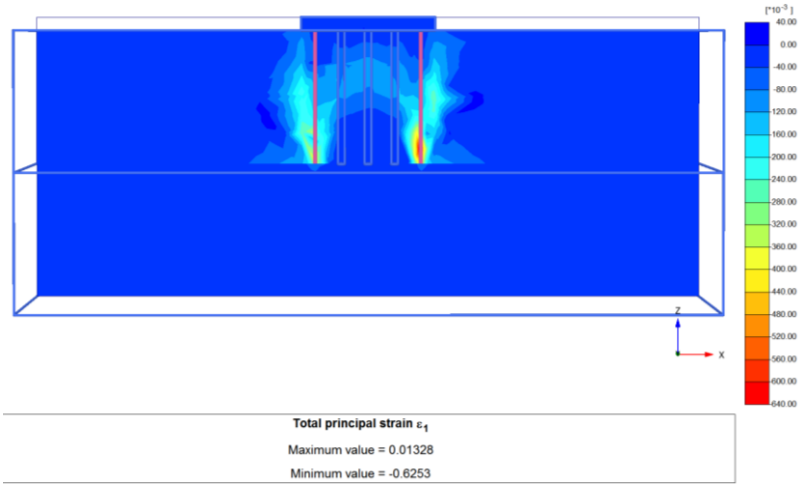
Set4



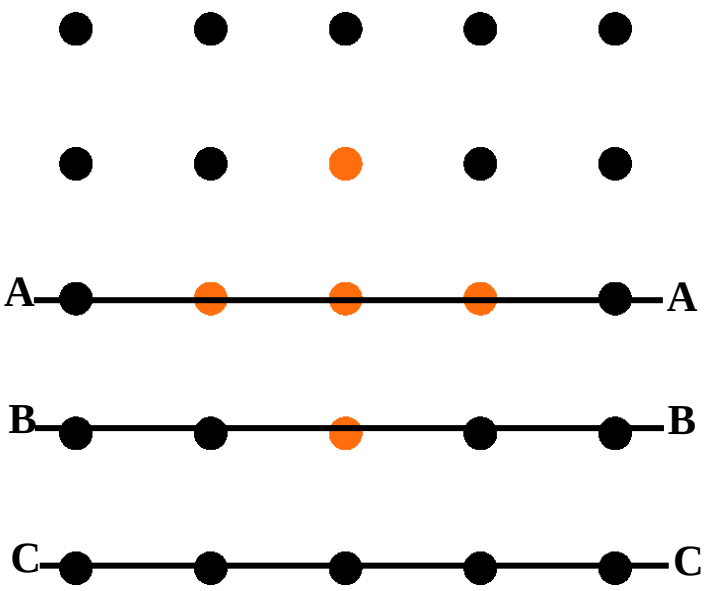
Set4 Section C-C



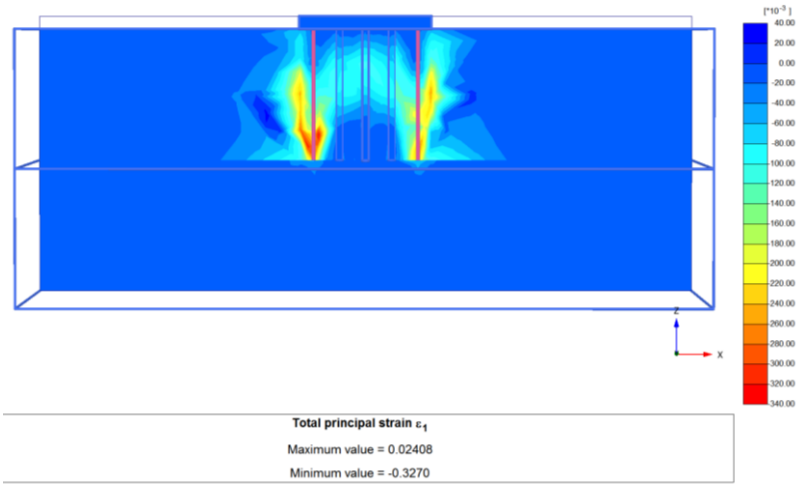
Set4 Section B-B



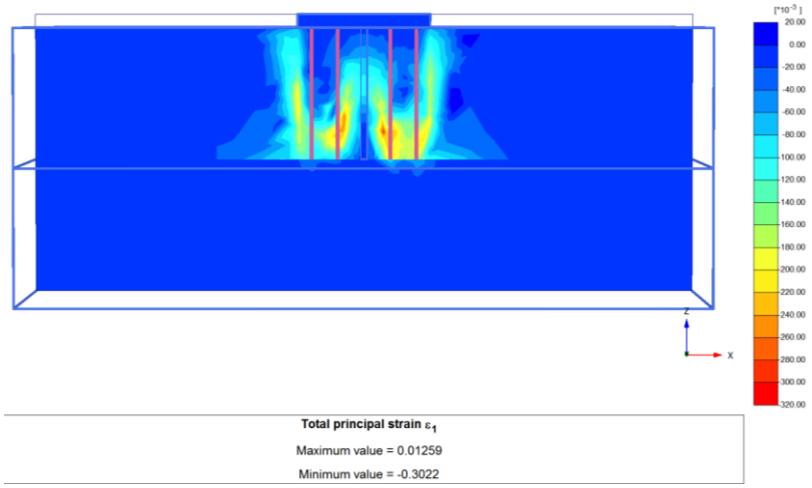
Set4 Section A-A



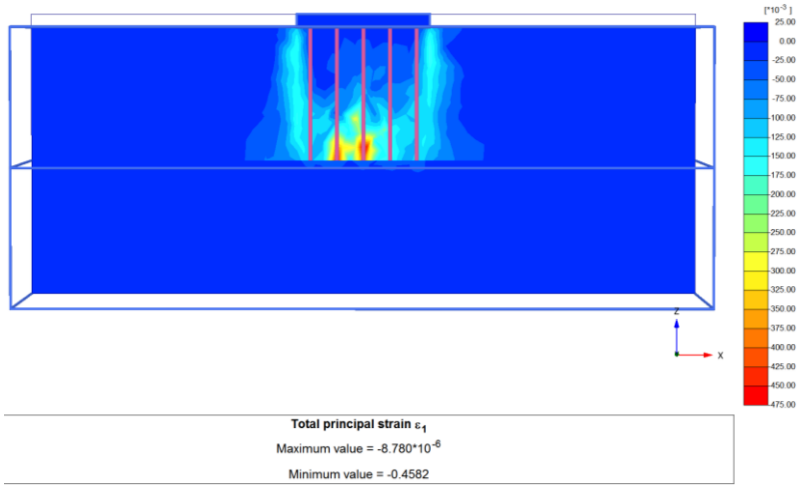
Set5



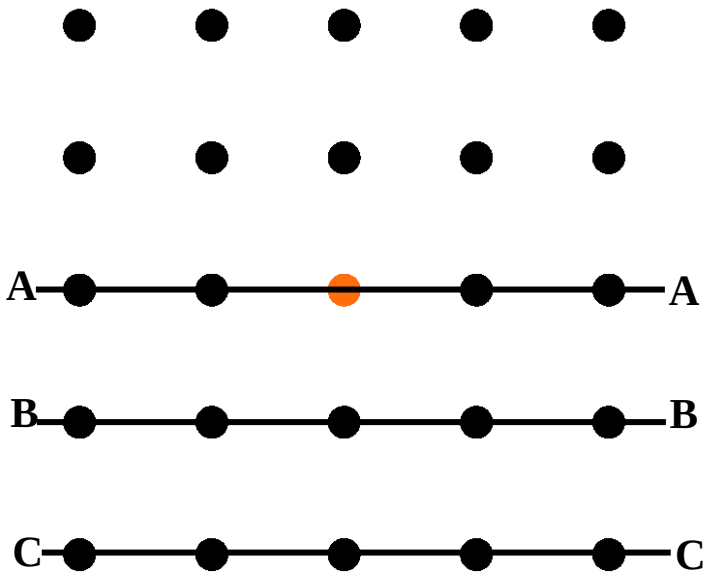
Set5 Section A-A



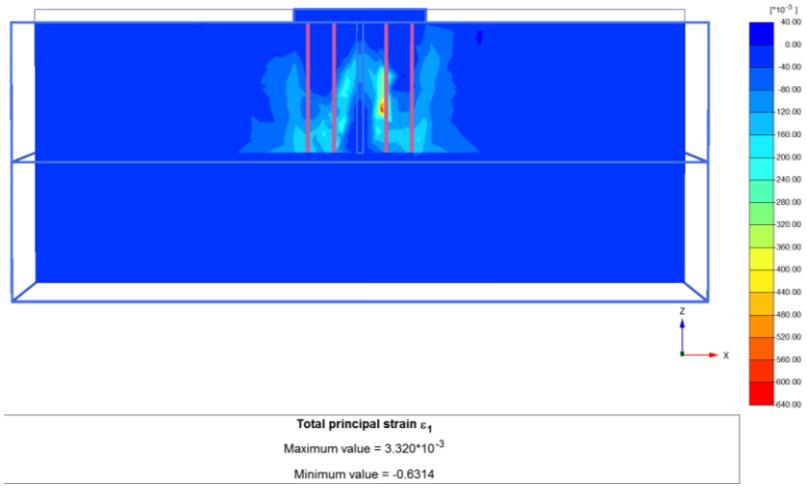
Set5 Section B-B



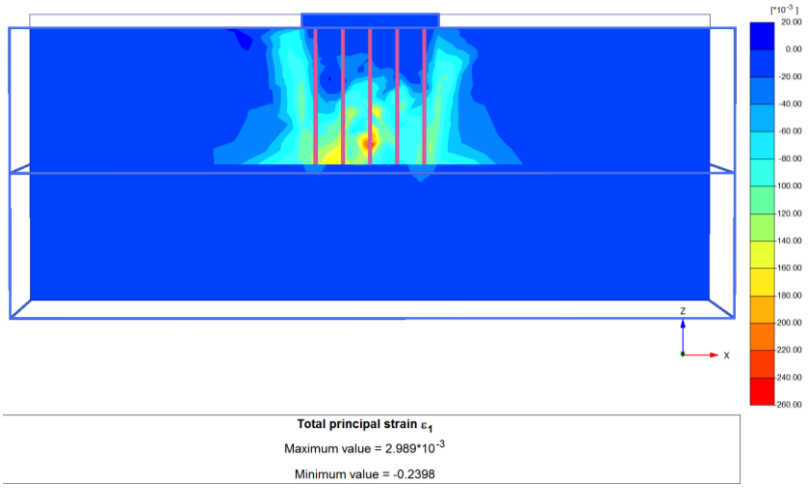
Set5 Section C-C



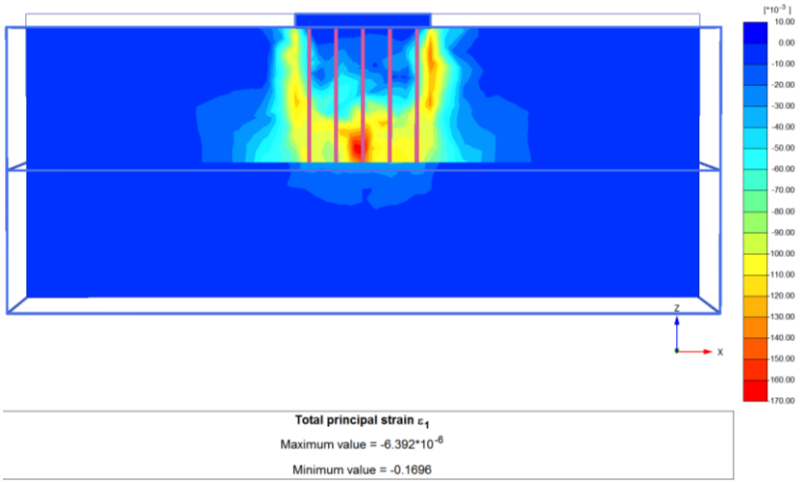
Set 6



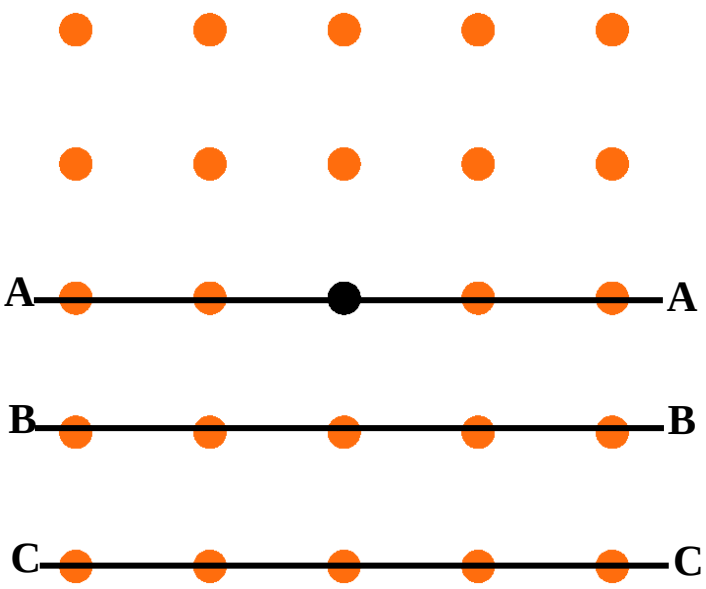
Set 6 Section A-A



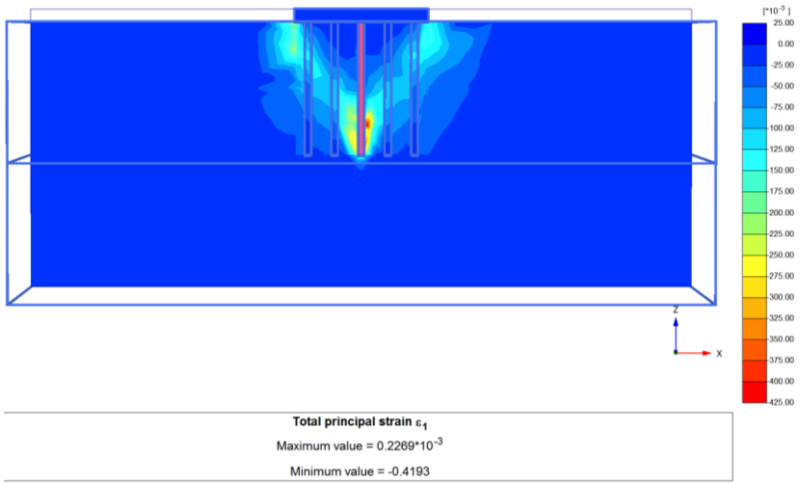
Set 6 Section B-B



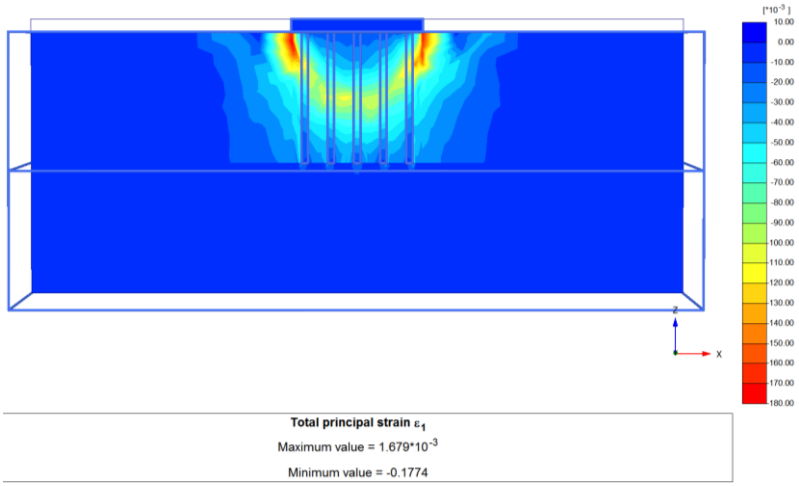
Set 6 Section C-C



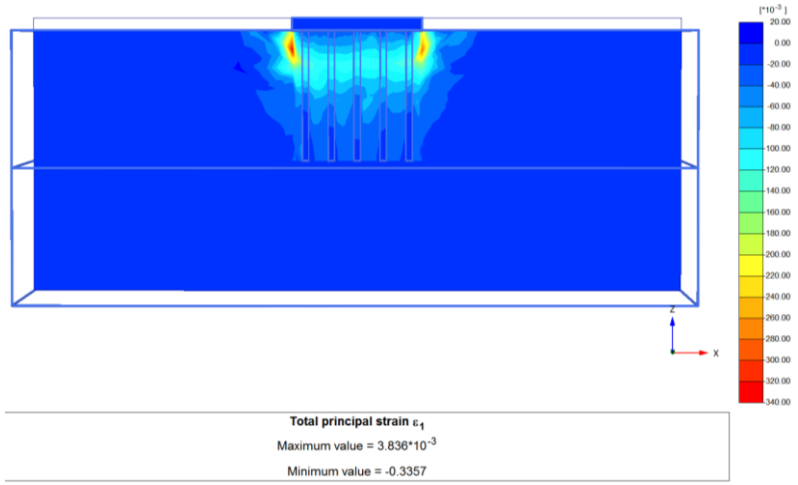
Set 7



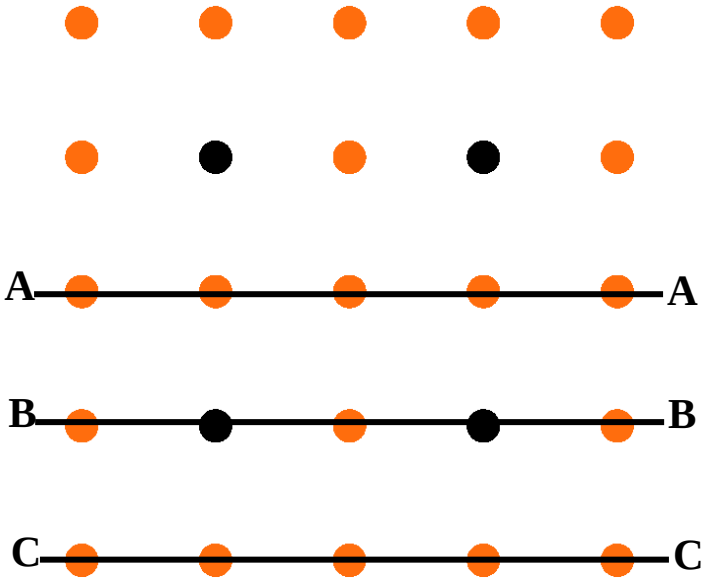
Set 7 Section A-A



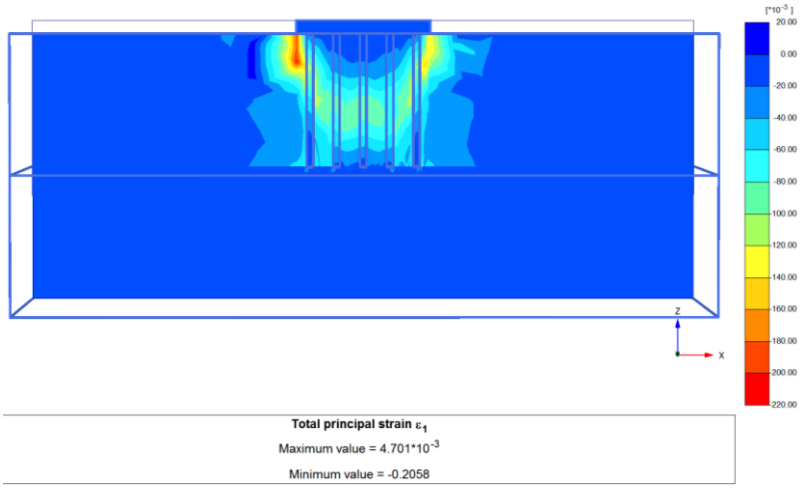
Set 7 Section B-B



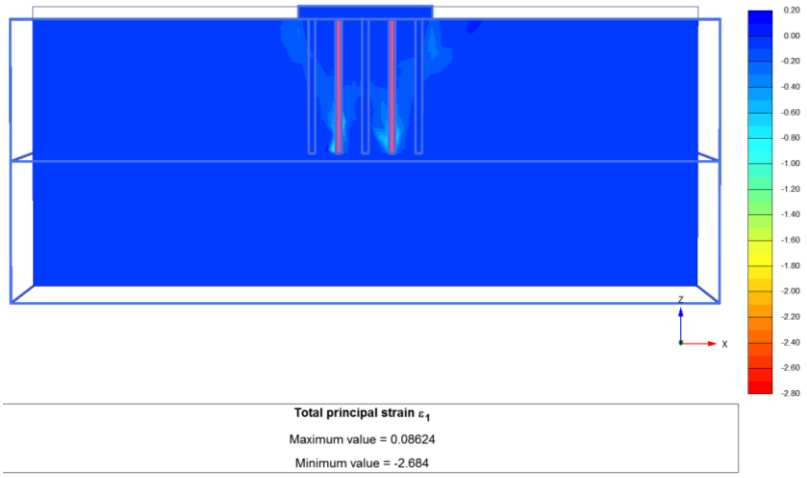
Set 7 Section C-C



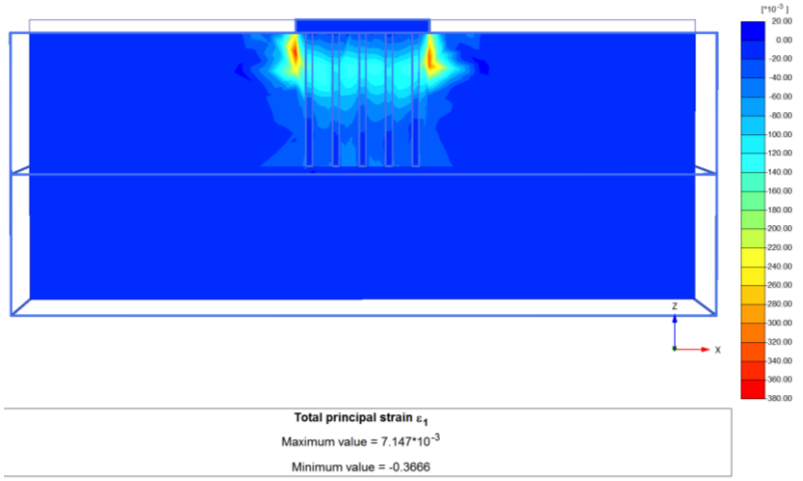
Set8



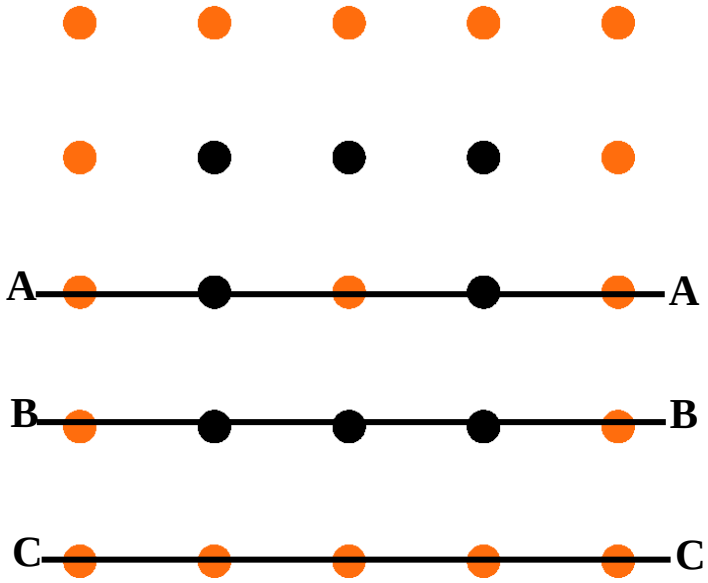
Set8 Section A-A



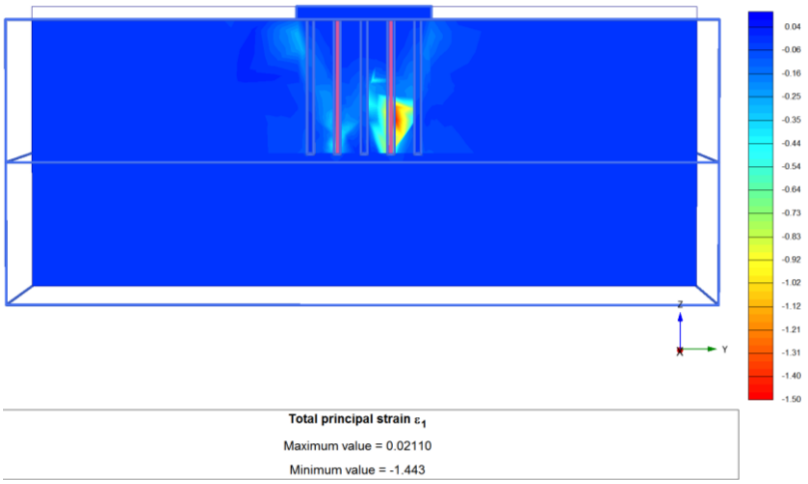
Set8 Section B-B



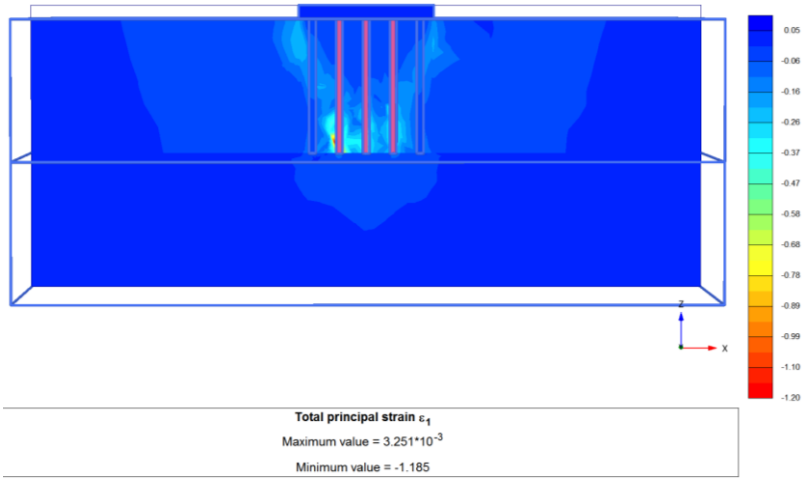
Set8 Section C-C



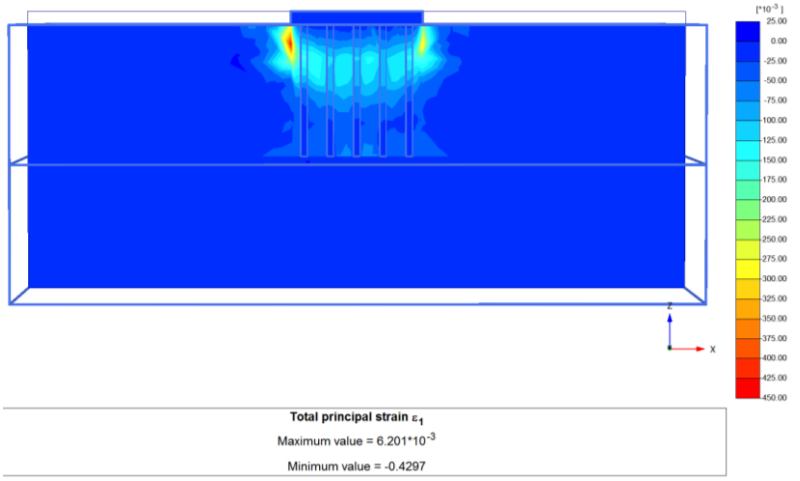
Set 9



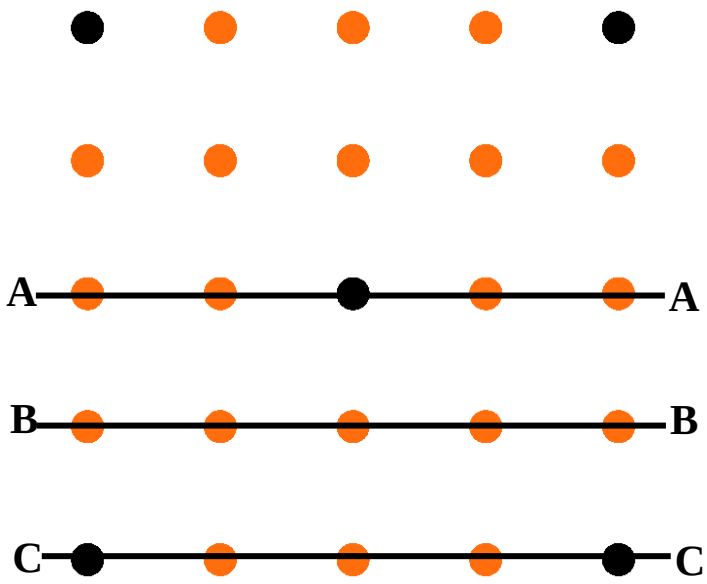
Set 9 Section A-A



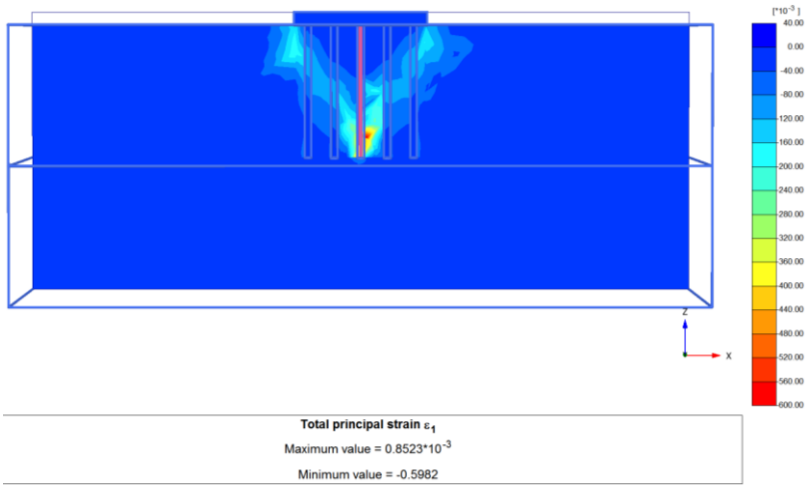
Set 9 Section B-B



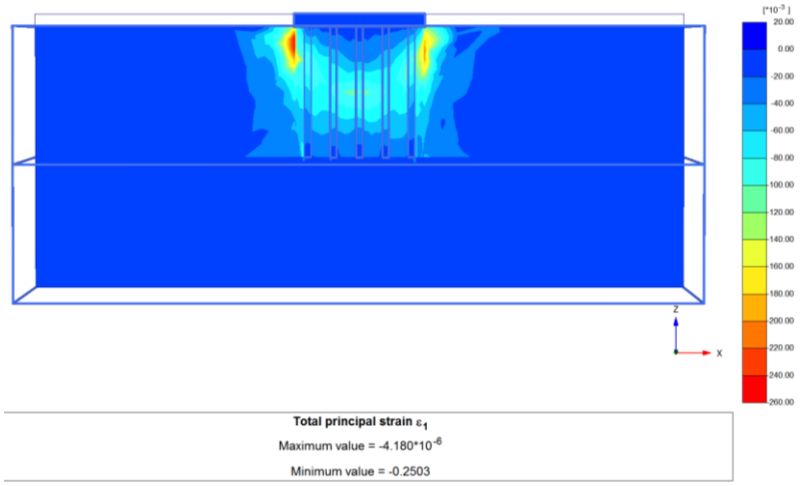
Set 9 Section C-C



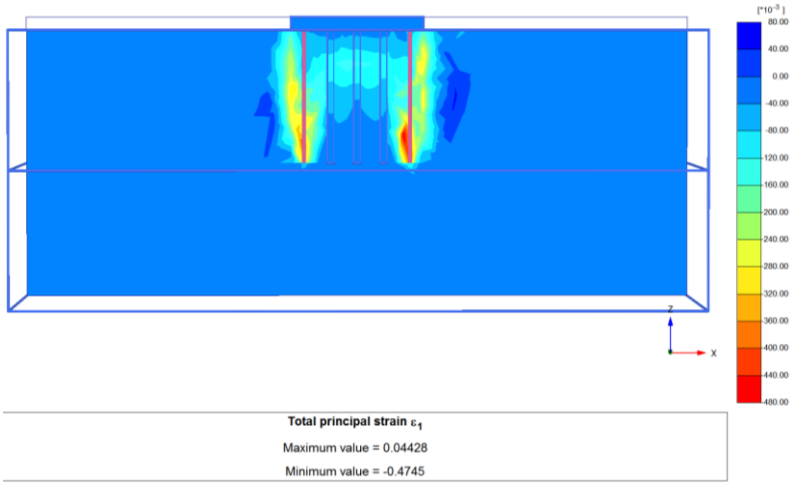
Set 10



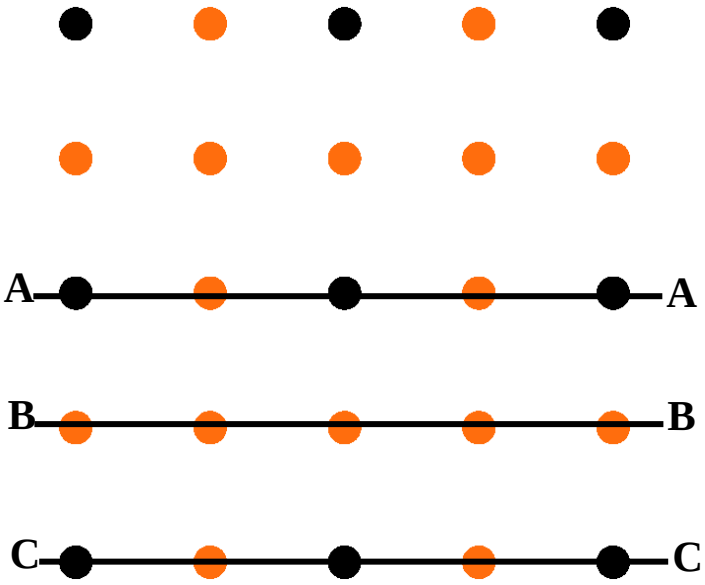
Set 10 Section A-A



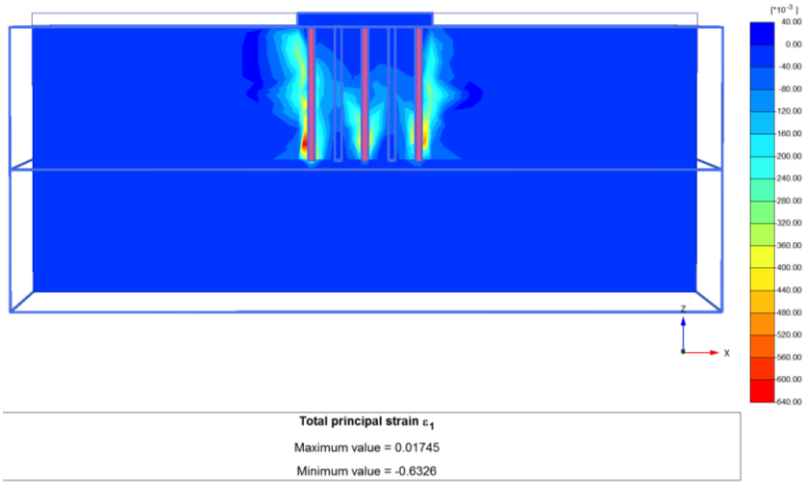
Set 10 Section B-B



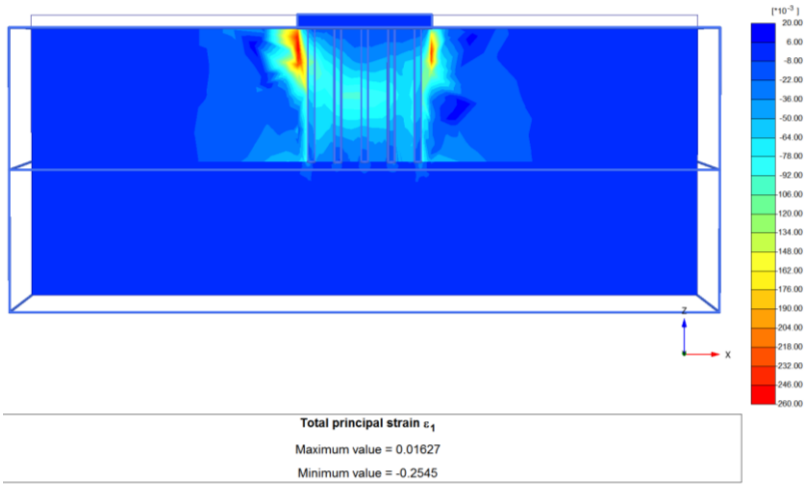
Set 10 Section C-C



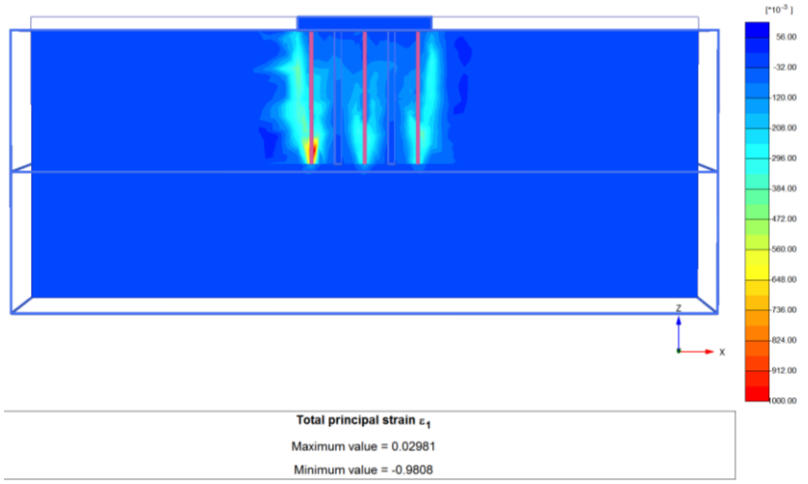
Set 11



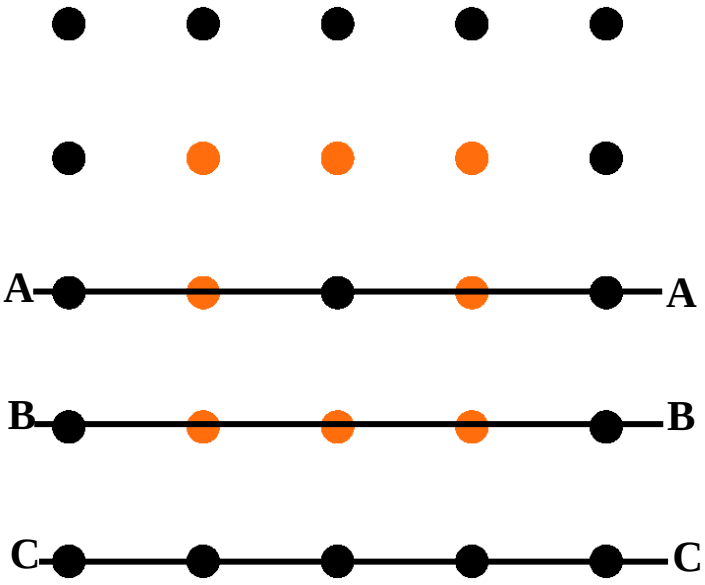
Set 11 Section A-A



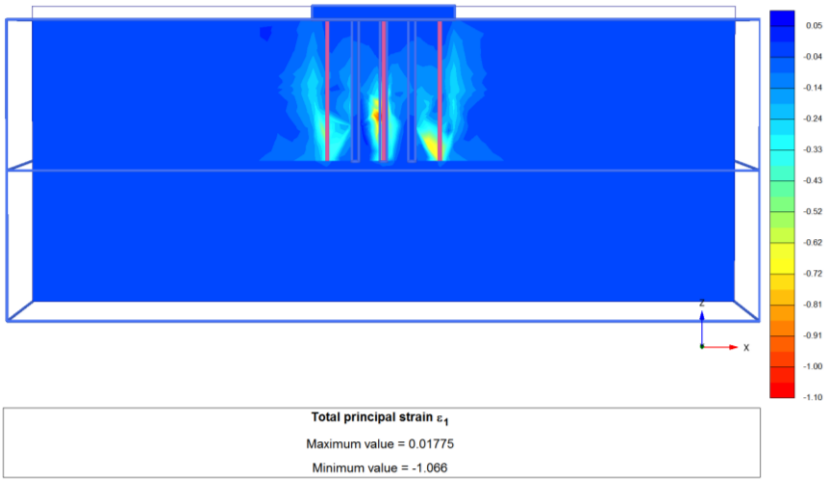
Set 11 Section B-B



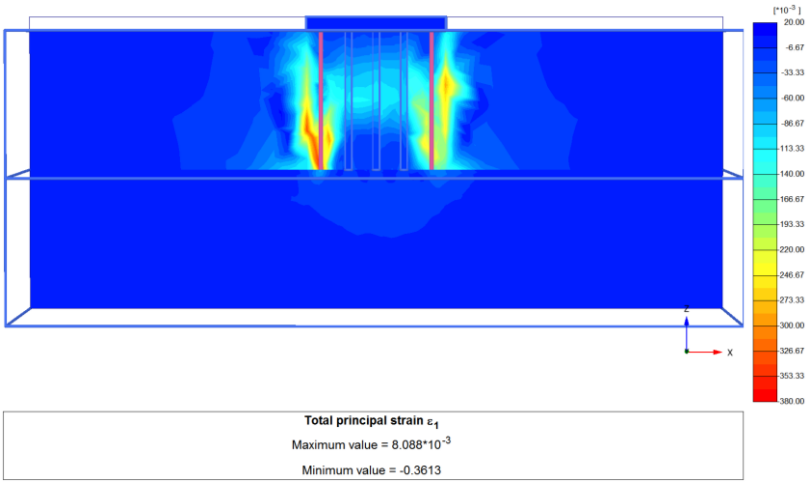
Set 11 Section C-C



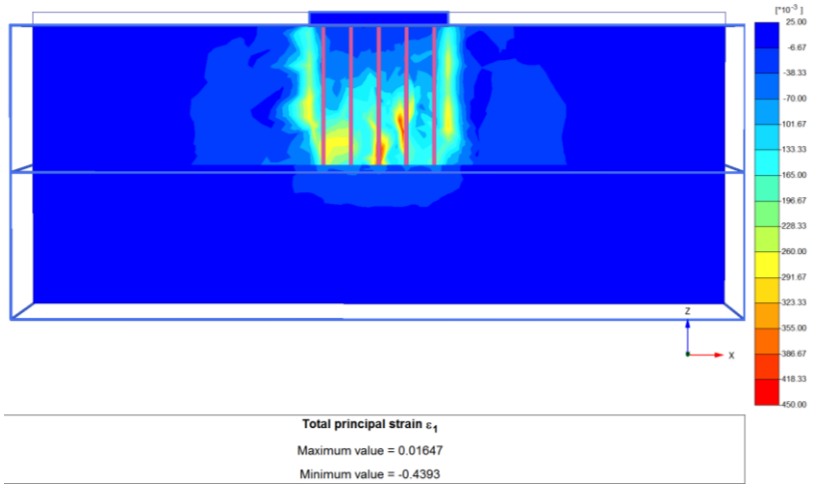
Set 12



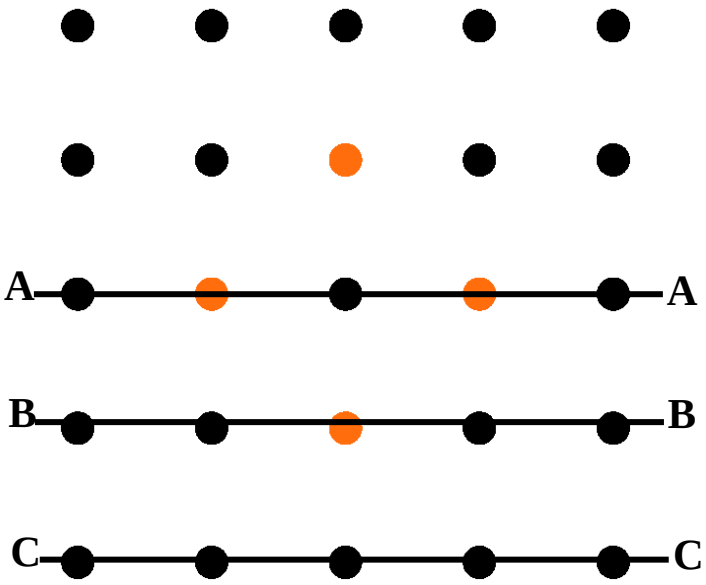
Set 12 Section A-A



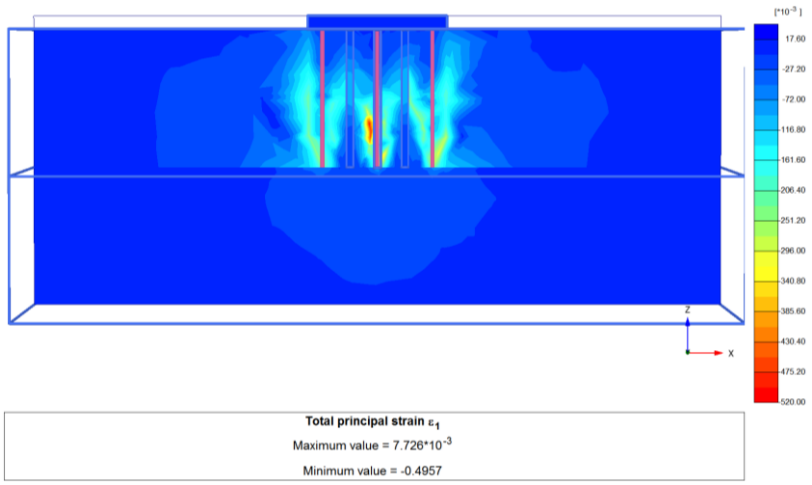
Set 12 Section B-B



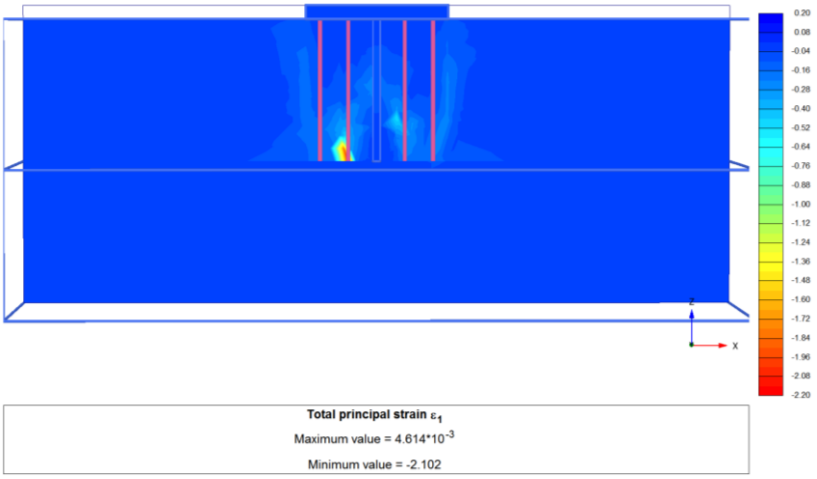
Set 12 Section C-C



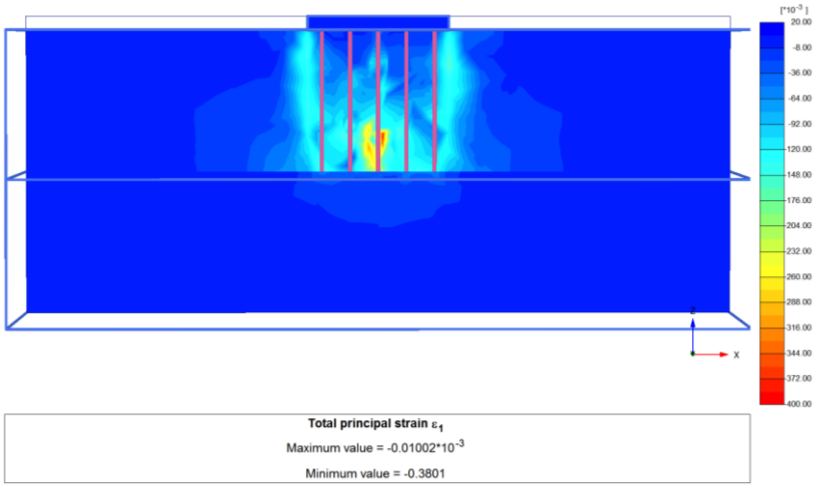
Set 13



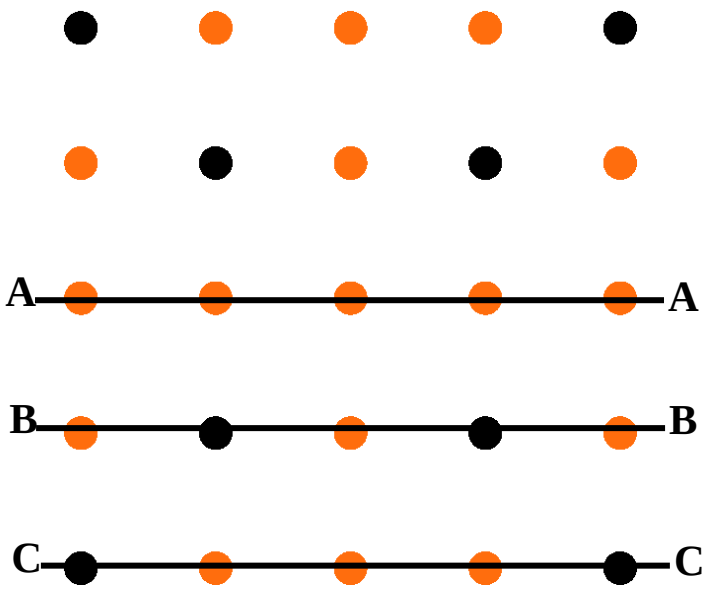
Set 13 Section A-A



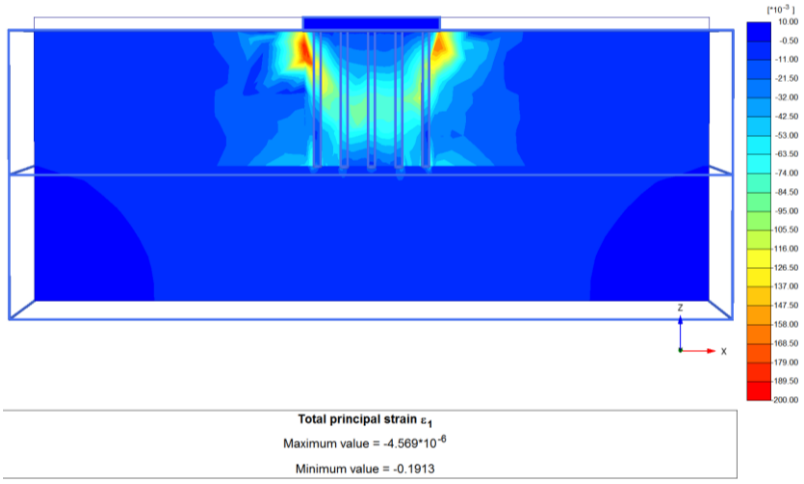
Set 13 Section B-B



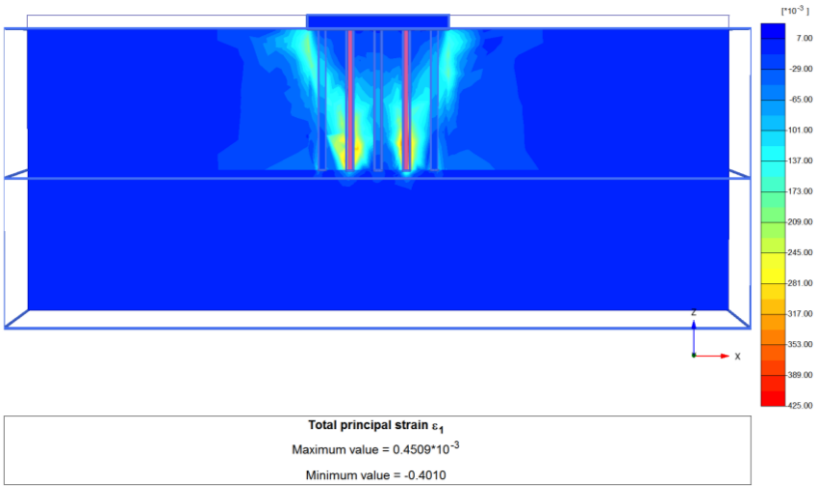
Set 13 Section C-C



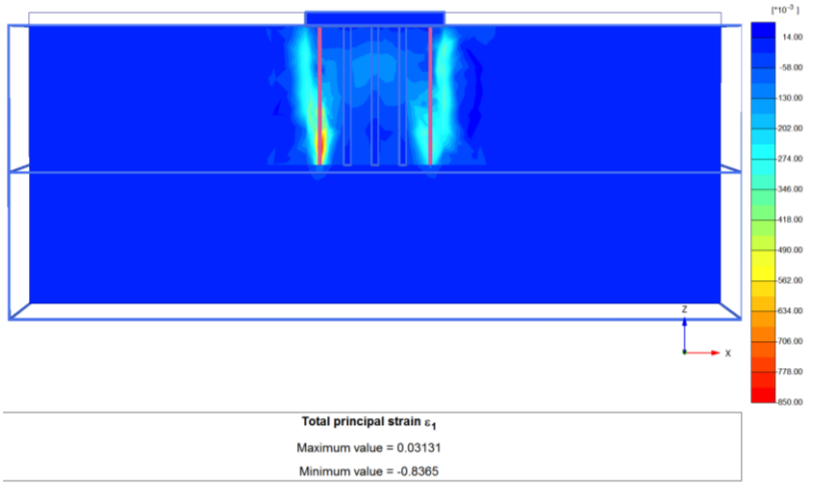
Set 14



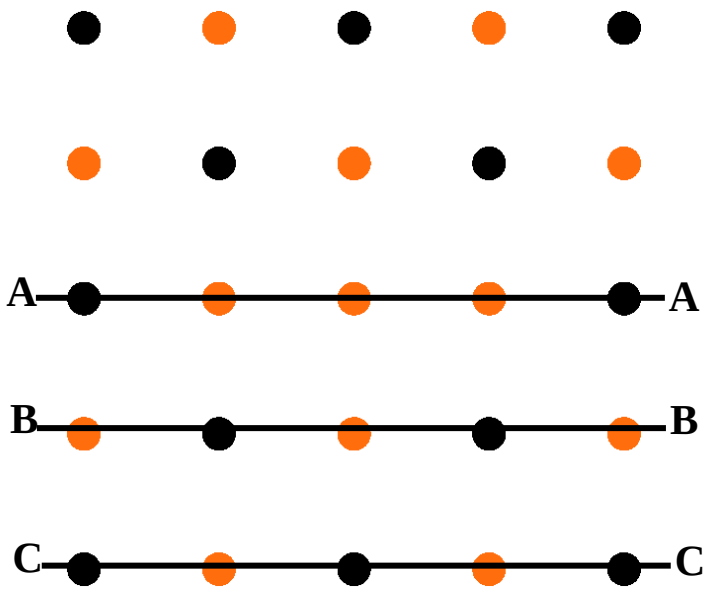
Set 14 Section A-A



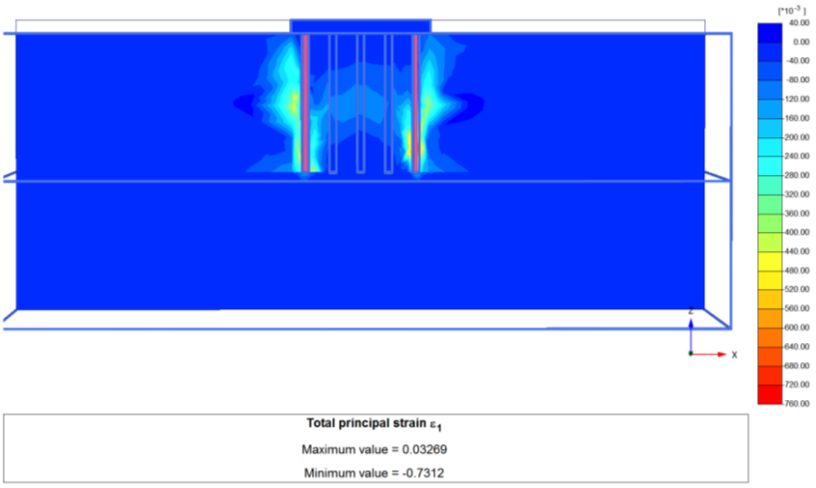
Set 14 Section B-B



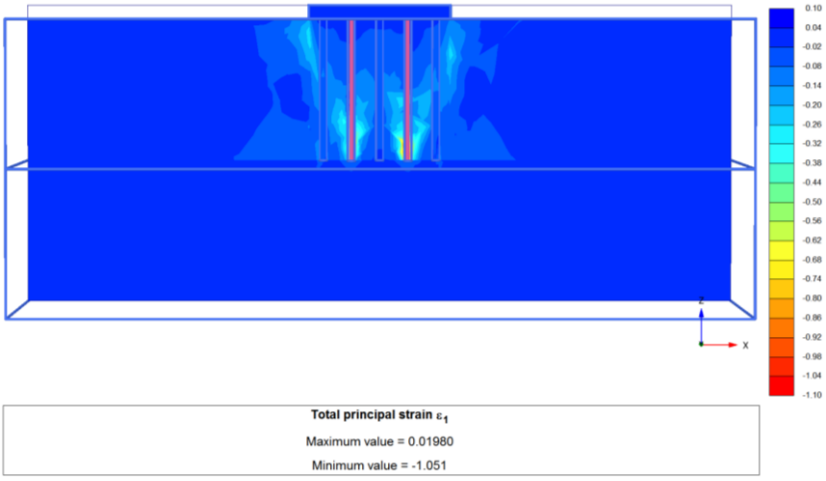
Set 14 Section C-C



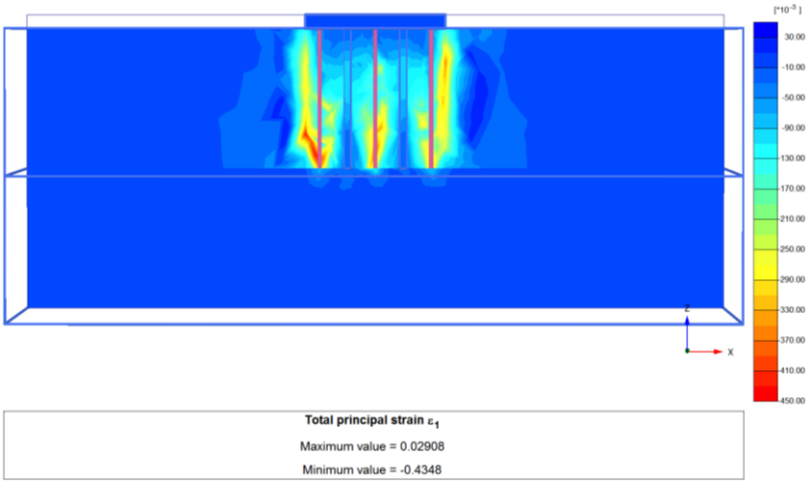
Set 15



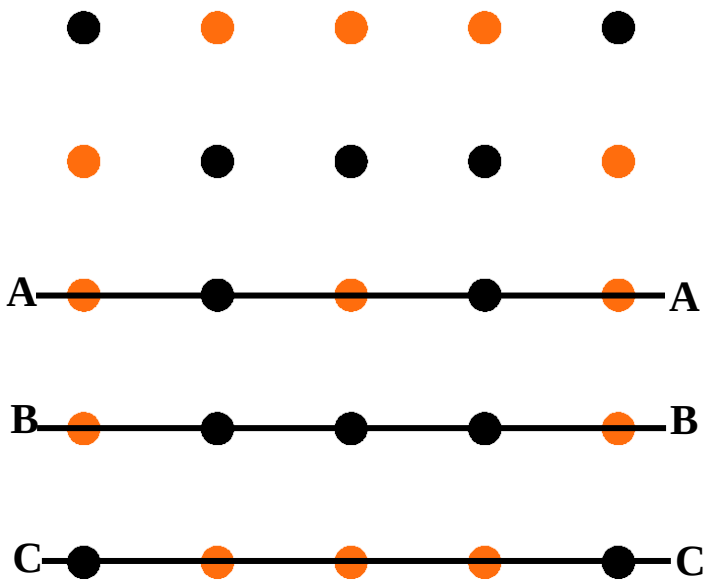
Set 15 Section A-A



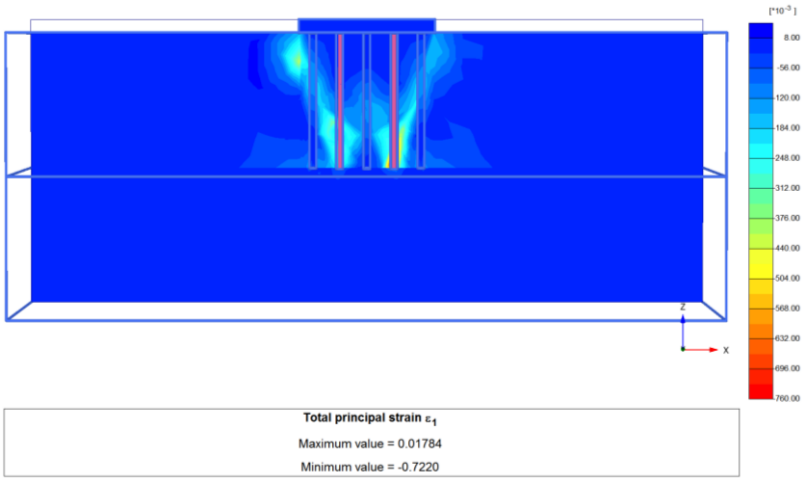
Set 15 Section B-B



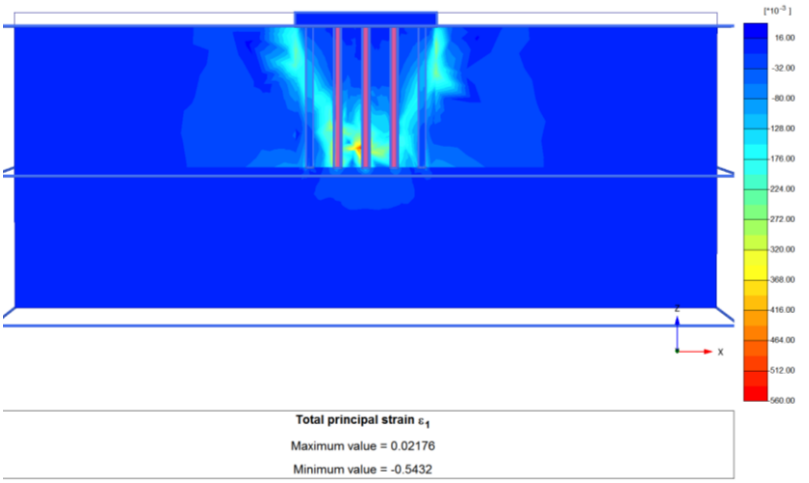
Set 15 Section C-C



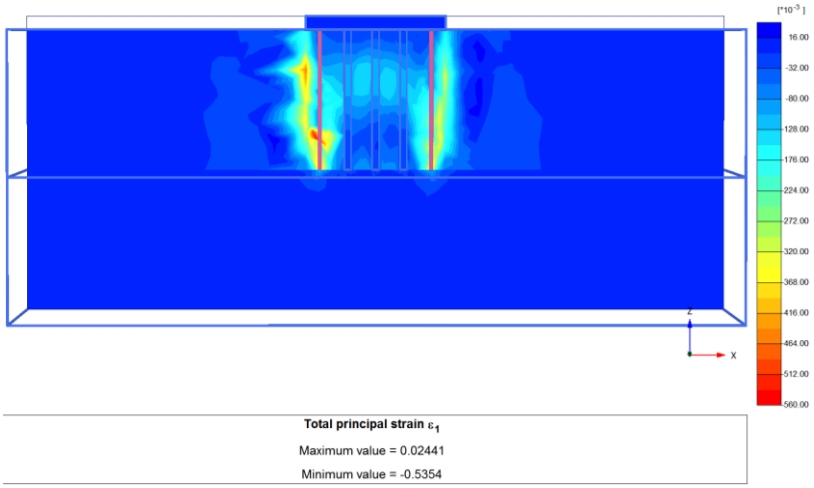
Set 16



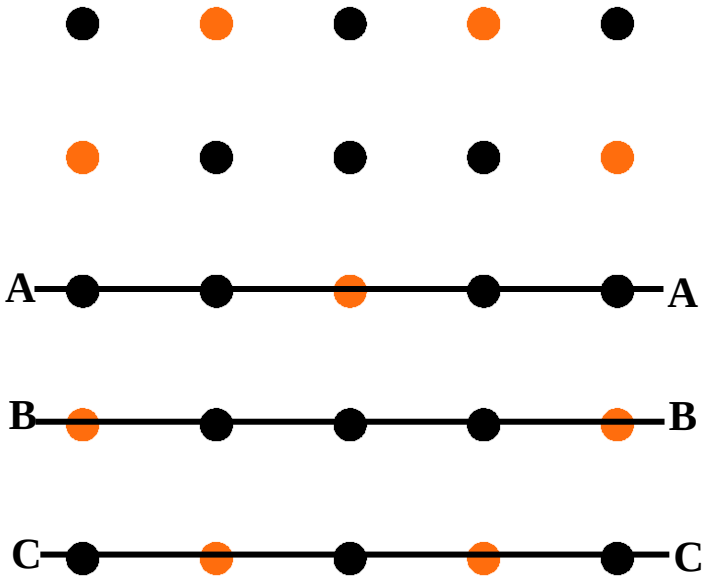
Set 16 Section A-A



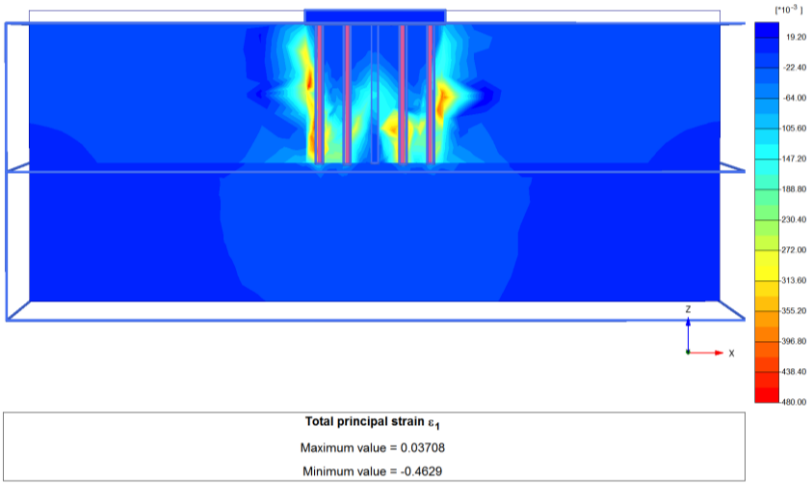
Set 16 Section B-B



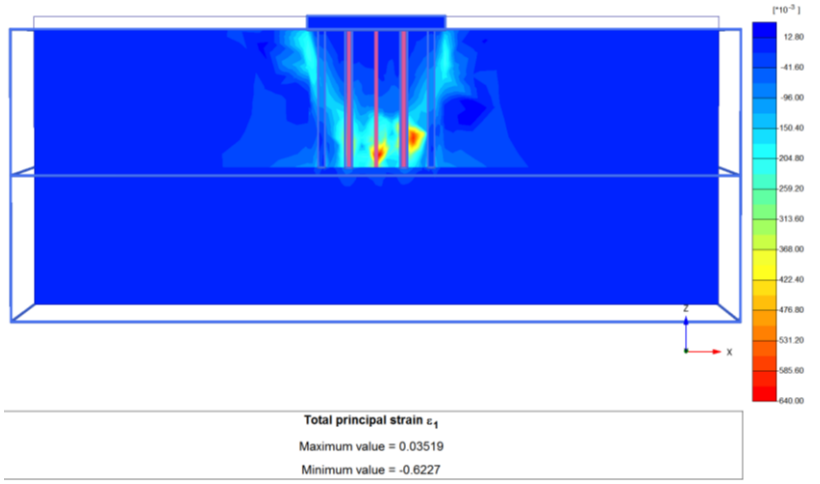
Set 16 Section C-C



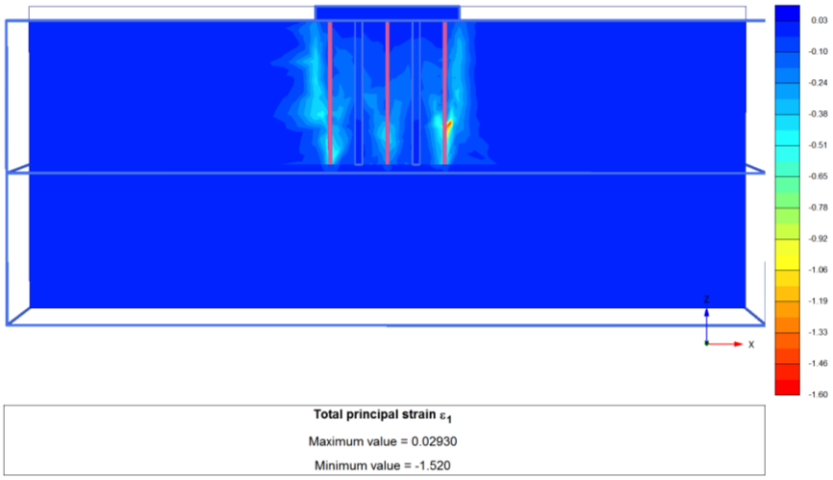
Set 17



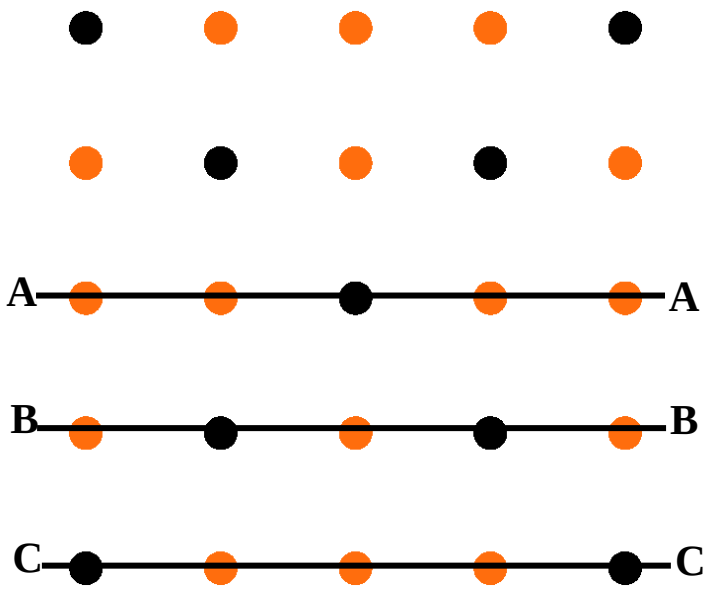
Set 17 Section A-A



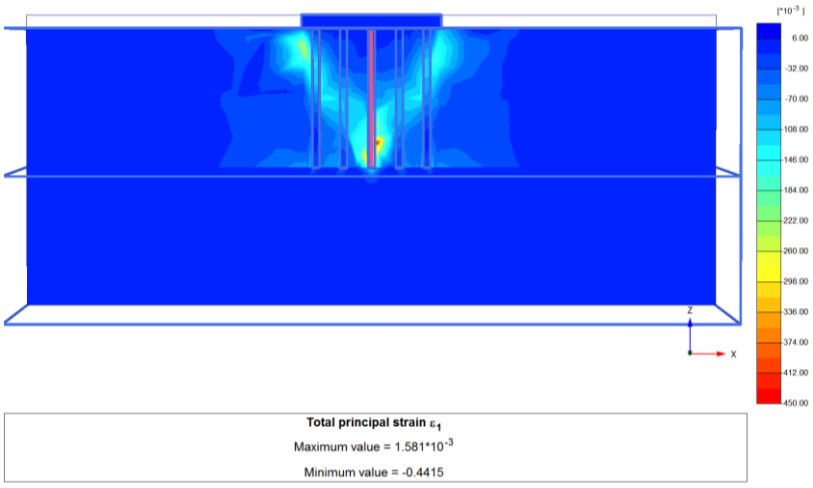
Set 17 Section B-B



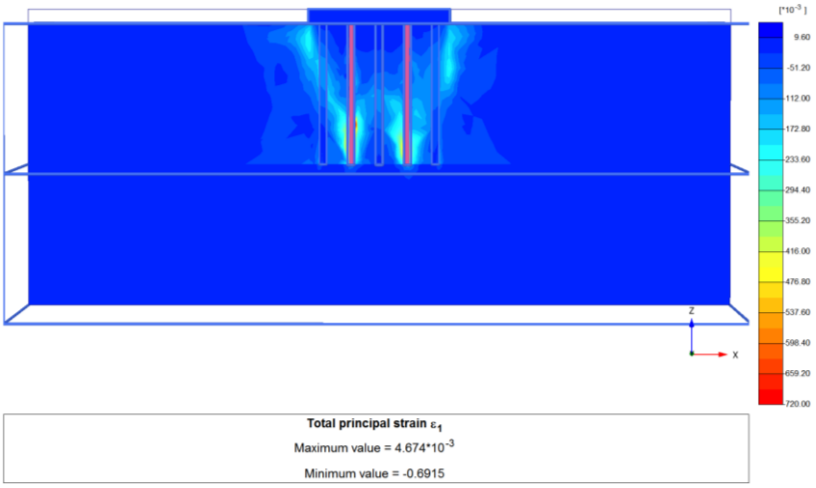
Set 17 Section C-C



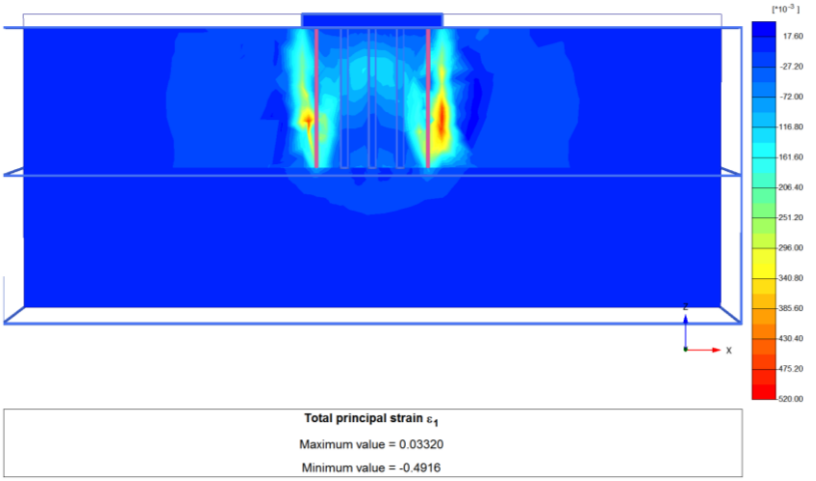
Set 18



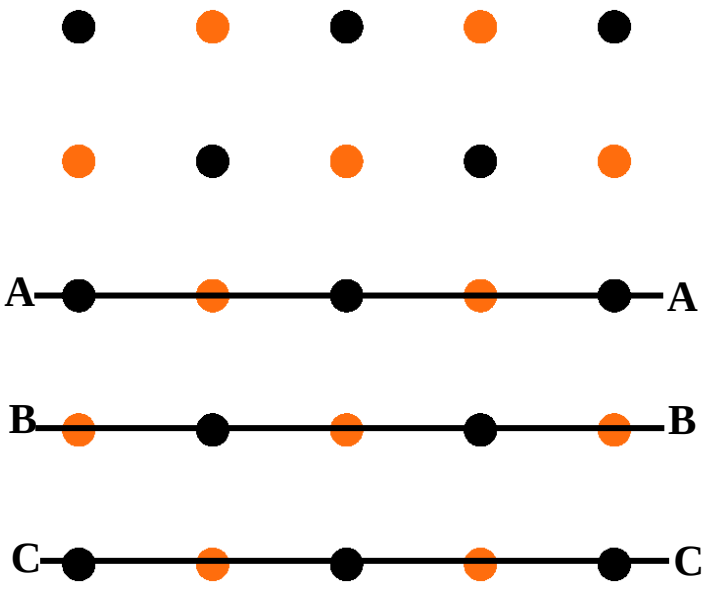
Set 18 Section A-A



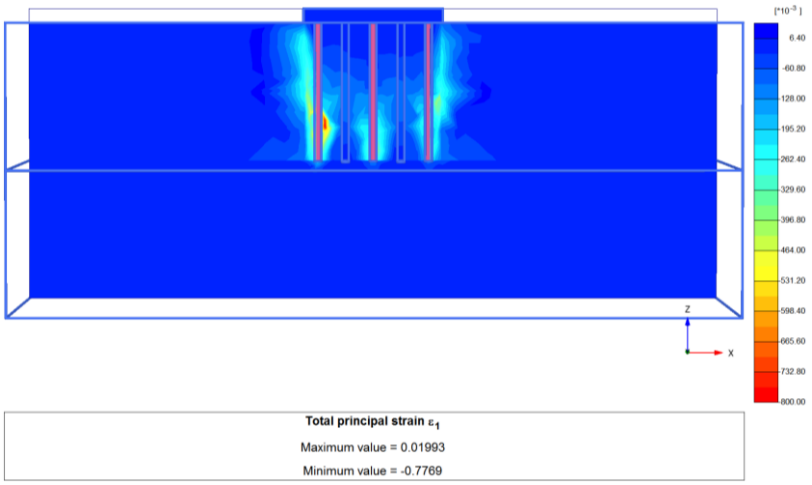
Set 18 Section B-B



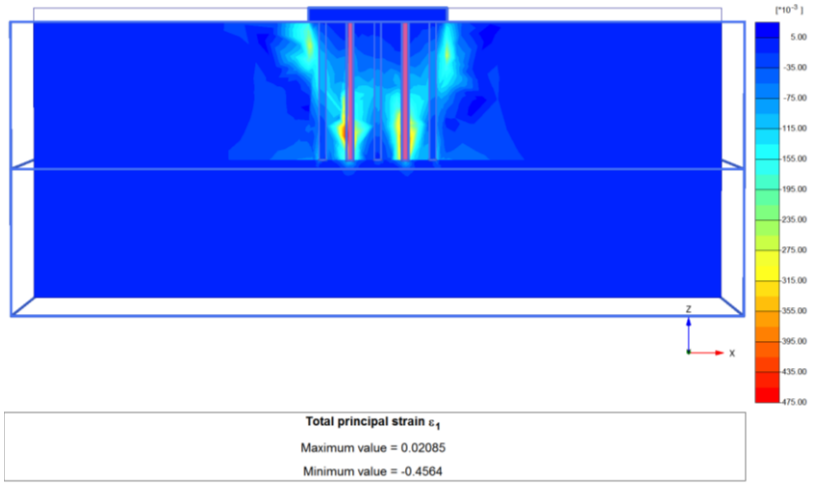
Set 18 Section C-C



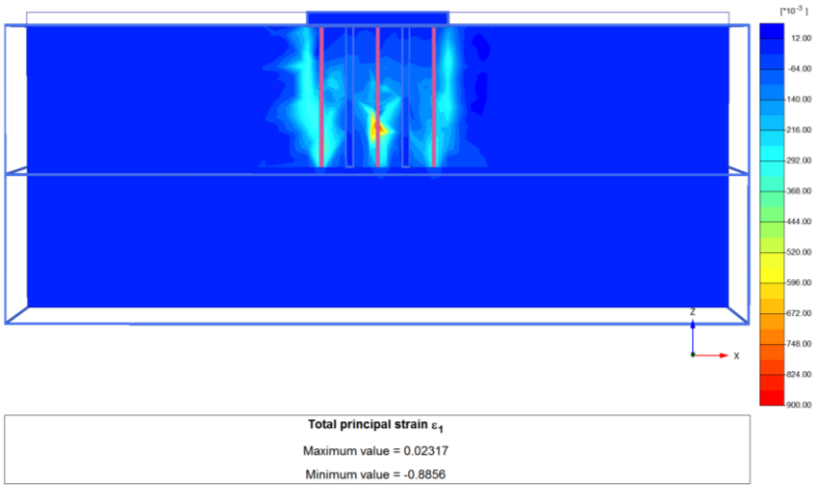
Set 19



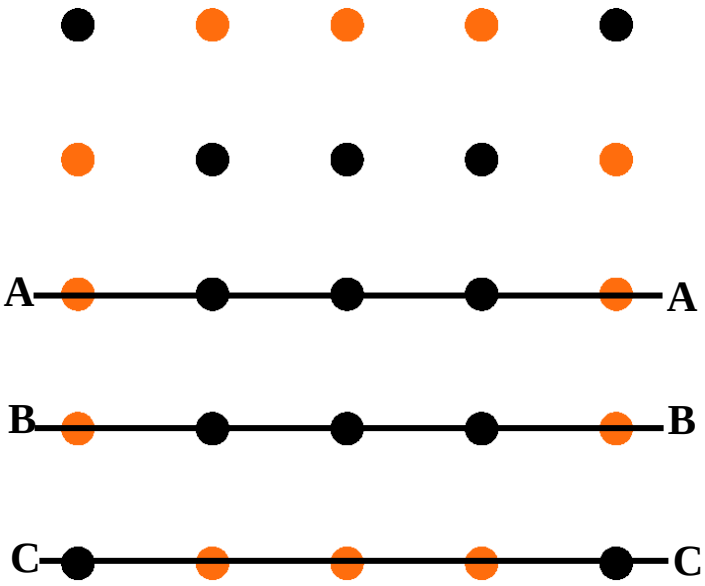
Set 19 Section A-A



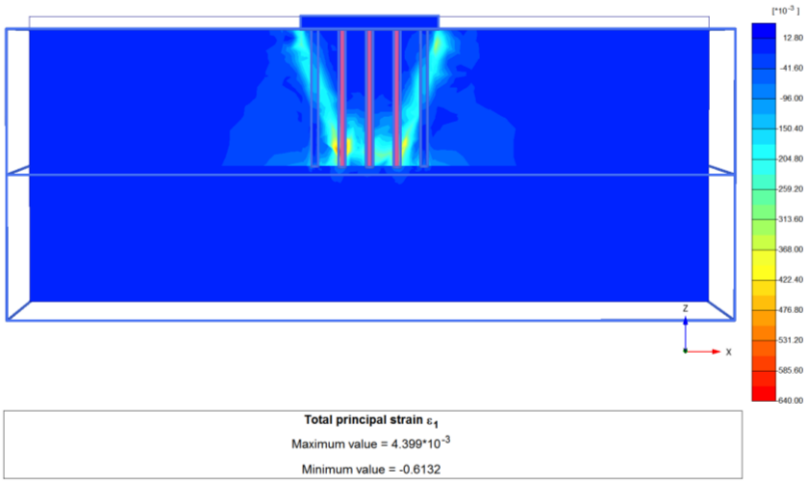
Set 19 Section B-B



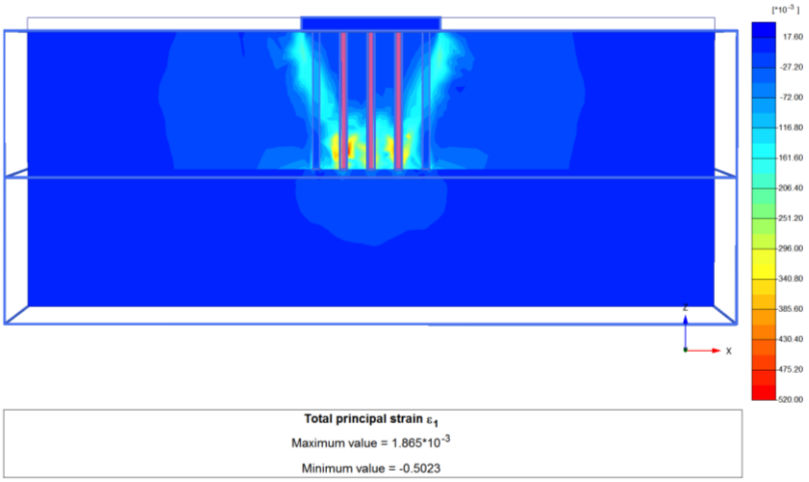
Set 19 Section C-C



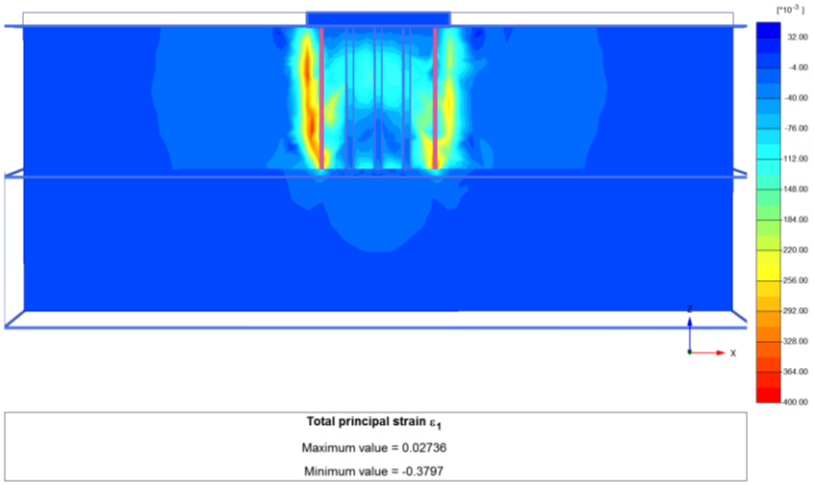
Set 20



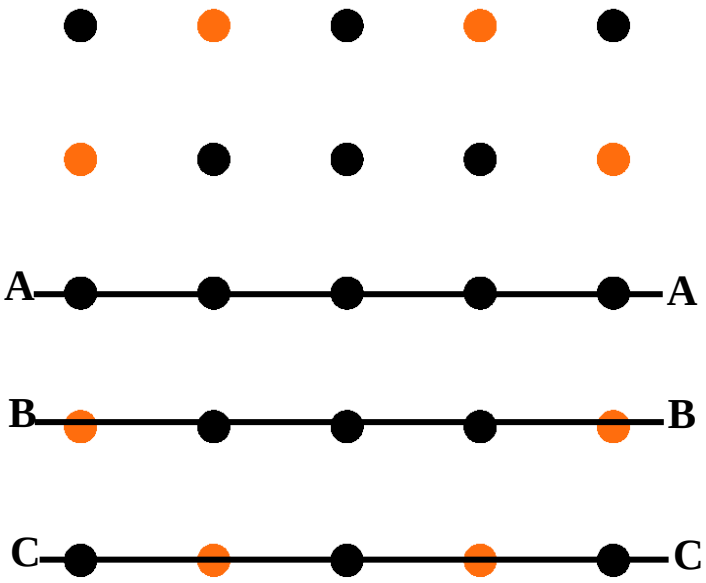
Set 20 Section A-A



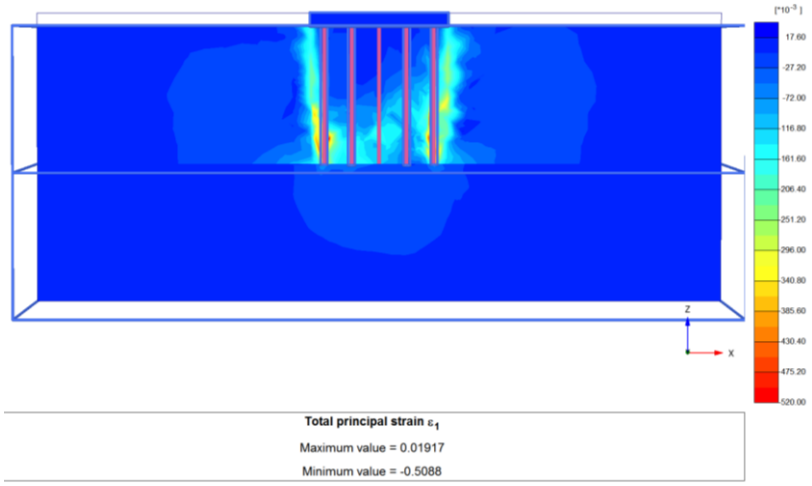
Set 20 Section B-B



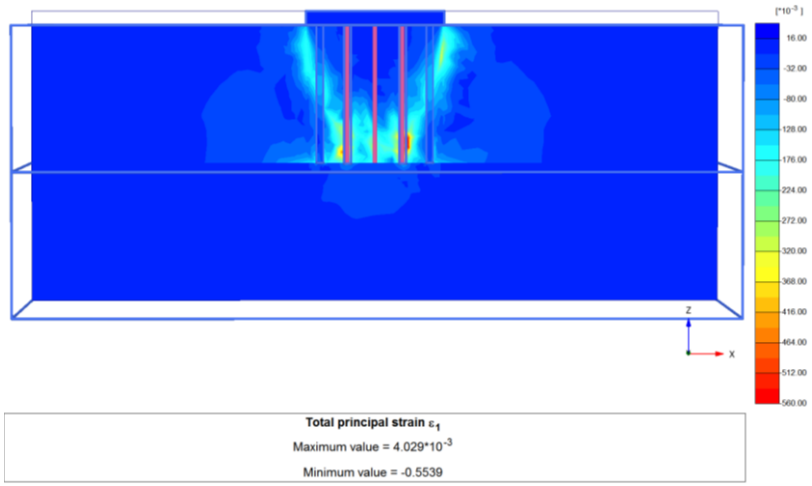
Set 20 Section C-C



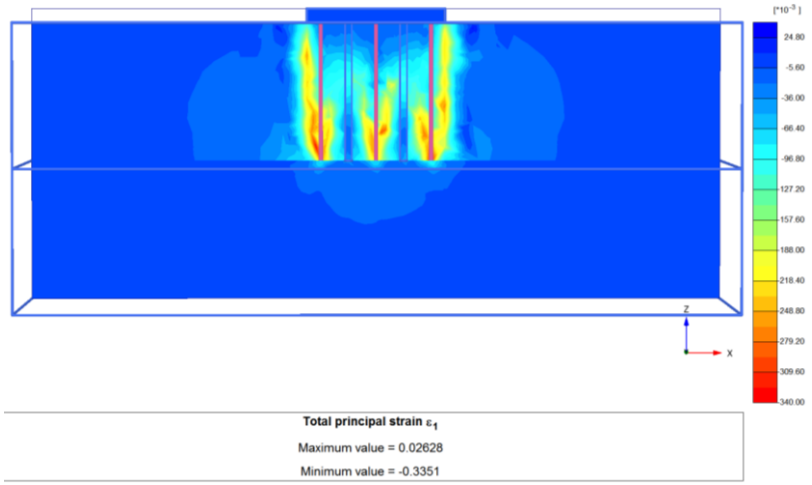
Set 21



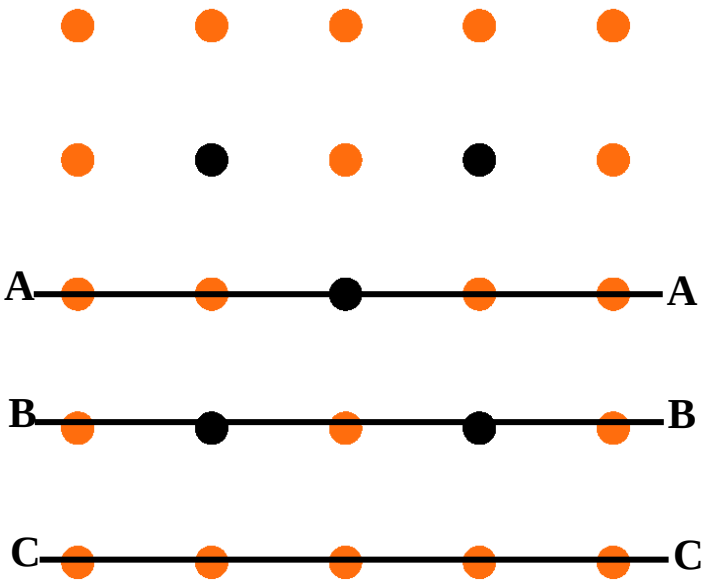
Set 21 Section A-A



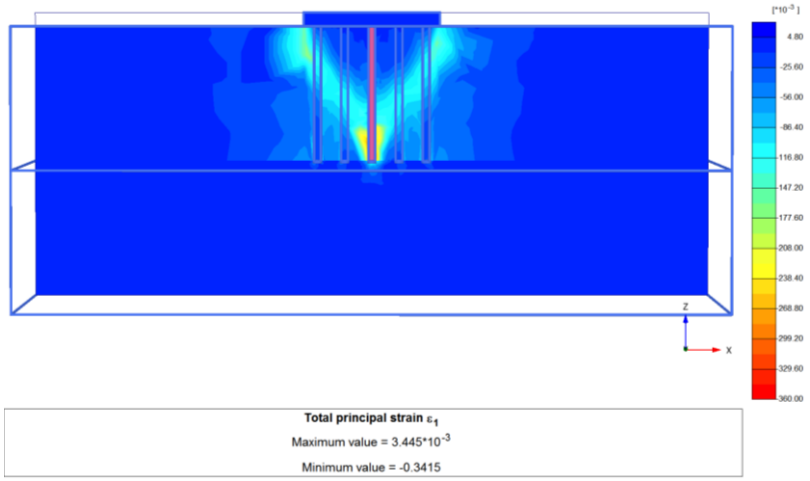
Set 21 Section B-B



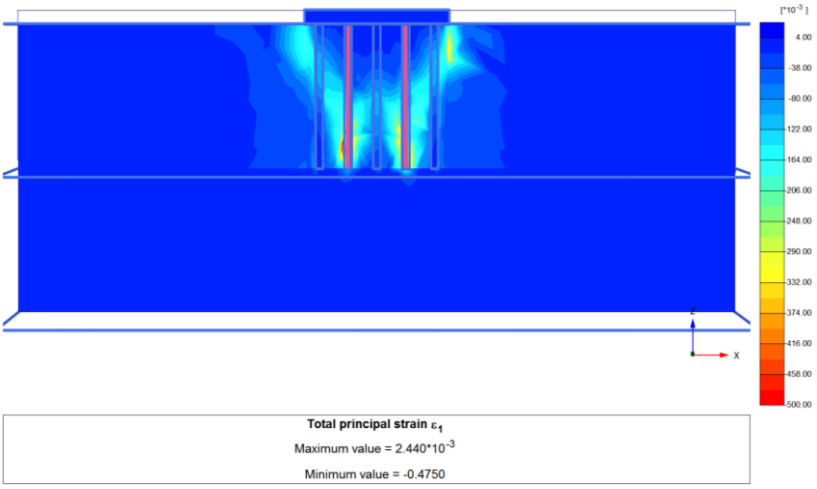
Set 21 Section C-C



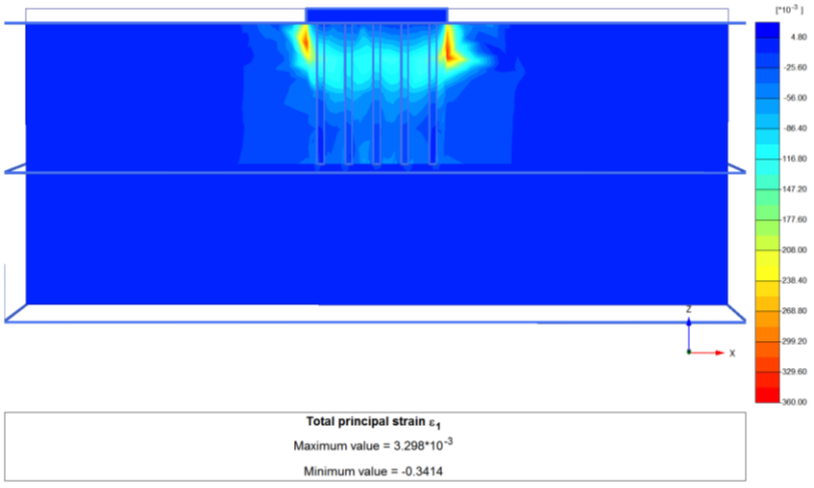
Set 22



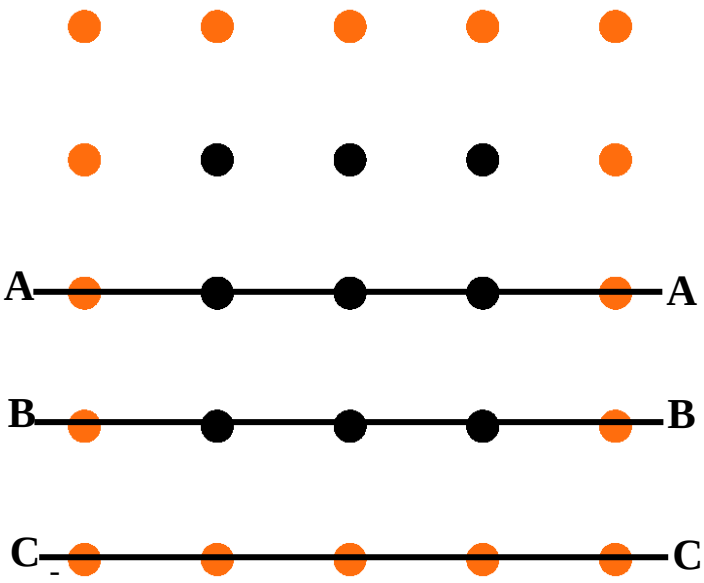
Set 22 Section A-A



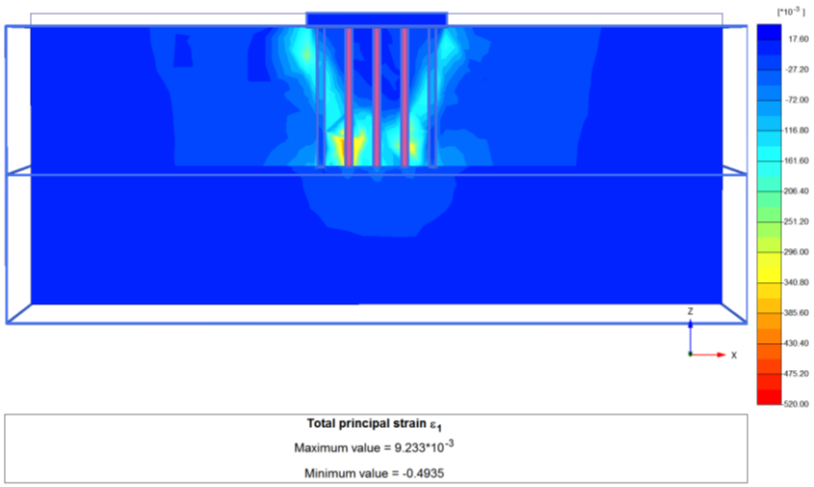
Set 22 Section B-B



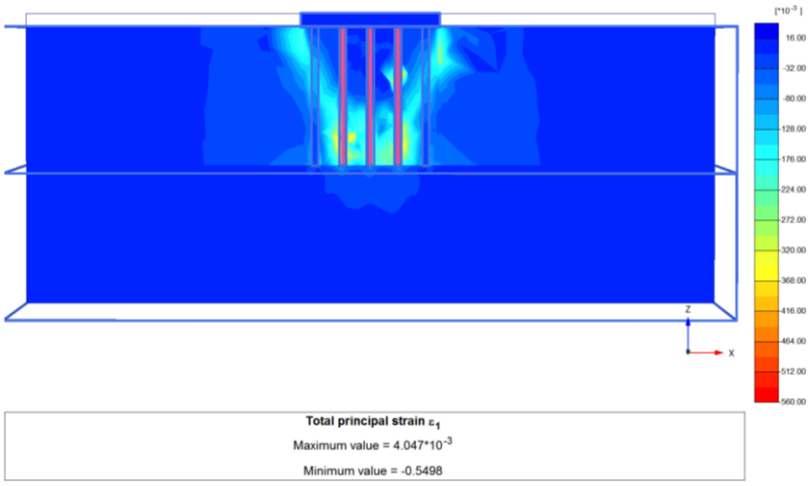
Set 22 Section C-C



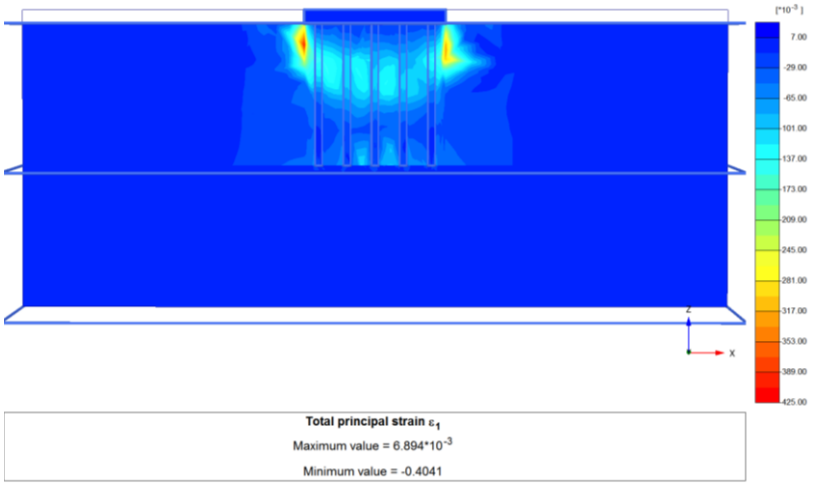
Set 23



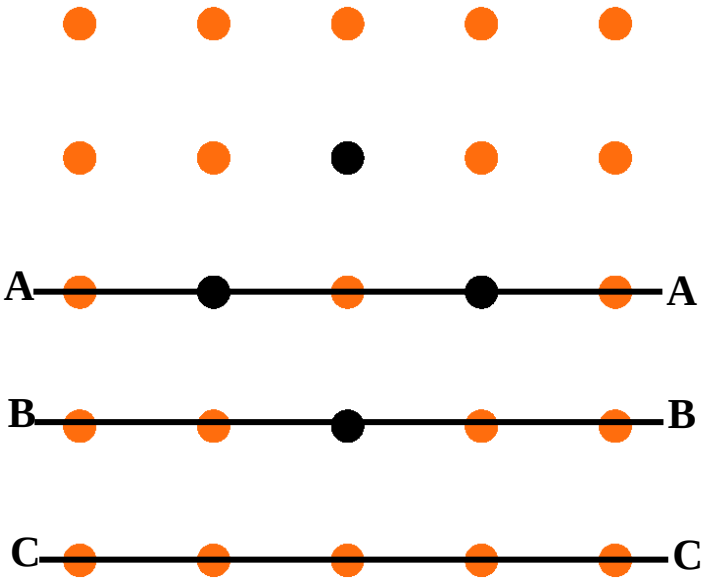
Set 23 Section A-A



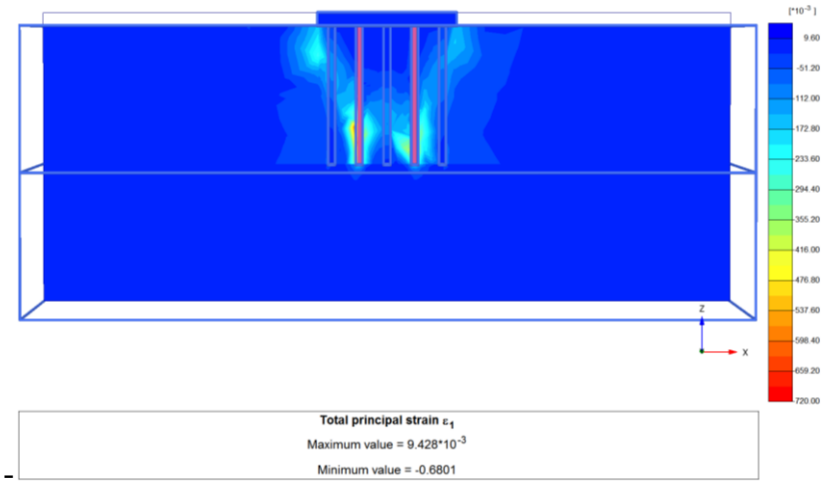
Set 23 Section B-B



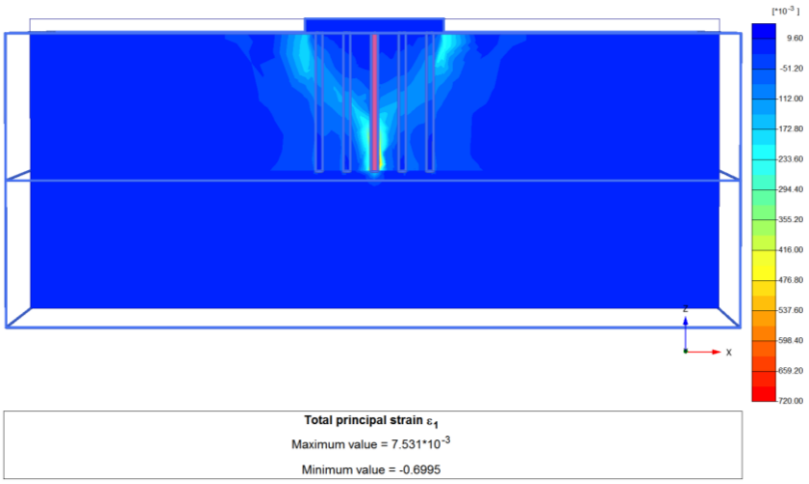
Set 23 Section C-C



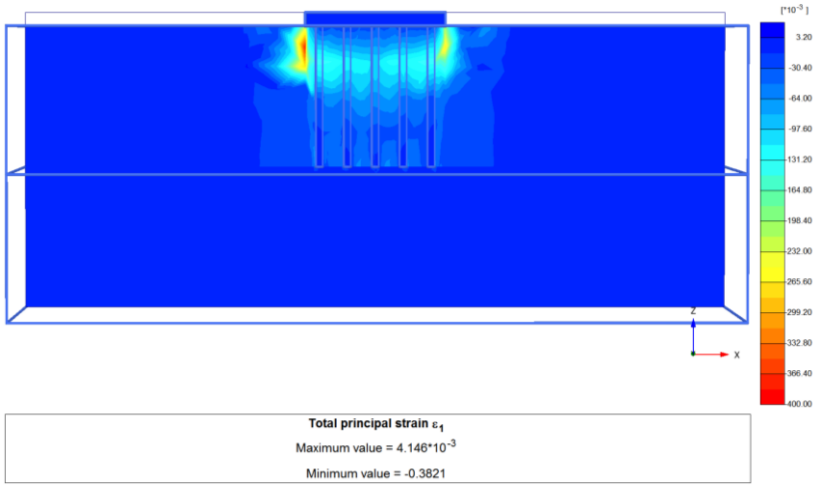
Set 24



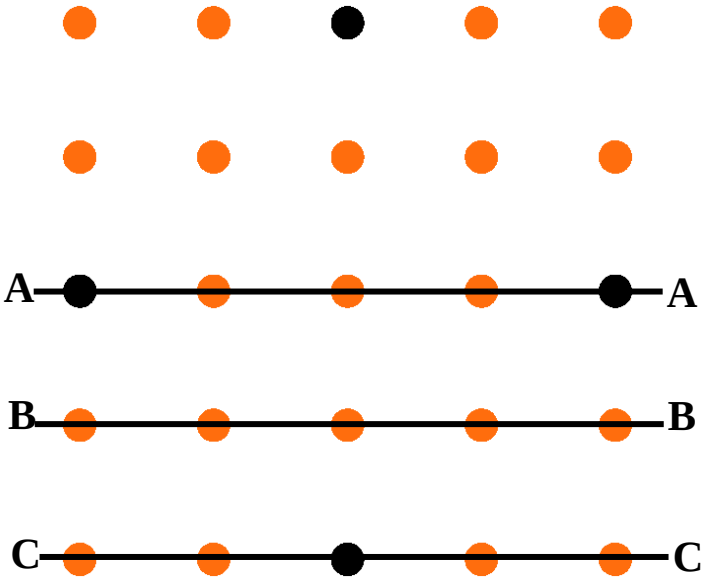
Set 24 Section A-A



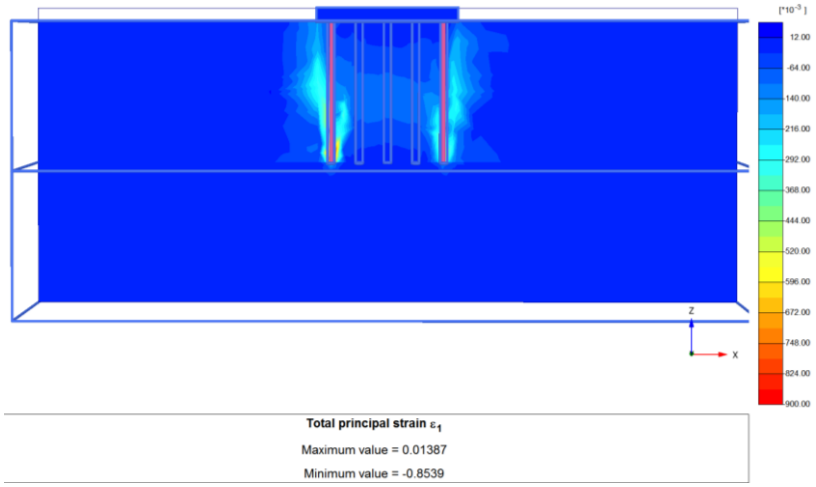
Set 24 Section B-B



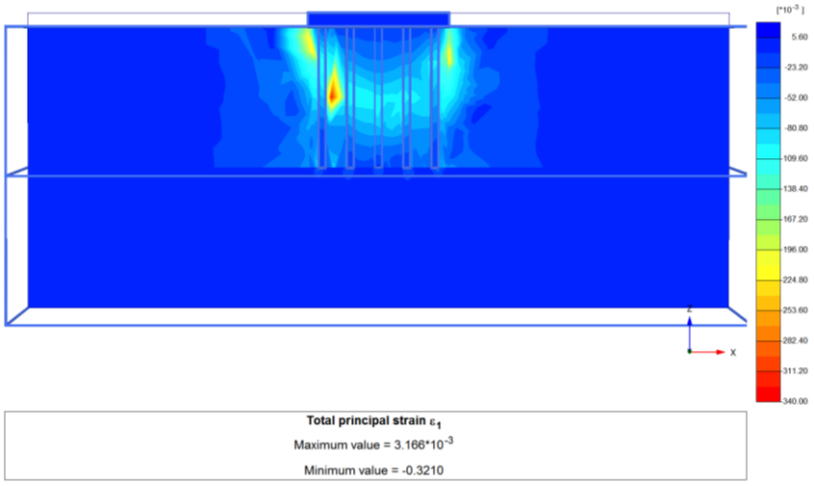
Set 24 Section C-C



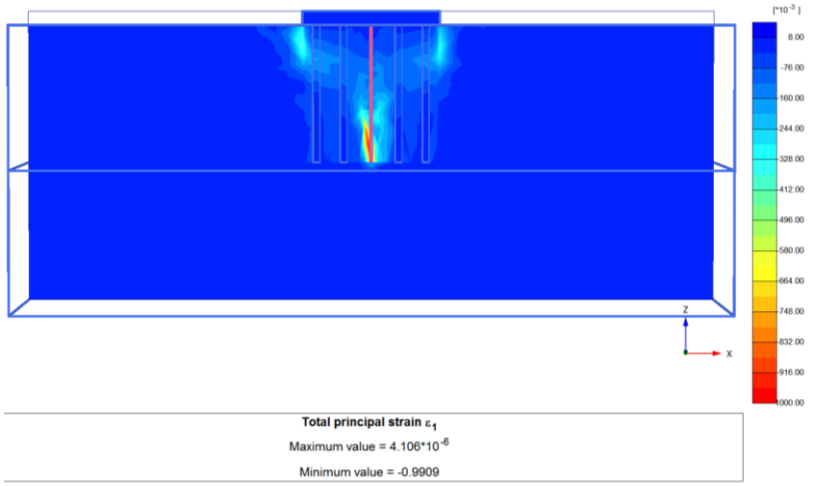
Set 25



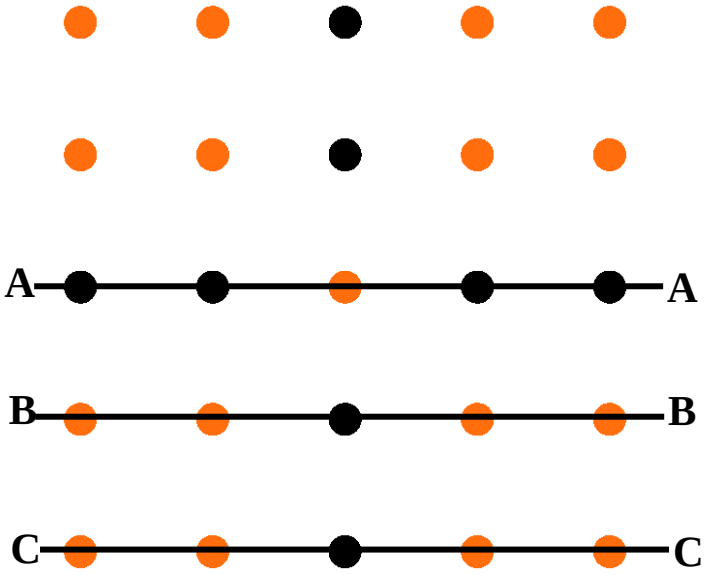
Set 25 Section A-A



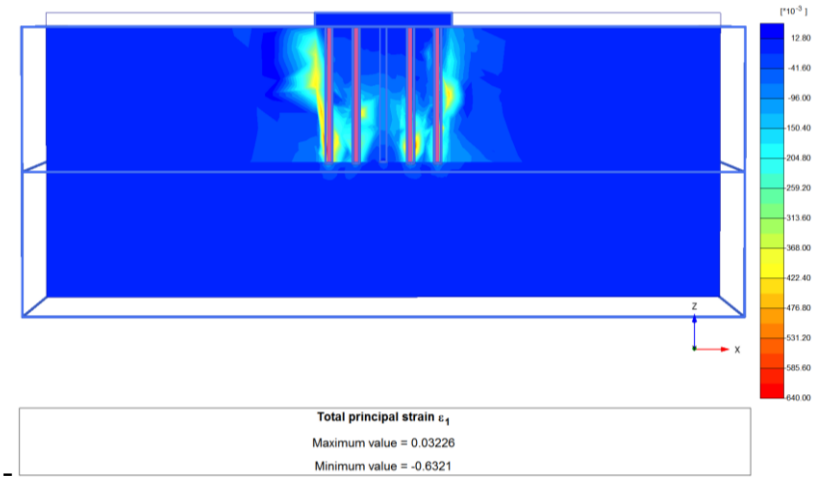
Set 25 Section B-B



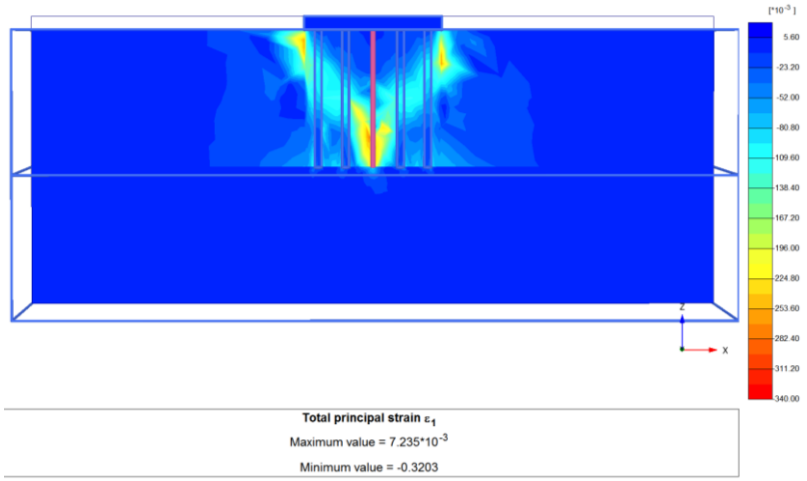
Set 25 Section C-C



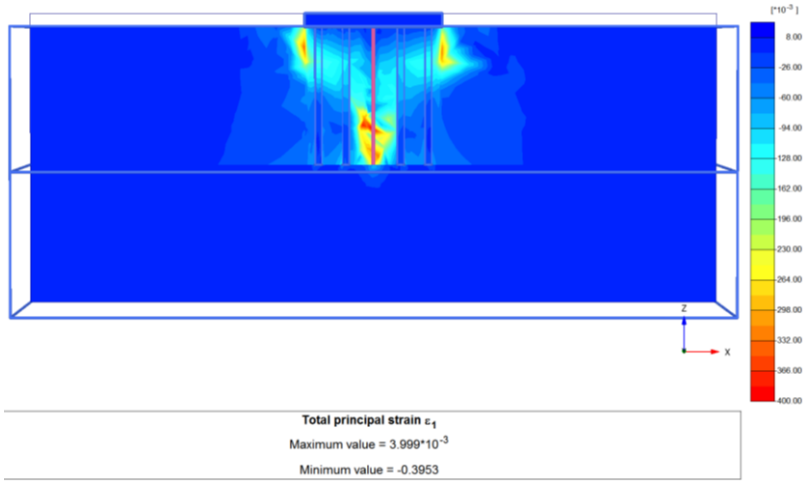
Set 26



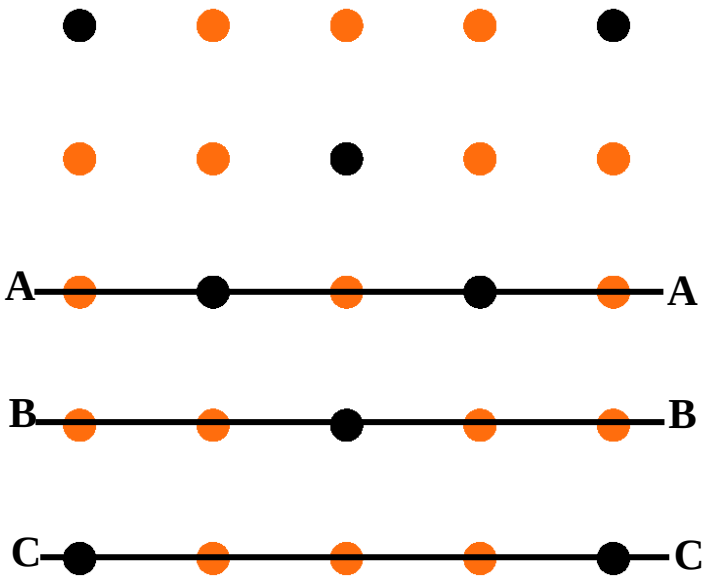
Set 26 Section A-A



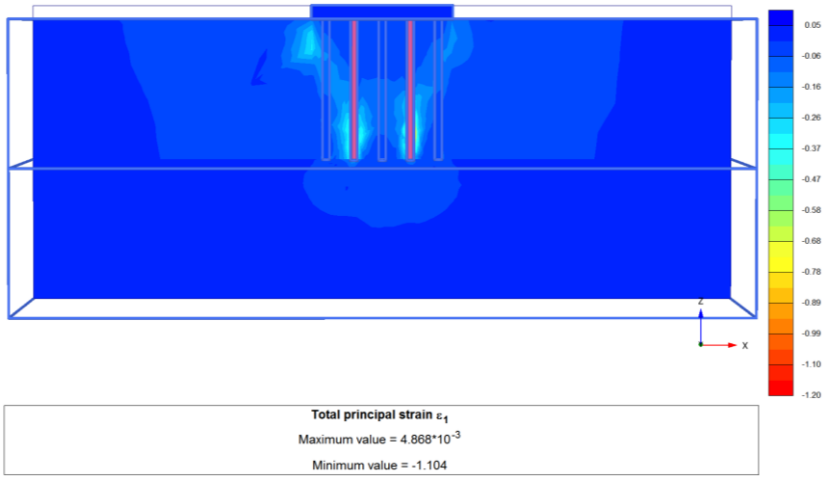
Set 26 Section B-B



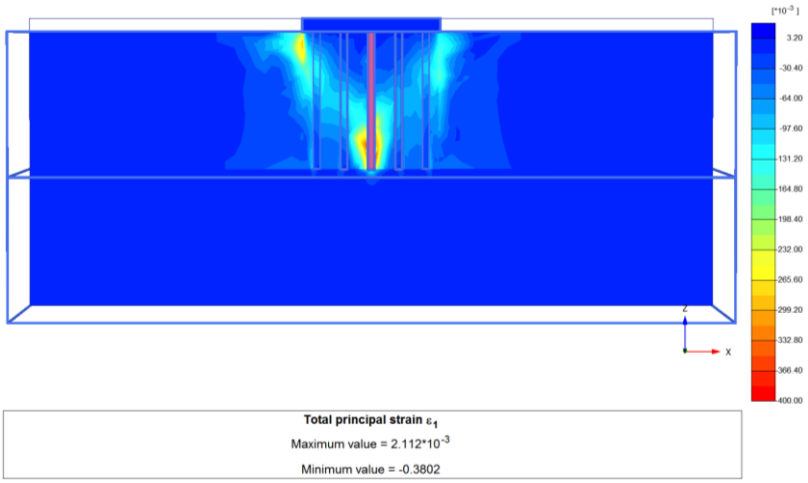
Set 26 Section C-C



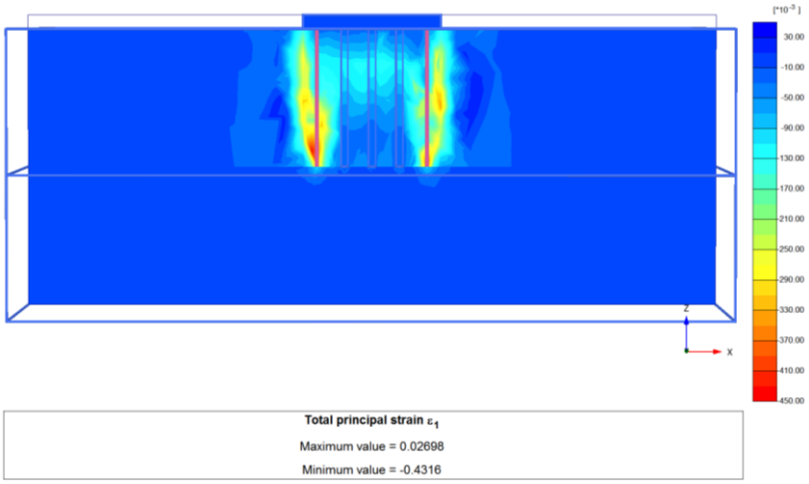
Set 27



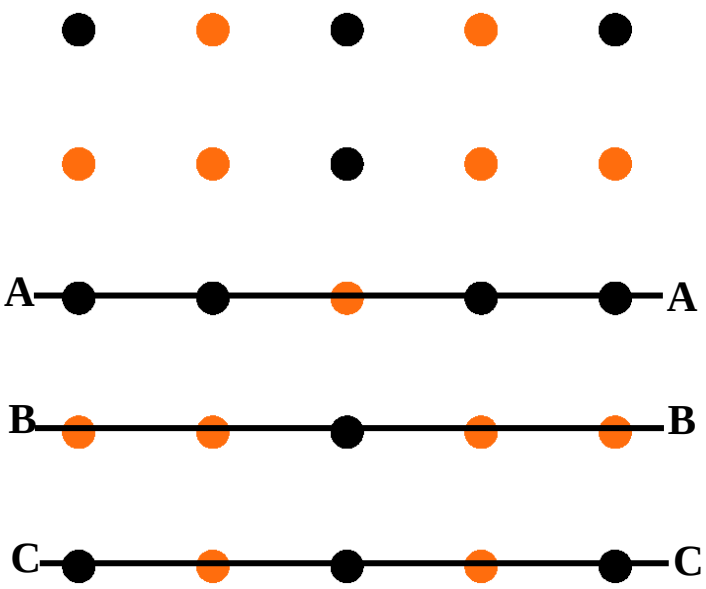
Set 27 Section A-A



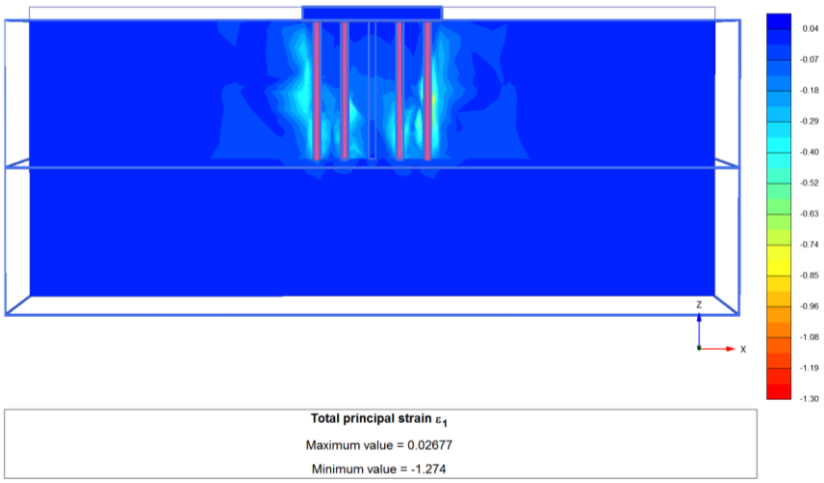
Set 27 Section B-B



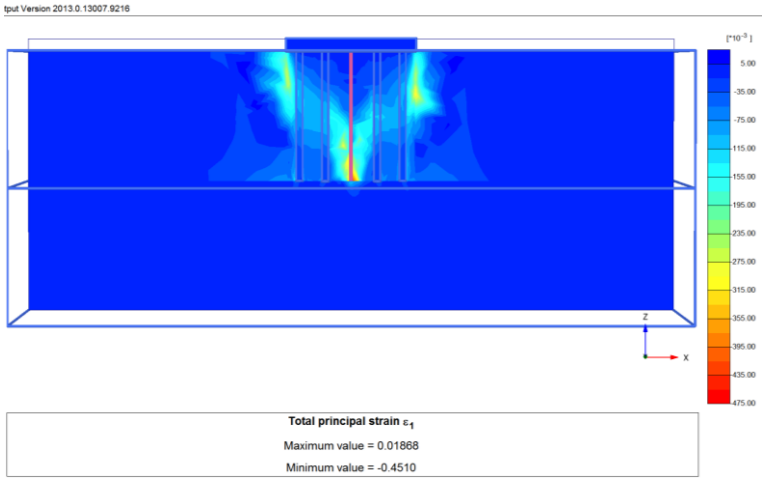
Set 27 Section C-C



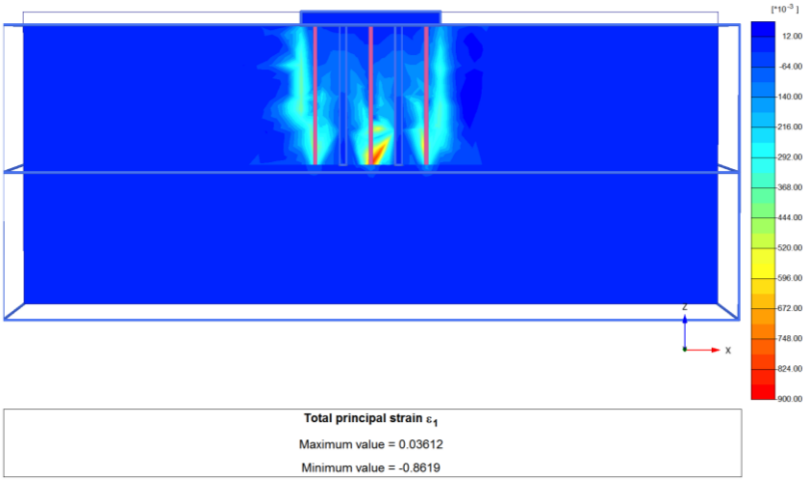
Set 28



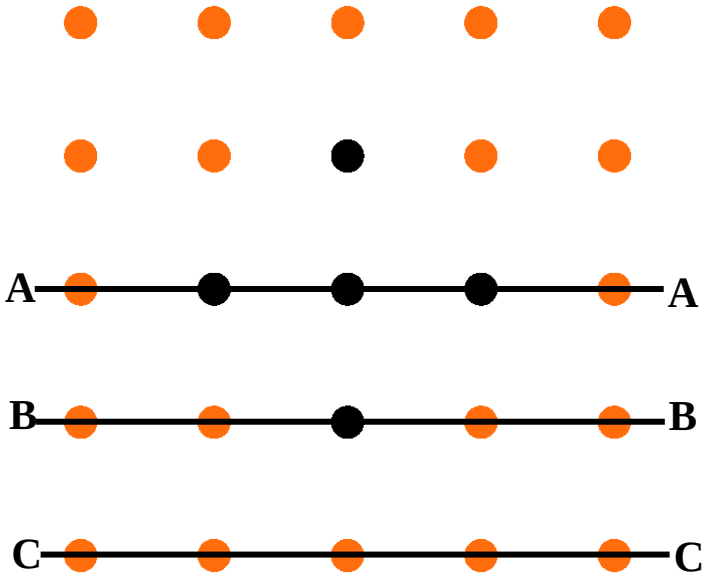
Set 28 Section A-A



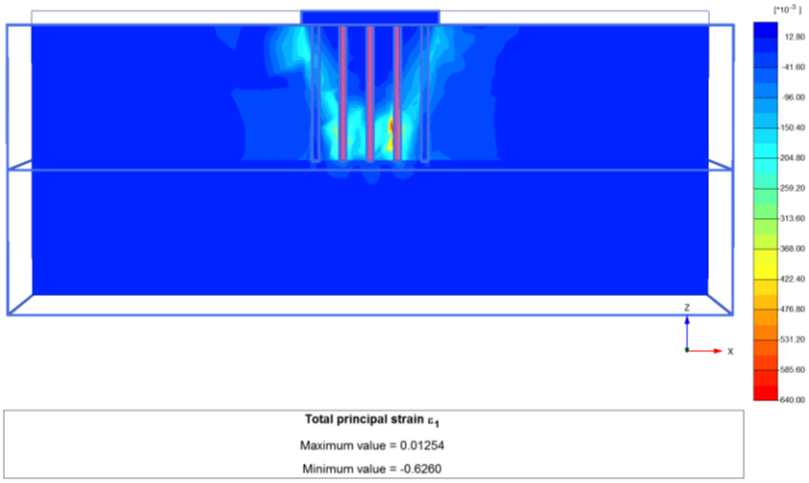
Set 28 Section B-B



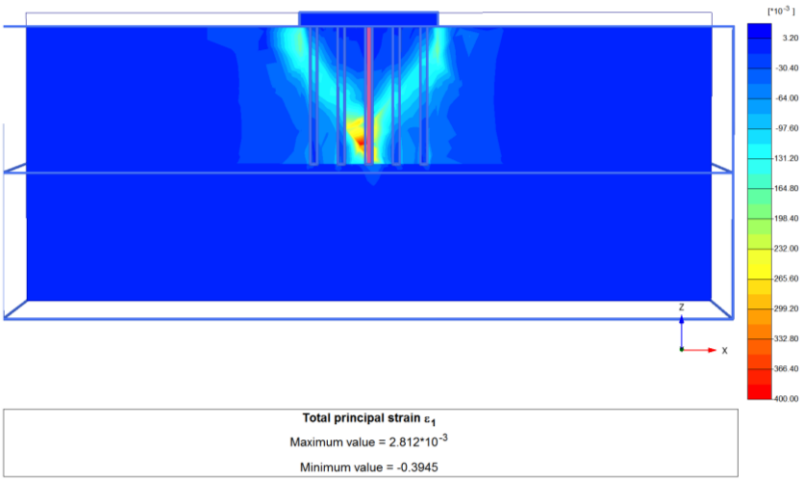
Set 28 Section C-C



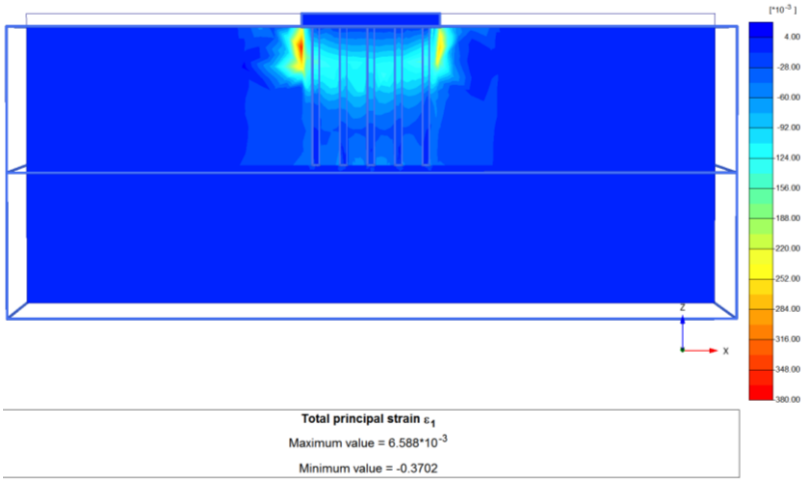
Set 29



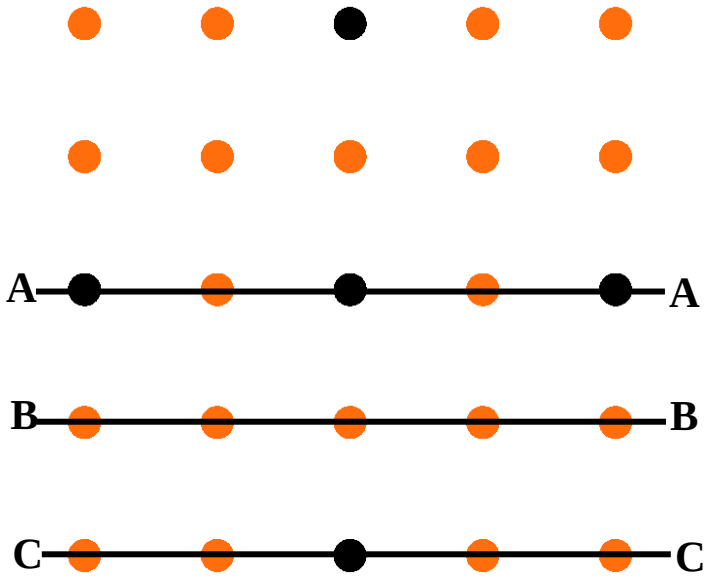
Set 29 Section A-A



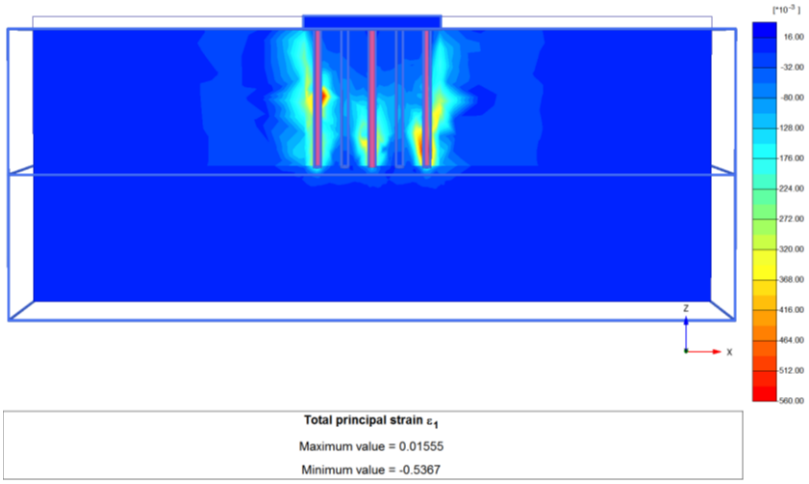
Set 29 Section B-B



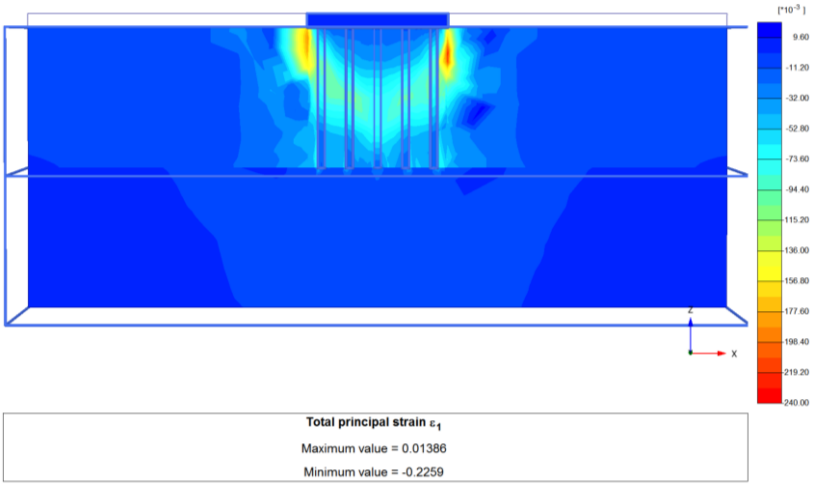
Set 29 Section C-C



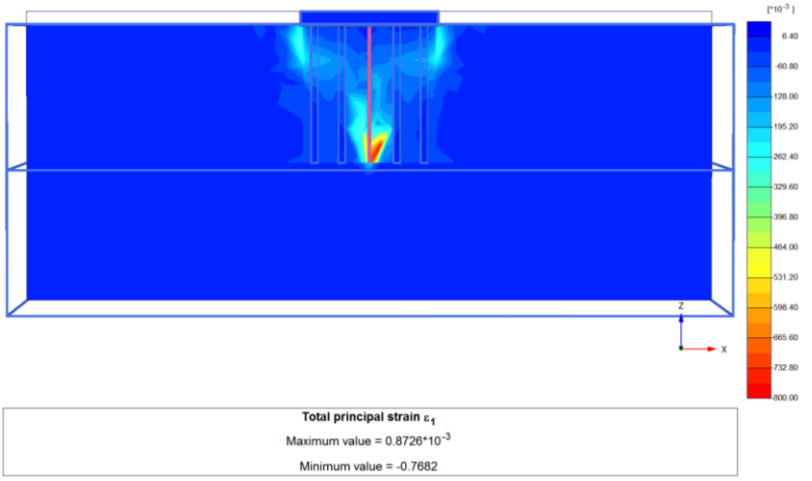
Set 30



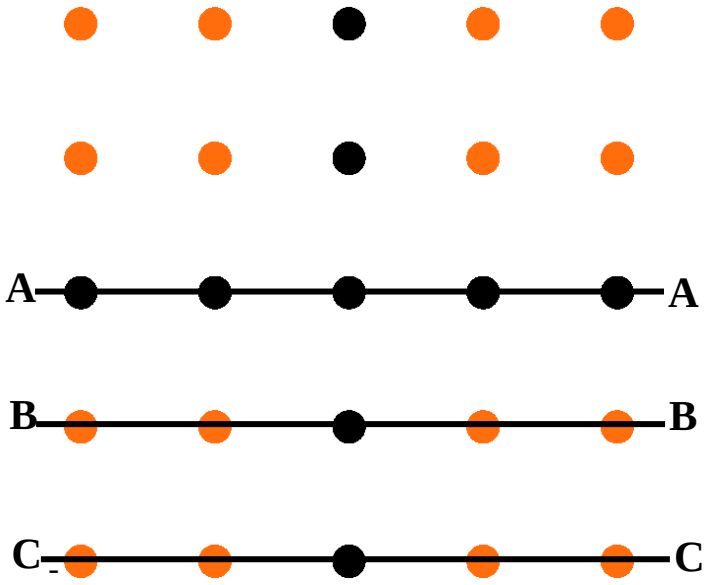
Set 30 Section A-A



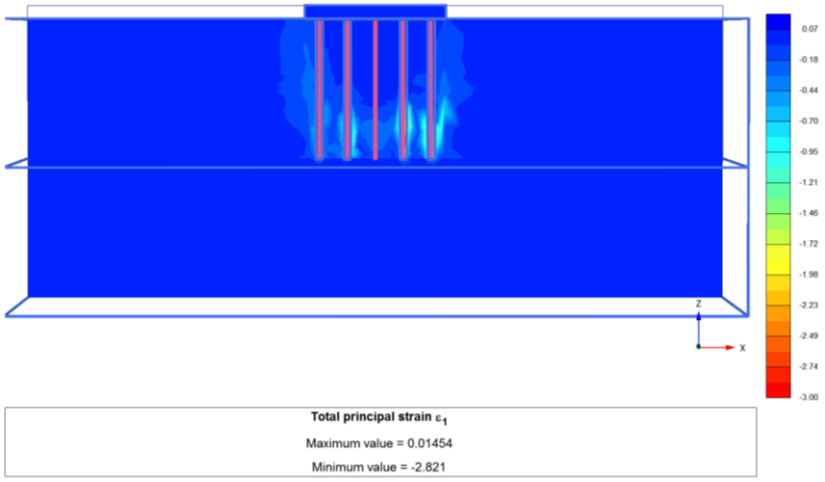
Set 30 Section B-B



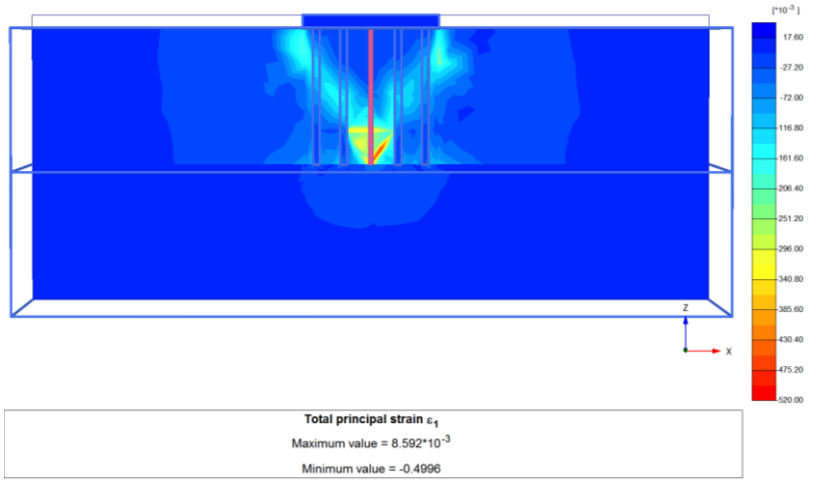
Set 30 Section C-C



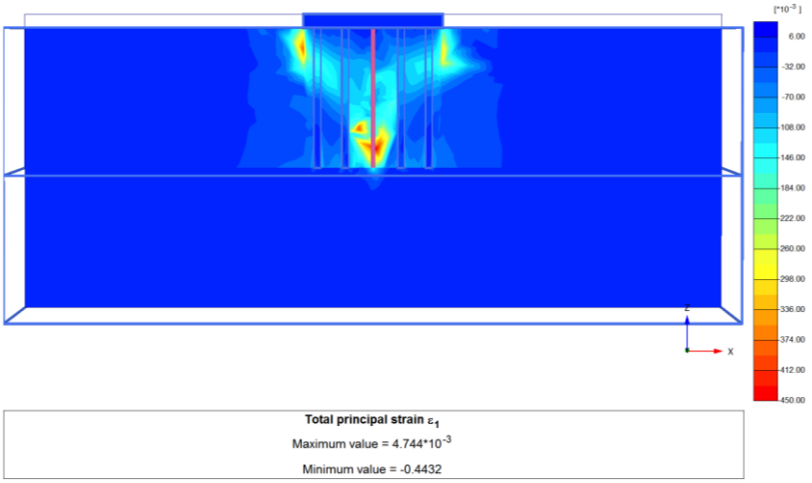
Set 31



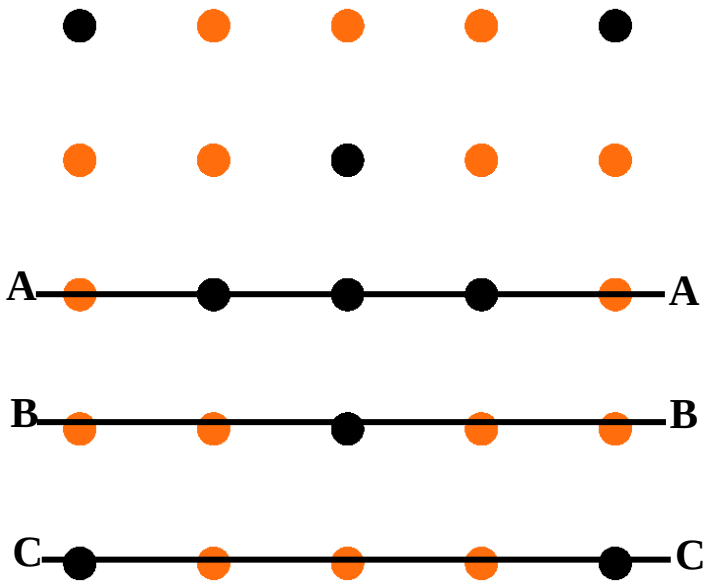
Set 31 Section A-A



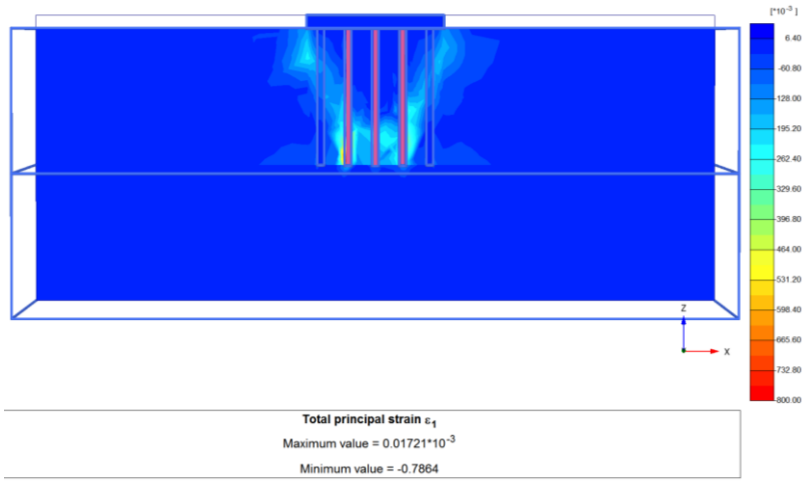
Set 31 Section B-B



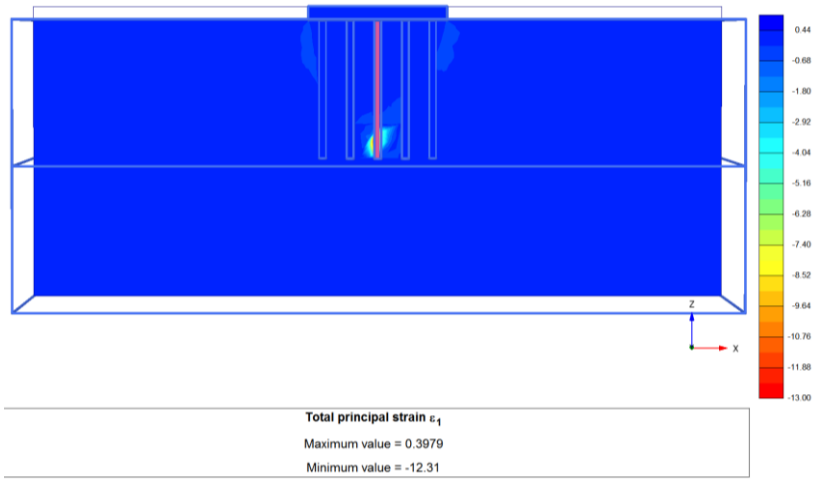
Set 31 Section C-C



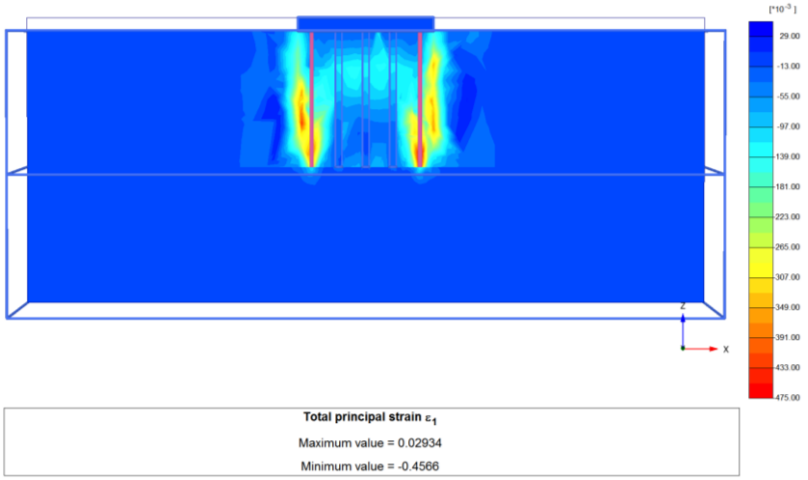
Set 32



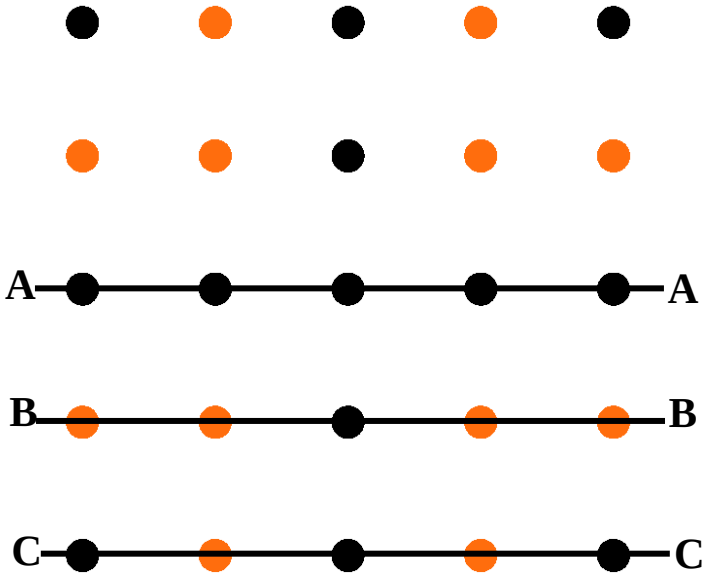
Set 32 Section A-A



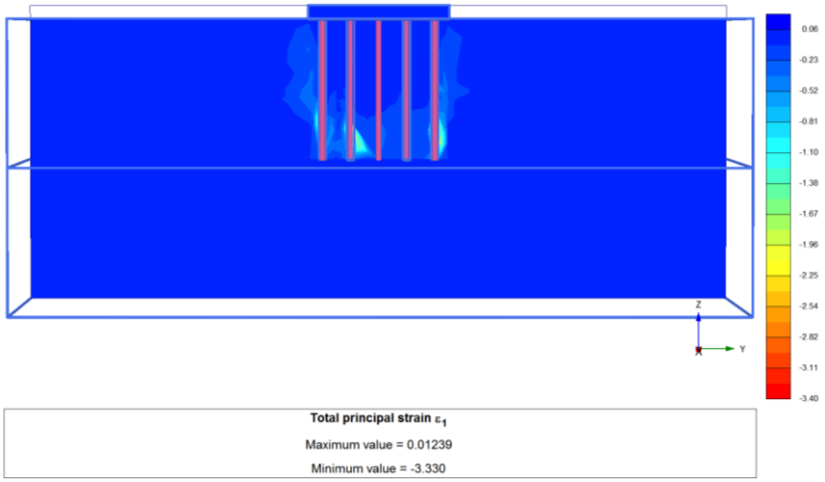
Set 32 Section B-B



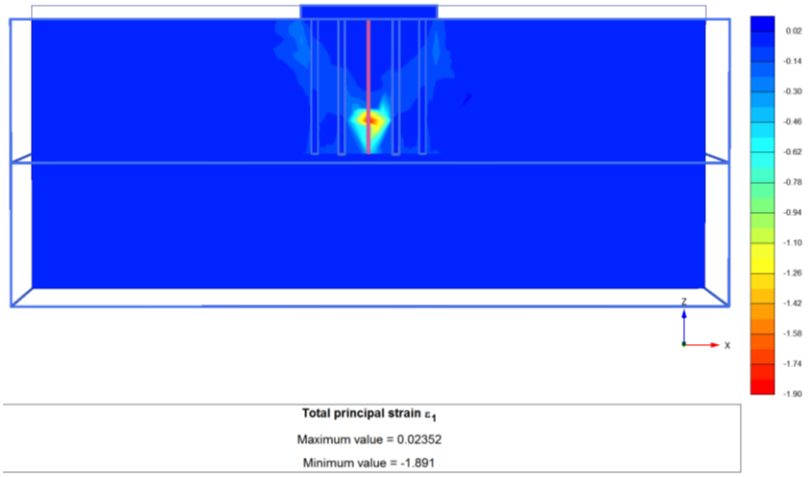
Set 32 Section C-C



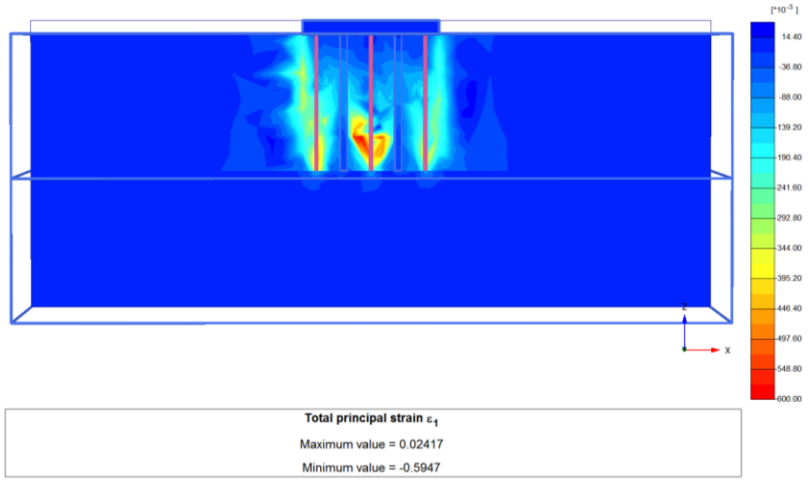
Set 33



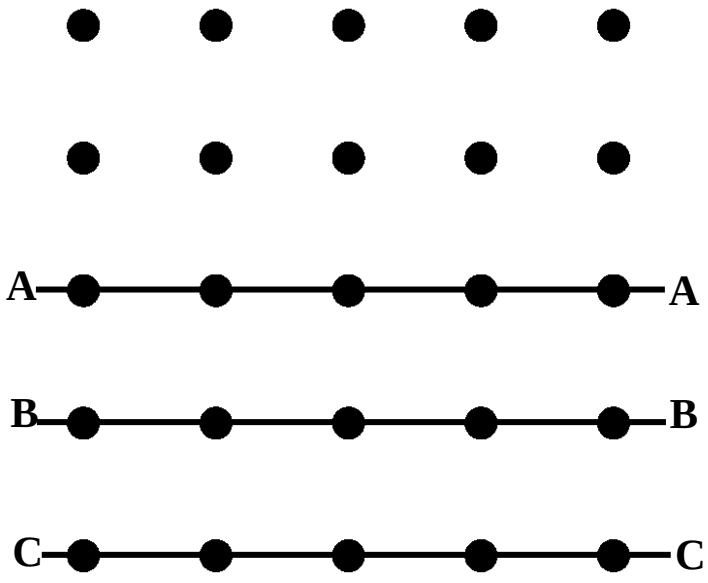
Set 33 Section A-A



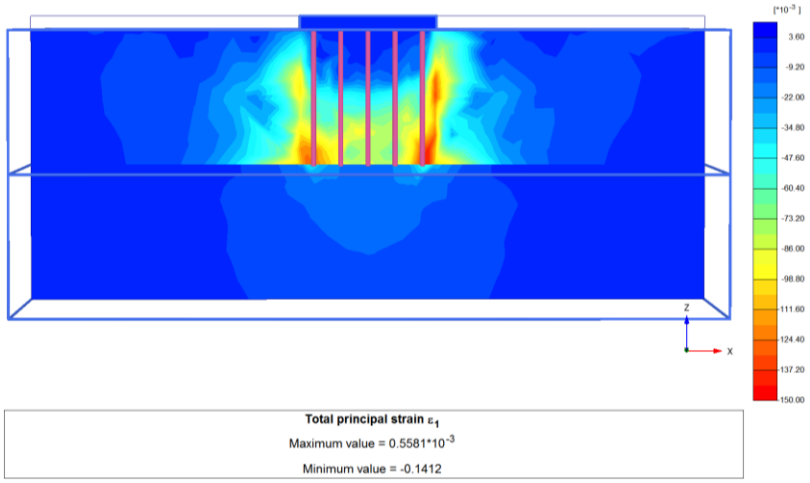
Set 33 Section B-B



Set 33 Section C-C



Set 34



Set 34 Section A-A

Appendix H (Configuration factor $\boldsymbol{\alpha}$)

Set No.	n_1 (number of piles)	n_c (number of columns)	α
2	4	21	0.74
8	4	21	0.68
24	4	21	0.69
25	4	21	0.71
10	5	20	0.72
22	5	20	0.69
29	5	20	0.69
30	5	20	0.71
3	8	17	0.72
9	8	17	0.69
14	8	17	0.71
26	8	17	0.68
27	8	17	0.71
11	9	16	0.72
18	9	16	0.71
23	9	16	0.71
31	9	16	0.70
32	9	16	0.70
15	12	13	0.73
16	12	13	0.70
28	12	13	0.72
19	13	12	0.71
20	13	12	0.66
33	13	12	0.73
4	16	9	0.80
17	16	9	0.72
12	17	8	0.80
21	17	8	0.68
5	20	5	0.89
13	21	4	0.94
6	24	1	1.00

Journal Publications

1. **Ahmed, D**., Linda bt Taib, S. N., Ayadat, T., & Hasan, A. (2022). Geotechnical performance of combined stone columns/piles capped with reinforced concrete raft foundation in soft clay soil. *Acta Geodynamica et Geomaterialia (AGG)*. DOI: 10.13168/AGG.2022.0016 (**Published**)
2. **Ahmed, D**., Linda bt Taib, S. N., Ayadat, T., & Hasan, A. (2022). Carrying Capacity of Piled Raft Foundation in Soft Clayey Soils. *Civil Engineering Journal*. Vol. 8, No. 04. **(Published)**
3. **Ahmed, D**., Linda bt Taib, S. N., Ayadat, T., & Hasan, A. (2021). A review on the behaviour of combined stone columns and pile foundations in soft soils when placed under rigid raft foundation. *ASM Science Journal*. Vol. 16. DOI: 10.32802/asmscj.2021.709. (**Published**)
4. **Ahmed, D**., Linda bt Taib, S. N., Ayadat, T., & Hasan, A. (2020). Numerical investigation on the performance of stone columns under raft foundation in soft clayey soils. *IOP Conference Series: Materials Science and Engineering*, Volume 1101, The conference proceedings 13th International UNIMAS Engineering Conference 2020 (ENCON 2020), Oct 2020, Kuching, Malaysia. DOI: 10.1088/1757-899X/1101/1/012015 **(Published, Conference proceeding)**

Conference Publications

1. **Ahmed, D**., Linda bt Taib, S. N., Ayadat, T., & Hasan, A. (2021). Geotechnical Performance of Combined Foundation System Composed of Stone Columns, Piles and

Rigid Mat Foundation in Soft Soils. *1st Mediterranean Geosciences Union*, Istanbul, Turkey, 25-28 November. (**Presented)**

2. **Ahmed, D**., Linda bt Taib, S. N., Ayadat, T., & Hasan, A. (2020). Numerical Investigation on the Performance of Stone Columns under Raft Foundation in Soft Clayey Soils. *13th International UNIMAS Engineering Conference* (EnCon 2020). **(Presented)**
3. **Ahmed, D**., Linda bt Taib, S. N., Ayadat, T., & Hasan, A. (2020) Numerical investigation on the performance of Piled Raft Foundation in Soft Clayey Soils. *5th International Conference on Geotechnical Research and Engineering* (ICGRE'20), Lisbon, Portugal, October 18-20. (**Presented & published**)